

Copyright is owned by the Author of the thesis. Permission is given for a copy to be downloaded by an individual for the purpose of research and private study only. The thesis may not be reproduced elsewhere without the permission of the Author.

**THE SYNTHESIS AND  
PROPERTIES OF POLYETHER  
SUBSTITUTED  
OLIGOTHIOPHENES**

**A thesis presented in partial fulfillment of the requirements  
for the degree of**

**Doctor of Philosophy**

**in**

**Chemistry**

**at Massey University, Palmerston North, New Zealand.**

**Daina Kim Grant**

**July 2003**

## **Abstract**

A number of novel dialkoxystyryl-substituted terthiophenes were synthesised as precursors to form conducting polymers. These compounds contained either crown ethers or polyether chains designed to complex metal cations, and polymerisable terthiophene moieties. Two isomeric cross-linked bis(terthiophene) crown ethers were also synthesised as monomers for conducting polymer synthesis, but could not be investigated further due to their insolubility. The solubility issue was circumvented by the formation of hemicrown compounds, containing two styryl-terthiophene units linked by a polyether chain. Thiophene analogues of the crown ether, open-chain ether, bis(terthiophene) crown ether and hemicrown compounds were also successfully synthesised and characterised.

The response of the terthiophene crown compounds, open-chain compounds and hemicrowns to a large range of metal cations was investigated by UV and fluorescence spectroscopy. The results obtained from this work were consistent with complexation based on size-fit and charge density of ions, and with hard-soft-acid-base theory.

Chemical polymerisation of the terthiophene crown monomers and open-chain ether terthiophene compounds was carried out using  $\text{FeCl}_3$ . This led to the isolation of dimeric sexithiophene compounds in high yield. Characterisation of the pure sexithiophene derivatives showed that they were the product of regioselective dimerisation, caused by the asymmetric reactivity of the terthiophene-based monomers. This is believed to be due to uneven electron spin-density distribution, and theoretical calculations on the radical cation support this view. Producing dialkoxystyryl-substituted sexithiophenes by this synthetic route gave excellent yields of isomerically-pure product.

Chemical oxidation of terthiophene compounds using  $\text{Cu}(\text{ClO}_4)_2$  was observed with UV/VIS/NIR spectroscopy. This allowed the observation and identification of absorption bands due to oxidised species. Reduction of these species led to sexithiophene dimers, as seen for chemical polymerisation using  $\text{FeCl}_3$ .

Electrochemical polymerisations of the terthiophene, thiophene and sexithiophene compounds were carried out by cyclic voltammetry. Those that formed adherent films were analysed by UV/VIS/NIR spectroscopy in both the neutral and oxidised form. The electrochemical and spectroscopic evidence again pointed to the formation of dimers as the primary product of oxidation from terthiophene-based monomers. The surface morphology of the films was investigated by scanning electron microscopy, and showed a variety of morphologies.

### CANDIDATE'S DECLARATION

This is to certify that the research carried out for my Doctoral thesis entitled "The Synthesis and Properties of Polyether Substituted Oligothiophenes" in the Institute of Fundamental Sciences, Massey University, Turitea, New Zealand is my own work and that the thesis material has not been used in part or in whole for any other qualification.

**Candidate's Name:** DAINA K. GRANT

**Signature:** 

**Date:** 5/12/03

### CERTIFICATE OF REGULATORY COMPLIANCE

This is to certify that the research carried out in the Doctoral Thesis entitled “The Synthesis and Properties of Polyether Substituted Oligothiophenes” in the Institute of Fundamental Sciences at Massey University, New Zealand:

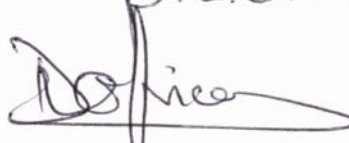
- (a) is the original work of the candidate, except as indicated by appropriate attribution in the text and/or in the acknowledgements;
- (b) that the text, excluding appendices/annexes, does not exceed 100,000 words;
- (c) all the ethical requirements applicable to this study have been complied with as required by Massey University, other organisations and/or committees which had a particular association with this study, and relevant legislation.

Candidate's Name: D.K. GRANT

Supervisor's Name: D.L. OFFICER

Signature: 

Signature:



Date: 5/12/03

Date:

05/12/03

## ***Publications***

Grant, D. K. (2002). "Synthesis and polymerisation of fully conjugated polyether-substituted terthiophenes." Synthetic Metals **135-136C**: 101-102.

Burrell, A. K., D. L. Officer and D. K. Grant (2002). "Functionalised poly(terthiophenes)." Synthetic Metals **135-136C**: 95-96.



## ***Acknowledgements***

Thank-you the management of Crop & Food Research for giving me the opportunity and the resources to undertake a PhD. In particular I would like to thank Dr Chris Downs for his unfailing support, for asking me how I was and genuinely caring about the reply.

To my chief supervisor Dr David Officer: this project wouldn't have gone ahead without your generous provision of financial support, equipment and space.

Thank-you to the staff and students of the Nanomaterials Research Centre and the Institute of Fundamental Sciences for long discussions that occasionally involved chemistry. In particular I would like to acknowledge Dr Wayne Campbell, who has made his friendship and chemical expertise freely available to me over many years. Thank-you also to Dr Gavin Collis and Dr Paul Plieger for teaching me the intricacies of pinball.

Thank-you to the support staff at both Massey University and Crop & Food Research (stores, workshop, electronics and administration) for doing what you could to help.

A special thank-you to Dr Simon Hall and Dr Keith Gordon for helpful discussions on electrochemistry and spectroscopy.

Thank-you to the staff of the Intelligent Polymer Research Institute in Wollongong and Industrial Research Ltd in Wellington for the opportunity to undertake research using your facilities and expertise.

Finally to my family and friends, especially my mother Lorraine, Koryn & Helga, Andy & Rachel, Jobee and Blake: thank-you for graciously accepting my unavailability at times during the course of this research and loving me anyway, and also for distracting me when I needed a break!



# Table of Contents

<b>Abbreviations</b>	<b>xix</b>
<b>Index of Figures</b>	<b>xxi</b>
<b>Index of Synthetic Schemes</b>	<b>xxix</b>
<b>Index of Tables</b>	<b>xxxii</b>
<b>Index of Compounds</b>	<b>xxxiii</b>
<b>1 INTRODUCTION AND LITERATURE REVIEW</b>	<b>1</b>
1.1 Research Objectives	2
1.2 Crown Ethers	3
1.3 Conducting Polymers	6
1.3.1 Polymer growth	7
1.3.2 Charge transport in conducting polymers	8
1.3.3 Functionalised polymers based on thiophene	10
1.4 Past Work on Ether Functionalised Thiophenes	15
1.4.1 Open-chain ethers	15
1.4.2 Pseudo crown ethers	21
1.4.3 Alkyl spaced crown ethers	24
1.4.4 Directly bonded crown ethers	27
1.5 Past Work on Vinyl-Substituted Polythiophenes	32
1.6 Vinyl Linked Terthiophene Crown Ether Target Molecules	34
<b>2 SYNTHESIS OF ETHER FUNCTIONALISED (TER)THIOPHENES</b>	<b>35</b>
2.1 Literature Synthetic Methods	37
2.1.1 The synthesis of vinyl-substituted benzo-crown ethers	37
2.1.2 The synthesis of 3'-vinyl-substituted terthiophenes	44
2.1.3 The synthesis of vinyl-substituted thiophenes	45
2.2 Synthetic Studies Toward Monostyryl (Ter)thiophene Crowns	47
2.2.1 Synthesis of crown phosphonium salts	47
2.2.2 Wittig reactions using crown phosphonium salts	50
2.2.3 Synthesis of crown phosphonates	53
2.2.4 Horner-Emmons reactions using phosphonates	55
2.2.5 Synthesis of crown-functionalised thiophenes	58
2.3 Synthesis of Open-Chain Ether Functionalised (Ter)thiophenes	62
2.3.1 Open-chain terthiophenes	62
2.3.2 Open-chain thiophenes	68

<b>3</b>	<b>SYNTHESIS OF ETHER FUNCTIONALISED BIS(TER)THIOPHENES</b>	<b>73</b>
3.1	Literature Synthetic Methods	76
3.2	Synthesis of Bis(styryl (Ter)thiophene) Crowns	77
3.2.1	Synthesis of crown bis(phosphonium salt) and bis(phosphonate)	77
3.2.2	Wittig/Horner-Emmons reactions using mixed bis(phosphonium salt)s and bis(phosphonate)s	81
3.2.3	Synthesis of <i>syn</i> -bis(formylbenzo)-18-crown-6 <b>XLV</b>	83
3.2.4	Horner-Emmons reaction using <i>syn</i> -bis(formylbenzo)-18-crown-6	88
3.2.5	Synthesis of <i>anti</i> -bis(formylbenzo)-18-crown-6 <b>XLVI</b>	90
3.2.6	Horner-Emmons reaction using <i>anti</i> -bis(formylbenzo)-18-crown-6	94
3.2.7	Formation of bis(styryl thiophene) crowns	96
3.3	Synthesis of (Ter)thiophene Hemicrowns	98
3.3.1	Synthesis of terthiophene hemicrowns	98
3.3.2	Synthesis of thiophene hemicrowns <b>LXIV - LXVI</b>	103
3.4	Synthetic Summary	105
<b>4</b>	<b>SPECTROSCOPIC ION BINDING STUDIES</b>	<b>107</b>
4.1	UV/VIS Spectroscopy	108
4.1.1	Literature review	108
4.1.1.1	Absorbance of substituted terthiophenes	108
4.1.1.2	Effect of cation complexation on absorbance of functionalised crown ethers	110
4.1.1.3	Effect of cation complexation on polyether-substituted polythiophenes	114
4.1.2	UV/VIS spectra of polyether-substituted oligothiophenes	118
4.1.2.1	Absorbance of terthiophene monomers	118
4.1.2.2	Absorbance of thiophene monomers	121
4.1.2.3	Absorbance of terthiophene dimers	122
4.1.3	Effect of cation complexation on terthiophene monomer UV/VIS spectra	124
4.1.3.1	Experimental procedure	125
4.1.3.2	Discussion	127
4.2	Fluorescence Spectroscopy	131
4.2.1	Literature review	131
4.2.1.1	Fluorescence of substituted crown ethers	131
4.2.1.2	Fluorescence of substituted terthiophenes	133
4.2.1.3	Fluorescence of crown ether-substituted thiophenes	135
4.2.2	Fluorescence of polyether-substituted oligothiophenes	137
4.2.3	Effect of cation complexation on terthiophene monomer fluorescence spectra	139
4.2.3.1	Experimental procedure	139
4.2.3.2	Discussion	142
4.3	Summary	145

<b>5</b>	<b>CHEMICAL AND ELECTROCHEMICAL POLYMERISATION</b>	<b>147</b>
<b>5.1</b>	<b>Chemical Polymerisation</b>	<b>148</b>
5.1.1	Literature review	148
5.1.2	FeCl <sub>3</sub> polymerisation of terthiophene monomers	150
5.1.3	Cu(ClO <sub>4</sub> ) <sub>2</sub> polymerisation of terthiophene monomers	160
<b>5.2</b>	<b>Electropolymerisation</b>	<b>168</b>
5.2.1	Cyclic voltammetry in a three-electrode cell	168
5.2.2	Experimental procedures	172
5.2.3	Electropolymerisation of reference compounds	175
5.2.3.1	Terthiophene	177
5.2.3.2	Styryl terthiophene LXXVI	179
5.2.3.3	Methoxystyryl terthiophene LXXVII	182
5.2.4	Electropolymerisation of dialkoxystyryl-substituted terthiophene compounds	188
5.2.4.1	Dimethoxystyryl terthiophene XXIX	188
5.2.4.2	Styryl-15-crown-5 terthiophene I	192
5.2.4.3	Styryl-18-crown-6 terthiophene II	200
5.2.4.4	Open-chain substituted terthiophenes XXIII - XXVIII	201
5.2.4.5	Terthiophene hemicrowns LXI - LXIII	210
5.2.4.6	Styryl-15-crown-5 terthiophene copolymer formation	218
5.2.5	Electropolymerisation of thiophene monomers	229
5.2.5.1	Electropolymerisation of dialkoxystyryl-substituted thiophene compounds	229
5.2.5.2	Electropolymerisation of thiophene hemicrown compounds	230
5.2.5.3	Styryl-15-crown-5 thiophene copolymer formation	232
5.2.6	Electropolymerisation of sexithiophene compounds	236
5.2.7	Summary	239
<b>6</b>	<b>CONCLUSIONS</b>	<b>241</b>
<b>7</b>	<b>EXPERIMENTAL DETAILS</b>	<b>245</b>
	<b>References</b>	<b>343</b>



## Abbreviations

AFM	atomic force microscopy
Anal.	analysis
aq.	aqueous
ArC	aromatic carbon atom
ArH	aromatic proton
AU	absorbance units
c.	concentrated
<i>ca.</i>	circa
calc	calculated
CV	cyclic voltammetry or cyclic voltammogram
DBU	1,8-diazabicyclo[5.4.0]undec-7-ene
DMF	dimethylformamide
<i>E</i>	potential
Em	emission
ESR	electron spin resonance
Et	ethyl
EtOH	ethanol
eq.	equivalents
Ex	excitation
FAB-MS	fast atom bombardment mass spectrometry
Fig.	Figure
GPC	gel permeation chromatography
HOMO	highest occupied molecular orbital
HRMS	high-resolution mass spectrometry
h	hours
IR	infrared
ITO	indium tin oxide
<i>J</i>	coupling constant
L	litre
LDI-MS	laser desorption of ions mass spectrometry

LUMO	lowest unoccupied molecular orbital
μL	microlitre
mA	milliampere
MALDI-MS	matrix assisted laser desorption of ions mass spectrometry
max	maximum
Me	methyl
MeCN	acetonitrile
MeOH	methanol
min	minutes
mL	millilitre
mM	millimole/litre
mmol	millimole
mol	mole
NIR	near infrared
NMR	nuclear magnetic resonance
Ph	phenyl
SEM	scanning electron microscopy or scanning electron micrograph
TBAP	tetrabutylammonium perchlorate
ThC	thienyl carbon atom
ThH	thienyl proton
THF	tetrahydrofuran
r.t.	room temperature
sat.	saturated
TLC	thin layer chromatography
UV	ultraviolet
ν	scanning speed
V	volt
VIS	visible

## ***Index of Figures***

<b>Figure</b>	<b>Page</b>	
1.1	Examples of crown ethers	3
1.2	Crown ether – metal ion complexation	4
1.3	Schematic representation of 2:1 and 3:2 ‘sandwich’ complexes	4
1.4	Examples of conjugated polymers	6
1.5	Redox activity of polythiophene	7
1.6	Polymer growth mechanism including oxidation, radical cation coupling and deprotonation	7
1.7	Degeneracy of poly( <i>trans</i> -acetylene) and non-degeneracy of polythiophene ground states	8
1.8	Thiophene	10
1.9	Coupling orientations of 3-substituted thiophenes	11
1.10	Regioregular polymers from disubstituted bithiophenes and terthiophenes	12
1.11	Regioselective chemical polymerisations by Gallazzi and McCullough, and Chen and Lere-Porte	13
1.12	Functionalisation space of polythiophene	14
1.13	Alkoxy substituted polythiophenes	16
1.14	3-Alkoxy substituted thiophenes synthesised by Roncali <i>et al.</i>	17
1.15	Cyclic voltammograms of poly[3-(3,6-dioxaheptyl)thiophene] in LiClO <sub>4</sub> and TBAP	18
1.16	Heteroatom substituted polythiophenes synthesised by McCullough <i>et al.</i>	18
1.17	3-Alkoxy and 3-alkoxy-4-methylthiophenes synthesised by Feldhues <i>et al.</i>	19
1.18	Poly(3-alkoxythiophenes) studied by Chen and Tsai	20
1.19	Alkoxy chain substituted polythiophenes (Scheib & Bauerle)	20
1.20	Formation of pseudo crown ether cavities during polymerisation	21
1.21	Oxyethylene linked bis(bithiophene) monomers of Roncali and Scheib	22

1.22	Oligo(oxyethylene) bridged EDOT monomers	22
1.23	Metal ion induced twisting of bithiophene monomer	23
1.24	Macrocyclic psuedo-crown ether cavities synthesised by Fabre <i>et al.</i>	24
1.25	Alkoxy spaced crowns synthesised by Bauerle and Scheib	25
1.26	Poly(3-alkoxy-4-methylthiophene)s	26
1.27	Planar and perpendicular bithiophene monomers designed by Sannicolo <i>et al.</i>	26
1.28	Crown ether functionalised thiophenes synthesised by Bicknell <i>et al.</i>	27
1.29	Directly $\pi$ -conjugated monomers of Bauerle and Scheib	28
1.30	Crown ether functionalised thiophenes studied by Berlin <i>et al.</i>	29
1.31	Polymers synthesised by Yamamoto <i>et al.</i>	30
1.32	Crown containing copolymers by Bouachrine <i>et al.</i>	31
1.33	2- and 3-substituted styrylthiophenes	32
1.34	Nitrostyryl terthiophene synthesised by Cutler <i>et al.</i>	33
1.35	Vinyl linked terthiophene crown ether target molecules	34
2.1	Target compounds styryl-15-crown-5 and styryl-18-crown-6 terthiophene	36
2.2	Heck arylation of olefins	37
2.3	Synthesis of vinyl-substituted crown ethers <i>via</i> alcohol dehydration	38
2.4	Formation of vinyl-substituted dibenzo-18-crown-6	38
2.5	Vinylation of benzo-15-crown-5 <i>via</i> Knoevenagel condensation	39
2.6	Extension of Knoevenagel condensation method	39
2.7	Claisen-Schmidt condensation of crown derivatives	40
2.8	Formation of mono- and bis-crown ether styryl dyes according to the method of Gromov <i>et al.</i>	41
2.9	Formation of stilbene bis-crown ethers	42
2.10	Wittig reaction between ferrocene phosphonium salt and formylbenzo-15-crown-5	43

2.11	Formation of vinyl substituted crown <i>via</i> Wittig (or Horner Emmons) reaction	44
2.12	Synthesis of 3'-vinyl-2,2':5',2"-terthiophene <i>via</i> Grignard chemistry	44
2.13	Wittig/Horner-Emmons reactions used to synthesise vinyl-substituted terthiophenes	45
2.14	The use of Wittig reactions to synthesise vinyl thiophenes	46
2.15	<sup>1</sup> H NMR spectrum of styryl-15-crown-5 terthiophene <b>I</b>	52
2.16	<sup>1</sup> H NMR spectrum for benzo-15-crown-5 phosphonate <b>XIII</b>	55
2.17	Fully assigned <sup>1</sup> H NMR spectrum of styryl-15-crown-5 thiophene <b>XV</b>	60
2.18	Open-chain polyether styryl-substituted terthiophenes targeted	62
2.19	Formation of open-chain ether functionalised terthiophenes	63
2.20	<sup>1</sup> H NMR spectra of open-chain terthiophenes <b>XXIII-XXV</b> (ether region)	66
2.21	Comparison of aromatic regions in <sup>1</sup> H NMR spectra of compounds <b>XXIII</b> and <b>XXVI</b>	67
2.22	Styryl terthiophene reference compounds	68
2.23	<sup>1</sup> H NMR assignment for open-chain thiophene <b>XXX</b>	70
3.1	Potential for actuation effect caused by metal complexation	74
3.2	The two isomeric forms of bis(styryl terthiophene)-18-crown-6	75
3.3	MALDI-MS of <i>syn</i> -bis(styryl terthiophene)-18-crown-6 <b>XVI</b> after acid wash	89
3.4	Isomeric terthiophene hemicrowns targeted	98
3.5	Assigned <sup>1</sup> H NMR spectrum of isovanillin-derived terthiophene hemicrown <b>LXI</b>	101
3.6	Comparison of <sup>1</sup> H NMR spectra for terthiophene hemicrowns <b>LXI</b> , <b>LXII</b> and <b>LXIII</b>	102
4.1	The structure of terthiophene	108
4.2	Crown ether styryl dyes	111
4.3	Aza crown ether styryl dyes investigated by UV/VIS spectroscopy	112

4.4	Polyether substituted polythiophenes investigated by UV/VIS spectroscopy	115
4.5	Ionochromic polythiophenes synthesised by Marsella <i>et al.</i>	116
4.6	Crown ether functionalised (ter)thiophenes	117
4.7	Absorbance spectra of terthiophene monomers in MeCN	118
4.8	Solution and thin film UV/VIS spectra of 18-crown-6 terthiophene dimer <b>LXVII</b>	123
4.9	Change in absorbance maxima caused by addition of metal cations to terthiophene monomers	126
4.10	Styryl-15-crown-5 terthiophene <b>I</b> before and after addition of Mg <sup>2+</sup>	128
4.11	Crown ether styryl dyes of Barzykin and Shin	132
4.12	Styryl-substituted aza crown ethers	133
4.13	Benzo-crown ether fluorophore synthesised by Cielen <i>et al.</i>	135
4.14	Pyridino crown ethers containing thiophene-based fluorophore(s)	136
4.15	Absorbance and fluorescence spectra for polyether-substituted terthiophene <b>XXVII</b> and polyether-substituted sexithiophene <b>LXIX</b> in CH <sub>2</sub> Cl <sub>2</sub>	138
4.16	Absorption and fluorescence spectra of styryl-15-crown-5 terthiophene <b>I</b> before and after addition of Mn <sup>2+</sup>	140
4.17	Fluorescence quenching caused by addition of metal cations to terthiophene monomers	141
5.1	Chemical polymerisation of 15-crown-5 terthiophene to form head-to-tail, head-to-head or tail-to-tail linked dimers	151
5.2	<sup>1</sup> H NMR spectra (aromatic region) of styryl-15-crown-5 terthiophene <b>I</b> and 15-crown-5 terthiophene dimer <b>LXVII</b>	152
5.3	Fully assigned <sup>1</sup> H NMR spectrum for terthiophene dimer <b>LXXIII</b>	155
5.4	Potential oligomers formed from chemical polymerisation of terthiophene hemicrown <b>LXI</b>	159
5.5	Oxidation and reduction of methoxystyryl terthiophene <b>LXXVII</b> as observed by UV/VIS spectroscopy	162
5.6	Schematic representation of a three electrode cell	169

5.7	Applied voltage, measured current and final cyclic voltammogram for ferrocene	170
5.8	Cyclic voltammetry for terthiophene	175
5.9	Post-polymerisation CVs of terthiophene in 0.1 M TBAP and 0.1 M LiClO <sub>4</sub>	176
5.10	Growth CV and surface morphology of terthiophene film on ITO-coated mylar	177
5.11	UV/VIS/NIR spectra of poly(terthiophene) in the neutral and oxidised forms	178
5.12	Cyclic voltammetry for styryl terthiophene <b>LXXVI</b>	179
5.13	Post-polymerisation CVs for styryl terthiophene <b>LXXVI</b> in 0.1 M TBAP and 0.1 M LiClO <sub>4</sub>	180
5.14	Growth CV and surface morphology of styryl terthiophene <b>LXXVI</b> film on ITO-coated mylar	181
5.15	UV/VIS/NIR spectra of poly(styryl terthiophene) in the oxidised form	182
5.16	Cyclic voltammetry for methoxystyryl terthiophene <b>LXXVII</b>	183
5.17	Post-polymerisation CVs of methoxystyryl terthiophene <b>LXXVII</b> in 0.1 M TBAP and 0.1 M LiClO <sub>4</sub>	184
5.18	Growth CV and SEM for methoxystyryl terthiophene <b>LXXVII</b> film	186
5.19	UV/VIS/NIR spectra of poly(methoxystyryl terthiophene) in the neutral and oxidised forms	187
5.20	Cyclic voltammetry for dimethoxystyryl terthiophene <b>XXIX</b>	188
5.21	Post-polymerisation CVs of dimethoxystyryl terthiophene <b>XXIX</b> in 0.1 M TBAP and 0.1 M LiClO <sub>4</sub>	190
5.22	Growth CV and SEM of dimethoxystyryl terthiophene <b>XXIX</b> film on ITO-coated mylar	191
5.23	UV/VIS/NIR spectra of poly(dimethoxystyryl terthiophene) in the neutral and oxidised forms	192
5.24	Cyclic voltammetry for styryl-15-crown-5 terthiophene <b>I</b>	193

5.25	Post-polymerisation CVs of styryl-15-crown-5 terthiophene <b>I</b> in 0.1 M TBAP and 0.1 M LiClO <sub>4</sub>	195
5.26	Growth CV for styryl-15-crown-5 terthiophene <b>I</b>	196
5.27	Post-polymerisation CVs of styryl-15-crown-5 terthiophene <b>I</b> in 0.1 M TBAP and 0.1 M LiClO <sub>4</sub>	197
5.28	Growth CV and SEM of styryl-15-crown-5 terthiophene <b>I</b> film	198
5.29	UV/VIS/NIR spectra of styryl-15-crown-5 terthiophene <b>I</b> in the neutral and oxidised forms	199
5.30	Overoxidation of styryl-15-crown-5 terthiophene <b>I</b>	200
5.31	Cyclic voltammetry for styryl-18-crown-6 terthiophene <b>II</b>	200
5.32	Cyclic voltammetry for open-chain terthiophene <b>XXIII</b>	202
5.33	Post-polymerisation CVs of open-chain terthiophene <b>XXIII</b> in 0.1 M TBAP and 0.1 M LiClO <sub>4</sub>	203
5.34	UV/VIS/NIR spectra of open-chain terthiophene <b>XXIII</b> in the neutral and oxidised forms	204
5.35	Growth CV and SEM image of <b>XXVI</b> film on ITO-coated mylar	205
5.36	Cyclic voltammetry for open-chain terthiophene <b>XXVI</b>	206
5.37	Post-polymerisation CVs of open-chain terthiophene <b>XXVI</b> in 0.1 M TBAP and 0.1 M LiClO <sub>4</sub>	207
5.38	Growth CV and SEM image of open-chain terthiophene <b>XXVI</b> film on ITO-coated mylar	208
5.39	UV/VIS/NIR spectrum of poly( <b>XXVI</b> ) in the oxidised form	209
5.40	Cyclic voltammetry for open-chain terthiophene <b>XXVII</b>	209
5.41	Cyclic voltammetry for isovanillin hemicrown <b>LXI</b>	211
5.42	Post-polymerisation CVs of hemicrown <b>LXI</b> in 0.1 M TBAP and 0.1 M LiClO <sub>4</sub>	213
5.43	Growth CV and surface morphology of isovanillin hemicrown <b>LXI</b> film from 1:1 MeCN:CH <sub>2</sub> Cl <sub>2</sub>	215
5.44	Growth CV and scanning electron micrograph of isovanillin hemicrown <b>LXI</b> film grown from CH <sub>2</sub> Cl <sub>2</sub>	216
5.45	Schematic diagram of terthiophene hemicrown surface deposition	217
5.46	UV/VIS/NIR spectra of hemicrown <b>LXI</b> in the neutral and oxidised forms	218

5.47	Cyclic voltammetry for styryl-15-crown-5 terthiophene: terthiophene copolymer	219
5.48	Post-polymerisation CVs of 15-crown-5:terthiophene copolymer in 0.1 M TBAP and 0.1 M LiClO <sub>4</sub>	220
5.49	Growth CV and surface morphology of 15-crown-5 terthiophene: terthiophene copolymer film on ITO-coated mylar	221
5.50	UV/VIS/NIR spectra of styryl-15-crown-5 terthiophene: terthiophene copolymer in the neutral and oxidised forms	222
5.51	Cyclic voltammetry for 15-crown-5 terthiophene:terthiophene hemicrown copolymer	223
5.52	Post-polymerisation CVs of 15-crown-5 terthiophene: hemicrown copolymer in 0.1 M TBAP and 0.1 M LiClO <sub>4</sub>	224
5.53	Growth CV and surface morphology of 15-crown-5 terthiophene: hemicrown copolymer film on ITO-coated mylar	225
5.54	UV/VIS/NIR spectra of styryl-15-crown-5 terthiophene: hemicrown:copolymer in the neutral and oxidised forms	226
5.55	Cyclic voltammetry for styryl-15-crown-5 thiophene <b>XV</b>	227
5.56	Cyclic voltammetry for thiophene hemicrown <b>LXV</b>	231
5.57	Cyclic voltammetry for styryl-15-crown-5 thiophene: terthiophene copolymer	232
5.58	Post-polymerisation CVs of terthiophene:thiophene crown copolymer in 0.1 M TBAP and 0.1 M LiClO <sub>4</sub>	233
5.59	Growth CV and SEM of thiophene crown:terthiophene copolymer on ITO-coated mylar	234
5.60	UV/VIS/NIR spectra of thiophene crown:terthiophene copolymer in the neutral and oxidised forms	235
5.61	Cyclic voltammetry for open-chain sexithiophene <b>LXXIII</b>	237
5.62	Cyclic voltammetry for open-chain sexithiophene <b>LXXII</b>	237
5.63	Cyclic voltammetry for open-chain sexithiophene <b>LXX</b>	238



## ***Index of Synthetic Schemes***

<b>Scheme</b>	<b>Page</b>
1     Alternative routes toward target compounds <b>I</b> and <b>II</b>	48
2     Formation of benzo-crown phosphonium salts <b>III</b> and <b>IV</b>	49
3     Wittig reactions between phosphonium salts <b>III-IV</b> and nitrobenzaldehyde	51
4     Wittig reactions between phosphonium salts <b>III-IV</b> and terthiophene aldehyde	53
5     Formation of benzo-crown phosphonates <b>XIII</b> and <b>XIV</b>	54
6     Horner-Emmons reactions between phosphonates <b>XIII-XIV</b> and terthiophene aldehyde	57
7     Formation of styryl terthiophene crowns <b>I</b> and <b>II</b> from terthiophene phosphonate	58
8     Formation of styryl-15-crown-5 thiophene <b>XV</b>	59
9     Synthesis of styryl-18-crown-6 thiophene <b>XVI</b>	61
10    Formation of tosylated glycols according to Lauter <i>et al.</i>	63
11    Formation of polyether-substituted benzaldehydes <b>XVII-XXII</b>	64
12    Horner-Emmons reaction to form open-chain terthiophenes	65
13    Synthesis of dimethoxystyryl terthiophene	68
14    Open-chain ether functionalised thiophenes <b>XXX-XXXV</b>	69
15    Synthesis of dimethoxystyryl thiophene	71
16    Alternative routes toward target crown linked bis(terthiophene)s <b>XXXVII</b> and <b>XXXVIII</b>	78
17    Formation of <i>syn/anti</i> isomeric mixture of crown bis(phosphonium salt)s <b>XXXIX</b> and bis(phosphonate)s <b>XL</b>	79
18    Wittig-type reactions between disubstituted crowns <b>XXXIX-XL</b> and 4-nitrobenzaldehyde	83
19    Alternative routes toward <i>syn</i> -bis(formylbenzo)-18-crown-6 <b>XLV</b>	84
20    Products formed from attempted demethylation of 1,5-bis(2'- methoxy-4'-formylphenoxy)-3-oxapentane <b>XLIX</b>	85

21	$S_N2$ and $S_NAr$ reactions between the thioethoxide ion and a substituted benzaldehyde	86
22	Horner-Emmons reaction between dialdehyde <b>XLV</b> and terthiophene phosphonate	88
23	Formation of <i>anti</i> -bis(formylbenzo)-18-crown-6 <b>XLVI</b>	92
24	Products formed from demethylation of 1-(2'-methoxy-4'-formylphenoxy)-5-(2''-methoxy-5''-formylphenoxy)-3-oxapentane <b>LIV</b>	94
25	Horner-Emmons reaction between dialdehyde <b>XLVI</b> and terthiophene phosphonate	95
26	Formation of <i>syn</i> -bis(styryl thiophene)-18-crown-6 <b>LIX</b>	96
27	Synthesis of <i>anti</i> -bis(styryl thiophene)-18-crown-6 <b>LX</b>	97
28	Formation of bis(terthiophene) hemicrowns <b>LXI-LXIII</b>	99
29	Synthesis of bis(thiophene) hemicrowns <b>LXIV-LXVI</b>	104

## ***Index of Tables***

<b>Table</b>		<b>Page</b>
4.1	Crown ether cavity sizes	111
4.2	Metal cation ionic diameters	112
4.3	Solution absorbance maxima of terthiophene monomers	120
4.4	Solution absorbance maxima of thiophene monomers	121
4.5	Solution and solid-state absorbance maxima of terthiophene dimers	122
4.6	Misono softness values for metal cations	129
4.7	Fluorescence data for terthiophene and sexithiophene monomers obtained in CH <sub>2</sub> Cl <sub>2</sub>	137
5.1	Calculated spin density values for styryl-substituted terthiophenes	157
5.2	Oxidation and reduction absorbance data for terthiophene monomers treated with Cu(ClO <sub>4</sub> ) <sub>2</sub> and hydrazine	161
5.3	Absorption maxima for electrochemically produced films and chemically produced dimer films	227
5.4	Peak oxidation and reduction potentials obtained on electro-polymerisation by cyclic voltammetry over the range $\pm 1.0$ V	228

⋮

## ***Index of Compounds***

For structures and systematic names of all compounds, refer to Chapter 7. A fold-out reference guide to the structures of terthiophene- and sexithiophene-based compounds is provided inside the back cover.

<b>I</b>	styryl-15-crown-5 terthiophene
<b>II</b>	styryl-18-crown-6 terthiophene
<b>III</b>	benzo-15-crown-5 phosphonium salt
<b>IV</b>	benzo-18-crown-6 phosphonium salt
<b>V</b>	formylbenzo-15-crown
<b>VI</b>	formylbenzo-18-crown-6
<b>VII</b>	hydroxymethylbenzo-15-crown-5
<b>VIII</b>	hydroxymethylbenzo-18-crown-6
<b>IX</b>	chloromethylbenzo-15-crown-5
<b>X</b>	chloromethylbenzo-18-crown-6
<b>XI</b>	nitrostyryl-15-crown-5
<b>XII</b>	nitrostyryl-18-crown-6
<b>XIII</b>	benzo-15-crown-5 phosphonate
<b>XIV</b>	benzo-18-crown-6 phosphonate
<b>XV</b>	styryl-15-crown-5 thiophene
<b>XVI</b>	styryl-18-crown-6 thiophene
<b>XVII</b>	isovanillin short-chain benzaldehyde
<b>XVIII</b>	isovanillin medium-chain benzaldehyde
<b>XIX</b>	isovanillin long-chain benzaldehyde
<b>XX</b>	vanillin short-chain benzaldehyde
<b>XXI</b>	vanillin medium-chain benzaldehyde
<b>XXII</b>	vanillin long-chain benzaldehyde
<b>XXIII</b>	isovanillin short-chain terthiophene
<b>XXIV</b>	isovanillin medium-chain terthiophene
<b>XXV</b>	isovanillin long-chain terthiophene
<b>XXVI</b>	vanillin short-chain terthiophene

<b>XXVII</b>	vanillin medium-chain terthiophene
<b>XXVIII</b>	vanillin long-chain terthiophene
<b>XXIX</b>	dimethoxystyryl terthiophene
<b>XXX</b>	isovanillin short-chain thiophene
<b>XXXI</b>	isovanillin medium-chain thiophene
<b>XXXII</b>	isovanillin long-chain thiophene
<b>XXXIII</b>	vanillin short-chain thiophene
<b>XXXIV</b>	vanillin medium-chain thiophene
<b>XXXV</b>	vanillin long-chain thiophene
<b>XXXVI</b>	dimethoxystyryl thiophene
<b>XXXVII</b>	<i>syn</i> -bis(styryl terthiophene)-18-crown-6
<b>XXXVIII</b>	<i>anti</i> -bis(styryl terthiophene)-18-crown-6
<b>XXXIX</b>	18-crown-6 bisphosphonium salt (isomeric mixture)
<b>XL</b>	18-crown-6 bisphosphonate (isomeric mixture)
<b>XLI</b>	bis(formylbenzo)-18-crown-6 (isomeric mixture)
<b>XLII</b>	bis(hydroxymethylbenzo)-18-crown-6 (isomeric mixture)
<b>XLIII</b>	bis(chloromethylbenzo)-18-crown-6 (isomeric mixture)
<b>XLIV</b>	bis(nitrostyryl)-18-crown-6 (isomeric mixture)
<b>XLV</b>	<i>syn</i> -bis(formylbenzo)-18-crown-6
<b>XLVI</b>	<i>anti</i> -bis(formylbenzo)-18-crown-6
<b>XLVII</b>	isovanillin methoxy hemicrown
<b>XLVIII</b>	isovanillin hydroxy hemicrown
<b>XLIX</b>	vanillin methoxy hemicrown
<b>L</b>	vanillin hydroxy hemicrown
<b>LI</b>	4-ethylsulfanyl-3-hydroxy-benzaldehyde
<b>LII</b>	3-hydroxy-4-[2-(2-hydroxy-ethoxy)-ethoxy]-benzaldehyde
<b>LIII</b>	3-[2-(2-chloro-ethoxy)-ethoxy]-4-methoxy-benzaldehyde
<b>LIV</b>	mixed methoxy hemicrown
<b>LV</b>	mixed hydroxy hemicrown
<b>LVI</b>	4-[2-(2-chloro-ethoxy)-ethoxy]-3-methoxy-benzaldehyde
<b>LVII</b>	4-ethylsulfanyl-3-methoxy-benzaldehyde
<b>LVIII</b>	4-hydroxy-3-[2-(2-hydroxy-ethoxy)-ethoxy]-benzaldehyde
<b>LIX</b>	<i>syn</i> -bis(styryl thiophene)-18-crown-6

<b>LX</b>	<i>anti</i> -bis(styryl thiophene)-18-crown-6
<b>LXI</b>	isovanillin terthiophene hemicrown
<b>LXII</b>	vanillin terthiophene hemicrown
<b>LXIII</b>	mixed terthiophene hemicrown
<b>LXIV</b>	isovanillin thiophene hemicrown
<b>LXV</b>	vanillin thiophene hemicrown
<b>LXVI</b>	mixed thiophene hemicrown
<b>LXVII</b>	15-crown-5 terthiophene dimer
<b>LXVIII</b>	18-crown-6-terthiophene dimer
<b>LXIX</b>	isovanillin short-chain terthiophene dimer
<b>LXX</b>	isovanillin medium-chain terthiophene dimer
<b>LXXI</b>	isovanillin long-chain terthiophene dimer
<b>LXXII</b>	vanillin short-chain terthiophene dimer
<b>LXXIII</b>	vanillin medium-chain terthiophene dimer
<b>LXXIV</b>	vanillin long-chain terthiophene dimer
<b>LXXV</b>	dimethoxystyryl terthiophene dimer
<b>LXXVI</b>	styryl terthiophene
<b>LXXVII</b>	methoxystyryl terthiophene
<b>LXXVIII</b>	styryl terthiophene dimer
<b>LXXIX</b>	methoxystyryl terthiophene dimer

**1**

**INTRODUCTION**

**AND**

**LITERATURE**

**REVIEW**

## **1.1 Research Objectives**

The overall aim of this work was to produce chemical compounds that could be used to form conducting polymers with a sensing capability. A successful chemical sensor must possess two attributes. Firstly it must be able to selectively recognize the desired analyte, and then it must be capable of producing a measurable signal.<sup>1</sup> It can also be added that if the functionalities fulfilling these two roles are separated within the molecule, then there must be some form of electronic communication between them. Combining the well-known ion recognition ability of crown ethers with the electrical conductivity of conducting polymers has the potential to satisfy both these requirements, and could result in the fabrication of a range of metal ion sensors.

The specific objectives of this work were to:

- i) Carry out a survey of the literature to investigate the chemistry of crown ethers, conducting polymers, and how these areas have previously been merged in order to produce conducting polymers functionalised with crown ethers that can be used as metal ion sensors (Chapter 1).
- ii) Design and synthesise a range of polyether-substituted monomers that have the potential both to selectively complex metal ions, and to form conducting polymers (Section 1.6, Chapters 2, 3 and 7).
- iii) Investigate the response of the monomers to a variety of metal ions (Chapter 4).
- iv) Investigate the polymerisation of the monomers both chemically and electrochemically, and investigate the response of the polymers to metal ions (Chapter 5).

## 1.2 Crown Ethers

Since the serendipitous discovery of crown ethers by Charles Pedersen in 1967,<sup>2, 3</sup> there has been a huge volume of work published on their synthesis and applications. The crown ethers originally reported by Pederson consisted of a cyclic polyether chain, and included compounds containing either benzo or cyclohexyl rings (Fig. 1.1).

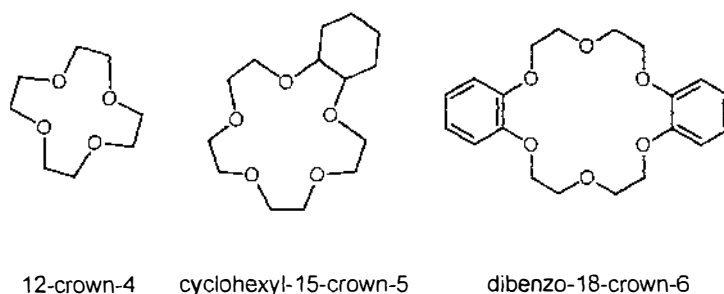


**Figure 1.1** Examples of crown ethers

The crown nomenclature was applied to the compounds due to their ability to crown alkali metal ions and form stable complexes. This was visualized by Pedersen to be the result of ion-dipole interactions between the cation and the oxygen atoms, with the ion sitting inside the crown ring. His hypothesis was later shown by X-ray crystallographic studies to be correct. The term ‘supramolecular chemistry’ was subsequently introduced to describe this type of work involving “two or more chemical species held together by intermolecular forces”.<sup>4</sup> A typical ion-dipole interaction has an energy of *ca.* 15 kJ/mol, certainly less than the 250 kJ/mol for an ion-ion interaction, or 370 kJ/mol for a covalent C-C bond.<sup>5, 6</sup> The strength of a crown-cation complex comes from having multiple ion-dipole interactions, and because of this, size is one of the main factors determining the stability of such complexes. When this ratio of the ionic diameter of the metal ion to the ‘hole’ in the center of the crown is close to unity, 1:1 complexes will be formed (Fig. 1.2). Complexes of this type are formed between Li<sup>+</sup> and 12-crown-4, Na<sup>+</sup> and 15-crown-5,

and  $K^+$  and 18-crown-6. In addition, when the ion is larger than the crown cavity, sandwich type 2:1 and 3:2 complexes can be formed (Fig. 1.3).<sup>7,9</sup>

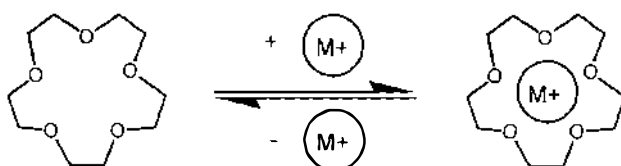


**Figure 1.2 Crown ether – metal ion complexation**

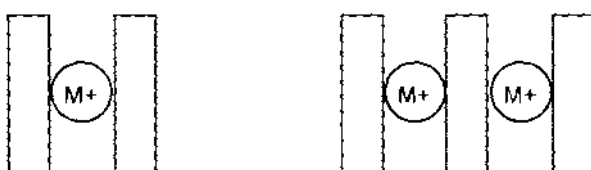


**Figure 1.3 Schematic representation of 2:1 and 3:2 ‘sandwich’ complexes**

Crown compounds bind metal cations much more strongly than their open-chain equivalents, called podands.<sup>10</sup> This is due to the level of preorganisation inherent in the crown molecules. While podands can exist in hundreds of conformations, only a few of these are suitable for ion binding. The energy gained by a podand on complexation must be greater than the loss in free energy associated with organizing the chain into a suitable conformation. For crown ethers however, this rearrangement has already occurred during synthesis, so that the molecule has substantially less freedom of movement and the oxygen atoms are held in a conformation more suitable for ion binding. The more preorganised a compound is for binding, the more stable its resulting complexes will be.<sup>10</sup>

The incorporation of benzene rings into the structure of crown ethers reduces both their flexibility<sup>11</sup> and their solubility in water<sup>12</sup>, affecting their complexation properties. The benzene ring also reduces the electron density at two of the oxygen binding sites, further altering cation selectivity.<sup>13</sup> Benzo-crown ethers are frequently exploited in synthesis, as they are easily functionalised by electrophilic aromatic

substitution. However, the introduction of electron-withdrawing or electron-donating groups onto the aromatic rings affects the basicity of the oxygen atoms, again modifying complexing ability.<sup>14</sup> Normal cation selectivity can be altered<sup>15, 16</sup> or even reversed<sup>17</sup> by this process, the effect being greater for benzo-15-crown-5 than for benzo-18-crown-6. Not surprisingly, the nature of the solvent used when measuring cation selectivity also has a large effect.<sup>13, 18</sup>

Since their discovery, crown compounds have been synthesised that incorporate nitrogen and sulphur donor atoms rather than oxygen. This is another factor that changes the crowns complexing abilities, allowing complexes to be formed with transition metal and heavy metal ions.<sup>9</sup> In addition, the field of supramolecular chemistry has been extended to lariat crown ethers,<sup>19-22</sup> cryptands<sup>23</sup> and spherands<sup>10, 24</sup>. The pioneers of the field of supramolecular chemistry, Charles Pedersen, Donald Cram and Jean-Marie Lehn, were awarded the Nobel Prize in Chemistry in 1987 for their work in this area.<sup>10</sup>

Applications of crown ethers range from their archetypal use as phase transfer catalysts in synthetic chemistry<sup>25</sup>, to the study of ion transport through membranes,<sup>26, 27</sup> metal ion separation<sup>20, 28</sup> or isotope fractionation<sup>29</sup>, chirality sensing of amino acids<sup>30</sup>, solid phase microextraction<sup>31</sup> and ion selective electrodes<sup>21, 32</sup>. They have also been used in chromatography as additives in the eluent<sup>33</sup>, adsorbed on<sup>34</sup> or covalently attached to<sup>35, 36</sup> various stationary phases or as a coating on a piezoelectric quartz crystal for detection<sup>37</sup>.

## 1.3 Conducting Polymers

Ten years after Pedersen reported the discovery of crown ethers, Alan MacDiarmid, Alan Heeger and Hideki Shirakawa published papers announcing that they had formed a film of polyacetylene that was capable of conducting electricity.<sup>38-41</sup> Like the discovery of crown ethers, this startling news caused a flurry of research activity in what was a completely new area, and led to their being jointly awarded the Nobel Prize in Chemistry in 2000.<sup>42-47</sup> Figure 1.4 shows the structural variety in types of polymers that have since been shown to be conducting.

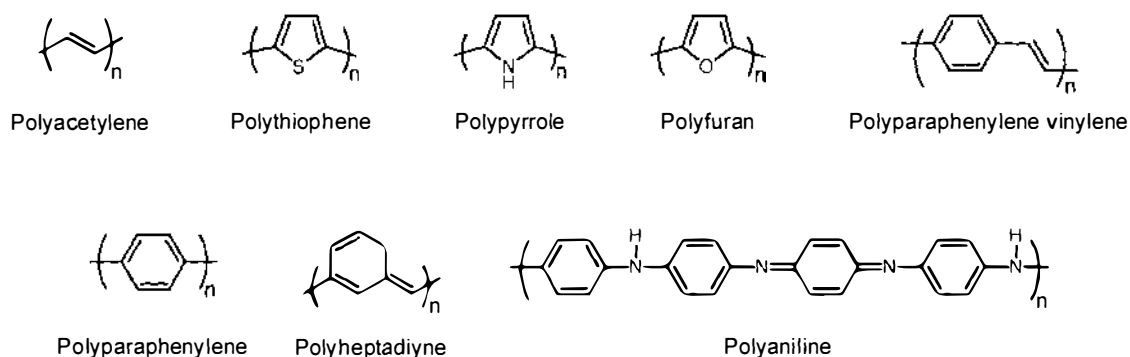


**Figure 1.4** Examples of conjugated polymers

All the polymers illustrated in Fig. 1.4 share one structural feature, their conjugated  $\pi$ -system of alternating single and double bonds. Polymers such as these may be transformed from insulating to semi-conducting by doping.<sup>46, 48</sup> The mechanisms of charge transport in conducting polymers will be further discussed in Section 1.3.2. Figure 1.5 shows the interconversion of polythiophene between the neutral insulating and the conductive oxidised form. Oxidation requires the incorporation of counter-ions into the polymer in order for the polymer to remain electrically neutral, and these counter-ions can be exploited to add functionality to the polymer e.g. recognition sites.<sup>49</sup>

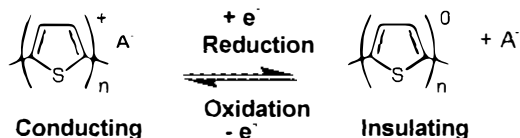


**Figure 1.5 Redox activity of polythiophene**

In addition to the change in conductivity on switching between the oxidised and reduced form of a polymer, there may also be changes in physical properties such as colour and morphology. In particular, the electrochromic properties of polythiophene have drawn attention due to possible applications in eyewear, 'smart windows' and optical information storage.<sup>50-54</sup>

### 1.3.1 Polymer growth

The polymerisation of heterocycles is believed to proceed *via* the coupling of radical cations.<sup>49, 55-57</sup> This is a multi-step process illustrated for thiophene in Fig. 1.6.

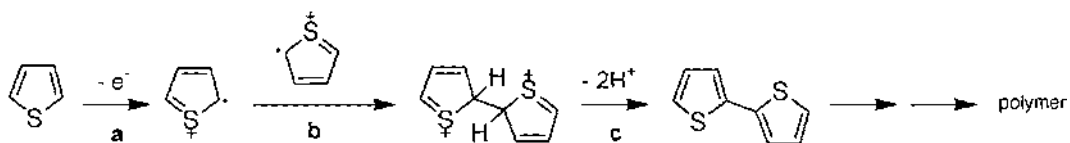


**Figure 1.6 Polymer growth mechanism including oxidation (a), radical cation coupling (b) and deprotonation (c)**

The first step involves oxidation of a monomer to form a radical cation. Two radical cations then couple to form a dication, which can be deprotonated to form the aromatic dimer. If nothing occurs to stop this process repeating, a polymer will be formed. Depending on the nature of the polymer and the conditions under which it is grown, a precipitate or deposit on the working electrode may be formed.<sup>49</sup>

### 1.3.2 Charge transport in conducting polymers

In an infinite polymer chain, delocalisation of  $\pi$ -electrons over the molecule, and overlap of the individual atomic orbitals, effectively produces a valence and a conduction band.<sup>58</sup> In the neutral state, the valence band is full, the conduction band is empty, and there is a significant energy gap between the two *ie.* the polymers are insulators.<sup>45, 59</sup> This band-gap can be altered by the incorporation of substituents on the monomer.<sup>45, 57, 60</sup> The polymers can become conducting (or semi-conducting), by chemical or electrochemical doping (Fig. 1.5).<sup>49</sup> On doping, self-localized excitations are formed that create new energy levels between the valence and conduction bands,<sup>61</sup> and allow electrons to move.<sup>59</sup> Doping can take two forms: n-doping (reduction) involves the addition of electrons leaving a negatively charged polymer, while p-doping (oxidation) removes electrons and leaves a positively charged polymer backbone.<sup>46, 49, 62</sup> Cations or anions are then incorporated into the polymer matrix in order to maintain electrical neutrality.<sup>46, 49</sup> One counter-ion is incorporated per charge on the polymer backbone, for polythiophene this gives a ratio of approximately 1 counter-ion per 3-4 thiophene rings.<sup>49, 63</sup>

Conducting polymers can be classified into two groups based on the energy of their ground state isomers.<sup>63</sup> The two resonance forms of poly(*trans*-acetylene) have the same energy, and are called degenerate states (Fig. 1.7a). This is not the case for most other conducting polymers, where the energies of the isomers are different (eg. polythiophene Fig. 1.7b).<sup>58, 64</sup>

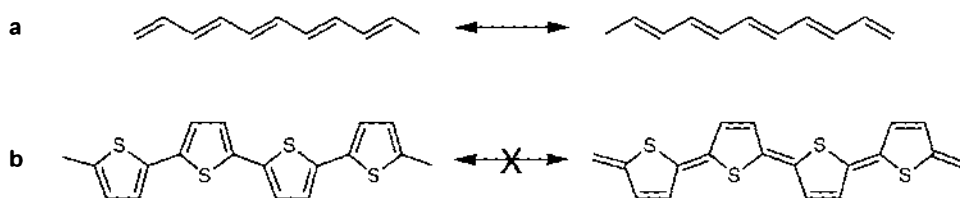


**Figure 1.7 Degeneracy of poly(*trans*-acetylene) (a) and non-degeneracy of polythiophene (b) ground states**

The particular type of self-localized excitation formed on oxidation or reduction depends on the degeneracy of the polymer ground state. For polymers with degenerate ground states, solitons are formed. Positive, negative and neutral solitons are the physics terms for the cations, anions and neutral radicals that are the charge carriers in these types of polymers.<sup>58</sup> For other conducting polymers, polarons and bipolarons are formed.<sup>45</sup> A positive polaron is the same as a radical cation, and is formed when an electron is removed from a polymer by oxidation.<sup>58</sup> Positive polarons are also sometimes described as the positive 'hole' left on removal of an electron. Polarons are able to move along polymer chains, and if two polarons meet they can combine to form a dication (positive bipolaron).<sup>49</sup> An equivalent mechanism also operates for negative polarons (radical anions).

The self-localised excitations formed can be studied by UV/VIS/NIR, IR, Raman and ESR spectroscopy.<sup>58</sup> ESR spectra of polymers containing radical species (polarons) will give signals attributable to the unpaired electrons present. Polymers with bipolaron charge carriers will give no response to ESR, making this a valuable technique for distinguishing between these types of excitations. UV/VIS/NIR spectra of conducting polymer films in the oxidised state show an absorbance in the NIR region.<sup>63</sup> This is due to the strong absorbances characteristic of organic radical cations and dications, and as such its exact position depends on the nature of the oxidised species.<sup>65</sup> This so-called 'free carrier tail' is often referred to in the literature as proof of a conducting polymer.<sup>63, 64, 66</sup>

### 1.3.3 Functionalised polymers based on thiophene

Thiophene is easily synthetically manipulated, and has therefore often been exploited as a suitable monomer for functionalisation.<sup>67</sup> Substitution is possible at either the  $\alpha$  (2 and 5) or  $\beta$  (3 and 4) positions as shown in Fig. 1.8. Polymerisation occurs preferentially at the more reactive  $\alpha$ -position<sup>68</sup>, so that thiophenes substituted at that position are less active to polymerisation than those substituted at the  $\beta$ -position.<sup>69</sup> Defects in the polymer structure caused by linkages through the  $\beta$ -position manifest in reduced conjugation length, higher oxidation potentials and lower conductivities.<sup>68</sup> Substituting at the  $\beta$ -position, as well as modifying physical properties such as solubility of the resulting polymer, decreases the probability of such undesirable  $\alpha$ - $\beta$  or  $\beta$ - $\beta$  linkages.

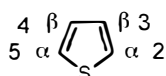


**Figure 1.8 Thiophene**

An important consideration when designing functionalised thiophenes, is that the functional groups incorporated must be able to withstand the positive potentials necessary for polymerisation. As thiophene requires a high positive potential for electropolymerisation ( $> 2.0$  V vs. SCE), bithiophene and terthiophene, which have lower oxidation potentials, can be used instead to limit overoxidation of the resulting polymer.<sup>70, 71</sup> This has the added advantage of reducing unfavorable  $\beta$ -linkages.<sup>72</sup> It has been acknowledged, however, that the functionalisation of bithiophene and terthiophene requires more complex synthetic chemistry.<sup>73</sup>

One crucial issue with both chemical and electrochemical polymerisation of 3-substituted thiophenes, is the regioselectivity of the polymers produced. Thiophene can couple in a 'head-to-head', 'head-to-tail' or 'tail-to-tail' manner (Fig. 1.9a-c), leading to four different regioisomers for a three-thiophene chain, as shown in Fig. 1.9d-g.<sup>68</sup> While 'head-to-tail' couplings are sterically preferred, 10-50% 'head-to-head' linkages have been observed,<sup>74, 75</sup> with 'tail-to-tail' linkages rare. The steric

hindrance caused by 'head-to-head' couplings induces twisting of the polymer backbone, reducing conjugation.<sup>76, 77</sup> The regioregularity of polymers can usually be clearly established by NMR analysis,<sup>78-84</sup> provided that they are sufficiently soluble in the deuterated solvents used.

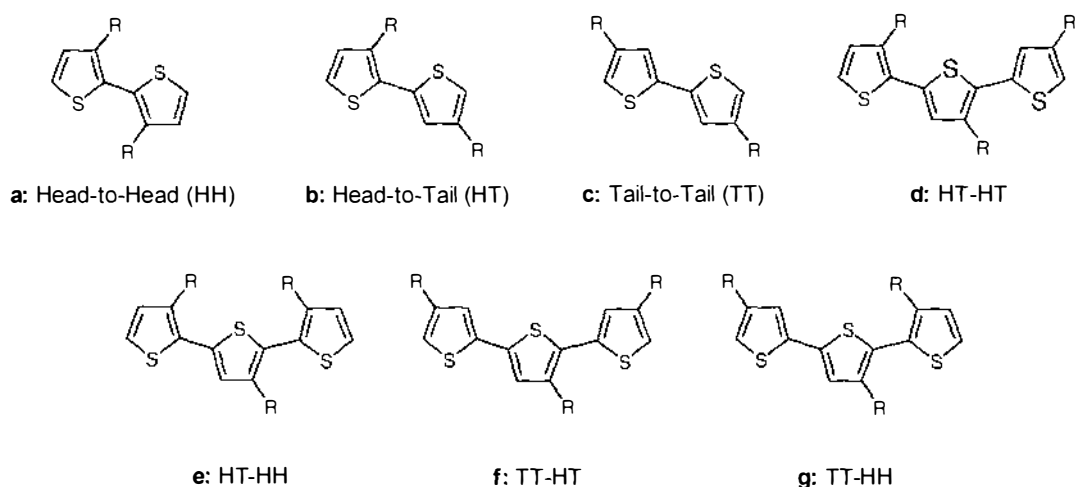


**Figure 1.9 Coupling orientations of 3-substituted thiophenes**

One approach to the formation of regioregular polymers, is the synthesis of symmetrical disubstituted bithiophene and terthiophene derivatives as shown in Fig. 1.10. This approach has been utilized by a number of researchers.<sup>70, 74, 76, 85-97</sup>

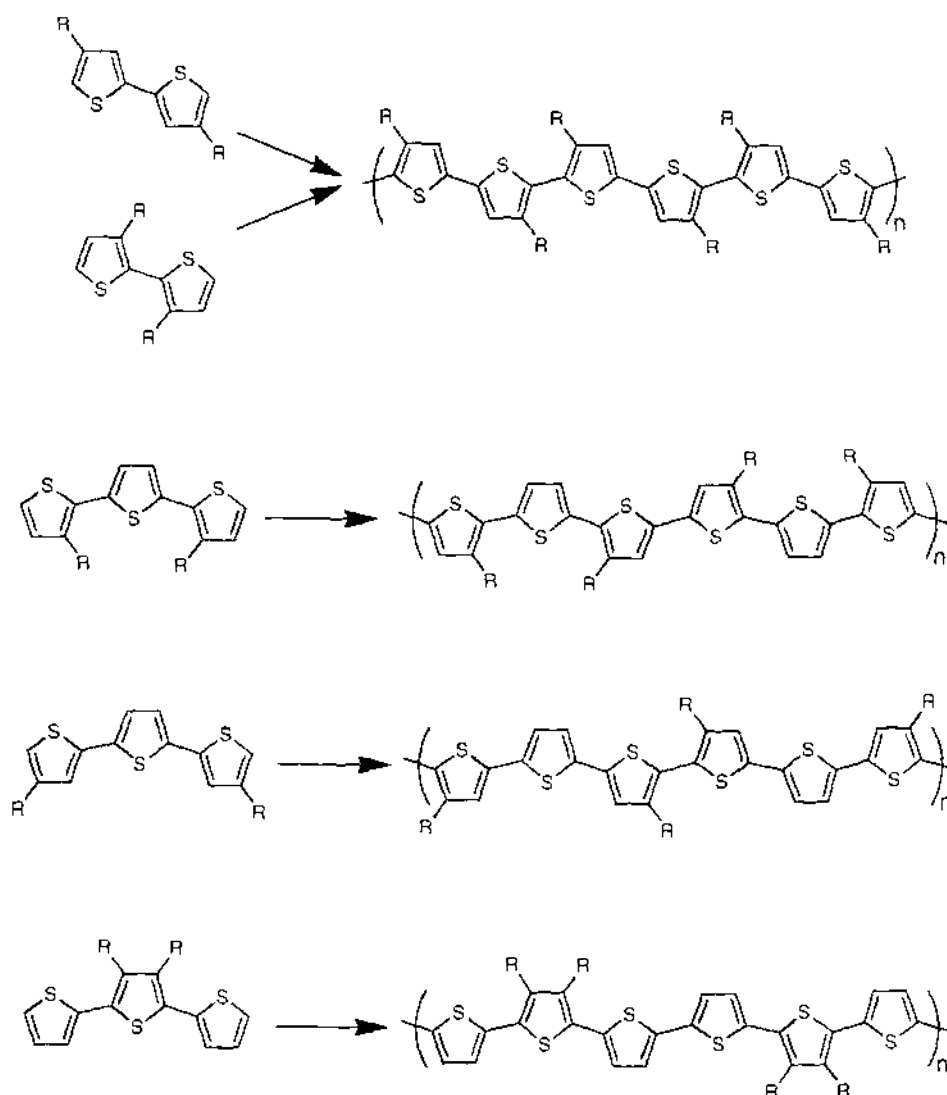


**Figure 1.10 Regioregular polymers from disubstituted bithiophenes and terthiophenes**

Gallazzi<sup>98</sup>, and later McCullough<sup>77, 99-103</sup>, used a nickel-catalysed Grignard reaction to form regioregular polymers. Chen *et al.*<sup>104-107</sup> used a similar nickel-catalysed dehalogenation polycondensation reaction, with the corresponding zinc reagent. They observed in this system that the regioregularity of the polymers produced was dependent on the catalyst.<sup>104, 107</sup> Lere-Porte<sup>84</sup> used Stille coupling, for the self-condensation of a bromotributylstannyl thiophene monomer with a palladium catalyst. These organometallic polymerisation methods are shown in Fig. 1.11.

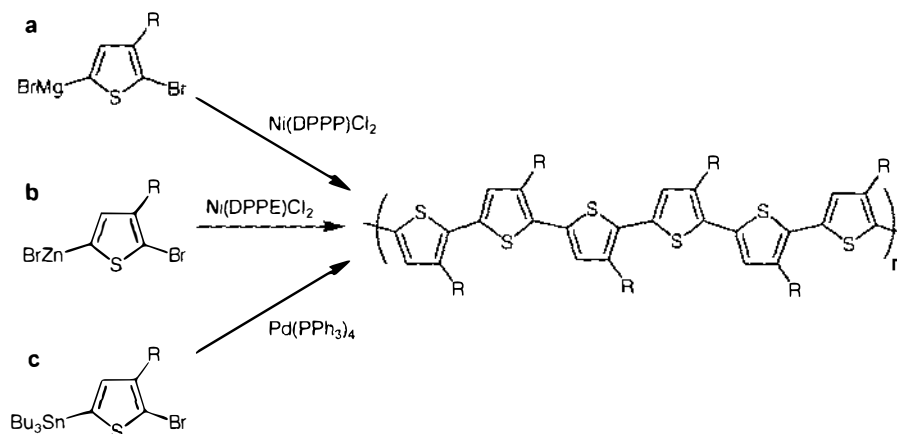


**Figure 1.11 Regioselective chemical polymerisations by Gallazzi and McCullough (a), Chen (b) and Lere-Porte (c)**

While this approach is effective, it requires extremely pure monomers and involves more complex chemistry than polymerisation of monomers using ferric chloride ( $\text{FeCl}_3$ ).

Ferric chloride is the most common chemical oxidant used to prepare polythiophenes. Its advantages include its simplicity of use and suitability for large-scale production due to its low cost. In addition, such polymerisations generally give high molecular weight polymers.<sup>82</sup> While early publications involving polymerisation by  $\text{FeCl}_3$  reported the production of irregular polymers only,<sup>81, 98, 108</sup> in 1994 Andersson *et al.* published work detailing the first example of a regioselective polymerisation from a non-symmetrical thiophene monomer (3-(4-octylphenyl)thiophene)<sup>82</sup>. Later, Goldoni *et al.*<sup>80</sup> reported the selective formation of one of the possible four regioisomers of tris(3-butylsulfanyl bithiophene) using  $\text{FeCl}_3$ , and more recently regioregular polymerisation of thiophene 3-substituted with a functionalised phenoxy group was achieved by Miyasaka<sup>109</sup>. It has been well established that 3-alkoxy thiophenes form well-defined head-to-tail linkages (>95%) when treated with  $\text{FeCl}_3$ , due to an asymmetric reactivity of the monomer.<sup>55, 78, 79, 110, 111</sup> Other research groups have chosen either not to comment on this issue<sup>112-116</sup>, or to admit their uncertainty about the regioregularity of polymers produced<sup>117, 118</sup>. The issue of polymer structure can be eliminated by chemically polymerising symmetrical monomers.<sup>70, 91, 98, 111</sup>

Regardless of the synthetic method used, regioregular polymers are reported to have enhanced magnetic, optical and electrochemical properties when compared with their regiorandom analogues.<sup>68, 74, 106, 119-122</sup> Recently a report was published detailing superconductivity from a regioregular film of poly(3-hexylthiophene), albeit a very thin film at a very low temperature.<sup>123</sup>

'Functionalisation space' (Fig. 1.12) is another concept that must be considered when designing substituted thiophene monomers for polymerisation.<sup>124-126</sup> Functionalisation space is defined as "the volume in which the introduction of bulky substituents exerts only a minor effect on the properties of the corresponding polymer". For polythiophene this allows the introduction of a chain 10 atoms long that can branch to 3-4 atoms wide. The size of the substituent allowable depends on the spacer length between the thiophene unit and the branched chain. It follows that substituents on bi- or ter-thiophene can be correspondingly larger. This concept is well illustrated by the work of Kankare *et al.*<sup>127</sup>, who studied the properties of a series of terthiophenes substituted at the 3'-position with a range of 5- and 6-membered aromatic rings. UV/VIS, NMR and X-ray diffractometry data led them to conclude that the steric hindrance caused by incorporating a ring substituent so closely to the oligothiophene backbone was too large to allow a coplanar (and therefore conjugated) configuration.

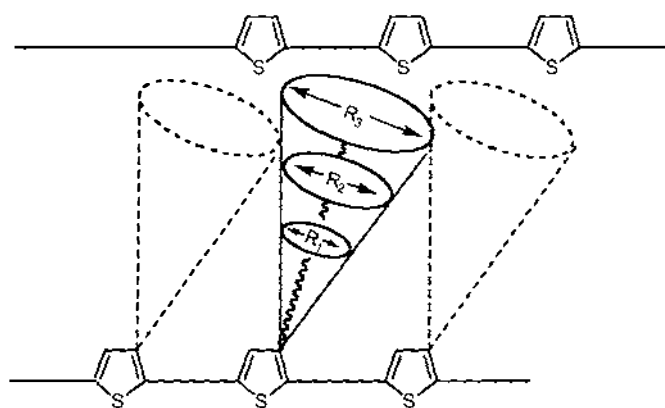


**Figure 1.12 Functionalisation space of polythiophene**

## **1.4 Past Work on Ether Functionalised Thiophenes**

With the issues raised in the previous section in mind, the literature was surveyed in order to find out what work had been previously carried out in the area of polyether functionalised thiophenes.

Four main types of compounds were evident and will be discussed here:

- a) Thiophenes substituted with polyether chains
- b) Thiophenes substituted with polyether chains designed such that psuedo crown cavities were formed on polymerisation
- c) Thiophenes substituted with crown ethers attached *via* alkyl or alkoxy spacers
- d) Thiophenes with directly bonded crown ether moieties

### **1.4.1 Open-chain ethers**

Bryce *et al.*<sup>128</sup> were the first to report the synthesis of thiophene 3-substituted with alkoxy chains. While they did look at the conductivity of the resulting polymer films illustrated in Fig. 1.13, they did not report any other electrochemical properties. Their results showed a very low conductivity for the compound that contained an oxygen atom directly bonded to the thiophene moiety, and that the conductivity increased with the length of the alkoxy chain for the remaining compounds.

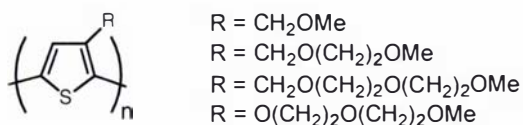


**Figure 1.13 Alkoxy substituted polythiophenes**

Roncali *et al.*<sup>124, 129, 130</sup> looked at several 3-alkoxy substituted thiophenes to determine the importance of both the position of the first oxygen atom in the side chain, and the number of ether groups in the chain (Fig. 1.14). Chang *et al.*<sup>131</sup> had earlier shown for 3-methoxy thiophene, that the electron donating effect of the oxygen resulted in the formation of soluble short-chain oligomers. A later review by Roncali<sup>125</sup> suggested that the oxygen atom has the effect of stabilizing the radicals produced by polymerisation, which would favour the formation of such soluble short-chain oligomers. This effect was somewhat lessened by the insertion of a methylene group between the oxygen atom and the thiophene backbone (Fig. 1.14d, g), but the polymer yield was still low due to the formation of large amounts of soluble products, and the polymer that was formed had low conductivity. In addition, the oxidation potentials of the monomers were higher than the comparable alkyl-substituted thiophenes. The inclusion of an additional methylene group between the oxygen atom and the thiophene ring (Fig. 1.14c, h, i) led to the formation of highly conductive films with a considerably larger mean conjugation length as evidenced by UV/VIS spectroscopy. However, the conductivity of these films was still significantly lower than the equivalent alkyl substituted thiophenes.

In systematically varying the number of ether groups in the chain with a constant  $-\text{CH}_2\text{CH}_2-$  spacer (Fig. 1.14c-e) they found the most conductive films were formed from the intermediate five-carbon compound containing two ether groups (Fig. 1.14d). It was postulated that the lower conductivity for the shorter chain compound was due to a perturbation of the lipophilic interactions between the side chains caused by the shortness of the chain, and that the lower conductivity for the longer chain compound was a result of the increase in the number of ether groups.

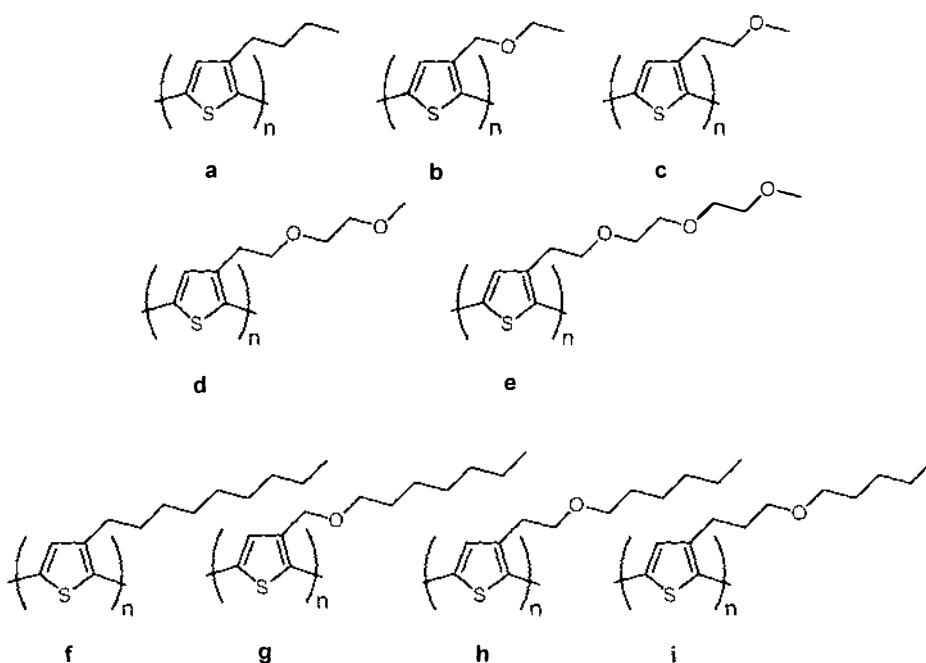


**Figure 1.14 3-Alkoxy substituted thiophenes synthesised by Roncali *et al.***

More information was later published on poly[3-(3,6-dioxaheptyl)thiophene] (Fig. 1.14d), which was the first example of a conjugated polymer with a covalently bonded functional group capable of ion complexation.<sup>130, 132, 136</sup> This polymer is more conjugated than its alkyl equivalent poly(3-heptylthiophene), which it was suggested was caused by the ether group stabilizing preferential conformations corresponding to longer effective mean conjugation lengths. Two waves were seen in the cyclic voltammogram, attributed to electrochemical doping of polymer chains of different mean conjugation lengths. It also showed a change in electroactivity in the presence of lithium cations, namely a narrowing of voltammetric waves and a shift toward less anodic peak potentials (Fig. 1.15). This was attributed to a change in conformation of the polythiophene backbone upon  $\text{Li}^+$  complexation by the polyether chain.<sup>137</sup>

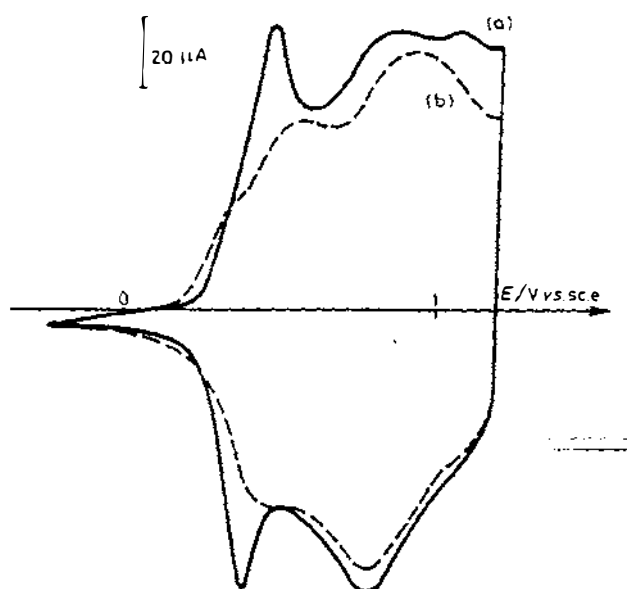


**Figure 1.15** Cyclic voltammograms of poly[3-(3,6-dioxaheptyl)thiophene] (a) in  $LiClO_4$  (b) in TBAP

McCullough *et al.*<sup>100</sup> chemically synthesised a series of regioregular polymers, with side chains as shown in Fig. 1.16.

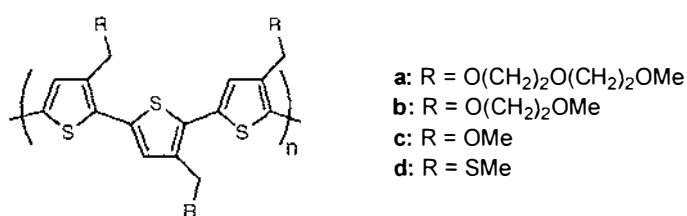


**Figure 1.16** Heteroatom substituted polythiophenes synthesised by McCullough *et al.*

They found that for the two compounds with short side chains, only low molecular weight polymers were formed due to insolubility of the propagating species during chemical polymerisation. The highest molecular weight polymers were produced from the monomers with the longest side chain (Fig. 1.16a). In addition to a marked change in solubility,  $\lambda_{max}$  for this polymer was blue-shifted by 11 nm on addition of  $Li^+$ . Later work on this compound showed that addition of  $Pb^{2+}$  or  $Hg^{2+}$  to a dilute solution of polymer caused the polymer backbone to twist in such a way that

conjugation was completely removed. This effect was irreversible however, and polymer conjugation could not be restored.<sup>138</sup>

Lévesque and Leclerc<sup>110</sup> synthesised 3-oligo(oxyethylene)-4-methylthiophene with a mixture of side chains from 3 to 10 oxyethylene units long. An ionochromic effect was noted in methanol, where the magnitude of the effect was  $K^+ \gg Na^+ > NH_4^+$ , with no effect seen on addition of  $Li^+$ . Cation complexation caused a twisting in the conjugated polymer backbone, manifested by a decrease in absorbance at a higher wavelength and a simultaneous increase in absorbance at a lower wavelength. A clear isobestic point indicated the co-existence of both the twisted and non-twisted forms of the polymer.

Three years later Feldhues *et al.*<sup>139</sup> published results on a series of 3-alkoxythiophenes and a few 3-alkoxy-4-methylthiophenes as illustrated in Fig. 1.17. The shorter alkoxy-substituted thiophenes would only form oligomers, while the long chain derivatives could be successfully polymerised. The 3-alkoxy-4-methyl compounds formed polymers with considerably higher electrical conductivity, although it decreased with increasing length of the substituent chain.

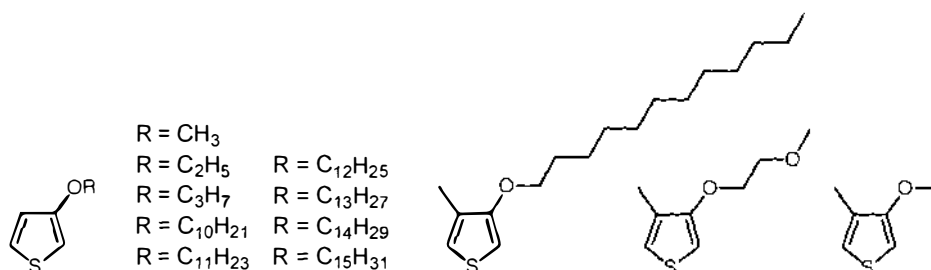


**Figure 1.17 3-Alkoxy (left) and 3-alkoxy-4-methylthiophenes (right) synthesised by Feldhues *et al.***

Similar work was carried out by Chen and Tsai<sup>113</sup> who looked at poly(3-alkoxythiophenes) and poly(3-alkoxy-4-methylthiophenes) with 8-atom substituent chains as depicted in Fig. 1.18.



## 1.4.2 Psuedo crown ethers

Another approach toward crown ether functionalisation of thiophenes was taken by Roncali *et al.*<sup>125, 126</sup> who synthesised monomers consisting of two thiophene units joined by a polyether chain. They envisaged that during polymerisation, in the presence of a suitable templating ion, these chains would form psuedo crown ether cavities (Fig. 1.20).

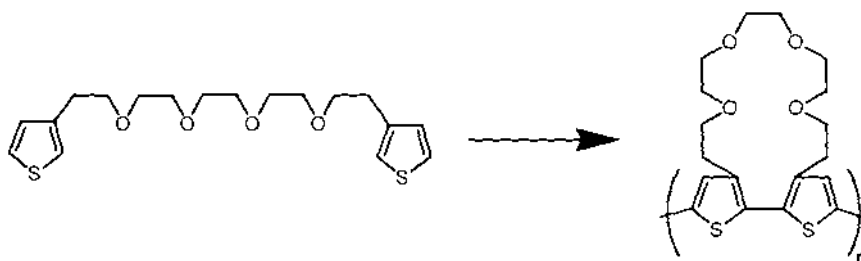


**Figure 1.20** Formation of psuedo crown ether cavities during polymerisation

A later review by Fabre and Simonet<sup>141</sup> cast doubt on the ‘templating ion’ mechanism, quoting research by Simonet<sup>142</sup> in which the nature of the electrolyte cation had no effect on the oxidation potential of the monomer. Taking into account this result and other electrochemical and UV/VIS data, they proposed the formation of a structure consisting of a polymer with pendant oligomeric thiophene chains that might also possibly contain pendant polyether chains. Further electropolymerisation could then result in the formation of polyether cages.

A few years later, Roncali *et al.* published a report on the bithiophene equivalent of their earlier work (Fig. 1.21a).<sup>143</sup> In this report they acknowledge that the polymers formed from these types of monomers could contain three different types of structure: a polythiophene chain with crown ether cavities, a ladder-like structure with oxyethylene ‘rungs’ or a randomly cross-linked three-dimensional polymer. In reality, it is likely that any polymer formed has elements of all three structures. They believed their new monomer to be superior due to its lower oxidation potential,

reduced steric hindrance, lower concentration required for electropolymerisation, and its potential ability to form larger cavities than the original thiophene monomer.

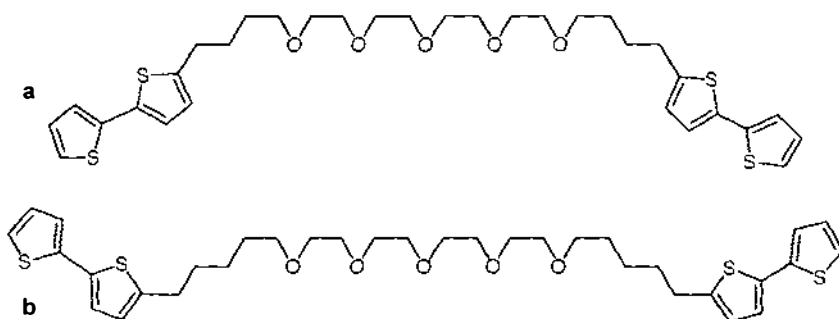


**Figure 1.21 Oxyethylene linked bis(bithiophene) monomers of Roncali (a) and Scheib (b)**

Polymer films grown in the presence of different cations gave distinctly different post-polymerisation CVs, confirming a templating effect. This was also seen by Scheib and Bauerle<sup>140</sup> who published data on a very similar compound around the same time (Fig. 1.21b). They found that polymers grown in TBAHFP showed no change in response on post-polymerisation cycling in solutions containing  $\text{Li}^+$ ,  $\text{Na}^+$  or  $\text{K}^+$ . However, growing polymers from alkali metal solutions did change the properties of the polymers, giving lower peak potentials and red-shifted UV/VIS maxima. This was attributed to a preorganisation of the bithiophene monomers in the presence of alkali metal ions, leading to a polymer with a longer mean conjugation length.

Recently Roncali *et al.* published another paper, this time on a series of oligo(oxyethylene) linked EDOT compounds (Fig. 1.22).<sup>144</sup>

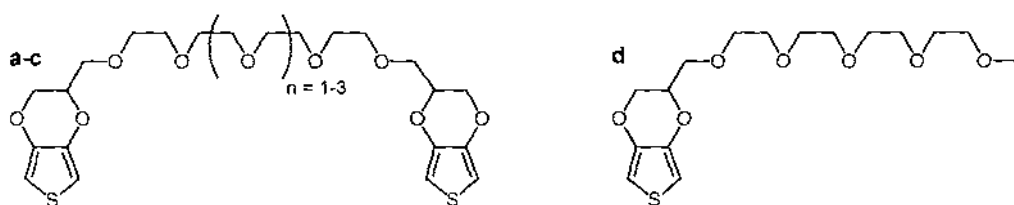


**Figure 1.22 Oligo(oxyethylene) bridged EDOT monomers**

It was observed that while the three bis(EDOT) monomers (Fig. 1.22a-c) electropolymerised easily at the same potential as EDOT, the reference compound with a single EDOT ring (Fig. 1.22d) did not polymerise at all on ITO, and required the application of a 100 mV overpotential on platinum. This behaviour is the same as that observed by Lemaire<sup>124</sup> for polythiophenes with polyether side chains, where the increasing length of the polyether chain caused the electropolymerisation to become more difficult. The ease with which the bridged monomers polymerised to form strongly adherent films was attributed to their ability to form multi-dimensional polymer structures. Post-polymerisation CVs carried out in the presence of various alkali and alkaline metal ions showed distinct changes in their redox peak positions for all the monomers studied.

Marsella and Swager<sup>67, 145-147</sup> used a similar methodology to create a system that gave an optical response to cation complexation. In their compound, Fig. 1.23, complexation caused rotation of the thiophene rings, leading to a loss of planarity and hence conjugation, and a resulting large change in  $\lambda_{\text{max}}$ . While the binding constants for the monomers with alkali metal ions were very low because of their inherent inflexibility, ionochromic shifts were large, as the twisting mechanism affected not just the immediate thiophene rings, but neighbouring rings as well. The introduction of an additional methylene group between the thiophene units and the first oxygen atoms in the polyether chain resulted in less conjugated polymers of lower molecular weight. These polymers had a lower binding affinity for alkali metal ions, which resulted in a failure of the twist-inducing mechanism, and hence poor ionochromic activity.

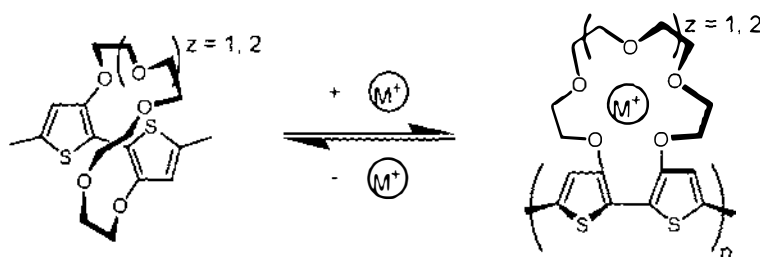


**Figure 1.23** Metal ion induced twisting of bithiophene monomer

Fabre *et al.*<sup>148</sup> also use the principle of creating pseudo-crown ether cavities during polymerisation. Their systems consist of two different aromatic units linked by a polyether chain, which creates a homopolymer with pendant polyether substituted aromatic moieties when a low anodic potential is applied. If the polymer is subsequently subjected to a more positive potential, polymerisation of the second aromatic group occurs (Fig. 1.24).

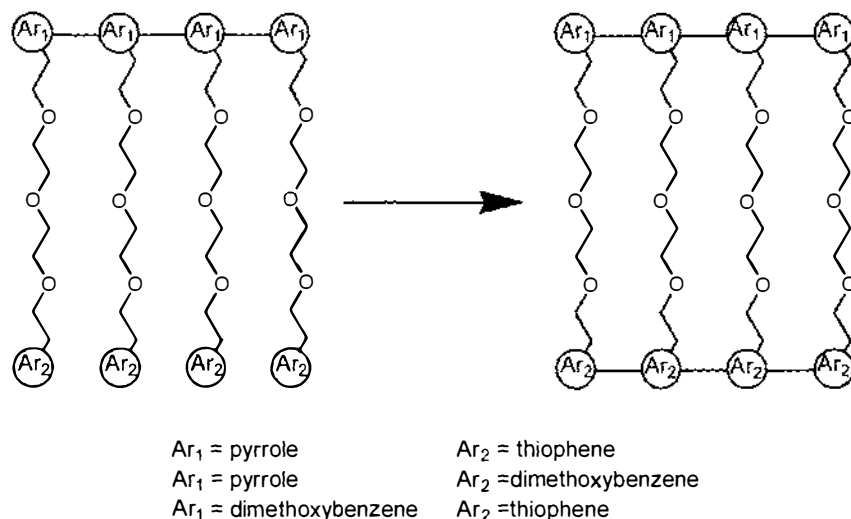


**Figure 1.24** Macrocylic psuedo-crown ether cavities synthesised by Fabre *et al.*

### 1.4.3 Alkyl spaced crown ethers

In order to improve the specificity of cation complexation, the polyether chain used in prior attempts at sensor fabrication needs to be preorganised into a crown ether.<sup>137</sup> Initial attempts to synthesise compounds of this type focused on crown ethers attached to polythiophene *via* a long alkyl or alkoxy chain.

The first series of such molecules was reported by Bauerle and Scheib in 1993.<sup>141, 149</sup> Their compounds, illustrated in Fig. 1.25, consist of thiophene, bithiophene and terthiophene connected to 12-crown-4.

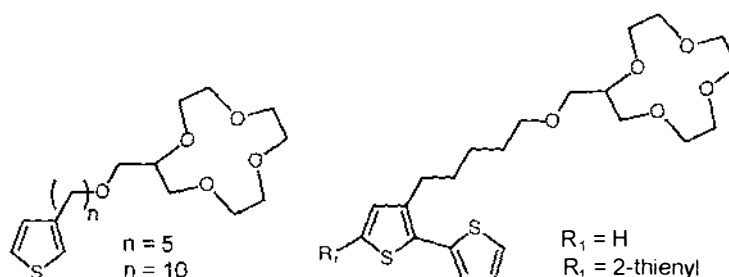


**Figure 1.25 Alkoxy spaced crowns synthesised by Bauerle and Scheib**

Polymerisation of the two monothiophene derivatives led to the formation of soluble oligomeric species that did not form adhering films on the working electrode, an observation that was attributed to steric repulsion. In contrast, both the bithiophene and terthiophene based monomers formed electroactive films. On addition of alkali metal ions, the cyclic voltammograms of these compounds moved to more positive potentials, indicating that the polymer was becoming more difficult to oxidise. The sensitivity of the bithiophene based polymer was  $\text{Li}^+ > \text{Na}^+ > \text{K}^+$ , and it gave a greater response to these ions than the terthiophene based polymer.

In later work,<sup>140</sup> it was demonstrated that the length of the oxaalkyl chain connecting 12-crown-4 to bithiophene had little effect on the polymerisation properties of the monomer. Equivalent monomers substituted with 18-crown-6 however, formed large amounts of soluble oligomeric material during polymerisation, presumably due to increased steric hindrance.

More recently, Boldea, Lévesque and Leclerc<sup>78</sup> reported the synthesis and ionochromic ability of poly(3-alkoxy-4-methylthiophene)s as shown in Fig. 1.26.

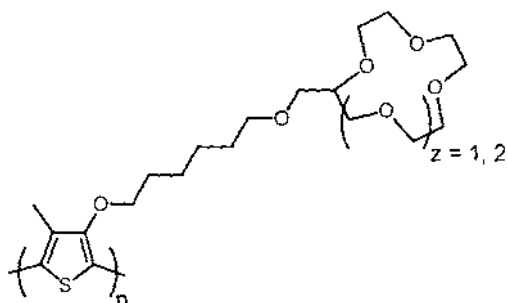


**Figure 1.26 Poly(3-alkoxy-4-methylthiophene)s**

Chemical polymerisation gave high molecular weight polymers that demonstrated substantial ionochromic effects. In acetone, complexation led to a more planar conformation, a clear isobestic point on the UV/VIS spectra indicating the coexistence of both planar and non-planar species. The selectivity of the polymers was not what was expected from a simple 1:1 crown:cation species, but appeared instead to be the result of 2:1 complexation.

Sannicolo *et al.*<sup>150</sup> designed two bithiophene monomers with rigidly tethered crown ethers. The design was such that in one monomer the crown was coplanar with the bithiophene moiety, while in the other monomer a perpendicular crown ether was present (Fig. 1.27).

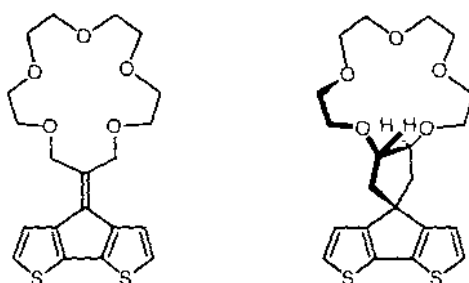


**Figure 1.27 Planar and perpendicular bithiophene monomers designed by Sannicolo *et al.***

Both of these monomers produced electroactive films with similar conductivities. While EQCM analysis showed that both polymers incorporated one alkali metal ion per crown, changes were only seen in the cyclic voltammogram for the planar species.

In this case, the redox potential of the polymer moved to more positive values on addition of lithium and sodium, with sodium having the greater effect.

#### 1.4.4 Directly bonded crown ethers

The first example of a crown ether in direct  $\pi$ -conjugation with the thiophene backbone was published by Bicknell *et al.* in 1994.<sup>151</sup> While they report successfully synthesising a monomer consisting of 15-crown-5 directly bonded to a thiophene ring (Fig. 1.28a), due to synthetic difficulties they changed focus to the corresponding thiophene vinylene system. This was achieved by polymerisation of the 2,5-bis(chloromethyl) derivative using potassium tert-butoxide (Fig. 1.28b-c).

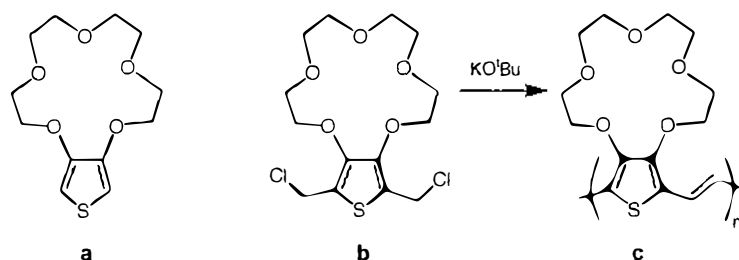


**Figure 1.28** Crown ether functionalised thiophenes synthesised by Bicknell *et al.*

Very soon after this, Bauerle and Scheib also published data on the same 15-crown-5-thiophene<sup>152</sup> which they synthesised in good yield following the method of Sone *et al.*<sup>153</sup> In addition they synthesised the analogous bithiophene and terthiophene monomers (Fig. 1.29).

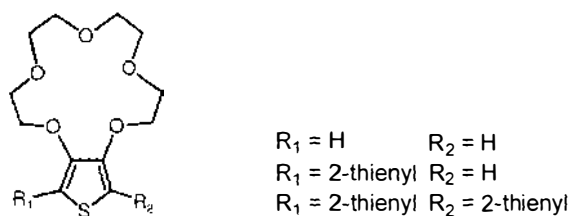


**Figure 1.29** Directly  $\pi$ -conjugated monomers of Bauerle and Scheib

Of the three monomers, only the terthiophene based compound did not form adhering films on the working electrode during electropolymerisation. However, the polymer based on bithiophene was not affected by alkali metal cations. The addition of alkali metal ions to the electrolyte in a multi-sweep cyclic voltammetric experiment caused the first oxidation wave of the thiophene based polymer to gradually shift to more positive potential, the effect being greatest for  $\text{Na}^+$  ions. The rationale for this result was that the complexation of positively charged ions made it harder to remove electrons from the polymer, hence increasing its oxidation potential. Due to substitution at the  $\beta$  positions, the thiophene-based monomer could only polymerise through ideal  $\alpha$ - $\alpha$  couplings, resulting in a fairly rigid polymer. This relative rigidity meant that transport and migration of metallic ions was slow in comparison to their earlier work using alkyl spaced crowns (Fig. 1.25) where equilibrium conditions were reached in just one scan. A later article details success in polymerizing the less bulky 12-crown-4 monothiophene, giving a polymer with a slightly greater mean conjugation length than that obtained for 15-crown-5 monothiophene, but which was only marginally affected by the addition of alkali metal ions. The same paper reported that 18-crown-6 monothiophene could not be polymerised “probably due to steric reasons”.<sup>140</sup>

A recent investigation into this work has been carried out by Berlin *et al.* They also synthesised the 18-crown-6 thiophene monomer using the method of Sone<sup>153</sup>, and in addition synthesised several other related compounds designed to provide an insight into Bauerle and Scheib’s earlier results (Fig. 1.30).<sup>154</sup>

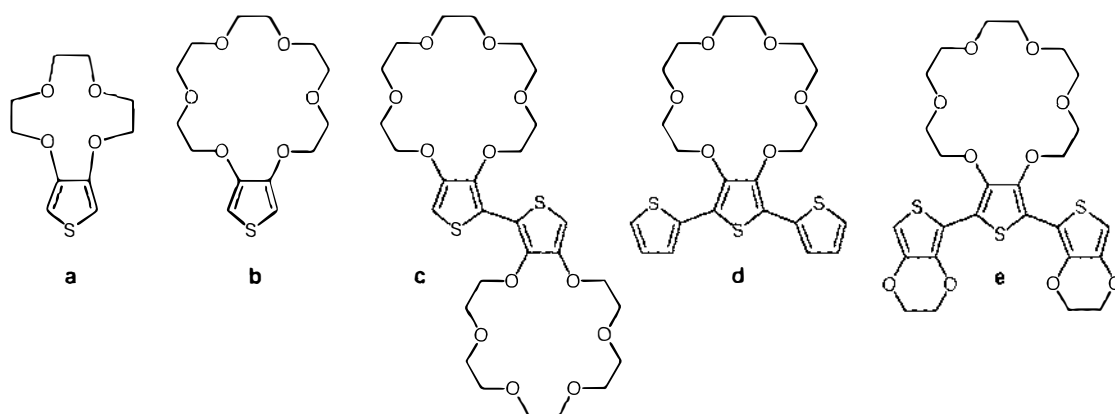


**Figure 1.30** Crown ether functionalised thiophenes studied by Berlin *et al.*

In agreement with the earlier data, no polymer was formed from repetitive CV cycling of 18-crown-6-thiophene. Electrolysis of a solution of the monomer gave a light red solution ( $\lambda_{\text{max}} = 365 \text{ nm}$ ) after reduction, which was shown by MALDI-MS to contain only dimers (*ca.* 10%) and monomeric products of overoxidation. It appeared that while coupling was occurring, it was sufficiently slow that there was significant competition from undesired side-reactions. In order to investigate more fully, the dimer (Fig. 1.30c) was synthesised. Again, no polymer was deposited by CV cycling, but a reversible redox signal was seen due to an electroactive species in solution. Bulk electrolysis of this compound, followed by reduction, gave a red solution ( $\lambda_{\text{max}} = 480 \text{ nm}$ ). Analysis by MALDI-MS showed the solution to consist mainly of trimers (sexithiophenes), with decreasing amounts of higher oligomers up to that containing sixteen thiophene rings. This finding clearly showed that steric hindrance was not the reason that polymer films were not deposited, rather the problem lay with the solubility of the oligomers formed. Two related terthiophene compounds were also investigated. The CV of a film formed from the terthiophene based monomer (Fig. 1.30d) showed no change in the presence of  $\text{Li}^+$ , and dissolved when either  $\text{Na}^+$  or  $\text{K}^+$  was introduced to give yellow solutions ( $\lambda_{\text{max}} = 430, 434 \text{ nm}$  respectively). This polymer film could be made insoluble by prior cycling in acetonitrile to oxidise trapped oligomers and potentially cross-link the film<sup>155</sup>, but afterward showed no response to either  $\text{Na}^+$  or  $\text{K}^+$ . Films of the EDOT-derived compound (Fig. 1.30e) showed no change by CV or UV/VIS on addition of  $\text{Li}^+$ ,  $\text{Na}^+$  or  $\text{K}^+$ . Both of the



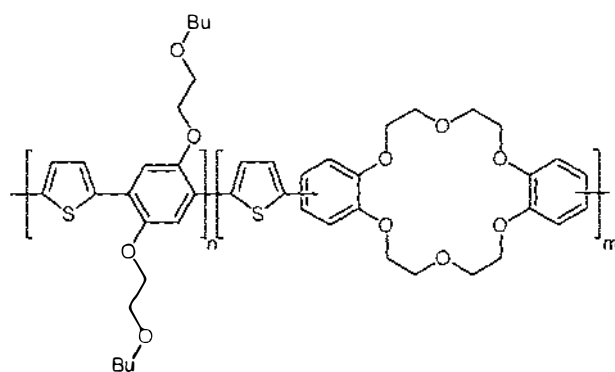
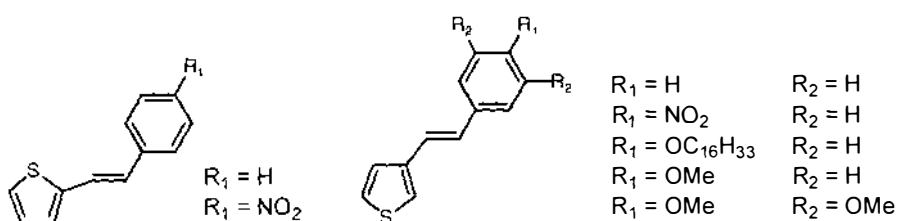


Figure 1.32 Crown containing copolymers by Bouachrine *et al.*

## 1.5 Past Work on Vinyl-Substituted Polythiophenes

There is a large amount of literature on vinyl-substituted thiophenes, the most relevant of which is reviewed below.

Smith, Campbell, Ratcliffe and Dunleavy synthesised a range of 2- and 3-styrylthiophenes, as illustrated in Fig. 1.33, in order to study their electrochemical properties.<sup>160, 161</sup>



**Figure 1.33** 2- and 3-substituted styrylthiophenes

In the case of both the 2- and 3-styrylthiophenes, the films that were formed were found to have low conductivity, and were redox inactive. This was attributed to simultaneous oxidation of both the thiophene and the alkene bond during polymerisation, resulting in a cross-linked polymeric matrix. Steric interactions between adjacent substituents were also believed to contribute to the inhibition of redox activity.

Welzel *et al.*<sup>162</sup> synthesised 3-(2,4-dinitrostyryl)thiophene and 3-(2,4,6-trinitrostyryl)thiophene. In both cases, homopolymerisation produced a film on the working electrode surface, however the films were not redox active. Copolymers were formed from a mixture of the nitrated monomer and 3-methylthiophene, and these films did show stable reversible redox systems.

Cutler *et al.*<sup>163-166</sup> were also unsuccessful in growing electroactive homopolymers from substituted 3-styrylthiophenes. Copolymers with bithiophene were redox active, and used in the fabrication of photoelectrochemical cells. In order to decrease steric interactions, and to lower the potential necessary for electropolymerisation, substituted styrylterthiophenes were synthesised (Fig. 1.34).

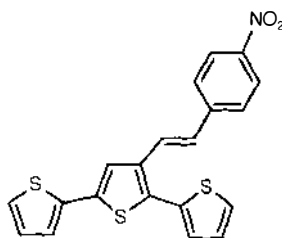


**Figure 1.34 Nitrostyryl terthiophene synthesised by Cutler *et al.***

Kagan and Liu<sup>167</sup> looked at the polymerisation of 3'-vinyl-[2,2':5',2'']-terthiophene alone and as a copolymer with styrene. They used AIBN and carried out the reactions under typical free radical conditions. They believed that the substantially unchanged UV/VIS spectrum seen for the homopolymer indicated that polymerisation occurred through the vinyl bond rather than through the terthiophene moiety. In both cases, high molecular weight polymers were produced. The polymerisation product formed from a similar molecule, 5-vinyl-2,2':5',2'']-terthiophene, was shown to consist of oligomers with some sexithiophene character caused by coupling of the pendant terthiophene radical cation.<sup>168</sup> A subsequent publication describes results obtained for the homologous 5-vinyl-quaterthiophene, and alkyl substituted 5-vinyl-quinquethiophene and -sexithiophene compounds.<sup>169</sup> These results showed a decrease in cross-linking of the polymers with increasing thiophene length. This was attributed to the increased stability of the pendant oligothiophene radical cations, slowing the coupling reaction in comparison to polymerisation through the vinyl bond. A recent investigation carried out by Pagels *et al.*<sup>170</sup> into the polymerisation of 5-vinyl-[2,2':5',2'']-terthiophene and 5-ethyl-5''-vinyl-2,2':5',2'']-terthiophene confirmed these results, disagreeing with those of Kagan and Liu. They found that blocking the spare  $\alpha$ -position in the molecule with an ethyl group drastically reduced the ability of the molecule to polymerise, an effect that would not be seen if polymerisation occurred only through the vinyl bond.

## 1.6 Vinyl Linked Terthiophene Crown Ether Target Molecules

In this work, molecules of the type illustrated below in Fig. 1.35 were targeted. The incorporation of a conjugated spacer between the crown ether moiety and the polymer backbone serves a dual purpose. Not only should it help ensure that the steric requirements imposed by the thiophene functionalisation space are met, but also that there is no hindrance to electronic communication between the crown ether and the polymer backbone. The use of terthiophene, rather than thiophene, will also assist in minimizing steric strain. In addition, this will lower the oxidation potential of the monomer, removing the problems encountered with polymerisation through the double bond as seen earlier by other researchers for substituted styrylthiophenes (Section 1.5). In turn, this should allow homopolymers to be formed, eliminating the compositional and structural uncertainty associated with the formation of copolymers.

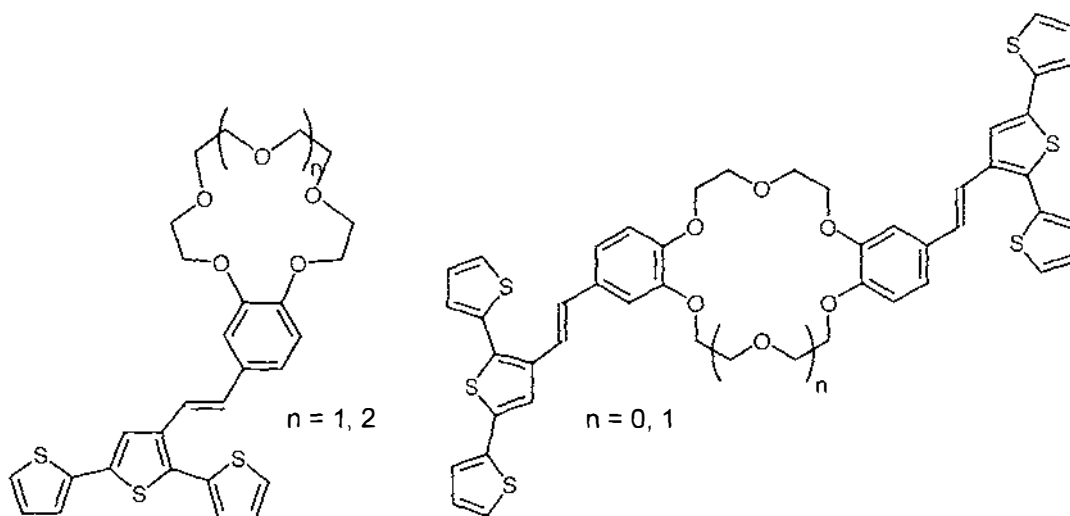


Figure 1.35 Vinyl linked terthiophene crown ether target molecules

**2**

**SYNTHESIS**

**OF**

**ETHER**

**FUNCTIONALISED**

**(TER)THIOPHENES**

The types of ether functionalised target molecules focused on in this research are described in Section 1.6 (Fig. 1.35). Two monostyryl-terthiophene compounds were initially targeted, and are illustrated below in Fig. 2.1. Each contains a single polymerisable terthiophene moiety connected by an alkene linker to a benzo-crown ether group. It was anticipated that using two different crown ethers would be sufficient to allow different cation selectivities to be observed.

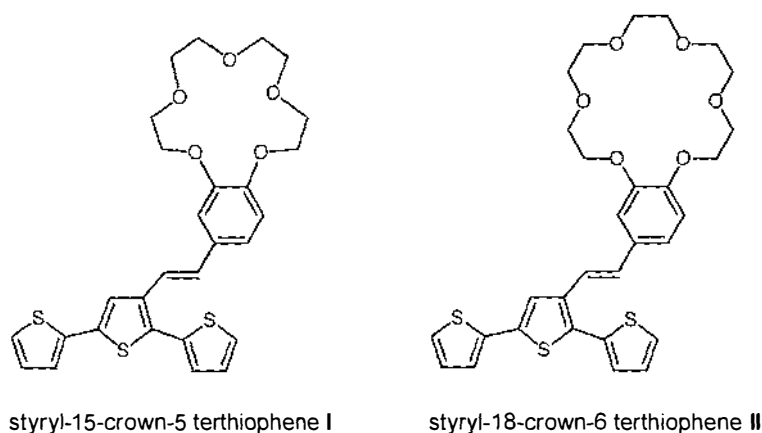


**Figure 2.1 Target compounds styryl-15-crown-5 and styryl-18-crown-6 terthiophene**

Molecules of the type depicted in Fig. 2.1 can be viewed either as vinyl-substituted benzo-crown ethers, or as vinyl-substituted terthiophenes. In order to design an efficient synthetic route toward the target molecules **I** and **II**, a survey of the literature was conducted to assess synthetic methods previously used to make vinyl-substituted crowns and terthiophenes. As the analogous thiophene crown compounds had not previously been made, synthetic strategies toward vinyl-substituted thiophenes were also of relevance.

## 2.1 Literature Synthetic Methods

### 2.1.1 The synthesis of vinyl-substituted benzo-crown ethers

There are a number of examples of vinyl-substituted benzo-crown ethers in the literature, and their syntheses can be divided into seven synthetic approaches.

Kikukawa *et al.*<sup>171</sup> published a method in 1980 utilizing a Heck arylation reaction between 4'-iodo- (or bromo-)benzo-15-crown-5 or benzo-18-crown-6 and various alkenes as shown in Fig. 2.2. Their procedure used a palladium catalyst, which was later modified by Yi, Zhuangyu and Hongwen,<sup>172</sup> to a polymeric palladium catalyst. This change removed some of the practical difficulties inherent in the earlier synthesis.

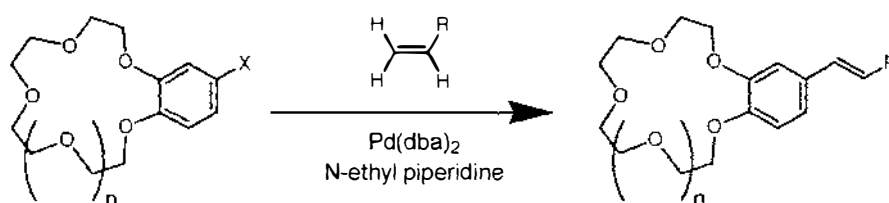


**Figure 2.2 Heck arylation of olefins**

Beer and co-workers<sup>173-177</sup> begin with a formylated crown, reacting it with a mono- or di-lithiated bipyridine derivative, and then dehydrate the intermediate alcohol to form products of the type shown in Fig. 2.3. Stepwise lithiation and addition of two different formylated compounds provides access to non-symmetrical bifunctionalised molecules.<sup>178</sup>

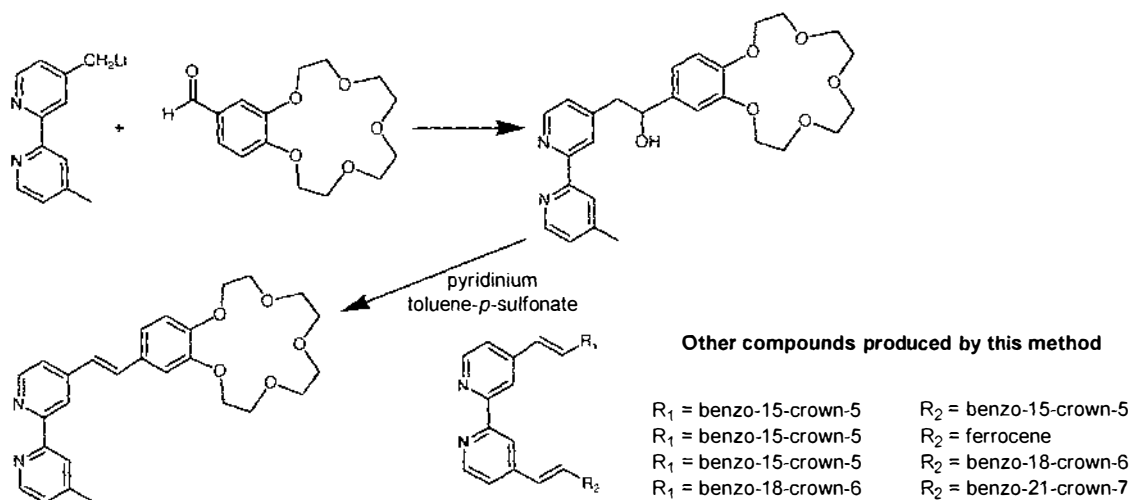


**Figure 2.3** Synthesis of vinyl-substituted crown ethers *via* alcohol dehydration

The only literature example of a vinyl-substituted dibenzo-18-crown-6 was also synthesised using this method, where an isomeric mixture of diformylbenzo-18-crown-6 was used as the aldehyde as illustrated in Fig. 2.4.<sup>179</sup>

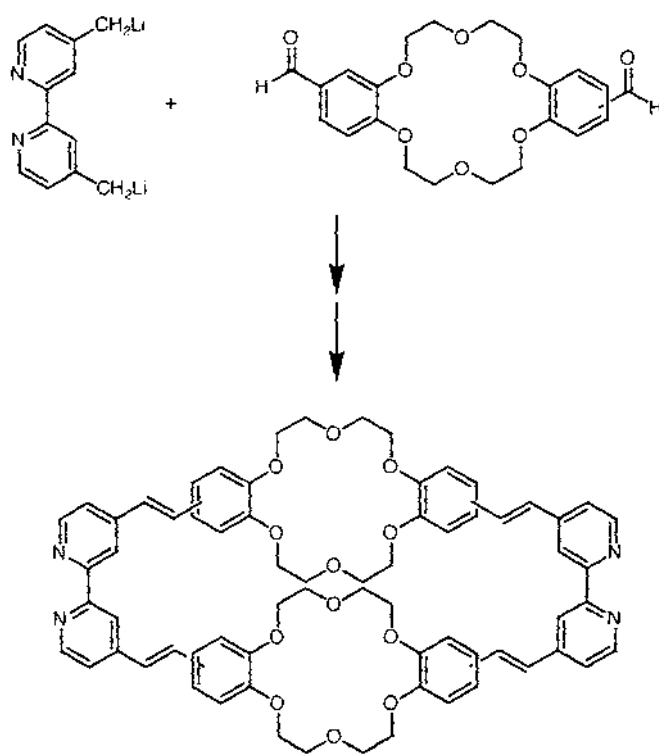


**Figure 2.4** Formation of vinyl-substituted dibenzo-18-crown-6

In the work of Brown and Foubister<sup>180</sup> the vinyl linkage is formed from the corresponding formylated crown and malonic acid using Knoevenagel condensation (Fig. 2.5).

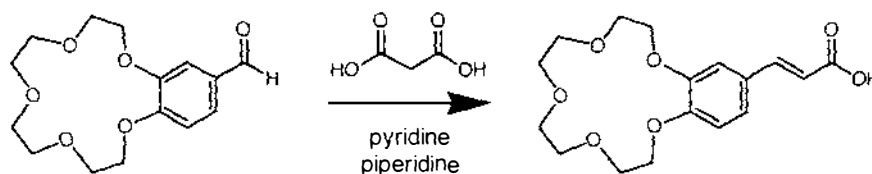


**Figure 2.5** Vinylation of benzo-15-crown-5 via Knoevenagel condensation

A few years later Shirai *et al.*<sup>181-186</sup> used Brown's synthesis as the initial step in their synthesis of vinyl substituted crowns, which also contained a terminal alkene (Fig. 2.6). These molecules could then be polymerised through the terminal alkene using boron trifluoride etherate as initiator, and further photodimerised through the remaining double bond.

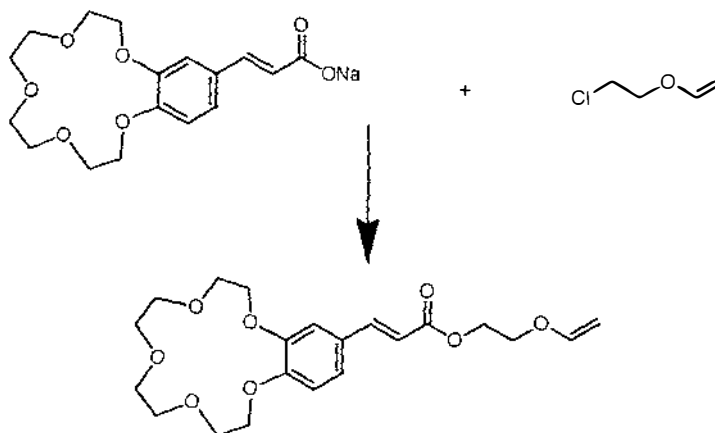


**Figure 2.6** Extension of Knoevenagel condensation method

Another method, published by Luboch, Cygan and Biernat<sup>187</sup> involved a Claisen-Schmidt condensation reaction between formyl- and aceto-substituted benzo crown ethers, as shown in Fig. 2.7.

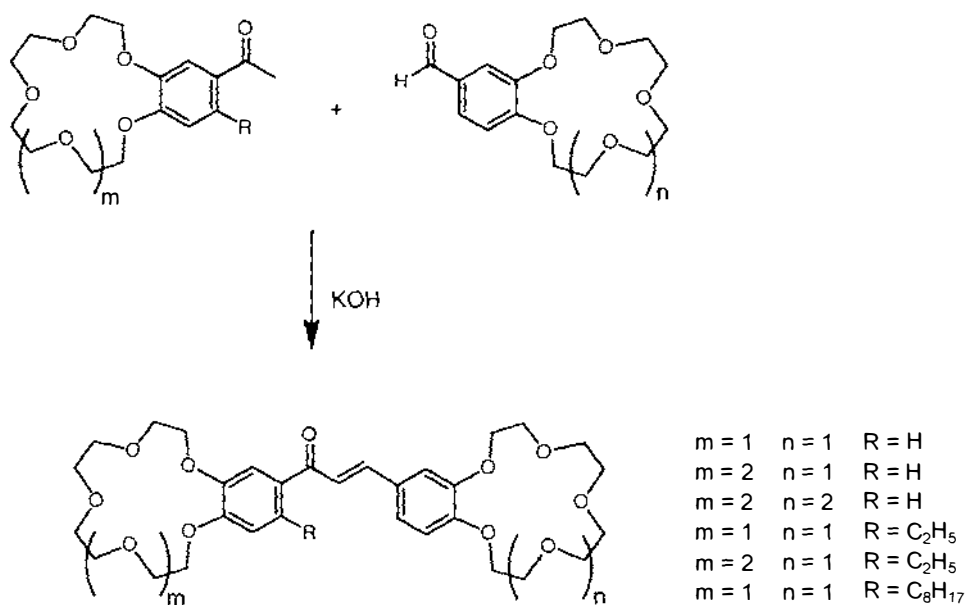


**Figure 2.7 Claisen-Schmidt condensation of crown derivatives**

Gromov *et al.*<sup>188-196</sup> used the reaction between the active methylene group of a benzothiazolium salt and a formylated crown in the presence of pyridine, (Fig. 2.8). Figure 2.8 also shows benzo-18-crown-6 based products,<sup>197-202</sup> and a bis(crown ether) derivative resulting from an extension of the methodology.<sup>203, 204</sup>

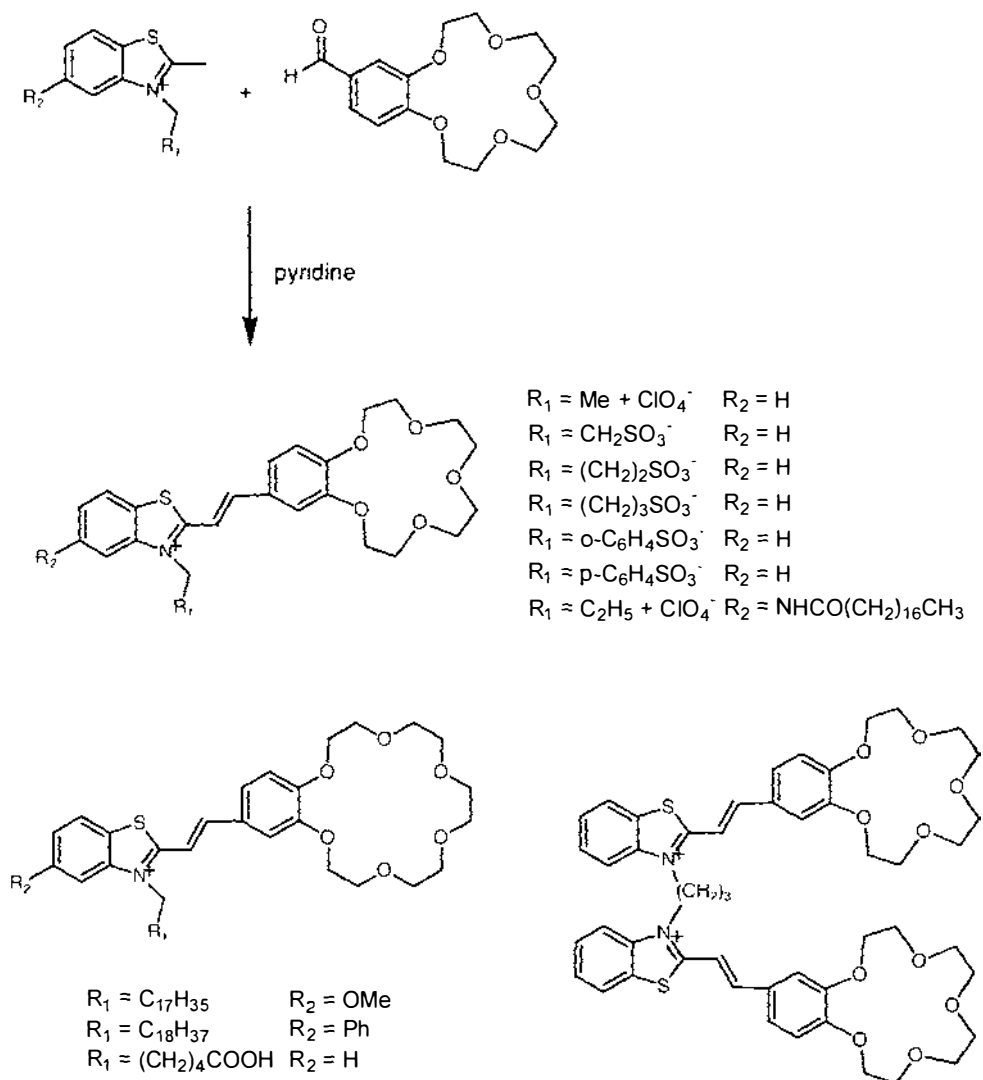


**Figure 2.8** Formation of mono- and bis-crown ether styryl dyes according to the method of Gromov *et al.*

Lindsten *et al.*<sup>205</sup> formed symmetrical stilbene crown ethers by the titanium-mediated (McMurry) reductive coupling of two molecules of a formylated benzo-crown ether as shown in Fig. 2.9. These compounds were interconverted between the *E* and *Z* isomeric forms by irradiation.

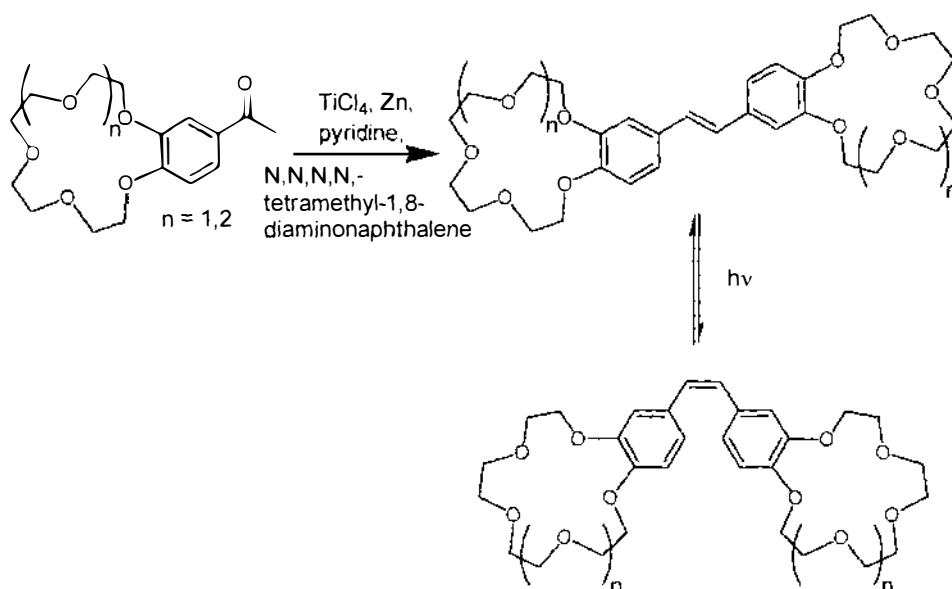


**Figure 2.9 Formation of stilbene bis-crown ethers**

The final synthetic approach uses a Wittig or Horner-Emmons reaction to form the double bond. Beer, Sikanyika, Blackburn and McAleer<sup>206, 207</sup> report a Wittig reaction between one or two molecules of formyl-benzo-15-crown-5 and ferrocene mono- or di-phosphonium salt respectively (Fig. 2.10). While the product resulting from a single Wittig reaction was successfully separated into the *cis* and *trans* isomeric forms by column chromatography, the isomeric mixture of products resulting from a dual Wittig reaction could not be separated.

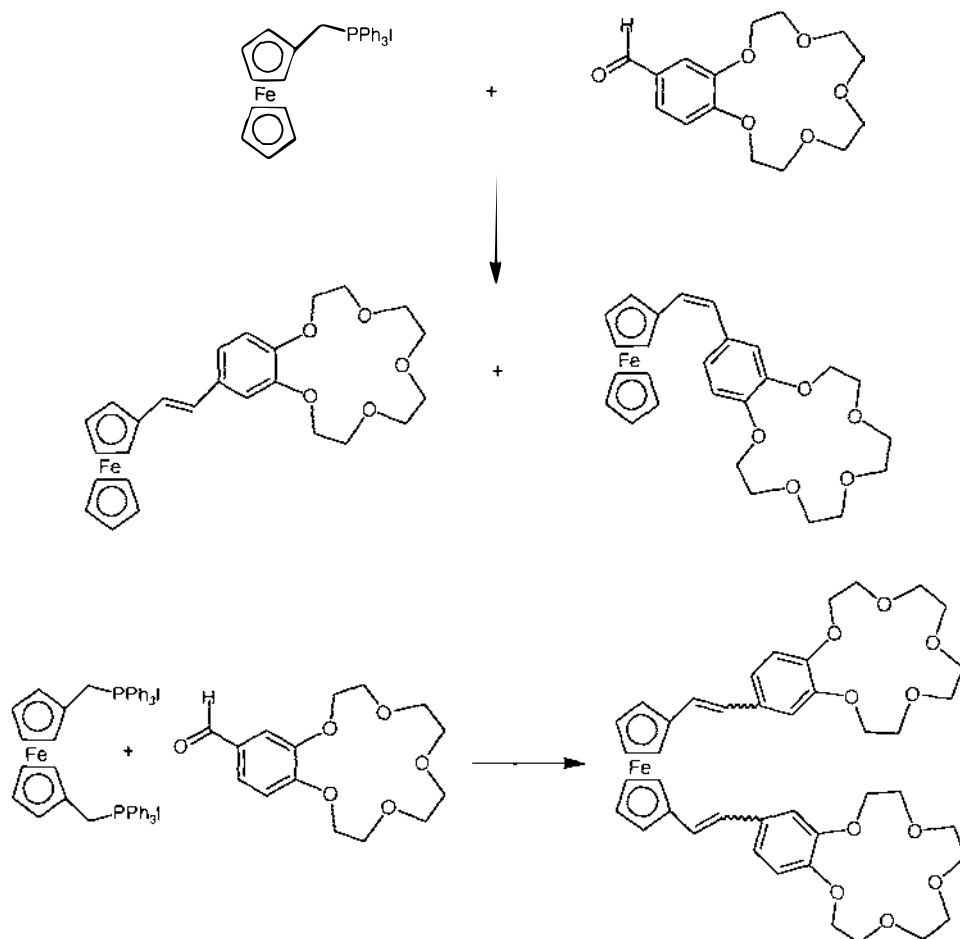


**Figure 2.10** Wittig reaction between ferrocene phosphonium salt and formylbenzo-15-crown-5

Winkler *et al.*<sup>208</sup> also used a Wittig (or Horner-Emmons) reaction, but reacted a disubstituted crown ether phosphonium salt (or phosphonate) with terephthalaldehyde to form oligomers as shown in Fig. 2.11. The *cis* isomer produced by the Wittig reaction was thermally isomerised into the *trans* isomer in the presence of  $I_2$ .

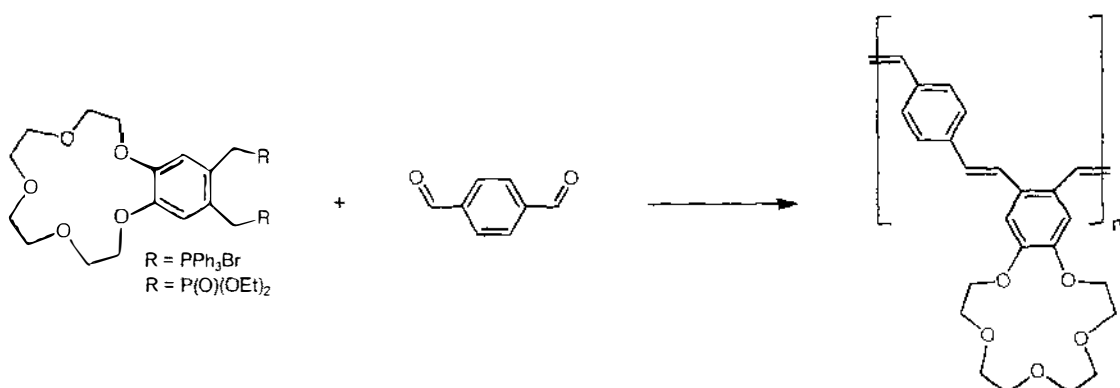


**Figure 2.11** Formation of vinyl substituted crown *via* Wittig (or Horner Emmons) reaction

## 2.1.2 The synthesis of 3'-vinyl-substituted terthiophenes

In contrast to the wealth of literature available on vinyl-substituted crowns, to the best of our knowledge at the beginning of this research there was only one report detailing synthesis of a 3'-vinyl-substituted terthiophene. Kagan and Liu synthesised 3'-vinyl[2,2';5',2'']terthiophene using Grignard chemistry as shown in Fig. 2.12.<sup>167</sup>

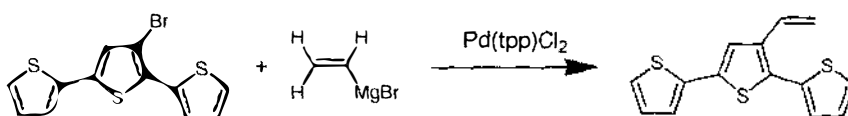


**Figure 2.12** Synthesis of 3'-vinyl-2,2':5',2''-terthiophene *via* Grignard chemistry

During the course of this research, Collis *et al.*<sup>209</sup> synthesised  $\beta$ -terthiophene aldehyde and  $\beta$ -terthiophene phosphonate. These compounds were then used in Wittig or Horner-Emmons reactions to produce a range of 3'-vinyl-substituted

terthiophenes (Fig. 2.13). This is a versatile method, applicable to a wide range of molecules. Compounds produced by this method and published to date include nitrophenyl,<sup>164</sup> pyridyl,<sup>209</sup> ferrocene<sup>165</sup> and porphyrin<sup>166</sup> derivatives.

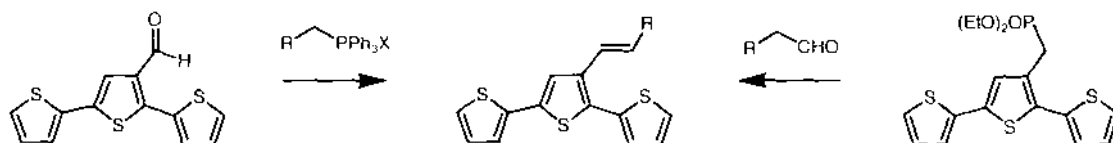


**Figure 2.13** Wittig/Horner-Emmons reactions used to synthesise vinyl-substituted terthiophenes

### 2.1.3 The synthesis of vinyl-substituted thiophenes

Due to the sparse literature available on the synthesis of 3'-vinyl-substituted terthiophenes, the synthetic method employed by Smith *et al.*<sup>160, 161</sup> to make the 3-styrylthiophenes discussed in Section 1.5 was also investigated. Their method of choice was Wittig/Horner-Emmons chemistry, forming the compounds shown in Fig. 2.14 by a reaction between thiophenecarboxaldehyde and a 3-substituted thiophene phosphonium salt or phosphonate.

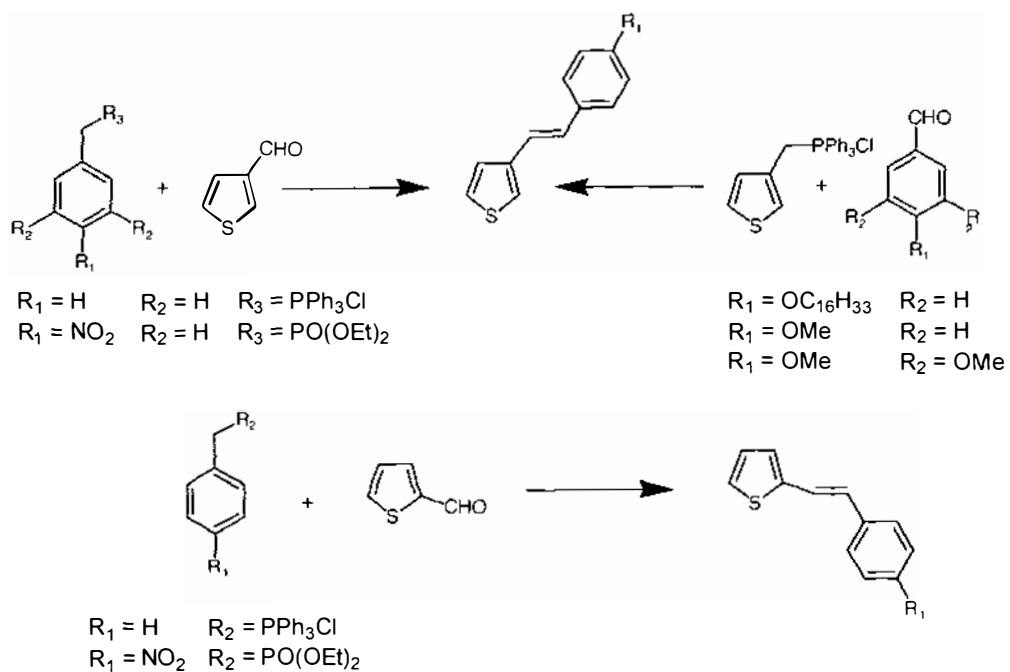


**Figure 2.14** The use of Wittig reactions to synthesise vinyl thiophenes

Given these reports and the work carried out in our laboratories, it would appear that the most expedient synthetic approach employed Wittig chemistry to form the central alkene linkage in molecules **I** and **II**.

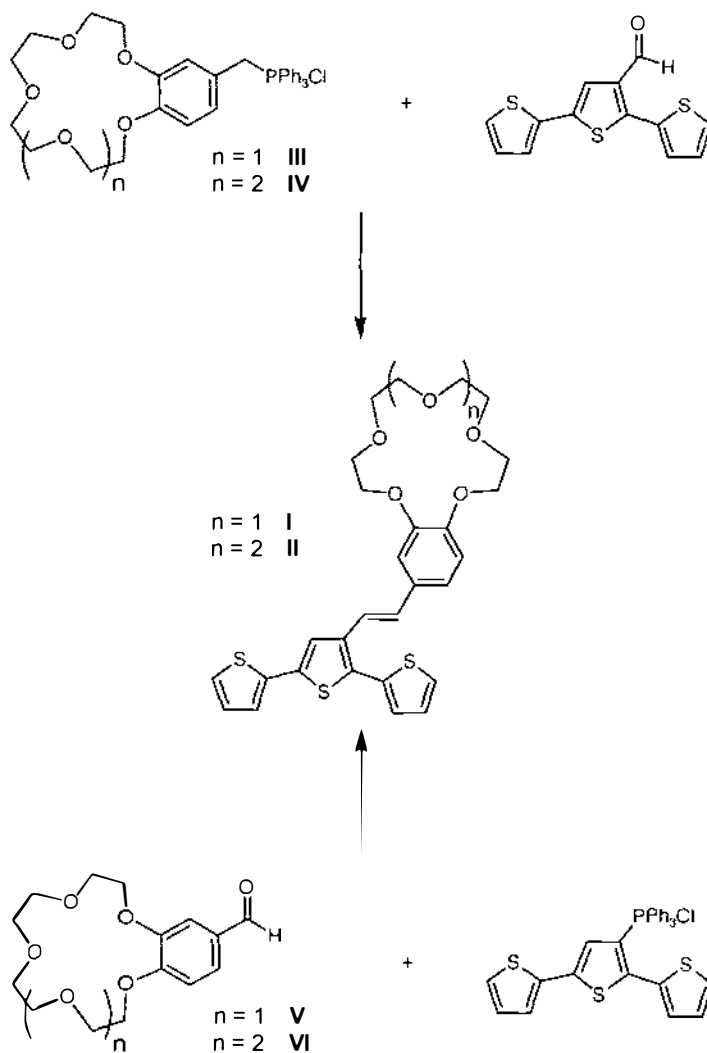
## 2.2 Synthetic Studies Toward Monostyryl (Ter)thiophene Crowns

### 2.2.1 Synthesis of crown phosphonium salts

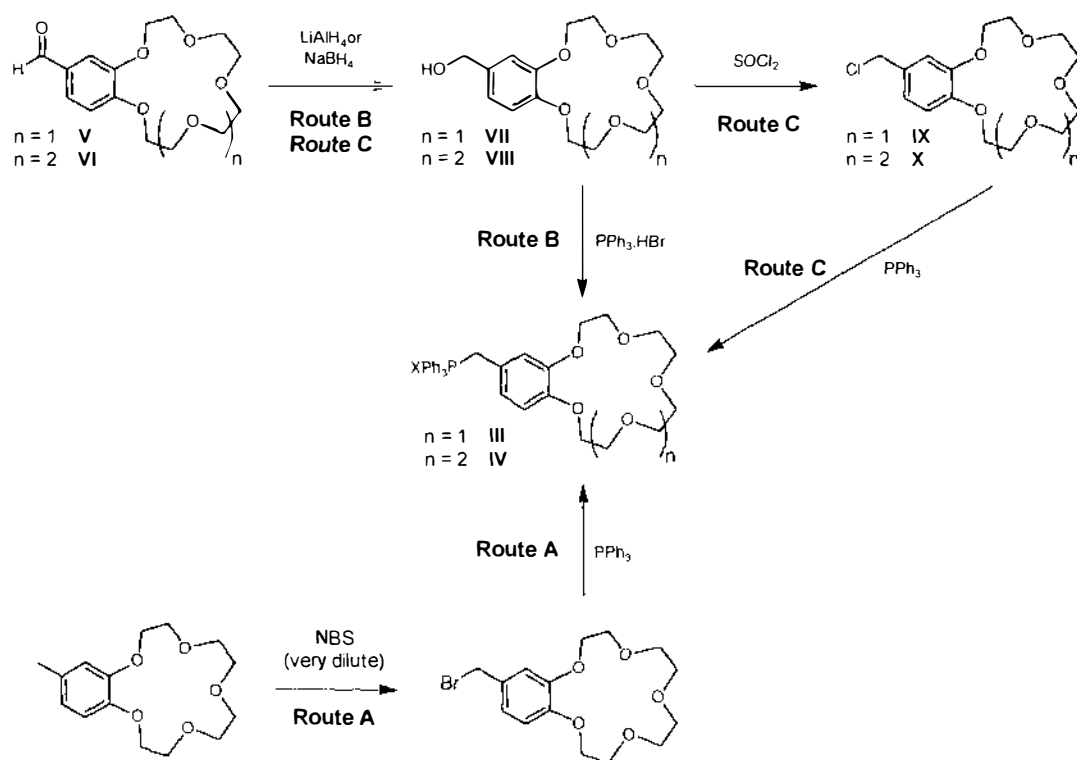
As discussed in the previous section, the preferred synthetic method toward compounds **I** and **II** utilizes a Wittig reaction to form the alkene bond. Scheme 1 illustrates how this could be achieved either by a reaction between a crown ether phosphonium salt and [2,2';5',2'']terthiophene-3'-carbaldehyde, or by a reaction between a terthiophene based phosphonium salt and a crown ether aldehyde.

Due to the availability of [2,2';5',2'']terthiophene-3'-carbaldehyde, the route utilizing crown phosphonium salts was explored. This method required the synthesis of the unknown benzo-15-crown-5 and benzo-18-crown-6 phosphonium salts. The phosphonium salt synthesis itself could be approached in three ways, as illustrated below (Scheme 2). Initially the synthesis involving the least number of steps was investigated, namely the bromination of a methylbenzo-crown (Scheme 2, Route A).

Wong and Ng<sup>210</sup> report the bromination of methylbenzo-15-crown-5 by N-bromosuccinimide at the methyl position when the reaction was carried out at high dilution (0.014 M). In more concentrated solutions bromination occurred on the aromatic ring. However, an initial attempt on a related benzo-crown using N-bromosuccinimide failed, instead giving electrophilic aromatic substitution on the benzene ring as evidenced by <sup>1</sup>H NMR. Two further attempts were made using N-bromosuccinimide and a radical initiator (1,1'-azobis(cyclohexanecarbonitrile)) but this route was abandoned when these also brominated in the wrong position. Consequently, the route with the least number of steps beginning with the crown aldehyde (Scheme 2, Route B) was investigated.



**Scheme 1** Alternative routes toward target compounds I and II



**Scheme 2** Formation of benzo-crown phosphonium salts **III** and **IV**

Formylbenzo-15-crown-5 **V** and formylbenzo-18-crown-6 **VI** were prepared according to the method of Ungaro *et al.*<sup>16</sup> (41% yield, literature value 40%) then reduced to the corresponding known alcohols using lithium aluminium hydride (yield 44%, literature value 64%).<sup>211</sup> It was later found that modifying this procedure to use the milder reducing agent sodium borohydride led to higher yields (86%) of the hydroxymethyl substituted crowns **VII** and **VIII**.

In some instances, alcohols can be converted directly into phosphonium salts by the use of triphenylphosphine hydrogen bromide,<sup>212</sup> but this method was unsuccessful in this case. The hydroxymethyl crowns **VII** and **VIII** were instead chlorinated<sup>211</sup> to give the chloromethyl derivatives **IX** and **X** (Scheme 2, Route C). These were then refluxed in toluene with triphenylphosphine to give benzo-15-crown-5 phosphonium salt **III** and benzo-18-crown-6 phosphonium salt **IV**. Isolation of these compounds was facilitated by their marked change in solubility in toluene during the course of the reaction. As well as the appearance of a large group of signals in the aromatic region, the <sup>1</sup>H NMR spectrum showed a distinct downfield shift in the position of the

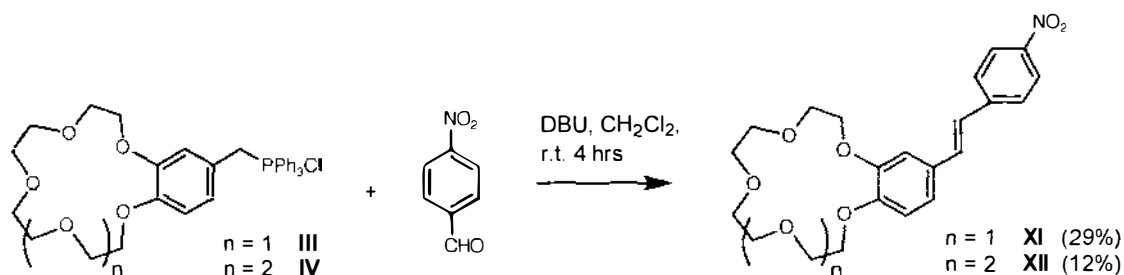
methylene proton signal, from 4.5 to 5.1 ppm. In addition, the signal at 5.1 ppm was split due to coupling with phosphorus ( $^2J_{\text{H,P}} = 13.8$  Hz).  $^{31}\text{P}$  NMR spectra of these compounds revealed a peak at 24 ppm, attributable to the newly incorporated phosphorus atom. Further evidence for phosphonium salts **III** and **IV** was provided by high-resolution mass spectrometry.

## 2.2.2 Wittig reactions using crown phosphonium salts

In order to investigate the reactivity of the newly synthesised crown ether phosphonium salts **III** and **IV**, Wittig reactions with 4-nitrobenzaldehyde were carried out (Scheme 3). It was envisaged that the products from this reaction would be highly coloured, and therefore easily separated and identified. The reaction between benzo-15-crown-5 phosphonium salt (**III**) and 4-nitrobenzaldehyde was carried out at room temperature, giving a product containing only a small amount (<10 %) of the *cis* isomer. Repetitive column chromatography on silica gave a pure fraction of *trans*-**XI** (29%), free of triphenylphosphine oxide but with a considerable loss of material. The  $^1\text{H}$  NMR spectra of this bright yellow product showed distinct *trans*-proton doublets at 7.0 and 7.2 ppm ( $^3J = 16.2$  Hz). The chemical shifts of two doublets seen at 7.6 and 8.2 ppm, each integrating to two protons, are typical of nitro-substituted benzene rings.<sup>213</sup> In addition, there was no sign of an aldehyde proton evident in the spectra.  $^{13}\text{C}$  NMR and UV/VIS data was also consistent with the structure of **XI**. While thermal isomerisation usually favours the *trans* isomer, in this case refluxing in 1,2-dichloroethanol led to approximately 20% of the *trans* isomer converting to the *cis* form.

A reaction between benzo-18-crown-6 phosphonium salt **IV** and 4-nitrobenzaldehyde was carried out under the same conditions used for benzo-15-crown-5.  $^1\text{H}$  NMR analysis of the crude product revealed it to consist of an approximately 1:1 mixture of the *cis* and *trans* isomers. After removal of excess aldehyde, this was successfully isomerised with iodine to leave a mixture of *trans*-**XII** and triphenylphosphine oxide.

Column chromatography yielded a small fraction of *trans*-**XII** (12%) free of triphenylphosphine oxide. The  $^1\text{H}$  NMR of this compound showed the same essential features as that obtained for *trans*-**XI**, high-resolution mass spectrometry giving further evidence for the desired product.



**Scheme 3** Wittig reactions between phosphonium salts **III-IV** and nitrobenzaldehyde

Following this success, Wittig reactions were carried out between crown phosphonium salts **III** and **IV** and [2,2';5',2'']terthiophene-3'-carbaldehyde. The reaction involving benzo-15-crown-5 appeared, from analysis of its  $^1\text{H}$  NMR spectra, to yield exclusively the *trans* isomer of the product. While one of the vinyl proton doublets ( $\delta$  6.97) was clear in the spectra of the crude product, the second vinyl doublet and most of the terthiophene protons could not be easily distinguished due to interference by triphenylphosphine oxide. Removal of this by-product was again difficult, column chromatography yielding only a small fraction of the pure *trans* styryl-15-crown-5 terthiophene **I** (17%). Inspection of the  $^1\text{H}$  NMR spectra of the pure product revealed the presence of six new terthiophene doublet of doublet signals, and one characteristic downfield singlet ( $\delta$  7.40) caused by the proton in the 4'''-position.  $^{13}\text{C}$  NMR, along with various 2D experiments (COSY, LR-COSY, HMQC and HMBC), allowed a complete assignment of the compound as shown in Fig. 2.15. The UV/VIS spectrum of this compound consisted of a single broad peak at 329 nm ( $\log \epsilon_{\text{max}} = 4.57$ ). Given that compound **I** contains two chromophores, namely the terthiophene and central styryl-thiophene moieties, it was not immediately clear what was being observed. In comparison, terthiophene absorbs at 354 nm ( $\log \epsilon_{\text{max}} = 4.25$ )<sup>214</sup>, and styryl-thiophene absorbs at 291 nm ( $\log \epsilon_{\text{max}} = 4.40$ )<sup>163</sup>. The UV spectra of these types of compounds are further discussed in Section 4.1.2.1. High-resolution

mass spectrometry was used as additional verification of the successful synthesis of the target molecule **I**.

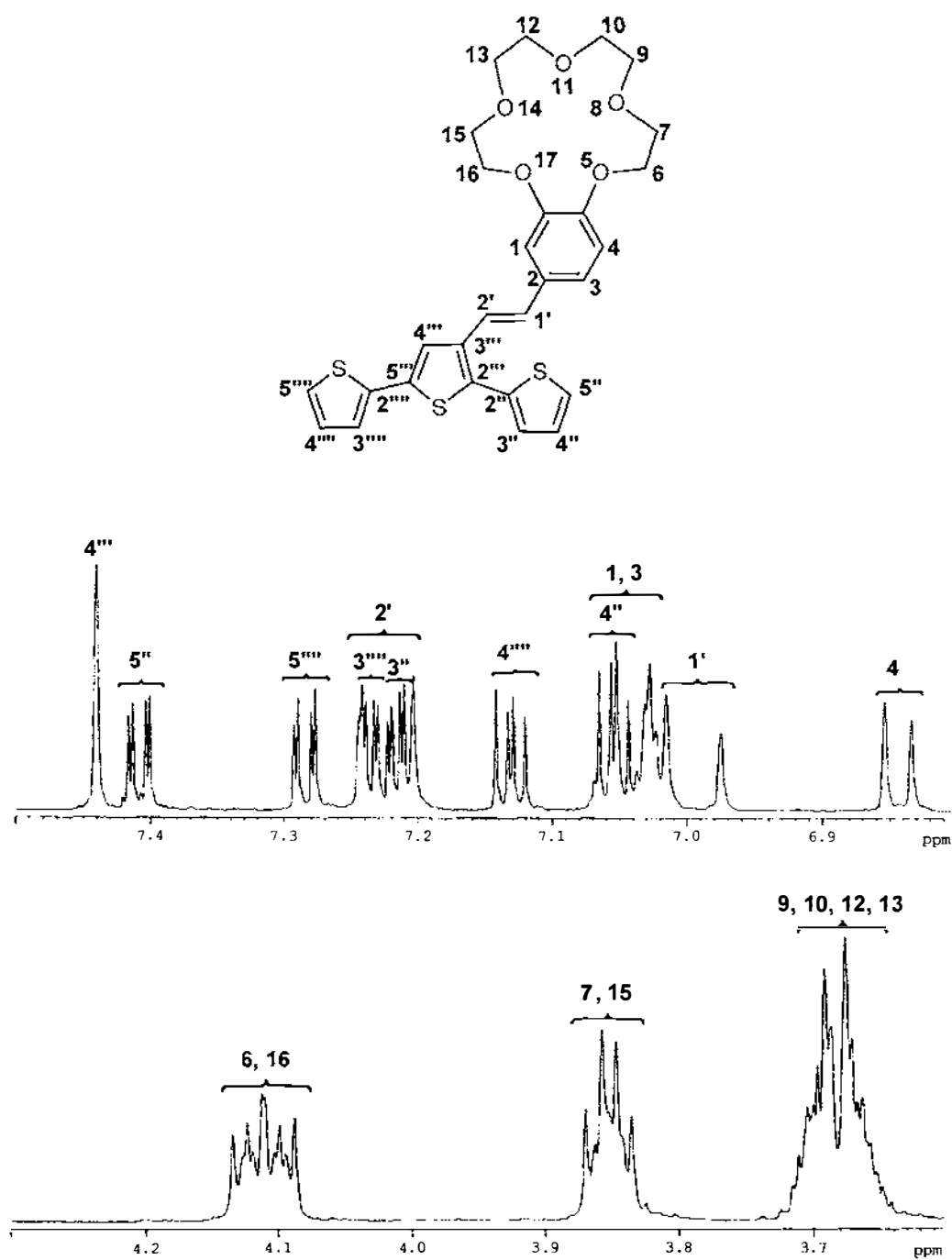
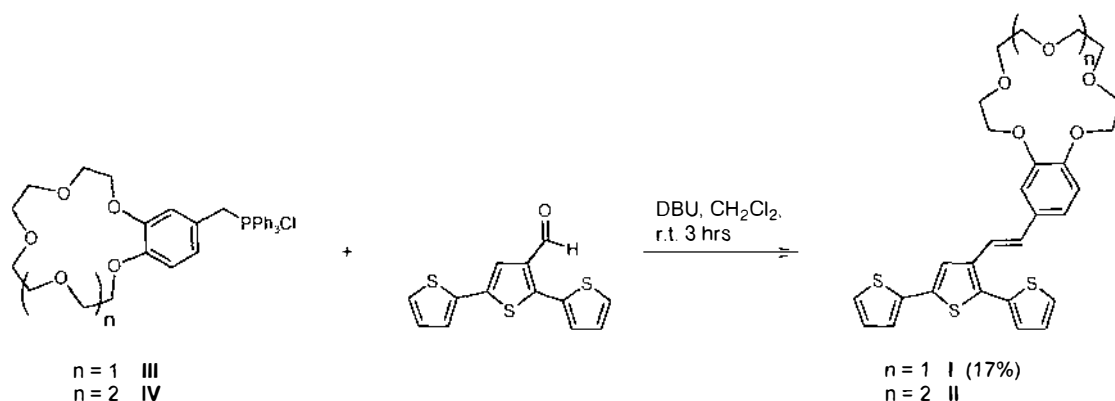


Figure 2.15  $^1\text{H}$  NMR spectrum of styryl-15-crown-5 terthiophene **I**

As in the earlier reaction with 4-nitrobenzaldehyde, the reaction between benzo-18-crown-6 phosphonium salt **IV** and [2,2';5',2'']terthiophene-3'-carbaldehyde yielded an approximately 1:1 *cis:trans* isomeric mixture. In this case, isomerisation with iodine was unsuccessful and resulted in the loss of the characteristic terthiophene proton signals in the  $^1\text{H}$  NMR spectra. The reaction was repeated and isomerisation attempted using irradiation, however this was also ineffective. Attempts to separate the product and triphenylphosphine oxide by column chromatography were fruitless. This difficulty in removing triphenylphosphine oxide has also been experienced by other researchers in our laboratory investigating terthiophene chemistry.<sup>209</sup> One potential solution to this problem was to utilise Horner-Emmons rather than Wittig chemistry.



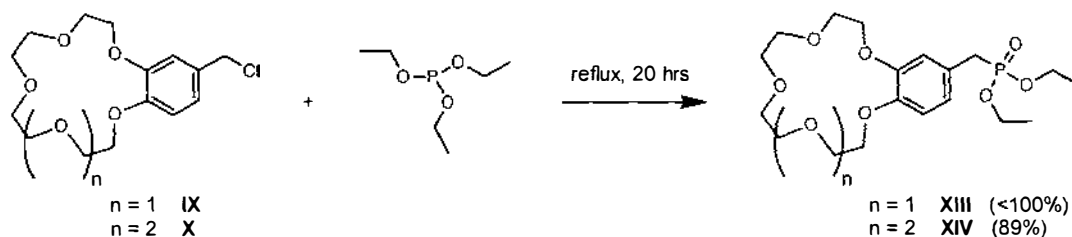
**Scheme 4** Wittig reactions between phosphonium salts III-IV and terthiophene aldehyde

### 2.2.3 Synthesis of crown phosphonates

Using phosphonates to carry out Horner-Emmons reactions has three main advantages over using phosphonium salts to perform Wittig reactions.<sup>215</sup> Ylides prepared from phosphonates are more reactive than those prepared from phosphonium salts, the by-product is water soluble and hence easily removed from the reaction mixture, and the

reaction generally gives exclusively the *trans* product, eliminating the need for isomerisation.

As it appeared that using phosphonates rather than phosphonium salts would solve the issues with both isomerisation and removal of by-product, the syntheses of benzo-15-crown-5 phosphonate **XIII** and benzo-18-crown-6 phosphonate **XIV** were investigated. Phosphonates are synthesised from halomethyl compounds and triethyl phosphite by the Arbuzov reaction<sup>216</sup>.



**Scheme 5** Formation of benzo-crown phosphonates **XIII** and **XIV**

The chloromethylbenzo crowns **IX** and **X** had been previously synthesised (Scheme 2) and their reaction with triethyl phosphite was straightforward (Scheme 5). Purification of the phosphonates was hampered by their high boiling points, rendering distillation ineffective, and consequently they were used with some impurities remaining. Despite this difficulty, several features were apparent in the <sup>1</sup>H NMR spectrum. As in the case of the phosphonium salt, the methylene proton signal had moved considerably, this time upfield to 3.1 ppm. The splitting of this signal (<sup>2</sup>J<sub>H,P</sub> = 21.2 Hz) was clear evidence of the presence of a phosphorus atom, confirmed by the appearance of a new signal at 28 ppm in the <sup>31</sup>P NMR spectra. The OCH<sub>2</sub> signal from the ethyl ester appeared in the same region as the OCH<sub>2</sub> signals from the crown ether, while the ester CH<sub>3</sub> signals are distinctive as a triplet at δ 1.2. The fully assigned <sup>1</sup>H NMR spectrum is shown below in Fig. 2.16. <sup>13</sup>C NMR spectroscopy and high-resolution mass spectrometry also supported the identity of the desired products **XIII** and **XIV**.

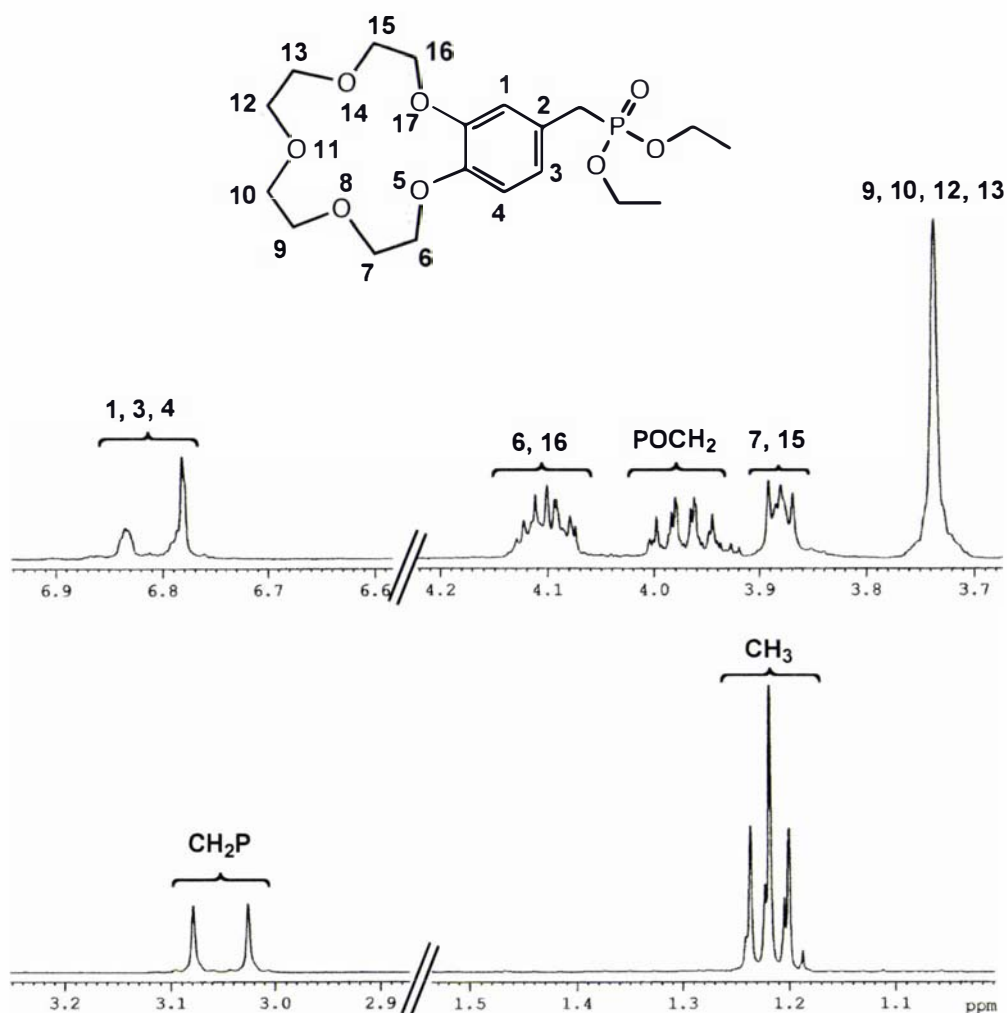


Figure 2.16 <sup>1</sup>H NMR spectrum for benzo-15-crown-5 phosphonate XIII

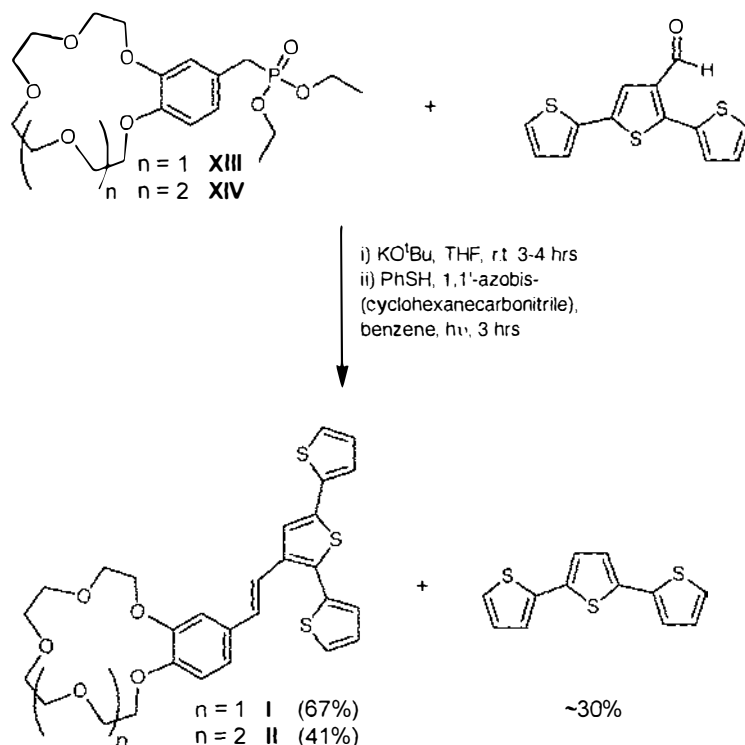
## 2.2.4 Horner-Emmons reactions using phosphonates

The Horner-Emmons reaction carried out at room temperature between benzo-15-crown-5 phosphonate XIII, [2,2';5',2'']terthiophene-3'-carbaldehyde and KO<sup>t</sup>Bu gave a good yield (73%) of the desired product I containing approximately 4% of the *cis* isomer after column chromatography. The crude product was then isomerised using

thiophenol, 1,1'-azobis(cyclohexanecarbonitrile) as a radical initiator with simultaneous heating and irradiation. After further purification by column chromatography, the pure *trans* isomer of styryl-15-crown-5 terthiophene **I** was obtained as a yellow oily solid (67%). The spectroscopic properties of the product were identical to that of the sample prepared by the Wittig route.

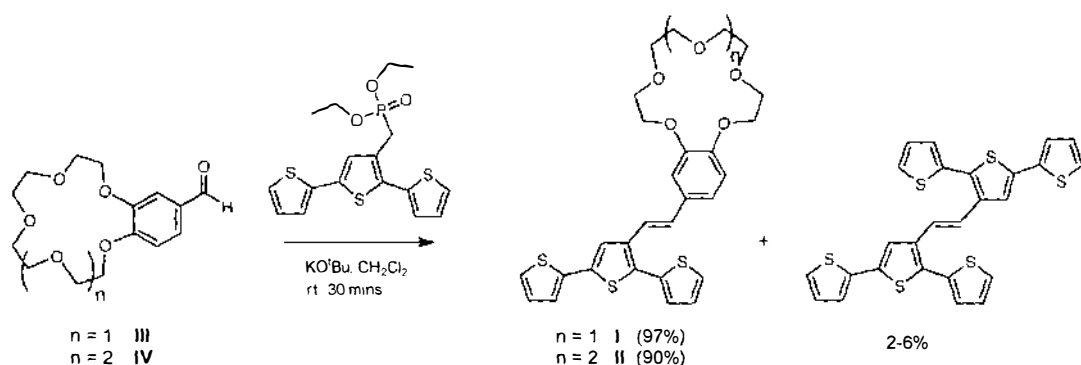
Of interest was the significant amount (*ca.* 30%) of terthiophene separated from the crude reaction mixture. It seems most probable that this was formed from the decarbonylation of [2,2';5',2'']terthiophene-3'-carbaldehyde by potassium tert-butoxide, a reaction that is not without precedent in other systems.<sup>217</sup> Mohanakrishnan and co-workers were the first to publish data on decarbonylation of thiophene derivatives<sup>218, 219</sup> by potassium tert-butoxide. Their studies involved thiophenes formylated at the  $\alpha$ -position only, and they were able to separate decarbonylated products in yields from 41-77%. As decarbonylation has not been seen in reactions involving [2,2';5',2'']terthiophene-3'-carbaldehyde and other non-crown phosphonium salts<sup>212</sup> it appears that the  $\beta$ -position of thiophene is less active than the  $\alpha$ -position. The increased activity in this system could well be due to the crown ether complexing potassium, allowing the 'naked' tert-butoxide anion to act as a much stronger base.<sup>220-222</sup>

The analogous reaction between benzo-18-crown-6 phosphonate **XIV** and [2,2';5',2'']terthiophene-3'-carbaldehyde progressed similarly, yielding 56% of the crude product **II** comprising approximately 2% of the *cis* isomer. After isomerisation and column chromatography the pure *trans* product **II** was isolated as a yellow oily solid (41%). As in the equivalent reaction utilizing benzo-15-crown-5 phosphonate, a significant amount of terthiophene was separated from the crude reaction mixture before isomerisation.



**Scheme 6 Horner-Emmons reactions between phosphonates XIII-XIV and terthiophene aldehyde**

During the course of this work, terthiophene phosphonate was synthesised in our laboratories.<sup>209</sup> The two styryl-crown terthiophenes **I** and **II** were then synthesised, in excellent yields, from a Horner-Emmons reaction between this phosphonate and the appropriate formylbenzo-crown as shown in Scheme 7. In these reactions, <sup>1</sup>H NMR analysis revealed that only the *trans* isomer of the desired products was formed. A small amount of a bright yellow by-product was also isolated during column chromatography, MALDI-MS indicating that the species still contained six thiophene rings. Comparison of the <sup>1</sup>H NMR spectrum for this product with the spectrum of a sample of cross-linked terthiophene previously synthesised in our laboratories revealed it to be 1,2-bis([2',2'';5''',2'''']terthiophen-3''-yl)ethene.<sup>212</sup> In phosphonium salt chemistry, the presence of water has been shown to lead to the formation of an aldehyde from the initial phosphonium salt.<sup>223</sup> If this were also the case here, it is anticipated that a reaction between the newly-formed terthiophene aldehyde and terthiophene phosphonate would lead to the cross-linked by-product seen.



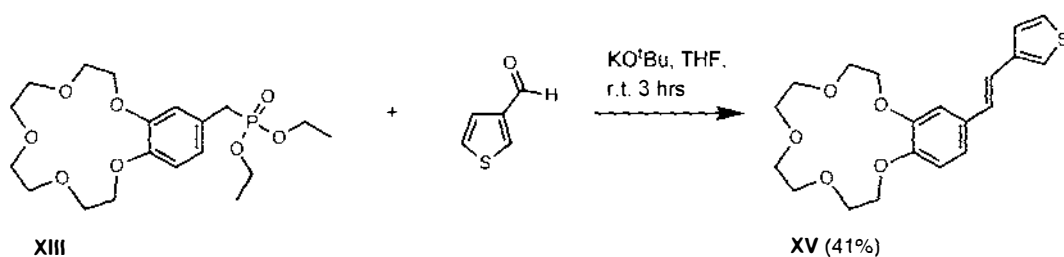
**Scheme 7** Formation of styryl terthiophene crowns I and II from terthiophene phosphonate

This procedure is clearly superior in a number of ways. Several steps are taken out of the synthetic scheme, as it is no longer necessary to transform the formylbenzo-crowns into phosphonates, the *cis* isomer of the product is not formed thereby eliminating the need for isomerisation, and yields are considerably higher since there is no competing decarbonylation reaction occurring.

## 2.2.5 Synthesis of crown-functionalised thiophenes

In order to more fully understand the electrochemical and spectroscopic properties of styryl-15-crown-5 terthiophene **I** (Chapter 4), it was desirable to synthesise the corresponding thiophene compound. All the necessary starting materials were available from previous work, so styryl-15-crown-5 thiophene **XV** was synthesised by a Horner-Emmons reaction as detailed in Scheme 8. This reaction proceeded smoothly, with no need for chromatography or isomerisation. The crude product was recrystallised to yield the pure *trans*-styryl-15-crown-5 thiophene **XV** as an off-white solid (41%). The  $^1\text{H}$  NMR spectrum of this compound (Fig. 2.17) shows all the expected features. Two doublets assigned to the two vinyl protons are seen at  $\delta$  6.87 and 6.98, with a typical *trans* splitting of 16 Hz. No *cis* signals are observed. Signals

due to the three aromatic protons are seen in the same region, showing both  $^3J$  and  $^4J$  coupling around the benzene ring. The thiophene proton signals are observed further downfield, at  $\delta$  7.2-7.4. The two multiplets in this area can be assigned to the 2'' and 5'' protons, and the 4'' thienyl protons. The crown proton signals occur in the region  $\delta$  3.7-4.3, and are divided into three groups by their proximity to the benzene ring.  $^{13}\text{C}$  NMR results are also consistent with the proposed structure, with the anticipated 8 ethereal and 12 aromatic protons all clearly visible. Long range COSY, HMQC and HMBC experiments allowed all of the NMR signals to be unequivocally assigned. UV/VIS spectroscopy showed absorbance maxima at 216 nm ( $\log \epsilon_{\text{max}} = 4.27$ ), 299 nm ( $\log \epsilon_{\text{max}} = 4.39$ ) and 318 nm ( $\log \epsilon_{\text{max}} = 4.41$ ). Compound **XV** is similar to *trans*-stilbene, which shows strong peaks at 295 and 308 nm ( $\log \epsilon_{\text{max}} = 4.40$ ), with a shoulder at 320 nm and a smaller peak at 229 nm ( $\log \epsilon_{\text{max}} = 4.20$ ).<sup>213</sup> These compare well to the peak positions and intensities observed for **XV**, and provide further evidence for a planar conjugated system. Previous work has been carried out on styryl-substituted thiophene derivatives of this type, where the benzene ring was functionalised in the *para* position with nitro, cyano, hydrogen, methoxy or dimethylamino groups. UV/VIS spectra for these compounds showed absorbance peaks at 199-248 nm ( $\log \epsilon_{\text{max}} = 2.34-4.32$ ) and 291-357 nm ( $\log \epsilon_{\text{max}} = 4.27-4.56$ ).<sup>163</sup> The current results appear in the middle of this range, and thus are consistent with past research. High-resolution mass spectrometry confirmed the formation of styryl-15-crown-5 thiophene **XV**.



**Scheme 8** Formation of styryl-15-crown-5 thiophene **XV**

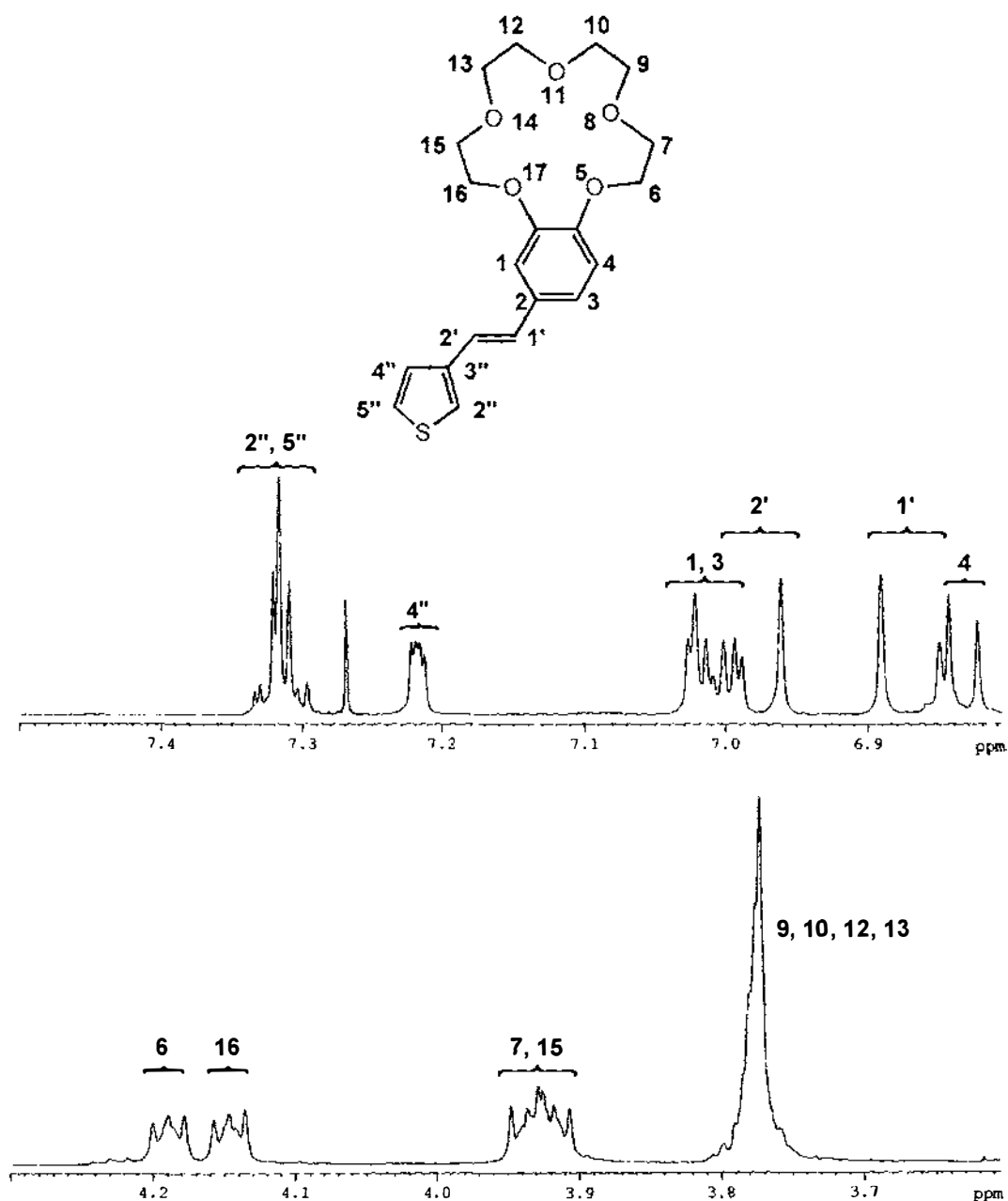
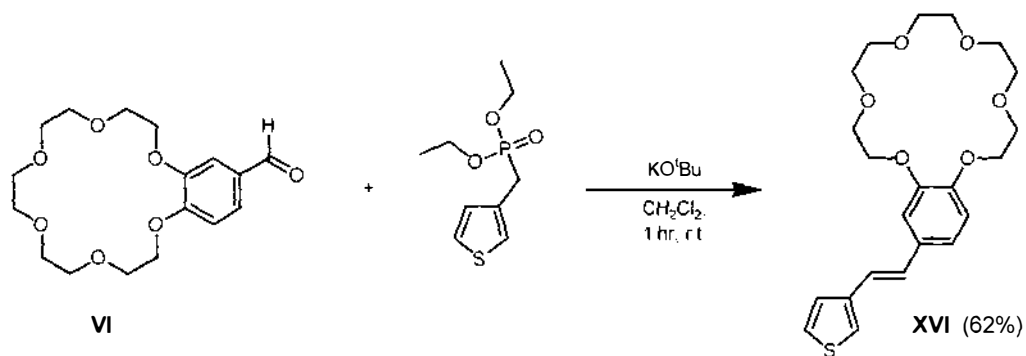


**Figure 2.17** Fully assigned  $^1\text{H}$  NMR spectrum of styryl-15-crown-5 thiophene **XV**

Styryl-18-crown-6 thiophene was also synthesised, as detailed in Scheme 9. A Horner-Emmons reaction between formylbenzo-18-crown-6 (**VI**) and thiophene phosphonate was carried out in  $\text{CH}_2\text{Cl}_2$  at room temperature. The crude product was purified by column chromatography on silica, giving the product **XVI** entirely in the *trans* form. LDI and FAB mass spectrometry showed the compound to be free from

Na<sup>+</sup> and K<sup>+</sup> ions. The <sup>1</sup>H NMR spectrum of the product was very similar to that obtained previously for styryl-15-crown-5 thiophene **XV**, with the expected changes in the ether region ( $\delta$  3.5-4.2) caused by expansion of the crown ether ring.



**Scheme 9** Synthesis of styryl-18-crown-6 thiophene **XVI**

## 2.3 Synthesis of Open-Chain Ether Functionalised (Ter)thiophenes

### 2.3.1 Open-chain terthiophenes

A further series of compounds was synthesised that included a polyether chain in place of the crown ether. The anticipated advantage of this system was that cations would be complexed less strongly, therefore releasing more easily, an attribute that would be important in a real-time sensing application. Compounds of the type depicted in Fig. 2.18 were targeted.

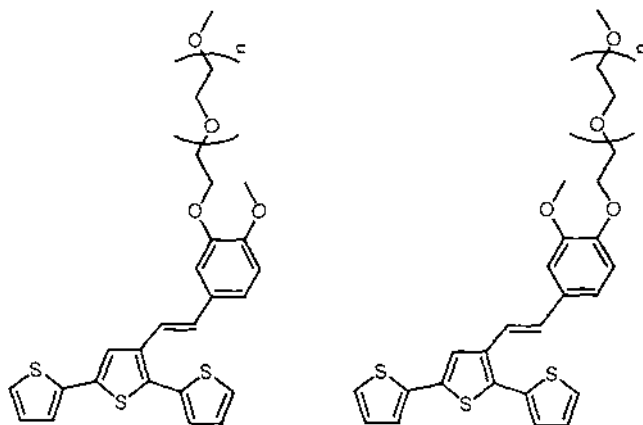


**Figure 2.18** Open-chain polyether styryl-substituted terthiophenes targeted

It was envisaged that these compounds could be synthesised from a reaction between terthiophene phosphonate and a substituted benzaldehyde in the same way that the crown-substituted terthiophenes were formed, as shown in Fig. 2.19.

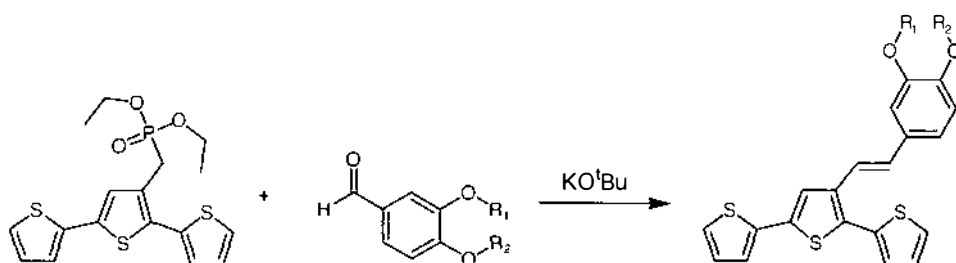
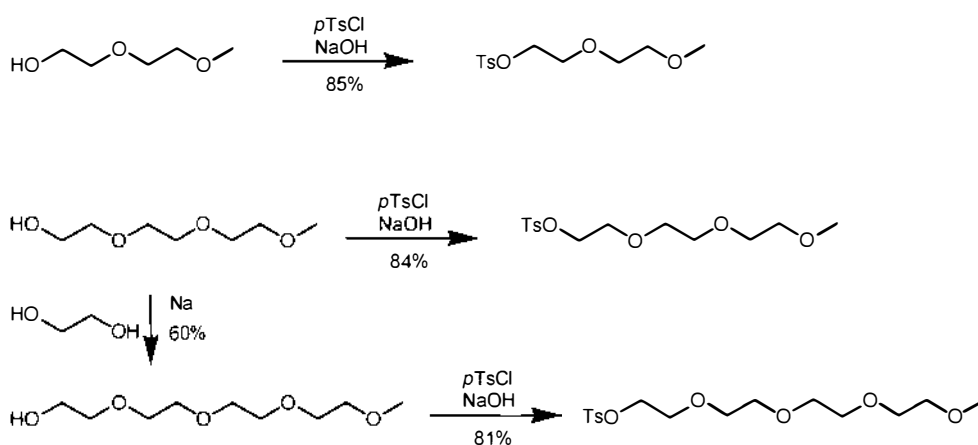


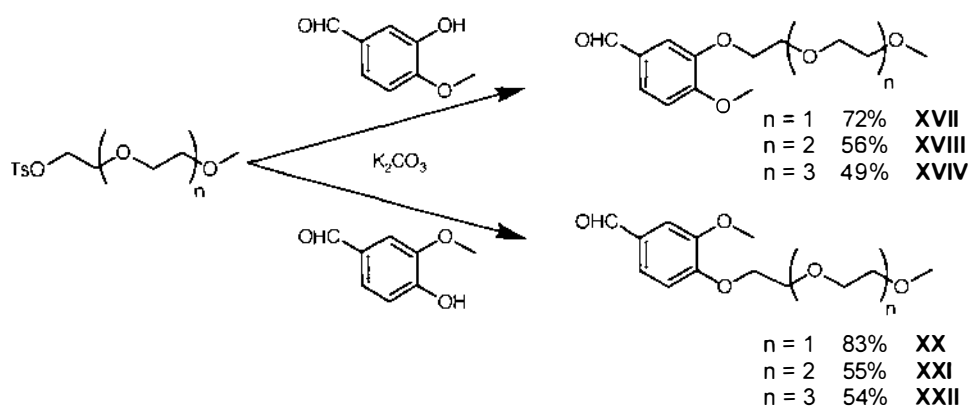
**Figure 2.19** Formation of open-chain ether functionalised terthiophenes

The first step toward making these products was the formation of the polyether-substituted benzaldehydes. These could clearly be made by the reaction of an appropriate tosylated oligo(ethyleneglycol) monomethyl ether together with either isovanillin or vanillin, in a Williamson ether synthesis reaction. A paper by Lauter, Meyer and Wegner<sup>224</sup> details the synthesis of these tosylated polyethers from their glycol counterparts. While both diethylene glycol and triethylene glycol monomethyl ethers are commercially available, any longer chain ethers must themselves be synthesised. The same paper by Lauter *et al.* describes the formation of tetra(ethyleneglycol) monomethyl ether from a Williamson-type etherification reaction between tri(ethyleneglycol) monomethyl ether and ethylene glycol.<sup>224</sup> These reactions are summarized in Scheme 10.



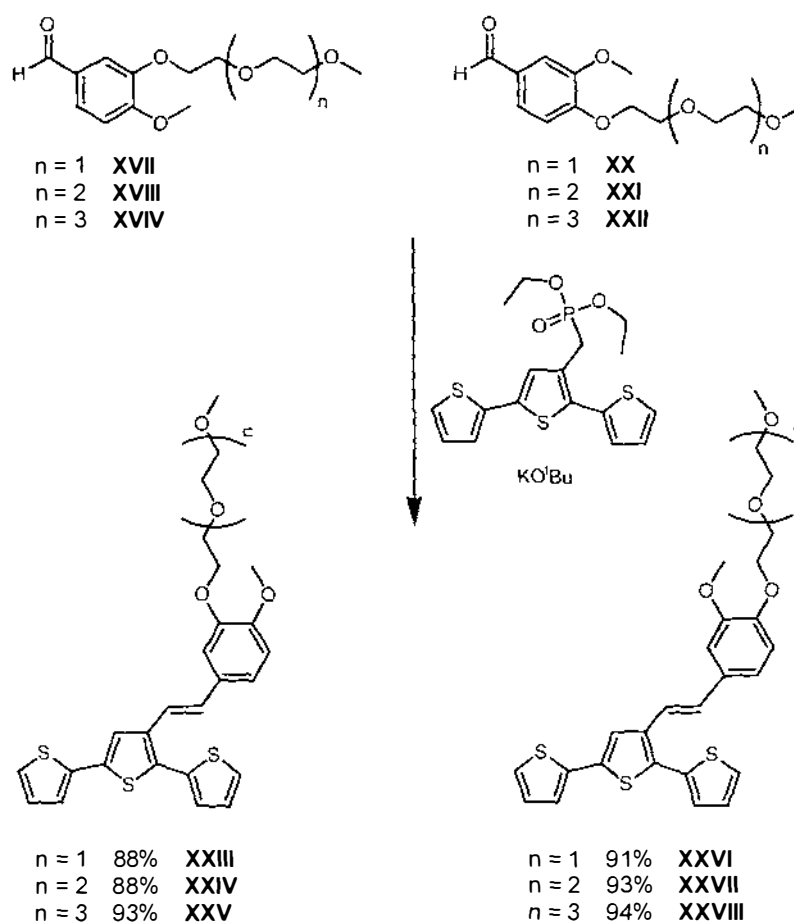
**Scheme 10** Formation of tosylated glycols according to Lauter *et al.*

Once these starting materials had been synthesised, the reactions with vanillin and isovanillin under Williamson conditions were straightforward. Purification by column chromatography led to the polyether-substituted benzaldehyde products **XVII-XXII** (Scheme 11) in 50-80% yield. All of the products were isolated as faintly coloured liquids and characterised by NMR and UV/VIS spectroscopy, and high-resolution mass spectrometry. A typical  $^1\text{H}$  NMR spectrum exhibited, in addition to an aldehyde peak at  $\delta$  9.8, three sets of signals due to aromatic protons in the region  $\delta$  6.9-7.5. Distinct  $^3J$  and  $^4J$  coupling allowed these to be unequivocally assigned. The use of a long-range COSY spectrum assisted in the assignment of the alkoxy signals ( $\delta$  3.3-4.3), while HMQC and HMBC experiments provided the remaining connectivity information necessary to completely assign the  $^{13}\text{C}$  spectrum.



**Scheme 11** Formation of polyether-substituted benzaldehydes **XVII-XXII**

A series of Horner-Emmons reactions between **XVII-XXII** and terthiophene phosphonate were carried out (Scheme 12), utilizing the same conditions employed for the synthesis of styryl-15-crown-5 terthiophene **I**. Allowing the reaction to proceed for 30-60 minutes at room temperature, followed by solvent extraction and silica-gel chromatography yielded the products **XXIII-XXVIII** in excellent 88-94% yields.



**Scheme 12 Horner-Emmons reaction to form open-chain terthiophenes**

The  $^1\text{H}$  NMR spectra of these compounds were very similar to that of styryl-15-crown-5 terthiophene **I**. The spectra obtained for the three isovanillin-derived compounds were identical in the aromatic region ( $\delta$  6.8-7.5), as were the spectra for the three vanillin-derived compounds, only differing as expected in the ether region ( $\delta$  3.3-4.3, Fig. 2.20) due to the differing lengths of the polyether chain attached. The slight differences in chemical shift in the aromatic region between the isovanillin-derived compounds **XXIII-XXV** and their vanillin-derived analogues **XXVI-XXVII** are illustrated in Fig. 2.21.  $^{13}\text{C}$  NMR and 2D NMR experiments (COSY, LR-COSY, HMQC and HMBC) allowed the spectra for all of the products to be completely assigned. The UV/VIS spectra of these compounds were virtually identical to that obtained for **I** and **II**, with  $\lambda_{\text{max}} = 329$  nm. High-resolution mass spectrometry

provided further evidence for the formation of the desired open-chain ether terthiophenes **XXIII-XXVIII**. A fraction containing 1,2-bis([2',2'';5'',2''']terthiophen-3''-yl)ethene (3-15%) was also isolated from each of the reactions in Scheme 12, as described earlier during the formation of styryl-15-crown-5 terthiophene **I** and styryl-18-crown-6 terthiophene **II** (Section 2.2.4)

The structures shown in Scheme 12 can be considered as open-chain equivalents of 12-crown-4, 15-crown-5 and 18-crown-6 when  $n = 1, 2$  or  $3$  respectively.

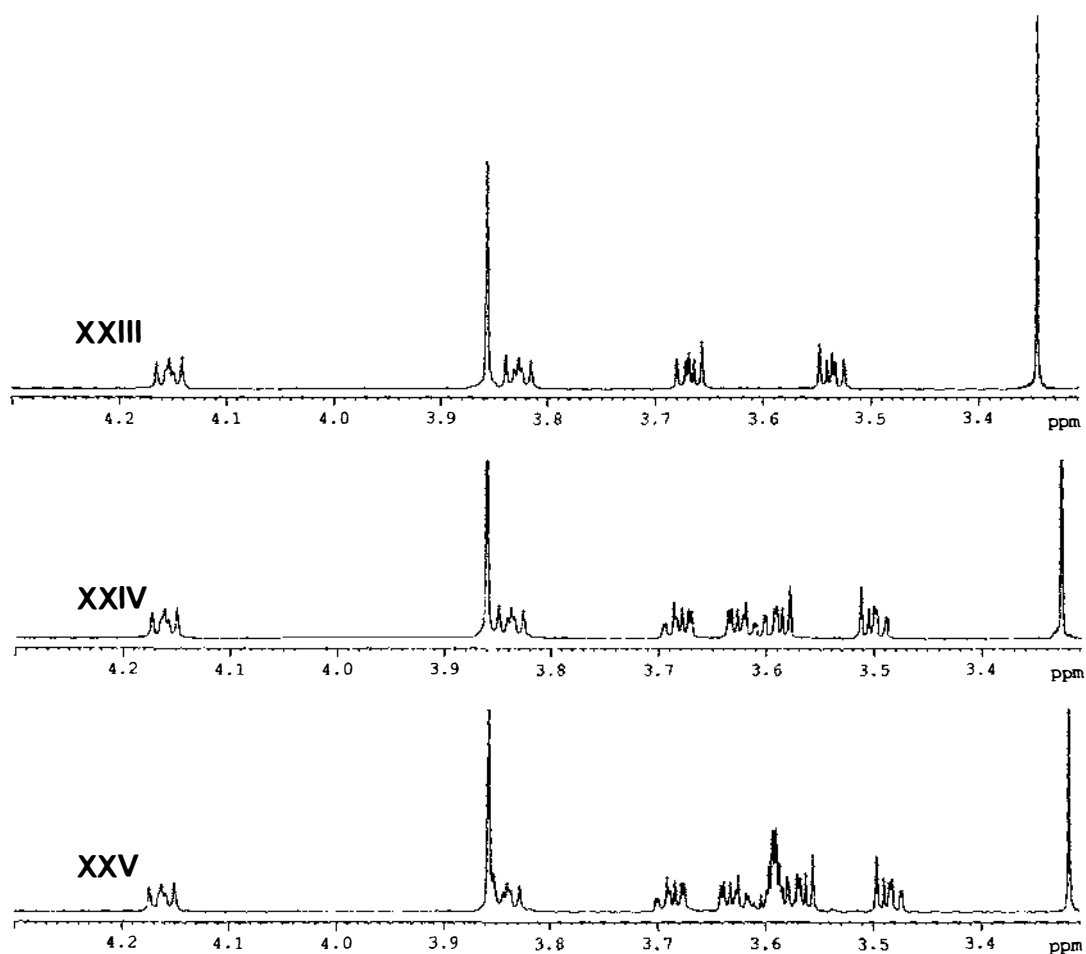


**Figure 2.20** <sup>1</sup>H NMR spectra of open-chain terthiophenes **XXIII-XXV**  
(ether region)

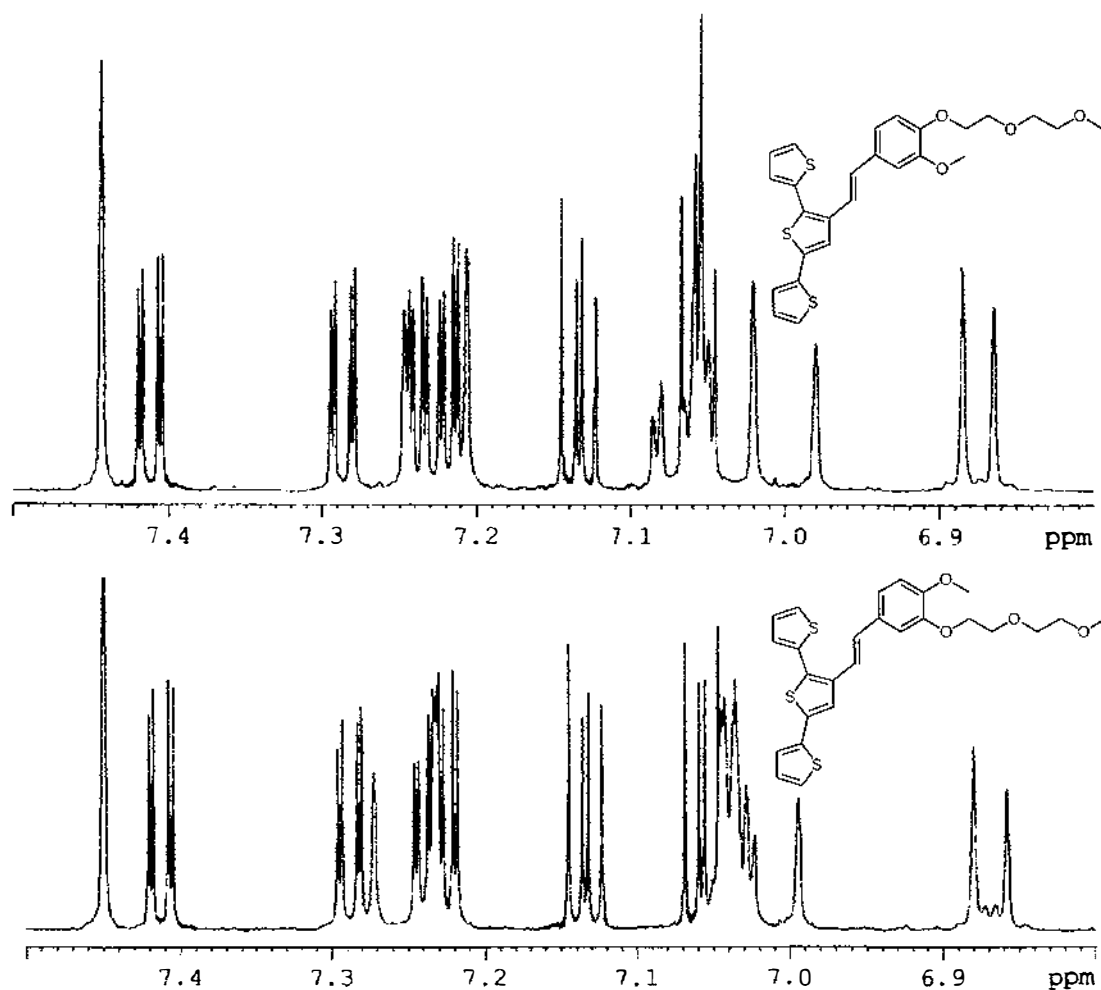
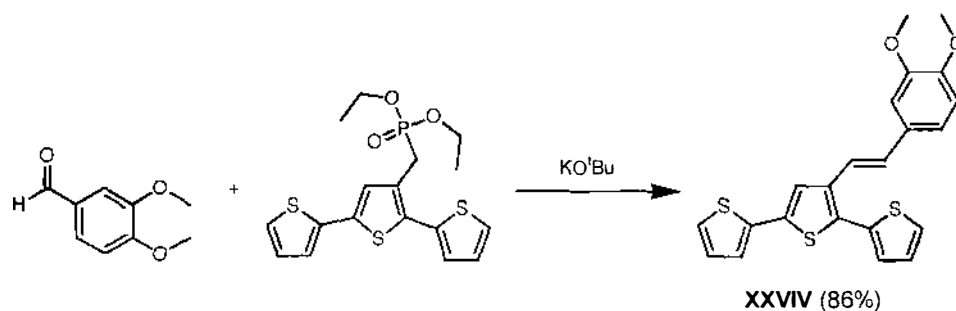


**Figure 2.21 Comparison of aromatic regions in  $^1\text{H}$  NMR spectra of compounds XXIII and XXVI**

An analogous styryl-terthiophene compound that didn't contain a polyether chain (**XXVIV**) was synthesised as a reference (Scheme 13). The cation complexing ability of this monomer was expected to be negligible when compared to the crown and open-chain compounds. It was prepared from a Horner-Emmons reaction between terthiophene phosphonate and 3,4-dimethoxybenzaldehyde in the same way as for the longer chain compounds.  $^1\text{H}$  NMR analysis of the product after purification by silica gel chromatography showed it to consist exclusively of the *trans* isomer.  $^{13}\text{C}$  NMR gave the expected number of signals, which, along with the  $^1\text{H}$  NMR signals, could be confidently assigned after inspection of relevant COSY, HMQC and HMBC data.

The UV/VIS spectrum was identical to that of the other polyether- and crown-substituted terthiophenes, with  $\lambda_{\text{max}} = 329 \text{ nm}$ . Samples analysed by high-resolution mass spectrometry and elemental analysis verified the successful synthesis of monomer **XXIV**.



**Scheme 13** Synthesis of dimethoxystyryl terthiophene

A further two reference compounds, that had been previously synthesised in our laboratories, were included in spectroscopic (Chapter 4) and polymerisation (Chapter 5) studies.<sup>225</sup> The structures of these compounds are illustrated below (Fig. 2.22).

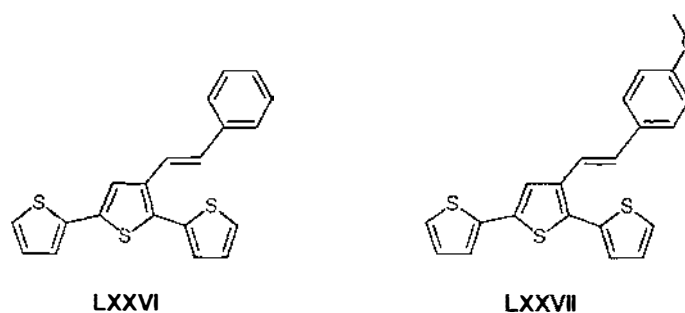
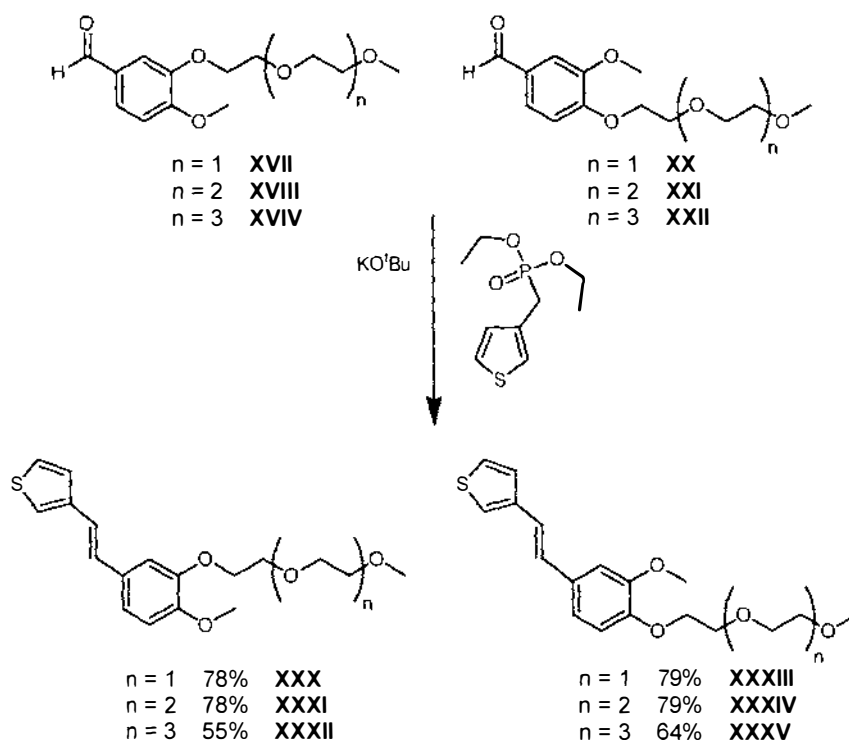


**Figure 2.22** Styryl terthiophene reference compounds

### 2.3.2 Open-chain thiophenes

As the benzaldehyde starting materials and thiophene phosphonate were available from previous work, the thiophene equivalents of compounds **XXIII-XXVIII** were also synthesised (Scheme 14). While it seemed unlikely that these compounds would form homopolymers given literature results<sup>160, 161, 163-166</sup>, they have been shown to be of

use in copolymer systems. In addition, it was anticipated that an investigation into the spectroscopic properties of these compounds would assist in understanding the behaviour of their terthiophene analogues.



#### Scheme 14 Open-chain ether functionalised thiophenes XXX-XXXV

These compounds were formed from a Horner-Emmons reaction between thiophene phosphonate and the polyether-substituted benzaldehydes that had been previously synthesised as described in Scheme 11. Utilising the same conditions employed for the terthiophene analogues ( $\text{KO}^t\text{Bu}$ ,  $\text{CH}_2\text{Cl}_2$ , room temperature, 1 hour) followed by solvent extraction and flash column chromatography yielded the desired products **XXX-XXV** as solids or semi-solids in 55-79% yield. The UV/VIS spectra for all these compounds compared well with those obtained previously for styryl-15-crown-5 thiophene **XV**, with bands at 216, 298 and 318 nm. The  $^1\text{H}$  and  $^{13}\text{C}$  NMR spectra were assigned with the aid of 2D spectra, and compared well with the results for the crown compounds **XV** and **XVI**. As seen for the open-chain terthiophene derivatives **XXIII-XXVIII**, the aromatic region of the spectra remained very similar, while the ethereal region increased in complexity with increasing polyether chain length. As an

example, a fully assigned  $^1\text{H}$  NMR spectrum for compound **XXX** is shown below in Fig. 2.23.

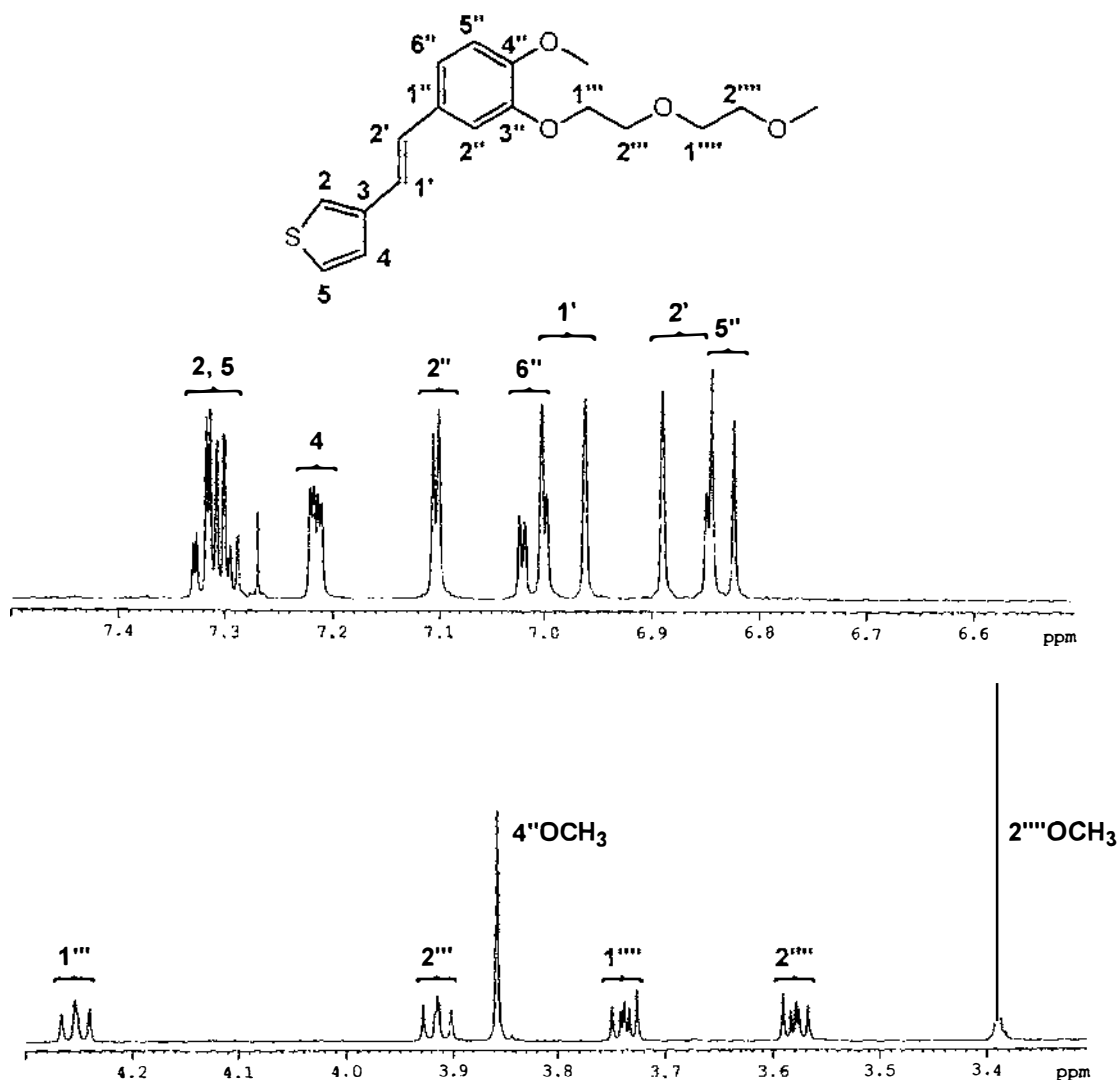
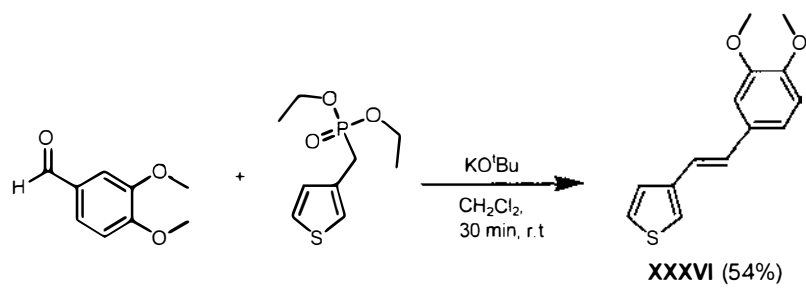


**Figure 2.23**  $^1\text{H}$  NMR assignment for open-chain thiophene **XXX**

In addition, a reference compound lacking a polyether chain was synthesised from thiophene phosphonate and 3,4-dimethoxybenzaldehyde as shown in Scheme 15. This reaction proceeded quickly at room temperature on addition of potassium tert-butoxide, and gave a product that was easily purified by filtering through a plug of silica. LDI mass spectrometry confirmed the presence and purity of the product, which was then fully characterised by  $^1\text{H}$ ,  $^{13}\text{C}$  and 2D NMR experiments, and UV/VIS spectroscopy.



**Scheme 15** Synthesis of dimethoxystyryl thiophene



**3**

**SYNTHESIS**

**OF**

**ETHER**

**FUNCTIONALISED**

**BIS(TER)THIOPHENES**

Extending the methodology developed in the formation of styryl-crown terthiophenes **I** and **II** to make bis-functionalised crowns could lead to cross-linked polymers with interesting properties. In particular, there is potential for an actuation effect on metal binding (Fig. 3.1). Polymers with a high degree of cross-linking also generally have better mechanical properties than those that only polymerise in one direction, and for these reasons the syntheses of bisterthiophene crown ethers were investigated next.

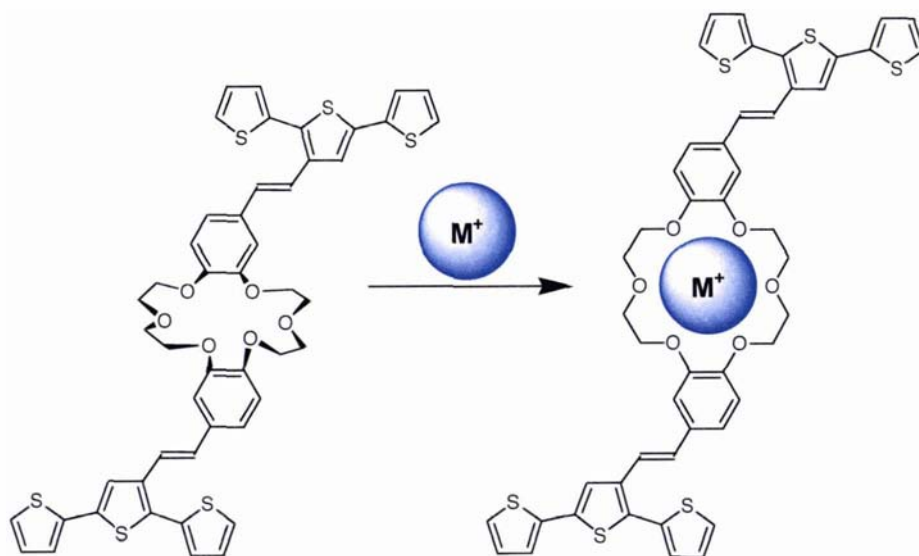
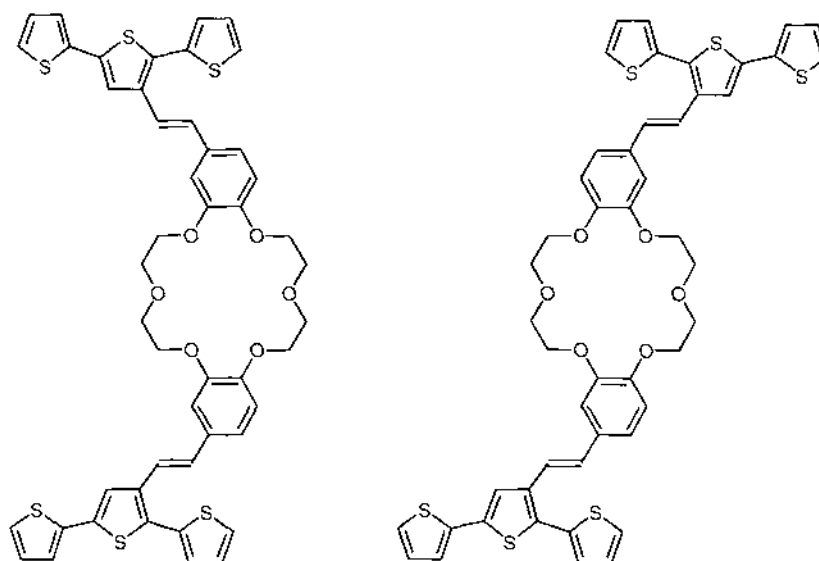


**Figure 3.1** Potential for actuation effect caused by metal complexation

There are two possible isomeric forms of the target 18-crown-6 compound, as shown in Fig. 3.2, that could potentially polymerise quite differently.



*Syn*-bis(styryl terthiophene)-18-crown-6 **XXXVII** *Anti*-bis(styryl terthiophene)-18-crown-6 **XXXVIII**

**Figure 3.2** The two isomeric forms of bis(styryl terthiophene)-18-crown-6

It was anticipated that these compounds could be made by the same Wittig or Horner-Emmons routes that were used to prepare the polyether-substituted terthiophenes discussed in Chapter 2. The starting materials in this case would be the terthiophene phosphonate or aldehyde already utilized in earlier reactions, and two isomeric forms of bis(formylbenzo)-18-crown-6 or the phosphonates/phosphonium salts prepared from these aldehydes. A literature survey was conducted in order to establish how the two isomers of bis(formylbenzo)-18-crown-6 had been previously synthesised and used.

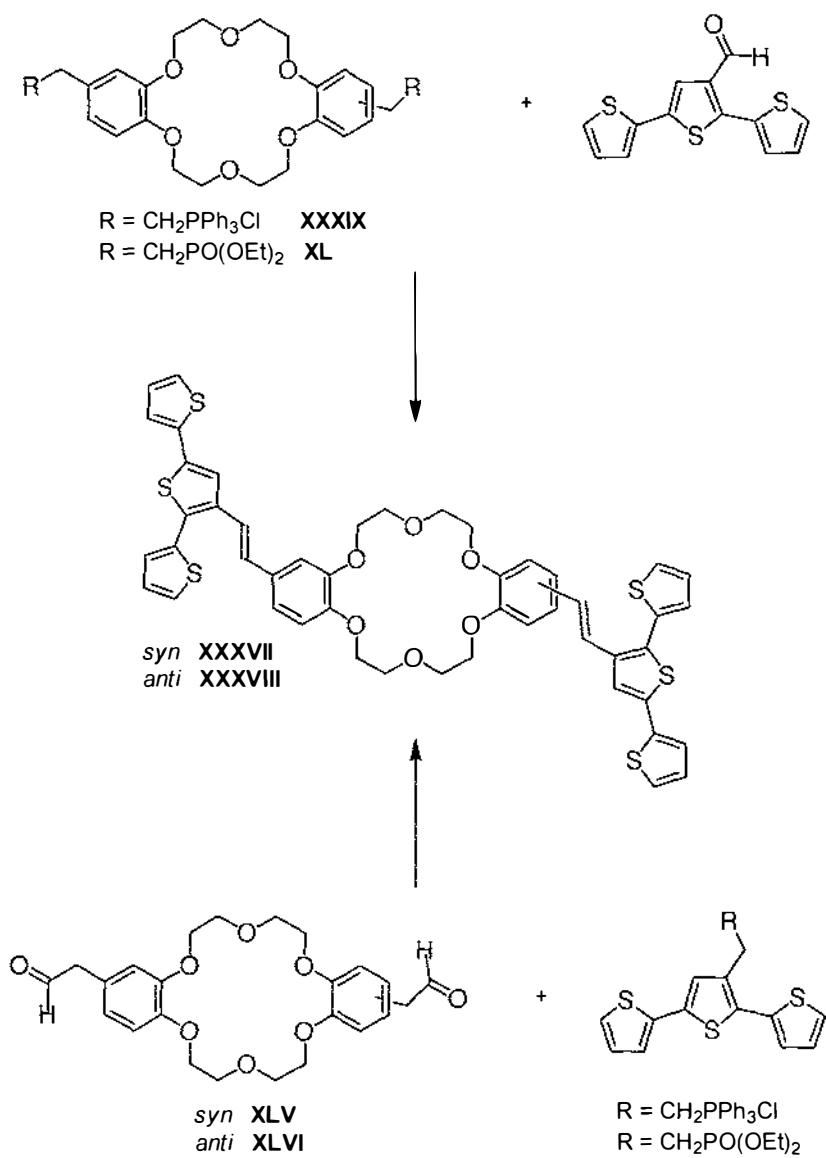
### 3.1 Literature Synthetic Methods

Bis-functionalised dibenzo-crowns have been approached in several different ways in the literature. Wada *et al.*<sup>177</sup> synthesised bis(formylbenzo)-18-crown-6 as an isomeric mixture utilizing the Smith modification of the Duff reaction (hexamethylenetetramine and methanesulfonic or trifluoroacetic acid), but conveniently ignore the issue of isomer formation, naming the product as 4',4''-diformyl-dibenzo-18-crown-6. More recently Ge and co-workers repeated this synthesis, using the bis(formylbenzo)-18-crown-6 produced as their starting material to make crown ethers substituted with both benzothiazolium styryl dye and fulleropyrrolidine moieties.<sup>226-228</sup> While in all three of their papers they consistently represent the product of the Wada formylation as the *syn* isomer only, in two of the papers they represent their final product as being an *anti* substituted dibenzo-18-crown-6. As the intermediate fulleropyrrolidine substituted crown is obtained in only 25% yield, and is purified by column chromatography, it is possible that the *syn* and *anti* products are separated during this step. However, it seems unlikely that only one isomer would be reported if both were successfully synthesised and separated. In addition, the inconsistencies between the three publications, and the low resolution of the majority of the NMR data (200 – 300 MHz), make it seem more probable that they were not aware of the existence of the two isomers. Bourgeois *et al.* did recognize that the Wada synthesis produces a mixture of isomers.<sup>229</sup> In their work they begin with the mixture, further modifying the product by converting the aldehyde functionalities to malonates, then using modified Bingel reaction conditions (I<sub>2</sub>, DBU) to incorporate a [60]fullerene moiety. This allowed the *syn* and *anti* isomers to be separated by column chromatography.<sup>230</sup> A bis(nitrophenyl)-18-crown-6 compound synthesised by Shchori<sup>14</sup> could be separated into the two isomeric forms based on solubility. Parish *et al.* looked at diacylating dibenzo-crowns and found that in some cases the isomers did not co-crystallise and could be separated.<sup>231</sup> In other research, compounds were used as isomeric mixtures with no attempt at separation.<sup>179, 232, 233</sup> Selectively synthesising either the *syn* or the *anti* isomer is another option, and this was the approach that Bourgeois *et al.* took in their synthesis of *anti*-bis(formylbenzo)-18-crown-6.<sup>230</sup>

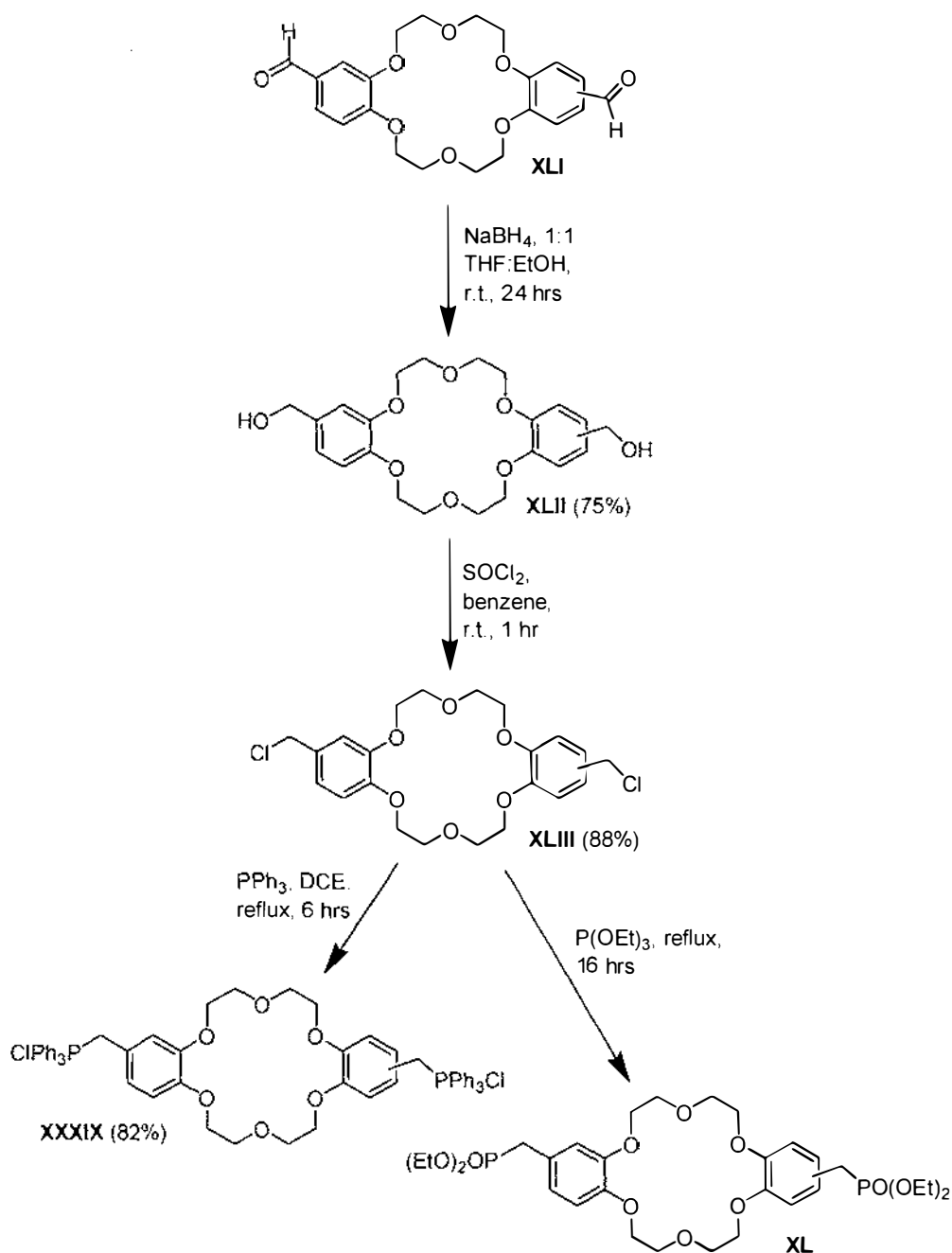
## 3.2 Synthesis of Bis(styryl (Ter)thiophene) Crowns

### 3.2.1 Synthesis of crown bis(phosphonium salt) and bis(phosphonate)

As with the crown linked terthiophenes **I** and **II**, the bis-substituted crowns **XXXVII** and **XXXVIII** could potentially be formed by Wittig (or Horner-Emmons) reactions between a crown phosphonium salt (or phosphonate) and [2,2';5',2'']terthiophene-3'-carbaldehyde, or from a bis-formylated crown and terthiophene phosphonium salt (or phosphonate) as shown in Scheme 16. Due to the availability at the beginning of this work of [2,2';5',2'']terthiophene-3'-carbaldehyde, the initial target was the crown bis(phosphonium salt) **XXIX**. A *syn/anti* isomeric mixture was investigated first to develop the methodology.



**Scheme 16** Alternative routes toward target crown linked bis(styryl terthiophene)s **XXXVII** and **XXXVIII**



**Scheme 17** Formation of *syn/anti* isomeric mixture of crown bis(phosphonium salt)s **XXXIX** and bis(phosphonate)s **XL**

The isomeric mixture of 18-crown-6 bisphosphonium salt was synthesised as illustrated in Scheme 17. Dibenzo-18-crown-6 was formylated using the Smith modification of the Duff reaction according to the method of Wada *et al.*<sup>177</sup> As established in the literature survey, this gave a 1:1 isomeric mixture of the *syn* and

*anti* forms. While only one aldehyde peak was visible by  $^1\text{H}$  NMR at 270 MHz, the same sample of **XLI** run at 400 MHz showed two aldehyde signals just 0.001 ppm apart. Duplicity of one of the aromatic signals was also observed at 400 MHz, where two aromatic doublets ( $^3J = 8.2$  Hz) were offset by 0.004 ppm. Thus it is clear, although not necessarily intuitive, that while the two isomers of bis(formylbenzo)-18-crown-6 are virtually identical, there is a very slight difference that can only be observed by NMR at high resolution.

The dialdehydes were then reduced to the dialcohols **XLII** using sodium borohydride under the same conditions used to reduce formylbenzo-15-crown-5 **V**. The changes in the  $^1\text{H}$  NMR spectrum of the reduction product were similar to those seen for the corresponding crown alcohols **VII** and **VIII**. A new signal appearing at  $\delta$  4.6 was attributed to the two methylene groups. A broad peak at  $\delta$  2.2 that reduced in size after a  $\text{D}_2\text{O}$  exchange experiment was assigned to the hydroxy protons. In addition, the aromatic protons shifted such that they were now overlapping as observed previously for **VII** and **VIII**.

Dialcohols **XLII** were then chlorinated with thionyl chloride, again using the same conditions that were successful in chlorinating the alcohols **VII** and **VIII**. While there were no large changes in the  $^1\text{H}$  NMR spectrum, there was a clear upfield shift in the position of the  $^{13}\text{C}$  methylene signal from  $\delta$  65 to  $\delta$  47 caused by the change in its chemical environment. High-resolution mass spectrometry provided additional evidence for the formation of the desired compounds **XLIII**.

The chloromethyl isomers **XLIII** were refluxed in toluene with an excess of triphenylphosphine. This yielded a mixture of mono- and bisphosphonium salts, presumably due to the limited solubility of the mono-phosphonium salt in toluene. This was overcome by replacing the toluene with 1,2-dichloroethane and continuing the reaction at reflux, yielding an isomeric mixture of the desired crown bis(phosphonium salt)s **XXXIX**. A careful examination of the  $^1\text{H}$  NMR spectrum showed that no starting material remained, as there was no signal at  $\delta$  4.5. Instead, the methylene signal was observed downfield at  $\delta$  5.2, and was split by the phosphorus atom as described earlier for benzo-15-crown-5 phosphonium salt **III**. A

<sup>31</sup>P NMR spectrum of the product showed a signal at  $\delta$  24, consistent with the results obtained for the mono-phosphonium salts **III** and **IV**. The UV spectrum for **XXXIX** was also similar to that obtained earlier, consisting of bands in the same position (270 and 276 nm) with extinction coefficients approximately double that seen for **III** and **IV**. High-resolution mass spectrometry was also consistent with these results.

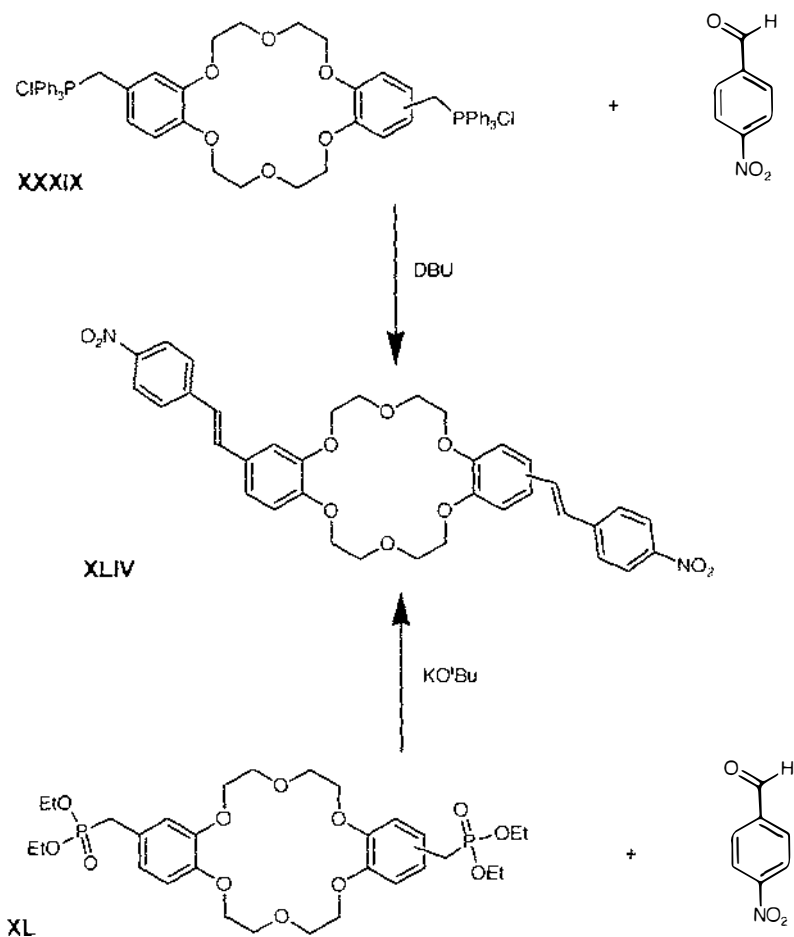
Bis(phosphonate)s **XL** were synthesised from bis(chloromethylbenzo)-18-crown-6 **XLIII**, by the Arbuzov reaction.<sup>216</sup> As in the case of benzo-15-crown-5 phosphonate **XIII** and benzo-18-crown-6 phosphonate **XIV**, bis(phosphonate)s **XL** were used as a crude product containing some high boiling point impurities. High resolution mass spectrometry provided evidence that the phosphonates were the major products.

### 3.2.2 Wittig/Horner-Emmons reactions using mixed bis(phosphonium salt)s and bis(phosphonate)s

The Wittig reaction between bis(phosphonium salt)s **XXXIX** and 4-nitrobenzaldehyde (Scheme 18) yielded a *syn/anti* isomeric mixture of the alkene product **XLIV** with a *cis:trans* ratio of approximately 7:6 as determined by <sup>1</sup>H NMR spectroscopy. While isomerisation with I<sub>2</sub> was successful in converting this to a pure *trans* product, the Na<sub>2</sub>S<sub>2</sub>O<sub>3</sub> wash used to remove excess iodine caused extensive emulsification and the formation of some insoluble orange material, presumably due to the complexation of sodium ions by the crown ether. To try to improve the yield of the *trans* isomers, the reaction was repeated at reflux in 1,2-dichloroethane. The isomeric ratio resulting from this reaction was approximately 6:8 *cis:trans*. Column chromatography of the crude product failed to remove triphenylphosphine oxide.

A Horner-Emmons reaction between the 18-crown-6 bis(phosphonate)s **XL** and 4-nitrobenzaldehyde (Scheme 18) with KO<sup>t</sup>Bu as base, yielded three yellow products after column chromatography. Two of these products had the same R<sub>f</sub> when checked by TLC (5% MeOH/CH<sub>2</sub>Cl<sub>2</sub>) and identical NMR spectra that showed similar features to that obtained previously for nitrostyryl crowns **XI** and **XII**. High-resolution mass spectrometry results were consistent with the *syn* and *anti* forms of the expected products **XLIV**, however the yields of these products were low (2% and 7%). The third product (7% yield) appeared to result from a single Horner-Emmons reaction between nitrobenzaldehyde and the dibenzo-18-crown-6 mono-phosphonates. It seems likely that the original formylation reaction was incomplete, and that a small amount of mono-formylated dibenzo-18-crown-6 had been carried through the intervening steps. This would result in contamination of the bisphosphonates **XL** with some mono-phosphonate, which could not be removed due to the high boiling points of the compounds. The end result of the incomplete formylation would be the observed mono-nitrated product.

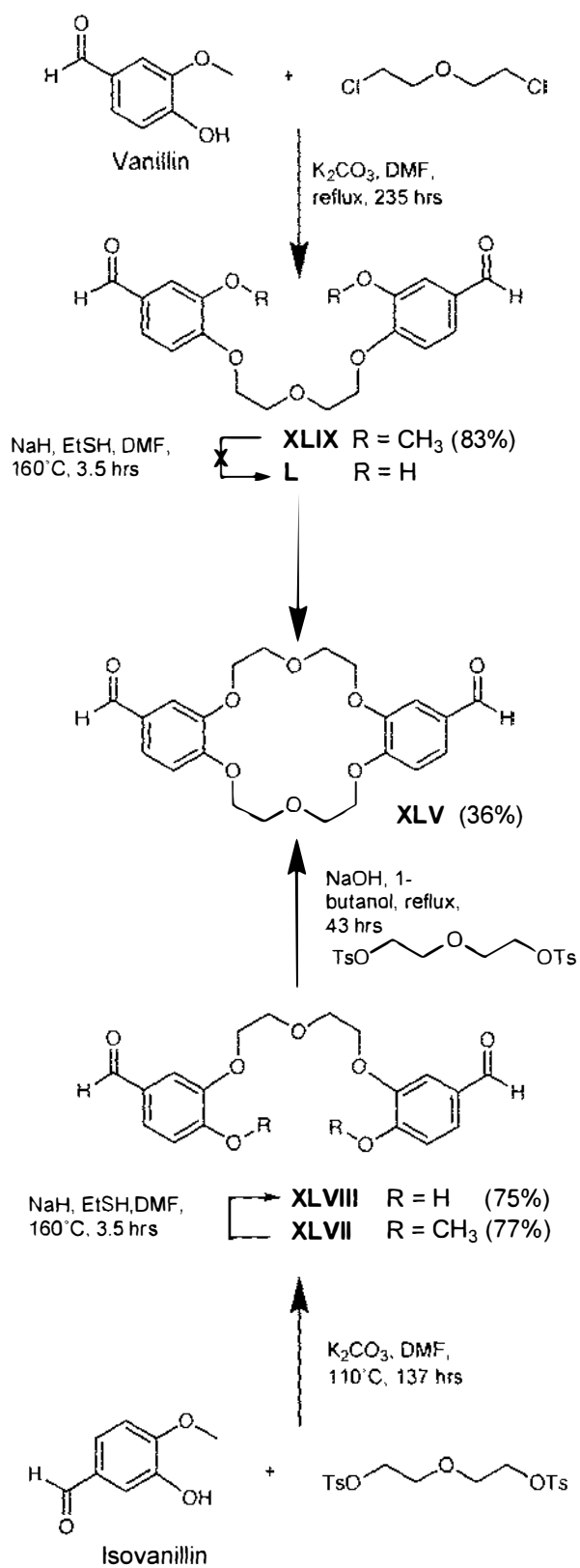
Given the low yields obtained on reaction of the bis(phosphonate)s **XL** with the activated aldehyde 4-nitrobenzaldehyde, it seemed unlikely that better yields would be obtained with [2,2';5',2'']terthiophene-3'-carbaldehyde. In addition, it was unclear whether the two isomeric products resulting from the Horner-Emmons reaction between bis(phosphonate)s **XL** and [2,2';5',2'']terthiophene-3'-carbaldehyde would be separable by chromatography. For these reasons it was decided to selectively synthesise the *syn* and *anti* forms of bis(formylbenzo)-18-crown-6, starting with the symmetrical *syn* isomer.



**Scheme 18** Wittig-type reactions between disubstituted crowns XXXIX-XL and 4-nitrobenzaldehyde

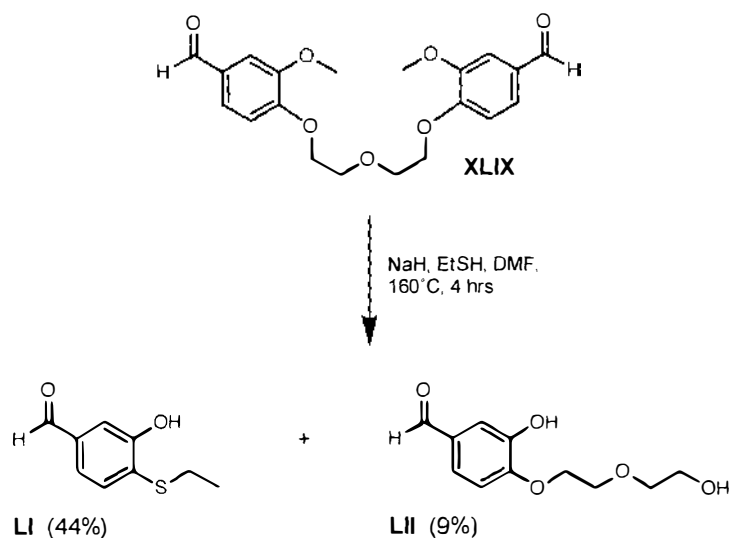
### 3.2.3 Synthesis of *syn*-bis(formylbenzo)-18-crown-6 XLV

In order to synthesise the target *syn*-bis(styryl terthiophene)-18-crown-6 **XXXVII**, it was necessary to first synthesise the corresponding starting material *syn*-bis(formylbenzo)-18-crown-6 **XLV**. As it was not possible to separate a mixture of the *syn* and *anti* dialdehydes,<sup>229</sup> selective synthesis was necessary. Scheme 19 shows two alternative routes to the target molecule **XLV**, starting from the inexpensive monomethyl protected dihydroxy benzaldehydes vanillin and isovanillin. Both routes were investigated in order to assess if one had a particular advantage over the other.



**Scheme 19** Alternative routes toward *syn*-bis(formylbenzo)-18-crown-6 XLV

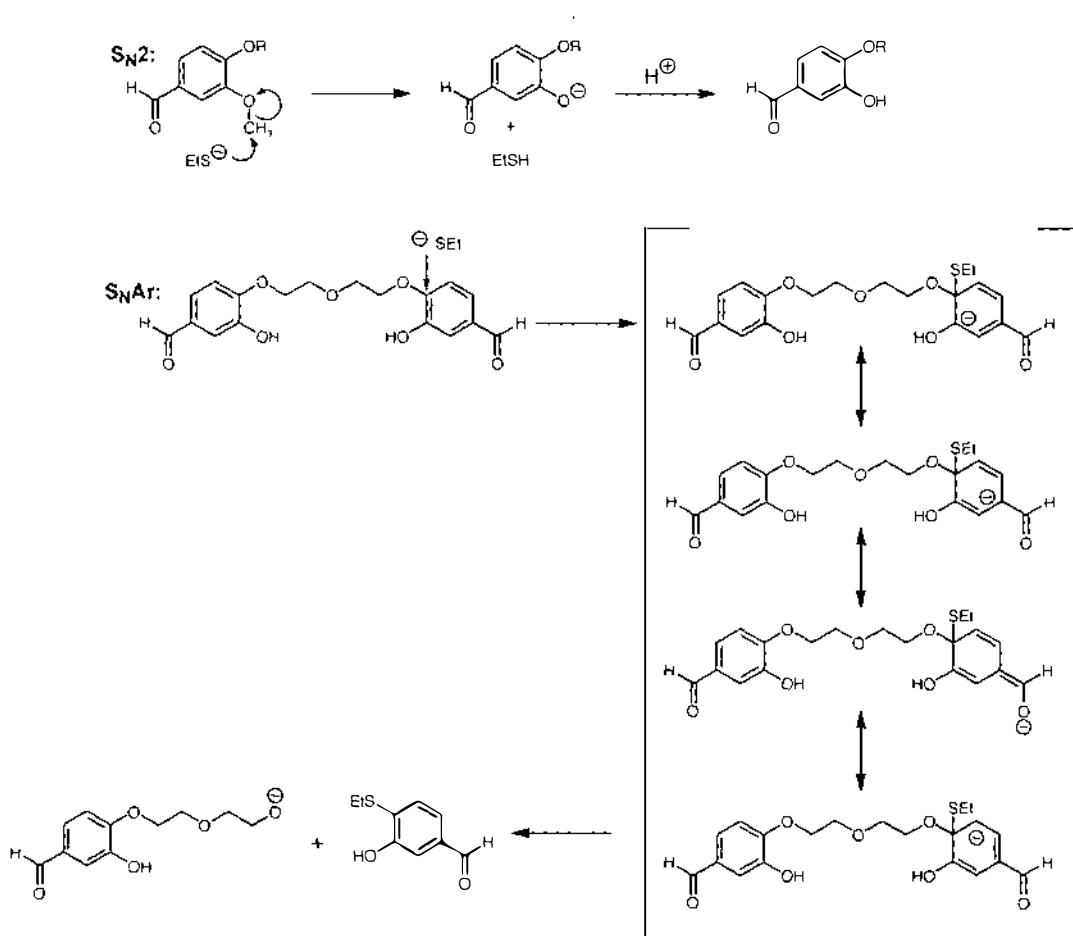
Starting with vanillin, the methoxy intermediate 1,5-bis(2'-methoxy-4'-formylphenoxy)-3-oxapentane **XLIX** was produced in high yield by reaction with dichloro diethyl ether according to the method of Tuncer and Erk.<sup>234</sup> The demethylation necessary to form the hydroxy intermediate **L** was unsuccessful using ethanethiol and sodium hydride.<sup>235, 236</sup> Instead of the desired product, two lower molecular weight materials were isolated from the crude reaction mixture using column chromatography. Careful examination of the <sup>1</sup>H NMR spectra for these compounds showed that one contained both a benzaldehyde moiety and a polyether chain. This product was identified as 3-hydroxy-4-[2-(2-hydroxyethoxy)ethoxy]-benzaldehyde **LII** (Scheme 20). The remaining product displayed <sup>1</sup>H NMR signals typical of an ethyl group, in addition to a benzaldehyde functionality, and was identified as 4-ethylsulfanyl-3-hydroxybenzaldehyde **LI** (Scheme 20). High-resolution mass spectrometry provided additional evidence for the formation of these compounds.



**Scheme 20** Products formed from attempted demethylation of 1,5-bis(2'-methoxy-4'-formylphenoxy)-3-oxapentane **XLIX**

It appeared that two reactions occurred during the attempted demethylation. The desired demethylation reaction is an S<sub>N</sub>2 reaction consisting of nucleophilic attack by the thioethoxide ion at the alkyl carbon, with the associated displacement of a substituted aryloxy ion (Scheme 21). However, in aryl methyl ethers containing strong electron-withdrawing substituents, substitution at the methoxy-bearing aromatic carbon atom has also been observed.<sup>235, 236</sup> In this case, the Meisenheimer

complex formed by the  $S_NAr$  addition of the thioethoxide moiety to the remaining alkoxy-bearing aromatic carbon atom would be resonance stabilized by the carbonyl group. Subsequent elimination of the substituted alkoxide ion would allow the isolation of 4-ethylsulfanyl-3-hydroxy-benzaldehyde **LI** and 3-hydroxy-4-[2-(2-hydroxy-ethoxy)-ethoxy]-benzaldehyde **LII** after an acidic work-up, as was observed (Scheme 21). Although lowering of the reaction temperature to 60°C led to no reaction, it is possible that an intermediate temperature might exist where only the desired  $S_N2$  reaction can proceed.



**Scheme 21**  $S_N2$  and  $S_NAr$  reactions between the thioethoxide ion and a substituted benzaldehyde

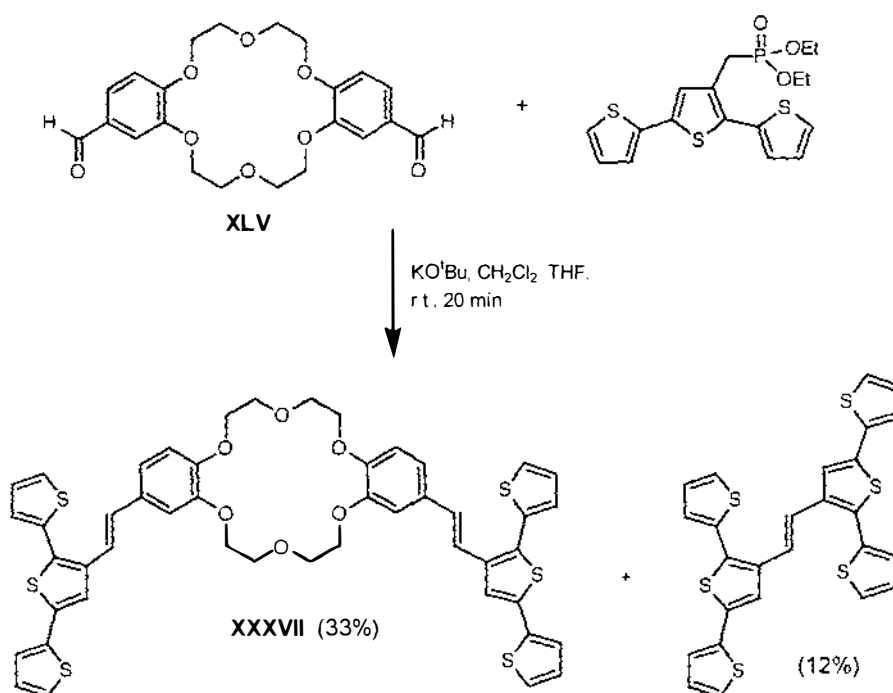
Attempted demethylations of **XLIX** using boron trichloride and boron tribromide<sup>237</sup> were also ineffective in producing the desired dialcohol **L**.

Consequently, the alternative approach to **XLV**, starting from isovanillin, was explored (Scheme 19). Diethylene glycol ditosylate was synthesised according to the method of Ouchi *et al.*<sup>238</sup> and then reacted with isovanillin using the method recently published by Kumar and Mashraqui<sup>239</sup> to synthesise 1,5-bis(2'-methoxy-5'-formylphenoxy)-3-oxapentane **XLVII**. The methoxy intermediate **XLVII** was now able to be demethylated using ethanethiol and sodium hydride<sup>235, 236</sup> to yield the required 1,5-bis(2'-hydroxy-5'-formylphenoxy)-3-oxapentane **XLVIII** in an excellent 75% yield. In this case, aromatic substitution by sulphur is not favoured, since the required Meisenheimer complex cannot be resonance stabilized by the carbonyl group. The demethylation was confirmed by the lack of the distinctive methoxy peak in the <sup>1</sup>H NMR ( $\delta$  3.89) and <sup>13</sup>C NMR ( $\delta$  56.0) spectra, while the ethereal, aromatic and aldehydic regions remained essentially the same. The UV/VIS spectrum of the hydroxy product was also similar to that of the methoxy starting material, with only minor changes to peak positions and intensities. High-resolution mass spectrometry confirmed the successful synthesis of compound **XLVIII**.

The formation of the target compound *syn*-bis(formylbenzo)-18-crown-6 **XLV** from the dialcohol **XLVIII** was accomplished using standard ether formation conditions, in a reasonable 36% yield. The <sup>1</sup>H NMR obtained for this compound was similar to that obtained for the isomeric mixture **XLI**. However, none of the duplication of aldehyde or aromatic signals discussed in Section 3.2.1 was evident here due to the isomerically pure nature of the product. Samples analysed by microanalysis and high-resolution mass spectrometry provided additional evidence for the production of *syn*-bis(formylbenzo)-18-crown-6 **XLV**.

### 3.2.4 Horner-Emmons reaction using *syn*-bis(formylbenzo)-18-crown-6

As terthiophene phosphonate had recently been synthesised in our laboratory, it seemed logical to react this directly with *syn*-bis(formylbenzo)-18-crown-6 **XLV** in a Horner-Emmons reaction as shown in Scheme 22.



**Scheme 22** Horner-Emmons reaction between dialdehyde **XLV** and terthiophene phosphonate

This reaction was carried out under the same conditions used to form styryl terthiophenes **I** and **II**. Analysis of the crude product by MALDI-MS revealed three species that corresponded to the desired product **XXXVII** ( $m/e = 904.1$ ), its potassium salt ( $m/e = 943.1$ ), and a product with a smaller molecular mass ( $m/e = 520.0$ ), that still appeared from the sulphur isomer ratios to contain six thiophene units. This by-product was identified as 1,2-bis([2',2'';5'',2''']terthiophen-3''-yl)ethene from a comparison of its <sup>1</sup>H NMR spectrum with that of a previously

characterised sample.<sup>212</sup> It is assumed that this by-product was formed in the same way as seen earlier for other Horner-Emmons reactions utilising terthiophene phosphonate (Sections 2.2.4 and 2.3.1). While column chromatography allowed this by-product to be isolated, it also appeared to lead to the formation of the sodium salt of **XXXVII**, giving a mixture of **XXXVII** and its sodium and potassium salts, as evidenced by MALDI-MS. It is not clear whether the ion-free product was actually present, or whether the appearance of this species was due to fragmentation during the MALDI-MS process. The eluted product mixture was insoluble in common solvents, and further characterization proved difficult. Numerous attempts were made to remove the metal ions by water and acid washing, but these proved futile possibly due to either the complexes strength or its insolubility (Fig. 3.3). Attempts were made to solubilise the product by introducing alkali metal cations with large organic counterions (*eg.* NaBPh<sub>4</sub>, NaPF<sub>6</sub>), however these were also unsuccessful. While these results are unusual, the low solubility of the product meant that it was of little value for polymerisation, and thus no further use was made of compound **XXVII**.

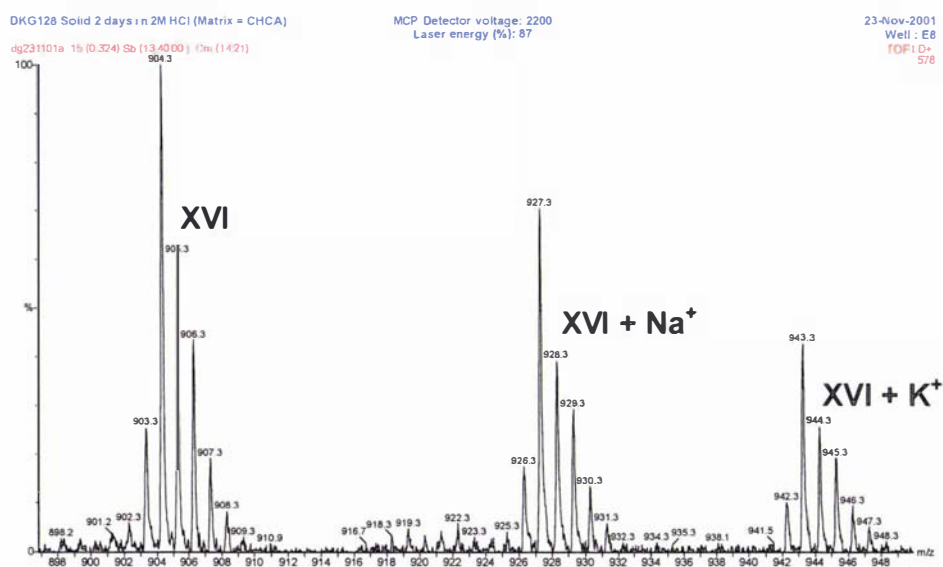


**Figure 3.3 MALDI-MS of *syn*-bis(styryl terthiophene)-18-crown-6 **XVI** after acid wash**

### 3.2.5 Synthesis of *anti*-bis(formylbenzo)-18-crown-6 XLVI

As in the case of *syn*-bis(formylbenzo)-18-crown-6 **XLV**, *anti*-bis(formylbenzo)-18-crown-6 **XLVI** can also be approached starting with either vanillin or isovanillin. This is illustrated in Scheme 23.

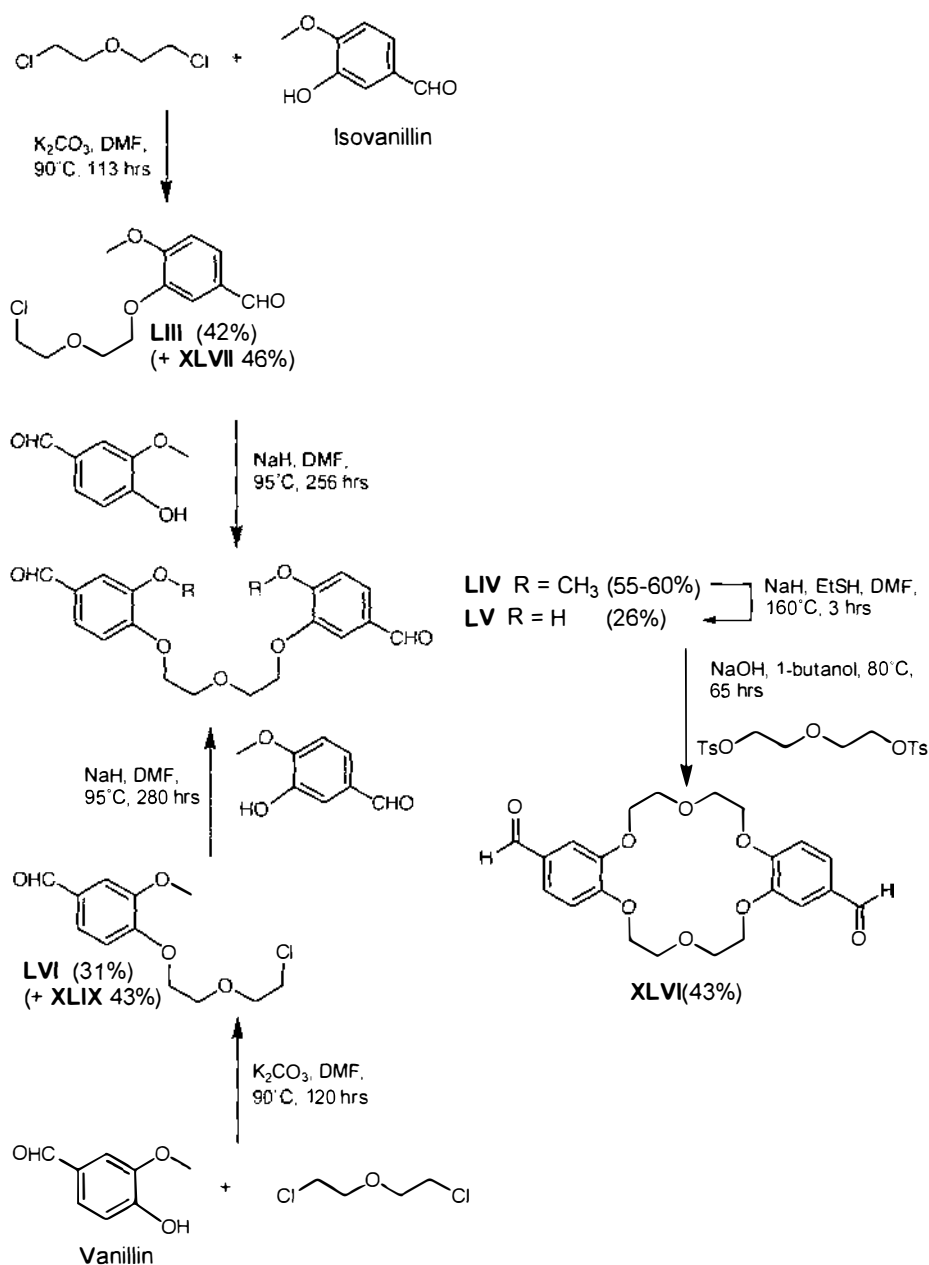
3-[2-(2-chloro-ethoxy)-ethoxy]-4-methoxy-benzaldehyde **LIII** was formed by the reaction of isovanillin and 2-chloroethyl ether. Two products were isolated from the reaction mixture by column chromatography, namely the desired product **LIII** (42%), and a substantial amount of **XLVII** (46%) resulting from the reaction of two molecules of isovanillin with one molecule of 2-chloroethyl ether. While the aromatic region of the  $^1\text{H}$  NMR spectrum obtained for **LIII** was identical to that previously observed for **XLVII**, the ethereal region of the spectrum was quite different due to the presence of the chlorine atom. This structural difference was also clearly visible in the  $^{13}\text{C}$  NMR spectrum of **LIII**, where the signal for the carbon atom next to the chlorine atom ( $\delta$  42.5) appeared in an area that was devoid of signals in the corresponding **XLVII**  $^{13}\text{C}$  NMR spectrum. The presence of the chlorine atom was apparent in the high-resolution mass spectrum obtained for **LIII**, with a typical  $M + 2$  peak of approximately 33% intensity due to the inclusion of the  $^{37}\text{Cl}$  isotope. The UV/VIS spectrum obtained was typical of those seen for the other dialkoxy-substituted benzaldehydes previously synthesised.

The chlorinated intermediate **LIII** was then reacted with vanillin under the same conditions used to form **XLVII** and **XLIX** (Scheme 19), yielding 1-(2'-methoxy-4'-formylphenoxy)-5-(2''-methoxy-5''-formylphenoxy)-3-oxapentane **LIV**. While the  $^1\text{H}$  NMR spectrum for this compound had the same features as the spectra previously obtained for **XLVII** and **XLIX**, each signal was duplicated due to the slight differences between the two benzene rings. A signal was observed for every carbon atom in the  $^{13}\text{C}$  NMR spectrum, in contrast to **XLVII** and **XLIX** where the symmetry of the molecule meant that there were only half as many signals as there were carbon

atoms in the molecule. Extra structural information obtained from 2-D experiments (LR-COSY, HMQC and HMBC) meant that the NMR data could be completely assigned. Elemental analysis, high-resolution mass spectrometry and UV/VIS spectroscopy all provided data consistent with the structure of **LIV**. It is important to note that this product could also been obtained using vanillin as the starting material, and this route was also investigated.

An analogous reaction between vanillin and 2-chloroethyl ether gave 4-[2-(2-chloroethoxy)-ethoxy]-3-methoxy-benzaldehyde **LVI** (31%) and a large amount of **XLIX** (43%) resulting from the reaction of two molecules of vanillin with one molecule of 2-chloroethyl ether (Scheme 23). The  $^1\text{H}$  and  $^{13}\text{C}$  NMR spectra obtained for **LVI** were very similar to those seen previously for **LIII**, with slight changes in chemical shift. The UV/VIS spectrum was also very similar, and the mass spectrometry data again clearly showed the presence of chlorine. Elemental analysis gave further evidence for the successful synthesis of **LVI**.

**LVI** was in turn reacted with isovanillin to give 1-(2'-methoxy-4'-formylphenoxy)-5-(2''-methoxy-5''-formylphenoxy)-3-oxapentane **LIV** (Scheme 22). The spectroscopic and physical properties of **LIV** produced *via* the two different synthetic routes were identical.



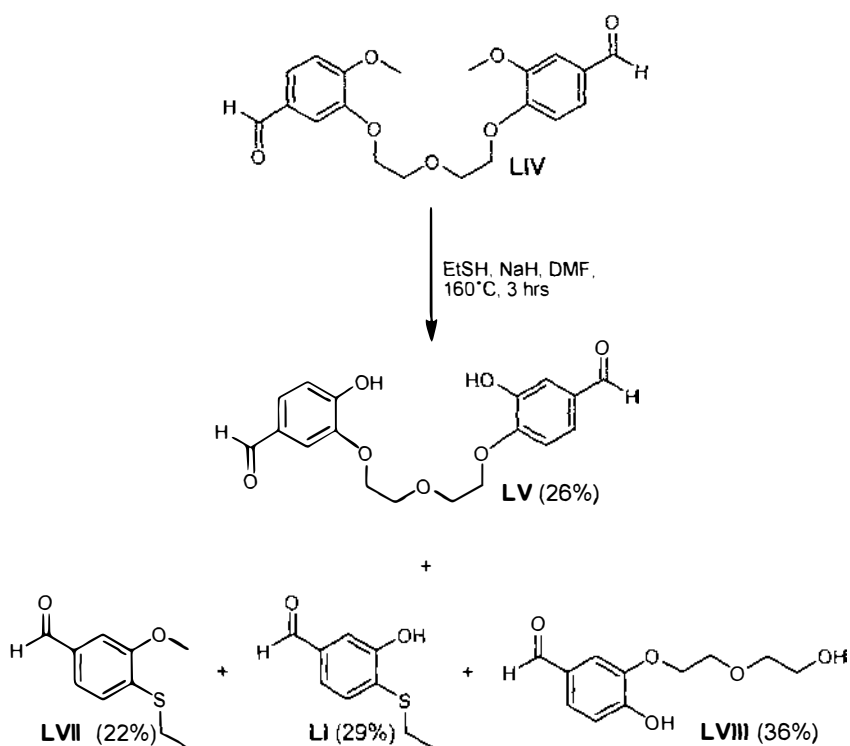
**Scheme 23** Formation of *anti*-bis(formylbenzo)-18-crown-6 **XLVI**

With the successful synthesis of **LIV**, the demethylation was explored. Reaction of **LIV** with ethanethiol and sodium hydride<sup>235, 236</sup> under the conditions previously used for 1,5-bis(2'-methoxy-5'-formylphenoxy)-3-oxapentane **XLVII**, yielded 4-ethylsulfanyl-3-methoxy-benzaldehyde **LVII**, 4-ethylsulfanyl-3-hydroxy-benzaldehyde **LI** and 4-hydroxy-3-[2-(2-hydroxy-ethoxy)-ethoxy]-benzaldehyde **LVIII** in addition to the desired product 1-(2'-hydroxy-4'-formylphenoxy)-5-(2'-

hydroxy-5''-formylphenoxy)-3-oxapentane **LV** (Scheme 24). The by-products appear to have formed from nucleophilic attack of the thioethoxide ion on the methoxy-bearing aromatic carbon as seen during the demethylation of **XLIX** (Scheme 20). All of these products were identified by NMR spectroscopy, mass spectrometry, and by comparison with the similar compounds previously observed. The intermediate Meisenheimer complex formed during this S<sub>N</sub>Ar reaction can only be stabilized by the carbonyl group in the aromatic ring where the alkoxy and carbonyl moieties are para to each other, explaining why only one isomer of each product is seen.

The dialcohol **LV** was then treated with sodium hydroxide and reacted with diethylene glycol ditosylate<sup>238</sup> to give *anti*-bis(formylbenzo)-18-crown-6 **XLVI**. The spectroscopic properties of this compound were virtually identical to those obtained for *syn*-bis(formylbenzo)-18-crown-6 **XLV**. The isomerically-pure nature of this product meant that only one aldehyde signal was seen in contrast to the two signals observed for the mixture **XLI** (Section 3.2.1). High-resolution mass spectrometry, elemental analysis and UV/VIS data were all consistent with the desired product **XLVI**.

It can be seen from Scheme 23 that the yields of both the chlorinated benzaldehyde isomers **LIII** and **LVI** were similar, as were the yields for the reaction of these products with vanillin or isovanillin respectively. However, the pathway beginning with isovanillin was advantageous in that the substantial amount of 1,5-bis(2'-methoxy-5'-formylphenoxy)-3-oxapentane **XLVII** isolated from the purification procedure could be demethylated and used in the synthesis of *syn*-bis(formylbenzo)-18-crown-6 **XLV** (Scheme 19).

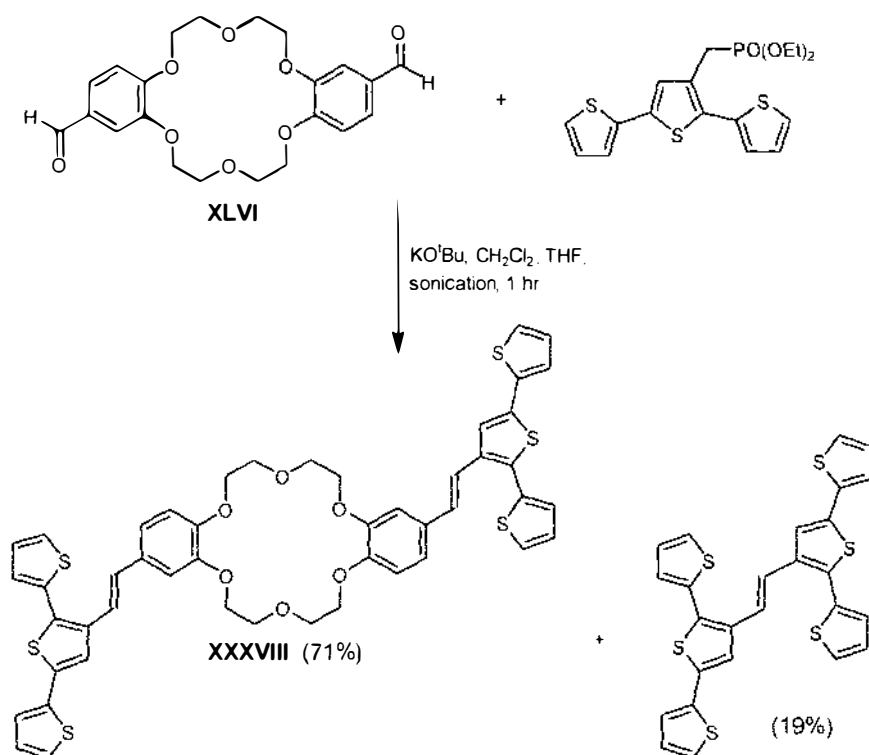


**Scheme 24** Products formed from demethylation of 1-(2'-methoxy-4'-formylphenoxy)-5-(2''-methoxy-5''-formylphenoxy)-3-oxapentane LIV

### 3.2.6 Horner-Emmons reaction using *anti*-bis(formylbenzo)-18-crown-6

*Anti*-bis(formylbenzo)-18-crown-6 **XLVI** was reacted with terthiophene phosphonate (Scheme 25) using the same reaction conditions as were used for *syn*-bis(formylbenzo)-18-crown-6 **XLV** (Scheme 22). Once again, analysis by MALDI-MS showed three species, the desired product **XXXVIII**, its potassium salt, and the terthiophene dimer seen earlier. As in the case of *syn*-bis(formylbenzo)-18-crown-6, it is uncertain whether the ion-free complex actually existed in the reaction mixture, or whether decomplexation was occurring during the MALDI-MS process. While

purification by column chromatography removed the by-product, it led to the formation of the sodium salt of **XXXVIII**. The product from this reaction was also insoluble, and again acid washing did not appear to remove the metal ions as evidenced by MALDI-MS. As in the case of **XXXVII**, the insolubility of the compound meant that further characterization was difficult, and **XXXVII** was not utilized in any further experiments.

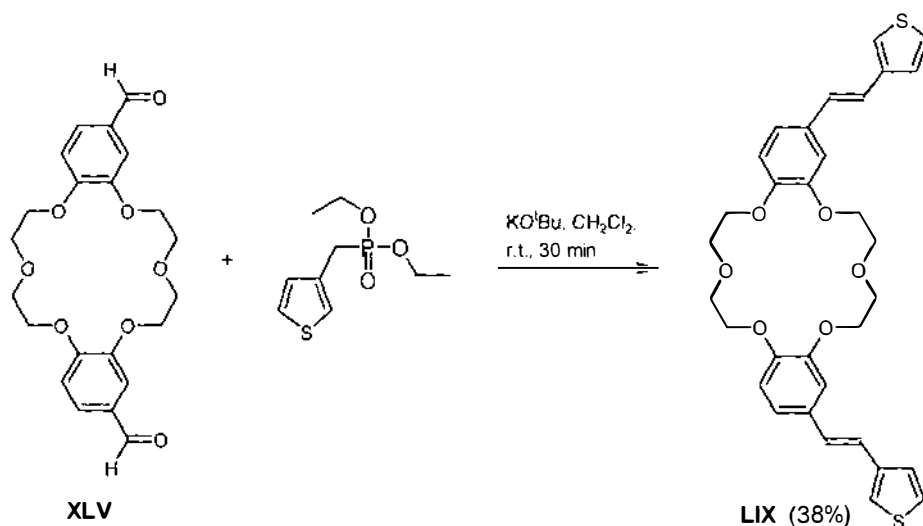


**Scheme 25** Horner-Emmons reaction between dialdehyde **XLVI** and terthiophene phosphonate

Given that the two bis(styryl terthiophene) crowns formed were too insoluble to be of further use, continued attempts to isolate pure materials were abandoned. However, it was anticipated that using the two bis(formylbenzo) crowns already synthesised and reacting them with thiophene phosphonate in Horner-Emmons reactions would provide cross-linked thiophenes that could be more soluble, and of use in copolymer systems.

### 3.2.7 Formation of bis(styryl thiophene) crowns

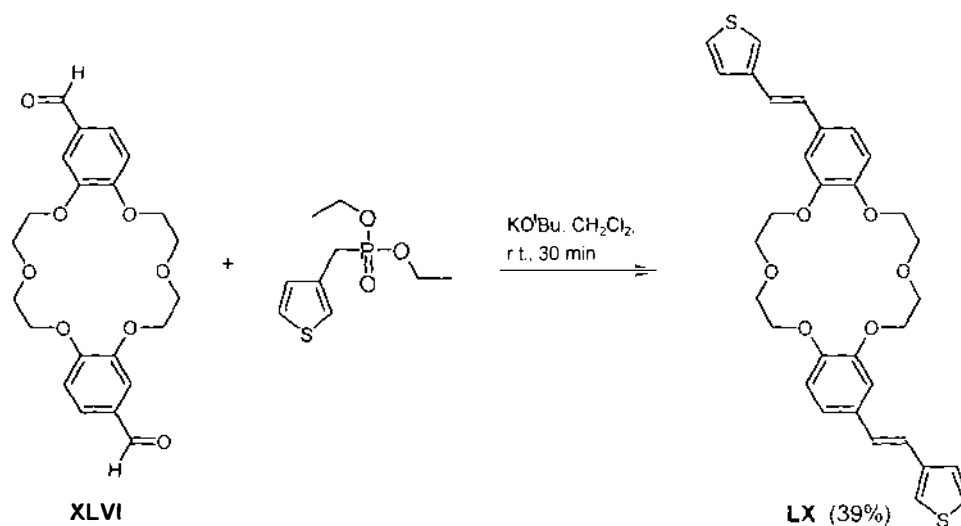
The Horner-Emmons reaction between *syn*-bis(formylbenzo)-18-crown-6 and thiophene phosphonate is detailed in Scheme 26. The reaction was carried out at room temperature, using KO<sup>t</sup>Bu as the base, and was complete within 30 minutes. The crude product was purified by flash column chromatography on silica to give a white powder. While slightly more soluble than the corresponding terthiophene derivative **XXXVII**, characterization was still limited. The <sup>1</sup>H NMR spectrum showed signals typical of a 3-substituted thiophene, in addition to two vinyl doublets ( $\delta$  6.91 and 7.03) and the expected aromatic and ether signals. High-resolution mass spectrometry data was also consistent with the proposed structure. UV/VIS analysis showed bands at 320.0 nm and 299.5 nm, the same positions as those seen for styryl-15-crown-5 thiophene **XV**. <sup>13</sup>C NMR and 2D NMR experiments requiring <sup>13</sup>C data were unable to be carried out due to the limited solubility of the product in CD<sub>2</sub>Cl<sub>2</sub>. A further complicating factor was the tendency of the compound to degrade in solution, turning from colourless to brown over a period of hours.



**Scheme 26** Formation of *syn*-bis(styryl thiophene)-18-crown-6 **LIX**

In the same way, *anti*-bis(styryl thiophene)-18-crown-6 **LX** was also formed from a Horner-Emmons reaction (Scheme 27). Thiophene phosphonate and *anti*-bis(formylbenzo)-18-crown-6 **XLVI** were reacted and purified under the same

conditions as described for **LIX**, yielding **LX** as a white powder in a similar yield. As observed for the equivalent *syn*-compound **LIX**, limited solubility hindered characterization. High-resolution mass spectrometry confirmed the formation of **LX**, and its UV/VIS spectra showed absorbances in the same positions as for **LIX**. A poorly resolved  $^1\text{H}$  NMR spectrum provided further evidence for the structure of **LX**, but the material was too insoluble in  $\text{CD}_2\text{Cl}_2$  and other deuterated solvents to obtain more NMR data.



**Scheme 27** Synthesis of *anti*-bis(styryl thiophene)-18-crown-6 **LX**

As the bis(styryl) crowns were all rather insoluble, this approach to forming monomers capable of forming cross-linked polymers was abandoned.

### 3.3 Synthesis of (Ter)thiophene Hemicrowns

Due to the insolubility of the cross-linked compounds **XXXVII** - **XXXVIII** and **LIX** - **LX**, and the availability of suitable starting materials, the monomers **LXI** - **LXIII** (Fig. 3.4) were instead targeted. It was anticipated that these compounds would bind metal ions less strongly, but still be capable of forming cross-linked polymeric structures.

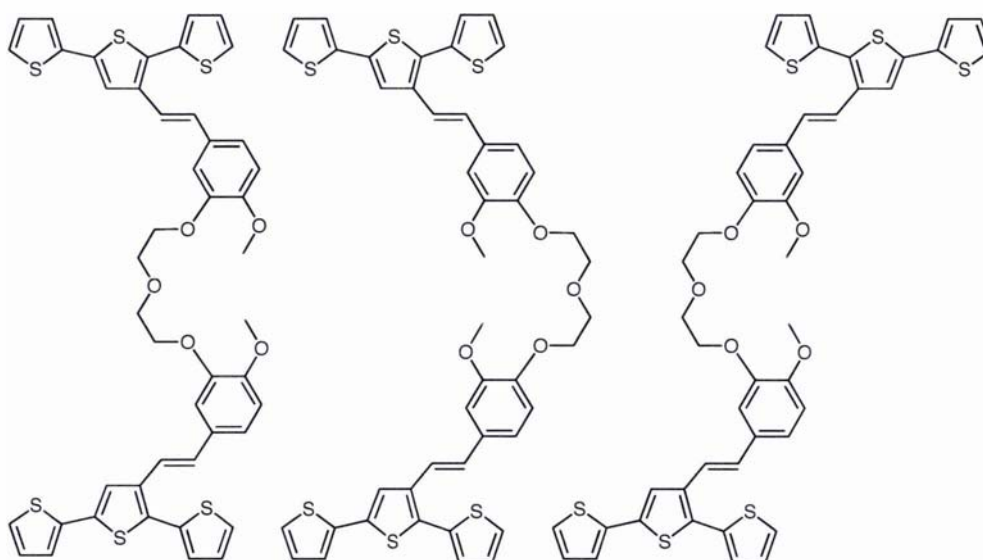
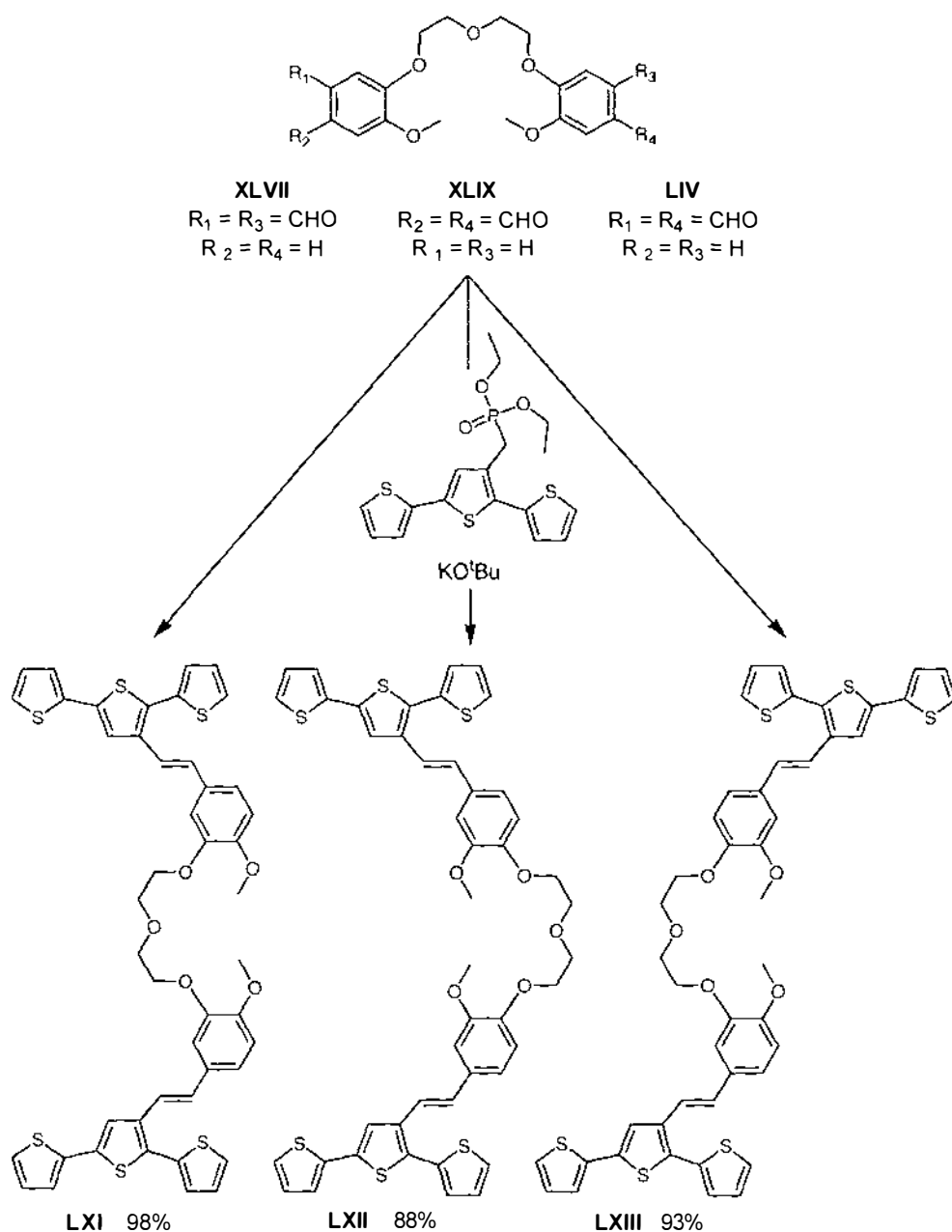


**Figure 3.4** Isomeric terthiophene hemicrowns targeted

#### 3.3.1 Synthesis of terthiophene hemicrowns

The starting dialdehydes necessary to form these compounds from a Horner-Emmons reaction with terthiophene phosphonate had been previously synthesised as

intermediates in the formation of **XLV** and **XLVI** (Schemes 19 and 23). The reactions to form target hemicrowns **LXI-LXIII** are shown below in Scheme 28.



**Scheme 28** Formation of bis(terthiophene) hemicrowns **LXI-LXIII**

The reaction to form the isovanillin-derived hemicrown compound **LXI** was carried out under the same conditions as previous Horner-Emmons reactions, utilizing  $\text{KO}^t\text{Bu}$  as the base. The reaction was complete within 1 hour at room temperature, and an aqueous work-up followed by silica gel chromatography yielded the pure *trans* **LXI**

as a yellow solid in an excellent 98% yield. The terthiophene-styryl peak at 330 nm was the only feature on the UV/VIS spectrum, identical to that observed for all other polyether-substituted terthiophenes. Due to the symmetry of the molecule, the  $^1\text{H}$  NMR spectrum was almost identical to that observed for the isovanillin-derived open-chain terthiophenes **XXVI-XXVII** in the aromatic region. The ether region of the spectrum contained two methylene multiplets and a singlet methoxy signal. Figure 3.5 shows the fully assigned  $^1\text{H}$  NMR spectrum for this compound. The assignment of the  $^1\text{H}$  and  $^{13}\text{C}$  NMR data was assisted by the collection of 2D NMR spectra, providing vital connectivity information. High-resolution mass spectrometry provided additional evidence to verify the successful synthesis of hemicrown **LXI**.

The remaining two hemicrowns **LXII** and **LXIII** were synthesised in an identical manner, again giving excellent yields of product (88 and 93% respectively). The aromatic regions of the  $^1\text{H}$  NMR spectra for the three hemicrowns are shown in Fig. 3.6. As previously shown in Fig. 2.19, the slight chemical shift differences between the isovanillin- and vanillin- derived compounds are small but distinct. The spectrum for the hemicrown containing both isovanillin- and vanillin-derived components appears almost as a straight addition of the two individual spectra, with separate signals seen for most protons. UV/VIS spectra for **LXII** and **LXIII** show a peak at 331 nm, as was observed previously for **LXI**. As seen for all previous Horner-Emmons reactions involving terthiophene phosphonate, a small fraction of 1,2-bis([2',2'';5'',2''']terthiophen-3''-yl)ethene (2%) was also isolated during column chromatography.

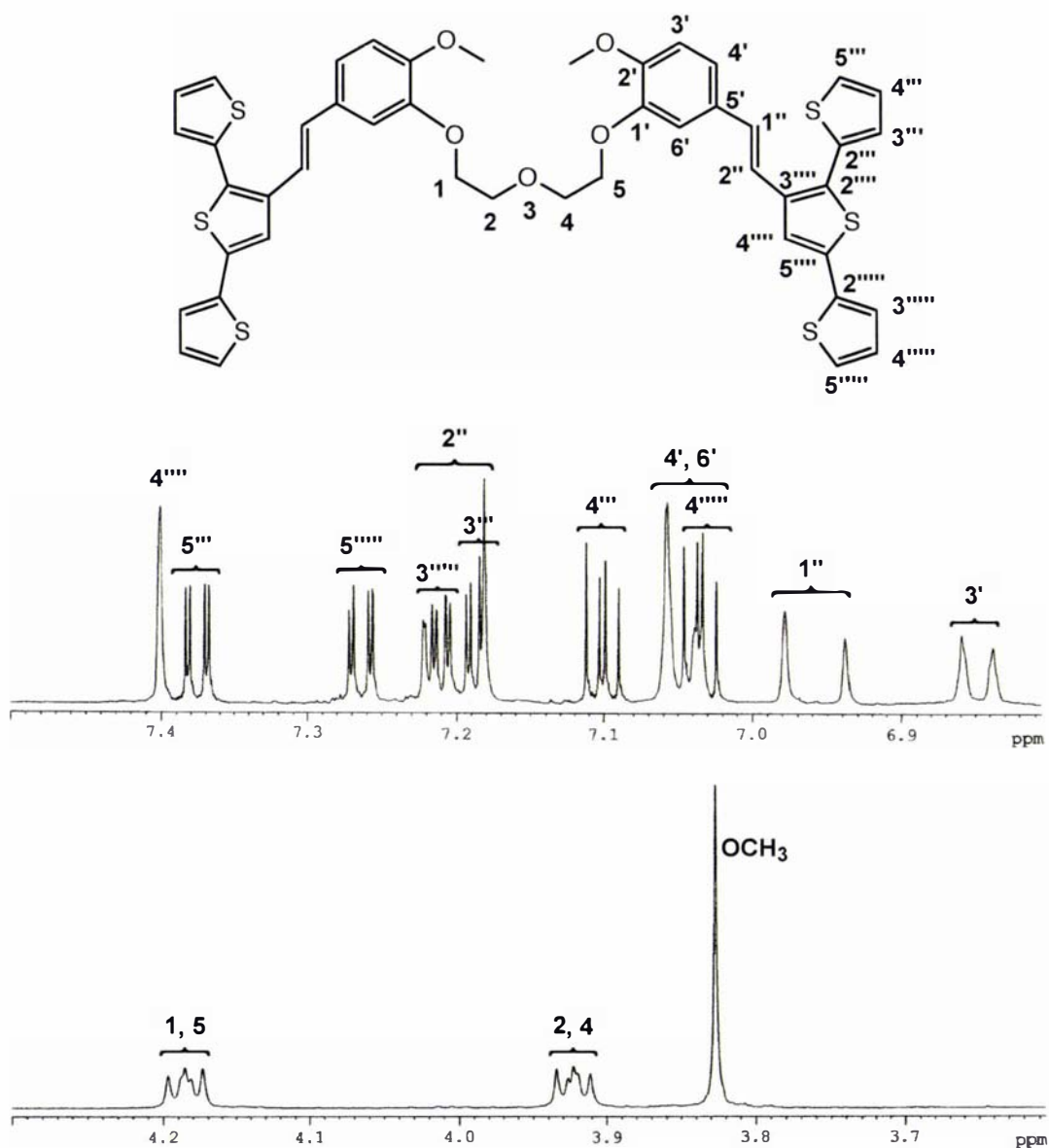


**Figure 3.5** Assigned  $^1\text{H}$  NMR spectrum of isovanillin-derived terthiophene hemicrown LXI

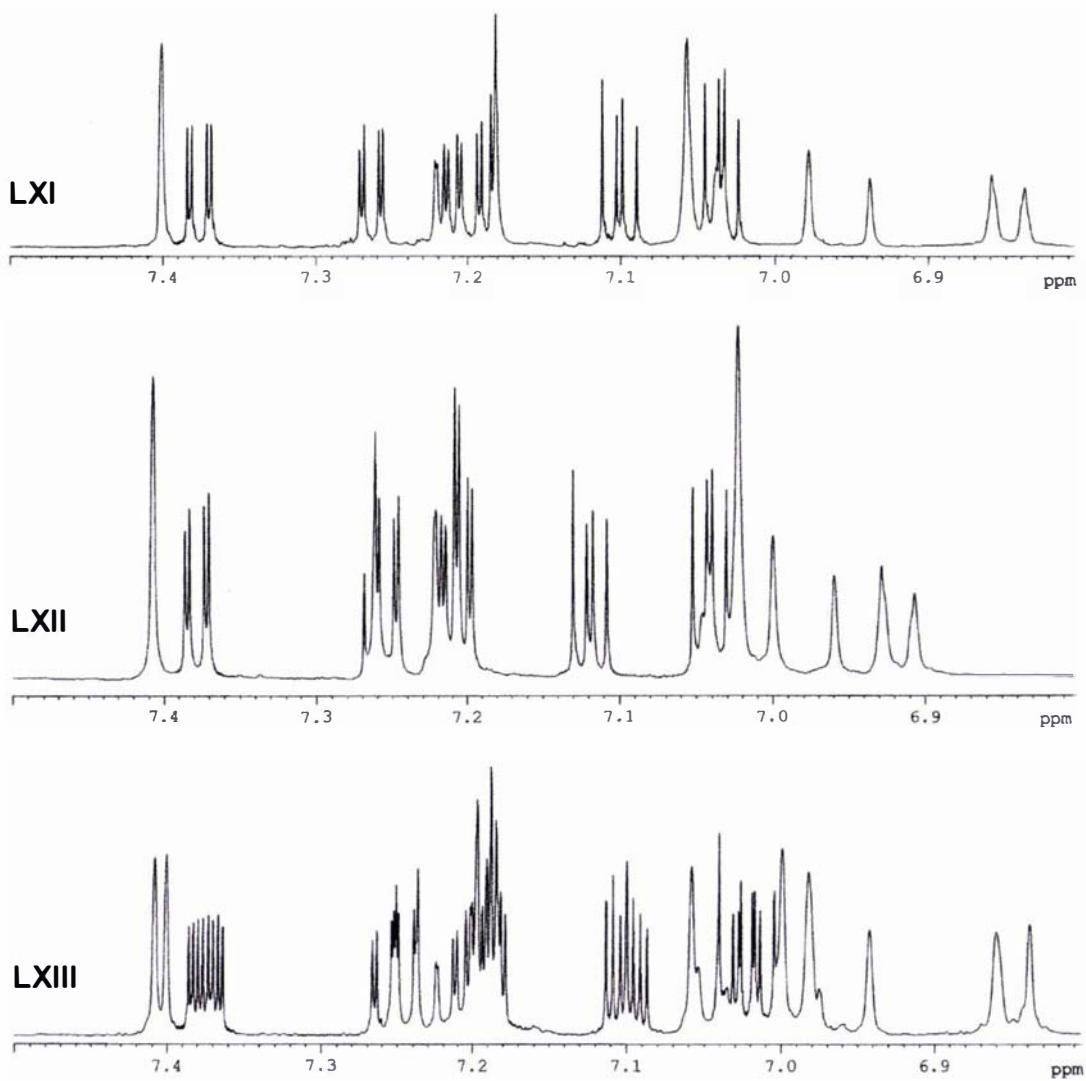
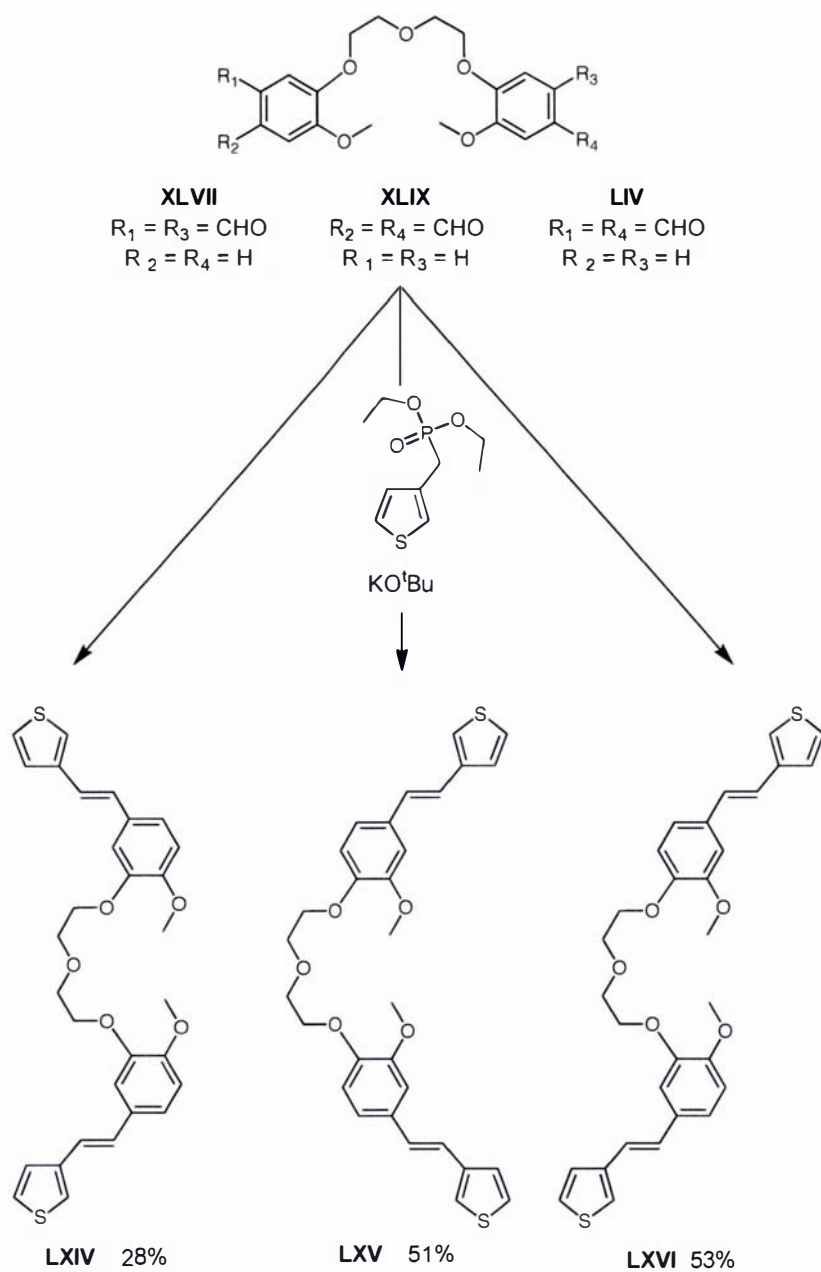


**Figure 3.6 Comparison of  $^1\text{H}$  NMR spectra for terthiophene hemicrowns LXI (top), LXII (middle) and LXIII (bottom)**

### 3.3.2 Synthesis of thiophene hemicrowns LXIV - LXVI

Due to the availability of starting materials and their potential use in copolymer systems, three isomeric thiophene hemicrowns, analogous to the terthiophene hemicrowns **LXI-LXIII**, were synthesised as shown in Scheme 29. The dialdehyde starting materials had been previously made, as detailed in Schemes 19 and 23, and were reacted with thiophene phosphonate in typical Horner-Emmons reactions. Purification by flash column chromatography produced white solids in all three cases. The lower yield of the isovanillin-derived compound **LXIV** reflects its lower solubility in organic solvents, but it is likely that this could be overcome by increasing the solvent volumes used during the workup. High-resolution mass spectrometry gave satisfactory results for all three compounds. UV/VIS spectra showed bands at 300 nm and 320 nm, as had been seen for all other ether-substituted styryl thiophenes synthesised. The signals in the ether region of the  $^1\text{H}$  NMR spectra were identical, with minor chemical shift differences seen in the aromatic region.  $^{13}\text{C}$  and 2D NMR experiments allowed the full assignment of all atoms in the three compounds.

No solubility difficulties were encountered with any of the three isomeric terthiophene hemicrowns, or the three isomeric thiophene hemicrowns, proving the worth of this approach.



**Scheme 29** Synthesis of bis(thiophene) hemicrowns LXIV-LXVI

### 3.4 Synthetic Summary

The aim of this synthetic work was to synthesise a number of mono- and bis(ter)thiophene compounds that contained dialkoxy-substituted conjugated styryl linkers. Incorporating a range of dialkoxy functionalities, including crown ethers and polyether chains, was desirable in order to investigate the different cation binding properties these would display. To this end, two crown ether functionalised styryl terthiophenes (Scheme 7) and three pairs of isomeric open chain ether compounds (Scheme 12) were synthesised. In addition, two cross-linked crown compounds (Schemes 22 and 25) and three isomeric hemicrowns (Scheme 28) were made. An analogous dimethoxy compound was also synthesised (Scheme 13) as a reference, as it was anticipated that this compound would be unable to bind metal cations. The synthesis of all these compounds was achieved by a Horner-Emmons reaction between terthiophene phosphonate and an appropriately substituted benzaldehyde. While other synthetic approaches were tried, this method proved superior due to the high yields of isomerically pure material that could be produced. In most cases the substituted benzaldehydes were themselves unknown and these also had to be synthesized, utilizing a variety of synthetic methodologies.

As thiophene phosphonate was available in our laboratories, it was reacted in a series of similar Horner-Emmons reactions with the substituted benzaldehydes that had been synthesised. This allowed a range of styryl-thiophene compounds to be made that were analogous to the styryl-terthiophene compounds already described. These included crown ethers (Schemes 8 and 9), open chain ethers (Scheme 14), bis(styryl thiophene)crown ethers (Schemes 26 and 27) and bis(styryl thiophene) hemicrowns (Scheme 29). While it was anticipated that these compounds would likely not form conducting homopolymers, they could be of great assistance in understanding the spectral properties of the styryl-terthiophenes.

The styryl terthiophene monomers synthesised had been designed to incorporate various crown and polyether functionalities that are capable of complexing metal cations. Thus it was important to investigate the ion binding of these monomers, to ensure that selectivity between metal ions could be observed. Therefore it was necessary that this selectivity resulted in a change in some measurable property of the monomer. As terthiophenes provide informative UV/VIS and fluorescence spectra, the effect of ion binding on the spectra of the monomers was investigated and is described in Chapter 4.

Another important aspect of the monomer design was the incorporation of a polymerisable terthiophene moiety, as it was desirable to be able to form a conducting polymer that could act as a sensor. An investigation into both the chemical and electrochemical polymerisation of these monomers was therefore carried out, and is detailed in Chapter 5.

The structures of the terthiophene and bis(terthiophene) compounds used in the spectroscopic and polymerisation studies are reproduced on a fold-out sheet inside the back cover as a reference.

4

**SPECTROSCOPIC**

**ION**

**BINDING**

**STUDIES**

## 4.1 UV/VIS Spectroscopy

UV/VIS spectroscopy is an important technique for gathering information about the electronic structure of conjugated compounds. In particular all the terthiophene compounds synthesised in this work are yellow, and therefore provide informative UV/VIS spectra. Cation binding could reasonably be expected to change the absorbance of these molecules, by effecting either electronic or conformational changes. It is also possible that the magnitude of this effect could provide information on the relative binding affinities of the synthesised crowns for various cations. For this reason an investigation into the effect of cation binding on the UV/VIS spectra of polyether-substituted terthiophenes was carried out.

### 4.1.1 Literature review

#### 4.1.1.1 Absorbance of substituted terthiophenes

A numbered structure of terthiophene is shown below (Fig. 4.1) to serve as a reference for the following literature discussion.

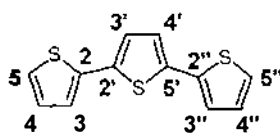


Figure 4.1 The structure of terthiophene

Terthiophene absorbs at 354 nm in dichloromethane solution,<sup>240</sup> and the broad and structureless nature of its  $\pi$ - $\pi^*$  peak has been attributed to the inherent flexibility of the molecule.<sup>241, 242</sup>

Substituted terthiophenes with both red- and blue-shifted absorbances are found in the literature. 3',4'-dihexylterthiophene shows an absorbance maxima that is hypsochromically shifted by 23 nm compared to terthiophene.<sup>241, 243, 244</sup> The observed shift was explained by the steric hindrance between the two adjacent alkyl groups creating torsion between the rings, decreasing conjugative interaction in the  $\pi$  system. A similar (19 nm) shift seen for 3,3''-dimethylterthiophene was also accounted for by a twisting of the molecule.<sup>243-245</sup> A considerably larger effect (63 nm) was noted for 3,3',4',3''-tetramethylterthiophene where the substituent interactions caused the thiophene rings to become almost perpendicular, drastically reducing conjugation.<sup>246</sup> In contrast, substitution with electron donating groups such as -OMe, or -Br causes a bathochromic shift in the position of the absorbance peak. Literature examples include 5-methoxyterthiophene ( $\Delta\lambda_{\text{max}} = 14$  nm)<sup>240</sup>, 5,5''-dibromoterthiophene ( $\Delta\lambda_{\text{max}} = 8$  nm)<sup>240</sup>, 5-bromo-5''-methoxyterthiophene ( $\Delta\lambda_{\text{max}} = 21$  nm)<sup>240</sup> and 3,3''-dimethoxyterthiophene ( $\Delta\lambda_{\text{max}} = 18$  nm)<sup>243-245</sup>. In addition, it would seem logical that any substituent containing multiple bonds would extend the  $\pi$  electron system, and therefore lead to a bathochromic shift of the absorption maxima. This has been shown to be the case in many examples, including a number of cyano- and dicyano-derivatives ( $\Delta\lambda_{\text{max}} = 15$ -29 nm)<sup>214</sup>, 5-nitroterthiophene ( $\Delta\lambda_{\text{max}} = 86$  nm)<sup>240</sup>, 5-bromo-5''-nitroterthiophene ( $\Delta\lambda_{\text{max}} = 76$  nm)<sup>240</sup>, 5,5''-diphenylterthiophene ( $\Delta\lambda_{\text{max}} = 50$  nm)<sup>247</sup>, two triphenylamino substituted terthiophenes ( $\Delta\lambda_{\text{max}} = 60$  and 86 nm), 5-formyl ( $\Delta\lambda_{\text{max}} = 48$  nm) 5-acetyl ( $\Delta\lambda_{\text{max}} = 41$  nm) 5-thenoyl ( $\Delta\lambda_{\text{max}} = 63$  nm) and 5-benzoylterthiophenes ( $\Delta\lambda_{\text{max}} = 52$  nm)<sup>248</sup>, among others<sup>241, 242, 249</sup>. The first electronic transition of terthiophenes ( $\pi$ - $\pi^*$ ) corresponding to that seen in UV/VIS spectra has been shown to be delocalized along the long molecular axis,<sup>241, 246</sup> and therefore substitution at the 5 and 5''-positions has the greatest effect on the energy of this transition. Kankare *et al.* looked at the UV/VIS spectra of a number of terthiophenes substituted at the 3'-position with aromatic moieties.<sup>127, 250</sup> They found that the long-wavelength absorption band was seen at the same position as for the parent terthiophene, and did not change on varying the attached substituent. This, along with

other supporting data, led them to conclude that the aromatic substituents were not appreciably conjugated with the terthiophene backbone. These results were attributed to steric hindrance between the aromatic substituent and the terthiophene moiety, forcing the aromatic ring out of coplanarity. It was anticipated that the incorporation of a conjugated spacer into the dialkoxystyryl-substituted terthiophenes synthesised in this work would overcome these steric issues.

#### **4.1.1.2 Effect of cation complexation on absorbance of functionalised crown ethers**

To the best of our knowledge, there are only two examples of styryl-substituted benzo crown ethers in the literature. Alfimov *et al.* synthesised crown ether styryl dyes as shown in Fig. 4.2a.<sup>188, 190</sup> The *trans* form of this dye showed a response to alkali metal ion perchlorates in acetonitrile, in the order  $Mg^{2+} > Ca^{2+} > Ba^{2+}$ , with hypsochromic shifts in the position of  $\lambda_{max}$  from 29- 42 nm. The dye could be converted into the *cis* form by irradiation, and again was affected by metal ions in the order  $Mg^{2+} > Ca^{2+} > Ba^{2+}$ . The peak maxima shifts were considerably larger this time (83-100 nm) and this was explained by the ability of the sulfonate group to interact with the complexed metal ion only in the *cis* configuration. The observed selectivity was rationalized on the basis that the smaller cation  $Mg^{2+}$  formed only 1:1 complexes with the dye, whereas the larger diameter cations tended to form 2:1 complexes with 2 dye molecules per cation.

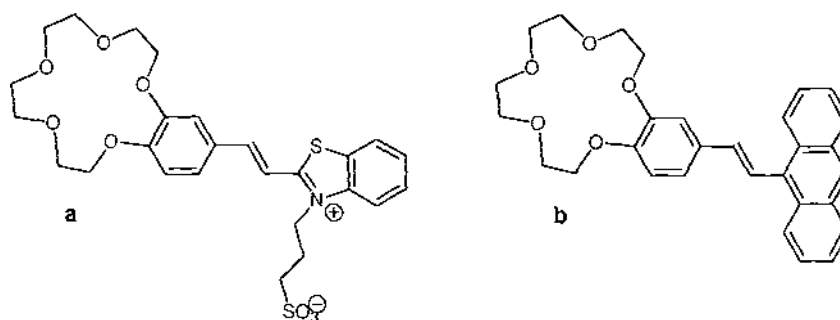


**Figure 4.2 Crown ether styryl dyes**

More recently, a crown ether styryl dye incorporating anthracene was reported (Fig. 4.2b).<sup>251</sup> Few experimental details are given, but the absorption maxima was reported to be blue-shifted on addition of  $\text{Li}^+$ ,  $\text{Na}^+$ ,  $\text{Mg}^{2+}$  and  $\text{Ca}^{2+}$ , and unaffected by  $\text{K}^+$  and  $\text{Cs}^+$ . Considering the alkali and alkaline-earth metal ion series separately, these shifts are easily rationalized based on size-fit from the data provided in Tables 4.1 and 4.2. The greater charge density of the alkaline-earth metal ions means that they have a larger influence than the alkali metal ions. It must be noted however, that the shifts observed were quite small, with the largest being just 4 nm.

**Table 4.1 Crown Ether cavity sizes<sup>252</sup>**

Crown Ether	Cavity Size / Å
14-crown-4	1.2-1.5
15-crown-5	1.7-2.2
18-crown-6	2.6-3.2
21-crown-7	3.4-4.3
24-crown-8	>4

**Table 4.2 Metal cation ionic diameters<sup>253</sup>**

Monocation	Ionic diameter / Å	Dication	Ionic diameter / Å
Li <sup>+</sup>	1.36	Mg <sup>2+</sup>	1.32
Na <sup>+</sup>	1.94	Ca <sup>2+</sup>	1.98
K <sup>+</sup>	2.66	Sr <sup>2+</sup>	2.24
Rb <sup>+</sup>	2.94	Ba <sup>2+</sup>	2.68
Cs <sup>+</sup>	3.34		
		Ni <sup>2+</sup>	1.38
Ag <sup>+</sup>	2.52	Co <sup>2+</sup>	1.44
NH <sub>4</sub> <sup>+</sup>	2.86	Zn <sup>2+</sup>	1.48
		Mn <sup>2+</sup>	1.60
		Cd <sup>2+</sup>	1.94
		Pb <sup>2+</sup>	2.40

In addition to the styryl-benzo crowns, there are several examples of styryl-linked aza crown ethers in the literature (Fig. 4.3).

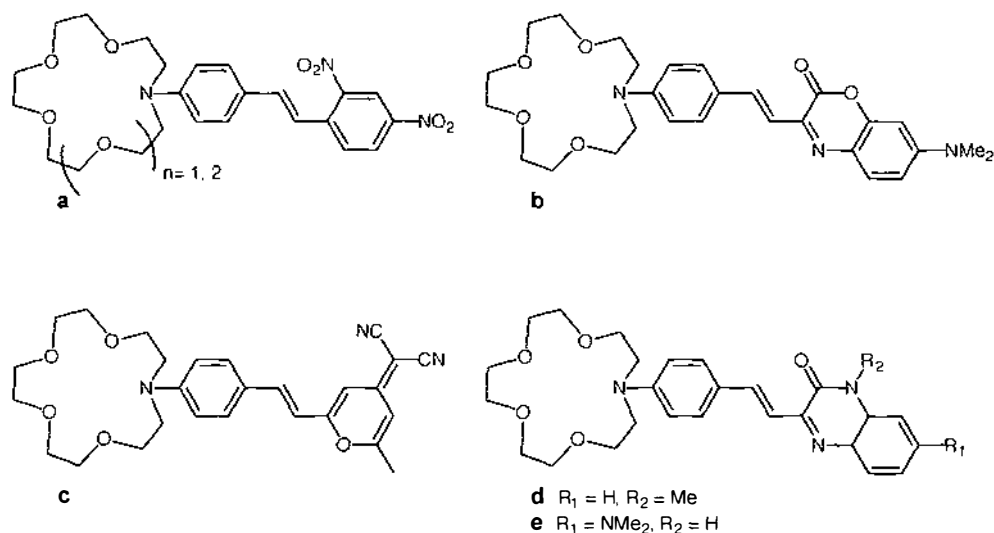


**Figure 4.3 Aza crown ether styryl dyes investigated by UV/VIS spectroscopy**

Löhr and Vögel<sup>254</sup> discuss several aza crown dyes, including the dinitro compounds shown in Fig. 4.3a. For the aza-15-crown-5 compound, the UV/VIS spectrum was most affected by  $Ca^{2+} > Ba^{2+} > Na^{+} > Li^{+} > K^{+}$ . The order for the 18-crown-6 compound was  $Ba^{2+} > Ca^{2+} > K^{+} > Na^{+} > Rb^{+}$ . It is easily rationalized based on size-fit, that  $Na^{+}$

would have a greater effect on the smaller crown, whereas the larger cation  $K^+$  would be a better fit for 18-crown-6 in the alkali metal ions. Similarly,  $Ca^{2+}$  would be a better fit for 15-crown-5 than  $Ba^{2+}$ , which had more of an effect on the larger crown. In each case, the alkaline earth metal ions had a greater effect than the alkali metal ions due to their greater charge density.

Figure 4.3b shows a benzoxazinone derivative of aza-15-crown-5 synthesised by Fery-Forgues *et al.*<sup>255</sup> This compound showed a blue-shift in the position of its absorption maxima on addition of  $Ca^{2+} > Mg^{2+} > Ba^{2+} > Na^+ > Li^+$ . This change was not seen on addition of metal ions to reference compounds containing the same chromophore without the crown ether moiety. It was noted that the spectrum of the crown dye became more like that of the unsubstituted chromophore on complexation, and that alkaline metal ions had a greater effect than alkali metal ions. Once again, these results are easily explained by size fit from the data provided in Tables 4.1 and 4.2.

Bourson and Valeur<sup>256</sup> investigated a series of merocyanine dyes, including one that incorporated an aza-crown (Fig. 4.3c). The greatest effects were caused by addition of alkaline earth metal ions  $Mg^{2+} > Ca^{2+} > Ba^{2+}$ , with  $Na^+$  having a larger effect than  $Li^+$  in the alkali metal ion series. They also observed that alkaline earth metal ions had a greater effect on the spectra than alkali metal ions, and that the shape of the spectra on addition of alkaline metal ions was reminiscent of the reference molecule that did not contain a donor substituent.

The structures in Fig. 4.3d-e are styrylbenzodiazinones synthesised by Cazaux *et al.*<sup>257</sup> Compound 4.3d shows no wavelength shift on addition of  $Mg^{2+}$  or  $Na^+$ , but large shifts are caused by  $Ca^{2+}$  and  $Ba^{2+}$ , with  $Zn^{2+}$  an intermediate case. As in other work, it is noted that the spectra of 4.3d complexed with  $Ca^{2+}$  or  $Ba^{2+}$  becomes more like the uncrowned reference chromophore. Compound 4.3e responds to metal ions in the same order, but the shift in wavelength is considerably smaller. Their complexation is further complicated by the formation of both 1:1 and 2:1 metal ion:ligand complexes

From these results, it is clear that the greatest effect on the wavelength maxima is caused by the cation (of the same charge) that best fits into the crown cavity. Doubly charged cations generally have a larger effect than monovalent cations, as their charge density is greater. In addition, the hypsochromic shifts seen on cation complexation cause the spectra to become more like that of the unsubstituted chromophore. Substitution of a chromophore by a saturated group with nonbonded electrons (an auxochrome e.g. OH, NH<sub>2</sub>) causes a bathochromic shift of the chromophores absorption bands.<sup>213</sup> Therefore, it seems logical that involving those electrons in a complex with a cation would reduce the auxochrome's effect, manifesting in a hypsochromic shift of the absorption band back toward the position of the original unsubstituted chromophore. The extent to which the cation 'neutralised' the effect of the auxochromes nonbonded electrons would determine how closely the spectra of the complexed auxochromically-substituted chromophore resembled that of the unsubstituted chromophore.

#### **4.1.1.3 Effect of cation complexation on polyether-substituted polythiophenes**

While there have been many polyether, pendant chain ether and crown ether functionalised polythiophenes previously synthesised (Section 1.4), there have been few systematic studies on the effect of cation complexation on their UV/VIS spectra.

McCullough and Williams synthesised regioregular head-to-tail poly(3-[2,5,8-trioxanonyl]thiophene (Fig. 4.4a).<sup>100</sup> They reported that, in addition to a marked change in solubility,  $\lambda_{\text{max}}$  for this polymer was blue-shifted by 11 nm on addition of Li<sup>+</sup>. Later work on this compound showed that addition of Pb<sup>2+</sup> or Hg<sup>2+</sup> to a dilute solution of polymer caused the polymer backbone to twist in such a way that conjugation was completely removed. This effect was irreversible however, and polymer conjugation could not be restored. In more concentrated solutions, the introduction of Pb<sup>2+</sup> caused a 50-100 nm blue-shift in the position of  $\lambda_{\text{max}}$ . The dramatic loss of conjugation caused by Pb<sup>2+</sup> was attributed primarily to the dissolved

soft metal binding to the thiophene sulphur atoms, with the polyether chain having only a 'supplemental' role.<sup>138</sup>

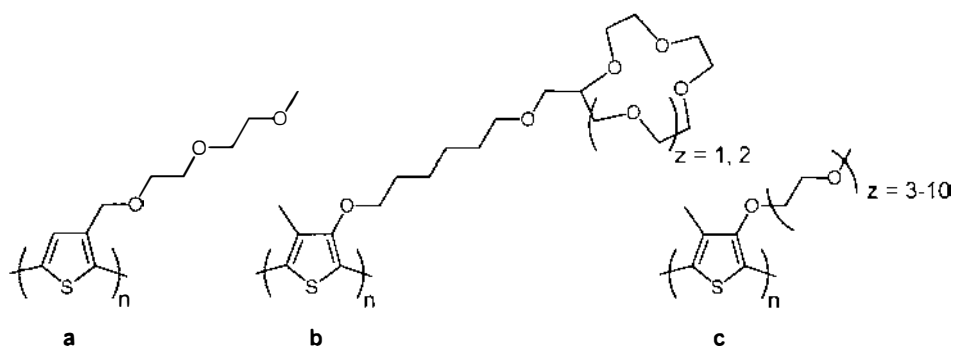


**Figure 4.4 Polyether substituted polythiophenes investigated by UV/VIS spectroscopy**

Lévesque and Leclerc synthesised 3-oligo(oxyethylene)-4-methylthiophene with a mixture of side chains from 3 to 10 oxyethylene units long (Fig. 4.4c).<sup>110, 258, 259</sup> An ionochromic effect was noted in methanol, where the magnitude of the effect was  $K^+ > Na^+ > NH_4^+$ , with no effect seen on addition of  $Li^+$ . Cation complexation caused a twisting in the conjugated polymer backbone, manifested by a decrease in absorbance at a higher wavelength and a simultaneous increase in absorbance at a lower wavelength. A clear isobestic point indicated the co-existence of both the twisted and non-twisted forms of the polymer. More recently, the same group reported the synthesis and ionochromic ability of poly(3-alkoxy-4-methylthiophene)s with pendant crown ethers as shown in Fig. 4.4b.<sup>78</sup> Chemical polymerisation gave high molecular weight polymers that demonstrated substantial ionochromic effects. For the 12-crown-4 compound, the largest response was seen for  $Na^+$ , followed by  $K^+$  and  $Li^+$ , whereas for 15-crown-5 the order was  $K^+ > Na^+ > Li^+$ . These selectivities are not what would be expected from a simple 1:1 crown:cation species, but were reported instead to be the result of 2:1 complexation.

Marsella and Swager<sup>67, 145-147</sup> synthesised molecules that gave a dramatic optical response to cation complexation. Their compounds consisted of bithiophene with a crown-like polyether chain tethering the two thiophene rings (Fig. 4.5a). In the uncomplexed state, the thiophene rings maintained their preferred *anti* geometry, but on complexation the thiophene rings were forced to rotate, leading to a loss of planarity and hence conjugation, resulting in a large change in  $\lambda_{\text{max}}$ . While the binding constants for the monomers with alkali metal ions were very low because of their inherent inflexibility, ionochromic shifts were large, as the twisting mechanism affected not just the immediate thiophene rings, but neighbouring rings as well. The polyether chains containing 5-oxygen atoms showed the greatest response to  $\text{Na}^+$ , followed by  $\text{Li}^+$  and  $\text{K}^+$  as would be expected by analogy with 15-crown-5. The larger 6-oxygen chains responded to  $\text{K}^+ > \text{Na}^+ > \text{Li}^+$ , due to its structural similarity to 18-crown-6. Incorporating an extra bithiophene unit into the polymer structure (Fig. 4.5b) gave polymers that responded with the same selectivity as the initial monomers. The observed wavelength shifts were smaller in this case, as would be expected due to the lower crown loading in the polymer. The introduction of an additional methylene group between the thiophene units and the first oxygen atoms in the polyether chain (Fig. 4.5c) resulted in less conjugated polymers of lower molecular weight. These polymers had a lower binding affinity for alkali metal ions, which resulted in a failure of the twist-inducing mechanism, and hence negligible wavelength shifts on complexation.

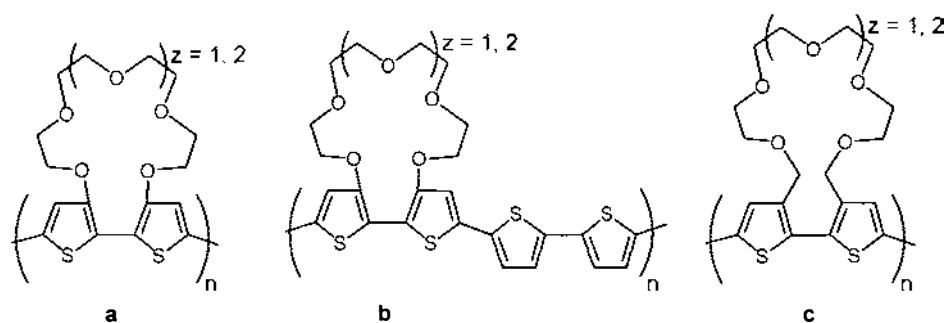


**Figure 4.5** Ionochromic polythiophenes synthesised by Marsella *et al.*

A recent investigation into crown ether functionalised thiophenes was carried out by Berlin *et al.*, who synthesised the monomers shown in Fig. 4.6.<sup>154</sup> The 14-crown-4

compound (Fig. 4.6a) showed no change by UV on addition of  $\text{Li}^+$ ,  $\text{Na}^+$  or  $\text{K}^+$ , whereas the 18-crown-6 compound (Fig. 4.6b) showed only very small changes on addition of  $\text{Na}^+$  and  $\text{K}^+$ . The terthiophene monomer (Fig. 4.6c) showed a larger and equal response to  $\text{Na}^+$  and  $\text{K}^+$ , and the EDOT-derived compound (Fig. 4.6d) showed a large UV/VIS response to  $\text{K}^+ > \text{Na}^+$ . Films of poly(4.6d) were shown to be insensitive to the presence of metal ions, whereas poly(4.6c) dissolved in solutions containing  $\text{Na}^+$  or  $\text{K}^+$ .

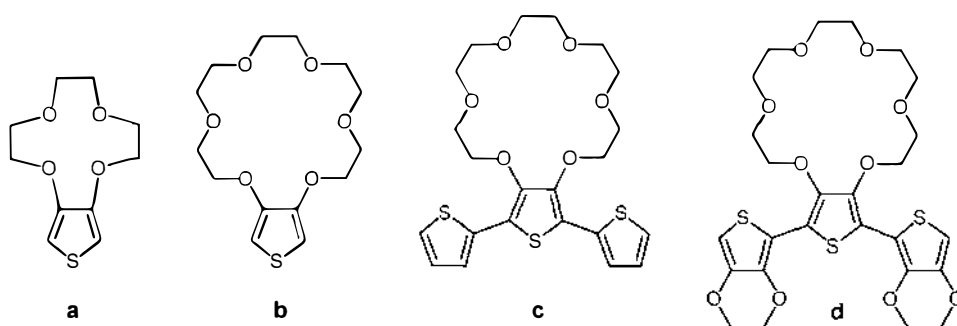


**Figure 4.6 Crown ether functionalised (ter)thiophenes**

While the research discussed in this section shows in places rather dramatic results, in many cases there is also a rather limited response to metal cations displayed. None of the work quoted employed a systematic approach to complexation using many different metals, instead preferring to concentrate on (at most) four different metals. In most cases, the alkali metal ions were chosen due to their well-known binding affinity with crown ethers. However, there are other cations that also have the potential to complex, and it was believed that investigating a larger range of metal ions would give a fuller picture of the binding ability of the polyether-substituted oligothiophenes synthesised. This was the approach taken in the remainder of this study.

## 4.1.2 UV/VIS spectra of polyether-substituted oligothiophenes

As a large range of crown ether, polyether chain and hemicrown terthiophene and thiophene monomers had been synthesised, along with a number of sexithiophene products of chemical polymerisation (Section 5.1), this provided a unique opportunity for an in-depth study of their UV/VIS properties.

### 4.1.2.1 Absorbance of terthiophene monomers

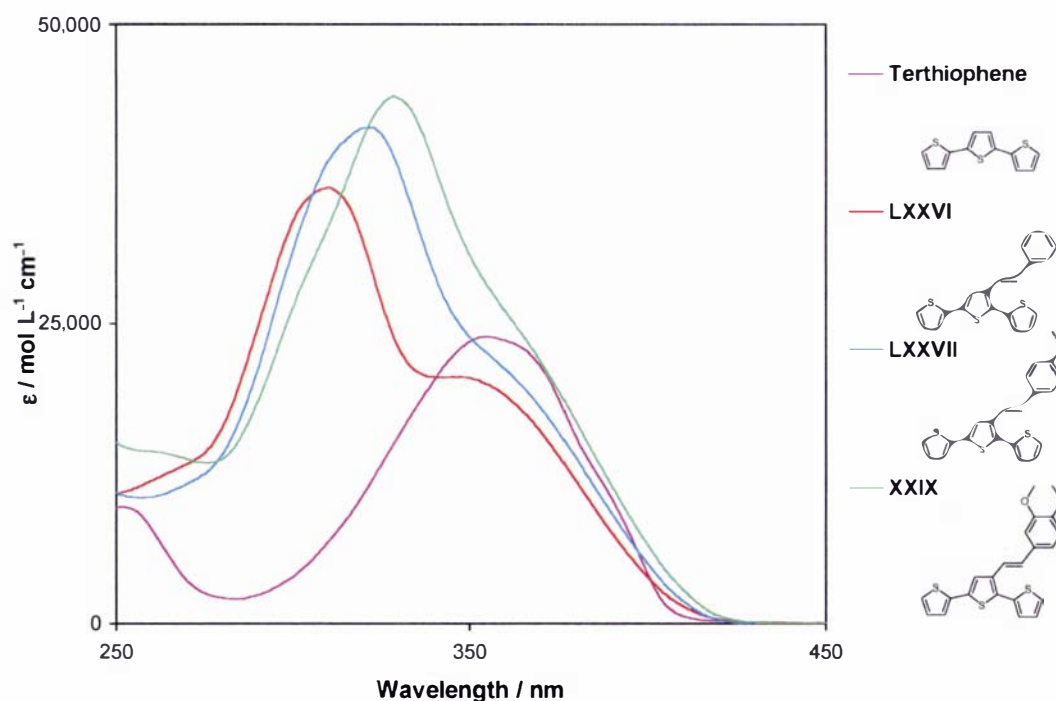


**Figure 4.7** Absorbance spectra of terthiophene monomers in MeCN

Figure 4.7 shows the UV/VIS spectra for styryl-, methoxystyryl- and dimethoxystyryl-terthiophenes **LXXVI**, **LXXVII** and **XXIX**, compared with the spectrum obtained for terthiophene under the same conditions. The spectrum obtained for styryl terthiophene **LXXVI** shows peaks at 310 and 345.5 nm. The

longer wavelength peak appears to result from the same electronic transition as that observed for terthiophene, with a slight hypsochromic shift and hypochromic effect caused by substitution. The band observed at 310 nm is attributed to the styryl-thiophene moiety, and can be compared to that observed for *trans*-stilbene (308 nm,  $\log \epsilon = 4.40$ ).<sup>213</sup> The only other possible chromophore that could give rise to this peak is the styrene moiety. However, the lowest energy band for styrene is observed at 282 nm ( $\log \epsilon = 2.65$ )<sup>213</sup>, and so it seems unlikely that the styrene chromophore is responsible for this peak. While none of the compounds synthesised in this research formed crystals of sufficient quality to be used for X-ray crystallographic structure determination, a related styryl terthiophene structure has been obtained. An analogous compound to **LXXVII**, substituted with a cyano functionality rather than a methoxy group, had a dihedral angle between the benzene and central thiophene ring of 26.5°. <sup>260</sup> Geometry optimizations (Gaussian 98, B3LYP/6-31G(d)) give dihedral angles of *ca.* 22° for the styryl, methoxystyryl and dimethoxystyryl terthiophenes.<sup>65, 261</sup> Thus available X-ray crystallographic and theoretical data supports conjugation of the styryl moiety with the central thiophene ring.

A comparison of the three styryl-substituted compounds shown in Fig. 4.7 shows a clear bathochromic shift of the lower wavelength absorbance on incorporation of an alkoxy auxochrome, an effect which is intensified on inclusion of a second alkoxy group. An increase in  $\epsilon$  accompanies these changes. It is well known that auxochromic substitution on benzene rings causes the observed absorbance peaks to move to longer wavelength, due to  $n-\pi$  conjugation, and usually also causes an increase in  $\epsilon$ .<sup>215</sup> Silverstein, Bassler and Morrill<sup>213</sup> state that for ortho-disubstituted benzenes, the shift effects of the two substituents on the primary  $\pi-\pi^*$  transition band are additive. For benzene, each of two adjacent methoxy substituents would be expected to cause a bathochromic shift of approximately 13 nm. It can be seen from Table 4.3 that the incorporation of a single alkoxy functionality causes a bathochromic shift of 12 nm, increasing to 20 nm on addition of a second alkoxy group. It is also clear that varying the length of the alkoxy chain grafted onto the molecule has no effect either on the position of the absorbance maxima or on its relative intensity.

**Table 4.3 Solution absorbance maxima of terthiophene monomers**

Compound	Solvent	Solution $\lambda_{\max}$ / nm (log $\epsilon$ )	
TTh=-Bz <b>LXXVI</b>	MeCN	310.0 (4.58)	345.5 (4.32)
TTh=-BzOMe <b>LXXVII</b>	MeCN	322.5 (4.62)	
TTh=-Bz(OMe), <b>XXIX</b>	MeCN	329.0 (4.65)	
TTh=-Bz15c5 <b>I</b>	MeCN	329.0 (4.57)	
TTh=-Bz18c6 <b>II</b>	MeCN	330.0 (4.58)	
TTh=-BzOCOCOC <b>XXIII</b>	MeCN	328.5 (4.61)	
TTh=-BzOCOCOC <b>XXVI</b>	MeCN	329.0 (4.59)	
TTh=-BzOCOCOCOC <b>XXIV</b>	MeCN	328.5 (4.60)	
TTh=-BzOCOCOCOCOC <b>XXVII</b>	MeCN	329.0 (4.60)	
TTh=-BzOCOCOCOCOCOC <b>XXV</b>	MeCN	328.5 (4.59)	
TTh=-BzOCOCOCOCOCOC <b>XXVIII</b>	MeCN	329.0 (4.64)	
TTh=-BzOCOCOBz=-TTh <b>LXI</b>	CH <sub>2</sub> Cl <sub>2</sub>	330.0 (4.88)	
TTh=-BzOCOCOBz=-TTh <b>LXII</b>	CH <sub>2</sub> Cl <sub>2</sub>	330.0 (4.86)	
TTh=-BzOCOCOBz=-TTh <b>LXIII</b>	CH <sub>2</sub> Cl <sub>2</sub>	331.0 (4.91)	

In summary, from a comparison of the data obtained for the series of styryl-terthiophenes, it appears that the UV spectra observed consists of the superimposition of the electronic transitions for the two constituent chromophores. The slightly shifted terthiophene absorbance can be seen clearly in the spectrum of the parent styryl-terthiophene **LXXVI**, as a shoulder in the spectrum of compound **LXXVII**, and is merged with the styryl-thiophene absorbance for the remaining dialkoxy-substituted styryl-terthiophenes. The higher energy styryl-thiophene absorbance gradually moves toward the red end of the spectrum with the incorporation of additional alkoxy groups on the benzene ring. The overlap of these two peaks leads to spectra for the dialkoxy-substituted compounds that display a single broad absorbance.

The terthiophene hemicrowns **LXI-LXIII** possess the same conjugated styryl-terthiophene moiety as do the simpler monomers, and would be expected to absorb at the same wavelength as the corresponding dialkoxy-substituted terthiophenes. This has been shown to be the case, and in addition the extinction coefficients of the bis(terthiophene) compounds are approximately double that obtained for the monomers containing a single styryl-terthiophene unit.

#### 4.1.2.2 Absorbance of thiophene monomers

The same trends observed for the terthiophene monomers are evident in the corresponding data for the thiophene monomers (Table 4.4).

**Table 4.4 Solution absorbance maxima of thiophene monomers**

Compound	Solvent	Solution $\lambda_{\max}$ / nm (log $\epsilon$ )		
Th=-Bz <sup>163</sup>	MeCN	225.0 (2.35)	291.0 (4.40)	
Th=-BzOMe <sup>163</sup>	MeCN	212.0 (4.22)	300.0 (4.49)	
Th=-Bz(OMe) <sub>2</sub> <b>XXXVI</b>	MeCN	216.5 (4.26)	297.5 (4.38)	318.0 (4.40)
Th=-Bz15c5 <b>XV</b>	MeCN	216.0 (4.27)	298.5 (4.39)	318.0 (4.41)
Th=-Bz18c6 <b>XVI</b>	MeCN	217.5 (4.21)	298.5 (4.31)	318.5 (4.34)
Th=-BzOCOCOC <b>XXX</b>	MeCN	216.0 (4.26)	298.0 (4.36)	317.0 (4.38)
Th=-BzOCOCOC <b>XXXIII</b>	MeCN	216.0 (4.24)	298.0 (4.33)	317.0 (4.35)
Th=-BzOCOCOCOC <b>XXXI</b>	MeCN	216.5 (4.25)	298.0 (4.28)	317.0 (4.30)
Th=-BzOCOCOCOC <b>XXXIV</b>	MeCN	216.0 (4.26)	298.0 (4.38)	317.5 (4.42)
Th=-BzOCOCOCOCOC <b>XXXII</b>	MeCN	216.0 (4.25)	298.0 (4.35)	317.0 (4.37)
Th=-BzOCOCOCOCOC <b>XXXV</b>	MeCN	216.0 (4.26)	298.0 (4.38)	317.5 (4.41)
<i>syn</i> Th=-Bz18c6Bz=-Th <b>LIX</b>	CH <sub>2</sub> Cl <sub>2</sub>		299.5 (4.55)	320.0 (4.57)
<i>anti</i> Th=-Bz18c6Bz=-Th <b>LX</b>	CH <sub>2</sub> Cl <sub>2</sub>		300.0 (4.49)	320.0 (4.51)
Th=-BzOCOCOBz=-Th <b>LXIV</b>	CH <sub>2</sub> Cl <sub>2</sub>		300.5 (4.63)	319.0 (4.67)
Th=-BzOCOCOBz=-Th <b>LXV</b>	CH <sub>2</sub> Cl <sub>2</sub>		300.5 (4.70)	320.0 (4.75)
Th=-BzOCOCOBz=-Th <b>LXVI</b>	CH <sub>2</sub> Cl <sub>2</sub>		300.5 (4.68)	319.5 (4.72)

Previously reported data indicates a bathochromic shift of 9 nm on incorporation of the alkoxy auxochrome into 3-styrylthiophene.<sup>163</sup> The inclusion of a second alkoxy functionality causes the appearance of an additional peak at 320 nm. It is possible that either a new peak has appeared, or that a hidden peak has been revealed due to a shift caused by the substituent. Given that the methoxy group is an auxochrome not a chromophore, and the large  $\epsilon$  values of the peaks, the latter explanation seems more likely. Furthermore, the same absorbances are seen for all the remaining structures. As seen for their terthiophene analogues, increasing the length of the polyether chain attached to the molecule has no effect on the position of the absorbance maximum. Again, the hemicrowns **LXIV-LXVI** absorb at the same wavelength as their thiophene equivalents, but with an extinction coefficient that has approximately

doubled. Due to the lack of solubility of the bis(thiophene) compounds in MeCN, their spectra were obtained in CH<sub>2</sub>Cl<sub>2</sub>, and hence the lowest wavelength band (*ca.* 216 nm) is not observed.

### 4.1.2.3 Absorbance of terthiophene dimers

The absorbance of terthiophene dimers was examined both in CH<sub>2</sub>Cl<sub>2</sub> solution and in the solid-state. Films used for solid-state UV measurements were prepared by repetitive evaporation of drops of a CH<sub>2</sub>Cl<sub>2</sub> solution containing the sexithiophene, onto polished quartz. The solution and thin film absorbance data is tabulated in Table 4.5, and example spectra are shown in Fig. 4.8.

**Table 4.5 Solution and solid-state absorbance maxima of terthiophene dimers**

Compound	Solution $\lambda_{\max}$ / nm		Thin film $\lambda_{\max}$ / nm		
	(log $\epsilon$ )				
(TTh=-Bz(OMe) <sub>2</sub> ) <sub>2</sub> <b>LXXV</b>	335.5 (4.80)	445.0 (4.55)	284.5	342.5	510.0 555.0 (s)
(TTh=-Bz15c5) <sub>2</sub> <b>LXVII</b>	336.0 (4.82)	450.0 (4.59)		357.0	499.0
(TTh=-Bz18c6) <sub>2</sub> <b>LXVIII</b>	335.5 (4.83)	445.5 (4.56)		346.0	480.0
(TTh=-BzOCOCOC) <sub>2</sub> <b>LXIX</b>	334.5 (4.83)	451.5 (4.61)	289.5	352.5	528.0
(TTh=-BzOCOCOC) <sub>2</sub> <b>LXXII</b>	336.0 (4.78)	458.5 (4.62)	291.0	380.0	510.5
(TTh=-BzOCOCOCOC) <sub>2</sub> <b>LXX</b>	334.5 (4.81)	446.0 (4.57)	278.5	348.0	499.5
(TTh=-BzOCOCOCOC) <sub>2</sub> <b>LXXIII</b>	335.5 (4.82)	448.0 (4.60)	279.5	348.5	489.0
(TTh=-BzOCOCOCOCOC) <sub>2</sub> <b>LXXI</b>	335.5 (4.80)	450.5 (4.61)	281.5	342.5	485.0
(TTh=-BzOCOCOCOCOC) <sub>2</sub> <b>LXXIV</b>	336.5 (4.81)	454.0 (4.63)	285.0	344.5	478.0

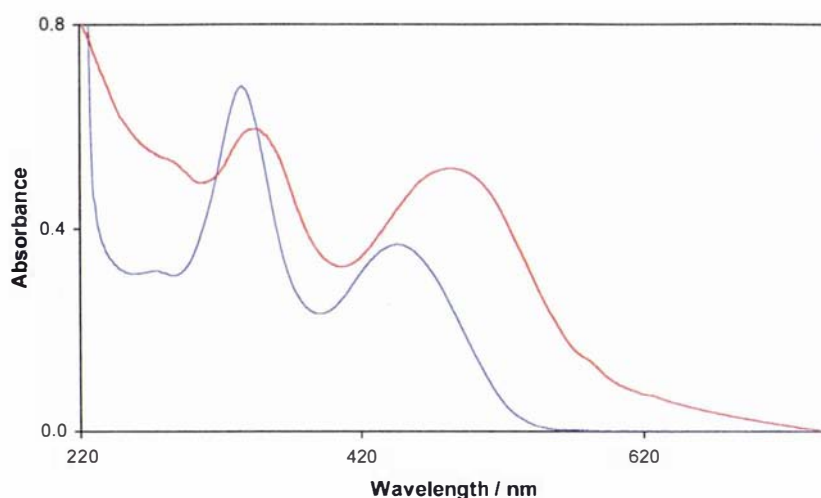


**Figure 4.8 Solution (blue) and thin film (red) UV/VIS spectra of 18-crown-6 terthiophene dimer LXVIII**

The red shift seen in the  $\pi$ - $\pi^*$  band on going from solution to the solid-state is characteristic of soluble polythiophenes, and has been attributed to conformational changes.<sup>97, 262</sup> It has been proposed that oligothiophenes adopt a flexible coil-like structure in solution where adjacent thiophene rings can deviate from coplanarity, and the increase in conjugation length seen in the solid-state is caused by a transition to a more rigid rod-like conformation.<sup>97, 263</sup>

There is a clear trend visible in the film data, with  $\lambda_{\text{max}}$  decreasing from 555 nm to 478 nm with increasing polyether chain length. This trend is not apparent in the solution data, and therefore is probably related to the conformation of the sexithiophenes in the solid-state. It seems likely that this is a steric effect rather than an electronic effect, and that the longer polyether chains are causing the molecules to adopt a less planar conformation. In addition, the effect is greater for the vanillin-derived compounds (LXXII - LXXIV) than for the isovanillin-derived equivalents (LXIX - LXXI). X-ray crystal structures could provide valuable information to assist in interpreting the spectral data, however numerous attempts to form suitable crystals from these compounds were unsuccessful. The evidence here implies that while all of the sexithiophenes have a similar conformation in solution, those with polyether chains are prevented to varying degrees from making the conformational transition to the more electronically delocalized rod structure.

While these  $\lambda_{\text{max}}$  values are at least as high as those reported by other researchers for polymerised terthiophene derivatives comprising up to 21 thiophene rings,<sup>97, 250</sup> only dimers were detectable by MALDI-MS. This implies that while longer oligomers were present in the quoted research, the effective conjugation length may have been as short as six thiophene rings. In turn, this suggests that the sexithiophenes synthesised here could potentially have electrochemical properties as good as some considerably longer oligothiophenes.

### **4.1.3 Effect of cation complexation on terthiophene monomer UV/VIS spectra**

An investigation was carried out into the UV/VIS spectra of the polyether-substituted terthiophenes, to see if the data could be used to determine cation binding affinities. UV/VIS spectroscopy gives a measure of the energy required to promote an electron from a bonding to an antibonding molecular orbital. In an extended  $\pi$ -system such as those existing in styryl terthiophenes, the energy of this transition is sufficiently low that it falls in the visible part of the electromagnetic spectrum, hence the yellow colour of the compounds. It was anticipated that the binding of cations to the polyether part of the molecules would pull electron density away from the molecule, therefore shifting its  $\pi$ - $\pi^*$  absorbance to higher energy (shorter wavelength). Different cations could be expected to bind to the molecules to varying degrees, thus affecting their spectra by differing amounts, so that observable changes in the UV/VIS spectra could be used as a measure of how well each cation bound.

#### 4.1.3.1 Experimental procedure

The effect of complexation on the UV/VIS spectra of the polyether-substituted terthiophenes synthesised during the course of this research was investigated by measuring the UV/VIS spectra before and after the addition of various metal ions. Terthiophene compounds (**I**, **II**, **XXIII** - **XXVIII**, **XXIX**, **LXXVI** - **LXXVII**, **LXI** - **LXIII**) were used at a concentration of  $1.5 \times 10^{-5}$  –  $2.8 \times 10^{-5}$  M in spectroscopy-grade acetonitrile. Stock solutions of the metal ions were prepared as either the perchlorate ( $\text{Li}^+$ ,  $\text{Na}^+$ ,  $\text{Ag}^+$ ,  $\text{N}(\text{Bu})_4^+$ ,  $\text{Mg}^{2+}$ ,  $\text{Ca}^{2+}$ ,  $\text{Sr}^{2+}$ ,  $\text{Ba}^{2+}$ ,  $\text{Ni}^{2+}$ ,  $\text{Co}^{2+}$ ,  $\text{Zn}^{2+}$ ,  $\text{Mn}^{2+}$ ,  $\text{Cd}^{2+}$ ,  $\text{Pb}^{2+}$ ) or hexafluorophosphate ( $\text{K}^+$ ,  $\text{NH}_4^+$ ) at 0.4 M in acetonitrile.  $\text{RbClO}_4$  and  $\text{CsClO}_4$  were used as a saturated solution in acetonitrile. 5-10  $\mu\text{L}$  of the relevant metal ion or acetonitrile blank was added to 3 mL of terthiophene derivative to give a metal ion excess of 50 fold. The change in the position of the absorbance maxima was measured from 310 nm (**LXXVI**), 322 nm (**LXXVII**) or 328.5 nm for all remaining compounds. In all cases, the position of the absorbance maxima was either unchanged (within the limits of experimental error estimated at  $\pm 1.5$  nm), or hypsochromically shifted on addition of metal ions.

Spectra were collected using a Shimadzu UV-3101PC UV/VIS/NIR Scanning Spectrophotometer controlled by a PC running standard Shimadzu software. Data was exported to Microsoft Excel for further processing.

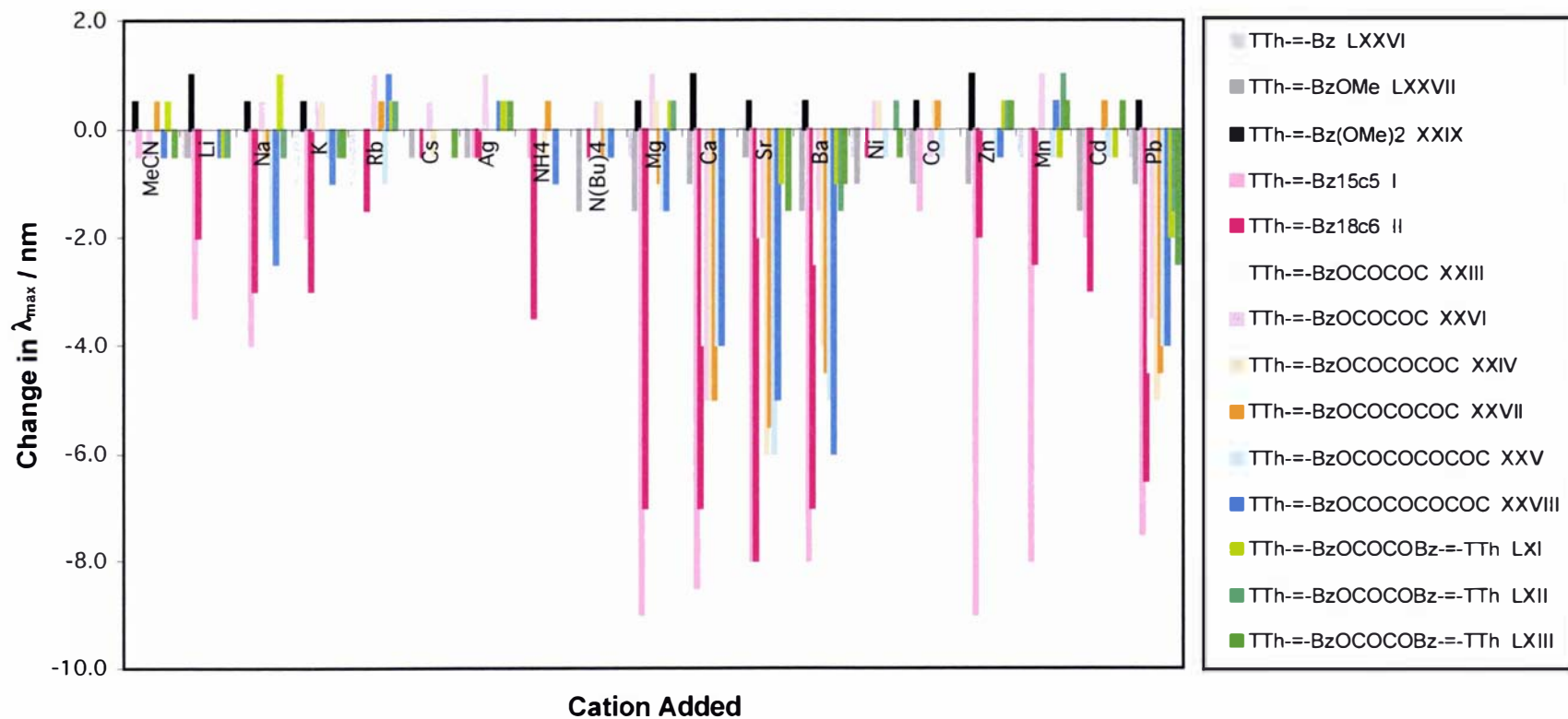


Figure 4.9 Change in absorbance maxima caused by addition of metal cations to terthiophene monomers

### 4.1.3.2 Discussion

The changes in absorbance maxima for all the styryl terthiophenes previously discussed with a variety of metal cations are summarized in Fig. 4.9. Given the change in absorbance maxima observed on addition of MeCN, it appears that the noise level in this data is approximately  $\pm 1.5$  nm. As the absorbances are rather broad for these types of compound, the peak values obtained tended to vary slightly from sample to sample, and this is thought to be the major contributor to the noise observed. Only responses greater than  $\pm 1.5$  nm are considered significant and discussed below.

The results obtained from this work can be most easily analysed by considering the cations used in their periodical groups.

It is clear from the data presented for the alkali metal cations ( $\text{Li}^+$ ,  $\text{Na}^+$ ,  $\text{K}^+$ ,  $\text{Rb}^+$ ,  $\text{Cs}^+$ ), that the crown ether terthiophenes **I** and **II** show a greater response than do the open-chain compounds. This is not surprising, given the free energy cost involved in organizing the polyether chain into the correct conformation for cation binding.<sup>10</sup> 15-crown-5 terthiophene **I** exhibits the largest  $\lambda_{\text{max}}$  shift when  $\text{Na}^+$  is added, with smaller effects caused by  $\text{Li}^+$  and  $\text{K}^+$ . In contrast, **II**, with its larger cavity size, shows a response of the order  $\text{Na}^+=\text{K}^>\text{Li}^>\text{Rb}^+$ . These results can be rationalized from the size data provided in Tables 4.1 and 4.2.

Only one response can be seen from any of the compounds investigated to the remaining three monocations  $\text{Ag}^+$ ,  $\text{NH}_4^+$  and  $\text{N}(\text{Bu})_4^+$ . 18-crown-6 terthiophene **II** showed a 3.5 nm shift of  $\lambda_{\text{max}}$  on complexation with  $\text{NH}_4^+$ . From the data given above in Tables 4.1 and 4.2, this is to be expected due to a size fit between the cation and the crown ether cavity. Neither  $\text{Ag}^+$  or  $\text{N}(\text{Bu})_4^+$  has any effect on UV/VIS spectra, and it seems most likely that it is due to the size of  $\text{N}(\text{Bu})_4^+$ , and electronic effects for  $\text{Ag}^+$ .

The next group of cations to be considered was the alkaline earth metal ions ( $\text{Mg}^{2+}$ ,  $\text{Ca}^{2+}$ ,  $\text{Sr}^{2+}$ ,  $\text{Ba}^{2+}$ ). 15-crown-5 terthiophene **I** showed the largest wavelength shift on addition of  $\text{Mg}^{2+}$ , followed by  $\text{Ca}^{2+}$ ,  $\text{Sr}^{2+}$  and  $\text{Ba}^{2+}$ , as would be expected by a

consideration of their relative sizes (Tables 4.1 and 4.2). It should be noted that although  $\text{Mg}^{2+}$  appears too small for the cavity, benzo-crown ethers will have slightly smaller cavities than those given in Table 4.1 due to the constraints imposed by the benzene ring. In contrast, the larger styryl-18-crown-6 terthiophene **II** should exhibit its largest wavelength shift with one of the larger alkaline metal cations. This is indeed the case, as shown in Fig. 4.9, where the greatest shift is caused by  $\text{Sr}^{2+}$ , followed by  $\text{Ba}^{2+}$ ,  $\text{Ca}^{2+}$  and  $\text{Mg}^{2+}$ .

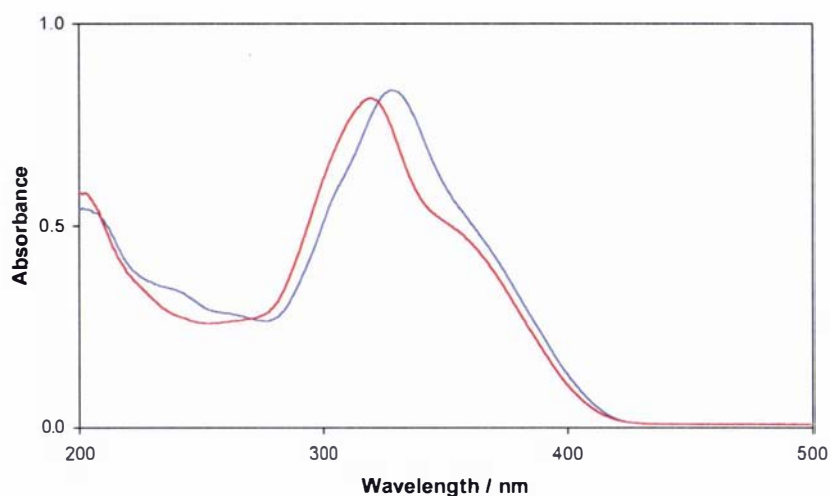


**Figure 4.10** Styryl-15-crown-5 terthiophene **I** before (blue) and after (red) addition of  $\text{Mg}^{2+}$

The spectra for styryl-15-crown-5 terthiophene before and after the addition of  $\text{Mg}^{2+}$  are shown in Fig. 4.10. On addition of the metal ion, the spectrum of **I** clearly starts to resemble the unsubstituted styryl-terthiophene monomer shown in Fig. 4.7. This is consistent with previous research (Section 4.1.1.2) where complexation by metal cations reduced the bathochromic effect of the ether auxochromes, resulting in a hypsochromic shift of the absorption maxima.

All three sets of open-chain compounds display size-related wavelength shifts. The compounds with the shortest chains, **XXIII** and **XXVI**, show the largest response to  $\text{Ca}^{2+}$ , with considerably smaller shifts caused by  $\text{Sr}^{2+}$  and  $\text{Ba}^{2+}$ . Intermediate chain length compounds **XXIV** and **XXVII** show responses in the order  $\text{Sr}^{2+} > \text{Ca}^{2+} > \text{Ba}^{2+}$ . The compounds containing the longest polyether chains, **XXV** and **XXVIII**, show an equal response to  $\text{Sr}^{2+}$  and  $\text{Ba}^{2+}$ , with a lesser shift caused by  $\text{Ca}^{2+}$ .  $\text{Mg}^{2+}$  did not cause

an appreciable shift in the wavelength maximum for any of the open-chain compounds.

The remaining dications ( $\text{Ni}^{2+}$ ,  $\text{Co}^{2+}$ ,  $\text{Zn}^{2+}$ ,  $\text{Mn}^{2+}$ ,  $\text{Cd}^{2+}$  and  $\text{Pb}^{2+}$ ) will be considered together. While 18-crown-6 terthiophene **II** shows an increasing response with increasing size ( $\text{Pb}^{2+} > \text{Cd}^{2+} > \text{Mn}^{2+} > \text{Zn}^{2+} > \text{Co}^{2+} > \text{Ni}^{2+}$ ), a straight size-dependence is not observed for 15-crown-5 terthiophene **I**. The response for the five cations  $\text{Zn}^{2+} > \text{Mn}^{2+} > \text{Cd}^{2+} > \text{Co}^{2+} > \text{Ni}^{2+}$  is quite reasonable in terms of cation size, but the increased response for  $\text{Pb}^{2+}$  suggests that in this case, electronic factors also come into play. This idea is further strengthened by the fact that while the bis(terthiophenes) show no response to any of the alkali or alkaline metal ions, or any of the transition metal ions, they all show a wavelength shift caused by  $\text{Pb}^{2+}$ . Thus  $\text{Pb}^{2+}$  is having a greater effect on the absorbance of the polyether-substituted crowns than would be expected based on its size and charge alone. Hard-soft-acid-base theory states that hard cations will complex preferentially with hard ligands, and soft cations with soft ligands. One measure of the 'hardness' or 'softness' of a cation is the Misono softness parameter (Y), which is related to the ionic radius, valence charge and ionization potential of a cation. Misono softness values for various metal ions are given below in Table 4.6.

**Table 4.6 Misono softness values for metal cations**

Metal Ion	Misono Softness (Y)	Metal Ion	Misono Softness (Y)
$\text{Li}^+$	0.36	$\text{Mg}^{2+}$	0.87
$\text{K}^+$	0.92	$\text{Ca}^{2+}$	1.62
$\text{Na}^+$	0.93	$\text{Sr}^{2+}$	2.08
$\text{Rb}^+$	2.27	$\text{Zn}^{2+}$	2.34
$\text{Cs}^+$	2.73	$\text{Ba}^{2+}$	2.62
		$\text{Ni}^{2+}$	2.82
		$\text{Cu}^{2+}$	2.89
		$\text{Co}^{2+}$	2.96
		$\text{Mn}^{2+}$	3.03
		$\text{Cd}^{2+}$	3.04
		$\text{Fe}^{2+}$	3.09
		$\text{Sn}^{2+}$	3.17
		$\text{Pb}^{2+}$	3.58
		$\text{Hg}^{2+}$	4.25

Cations with Misono softness values  $Y < 2.5$  are classed as hard cations, and those with  $Y > 3.2$  as soft cations. Values of  $2.5 < Y < 3.2$  are borderline cases, where complexation will depend on environmental factors such as solvent. It is well known that oxygen is a hard ligand, and as such will preferentially complex hard cations. This is the reason why crown ethers complex alkali and alkaline earth metal cations so strongly, whereas they rarely form complexes with transition metal ions.<sup>9</sup> However, the particular monomers studied in this research also incorporate sulphur atoms. Sulphur is a soft ligand, and soft cations would preferentially bind to sulphur over oxygen. It can be seen from the data presented in Table 4.6 that the only metal ion studied here that can be classified as a soft cation is  $Pb^{2+}$ . The data in Fig. 4.9 shows that  $Pb^{2+}$  has an effect on the spectra of all the polyether-substituted terthiophenes, and it seems likely that this is due to complexation between the thienyl sulphur atoms and the dissolved soft metal ion. Given that the magnitude of this effect varies between the different types of polyether-substituted monomers, and that no change is seen in the spectra of the reference compounds, it is clear that the polyether chain is also playing a role. This is consistent with results published by McCullough and Williams (Section 4.1.1.3) where they see a particularly strong complexation effect on addition of  $Pb^{2+}$  or  $Hg^{2+}$  to a solution of poly(3-[2,5,8-trioxanonyl]thiophene).<sup>100</sup>

The absorption maxima for the three reference compounds **LXXVI**, **LXXVII** and **XXXIX** are unaffected by all of the cations tested. This shows that the wavelength shifts observed are not caused simply by the presence of the metal ion cations, but that the cations must be complexed to some degree in order to exert an effect. In addition, no significant wavelength changes were noted on addition of MeCN to any of the compounds tested.

## **4.2 Fluorescence Spectroscopy**

Given that terthiophene fluoresces, it seemed reasonable that the electronic changes caused by a cation binding to the crown ether cavity could affect the fluorescence output of the terthiophene monomers synthesised. Furthermore, the change in fluorescence observed could provide a measure of the binding affinity of a range of cations for a particular polyether monomer. A survey of the literature was therefore undertaken in order to see what research had been previously carried out in the areas of (i) determining cation binding to crowns by fluorescence spectroscopy, and (ii) terthiophene fluorescence.

### **4.2.1 Literature review**

#### **4.2.1.1 Fluorescence of substituted crown ethers**

Due to their well-known cation binding properties, crown ethers have been incorporated into many different types of molecules for use as ion-sensors. In general, these compounds consist of a crown ether covalently linked to a fluorophore, where it is expected that the electronic change caused by complexation will cause a change in the fluorescence properties of the molecule. Two main effects have been noted by researchers working in this area. By far the most common is complexation enhanced quenching of fluorescence (CEQF) whereby the binding of a cation by the crown ether causes a decrease in the fluorescence intensity observed. Less frequently observed is complexation enhanced fluorescence (CEF), where a binding event causes an increase in fluorescence. This is usually observed when the cation either interrupts

intramolecular quenching between functional groups in a molecule, or when a non- or weakly-quenching cation displaces a more strongly quenching cation.<sup>264</sup>

To the best of our knowledge, there are only two fluorescence studies into the cation binding of styryl-substituted benzo-crown ethers published in the scientific literature. Barzykin *et al.*<sup>190</sup> synthesised the benzo-crown ether styryl dye shown in Fig. 4.11a, and examined its fluorescence response to  $Mg^{2+}$ ,  $Ba^{2+}$  and  $Ca^{2+}$  in acetonitrile. They observed a hypsochromic shift of the fluorescence emission peak of the *trans* isomer, with a concomitant decrease in fluorescence intensity. Shin<sup>251</sup> looked at a vinylanthracene fluorophore (Fig. 4.11b) and saw a dramatic  $Mg^{2+}$  induced fluorescence enhancement effect. This was attributed to the complexed cation inhibiting intramolecular charge transfer from the crown ether moiety to the anthrylene moiety.

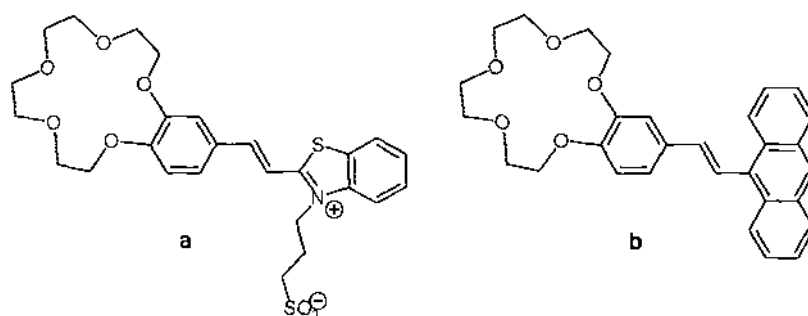


**Figure 4.11** Crown ether styryl dyes of Barzykin (a) and Shin (b)

Similar molecules exist in the form of styryl-substituted aza-crown ethers, and to date three investigations into the effect of cation complexation on their fluorescence spectra have been carried out.<sup>255-257</sup>

Fery-Forgues *et al.* looked at a benzoxazinone derivative of aza-15-crown-5 (Fig. 4.12a).<sup>255</sup> In their study they noted a hypsochromic shift of the fluorescence emission maxima, and an enhancement of the fluorescence signal. Bourson and Valeur<sup>256</sup> synthesised a crown-substituted merocyanine shown in Fig. 4.12b. On complexation of various cations, they describe a hypsochromic shift and reduction in intensity of the fluorescence peak. Two styrylbenzodiazinones studied by Cazaux *et al.*<sup>257</sup> are also

shown in Fig. 4.12c-d. While both compounds displayed hypsochromic shifts on cation complexation, for compound 4.12c the fluorescence intensity was increased, whereas for 4.12d it decreased. The results are explained by noting the donor/acceptor nature of compounds 4.12a and 4.12c, and their similarity of behaviour, which contrasts with the the two donor/acceptor/donor molecules 4.12b and 4.12d.

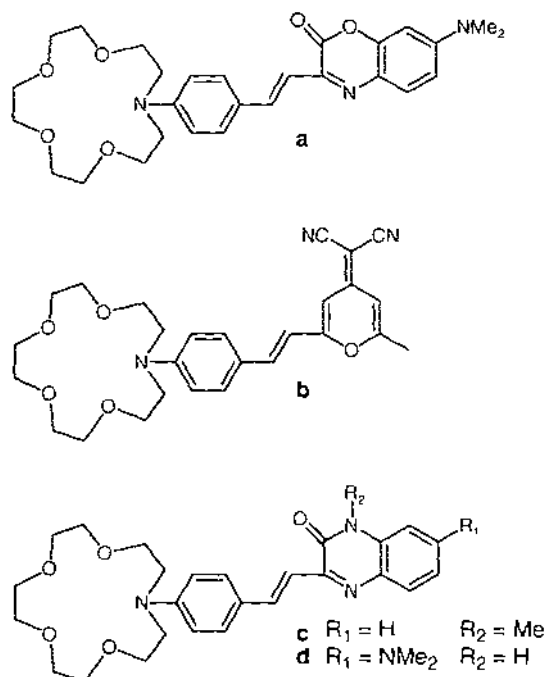


**Figure 4.12 Styryl-substituted aza crown ethers**

There are many other literature examples of fluorophores covalently linked to crown ethers,<sup>265-267</sup> benzo-crown ethers,<sup>268-272</sup> aza-crown ethers,<sup>256, 273-275</sup> pyridino crown ethers<sup>276</sup> and open-chain ethers<sup>277</sup> that display complexation enhanced fluorescence quenching.

#### 4.2.1.2 Fluorescence of substituted terthiophenes

The fluorescence of thiophene oligomers has been well studied,<sup>240, 246, 278-287</sup> and their emission spectra show two main peaks. For terthiophene in dichloromethane (absorbance  $\lambda_{max} = 354$  nm), the fluorescence maxima peaks are observed at 411 and

433 nm, with a fluorescence quantum yield ( $\Phi_F$ ) of 0.055.<sup>240</sup> The more structured fluorescence spectrum indicates that the molecule is more rigid in the first relaxed excited singlet state. This has been explained on the basis of the excited state having a quinoidal-like form that is essentially planar, while in the ground state the molecule is free to rotate.<sup>288</sup> The major deactivation pathway of the  $S_1$  excited state of oligothiophenes involves an intersystem crossing process from  $S_1$  to  $T_1$ .<sup>243</sup> While the sulphur atom in oligothiophenes has only a minor effect on the electronic spectra, essentially holding the molecule in a *cis*-diene configuration, it has a major influence on fluorescence.<sup>246</sup> It is well established that molecules containing moderately heavy atoms such as sulphur have large spin-orbit coupling. This allows unpairing of electron spins, and hence intersystem crossing from singlet to triplet excited states.<sup>5</sup> Clearly, the nature of substituents attached to oligothiophenes has an effect on the energy of the singlet and triplet excited states, and as the energy gap between  $S_1$  and  $T_1$  decreases, the rate of intersystem crossing will increase.<sup>243</sup> This effect is clearly evidenced by the collection of triplet quantum yield data where  $\Phi_T$  for substituted terthiophenes is as high as 0.99.<sup>246</sup> An increase in oligomer length shifts both the absorbance and fluorescence peaks to longer wavelength, with a concomitant increase in fluorescence quantum yield. This effect has been attributed to a decrease in nonradiative decay in longer oligothiophenes,<sup>284</sup> and is evidenced by a decrease in  $\Phi_T$ .<sup>279</sup> Despite the high value of  $\Phi_T$  (0.90) for terthiophene, no phosphorescence has been observed. This can only mean that the non-radiative rate constant from the lowest triplet state to the ground state is considerably larger than the corresponding radiative rate constant.<sup>279</sup> This high radiationless rate constant has been explained by inter-ring bond torsional coupling to the ground state, effectively quenching phosphorescence.<sup>288</sup> While a literature report claiming the first evidence of phosphorescence from poly(3-hexylthiophene), terthiophene and  $\alpha$ -bromoterthiophene can be found,<sup>289</sup> doubt has been cast on the results by other researchers<sup>279, 288</sup>. In addition, researchers previously investigating the photoexcitation of  $\alpha$ -terthiophene failed to observe any phosphorescence.<sup>262, 290, 291</sup>

Substituted terthiophenes with a large range of fluorescence peak maxima and quantum yields can be found in the literature. Some derivatives (eg. 3,4'-dihexylterthiophene and 3,3''-dimethoxyterthiophene) show significant changes in the

UV (Section 4.1.1.1), but very little difference in their fluorescence spectra.<sup>241, 243-245</sup> 5-theonylterthiophene and 5-benzoylterthiophene show significantly red-shifted fluorescence maxima, attributed to the additional aromatic ring stabilizing the excited state.<sup>248</sup> One of the more dramatic examples is that of 5-nitroterthiophene. The fluorescence maxima for this compound is shifted by almost 70 nm compared to terthiophene, and  $\Phi_F$  increases from 0.055 to 0.34. 5-bromo-5''-nitroterthiophene has an even larger  $\Phi_F$  of 0.55. These results are explained by intramolecular charge transfer occurring in the excited state, vastly increasing the lifetime of the excited state and presumably decreasing intersystem crossing.<sup>240</sup> To the best of our knowledge, at the time of this research, there was no fluorescence data published on terthiophenes mono-substituted at the 3'-position. Rather, the majority of the work (discussed above) has been carried out on symmetrical molecules, or on those substituted at the  $\alpha$ -positions.

#### 4.2.1.3 Fluorescence of crown ether-substituted thiophenes

Despite the ability of terthiophene to fluoresce, none of the crown- or polyether-substituted terthiophene compounds published to date have included an investigation of this property. However, there is an example of a thiophene-substituted benzo-crown ether synthesised by Cielen *et al.* that is of interest (Fig. 4.13).<sup>292</sup>

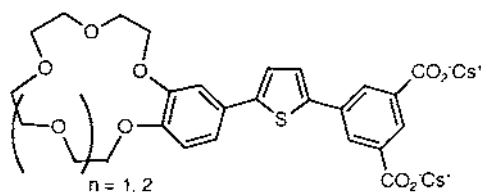


**Figure 4.13** Benzo-crown ether fluorophore synthesised by Cielen *et al.*

The carboxylated functionalities on the phenyl ring were designed to improve the solubility of the compound, allowing spectroscopy to be carried out in aqueous buffers. Under the conditions employed, the compounds showed no change in the

positions of the absorption or emission maxima upon addition of  $\text{Li}^+$ ,  $\text{Na}^+$ ,  $\text{K}^+$ ,  $\text{Cs}^+$ ,  $\text{Mg}^{2+}$  or  $\text{Ca}^{2+}$ , but did show a change in emission intensity. Interestingly some metal ions increased the fluorescence intensity, while other metal ions had the opposite effect and decreased the response. Although the 15-crown-5 compound showed no discrimination between  $\text{Na}^+$  and  $\text{K}^+$  ions, the 18-crown-6 based molecule displayed a selectivity of 3:1 for  $\text{K}^+$  over  $\text{Na}^+$ .

In later work utilizing the same fluorophore, the group tested three new (di)pyridino crown ethers (Fig. 4.14).<sup>276</sup>

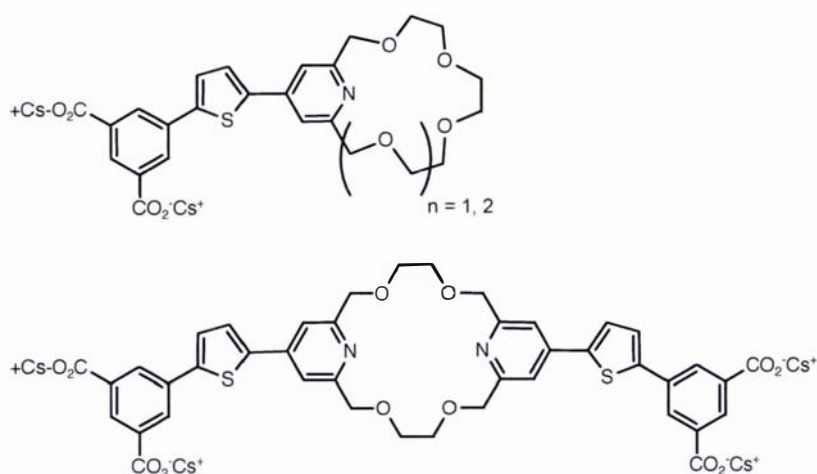


**Figure 4.14 Pyridino crown ethers containing thiophene-based fluorophore(s)**

As for the benzo-crown ethers, the positions of absorption and emission maxima were not altered by the addition of metal ions. However, in contrast to the results obtained for the benzo-crown derived materials, addition of metal ions caused a decrease in fluorescence intensity for all the ions studied. Again, the 15-membered ring showed little selectivity between metal ions, whereas both the 18-membered ring and the difunctionalised compound showed the greatest response to  $\text{K}^+$ .

## 4.2.2 Fluorescence of polyether-substituted oligothiophenes

Tabulated fluorescence data for the complete range of terthiophene and sexithiophene compounds is presented below in Table 4.7. The difference between the emission and absorption bands (Stokes shift) is calculated, and can be related to the stability of the excited state of the molecule.<sup>240</sup> Data for terthiophene and sexithiophene is also included for comparison.

**Table 4.7** Fluorescence data for terthiophene and sexithiophene monomers obtained in CH<sub>2</sub>Cl<sub>2</sub>

Compound	E <sub>x</sub> λ <sub>max</sub> / nm	E <sub>m</sub> λ <sub>max</sub> / nm	Δλ <sub>max</sub> / nm (Stokes shift)
Terthiophene <sup>240</sup>	354	411, 433	79
TTh=-Bz <b>LXXVI</b>	312	449	137
TTh=-BzOMe <b>LXXVII</b>	323	444	121
TTh=-Bz(OMe) <sub>2</sub> <b>XXIX</b>	330	443	113
TTh=-Bz15c5 <b>I</b>	330	446	116
TTh=-Bz18c6 <b>II</b>	330	444	114
TTh=-BzOCOCOC <b>XXIII</b>	330	443	113
TTh=-BzOCOCOC <b>XXVI</b>	330	445	115
TTh=-BzOCOCOCOC <b>XXIV</b>	330	442	112
TTh=-BzOCOCOCOCOC <b>XXVII</b>	330	445	115
TTh=-BzOCOCOCOCOCOC <b>XXV</b>	330	444	114
TTh=-BzOCOCOCOCOCOC <b>XXVIII</b>	330	445	115
TTh=-BzOCOCOBz=-TTh <b>LXI</b>	330	445	115
TTh=-BzOCOCOBz=-TTh <b>LXII</b>	330	445	115
TTh=-BzOCOCOBz=-TTh <b>LXIII</b>	330	448	118
Sexithiophene <sup>240</sup>	432	512, 548	116
(TTh=-Bz) <sub>2</sub>	320, 450	546	226, 96
(TTh=-BzOMe) <sub>2</sub>	330, 445	543	213, 98
(TTh=-Bz(OMe) <sub>2</sub> ) <sub>2</sub>	335, 445	545	210, 100
(TTh=-Bz15c5) <sub>2</sub> <b>LXVII</b>	335, 450	549	214, 99
(TTh=-Bz18c6) <sub>2</sub> <b>LXVIII</b>	335, 445	546	211, 101
(TTh=-BzOCOCOC) <sub>2</sub> <b>LXIX</b>	335, 450	545	210, 95
(TTh=-BzOCOCOC) <sub>2</sub> <b>LXXII</b>	335, 445	545	210, 100
(TTh=-BzOCOCOCOC) <sub>2</sub> <b>LXX</b>	335, 445	545	210, 100
(TTh=-BzOCOCOCOC) <sub>2</sub> <b>LXXIII</b>	335, 445	545	210, 100
(TTh=-BzOCOCOCOCOC) <sub>2</sub> <b>LXXI</b>	335, 445	545	210, 100
(TTh=-BzOCOCOCOCOC) <sub>2</sub> <b>LXXIV</b>	335, 455	546	211, 91

An example of the fluorescence spectra obtained for the terthiophene and sexithiophene monomers is shown in Fig. 4.15, along with their absorbance spectra.

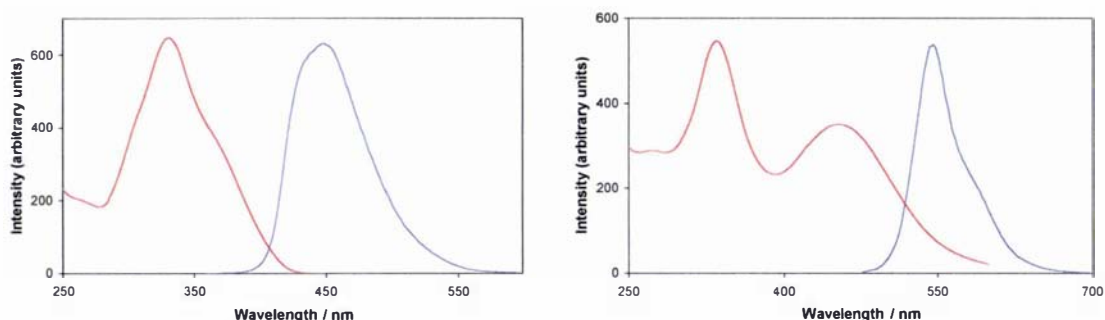


**Figure 4.15 Absorbance (red) and fluorescence (blue) spectra for polyether-substituted terthiophene XXVII (left) and polyether-substituted sexithiophene LXIX (right) in  $\text{CH}_2\text{Cl}_2$**

It can be seen from the tabulated data, that the fluorescence spectra of the styryl ter- and sexi-thiophenes show considerably less structure than the parent compounds. The reason given for the increase in structure seen for the fluorescence spectra of terthiophene and sexithiophene over their absorption spectra, is an increase in rigidity of the molecule in the first relaxed excited state.<sup>288</sup> Thus, it follows that this is likely not the case for the synthesised styryl-derivatives.

The Stokes shifts for all the dialkoxy-substituted compounds are larger than that obtained for terthiophene, indicating that the excited state is more stable.<sup>240</sup> A decrease in Stokes shift is seen on incorporation of alkoxy groups from styryl terthiophene **LXXVI** to methoxystyryl terthiophene **LXXVII** to dimethoxystyryl terthiophene **XXXVI**, indicating that the inclusion of these alkoxy groups destabilizes the excited state. The values are then fairly constant for all the crown and open-chain terthiophenes, and for the bis(terthiophene) hemicrowns. The sexithiophenes show the same pattern on incorporation of methoxy groups, with a decrease in Stokes shift. In addition, the emission wavelength for these compounds is independent of the wavelength chosen for excitation, indicating that the same first relaxed excited state is reached regardless of excitation wavelength.

## 4.2.3 Effect of cation complexation on terthiophene monomer fluorescence spectra

### 4.2.3.1 Experimental procedure

The effect of complexation on the fluorescence emission spectra of the polyether-substituted terthiophenes synthesised during the course of this research was investigated by measuring the fluorescence spectra before and after the addition of various metal ions. Terthiophene compounds (**I**, **II**, **XXIII-XXVIII**, **XXIX**, **LXXVI-LXXVII**) were used at a concentration of *ca.*  $6 \times 10^{-7}$  M, and bis(terthiophenes) (**LXI-LXIII**) at *ca.*  $3 \times 10^{-7}$  M in spectroscopy-grade acetonitrile. Stock solutions of the metal ions were prepared as either the perchlorate ( $\text{Li}^+$ ,  $\text{Na}^+$ ,  $\text{Ag}^+$ ,  $\text{N}(\text{Bu})_4^+$ ,  $\text{Mg}^{2+}$ ,  $\text{Ca}^{2+}$ ,  $\text{Sr}^{2+}$ ,  $\text{Ba}^{2+}$ ,  $\text{Ni}^{2+}$ ,  $\text{Co}^{2+}$ ,  $\text{Zn}^{2+}$ ,  $\text{Mn}^{2+}$ ,  $\text{Cd}^{2+}$ ,  $\text{Pb}^{2+}$ ) or hexafluorophosphate ( $\text{K}^+$ ,  $\text{NH}_4^+$ ) at 0.4M in acetonitrile.  $\text{RbClO}_4$  and  $\text{CsClO}_4$  were used as a saturated solution in acetonitrile.  $5\mu\text{L}$  of the relevant metal ion or acetonitrile blank was then added to 3 mL of terthiophene derivative to give a metal ion excess of *ca.* 1000. The excitation wavelength was 329 nm for all compounds except **LXXVI** (310 nm) and **LXXVII** (322 nm). The fluorescence emission was quantified at 453 nm (**LXXVI**), 445 nm (**LXXVII**) and 448.5 nm for all remaining compounds. In all cases, the fluorescence response was either unchanged or decreased on addition of metal ions. Figure 4.16 shows the effect of  $\text{Mn}(\text{ClO}_4)_2$  addition on both the absorption and fluorescence spectra of styryl-15-crown-5 terthiophene **I**. The results for all compounds with the series of metal cations are summarized in Fig. 4.17.

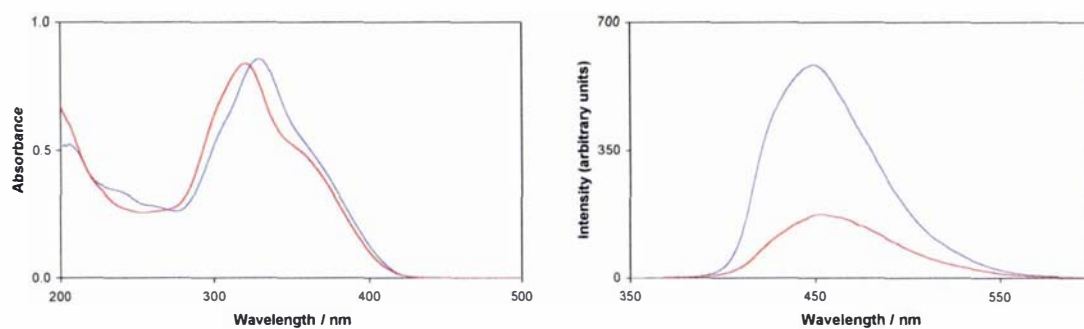


**Figure 4.16** Absorption (left) and fluorescence (right) spectra of styryl-15-crown-5 terthiophene I before (blue) and after (red) addition of  $\text{Mn}^{2+}$

Spectra were collected on a Perkin Elmer LS50B Luminescence Spectrometer controlled by a PC running standard Perkin Elmer software. Data was subsequently exported to Microsoft Excel for further processing.

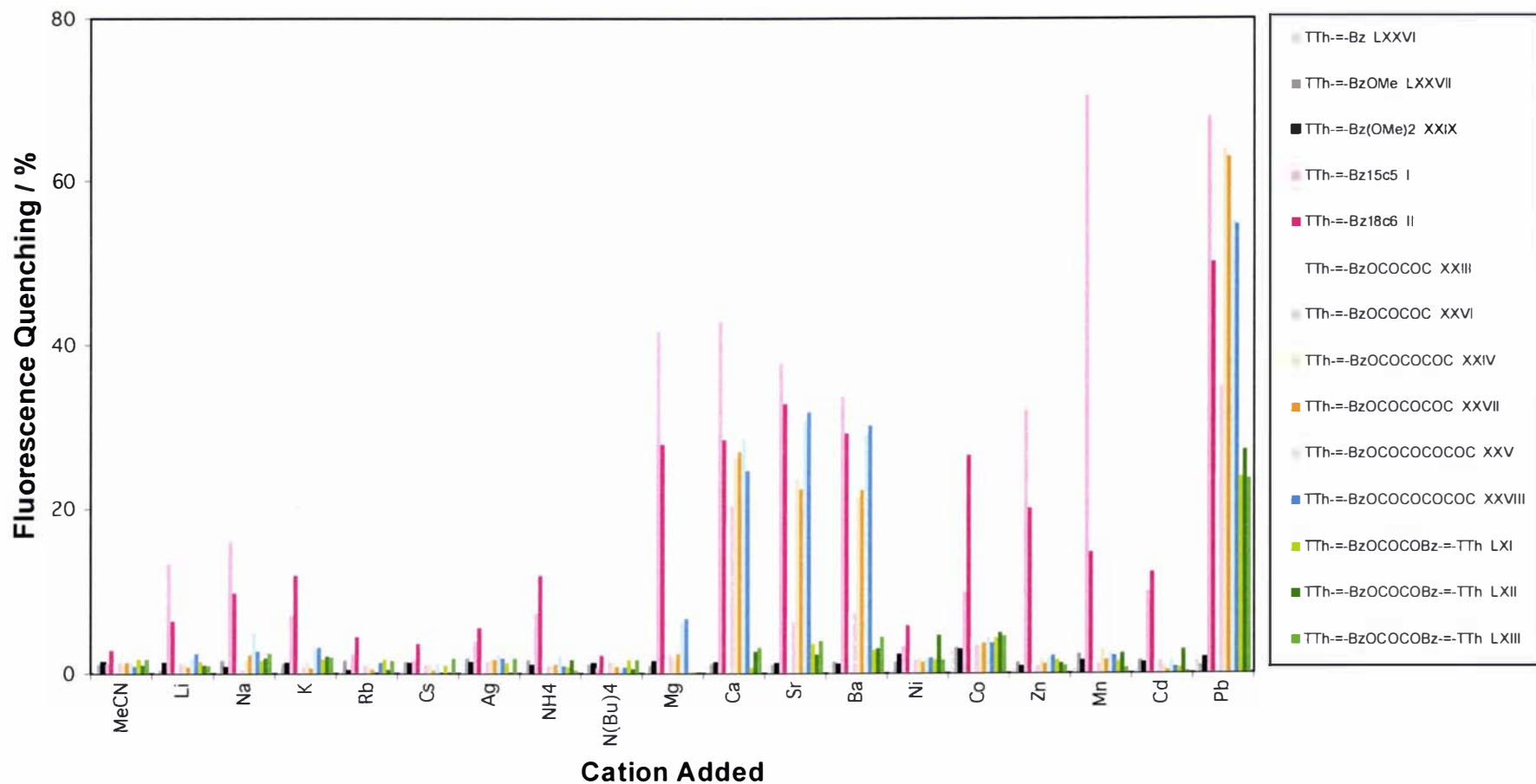


Figure 4.17 Fluorescence Quenching caused by addition of metal cations to terthiophene monomers

### 4.2.3.2 Discussion

The addition of MeCN to the substituted terthiophenes was intended as a reference to assess noise arising from both instrumental and procedural causes. In the same way, the large cation  $N(\text{Bu})_4^+$  was also intended as a control, as the large diameter of the cation ensures that it cannot be complexed by these molecules. An analysis of the data obtained on addition of these two solutions reveals the noise level to be *ca.* 3%. Only fluorescence quenching greater than this is considered significant. From an examination of the data presented in Fig. 4.17, with reference to Tables 4.1 and 4.2, the following observations can be made.

In the alkali metal ion series ( $\text{Li}^+$ ,  $\text{Na}^+$ ,  $\text{K}^+$ ,  $\text{Rb}^+$ ,  $\text{Cs}^+$ ), only the crown compounds **I** and **II** show a significant response. Styryl-15-crown-5 terthiophene **I** showed the greatest response to  $\text{Na}^+$ , followed by  $\text{Li}^+$  and  $\text{K}^+$ . This is what would be expected based purely on a size-fit between the crown ether cavity and the metal ion. Styryl-18-crown-6 terthiophene **II**, which possesses a larger cavity, is affected the most by  $\text{K}^+$ , then by the smaller ions  $\text{Na}^+$  and  $\text{Li}^+$ . A very slight effect is caused by the larger cations  $\text{Rb}^+$  and  $\text{Cs}^+$ . While none of the open-chain compounds show a large response, a small decrease in fluorescence intensity is observed for the longest chain compound **XXV** on addition of  $\text{Na}^+$ . It is not surprising that the crown ether compounds give larger responses than the open-chain ethers, given the preorganisation of the ether chain inherent in the crown molecules. The loss in free energy associated with organising the polyether chains into the correct conformation for binding in solution, must be exceeded by a gain in complexation free energy in order for binding to occur.<sup>10</sup> Thus it appears from Fig. 4.17, that the alkali metal ions do not provide sufficient energy incentive for the terthiophene derivatives to form complexes.

The remaining two monocations,  $\text{Ag}^+$  and  $\text{NH}_4^+$  both have large diameters more suited to complexation by **II** than **I**. This is reflected in the larger fluorescence quenching result for styryl-18-crown-6 terthiophene **II**.

No fluorescence quenching is observed on addition of any of the monocations to the hemicrown compounds **LXI-LXIII**. It is likely that this is due to their short ether chain, and greatly reduced ability to wrap around metal cations.

Considerably larger decreases in fluorescence intensity are evident on addition of alkaline metal cations ( $\text{Mg}^{2+}$ ,  $\text{Ca}^{2+}$ ,  $\text{Sr}^{2+}$ ,  $\text{Ba}^{2+}$ ), due to their greater charge density. Styryl-15-crown-5 terthiophene **I** responds in the order  $\text{Ca}^{2+} > \text{Mg}^{2+} > \text{Sr}^{2+} > \text{Ba}^{2+}$ , while for styryl-18-crown-6 terthiophene **II** the order is  $\text{Sr}^{2+} > \text{Ba}^{2+} > \text{Ca}^{2+} > \text{Mg}^{2+}$ . This difference between the two crowns clearly illustrates their different complexation properties, caused by the different sizes of their constituent crown ethers. The same size-fit principle can be seen in the data for the open-chain compounds. The two compounds with the shortest chain length (**XXIII** and **XXVI**) are affected most by addition of  $\text{Ca}^{2+}$ , with the larger cations  $\text{Sr}^{2+}$  and  $\text{Ba}^{2+}$  having a very small effect. For the medium length molecules **XXIV** and **XXVII**, while the greatest change is still seen for  $\text{Ca}^{2+}$ , both  $\text{Sr}^{2+}$  and  $\text{Ba}^{2+}$  also have a significant effect. **XXV** and **XXVIII**, which have the longest ether chains, show the greatest response to the larger ion  $\text{Sr}^{2+}$ , followed closely by  $\text{Ba}^{2+}$  and  $\text{Ca}^{2+}$ . Again as for the monocations, the three bis(terthiophenes) do not exhibit substantial fluorescence quenching on addition of any of these dications.

A contrast is seen between the responses observed for the open-chain compounds and the crown compounds, on addition of the transition metal cations  $\text{Ni}^{2+}$ ,  $\text{Co}^{2+}$ ,  $\text{Zn}^{2+}$ ,  $\text{Mn}^{2+}$  and  $\text{Cd}^{2+}$ . The ionic diameter of  $\text{Cd}^{2+}$  is very close to that of  $\text{Ca}^{2+}$ , and given that they have the same charge, the same response could be expected for both. This is not the case however, with none of the open-chain compounds showing any decrease in fluorescence intensity on addition of  $\text{Cd}^{2+}$ . Therefore, size is not the only factor governing the complexation of cations by polyethers, and electronic factors must also be considered. The crown ether terthiophenes **I** and **II** do show a fluorescence quenching response to these transition metal cations. 15-crown-5 terthiophene **I** is greatly affected by  $\text{Mn}^{2+}$ , and less so by  $\text{Zn}^{2+}$ ,  $\text{Co}^{2+}$  and  $\text{Cd}^{2+}$ . This can be rationalised on the basis of size fit, although the particularly large response obtained for  $\text{Mn}^{2+}$  implies that electronic factors may also be involved. The results for 18-crown-6 terthiophene **II** are less easily understood, as the response decreases with increasing

size from  $\text{Co}^{2+}$  to  $\text{Cd}^{2+}$ , rather than increasing as would be expected. Once again, it is clear that in the case of transition metals, complexation cannot be explained on the basis of size fit alone, and electronic factors are also exerting an influence.

The last cation remaining to be discussed is  $\text{Pb}^{2+}$ . As can be seen clearly from Fig. 4.16, the addition of  $\text{Pb}^{2+}$  causes fluorescence to be reduced for all of the polyether-substituted compounds studied. As explained in Section 4.1.3, it seems likely that this is caused by the affinity of the soft metal  $\text{Pb}^{2+}$  cations for the thienyl sulphur atoms, supplemented by a contribution from the polyether chain. There is another possibility in fluorescence spectra however, the heavy atom effect. Heavy atoms are well known to cause fluorescence quenching by increasing intersystem singlet-triplet crossing as a result of increased spin-orbit coupling.<sup>293</sup> The enhanced triplet formation reduces the population in the lowest excited singlet state, thus reducing fluorescence.<sup>294</sup> It seems unlikely that this is a major contributor to the fluorescence quenching seen, as the three reference compounds do not show any change on addition of  $\text{Pb}^{2+}$ .

As seen for the UV/VIS data earlier (Section 4.1.3), no significant change was seen for any compound on addition of MeCN, or on addition of any metal cation to the reference compounds **LXXVI**, **LXXVII** and **XXIX**.

### 4.3 Summary

Few UV and/or fluorescence complexation studies of this type have been carried out that involve alkali, alkaline earth and transition metal cations. Rather, most investigate only a handful of cations, usually alkali and/or alkaline earth. In addition, to the best of our knowledge, this is the first fluorescence study on the ion-complexing behaviour of polyether-substituted terthiophenes that has been undertaken.

A comparison of Figs. 4.9 and 4.17 shows that the UV/VIS complexation data obtained correlates well with the fluorescence quenching complexation data. This provides valuable evidence for the validity of these methods, and increases confidence in the results obtained.

Within both the alkali and alkaline earth metal cation series, the magnitude of the response correlates well to the typical crown ether size-fit model. Open-chain compounds consistently give smaller responses than do crown ethers, due to the energy required to organise the polyether chain into a conformation suitable for binding. Size discrimination is also evident based on polyether chain length. Alkaline-earth metal ions consistently cause larger spectral changes than alkali metal ions. As the changes observed are based on the complexed cation pulling electron density away from the chromophore, it is not surprising that the doubly charged alkaline cations exert a greater effect.

An exception to the size-based complexation is provided by  $\text{Pb}^{2+}$ . While a comparison of its ionic diameter (Table 4.2) with crown ether cavity sizes (Table 4.1) suggests that it would only be complexed significantly by 18-crown-6, all of the dialkoxystyryl-terthiophene derivatives showed changes in their UV/VIS and fluorescence spectra on addition of  $\text{Pb}^{2+}$ . This is thought to be due to the soft nature of the  $\text{Pb}^{2+}$  cation interacting with the sulphur atoms present in the thiophene rings.

The fact that no response was observed on addition of  $\text{Pb}^{2+}$  to the three reference compounds, and that the responses were different from compound to compound, suggests that the alkoxy functionalities must also play a role in this complexation. As  $\text{Pb}^{2+}$  was the only soft cation studied (Table 4.6), it is unclear how unique this response is, and further study would be required in order to clarify this issue.

**5**

**CHEMICAL**

**AND**

**ELECTROCHEMICAL**

**POLYMERISATION**

## 5.1 Chemical Polymerisation

Since a wide range of alkoxytyryl-substituted terthiophenes had been synthesised as precursors for conducting polymers, it remained to investigate this polymerisation. Two methods are commonly used to polymerise thiophenes, namely chemical and electrochemical polymerisation.<sup>45, 46</sup> Chemical polymerisation was investigated first, and as ferric chloride is the most frequently employed chemical oxidant for these types of monomers, it was the oxidizing agent of choice. A review of the literature was conducted to investigate polymers previously produced by this method, and their physical properties.

### 5.1.1 Literature review

Wang *et al.*<sup>97</sup> studied the polymerisation of 3',4'-dibutyl- $\alpha$ -terthiophene by ferric chloride. The polymer produced could be split into three fractions, based on solubility differences. The first fraction, soluble in  $\text{CHCl}_3$  at room temperature, had a number-average molecular weight  $M_n$  of 2600, corresponding to approximately 7 monomer units. The  $\lambda_{\text{max}}$  for this fraction was 446 nm in solution, and 488 nm as a thin film. The second fraction, soluble in  $\text{CHCl}_3$  at 80°C, consisted of polymer with  $M_n = 5700$  (16 terthiophene units), and  $\lambda_{\text{max}} = 449$  nm (solution) and 522 nm (solid-state). A small amount of insoluble material was also recovered, and this was believed to consist of even higher molecular weight polymer.

Somanthan and colleagues studied a non-symmetrical alkyl-substituted terthiophene, 3'-(2-ethylhexyl)-[2,2';5',2'']-terthiophene.<sup>122</sup> The polymer produced by  $\text{FeCl}_3$  oxidation had  $M_n = 2700$ , and  $\lambda_{\text{max}}$  ( $\text{CHCl}_3$  solution) = 451 nm.

The presence of alkoxy substituents on the outer rings of terthiophene can have a large influence on reactivity, clearly seen in the work of Gallazzi *et al.*<sup>91</sup> A polymer formed from chemically oxidised 3,3''-dihexylterthiophene had  $M_n = 6000$ ,  $\lambda_{\max}$  (solution) = 456 nm and  $\lambda_{\max}$  (film) = 535 nm. The equivalent alkoxy-substituted compound, 3,3''-dipentoxyterthiophene, produced only low molecular weight material on treatment with  $\text{FeCl}_3$ . Gel permeation chromatography results on this product gave  $M_n = 1500$ . The UV/VIS spectra were also quite different, with  $\lambda_{\max}$  (solution) = 499 nm and  $\lambda_{\max}$  (solid) = 514 nm. This contrasts markedly with the results obtained for the isomeric compound 4,4''-dipentoxyterthiophene. In this monomer the  $\alpha$ -positions next to the alkoxy substituents are highly reactive, and a high molecular weight insoluble polymer resulted from ferric chloride oxidation. This was also observed in later work utilizing 4,4''-dipentoxy-4'-dicyanoethenyl-[2,2';5',2'']-terthiophene.<sup>295</sup> In this case, chemical oxidation using ferric chloride yielded an insoluble material, believed to consist of high molecular weight polymer. The same effect has been observed in the case of bithiophene, where a 3,3'-dialkoxy derivative was shown to be considerably less reactive than the corresponding 4,4'-dialkoxy derivative.<sup>85, 296</sup>

From these results, it appears that ferric chloride polymerisation is a viable route to produce long-chain polymers from substituted terthiophenes. To the best of our knowledge, at the time of this research, there had been no investigations carried out on the  $\text{FeCl}_3$  polymerisation of 3'-styryl-substituted terthiophenes, and hence the influence of the conjugated substituent was unknown. It was also uncertain how great an influence the oxygen atoms would have on polymerisation, given that they are some distance from, but directly conjugated to, the polymer backbone.

## 5.1.2 FeCl<sub>3</sub> polymerisation of terthiophene monomers

Chemical polymerisations were initially carried out using similar conditions to those of Wang *et al.*,<sup>97</sup> where a chloroform suspension of ferric chloride is added slowly to a chloroform solution of the monomer. The solution is then left to stir at room temperature for a considerable length of time, to allow complete conversion of the monomer to polymer. The polymer is simultaneously precipitated and dedoped by treatment with methanol, then recovered by filtration. Extraction in a soxhlet apparatus with methanol removes oligomers, also ensuring complete dedoping of the polymer. In addition, fractions of different molecular weights can often be obtained by exploiting solubility differences in common organic solvents.

Treatment of styryl-15-crown-5 terthiophene **I** with ferric chloride as described above, gave a red powder that was soluble in CH<sub>2</sub>Cl<sub>2</sub> at room temperature ( $\lambda_{\text{max}} = 336, 450 \text{ nm}$ ). The powder was sparingly soluble in MeCN, but became freely soluble on addition of NaClO<sub>4</sub>. A small fraction of insoluble material was also recovered. Analysis by MALDI-MS revealed the red powder to consist solely of dimer ( $m/e = 1078.20$ ). Assuming that dimerisation had occurred as expected through the two available  $\alpha$ -positions, there are three possible regioisomeric products resulting from this dimerisation, as shown in Fig. 5.1.

The solubility of the product in CD<sub>2</sub>Cl<sub>2</sub> allowed a complete set of 1-D and 2-D NMR experiments to be performed in order to investigate the regiospecificity of the dimeric product. The simplicity of the <sup>1</sup>H and <sup>13</sup>C NMR spectra made it clear that the product consisted of a single symmetrical isomer, eliminating the possibility of a regioisomeric mixture of compounds, and also excluding the presence of the head-to-tail linked dimer.

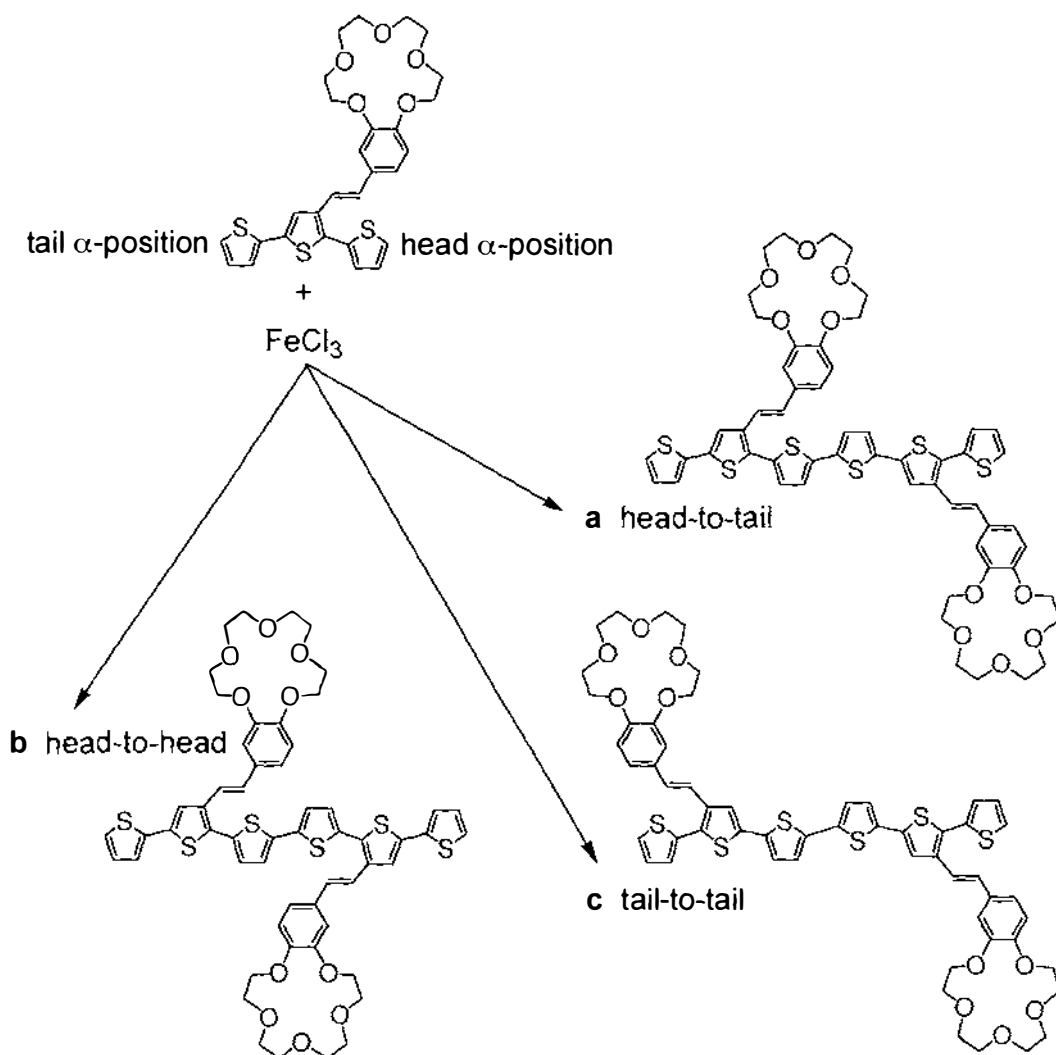


**Figure 5.1** Chemical polymerisation of 15-crown-5 terthiophene to form a) head-to-tail, b) head-to-head or c) tail-to-tail linked dimers

Further analysis of the 2-D connectivity information provided by the NMR spectra, and comparison with the spectra of the monomer (Fig. 5.2), led to the conclusion that the sole product of the oxidation was the head-to-head linked dimer. In particular, the disappearance of the head- $\alpha$  thiophene proton signal in both the  $^1\text{H}$  and  $^{13}\text{C}$  NMR spectra, while the tail- $\alpha$  thiophene proton signal remained, provided conclusive evidence for this assignment. The addition of two new thienyl doublets ( $\delta$  7.17, 7.26) gave support for the presence of two central  $\alpha$ -disubstituted thiophene rings. An example of a fully assigned dimer  $^1\text{H}$  NMR spectrum is shown in Fig. 5.3. The new band in the UV/VIS spectra at 450 nm is assigned to the  $\pi$ - $\pi^*$  transition for the

sexithiophene moiety, while the essentially unchanged band at 336 nm is attributed to the styryl-thiophene functionality. For comparative purposes,  $\lambda_{\max}$  for  $\alpha$ -sexithiophene has been reported as 432 nm (experimental)<sup>240</sup> and 434 nm (calculated)<sup>279</sup>.

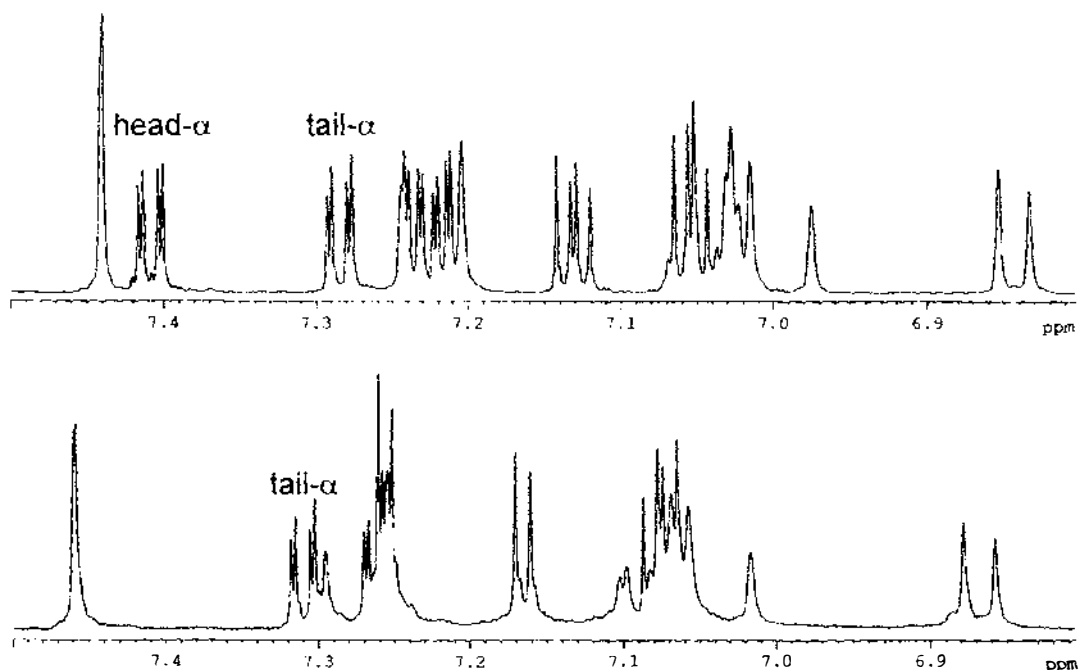


**Figure 5.2**  $^1\text{H}$  NMR spectra (aromatic region) of styryl-15-crown-5 terthiophene I (top) and 15-crown-5 terthiophene dimer LXVII (bottom)

In order for polymers prepared by chemical oxidation to be regioselective, there must be a sufficiently large difference in spin/charge density of the radical cation generated in the oxidative polymerisation process between the two available  $\alpha$  positions.<sup>68, 297</sup> The literature shows that this is not the case in 3-alkyl substituted thiophenes, explaining why only regiorandom polymers are formed from these monomers. The position of oxygen atoms is known to have a marked effect on regioselectivity, and the asymmetric reactivity of 3-alkoxy thiophenes discussed in Section 1.3.2 shows this clearly. Polymerisation of these monomers with  $\text{FeCl}_3$  leads to highly regioselective polymers. It was unclear from the literature whether alkyl or alkoxy substitution on the central ring of terthiophene would cause sufficient reactivity differences in the two available  $\alpha$ -positions on the outer rings to cause regioselective polymerisation. The majority of the literature published involving chemical polymerisation of

substituted terthiophenes avoids this issue by employing symmetrical compounds (Section 5.1.1).

The observed regioregularity in the product from 15-crown-5 terthiophene polymerisation, can only be explained by a difference in reactivity between the two available terthiophene  $\alpha$ -positions. This leads to the conclusion that the head  $\alpha$ -position is more reactive than the tail position, and therefore coupling occurs more quickly at this position. There are then two plausible reasons why the reaction does not appear to continue: either the tail position is sufficiently unreactive that the reaction proceeds very slowly or not at all, or the sexithiophene product is considerably less soluble than the terthiophene starting material, so that again the reaction comes to a standstill. In order to test the influence of solubility on polymerisation, dual polymerisations were carried out in 1,2-dichloroethane at room temperature (23°C), and at reflux (83°C). In both cases 93% of the material transferred into the soxhlet thimble was collected after extraction with CH<sub>2</sub>Cl<sub>2</sub> and precipitation with methanol, with no insoluble material able to be isolated. From this result it seems that while solubility may play a small part in determining the extent of polymerisation, it is the stability of the oxidised sexithiophene that plays the main role.

With the exact nature of the polymerisation product known, further experiments were carried out to ascertain if head-to-head dimerisation would occur for all the polyether-substituted terthiophenes.

Chemical polymerisation of styryl-18-crown-6 terthiophene **II** under the same conditions employed for **I** gave a red powder soluble in CH<sub>2</sub>Cl<sub>2</sub> along with a smaller insoluble fraction. Mass spectrometry data on the soluble product again revealed that it consisted exclusively of dimer. NMR and UV/VIS investigations confirmed the regioregularity and extent of polymerisation as that of a head-to-head linked dimer. The nature of the insoluble product meant that it was unable to be analysed by the spectroscopic techniques available to us, but it seems likely that it could be either a higher oligomer, or cross-linked material. Yamamoto and Hayashi<sup>298</sup> found that on

$\text{FeCl}_3$  oxidation of thiophenes substituted with aromatic rings, cross-linked material was produced due to oxidation of the benzene ring, as well as the thiophene ring.

The ferric chloride oxidation of the six open-chain terthiophenes **XXIII-XXVIII** was explored next. The yield of the  $\text{CH}_2\text{Cl}_2$  soluble red product ranged from 59-93%, with the recovery of 0-26% (by weight) of an insoluble solid. MALDI and FAB mass spectrometry showed no sign of oligomers higher than the dimer. Complete sets of NMR data ( $^1\text{H}$ ,  $^{13}\text{C}$ , COSY, HMQC and HMBC) were obtained for every product, and in each case verified the exclusive formation of a head-to-head linked product. The spectra were fully assigned in the same way previously discussed for styryl-15-crown-5 terthiophene dimer **LXVII**, and that of dimer **LXXIII** is shown as an example in Fig. 5.3. UV/VIS spectra for all of the products afforded a peak at *ca.* 450 nm, and a second more intense peak at *ca.* 335 nm. The solubility of the dimers increased markedly with increasing length of the attached polyether chain. The small amount of insoluble material that remained after soxhlet extraction is likely to consist of higher oligomers and/or cross-linked material, however the insolubility of this materials defies further characterisation by mass spectrometry or other available analytical techniques.

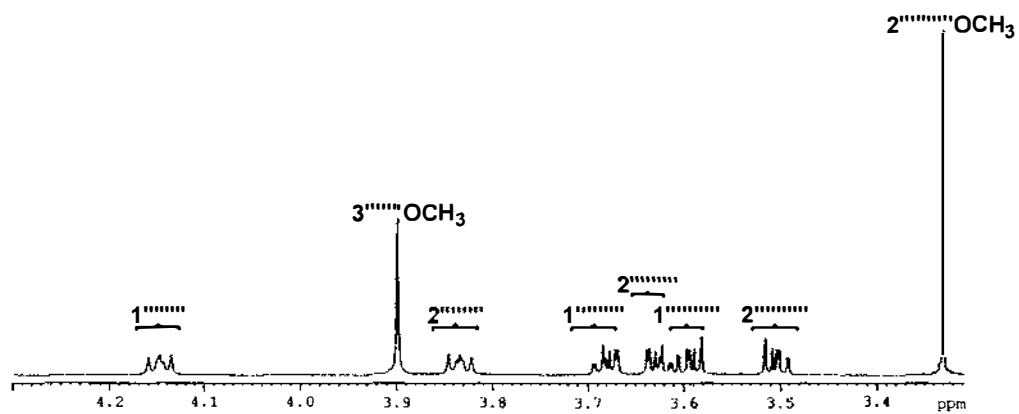
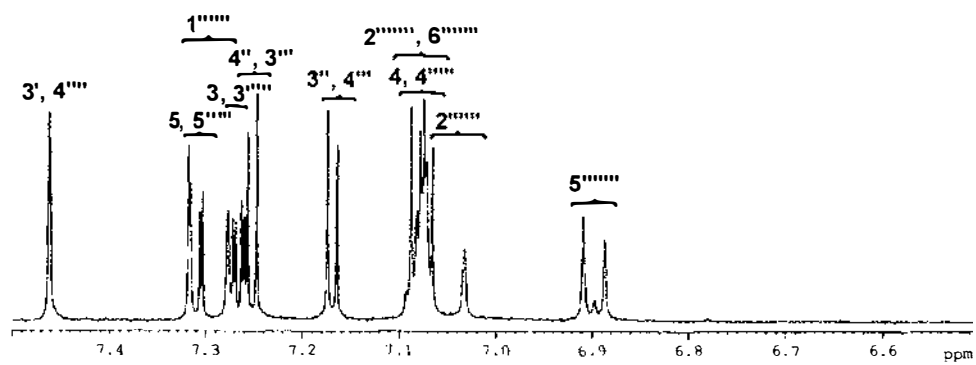
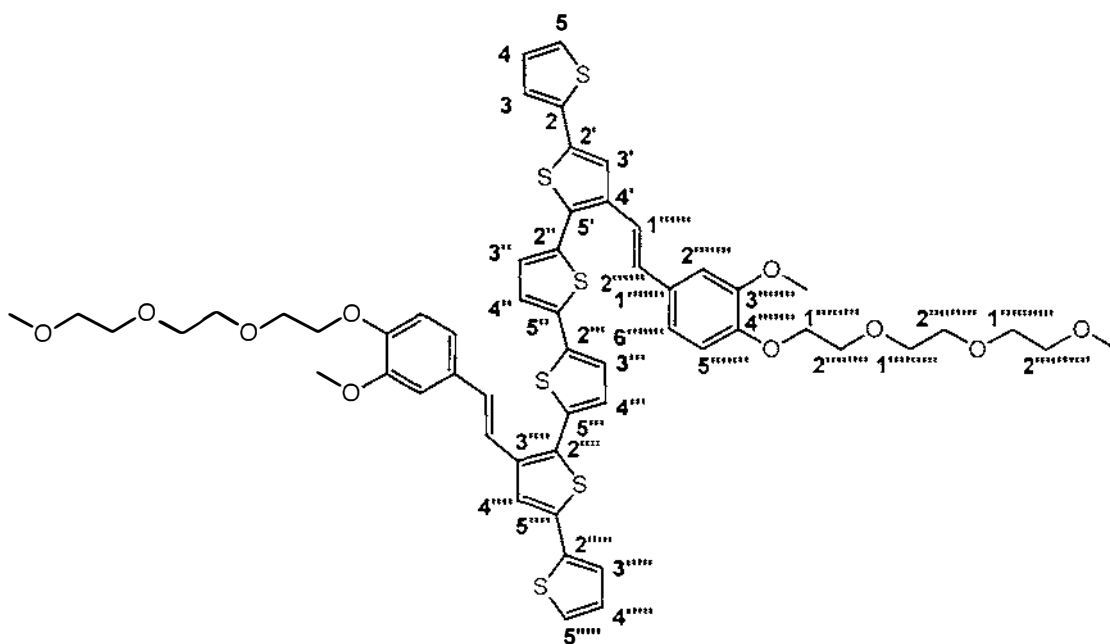


Figure 5.3 Fully assigned  $^1\text{H}$  NMR spectrum for terthiophene dimer LXXIII

An investigation into the  $\text{FeCl}_3$  polymerisation of the dimethoxy terthiophene **XXXVI** was less successful. A shortening of the reaction time to 30 minutes led to the isolation of a red powder in 79% yield. This product was again shown to consist only of dimer by MALD-MS, and gave the expected UV/VIS peaks at 336 and 445 nm. The dimer product was considerably less soluble in  $\text{CD}_2\text{Cl}_2$  than the dimers with longer polyether chains, therefore limiting the NMR data that could be obtained. The aryl and methoxy protons were clearly visible in the  $^1\text{H}$  NMR spectrum, however many of the thienyl protons were indistinct. It is uncertain whether this is due to the low solubility of the compound, or whether in fact the product from this dimerisation is not regioregular. Repeated recrystallisations and column chromatography did not help in obtaining a more useful NMR sample. While it seems unlikely that this compound would behave differently from the other polyether-substituted terthiophenes, this cannot be proven conclusively.

Chemical polymerisations were also carried out on the two reference compounds styryl-terthiophene **LXXVI** and methoxystyryl-terthiophene **LXXVII**. These reactions gave considerably lower yields of  $\text{CH}_2\text{Cl}_2$  soluble material (24% and 9% respectively) than were obtained for the corresponding compounds with attached polyether chains. Again, the limited solubility of the products restricted the NMR data that could be collected. The  $^1\text{H}$  NMR spectrum for the methoxystyryl dimer was consistent with those acquired for the other head-to-head linked dimers, however the lack of  $^{13}\text{C}$  and 2D data means that this cannot be proven. MALDI-MS data confirmed that this product consisted only of dimer. The styryl terthiophene dimer was even less soluble, and no useful NMR data could be obtained. MALDI mass spectrometry on this compound showed a large signal due to the dimer ( $m/e = 698.04$ ), as well as a small amount (*ca.* 2%) of trimer and tetramer. The considerably lower yields obtained from these compounds provide further evidence that it is the stability rather than the solubility of the oxidised sexithiophene that causes the polymerisation to stop at dimerisation for the ether-functionalised compounds. The dimers obtained from the styryl and methoxystyryl terthiophenes (**LXXVI** and **LXXVII**) were substantially less soluble than those obtained from the polyether-substituted terthiophenes. If solubility were the dominating factor, then these oxidations would have led to a higher yield of dimers than the more soluble polyether

compounds. This was not the case however, as the observed yields were substantially lower. Thus, the evidence points to the disubstituted polyether compounds forming a stable oxidised sexithiophene intermediate. The less stable intermediate formed from the styryl and methoxystyryl compounds would be sufficiently reactive to participate further in the polymerisation reaction.

Spin-density calculations on the radical cations of the styryl, methoxystyryl and dimethoxystyryl terthiophenes (**LXXVI**, **LXXVII** and **XXIX**) have been carried out by T. M. Clarke and K. C. Gordon at the University of Otago.<sup>299</sup> The method B3LYP/6-31G(d) was used to calculate the spin densities during each geometry optimisation. This level of theory (Becke-style 3-Parameter Density Functional Theory (DFT) using the Lee-Yang-Parr correlation function) was chosen as it includes the effects of electron correlation, making the results more reliable. The standard basis set 6-31G(d) was used since it is relatively large and contains polarisation functions which add d orbitals to the heavy atoms, necessary due to the presence of sulphur atoms.<sup>300</sup> The spin densities calculated for the head- $\alpha$  (5) and tail- $\alpha$  (5'') positions are tabulated below in table 5.1, along with the ratio of these two values. The spin densities over the entire radical cation are calculated to sum to 1.0, thus the values presented below are fractions and have no units.

**Table 5.1 Calculated spin density values for styryl-substituted terthiophenes**

Compound	Spin Density (head- $\alpha$ position)	Spin Density (tail- $\alpha$ position)	Spin Density Ratio (head/tail)
TTh=-Bz <b>LXXVI</b>	0.1962	0.1295	1.52
TTh=-BzOMe <b>LXXVII</b>	0.1642	0.0942	1.74
TTh=-Bz(OMe) <sub>2</sub> <b>XXIX</b>	0.1354	0.0740	1.83

The polymerisation of substituted thiophenes has been described as a “delicate balance between electronic and steric effects”.<sup>57, 301</sup> It has been shown that when thiophene monomers are alkyl substituted at the 3-position, head-to-head polymerisation is unfavourable due to steric interactions between the alkyl chains and

the lone pair on the adjacent sulphur atom.<sup>122</sup> Rather, they polymerise in a predominantly (*ca.* 80%) head-to-tail fashion.<sup>74, 120-122</sup> Steric issues were considered when designing these monomers (Section 1.6), and both the conjugated styryl-spacer and the terthiophene moiety were incorporated in order to minimize sterically-based barriers to polymerisation. The fact that regioselective head-to-head dimerisation is observed, shows that this approach was successful. In the absence of these steric interactions, coupling occurs preferentially between carbon atoms with higher spin densities.<sup>55, 297</sup> Further to this, a spin density ratio greater than 2.0 indicates a strong directing influence of the radical cations.<sup>297</sup> It can be seen from the data in Table 5.1 that the dimethoxy compound **XXIX** could be expected to give a greater proportion of head-to-head linked dimer than the methoxy compound **LXXVII** or the styryl terthiophene **LXXVI**. This is reflected in the yields of the corresponding chemical polymerisations, where the dialkoxystyryl-substituted terthiophenes produce excellent yields of head-to-head linked dimer. No head-to-tail or tail-to-tail dimer was isolated from any of the reaction mixtures. In the case of tail-to-tail dimer, it seems unlikely that this species would form due to the low electron spin-densities shown in Table 5.1. It is feasible that some head-to-tail dimer may have formed during chemical polymerisation, however the lack of isolation of such a compound implies that if it was formed, it must have reacted further. This could be the origin of some of the insoluble fraction isolated in some cases. The nature of the insoluble fractions obtained could not be elucidated, and, as indicated previously, could also have resulted from oxidation of other parts of the molecule.<sup>298</sup>

The last compounds to be subjected to ferric chloride polymerisation, were the terthiophene hemicrowns **LXI-LXIII**. In all cases, insoluble red solids were isolated. This insolubility meant that no spectroscopic analyses could be carried out, and the nature of the products are therefore unknown. It seems likely that these compounds would react preferentially at the head position as seen for all the previous ether-substituted terthiophenes. This could potentially lead to a large number of products, the smallest of which are shown in Fig. 5.4. One possible product consists of two monomers coupling at both available head positions (Fig. 5.4a). In this case, no head positions would be available for further polymerisation. Alternatively, if two monomers joined at just one head position, there would still be two available sites for

further polymerisation, forming a network-type structure (Fig. 5.4b, c). The maximum length of this type of oligomer would likely be determined by its solubility.

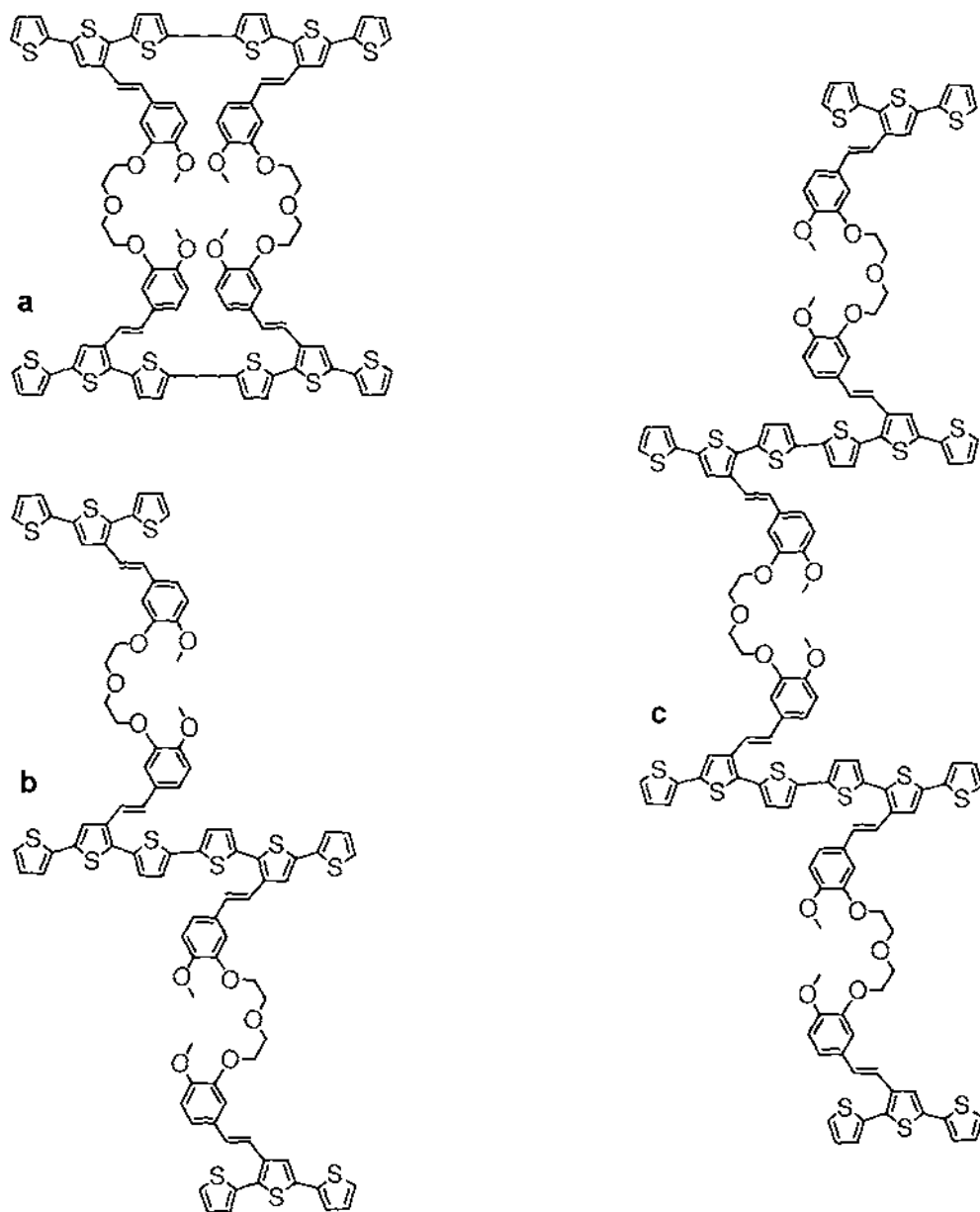


**Figure 5.4** Potential oligomers formed from chemical polymerisation of terthiophene hemicrown LXI

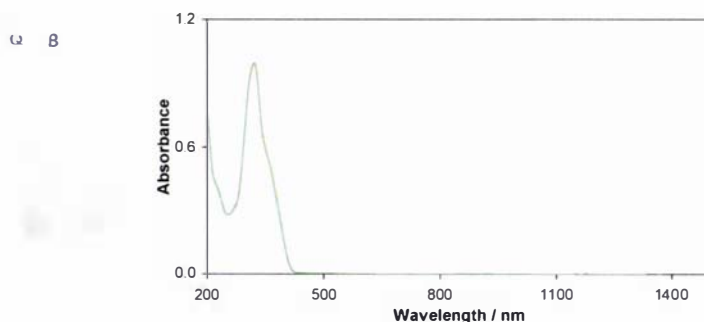
### 5.1.3 $\text{Cu}(\text{ClO}_4)_2$ polymerisation of terthiophene monomers

In order to further probe the nature of this dimerisation, oxidative polymerisation was carried out using  $\text{Cu}(\text{ClO}_4)_2$  in acetonitrile, following the reaction with UV/VIS/NIR spectroscopy. Measurements were carried out as follows: All spectra were measured in spectroscopy-grade acetonitrile from 190-1500 nm. Monomer concentrations used were  $2.3 \times 10^{-5}$  -  $2.8 \times 10^{-5}$  M (terthiophenes) and  $1.4 \times 10^{-5}$  M (bis-terthiophenes), giving maximum absorbances of 0.8-1.2 AU. The monomer spectrum was recorded before 50 equivalents of  $\text{Cu}(\text{ClO}_4)_2$  were added in a volume of 5-10  $\mu\text{L}$  from a stock solution of 0.4 M  $\text{Cu}(\text{ClO}_4)_2$  in MeCN, and the spectrum recorded again. This large excess was used in order to ensure that the compound was fully oxidised. Two drops of 2% aqueous hydrazine were added to effect the reduction, the solution was mixed thoroughly, and a final spectrum recorded. Tabulated data for all terthiophene-based monomers is presented in Table 5.2, and an example of the information collected is shown in Fig. 5.5 (photographs taken at higher concentrations for clarity).

**Table 5.2 Oxidation and reduction absorbance data for terthiophene monomers treated with Cu(ClO<sub>4</sub>)<sub>2</sub> and hydrazine**

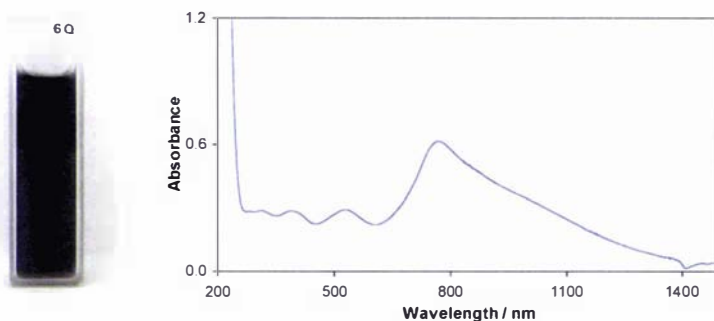
Compound	$\lambda_{\max} / \text{nm}$						
	Monomer	Oxidised with Cu(ClO <sub>4</sub> ) <sub>2</sub>				Reduced with hydrazine	
TTh--Bz <b>LXXVI</b>	348, 310	284, 370, 474			892, 986	314	432
TTh--BzOMe <b>LXXVII</b>	321	283, 314, 389	530	771		325	437
TTh--Bz(OMe) <sub>2</sub> <b>XXIV</b>	329	386	561	728		332	442
TTh--BzOCOCOC <b>XXIII</b>	328	363	593	777		332	443
TTh--BzOCOCOC <b>XXVI</b>	329	338	592	778		332	440
TTh--BzOCOCOCOC <b>XXIV</b>	329	352	582	782		332	440
TTh--BzOCOCOCOC <b>XXVII</b>	329	334, 386	574	782		330	439
TTh--BzOCOCOCOCOC <b>XXV</b>	329	332, 390	560	790		330	437
TTh--BzOCOCOCOCOC <b>XXVIII</b>	329	359	593	783		333	441
TTh--Bz15c5 <b>I</b>	330	319, 398	588	791		331	437
TTh--Bz18c6 <b>II</b>	330	326	588	787		330	434
TTh--BzOCOCOBz--TTh <b>LXI</b>	328	323, 416	564		931	333	440
TTh--BzOCOCOBz--TTh <b>LXII</b>	329	285, 331, 419	554		873	335	438
TTh--BzOCOCOBz--TTh <b>LXIII</b>	328	284, 331, 400	562		885	332	440

a) TTh--BzOMe



b) TTh--BzOMe

+ Cu(ClO<sub>4</sub>)<sub>2</sub>



c) TTh--BzOMe

+ Cu(ClO<sub>4</sub>)<sub>2</sub>

+ hydrazine

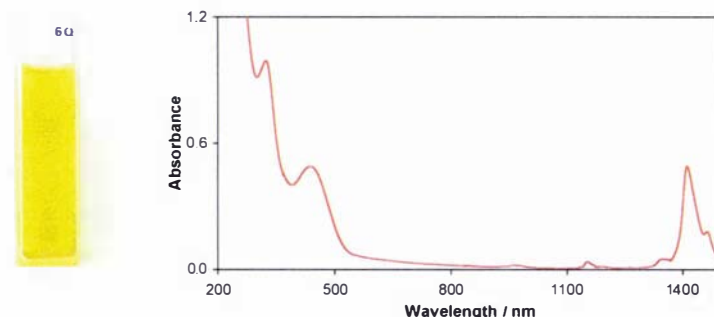
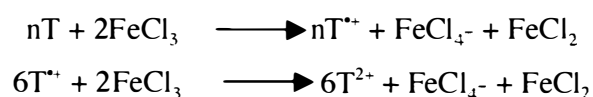


**Figure 5.5 Oxidation and reduction of methoxystyryl terthiophene LXXVII as observed by UV/VIS spectroscopy**

A similar experiment was carried out by Kankare *et al.* where they looked at the stepwise oxidation of 3'-aryl substituted terthiophenes by copper (II) triflate in acetonitrile.<sup>127</sup> They concluded that peaks observed between 600-800 nm and >1100 nm at low oxidant levels were due to dimer radical cations ( $6T^{•+}$ ). On addition of further oxidant, these peaks reduced while others were formed between 850-1000 nm, and were attributed to the presence of a dimer dication ( $6T^{2+}$ ). On reduction, a peak was seen at *ca.* 430 nm for all compounds, and this was assigned to the neutral dimer (6T).

Rapid coupling of terthiophene radical cations has also been observed by Fichou *et al.*, who used a  $\text{FeCl}_3/\text{CH}_2\text{Cl}_2$  system to examine the chemical oxidation of terthiophene (3T), quaterthiophene (4T), quinquethiophene (5T) and sexithiophene (6T).<sup>302, 303</sup> On addition of 2 equivalents of oxidizing agent, the monomer  $\pi$ - $\pi^*$  UV/VIS signal was lost, while others were formed at 646-780 and 1069-1476 nm. The strong colour observed is typical of organic radicals, further proof being provided by an intense e.s.r. signal. While the spectra for  $4\text{T}^{+\cdot}$ ,  $5\text{T}^{+\cdot}$  and  $6\text{T}^{+\cdot}$  were stable, the spectrum obtained for  $3\text{T}^{+\cdot}$  was identical to that of  $6\text{T}^{+\cdot}$ , indicating that the terthiophene radical cation was unstable and had immediately dimerised to the more stable sexithiophene radical cation. No changes were seen in the spectra for  $4\text{T}^{+\cdot}$  or  $5\text{T}^{+\cdot}$  on addition of a further two equivalents of  $\text{FeCl}_3$ . The spectrum obtained for  $6\text{T}^{+\cdot}$  however, underwent large changes, with the loss of the previously observed  $6\text{T}^{+\cdot}$  bands, and the appearance of a new signal at 1003 nm. In addition, the final solution was colourless and the e.s.r. signal disappeared, proving that the final species present in the case of sexithiophene was the dication  $6\text{T}^{2+}$ . These oxidations are represented by the equations below:



Terthiophene dimerisation has even been seen for terthiophene derivatives where the  $\alpha$ -positions are blocked.<sup>304</sup> In research by Guay *et al.*<sup>304</sup>, as in that of Fichou (above), dication formation was only observed for oligothiophenes with six or more thiophene rings. Dication formation was characterised by the loss of the e.s.r. signal associated with the unpaired electron in the radical cation.

Hill *et al.*<sup>305</sup> proposed that the reversible formation of a diamagnetic  $\pi$ -dimer could also be used to explain the loss of e.s.r. signal seen on oxidation. Their spectroelectrochemical system involved a terthiophene derivative that could not polymerise due to the presence of substituents at the  $\alpha$ -positions. Distinct UV/VIS peaks attributed to the monomer radical cation ( $\lambda_{\text{max}} = 572, >800 \text{ nm}$ ) and radical cation dimer ( $\lambda_{\text{max}} = 466, 708 \text{ nm}$ ) were seen with one electron oxidation. On incorporating a second electron, a new peak caused by the monomer dication was

observed at 570 nm. They concluded that a rapid equilibrium exists between monomer and dimer in solution, and that the weak bond thus created does not greatly affect the electronic structure of the monomer. The dimerisation was reported to be favoured at low temperature, and/or high concentration. Further evidence was provided by a later study utilizing photochemical oxidation in acidic solution. Peaks at 665 and 1150 nm were attributed to the radical cation  $3T^{+\bullet}$ , while the radical cation dimer  $(3T^{+\bullet})_2$  absorbed at 526 and 836 nm. This study also showed that dimer formation was more prevalent in polar solvents such as acetonitrile, as the dimer was better solubilised.<sup>306</sup>

Dimerisation has also been reported by Bauerle *et al.*<sup>307</sup>, who used a system involving an alkylated sexithiophene (a6T). They discuss the oxidation of a6T by  $FeCl_3$  in  $CH_2Cl_2$  to give a solution containing  $a6T^{+\bullet}$  ( $\lambda_{max} = 775, 1425$  nm), and  $(a6T)_2^{2+}$  ( $\lambda_{max} = 685, 1087$  nm) in reversible equilibrium. The formation of the “pimer” is favored at higher concentration and/or lower temperature. Further oxidation leads to the formation of  $a6T^{2+}$  ( $\lambda_{max} = 843, 946$  nm).

Apperloo *et al.*<sup>308</sup> looked at oligothiophenes where the  $\alpha$ -positions were substituted with solubilising poly(benzyl ether) dendrons. They also found that on oxidation, an equilibrium was formed between radical cations and  $\pi$ -dimers. The dimers were favoured at low temperature and were characterised by UV/VIS absorptions at 537 and 905 nm, in contrast to the radical cation peaks seen at 656 and 1068 nm. Two quinquethiophene derivatives were also investigated, forming a radical cation/ $\pi$ -dimer equilibrium at low oxidant concentration, then being further oxidised to dications on addition of more oxidizing agent. The longer oligothiophenes studied (containing 9, 11 and 17 thiophene units) did not form dimers, but could be oxidised to form dications. In addition it was discovered that while the doubly oxidised state for a nine-thiophene chain was present as a bipolaron, for longer oligothiophenes two independent polarons were present instead.

An alternative view is presented by Sato and Hiroi.<sup>309, 310</sup> In their work on alkyl substituted sexithiophenes, they also utilize chemical oxidation by  $FeCl_3$  in dichloromethane. Addition of two equivalents of oxidant caused the loss of the  $\pi$ - $\pi^*$

UV/VIS peak, and the formation of peaks at 780 and 1512 nm. An intense e.s.r. signal was also observed, results consistent with the formation of a radical cation, and consistent with that seen by other researchers. On addition of a further two equivalents of oxidant, the peaks at 780 and 1512 nm disappeared, and new peaks were formed at 551, 932 and 1060 nm. The unchanged e.s.r. signal led them to conclude that in this case, trication radicals, not dications, were formed.

From the literature results discussed above, it is clear that there are six possible species to be considered when interpreting the UV/VIS data presented in Table 5.2. The monomer itself 3T, the monomer radical cation  $3T^{+\bullet}$ , the radical cation dimer  $(3T^{+\bullet})_2$ , the dimer radical cation  $6T^{+\bullet}$ , the dimer dication  $6T^{2+}$ , and the neutral dimer 6T.

It is clear from the experimental results presented in Table 5.2 that only dimers were formed during the copper(II) perchlorate oxidation of these polyether-substituted styryl-terthiophenes. This is most easily evidenced by the presence of a UV/VIS absorbance at *ca.* 440 nm on reduction with hydrazine, attributed to the sexithiophene chromophore. This result is also consistent with that obtained by ferric chloride polymerisation discussed in Section 5.1.2. A peak is also seen at approximately the same position as the original  $\pi$ - $\pi^*$  peak for the monomer. The position of this peak has barely shifted, as would be expected given that the styryl-thiophene moiety is unchanged. It is noteworthy that while the styryl terthiophene monomer **LXXVI** originally shows two absorbances ( $\lambda_{\text{max}} = 310, 348 \text{ nm}$ ), only the smaller wavelength peak is restored after oxidation and reduction. This result gives further weight to the assignments previously given to these peaks (Section 4.1.2.1), as the styryl-thiophene chromophore exists in the dimerised product, but the terthiophene chromophore does not. The peak visible in Fig. 5.5 at *ca.* 1400 nm was seen in all of the reduced spectra and is due to hydrazine. For clarity, these peaks were not included in Table 5.2.

This leaves four possible oxidised species that could be responsible for the peaks observed on addition of  $\text{Cu}(\text{ClO}_4)_2$ . The cation radical  $\pi$ -dimer  $(3T^{+\bullet})_2$  observed in acetonitrile by Hill *et al.*<sup>305, 306, 311</sup> for their compounds is extremely unlikely in this case for two reasons. Firstly, the  $\pi$ -dimers were only observed in terthiophene

derivatives that were substituted at their  $\alpha$ -positions, precluding the otherwise rapid formation of  $\sigma$ -dimers. Secondly,  $\pi$ -dimers were only present at low oxidant concentrations, with the compounds being further oxidised to dications on addition of more oxidant. The data given in Table 5.2 is the UV absorbances observed in a solution containing a 50-fold excess of Cu(II). With this concentration of oxidant, it is unlikely that  $\pi$ -dimers would exist. It also seems improbable that monomer radical cations would be observed, given the propensity of terthiophene radical cations to rapidly couple. Thus, the most likely species in solution are the dimer radical cation and dimer dication. The general consensus in the literature is that peaks for  $6T^{+\cdot}$  would be expected at 600-800 nm and 1400-1500 nm, whereas  $6T^{2+}$  is more likely to absorb from 850-1000 nm.

Examining the data in Table 5.2, it is clear that all the alkoxyterthiophenes (**LXXVII, I-II, XXIII-XXVIII**) have absorbances at approximately the same wavelengths. Bands are seen for all these compounds at 728-791 nm, 530-593 nm and  $<400$  nm. Comparing these bands with previous research, it seems most likely that they are caused by the presence of the dimer radical cation  $6T^{+\cdot}$ . Styryl-terthiophene **LXXVI** shows peaks at higher wavelength (892, 986 nm), which could be due to the dimer cation  $6T^{2+}$ . Thus it appears that either the alkoxy substituents are stabilizing the dimer radical cation in the earlier cases such that copper(II) is insufficient to oxidise the compounds further to the dimer dication  $6T^{2+}$ , or that the dimer dication is itself unstable. The three isomeric hemicrown compounds **LXI-LXIII** appear to be intermediate cases, where bands at 873-931 nm and 554-564 nm indicate the presence of both  $6T^{2+}$  and  $6T^{+\cdot}$ . It is unclear why the hemicrown compounds behave differently to other dialkoxyterthiophenes, and further work would be needed to clarify this issue. It seems possible that an equilibrium between  $6T^{+\cdot}$  and  $6T^{2+}$  exists in solution that favours  $6T^{2+}$  for the styryl compound,  $6T^{+\cdot}$  for the alkoxyterthiophenes, and which allows both forms to be present for the hemicrown terthiophenes. In none of these cases is the dimer radical cation sufficiently reactive to couple further. This work was repeated by researchers at the University of Otago, adding  $\text{Cu}(\text{OSO}_2\text{CF}_3)_2$  slowly to an MeCN solution of the monomer. Their peak assignments agree with those given here. In addition, a solution of the dimethoxystyryl terthiophene dimer **LXXIX** was investigated by

resonance Raman spectroscopy. This produced a spectrum that agreed closely with that calculated for the head-to-head linked dimer.<sup>65, 261</sup>

In order to verify these conclusions, a similar oxidation was carried out on the most soluble sexithiophenes **LXXI** and **LXXIV**. The compounds were dissolved in  $\text{CH}_2\text{Cl}_2$  at *ca.*  $1.5 \times 10^{-5}$  M and a UV spectrum run from 250-1500 nm. Fifty equivalents of  $\text{Cu}^{2+}$  were added from a stock solution of 0.4 M  $\text{Cu}(\text{ClO}_4)_2$ , the solution was thoroughly mixed, and the UV spectrum recorded again. Finally, two drops of 2% aqueous hydrazine were added and the contents of the cuvette agitated until the solution turned yellow (forming an emulsion), before the final UV/VIS spectrum was recorded. In both of these cases, a very large peak in the spectrum of the oxidised compound was seen at 805/827 nm, with smaller peaks visible at 576/585, 412/415 and 329/339 nm. Taking into account the different solvent system, this appears to be consistent with the formation of  $6\text{T}^{*+}$  as seen for the dialkoxy terthiophenes in MeCN. On reduction with hydrazine, the original spectrum was restored, indicating that no coupling occurred.

The results of chemical polymerisation with both  $\text{FeCl}_3$  and  $\text{Cu}(\text{ClO}_4)_2$  agree closely, pointing to the almost exclusive production of head-to-head linked dimers. This is believed to be due to an asymmetric reactivity of the terthiophene monomers caused by uneven electron spin density distribution, rather than by any steric effects. Theoretical calculations support this view, showing a considerable difference in spin density between the two available  $\alpha$ -positions. UV/VIS/NIR spectra of the oxidised species in MeCN solution, indicate the presence of dimer radical cations for all alkoxyterthiophenes, however these do not couple further under these conditions.

## **5.2 Electropolymerisation**

An alternative to chemical polymerisation, is the formation of polymers from terthiophene monomers by electropolymerisation. The monomer is dissolved in a suitable solvent (eg. acetonitrile or dichloromethane) in the presence of an electrolyte (eg. tetrabutylammonium perchlorate, TBAP). A polymer can then be selectively deposited onto an electrode surface by cyclic voltammetry (CV, repetitive sweeping between two electrode potentials) or by applying a constant potential or current for an appropriate length of time. For this investigative electrochemical work, the technique selected was cyclic voltammetry in a three-electrode cell. The voltammograms arising from this process are referred to as 'growth CVs' in this thesis. CVs performed on such films after growth, in the absence of monomer, are termed 'post-polymerisation CVs'.

### **5.2.1 Cyclic voltammetry in a three-electrode cell**

A common laboratory setup for electrochemical polymerisation is the three electrode cell. In this system, reference, working and auxiliary electrodes are placed in a solution containing the monomer(s) and electrolyte(s). Current flows between the working and counter electrodes, and a potentiostat controls the potential difference between the working and reference electrodes.<sup>312</sup> A high concentration of electrolyte in solution, and a large surface area auxiliary electrode ensure that current flow is not limited. Electrochemical polymerisation is sensitive to many variables, including working electrode composition and size, electrolyte nature and concentration and monomer concentration. In particular, when electrochemistry is conducted in an organic solvent, the distance between the electrodes is critical. In order to minimise the effects of these variables, conditions need to be as reproducible as possible. The

experimental setup used throughout this research is illustrated in Fig. 5.6, and further described in Section 5.2.2.

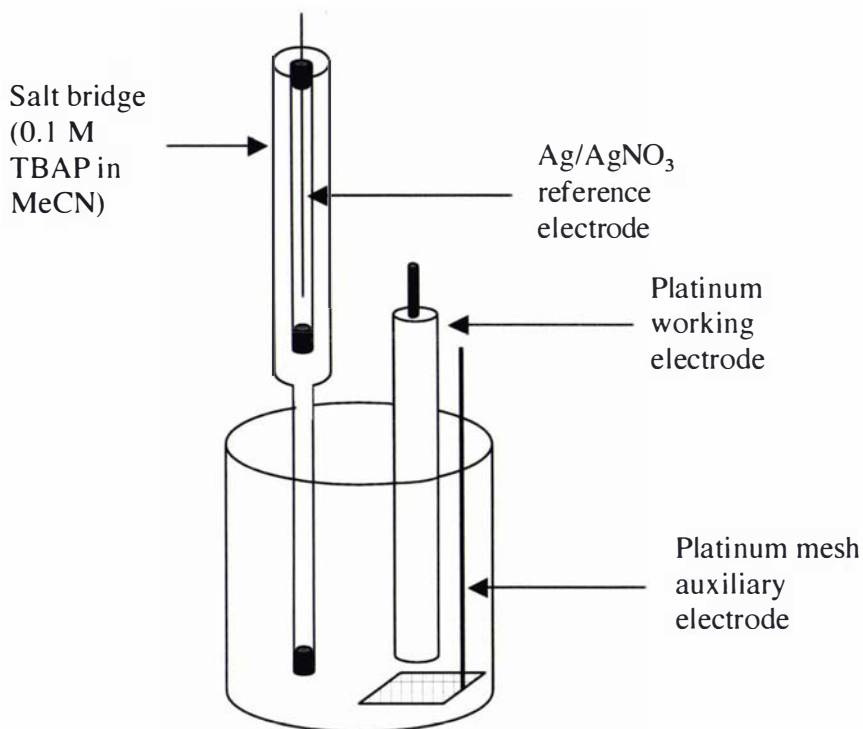


**Figure 5.6 Schematic representation of a three electrode cell**

The electrochemical technique utilised in this research was cyclic voltammetry. Cyclic voltammetry involves applying a potential that sweeps backward and forward between two set electrode potentials while measuring the current flowing between the electrodes. An example of both the applied potential and measured current is shown in Fig. 5.7. This figure shows two cycles, each comprising a forward (oxidizing) and reverse (reducing) sweep, between  $-0.5$  and  $+0.5$  V, for a solution of ferrocene and TBAP in MeCN. Species that are oxidised on the forward scan, may undergo reduction on the reverse scan. A measure of the reversibility of this process is the peak-to-peak separation between the forward and reverse scans. For a completely reversible one-electron process with both oxidised and reduced species in solution, the separation between oxidation and reduction peaks is  $57$  mV.<sup>313</sup> In a real system, diffusion of oxidised species from the electrode, deposition of solid material on the electrode, solvent and electrolyte composition and scanning speed can all affect the current response given by a chemical species.<sup>57</sup>

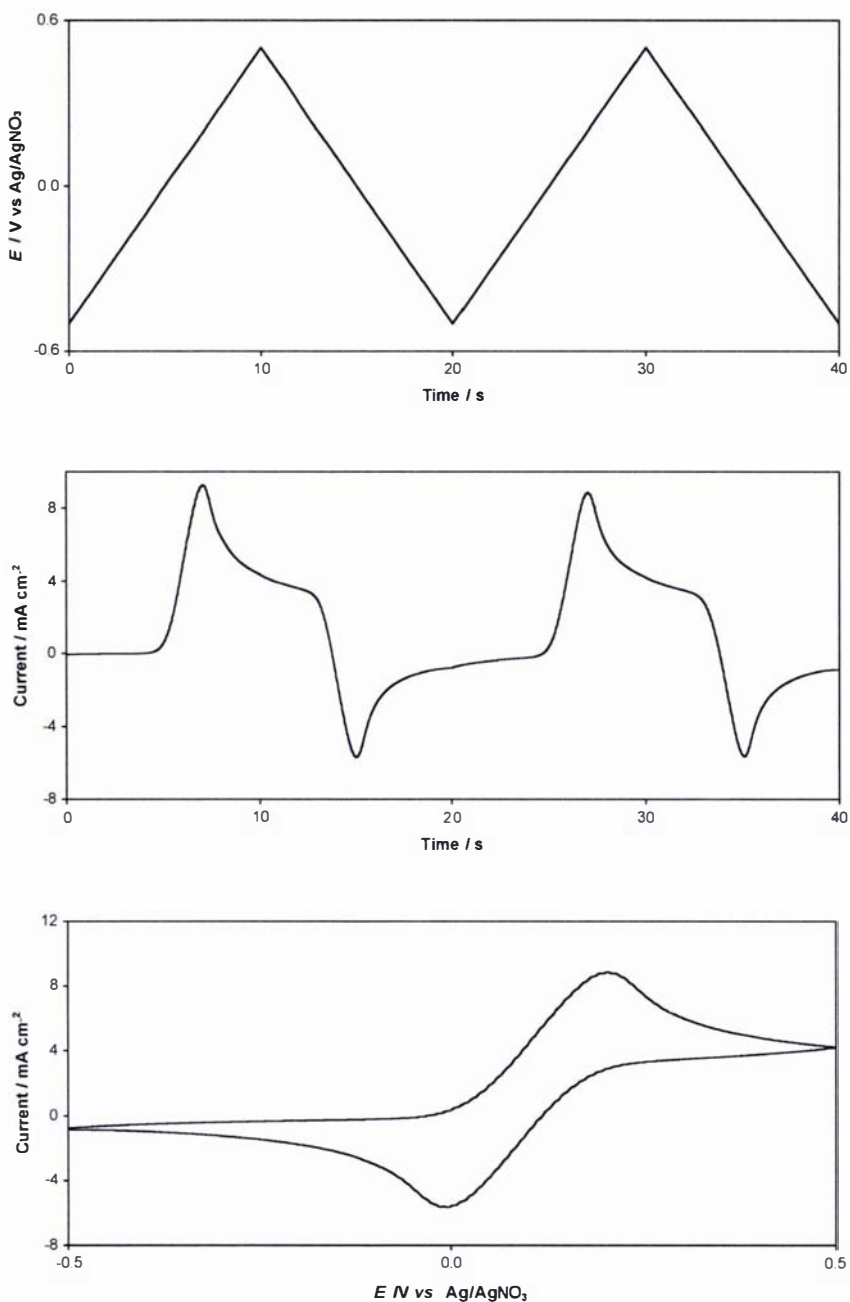


**Figure 5.7** Applied voltage (top), measured current (middle) and final cyclic voltammogram (bottom) for ferrocene

( $\nu = 100\ mV\ s^{-1}$ , 0.1 M TBAP, MeCN)

Cyclic voltammograms are more often displayed showing current as a function of applied potential. The data from Fig. 5.7 (top and middle) is represented in this form in Fig. 5.7 (bottom, second scan only). This format allows facile identification of peak oxidation and reduction potentials.

In the case of deposition by cyclic voltammetry, formation of a conductive polymer is indicated by an increase in current over consecutive cycles. Since current is directly proportional to the surface area of an electrode, depositing an electroactive polymer layer on an electrode surface may cause the surface area to enlarge with each scan, thus causing the observed current to increase. Oligomers formed from the coupling of two or more monomer units appear, on the second and subsequent scans, as oxidation peaks at lower potential than seen for oxidation of the monomer. This is due to the longer conjugation length present in oligomers, causing them to oxidise at lower potential.<sup>314</sup>

As discussed in Section 1.3, counter-ions move in and out of polymer films to balance charge during oxidation and reduction. In most cases the electrolyte anion migrates into the polymer to balance the positive charge formed by loss of an electron during oxidation.<sup>49</sup> The anion incorporated during electropolymerisation has been shown to have a large effect on the morphology and electroactivity of the resulting polymer.<sup>301</sup> For this reason, the anion used in the following electrochemical experiments was kept constant. Tetrabutylammonium perchlorate was chosen as the electrolyte for all film growth experiments, as the bulky tetrabutylammonium cation was not anticipated to complex with the crown or polyether chains present in the monomers. It was also assumed here that the tetrabutylammonium cation would not play a significant role in determining the properties of the polymer films, and that changing the cation would have no effect unless there were specific interactions between the cation and polymer. Where other metal cations were used to investigate complexation during post-polymerisation cyclic voltammetry, they were introduced as perchlorates at a concentration of 0.1 M, in order to cause as little disruption as possible to the polymer matrix. However, in cases where the anion is trapped inside the polymer, and cannot move out during reduction, the electrolyte cation must migrate into the polymer matrix to maintain electrical neutrality.<sup>49</sup> This possible complication must be considered when interpreting CV data.

## 5.2.2 Experimental procedures

For all electrochemical experiments, a three-electrode, one-compartment cell was used. The reference electrode was a non-aqueous Ag/AgNO<sub>3</sub>/MeCN system (BAS # MF-2062) housed in a 0.1 M TBAP/MeCN salt bridge (Fig. 5.6). All electrical potentials are quoted with respect to this reference, unless otherwise stated. Platinum mesh was used as the counter electrode. A platinum disc working electrode (0.0201 cm<sup>2</sup>) was used for all growth and post-polymerisation CVs. The surface was polished with alumina (0.05 μm) and rinsed with H<sub>2</sub>O and MeCN between each experiment. Use of a cell lid with drilled holes for the electrodes ensured that the distance between electrodes remained constant. Tetrabutylammonium or selected metal ion perchlorates were used as the electrolyte at a concentration of 0.1 M in acetonitrile, dichloromethane or a stated combination. Spectroscopy grade acetonitrile (0.001% w/w H<sub>2</sub>O) and dichloromethane were used as received, and all electrolytes were dried under high vacuum for at least 24 hours prior to use. Monomer and electrolyte solutions were deoxygenated by bubbling with oxygen-free nitrogen for five minutes before electrochemistry was commenced. Measurements were collected using an Autolab Potentiostat Galvanostat controlled by a PC running Autolab GPES software. Subsequent data processing was carried out using Microsoft Excel. All cyclic voltammograms were recorded at room temperature, with a sweep rate of 100 mV s<sup>-1</sup>, starting and finishing at the cathodic limit. The resulting films were rinsed with clean solvent (free of electrolyte and monomer) before being used further. While this removed monomer solution from the surface, it is acknowledged that surface washing could not remove monomers trapped deeper in the films.

Growth CVs were recorded for each terthiophene-based monomer, between potential limits of +1.0 V to -1.0 V, with a monomer concentration of 5-10 mM. Potential limits were not optimized further for each individual monomer. Rather, the work presented is a comparison of the electrochemical properties of the various monomers under the same conditions. Post-polymerisation CVs were recorded in 0.1 M metal ion perchlorate solution that contained no monomer and no tetrabutylammonium

cation, between identical potential limits. Again, this work was not intended to be an exhaustive electrochemical study, but to provide a broad survey of the various monomers' electrochemical response to selected metal cations.

Samples prepared for SEM analysis were grown onto ITO-coated mylar, due to the physical constraints imposed by the SEM sample chamber. All SEM samples were grown by cyclic voltammetry for 5 cycles, starting and ending at the cathodic limit. Concentrations of monomer and electrolyte used were identical to those used for growth onto platinum disc electrodes. The same potential limits employed during CV growth onto platinum were used to grow films onto ITO-coated mylar. As this led to films with visually uniform colour and gross morphology, alternate limits were not investigated. The estimated area of the ITO-coated mylar electrodes used in the production of samples for SEM analysis was 0.5 cm<sup>2</sup>. This area was not masked, so that meniscus effects and variations in size between individual pieces of mylar contribute to a lack of precision in this value. A sheet of mylar was prepared by washing in hot soapy water, before being thoroughly rinsed with H<sub>2</sub>O, MeOH and acetone. The non-conductive side was then marked, before the sheet was cut into small strips. SEM analysis was performed by D. Hopcroft at HortResearch, Palmerston North. Small pieces of sample (*ca.* 5 x 5 mm) were mounted on an aluminium specimen stub, sputter coated with *ca.* 100 - 150 nm of gold and studied using a Cambridge 250 Mk3 Scanning Electron Microscope in the secondary electron mode. Images were taken from the centre of the film to avoid edge effects, recorded on Ilford FP4 black and white film at the chosen magnifications and printed on Kodak multigrade paper.

UV/VIS/NIR spectroscopy was also used to characterise the electrochemically produced films. A Shimadzu UV-3101PC UV-VIS-NIR Scanning Spectrophotometer controlled by a PC running standard Shimadzu software was used to record spectra. In order to use this technique, samples were grown onto pieces of ITO-coated glass. The average area of polymer-coated ITO glass was estimated to be 0.7 cm<sup>2</sup>. Again, as for ITO-coated mylar, this value is imprecise. The glass was prepared by consecutive washes in hexane, MeOH and CH<sub>2</sub>Cl<sub>2</sub> with ultrasonication, and afterward handled only by the edges. A baseline correction was obtained on two pieces of this glass,

subsequent measurements being carried out with a pristine piece of glass as a reference. Both the sample and reference pieces of glass were mounted on a black screen perpendicular to the light beam. The screen had small holes positioned to allow the light beam to pass through. This experimental setup greatly reduced light scattering, and ensured that the samples were placed directly and reproducibly in the path of the light beam. Despite this, occasional noise was seen near the detector changeover that occurred at 830 nm. This noise was always small compared to the absorbance of the sample, and did not occur in a region containing absorbance peaks. Spectra were recorded from 250-1500 nm, with a data pitch of 1.0 nm. This experimental procedure was deemed more useful than spectroelectrochemistry in this case, due to the tendency of some samples to dissolve in electrolyte solution, as will be discussed in Section 5.2.4. Spectroelectrochemistry involves poisoning the film at a series of set potentials and recording a spectrum at each potential. This is achieved by setting up a three electrode cell within a glass or quartz cuvette.<sup>315</sup> The experimental setup described ensures that films are maintained in their oxidised or reduced forms, but has the disadvantage that solution species can interfere with the spectra collected. In this case, preliminary investigations revealed that many of the films formed were not stable under these conditions, so that spectroelectrochemistry would be a less useful technique. For these reasons, UV/VIS/NIR spectra were run on solid films grown onto ITO-coated glass. An early report by Kaneto *et al.* on thin films of polythiophene reported that the neutral film was very stable, but the oxidised film tended to reduce during exposure to air or protic solvents.<sup>316</sup> While the oxidised films prepared in this work maintained their blue hue over the time period required to collect UV/VIS/NIR spectra, it is possible that partial reduction occurred during this time. Hence, some unstable oxidised species may not have been observed. Separate films were grown for each spectrum recorded. Those left in the neutral form were grown by cyclic voltammetry, under the conditions used for growth experiments, starting and ending at the cathodic limit. The number of scans used varied depending on the density of the film deposited, and was between 1-3 cycles for all monomers. Films measured in the oxidised state were grown at a constant potential, + 0.8 V, for 5 seconds. All films had even coverage to the human eye, and maintained their red (neutral) or blue (oxidised) tint for weeks in contact with the atmosphere.

## 5.2.3 Electropolymerisation of reference compounds

In order to provide insight into the polymerisation of the new dialkoxy-styryl substituted terthiophene compounds, some preliminary electrochemistry was performed on terthiophene, styryl terthiophene **LXXVI**, methoxystyryl terthiophene **LXXVII** and dimethoxystyryl terthiophene **XXIX**.

### 5.2.3.1 Terthiophene

A growth CV for terthiophene is shown below in Fig. 5.8. The increasing current with scan number is indicative of the formation of an electroactive polymer. After 5 cycles the platinum disc working electrode surface was covered by an adherent dark red film. In previous work (Section 5.1), it was observed that both neutral and oxidised sexithienyl species were highly coloured, and it is reasonable to assume that longer chain oligomers would also absorb strongly in the visible part of the electromagnetic spectrum. As the solution colour remained unchanged during cyclic voltammetry, it seems unlikely that large amounts of soluble oligomeric species were being formed.

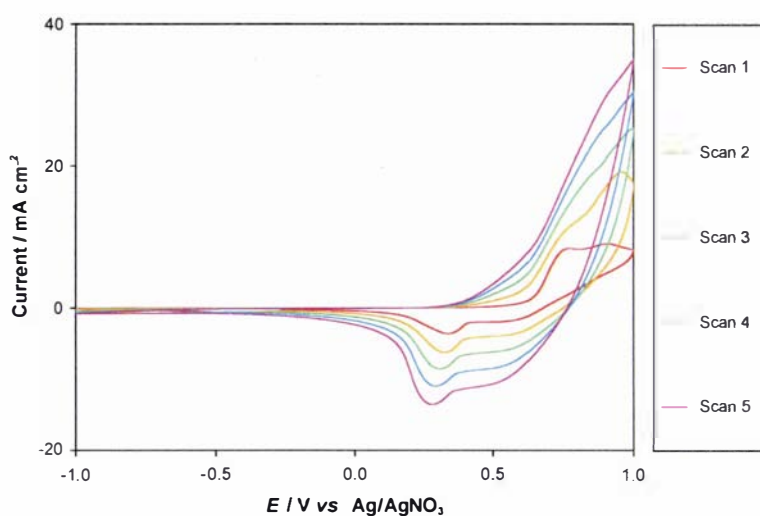


**Figure 5.8** Cyclic voltammetry for terthiophene  
( $\nu = 100 \text{ mV s}^{-1}$ , 10 mM terthiophene, 0.1 M TBAP, MeCN)

Post-polymerisation CVs in 0.1 M TBAP and 0.1 M LiClO<sub>4</sub> in the absence of monomer, are shown below in Fig. 5.9. A separate film, grown under identical conditions, was used for each different metal cation. Figure 5.9 shows that identical responses were obtained for films cycled in the presence of Li<sup>+</sup> and N(Bu)<sub>4</sub><sup>+</sup>. Similar responses were also observed for other metal cations tested (Na<sup>+</sup>, Mg<sup>2+</sup>, Mn<sup>2+</sup>). A current decline of approximately 25% was observed over 15 cycles. A similar type of oxidative degradation observed by Harada *et al.*<sup>317</sup> was attributed to nucleophilic attack on polythiophene in the oxidised state and was accelerated by the presence of small amounts of H<sub>2</sub>O and/or nucleophilic electrolyte anions.

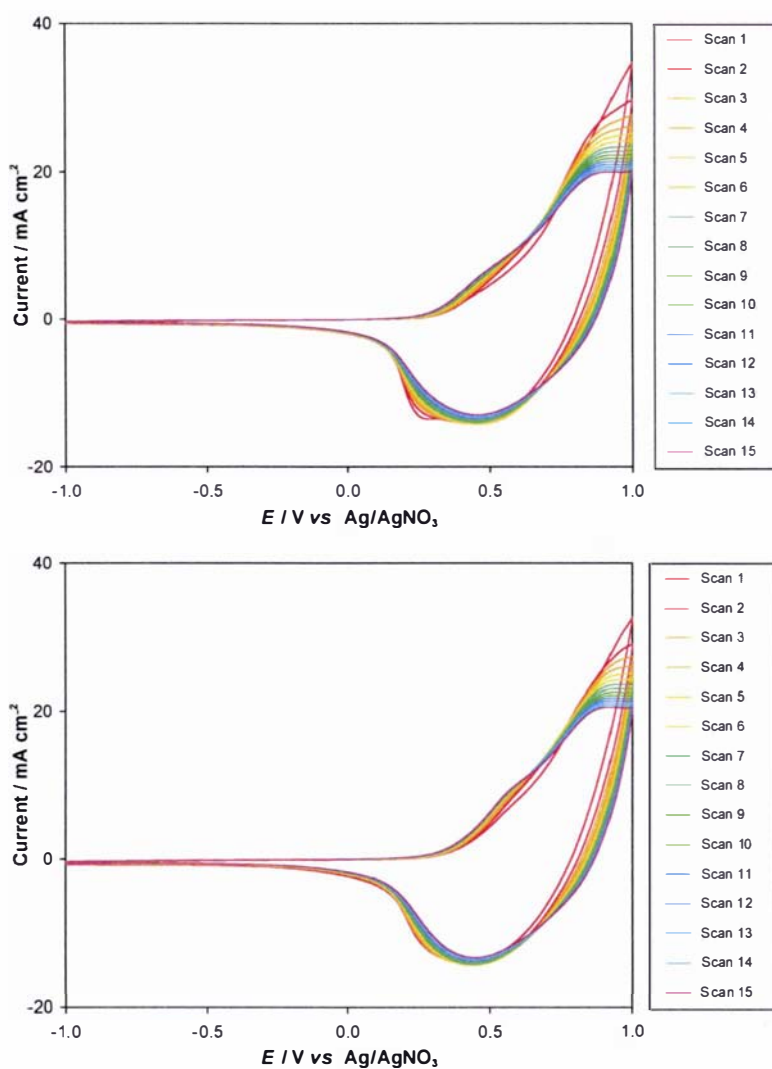


**Figure 5.9** Post-polymerisation CVs of terthiophene in 0.1 M TBAP (top) and 0.1 M LiClO<sub>4</sub> (bottom) ( $\nu = 100 \text{ mV s}^{-1}$ , MeCN)

A film was also prepared for analysis by SEM under the same conditions as above, but using ITO-coated mylar as the working electrode. The CV of the growth of this film is shown in Fig. 5.10 together with an SEM image of the films' surface.

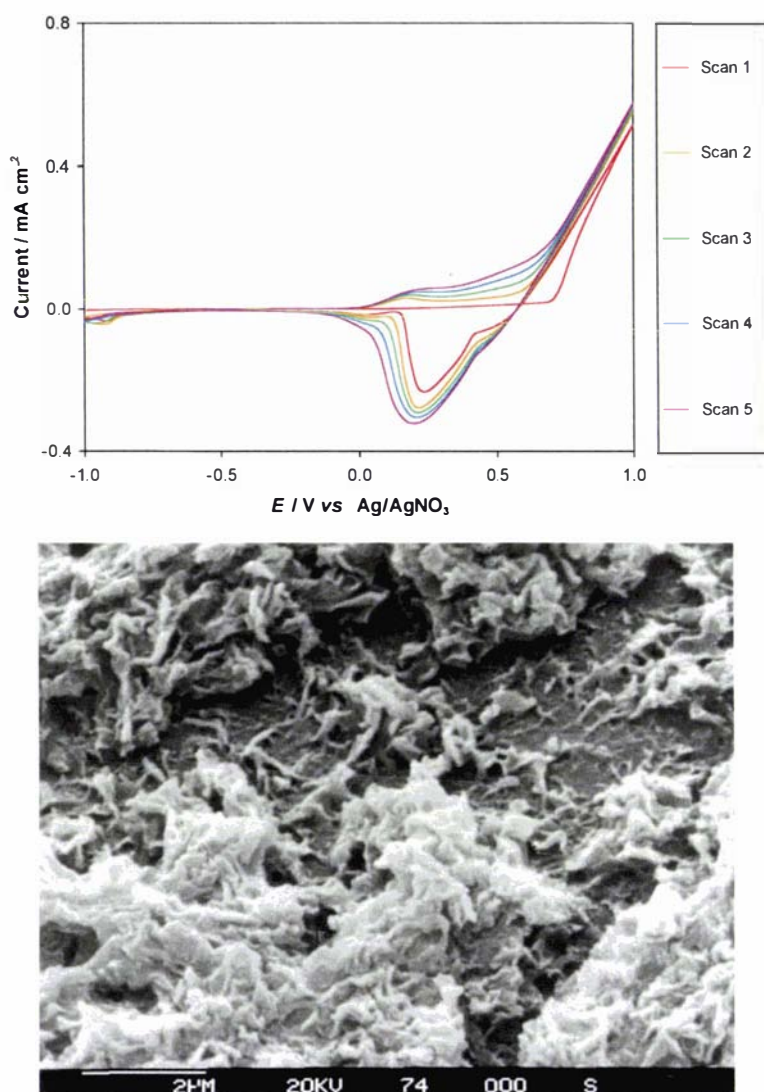


**Figure 5.10 Growth CV (top) and surface morphology of terthiophene film on ITO-coated mylar**

( $\nu = 100 \text{ mV s}^{-1}$ , 10 mM terthiophene, 0.1 M TBAP, MeCN)

It can be seen from a comparison of Figs. 5.8 and 5.10 that the current density obtained on ITO-coated mylar is a fraction of that obtained on a platinum working electrode surface. In addition, the monomer is less readily oxidised on mylar, so that by the oxidative limit (+1.0 V) the current has not attained a peak. Furthermore, if the anodic limit was extended to +1.2 V a peak was still not discernable. The increasing

current with scan number is consistent with deposition of an electroactive film on the mylar surface, increasing its surface area (Section 5.2.1). A scanning electron micrograph of this surface (Fig. 5.10 bottom) shows that under these conditions terthiophene forms a coarse film that appears to cover the surface of ITO-coated mylar.

Films of terthiophene in both the neutral and oxidised state were grown onto ITO-coated glass for analysis by UV/VIS/NIR spectroscopy (Fig. 5.11). The growth CV of terthiophene onto ITO-coated glass was similar in shape to that observed using an ITO-coated mylar working electrode (Fig. 5.10), with no current peak discernable before +1.0 V on the first oxidation scan.

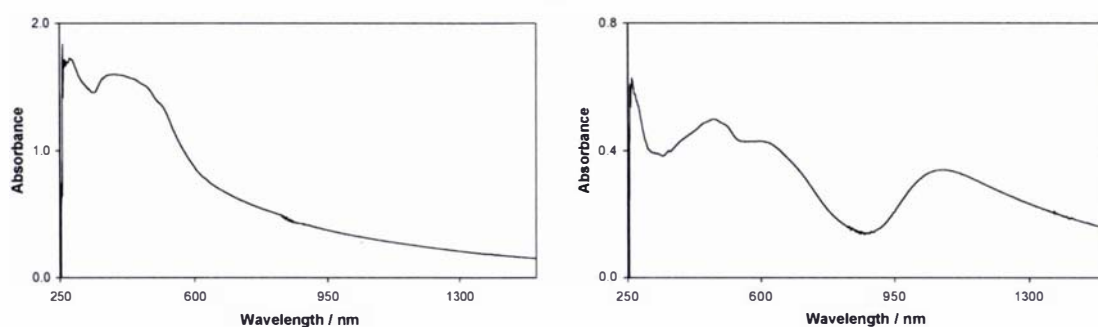


**Figure 5.11** UV/VIS/NIR spectra of poly(terthiophene) in the neutral (left) and oxidised (right) forms

The UV/VIS/NIR spectrum of the neutral poly(terthiophene) film exhibits a broad maximum at 380-410 nm, peaking at 393 nm. This value is in good agreement with that obtained by Roncali *et al.* (400 nm)<sup>318</sup>, Zotti *et al.* (370 nm)<sup>155</sup> and Visy *et al.* (395 nm)<sup>250</sup>, who concluded that poly(terthiophene) consists mostly of dimer and trapped monomer. The spectrum of poly(terthiophene) obtained in the oxidised state has absorption peaks at 478, 595 and 1075 nm, likely due to oxidised sexithienyl species.

### 5.2.3.2 Styryl terthiophene LXXVI

In order to investigate the effect that the conjugated styryl moiety would have on the polymerisation of terthiophene monomers, styryl terthiophene **LXXVI** was investigated next. Its growth CV is shown below in Fig. 5.12, and again points to the formation of an electroactive material on the working electrode surface. A bright red adherent film was visible on the working electrode surface after 5 cycles, and the monomer solution did not appear to have changed colour.

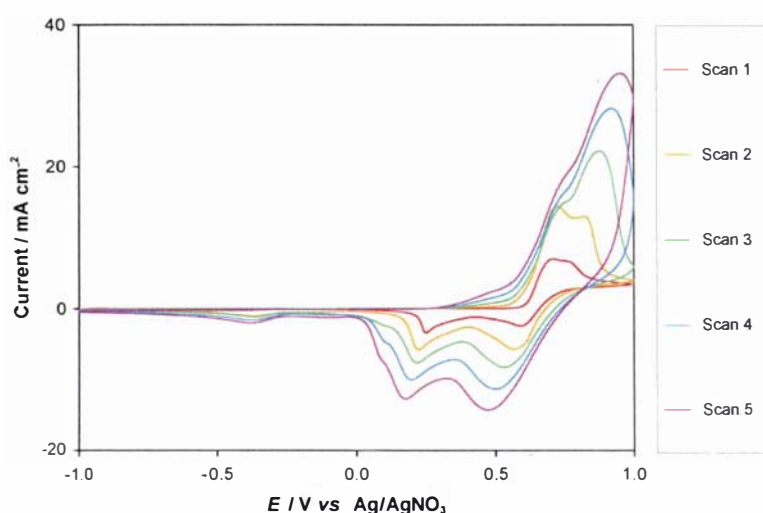


**Figure 5.12** Cyclic voltammetry for styryl terthiophene **LXXVI**

( $\nu = 100 \text{ mV s}^{-1}$ , 10 mM **LXXVI**, 0.1 M TBAP, MeCN)

The oxidation potential peak during the first cycle of electropolymerisation of styryl terthiophene **LXXVI** occurs at 0.72 V, compared to 0.76 V for terthiophene. This indicates that **LXXVI** is more readily oxidised, perhaps due to greater  $\pi$ -delocalisation. On subsequent oxidation sweeps, two peaks are seen at 0.68 and 0.84 V, which merge on further cycling, and gradually shift to higher oxidation potential. The reduction sweep is substantially different to terthiophene, with two peaks at 0.58 and 0.24 V evident in this case, as opposed to a single peak at 0.33 V.

Post-polymerisation CVs in both TBAP and  $\text{LiClO}_4$  are shown below in Fig. 5.13. It can be seen that there is no significant difference in the electrochemical response of the film in the two different electrolytes. In both cases, there is a main oxidation peak

at 0.94 V, with a shoulder at 0.73 V. Two reduction peaks are seen, at 0.42 and 0.13 V. In addition, the film appears to be quite stable, displaying only a small decline in current (6%) between cycles 3-15 in TBAP. The film did not appear to have degraded after this treatment, maintaining its red colour, and the electrolyte remaining colourless.

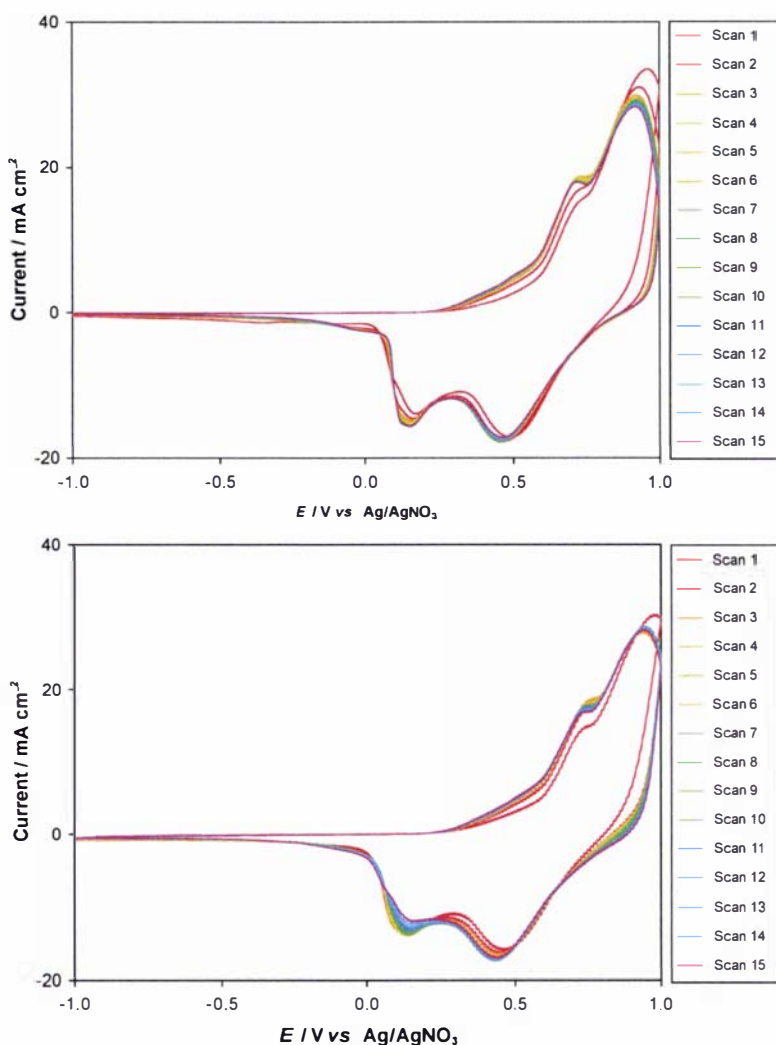


**Figure 5.13 Post-polymerisation CVs for styryl terthiophene LXXVI in 0.1 M TBAP (top) and 0.1 M LiClO<sub>4</sub> (bottom)**

( $\nu = 100 \text{ mV s}^{-1}$ , MeCN)

A scanning electron micrograph of a film of styryl terthiophene grown onto ITO-coated mylar is shown in Fig. 5.14, along with its growth CV. As seen for terthiophene, oxidation occurs at a considerably more anodic potential on this surface. The flat surface visible in the SEM image appears, from a comparison of this image

with a blank obtained on unused mylar, to be the mylar surface rather than a smooth polymer film. Thus it seems that, at least under these conditions, nucleation is sparse on ITO-coated mylar, and coherent films are not formed.

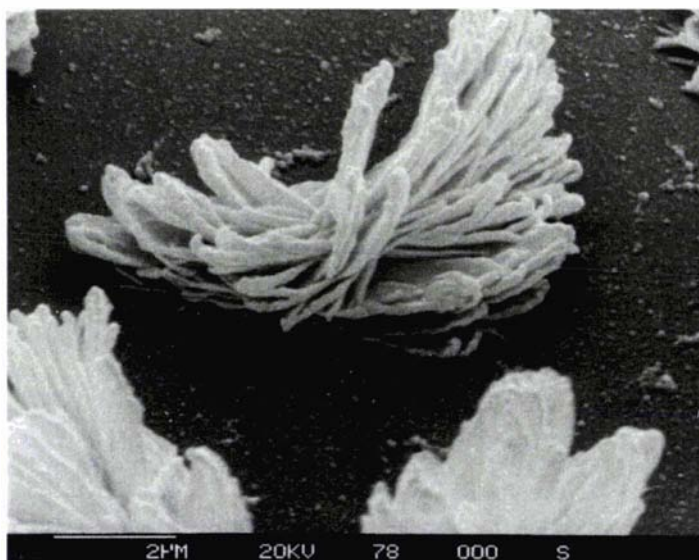
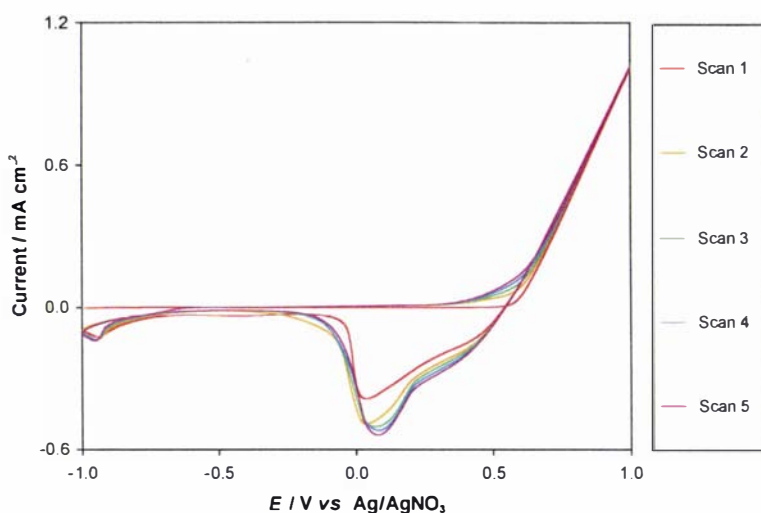


**Figure 5.14 Growth CV (top) and surface morphology of styryl terthiophene LXXVI film on ITO-coated mylar**

( $\nu = 100 \text{ mV s}^{-1}$ , 10 mM LXXVI, 0.1 M TBAP, MeCN)

Samples were also grown onto ITO-coated glass in both the neutral and oxidised forms, and the UV/VIS/NIR spectra of these films are shown in Fig. 5.15.

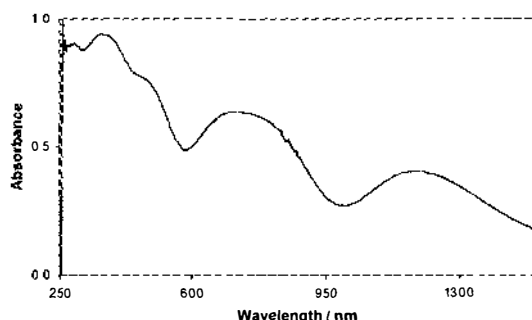


**Figure 5.15 UV/VIS/NIR spectra of poly(styryl terthiophene) in the oxidised form**

The UV/VIS/NIR spectrum of the neutral polymer shows an absorption maximum at 500 nm, that appears to indicate a longer mean conjugation length than seen for terthiophene. However, the data presented in Table 5.3 (page 225) shows that the absorbance maxima for the neutral electrochemically produced film are similar to that observed for the chemically produced dimer. During chemical polymerisation (Section 5.1.2), a small amount of soluble dimer, and a large amount of insoluble material was formed. MALDI-MS results on the sparingly soluble (<0.1 mg/mL) fraction indicated the presence of trace amounts of trimer and tetramer. The neutral sample used in this case was grown over two CV cycles, and it is possible that this was insufficient to form large quantities of higher oligomers, so that only dimers precipitated on the electrode. Conversely, growing a sample using a larger number of CV cycles produced a film that was too highly coloured to be useful for UV/VIS/NIR analysis. The UV/VIS spectrum obtained of the polymer in the oxidised form has peaks at 358, 727 and 1185 nm, with a shoulder at 482 nm. A comparison of the data presented in Table 5.4 (page 226) shows that these peaks are in similar positions to those observed for other dialkoxystyryl-substituted terthiophenes.

### 5.2.3.3 Methoxystyryl terthiophene LXXVII

It was uncertain what effect the incorporation of a methoxy group would have on the properties of the monomer and resulting polymer, as differing results have been reported in the literature for oligothiophenes. For example, alkoxy substituents in the  $\beta$ -position of thiophene oligomers increase the reactivity of the neighbouring  $\alpha$ -

position, and lead to the formation of more highly conjugated polymers. This has been observed for both chemically<sup>85, 91, 295, 296</sup> and electrochemically<sup>319</sup> produced materials. On the other hand, Visy *et al.* studied terthiophene substituted at the 3'-position with a phenyl or methoxyphenyl group,<sup>250</sup> and found no significant differences between the polymers produced. In order to investigate the effect that a methoxy group would have on the electropolymerisation of styryl terthiophene, a solution of monomer **LXXVII** was subjected to cyclic voltammetry (Fig. 5.16).

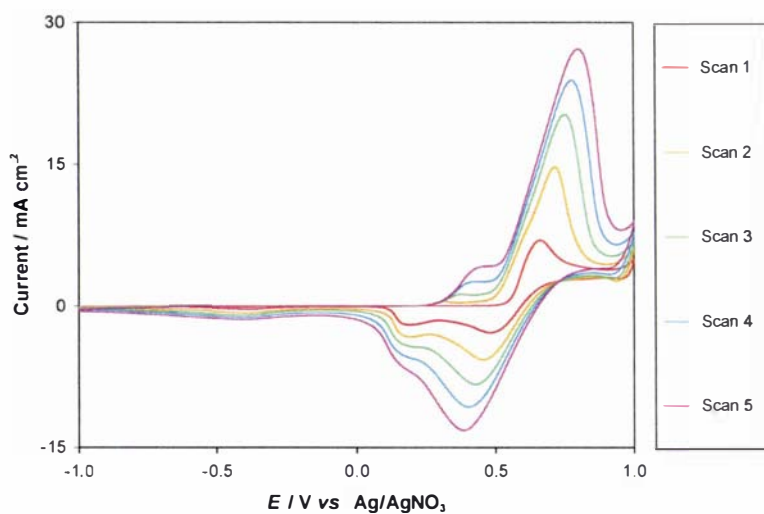


**Figure 5.16** Cyclic voltammetry for methoxystyryl terthiophene **LXXVII**  
( $\nu = 100 \text{ mV s}^{-1}$ , 10 mM **LXXVII**, 0.1 M TBAP, MeCN)

As in the cases of terthiophene and styryl terthiophene, methoxystyryl terthiophene appears to form an electroactive film from the increase in current with scan number evident in Fig. 5.16. The initial oxidation peak occurs at 0.66 V, a lower potential than was seen for either terthiophene (0.76 V) or styryl terthiophene (0.72 V). Therefore this compound appears to oxidise more readily, which could indicate that the methoxy group is having a stabilizing effect on the oxidised species. It has been previously reported that the electron-donating methoxy group can reduce oxidation potential by stabilizing the radical cation formed, reducing the extent of polymerisation and giving rise to polymers with inferior properties.<sup>57, 240, 250</sup> Scheib and Bauerle<sup>140</sup> saw a similar reduction in oxidation potential on moving from an alkyl-substituted bithiophene, to an alkoxy-substituted bithiophene. They suggested that this could be due to the higher ionic conductivity of the polyether groups. They postulated that this would allow easier diffusion of the counter ions that are necessary to balance the positive charges formed on the polymer backbone during oxidation.

The first reduction sweep for **LXXVII** shows two peaks at 0.48 and 0.16 V, which appear to be equivalent to those seen for styryl terthiophene at 0.58 and 0.24 V. On further scans these merge together to form a single reduction peak at 0.41 V. The second oxidation sweep gives two peaks, visible at 0.28 and 0.71 V. While these move to slightly higher potentials on further cycling, they remain well separated and distinct, in contrast to the merging of close oxidation peaks seen for styryl terthiophene.

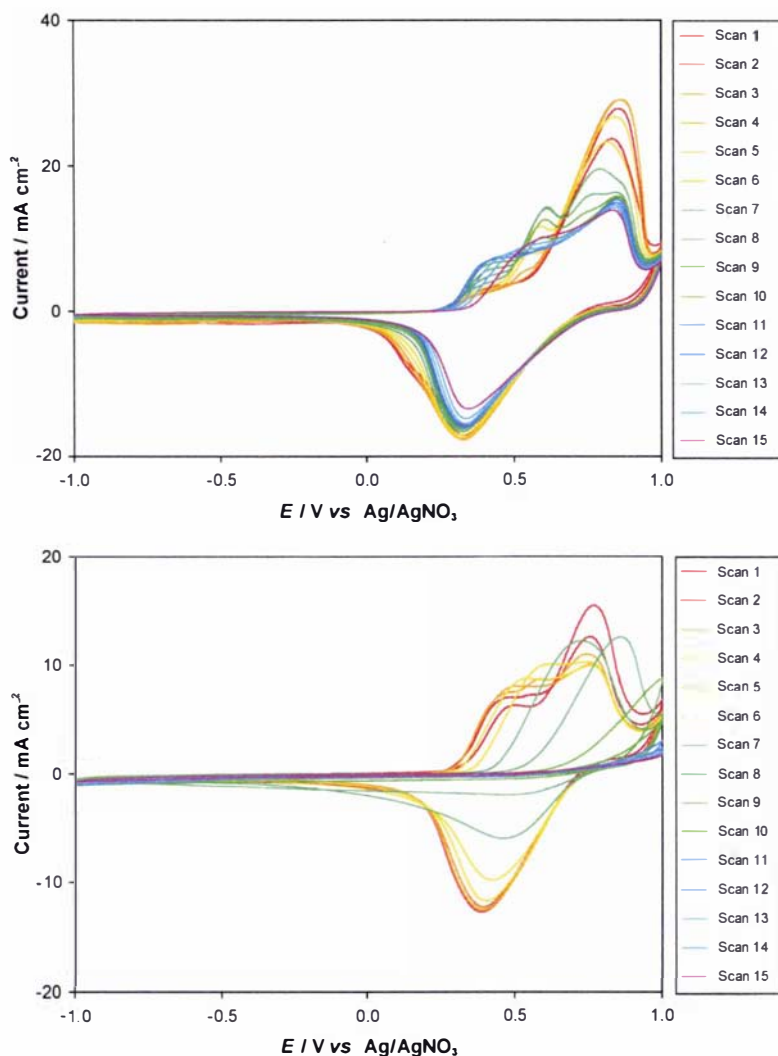


**Figure 5.17** Post-polymerisation CVs of methoxystyryl terthiophene **LXXVII** in 0.1 M TBAP (top) and 0.1 M LiClO<sub>4</sub> (bottom)  
( $\nu = 100 \text{ mV s}^{-1}$ , MeCN)

Post-polymerisation CVs for methoxystyryl terthiophene are shown in Fig. 5.17, and a substantial difference can be seen in the films' response to these electrolytes. While in TBAP the peak current value has dropped by 40% over 15 cycles, in  $\text{LiClO}_4$  the film has lost all electroactivity before 10 cycles have been completed. Since the same anion is present in both electrolytes, and it is generally the anion that moves in and out of the film to balance charge, it seems unlikely that this is due to a size-based mobility difference between the small  $\text{Li}^+$  and large  $\text{N}(\text{Bu})_4^+$  cations. It seems more probable that the increased rate of degradation in  $\text{LiClO}_4$  solution is due to an interaction between the lithium cation and the methoxy group. This loss of activity appears to be oxidative degradation rather than dissolution for two reasons. First, the electrolyte solutions do not appear to become coloured after post-polymerisation as would be expected if conjugated species were dissolving. Secondly, the presence of a sticky dark blue material on the working electrode surface indicates the presence of insoluble or sparingly soluble oxidised species.

A sample grown under the same conditions onto ITO-coated mylar is shown in Fig. 5.18, together with its growth CV. In this case, as for terthiophene and styryl terthiophene (Sections 5.2.3.1 and 5.2.3.2), the monomer oxidation potential has increased sufficiently so that a peak is not observed. The current density is again considerably lower than for the corresponding growth CV onto a platinum working electrode (Fig. 5.16), consistent with previous results. In contrast to the image obtained for styryl terthiophene (Fig. 5.14), methoxystyryl terthiophene appears to be forming overlapping sheet-like structures that cover the entire mylar surface under these conditions.

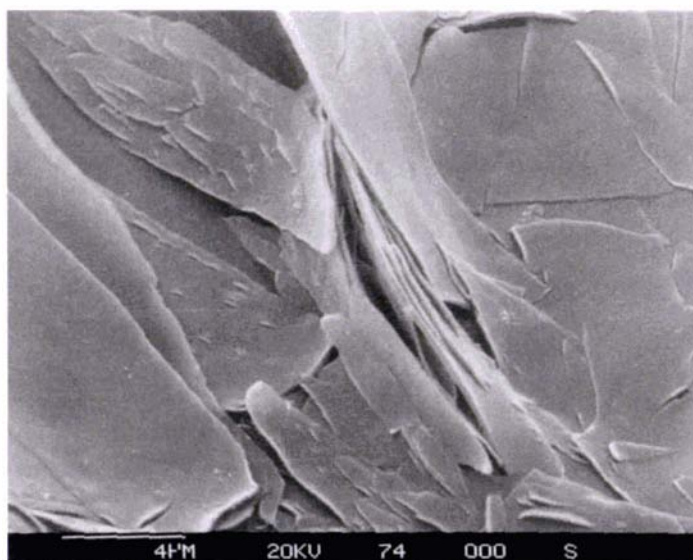
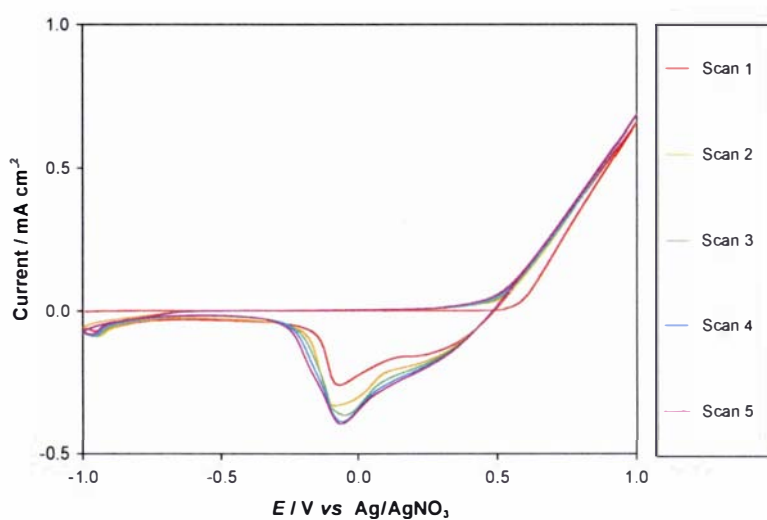


**Figure 5.18 Growth CV and SEM for methoxystyryl terthiophene LXXVII film**

( $v = 100 \text{ mV s}^{-1}$ , 10 mM LXXVII, 0.1 M TBAP, MeCN)

Films in both the neutral and oxidised forms were grown onto ITO-coated glass to be analysed by UV/VIS/NIR spectroscopy. The spectra obtained are shown below in Fig. 5.19.

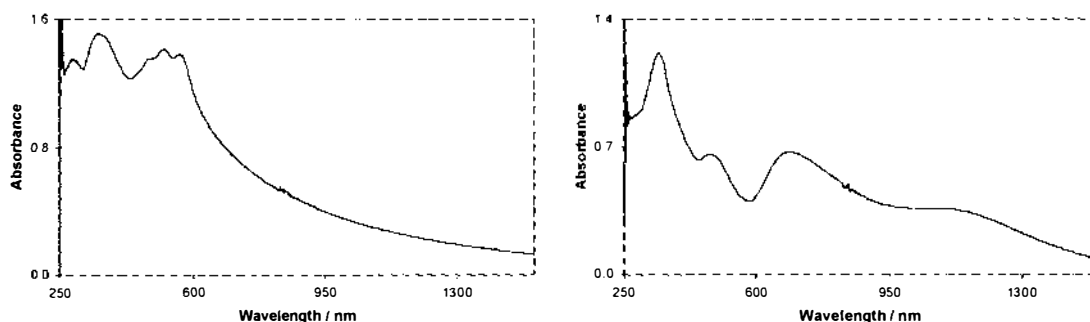


**Figure 5.19 UV/VIS/NIR spectra of poly(methoxystyryl terthiophene) in the neutral (left) and oxidised (right) forms**

The UV spectrum of the neutral poly(methoxystyryl terthiophene) film shows absorbance maxima at 357, 489, 524 and 563 nm. In contrast, a film of the dimer synthesised *via* chemical polymerisation shows maxima at 336 and 488 nm (Table 5.3). The peaks observed in the electrochemically produced film at 524 and 563 nm are not inconsistent with the formation of longer oligomers. This finding is in agreement with the results of chemical polymerisation, where only a small amount of dimer (9 %) was successfully isolated. The remaining insoluble material (89 %) is believed to consist of higher oligomers and/or cross-linked material, although its insolubility meant that it could not be analysed (Section 5.1.2). The spectrum of the oxidised form of monomer **LXXVII** shows absorption maxima at 345, 482, 689 and 1082 nm. No 'free carrier tail' absorption increasing into the NIR is evident.

An electrochemically grown film of poly(methoxystyryl terthiophene) was also studied independently by resonance Raman spectroscopy at Otago University. The spectrum of this film exhibited bands in the same position as seen for a solution of the chemically produced dimer (Section 5.1.2), which matched the spectrum calculated for the head-to-head linked dimer.<sup>65, 261</sup>

## 5.2.4 Electropolymerisation of dialkoxystyryl-substituted terthiophene compounds

### 5.2.4.1 Dimethoxystyryl terthiophene XXIX

Given the evidence for at least low levels of polymerisation obtained using styryl and methoxystyryl terthiophene, investigation of the electrochemical properties of dimethoxystyryl terthiophene **XXIX** allows the effect of an additional methoxy group to be evaluated. The growth CV, run under the same conditions used for the previous compounds, is shown in Fig. 5.20. A bright red adherent film was deposited on the working electrode surface, and no discolouration of the monomer solution was apparent.

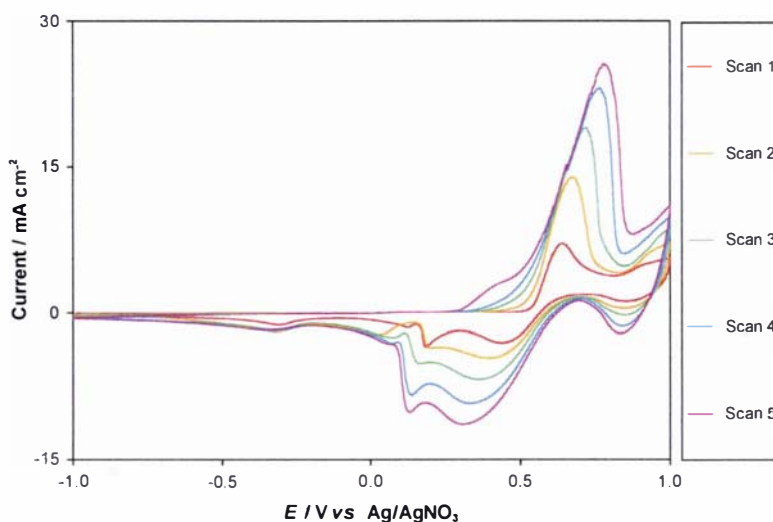
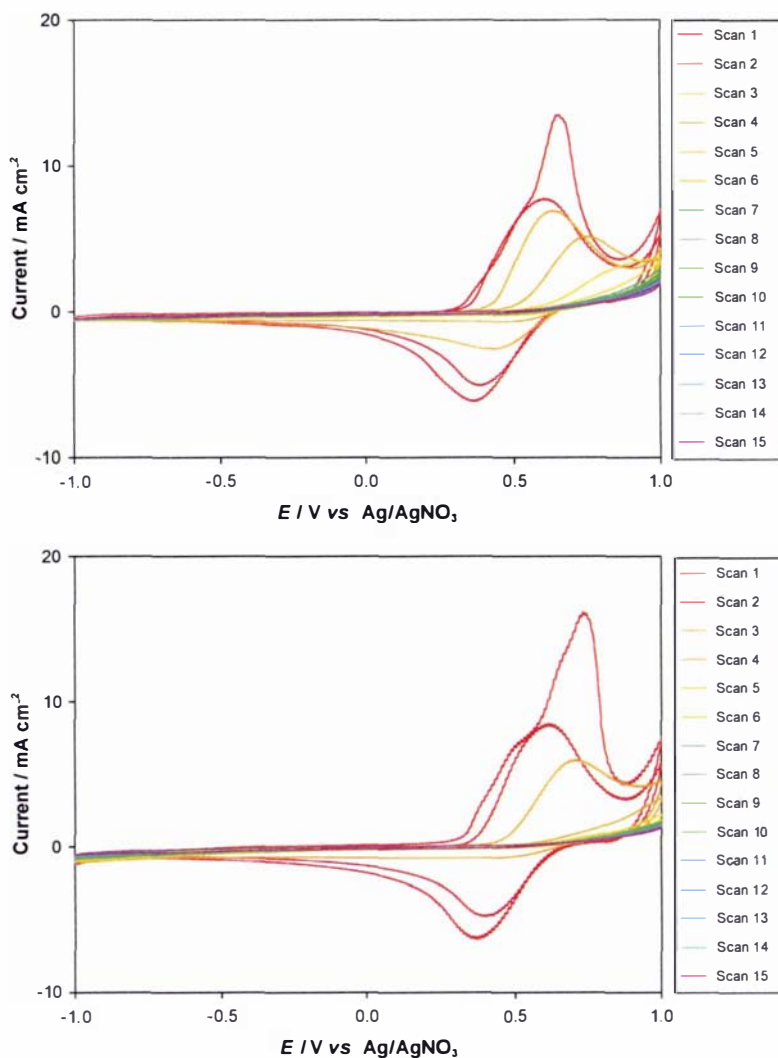


**Figure 5.20** Cyclic voltammetry for dimethoxystyryl terthiophene **XXIX**  
( $\nu = 100\ mV\ s^{-1}$ , 10 mM **XXIX**, 0.1 M TBAP, MeCN)

Figure 5.20 shows a growth CV, indicative of an electroactive polymer, from dimethoxystyryl terthiophene **XXIX**. The initial oxidation peak appears at 0.65 V, at almost the same position observed for methoxystyryl terthiophene (0.66 V). This indicates that the additional methoxy group does not substantially change the stability of the oxidised species. The two reduction peaks discernable on the first scan (0.43,

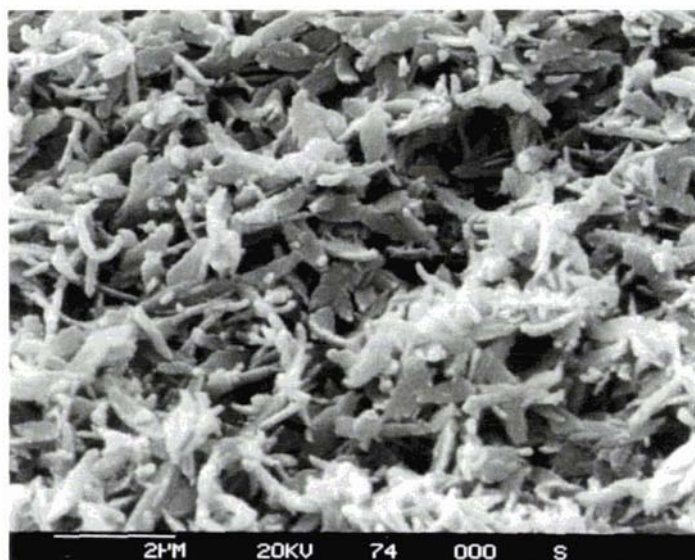
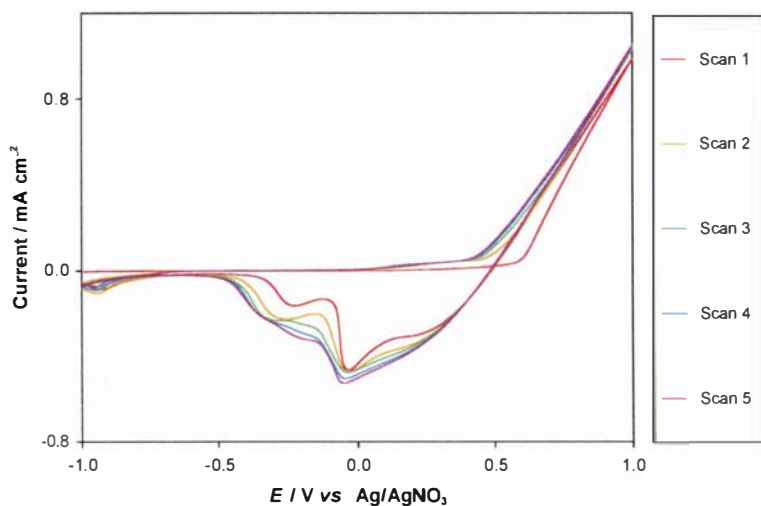
0.18 V) are also in a similar position to those observed for **LXXVII**. Subsequent scans, however, differ between the two compounds. In this case, one main oxidation peak is observed, with only a small shoulder evident at lower oxidation potential. This could imply the formation of shorter chain length material. Reduction sweeps show the continuation of the two peaks seen on the first scan. In addition, there is a broad, shallow peak evident at  $-0.32$  V.

Post-polymerisation CVs with TBAP and  $\text{LiClO}_4$  as electrolyte are shown in Fig. 5.21. Similar current densities are observed, with oxidative degradation occurring in both electrolytes although it appears slightly faster when  $\text{Li}^+$  is present. This indicates that the film is not stable over the potential range employed in its electrosynthesis. As this is not seen for terthiophene or styryl terthiophene, it may be due to the incorporation of methoxy groups. It has already been noted from a comparison of oxidation potentials (Table 5.4) that methoxystyryl and dimethoxystyryl terthiophene oxidise at lower potentials than terthiophene and styryl terthiophene. The increase in current at the anodic limit observed for the alkoxy-substituted compounds could indicate the start of this degradation. It seems likely that both oxidative degradation and polymerisation occur during cyclic voltammetry between these potential limits in a solution of monomer, with polymerisation being the dominant reaction. In monomer-free solution however, polymerisation cannot occur so that oxidative degradation alone is observed. These dual processes have been described by Mukoyama *et al.* for poly(3-methylthiophene).<sup>320</sup> The observation that the degradation is faster in the presence of  $\text{Li}^+$  for both this compound and methoxystyryl terthiophene, makes it seem likely that an interaction between  $\text{Li}^+$  and the methoxy groups present may also make a contribution to the observed instability.



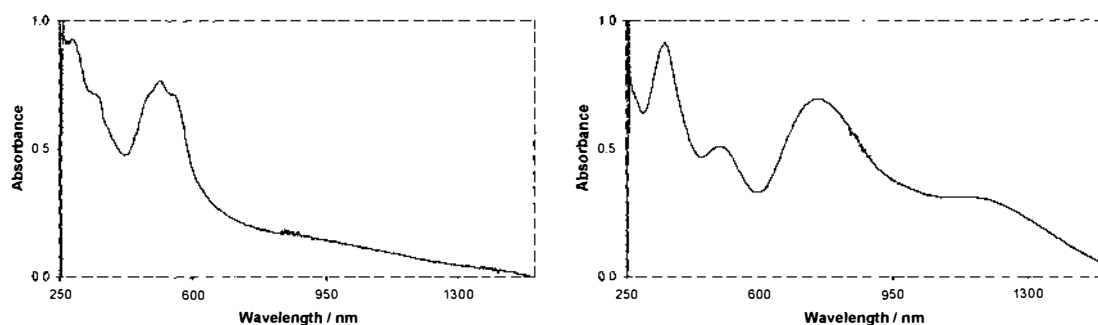
**Figure 5.21** Post-polymerisation CVs of dimethoxystyryl terthiophene **XXIX** in 0.1 M TBAP (top) and 0.1 M LiClO<sub>4</sub> (bottom)  
( $\nu = 100 \text{ mV s}^{-1}$ , MeCN)

Figure 5.22 shows the growth CV of dimethoxystyryl terthiophene **XXIX** onto ITO-coated mylar, and SEM analysis of the film produced. In this case, as for methoxystyryl terthiophene, the mylar surface is covered by a layer of polymer. The morphology is substantially different between the two compounds, with **XXIX** forming a more porous, less smooth structure.



**Figure 5.22 Growth CV and SEM of dimethoxystyryl terthiophene XXIX film on ITO-coated mylar**  
 ( $\nu = 100 \text{ mV s}^{-1}$ , 10 mM XXIX, 0.1 M TBAP, MeCN)

Samples were also grown onto ITO-coated glass, for analysis by UV/VIS/NIR spectroscopy. The spectra obtained are shown below in Fig. 5.23.



**Figure 5.23 UV/VIS/NIR spectra of poly(dimethoxystyryl terthiophene) in the neutral (left) and oxidised (right) forms**

In the UV spectrum obtained for the neutral film, peaks can be seen at 280, 347 and 513 nm, with a shoulder at 555 nm. On chemical polymerisation with  $\text{FeCl}_3$  a high yield of dimer was obtained, MALDI-MS confirming that no higher oligomers were present (Section 4.1.2.3). A thin film of this dimer cast onto a quartz surface by evaporation from  $\text{CH}_2\text{Cl}_2$ , afforded a UV spectrum with peaks in identical positions to that obtained here by electropolymerisation (Table 5.3). Therefore, there is no UV evidence for the presence of oligomers with greater chain length than dimers under these conditions. The spectrum obtained for the oxidised film shows peaks at 350, 496, 749 and 1147 nm, with no sign of a 'free carrier tail' extending into the near infrared.

#### 5.2.4.2 Styryl-15-crown-5 terthiophene I

The next compound to be electropolymerised was styryl-15-crown-5 terthiophene **I**. Growth by cyclic voltammetry indicated the formation of an electroactive polymer with two sets of redox peaks (Fig. 5.24). By the fourth scan, all four peaks are distinct and at this point the peak separations are *ca.* 60 mV for the lower potential couple, and *ca.* 160 mV for those at higher potential. This indicates that the peaks at lower potential are due to a reversible one-electron process. These separations increase slightly with increasing scan number.

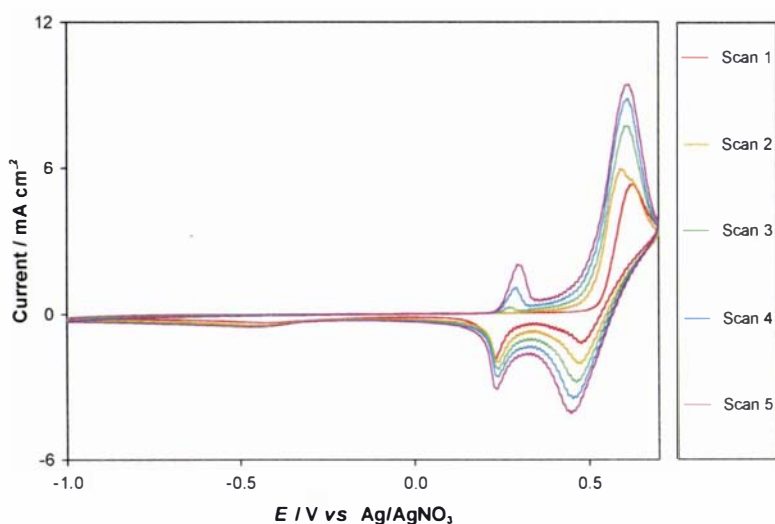


**Figure 5.24** Cyclic voltammetry for styryl-15-crown-5 terthiophene **I**  
( $\nu = 100 \text{ mV s}^{-1}$ , 10 mM **I**, 0.1 M TBAP, MeCN)

Electrochemical polymerisation of **I** under these conditions gave an adherent red film on the electrode surface, which after rinsing with solvent, was subjected to post-polymerisation cyclic voltammetry in monomer-free electrolyte solution (Fig. 5.25 top). A post-polymerisation CV on a new film, grown under the same conditions, was obtained in 0.1 M  $\text{LiClO}_4$  (Fig. 5.25 bottom).

The growth CV shown in Fig. 5.24 clearly shows two reversible redox peaks. One oxidation peak is seen on the initial scan (0.64 V), with a second peak appearing at 0.28 V on subsequent scans. The reduction is seen as two peaks at 0.47 and 0.22 V. It is assumed here that the oxidation peak at 0.64 V is due to oxidation of the monomer to its radical cation. Terthiophene radical cations are known to be very reactive and couple quickly to form dimers (sexithiophenes) as discussed in Section 5.1. The oxidation potential required to oxidise the terthiophene to its radical cation must be higher than the oxidation potential required to oxidise sexithiophene, so that the newly formed neutral sexithiophene would be oxidised immediately to its dication as it is formed. The two reduction peaks observed could then be caused by reduction of the sexithiophene dication to the radical cation, and then the radical cation to the neutral species. On further oxidation cycles, dimer would already be present and the new oxidation peak at 0.28 V could be a result of oxidizing the dimer to its radical cation. On each sweep, more terthiophene would be oxidised and couple to

sexithiophene, which could then be reduced and reoxidised, explaining why the peak currents enlarge with each subsequent scan. Oxidised sexithienyl species are well known to be very stable (Section 5.1.3), accounting for why no further polymerisation is observed. In addition, the oxidation peak at higher potential would be large due to the formation of dimer that then diffuses into the bulk solution. This was evidenced by a discolouration of the solution over time, from light yellow to bright yellow. MALDI-MS analysis of this solution indicated the presence of dimer, but no higher oligomers.

The post-polymerisation CV in TBAP (Fig. 5.25 top) shows the same two sets of redox peaks evident in the growth CV that were attributed to the formation of sexithiophene radical cation and dication respectively. After the first scan, during which any trapped monomer could be oxidised/polymerised, these peaks are similar in size, as would be expected for a reversible redox system. This CV strongly resembles that seen by Zotti *et al.* for 3'-pentoxy-3,3''-dioctyl-[2,2';5',2'']-terthiophene, where only dimers were formed on electropolymerisation.<sup>319</sup> A gradual decrease in current can also be seen on post-polymerisation cycling in monomer-free electrolyte (Fig. 5.25 top). This was attributed to a slow dissolution of the product in acetonitrile, as evidenced by the gradual yellow coloration of the electrolyte solution and eventual recovery of a mirror surface on the platinum working electrode. Very rapid dissolution was observed in solutions containing metal ions, and it was observed that the solution became coloured in the immediate vicinity of the working electrode. Again, the silver surface on the working electrode was recovered. MALDI-MS analysis of the metal ion electrolyte gave no evidence for oligomers longer than the dimer. Because of this almost instant dissolution, post-polymerisation cyclic voltammograms could not be obtained in metal cation solutions (Fig. 5.25 bottom). This was the case for all metal ion solutions tested ( $\text{Li}^+$ ,  $\text{Na}^+$ ,  $\text{K}^+$ ,  $\text{Mg}^{2+}$ ,  $\text{Ca}^{2+}$ ,  $\text{Mn}^{2+}$ ). As rapid dissolution of the electrochemically-produced film was observed only in the presence of metal ions, and not in TBAP, it is believed that the marked change in solubility was caused by complexation of the metal ions by the crown moiety. This is not surprising given the solubility properties of the product obtained from chemical polymerisation of styryl-15-crown-5 terthiophene **I**. The isolated crown dimer **LXVII** was slightly soluble in acetonitrile, but become freely soluble on addition of

Na<sup>+</sup>, mirroring the behaviour of the electrochemically produced film. Similar dissolution was observed by Berlin *et al.*<sup>154</sup> for a terthiophene compound containing a directly attached crown ether (Fig. 4.5c), and by McCullough and Williams for poly[3-(2,5,8-trioxanonyl)thiophene] (Fig. 1.15a)

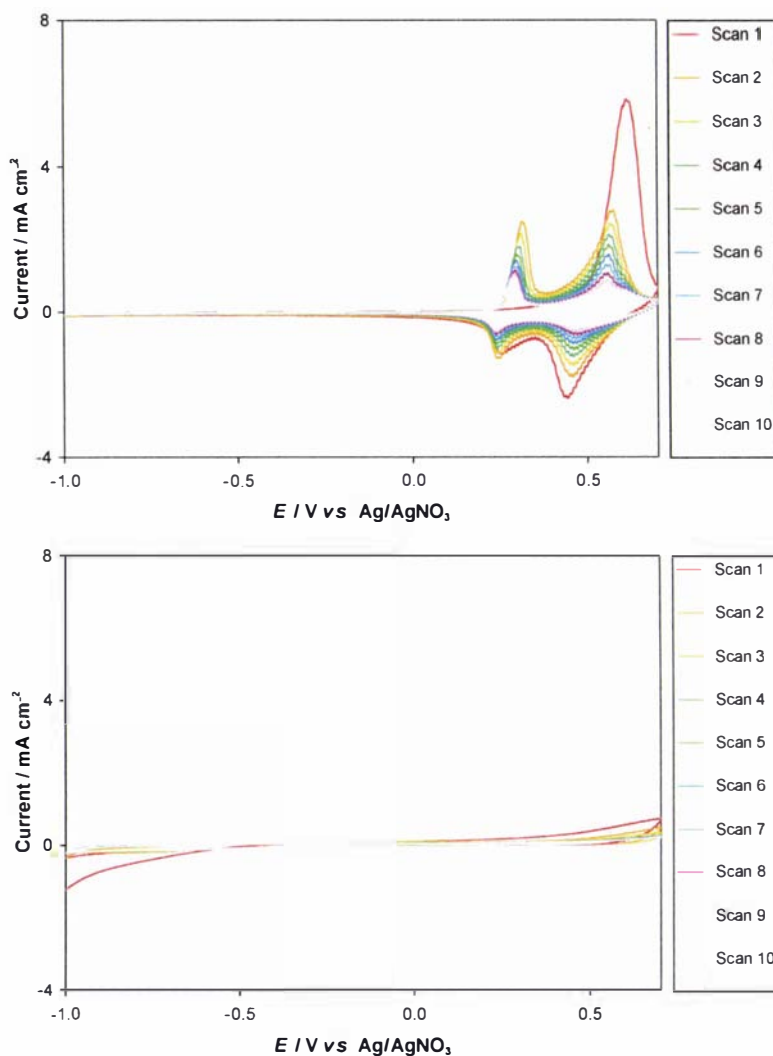


**Figure 5.25** Post-polymerisation CVs of styryl-15-crown-5 terthiophene **I** in 0.1 M TBAP (top) and 0.1 M LiClO<sub>4</sub> (bottom) ( $\nu = 100 \text{ mV s}^{-1}$ , MeCN)

In an attempt to form a more stable film from styryl-15-crown-5 terthiophene **I**, the upper potential limit was increased slightly to +1.0 V (Fig. 5.26).

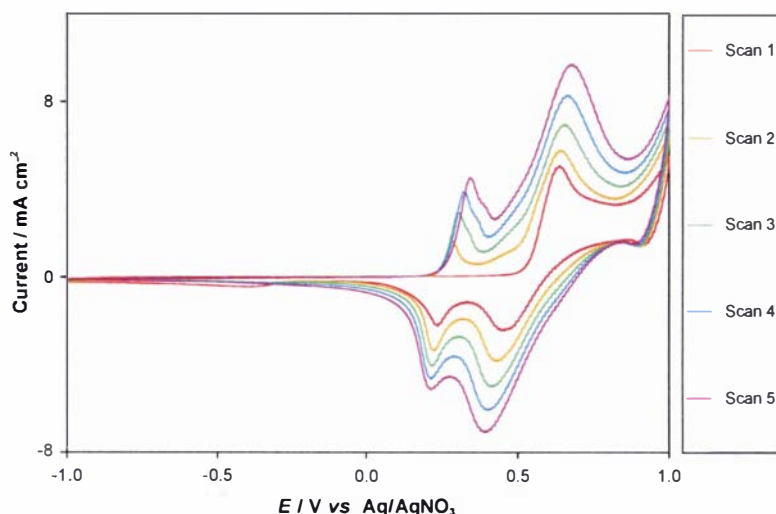


**Figure 5.26 Growth CV for styryl-15-crown-5 terthiophene I**

( $\nu = 100 \text{ mV s}^{-1}$ , 10 mM I, 0.1 M TBAP, MeCN)

The increasing current with scan number is indicative of the formation of an electroactive material on the working electrode. The initial oxidation (0.65 V) and reduction (0.44, 0.23 V) peaks are at potentials similar to those observed for dimethoxystyryl terthiophene, indicating an electronic similarity between the two compounds. The main difference between this growth CV and that shown in Fig. 5.24, is the start of a second oxidation peak at *ca.* 0.9 V. As this response occurs at a higher potential than is necessary for dimer formation, it cannot be due to a longer oligomeric species. It is possible that the oxidation responsible for this new peak is some type of cross-linking, perhaps through the alkene bond as seen by other researchers for styryl-thiophenes (Section 1.5). This new oxidation peak does not have a corresponding reduction peak, indicating that it is irreversible.

Post-polymerisation CVs in 0.1 M TBAP and 0.1 M LiClO<sub>4</sub> are shown below in Fig. 5.27. A comparison of the post-polymerisation CVs in Fig. 5.27 with those in Fig. 5.25 shows a number of differences. Immediately evident is that in this case, post-polymerisation cycling was possible in the presence of Li<sup>+</sup>. Although the film had degraded after 10 cycles had been run, this was a large improvement over the earlier attempt, and growing the film to a slightly higher oxidation potential had somehow stabilized the resulting film. It can also be seen that the shape of these cyclic voltammograms is quite different to those obtained at lower oxidation potential, with the two sets of redox peaks no longer distinguishable. This is attributed to the effects

of slightly overoxidising the film, which has improved its stability at the expense of reversibility. It seems likely that the overoxidised species are less soluble in MeCN, thereby slowing the dissolution process. The observation that the film cycled in  $\text{LiClO}_4$  had completely degraded after 10 scans, whereas the film cycled in TBAP still had a reasonable activity at that point, indicates that metal ion complexation is again playing a role in destabilizing the film.

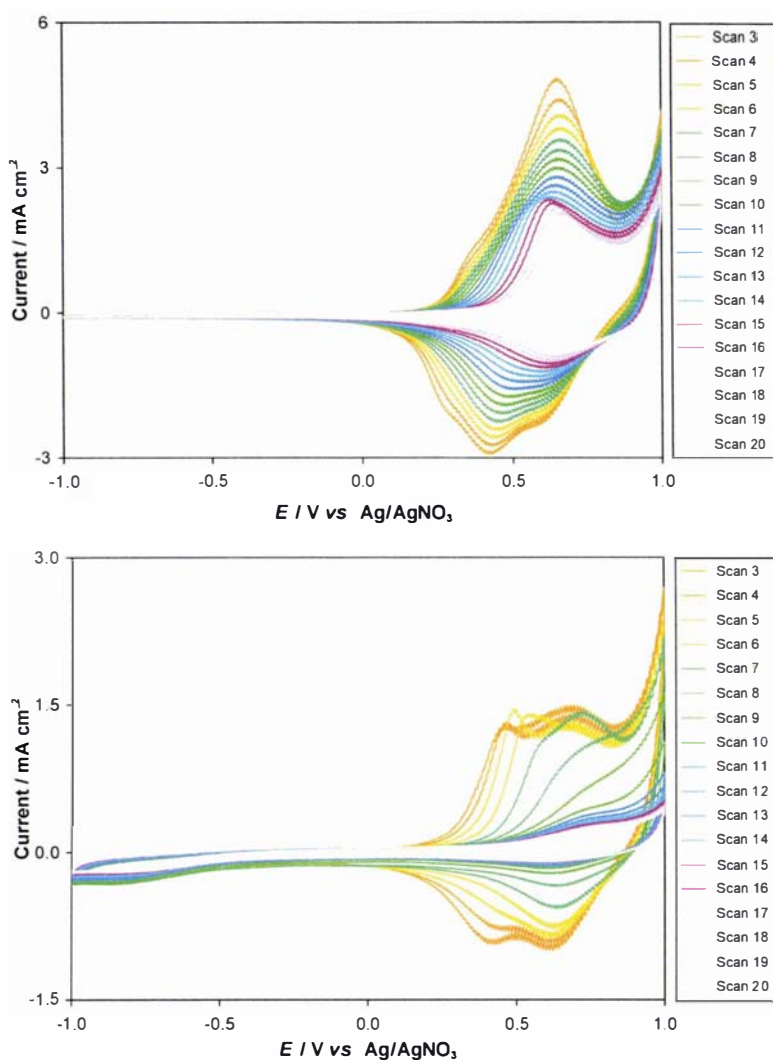


**Figure 5.27** Post-polymerisation CVs of styryl-15-crown-5 terthiophene **I** in 0.1 M TBAP (top) and 0.1 M  $\text{LiClO}_4$  (bottom) ( $\nu = 100 \text{ mV s}^{-1}$ , MeCN)

A scanning electron micrograph of a film of **I** grown onto ITO-coated mylar is shown, together with its growth CV, in Fig. 5.28.

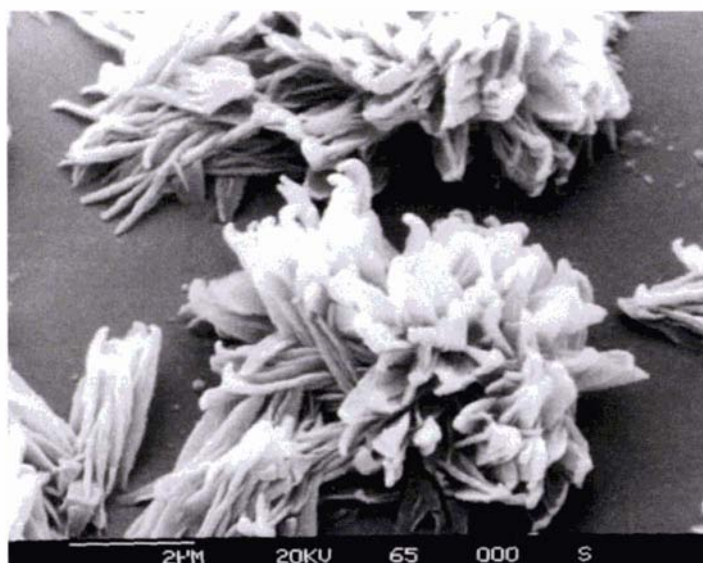
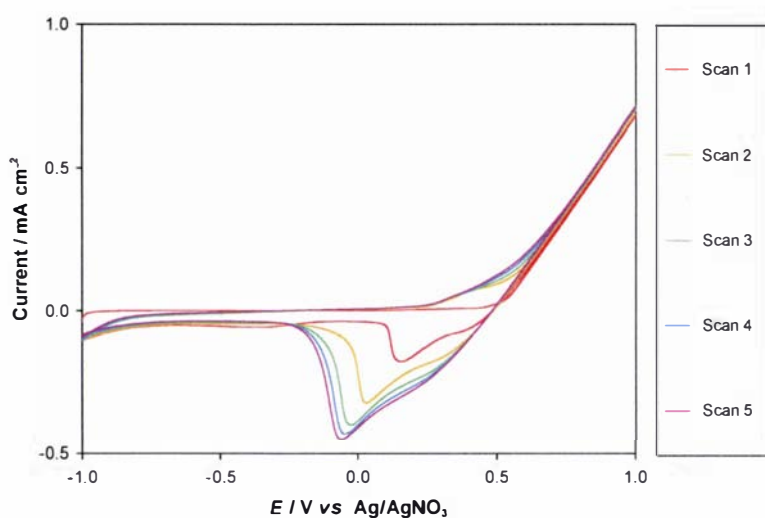


**Figure 5.28 Growth CV and SEM of styryl-15-crown-5 terthiophene I film**

( $v = 100 \text{ mV s}^{-1}$ , 10 mM I, 0.1 M TBAP, MeCN)

It appears from this SEM picture, that upon electropolymerisation under these conditions, styryl-15-crown-5 terthiophene I is not forming a continuous film, but rather numerous discrete coral-like structures. An increase in the density of nucleation on ITO-coated mylar would be necessary in order for these separate structure to merge and form a film.

Films were also grown onto ITO-coated glass, for analysis by UV/VIS/NIR spectroscopy. Separate films were grown in the neutral and oxidised state as described in Section 5.2.2, and their spectra are shown below in Fig. 5.29.

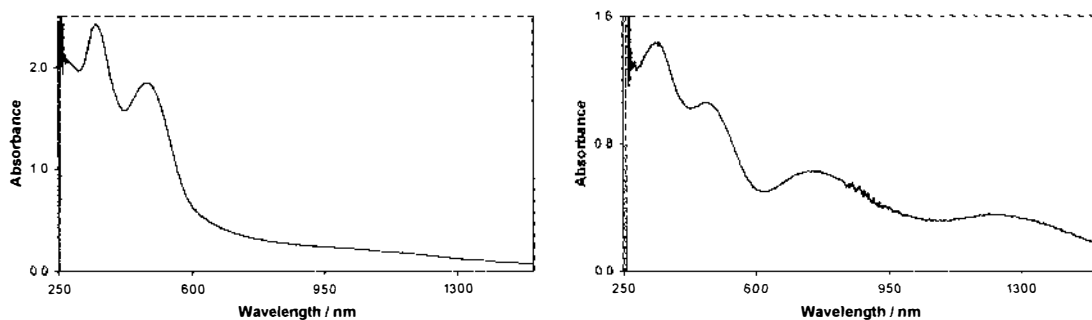


**Figure 5.29** UV/VIS/NIR spectra of styryl-15-crown-5 terthiophene **I** in the neutral (left) and oxidised (right) forms

The  $\lambda_{\max}$  peaks in the spectrum of the neutral film occur at 348 and 480 nm. A comparison of these values with those obtained for a film of the pure dimer (Table 5.3) gives a close correlation. This provides further evidence that under these conditions, polymerisation is stopping at the dimer. Furthermore, this is in agreement with the results previously obtained for chemical oxidation of **I** with  $\text{FeCl}_3$  and  $\text{Cu}(\text{ClO}_4)_2$  (Sections 5.1.2 and 5.1.3). In the spectrum of the oxidised film, additional peaks are observed at 753 and 1254 nm, at similar potentials to other oxidised sexithienyl species (Table 5.3).

Increasing the upper oxidation potential further during cyclic voltammetry, led to over-oxidation<sup>49</sup> of the polymer film (Fig. 5.30). This is evidenced by large oxidation peaks, but a lack of corresponding reduction peaks. In addition, the surface of the working electrode was covered in sticky blue material on removal from the monomer solution, the colour consistent with this material incorporating oxidised species.

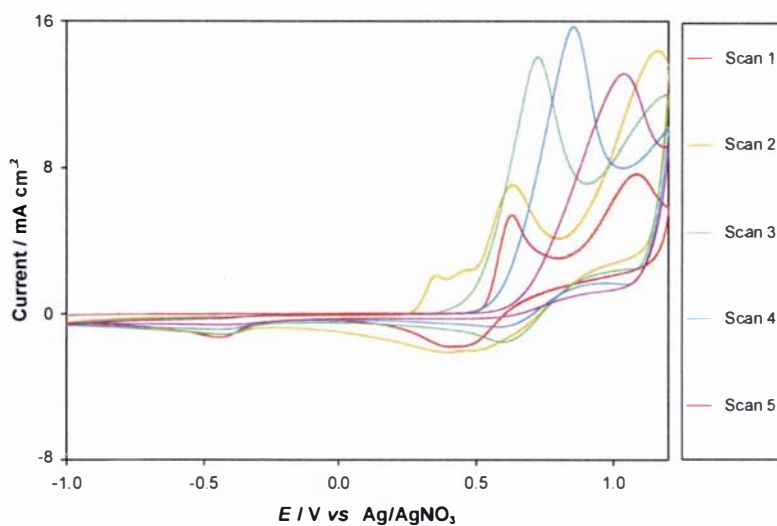


**Figure 5.30 Overoxidation of styryl-15-crown-5 terthiophene I**  
 ( $\nu = 100 \text{ mV s}^{-1}$ , 10 mM I, 0.1 M TBAP, MeCN)

### 5.2.4.3 Styryl-18-crown-6 terthiophene II

The same conditions that were successful in forming electroactive films from the previous monomers were employed in the cyclic voltammetry of a solution of styryl-18-crown-6 terthiophene **II** (Fig. 5.31).

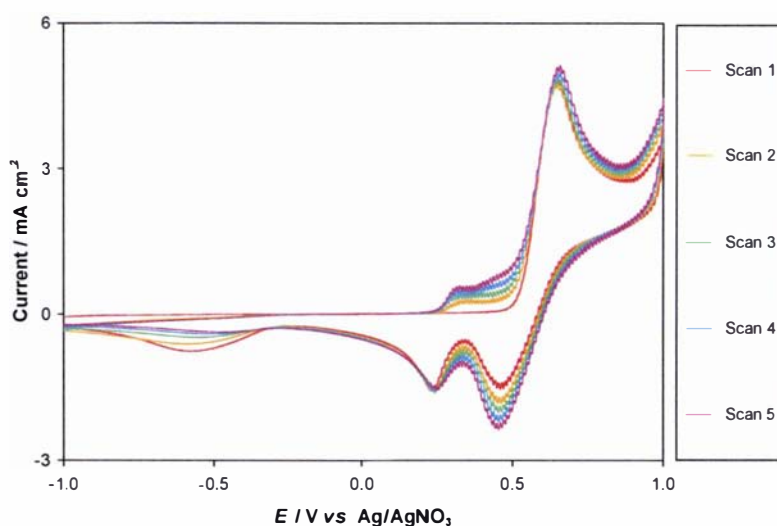


**Figure 5.31 Cyclic voltammetry for styryl-18-crown-6 terthiophene II**  
 ( $\nu = 100 \text{ mV s}^{-1}$ , 10 mM II, 0.1 M TBAP, MeCN)

Unlike all previous cases, no film was visible on the electrode after 5 cycles under these conditions. The oxidation (0.66 V) and reduction (0.45, 0.23 V) peaks are located at potentials close to those observed for dimethoxystyryl terthiophene and styryl-15-crown-5 terthiophene. This makes it seem unlikely that electronic factors are the reason for the lack of film formed. Given that both of those compounds only form dimers during electrochemical growth under these conditions, it seems likely that this is also the case for monomer **II**. During chemical polymerisation of the terthiophene monomers synthesised during this research (Section 5.1.2), it was noted that a lengthening of the polyether chain incorporated in the molecule markedly increased its solubility. It is possible that the lack of film formation here could be due to the increased solubility of the dimer in acetonitrile, rather than electronic effects. As there was no film formed for this compound, surface morphology and UV/VIS/NIR properties could not be investigated.

#### **5.2.4.4 Open-chain substituted terthiophenes XXIII - XXVIII**

The first open-chain compound to be electropolymerised, was the shortest chain isovanillin derivative **XXIII**, and its growth CV on platinum is shown in Fig. 5.32. The initial oxidation peak (0.65 V) and reduction peaks (0.86, 0.41, 0.23, -0.45 V) are in the same positions as those observed for other dialkoxystyryl terthiophene derivatives (Table 5.4). This shows that compound **XXIII** reacts similarly to the other compounds investigated. However, there is a difference apparent in later oxidation scans. It can be seen from Fig. 5.32 that the current reaches a maximum value after 4 oxidation scans, and then declines on the final oxidative sweep. This implies that oxidation of the monomer to its radical cation at the surface is becoming less efficient, perhaps due to non-conductive material being deposited on the working electrode. The film also appeared visually darker than other similar films. An added complication in this case was the tendency of the monomer to crystallize out from solution.

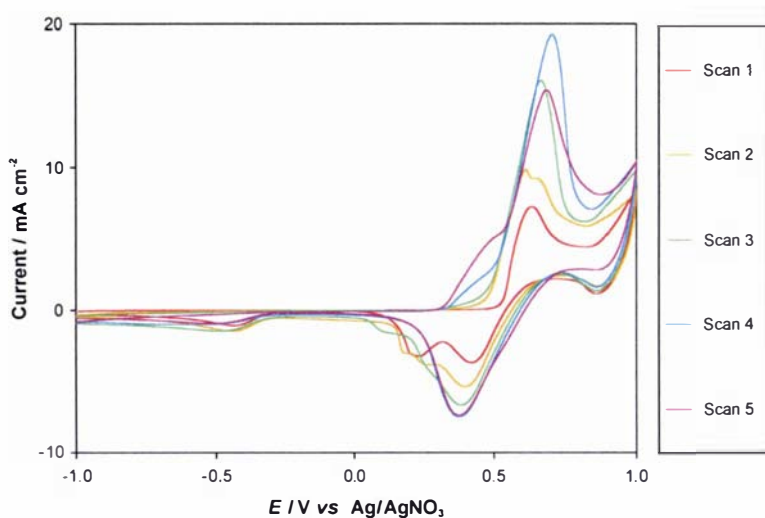


**Figure 5.32** Cyclic voltammetry for open-chain terthiophene XXIII  
 ( $\nu = 100 \text{ mV s}^{-1}$ , 10 mM XXIII, 0.1 M TBAP, MeCN)

Post-polymerisation CVs of this film in both TBAP and  $\text{LiClO}_4$  were also obtained, and are shown in Fig. 5.33. There, the film degrades at approximately the same rate regardless of electrolyte. As interpreted for methoxystyryl terthiophene and dimethoxystyryl terthiophene, it seems likely that this current decline is due to oxidative degradation. This is consistent with the lack of colouration of the electrolyte, and by the development of dark material on the working electrode surface, following post-polymerisation cycling. It is interesting that in this case, the current decline is independent of electrolyte composition, suggesting an absence of complexation between the polyether chain and the lithium cations.

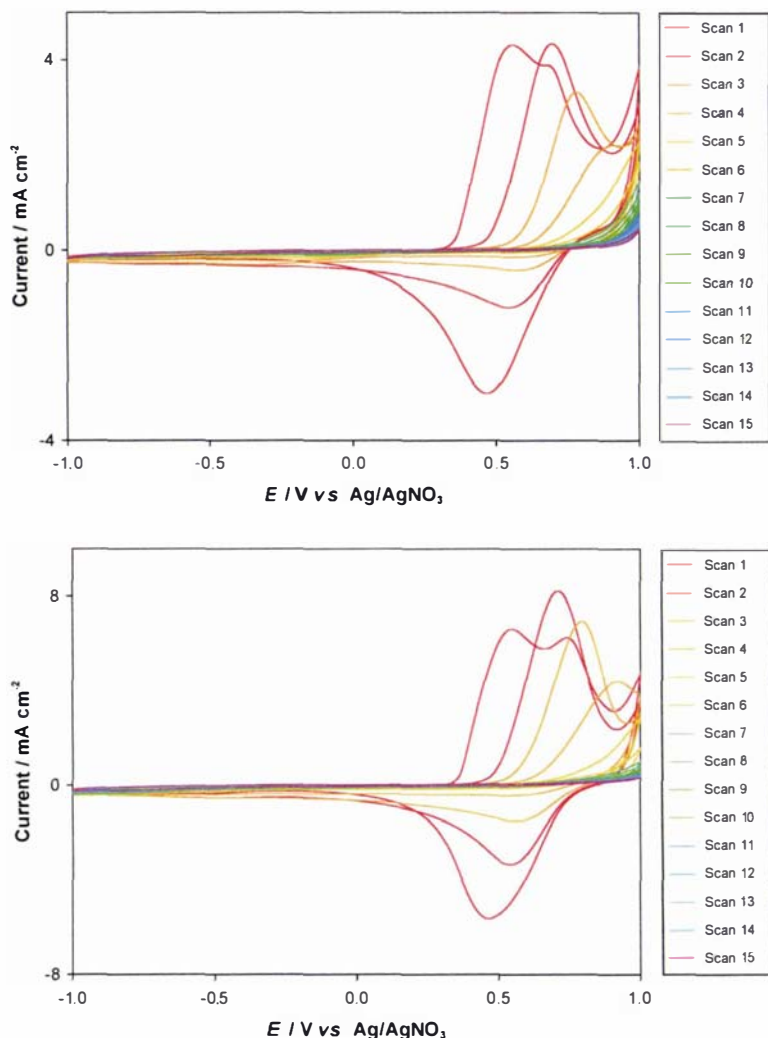


**Figure 5.33** Post-polymerisation CVs of open-chain terthiophene XXIII in 0.1 M TBAP (top) and 0.1 M LiClO<sub>4</sub> (bottom) ( $\nu = 100 \text{ mV s}^{-1}$ , MeCN)

As for previous dialkoxyethyl-substituted terthiophenes, films were grown onto ITO-coated glass for analysis by UV/VIS/NIR spectroscopy. The spectra obtained are shown below in Fig. 5.34. A main peak is seen in the neutral film, at 523 nm, with shoulders at 499 and 578 nm. While the main peak corresponds to that seen for the pure dimer film (528 nm, Table 5.3), the shoulder at 578 nm may well indicate the presence of a higher oligomer. This cannot be proven however, and it is also possible that this peak could be due to an overoxidised species on the surface.

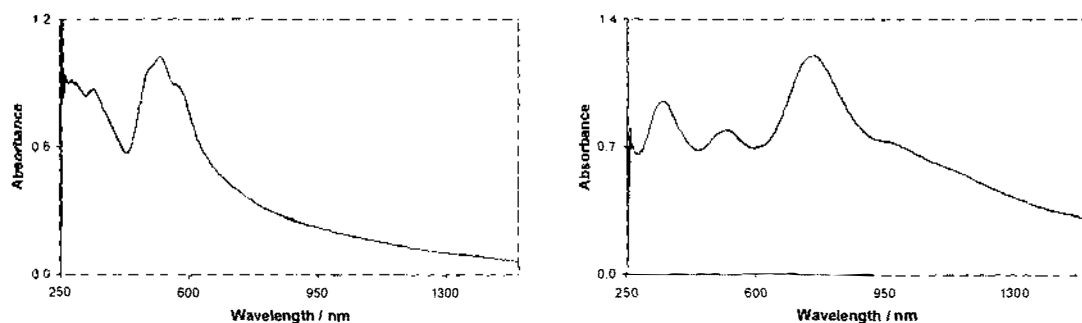


**Figure 5.34** UV/VIS/NIR spectra of open-chain terthiophene **XXIII** in the neutral (left) and oxidised (right) forms

A film was also grown onto ITO-coated mylar for SEM analysis, and both the growth CV and an SEM image are presented in Fig. 5.35. The growth CV indicates that (as seen for all the previous compounds) the oxidation of **XXIII** is more difficult on ITO-coated mylar than on platinum. The SEM shows that, under these conditions, open-chain compound **XXIII** has formed long fibre-like structures that partially cover the surface.

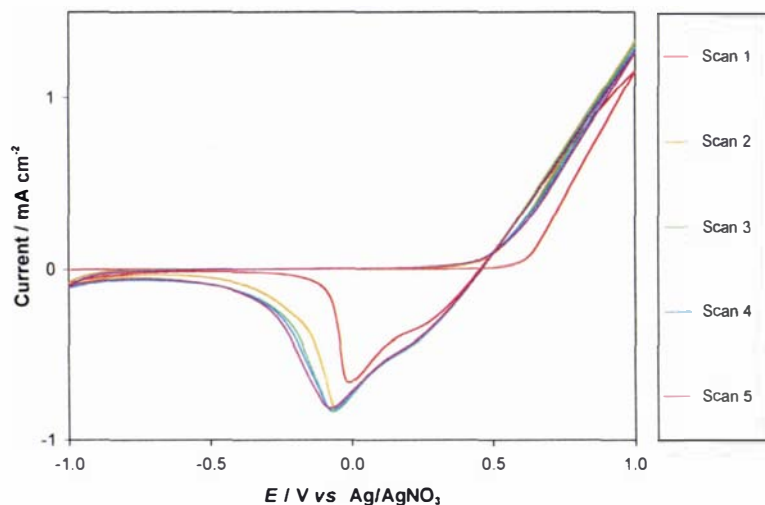


**Figure 5.35 Growth CV (top) and SEM image of XXVI film on ITO-coated mylar**

( $\nu = 100 \text{ mV s}^{-1}$ , 10 mM XXVI, 0.1 M TBAP, MeCN)

The analogous vanillin-derived monomer, **XXVI**, also formed an electroactive film, and its growth CV onto a platinum working electrode is presented in Fig. 5.36. The initial oxidation peak at 0.65 V, with an additional increase in current toward the anodic potential limit is similar to the other dialkoxystyryl-substituted terthiophenes investigated (Table 5.4). Two closely spaced peaks are seen on subsequent oxidative sweeps, indicating the formation of oligomeric material. The reduction peaks

observed are also at similar potentials to those seen for other related compounds (Table 5.4).

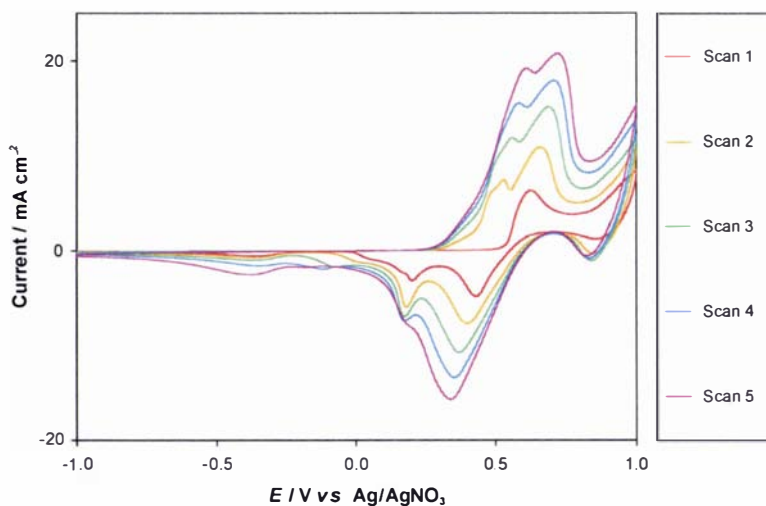


**Figure 5.36** Cyclic voltammetry for open-chain terthiophene **XXVI**  
( $\nu = 100\ mV\ s^{-1}$ , 10 mM **XXVI**, 0.1 M TBAP, MeCN)

Post-polymerisation CVs for separate electrochemically grown films of **XXVI** in TBAP and  $LiClO_4$  are shown below in Fig. 5.37. In contrast to the results obtained for methoxystyryl terthiophene, dimethoxystyryl terthiophene and styryl-15-crown-5 terthiophene (Sections 5.2.3.3, 5.2.4.1, 5.2.4.2) degradation appears to be faster in the presence of  $N(Bu)_4^+$  than  $Li^+$ . The decline in current evident in Fig. 5.37 appears to result from oxidative degradation rather than dissolution. This is evidenced by the lack of colouring of the electrolyte solutions, and by the presence of dark blue/black residue on the working electrode surface after cycling. It is unclear why this process is faster in TBAP than in  $LiClO_4$ .

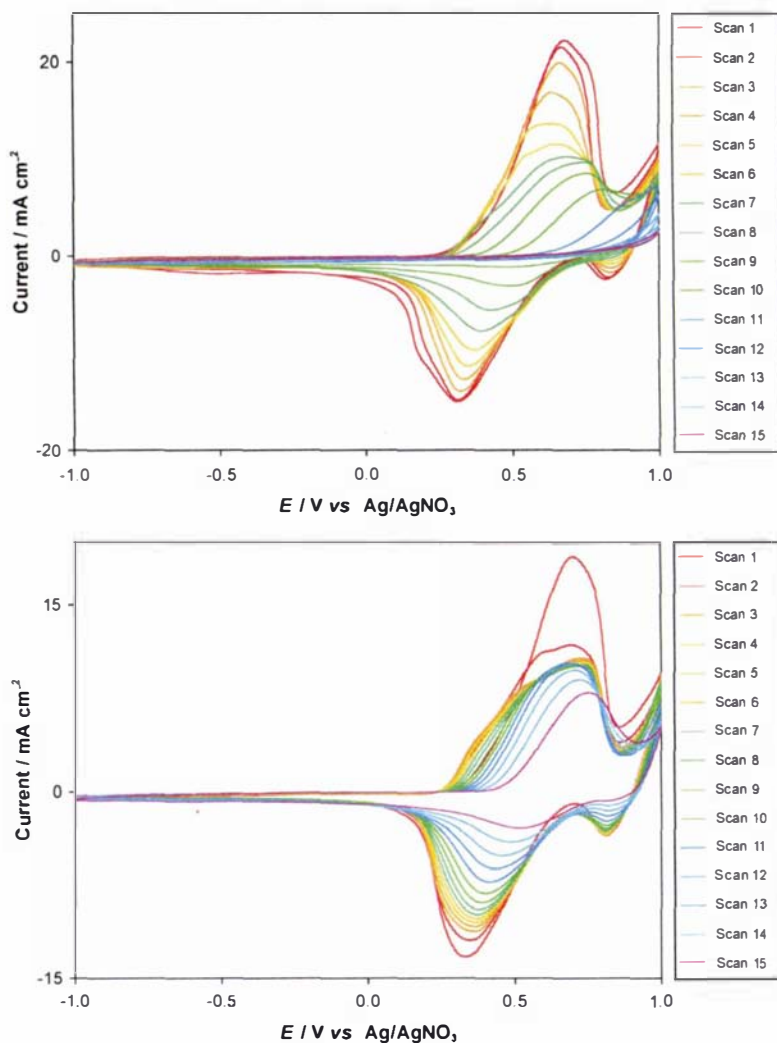


**Figure 5.37 Post-polymerisation CVs of open-chain terthiophene XXVI in 0.1 M TBAP (top) and 0.1 M LiClO<sub>4</sub> (bottom)**  
( $\nu = 100 \text{ mV s}^{-1}$ , MeCN)

A film of **XXVI** was also grown onto ITO-coated mylar, to be analysed by scanning electron microscopy. The growth CV and SEM image of the surface are shown below in Fig. 5.38. The surface morphology of **XXVI** most resembles that seen for 15-crown-5 terthiophene **I** (Fig. 5.28). While in both cases the film appeared homogeneous on a macroscopic scale, the SEM images show that coherent films are not formed. Nucleation appears to be sparse under these conditions, leading to the distinct coral-like structures seen in Fig. 5.38. This issue would need to be addressed in order to produce a film of **XXVI**.

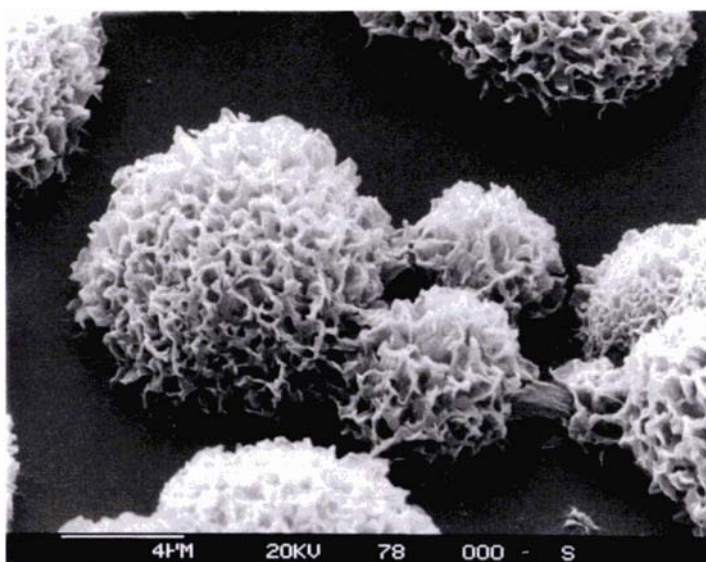
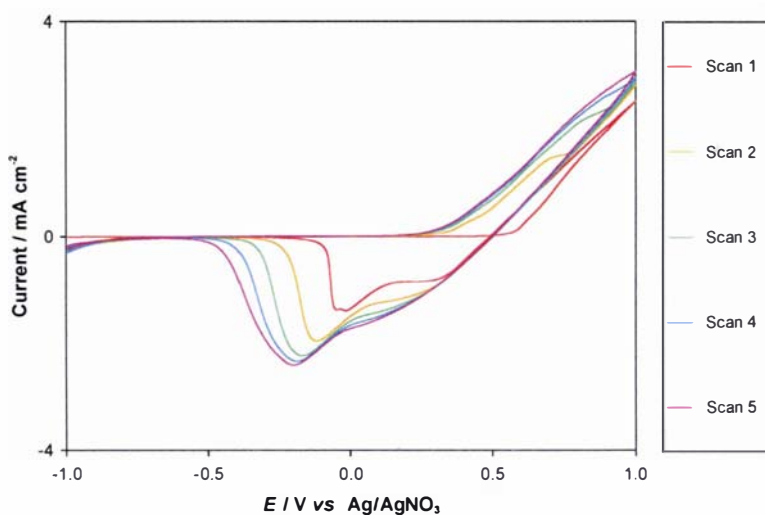


**Figure 5.38 Growth CV (top) and SEM image of open-chain terthiophene XXVI film on ITO-coated mylar**

( $\nu = 100 \text{ mV s}^{-1}$ , 10 mM XXVI, 0.1 M TBAP, MeCN)

A film was also grown, in the oxidised form, onto ITO-coated glass. Several attempts were made to obtain a spectrum of the film in the neutral oxidation state, but these proved futile. The UV/VIS/NIR spectrum of this film (Fig. 5.39) shows peaks at 357, 510, 695, and 978 nm. The three highest energy peaks are similar to those seen for other dialkoxystyryl-substituted terthiophenes. However, the shoulder at 978 nm and that seen for the isovanillin analogue at 995 nm, are not seen in the spectra of other compounds. Neither is there a peak at  $>1200 \text{ nm}$  in the spectra of these two short chain styryl terthiophenes.

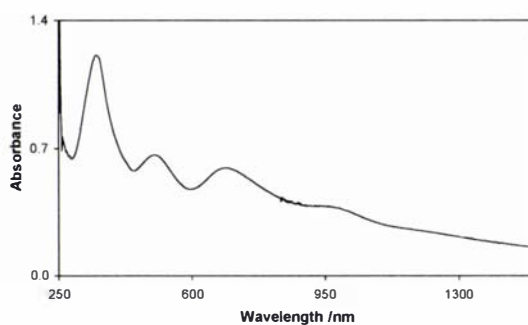


**Figure 5.39** UV/VIS/NIR spectrum of poly(XXVI) in the oxidised form

No films could be formed from cyclic voltammetry of the longer open-chain compounds **XXIV**, **XXV**, **XXVII** and **XXVIII**. The cyclic voltammograms recorded were similar in each case, and an example is shown below in Fig. 5.40. Peak potential data for all four compounds is presented in Table 5.4. The lack of film formation meant that SEM and UV/VIS/NIR analysis could not be used in these cases.

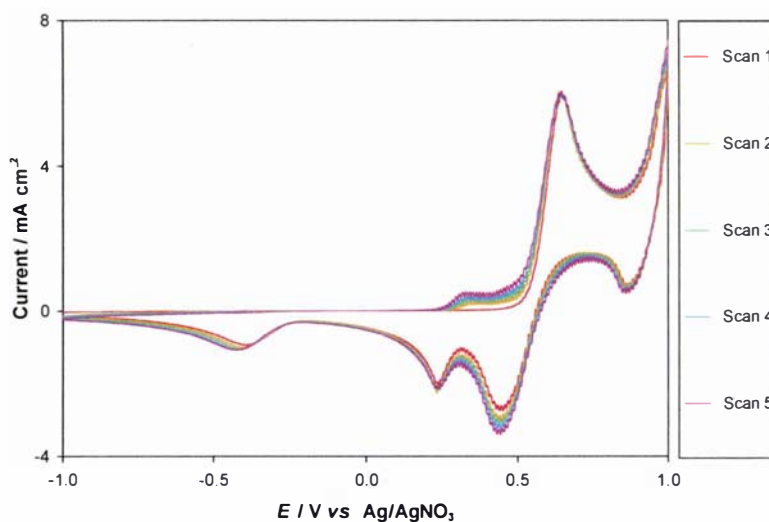


**Figure 5.40** Cyclic voltammetry for open-chain terthiophene **XXVII**  
( $\nu = 100 \text{ mV s}^{-1}$ , 10 mM **XXVII**, 0.1 M TBAP, MeCN)

As can be seen from Fig. 5.40 and Table 5.4, the cyclic voltammograms obtained for compounds **XXIV**, **XXV**, **XXVII** and **XXVIII** are very similar to that obtained for other dialkoxyethyl-substituted terthiophenes. The new peak appearing at 0.33-0.36 V on the second and subsequent oxidation sweeps indicates that an oligomeric species is being produced. In this case, however, a film is not formed. This appears

to suggest that the oligomeric species is soluble, and does not deposit significantly on the working electrode surface. During chemical polymerisation of the open-chain terthiophenes (Section 5.1.2), a marked increase in solubility with increasing polyether chain length was noted. It is not inconsistent with previous observations that the asymmetric reactivity of the terthiophene monomer is leading only to the formation of dimers, and that in these cases the sexithienyl species formed are sufficiently soluble that they do not form films on the electrode surface.

#### **5.2.4.5 Terthiophene hemicrowns LXI - LXIII**

The three isomeric terthiophene hemicrowns **LXI** - **LXII** produced virtually identical responses upon electropolymerisation, so that only one example will be discussed here. Cyclic voltammograms obtained in both  $\text{CH}_2\text{Cl}_2$  and 1:1  $\text{MeCN}:\text{CH}_2\text{Cl}_2$  for the isovanillin-derived hemicrown **LXI** are shown below in Fig. 5.41. Red adherent films were obtained from both of these solvent systems.

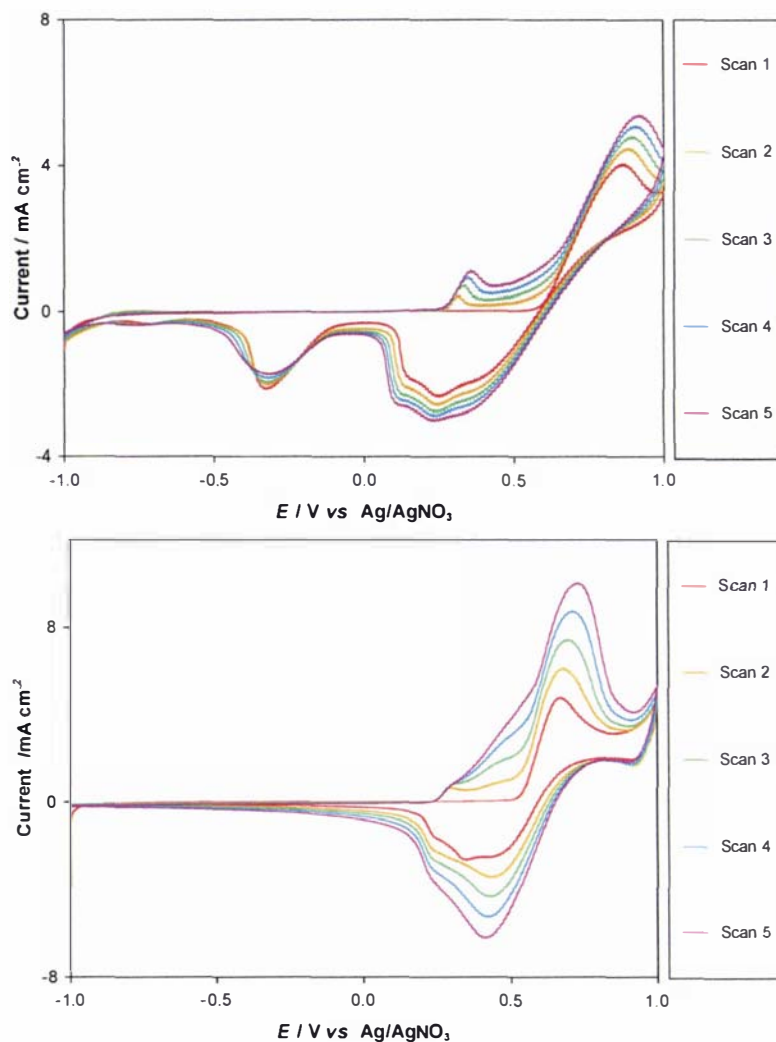


**Figure 5.41 Cyclic voltammetry for isovanillin hemicrown LXI**

( $\nu = 100 \text{ mV s}^{-1}$ , 5 mM LXI, 0.1 M TBAP,  $\text{CH}_2\text{Cl}_2$  - top)

( $\nu = 100 \text{ mV s}^{-1}$ , 5 mM LXI, 0.1 M TBAP, 1:1 MeCN: $\text{CH}_2\text{Cl}_2$  - bottom)

Due to the lack of solubility of the terthiophenes in MeCN ( $<0.1 \text{ mg/mL}$ ), cyclic voltammetry was investigated in both  $\text{CH}_2\text{Cl}_2$  alone, and MeCN/ $\text{CH}_2\text{Cl}_2$  mixes. In 1:1 MeCN/ $\text{CH}_2\text{Cl}_2$  the initial oxidation peak occurs at 0.68 V, not substantially different from that seen for other dialkoxy-substituted styryl terthiophenes in MeCN. The other isomeric hemicrowns also display initial oxidation peaks at similar potentials (Table 5.4). The reduction peak on the first scan is rather broad, with the main peak discernible at 0.23 V, and shoulders at 0.38 and 0.14 V. Hemicrowns **LXII** and **LXIII** display two clear peaks on reduction, at 0.46 and 0.25 V, and 0.47 and 0.29 V respectively. These peaks are in approximately the same positions as seen for the other dialkoxy-substituted styryl terthiophenes in MeCN (Table 5.4), and indicate that

very similar oxidised species may be forming in all of these cases. This is not surprising considering that the terthiophene hemicrown is really two dialkoxyethyl-substituted terthiophenes that are physically tethered, but electronically insulated, by the polyether chain. The initial oxidation peaks seen in  $\text{CH}_2\text{Cl}_2$  alone are considerably higher, at 0.82-0.88 V for the three hemicrowns. This shows that the hemicrowns are harder to oxidise in  $\text{CH}_2\text{Cl}_2$  than in MeCN: $\text{CH}_2\text{Cl}_2$  mixtures, possibly due to their higher solubility in this solvent. On further oxidation scans, a second distinct peak occurs for all three compounds, at 0.30-0.37 V. This peak is in a similar position to the shoulder seen during cyclic voltammetry of the same compounds in a MeCN: $\text{CH}_2\text{Cl}_2$  solvent mixture, implying that the oxidation potential of the new species is unaffected by solvent. The new species must be due to a higher oligomer of the hemicrown, containing sexithienyl moieties as seen for the previous compounds. This species, containing at least 12 thiophene rings, would likely be insoluble in both MeCN and  $\text{CH}_2\text{Cl}_2$ . This could explain why the oxidation potential does not change with solvent. In contrast, the hemicrown monomers are freely soluble in  $\text{CH}_2\text{Cl}_2$  but only sparingly soluble in MeCN, and it is possible that this could be causing the discrepancy in oxidation potentials seen between the two different solvent systems. The reduction peaks seen in  $\text{CH}_2\text{Cl}_2$  alone for the three hemicrowns are in approximately the same positions as seen in MeCN: $\text{CH}_2\text{Cl}_2$ , again implying that it is a solubility effect. An additional peak is observed between -0.21 and -0.38 V in the  $\text{CH}_2\text{Cl}_2$  solution that does not exist in the MeCN: $\text{CH}_2\text{Cl}_2$  data. This has been observed for a number of different monomers by other researchers, and has been attributed to a conformational change.<sup>321</sup> A slight decrease in current at the cathodic limit in the presence of  $\text{CH}_2\text{Cl}_2$  is likely due to the reduction of  $\text{H}^+$  from HCl in the solvent, as this was also noted in a background scan of TBAP in  $\text{CH}_2\text{Cl}_2$ .

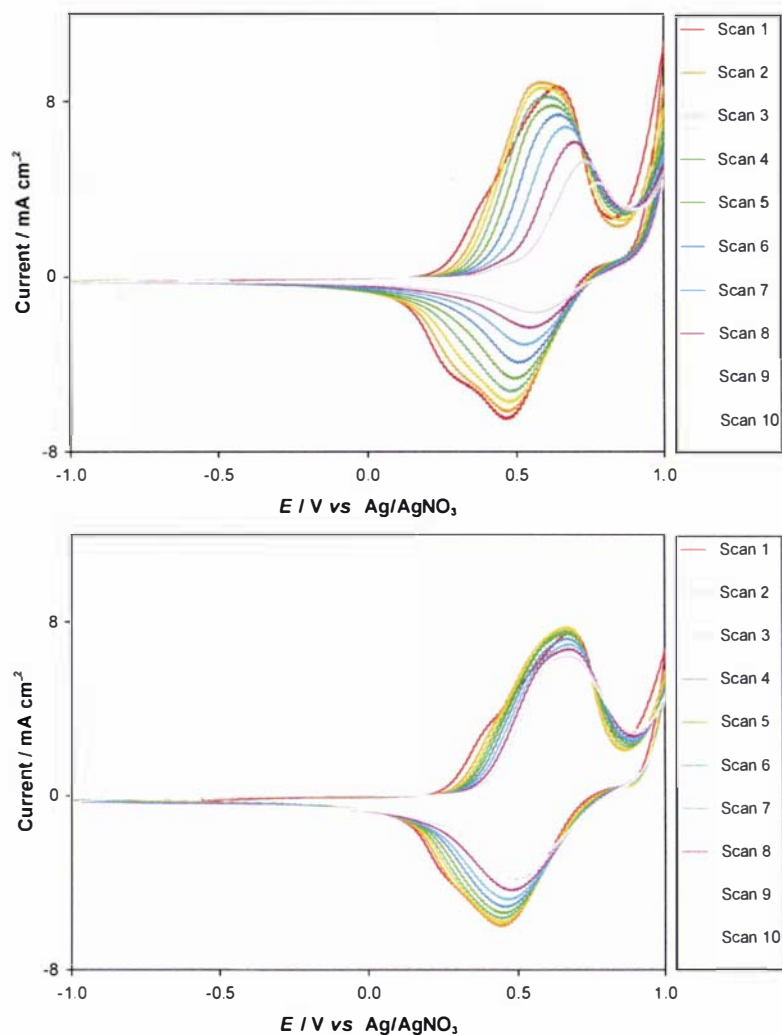


**Figure 5.42 Post-polymerisation CVs of hemicrown LXI in 0.1 M TBAP (top) and 0.1 M LiClO<sub>4</sub> (bottom)**

( $\nu = 100 \text{ mV s}^{-1}$ , MeCN)

Post-polymerisation CVs of hemicrown LXI in TBAP and LiClO<sub>4</sub> are shown above in Fig. 5.42. The positions of the peaks are very similar to those seen on formation of films in CH<sub>2</sub>Cl<sub>2</sub>:MeCN, with oxidation occurring at *ca.* 0.68 V, and the corresponding reduction at *ca.* 0.44 V. While the potentials are very similar between the two different electrolytes, in contrast to the results seen for the previous monomers, the hemicrown films appear to be less stable in the presence of N(Bu)<sub>4</sub><sup>+</sup> than Li<sup>+</sup>. In the examples shown above, the peak current measured in TBAP reduces by 50% over 10 CV cycles, whereas the decrease is only 16% over the same number of scans in

$\text{LiClO}_4$ . The same pattern was observed regardless of whether the films were originally grown from  $\text{CH}_2\text{Cl}_2$  or a  $\text{CH}_2\text{Cl}_2:\text{MeCN}$  solvent mixture. SEM images (Figs. 5.43 and 5.44) reveal that the hemicrown monomers form substantially less porous films. If these films were sufficiently dense that the electrolyte anions were trapped and could not migrate out of the film on reduction, then cations would have to migrate into the film to retain neutrality of charge. Lithium cations are very small, and may well be able to move in and out of the film more readily than bulky tetrabutylammonium cations. It is possible that this could lead to the degradation of the film in the presence of TBAP, as seen in Fig. 5.42.

Films of the terthiophene hemicrowns were grown onto ITO-coated mylar for surface analysis by SEM. The growth CVs for the isovanillin-derived hemicrown **LXI**, from  $\text{CH}_2\text{Cl}_2$  and  $\text{CH}_2\text{Cl}_2:\text{MeCN}$  solutions, are shown below in Figs. 5.43 and 5.44. SEM images of the films surface morphologies are also shown.

The growth CVs of this compound onto ITO-coated mylar are substantially different from those seen for previous monomers. The onset of oxidation occurs at *ca.* 0.5 V on the first scan, and 0.2 V on subsequent scans. In addition, a distinct oxidation peak that increases rapidly is seen at 0.4-0.5 V. These observations are not inconsistent with the formation of higher oligomers. In the case of the cyclic voltammetry carried out in  $\text{CH}_2\text{Cl}_2$  (Fig. 5.44), a decrease in current is seen toward the cathodic limit, and a small oxidation peak is evident at -0.4 V. It was noted that the mylar used was not completely stable in  $\text{CH}_2\text{Cl}_2$ , and softened if left sitting in this solvent. It is possible that the peaks seen in the cathodic region of Fig. 5.44 are due to chemical species dissolved from the surface of the mylar.

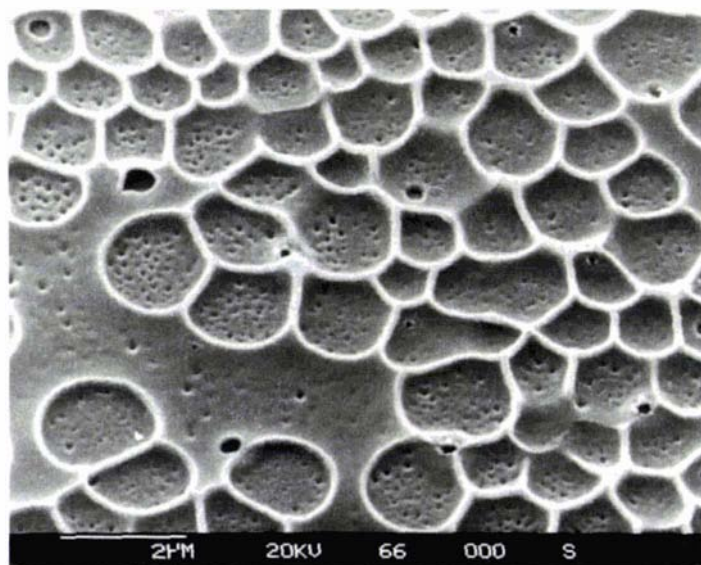
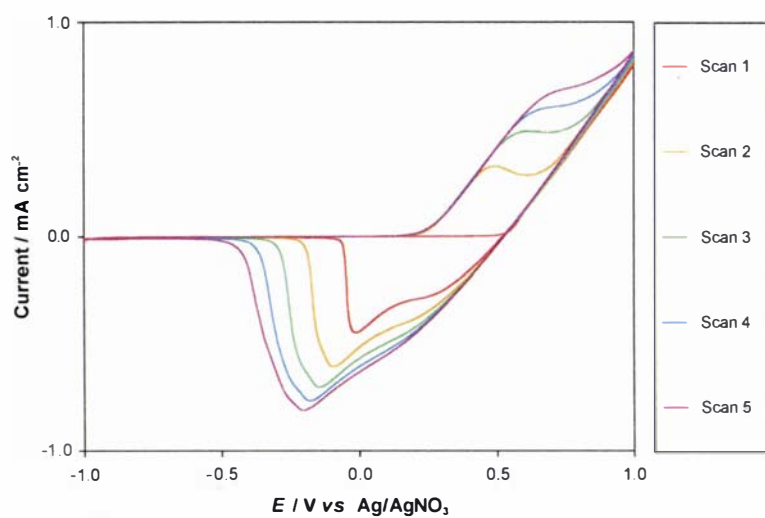


**Figure 5.43** Growth CV and surface morphology of isovanillin hemicrown LXI film from 1:1 MeCN:CH<sub>2</sub>Cl<sub>2</sub> ( $\nu = 100 \text{ mV s}^{-1}$ , 5 mM LXI, 0.1 M TBAP, 1:1 MeCN:CH<sub>2</sub>Cl<sub>2</sub>)

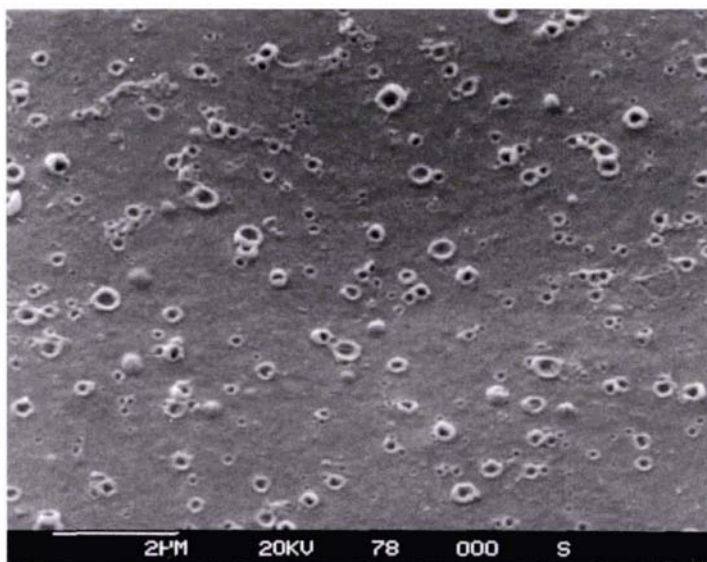
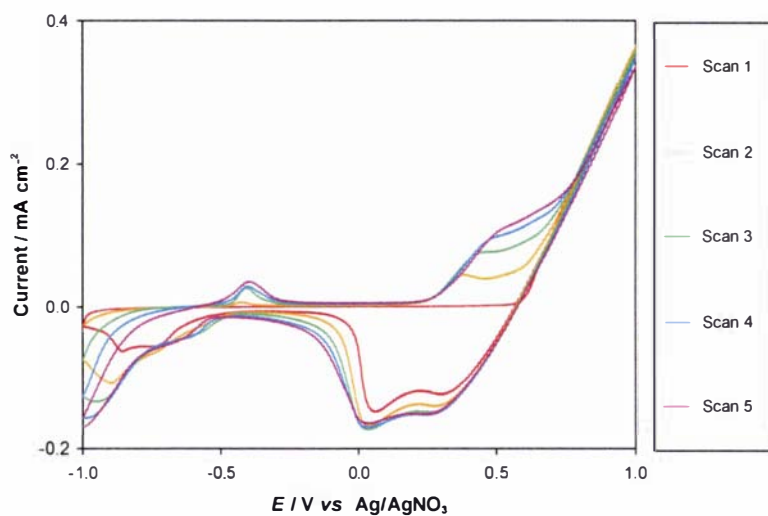


**Figure 5.44 Growth CV and scanning electron micrograph of isovanillin hemicrown LXI film grown from  $\text{CH}_2\text{Cl}_2$**   
 ( $\nu = 100 \text{ mV s}^{-1}$ , 5 mM LXI, 0.1 M TBAP,  $\text{CH}_2\text{Cl}_2$ )

In all cases, the hemicrowns showed a characteristic crater-like morphology, as seen in Figs. 5.43 and 5.44 for **LXI**. This morphology is not seen in films obtained from any of the other styryl terthiophenes investigated, and therefore must be primarily due to the properties of the monomer rather than the conditions employed during electropolymerisation. The main difference between the hemicrown monomers and the styryl terthiophene monomers is their solubility, and it seems likely that this

property has caused their unique morphology. During the oxidation phase of cyclic voltammetry, gas could be evolved due to trace amounts of dissolved water in the solvent. At the same time, the terthiophene-based monomers are oxidised to their radical cations  $TTh^{+\bullet}$  at the surface, these reactive materials then coupling to form higher oligomers. Diffusion of these materials also occurs, so that some of the radical cations and oligomers diffuse back into the solution rather than depositing onto the electrode surface. This diffusion will be less effective for compounds that are not very soluble, these materials tending to deposit on the surface of the electrode instead. As gas bubbles are evolved, an accumulation of  $TTh^{+\bullet}$  and oligomers could occur near the surface, lessening the effect of diffusion. While this does not seem to be an issue for the more soluble terthiophene-based monomers, the insolubility of the hemicrown monomers apparently causes them to deposit on the surface around the gas bubbles, as illustrated schematically in Fig. 5.45, and evidenced in the SEM pictures in Fig. 5.43 and Fig. 5.44. This could also explain why the 'craters' are more pronounced in  $MeCN:CH_2Cl_2$  solution, since the oligomers would be substantially less soluble in this system than in  $CH_2Cl_2$  alone.

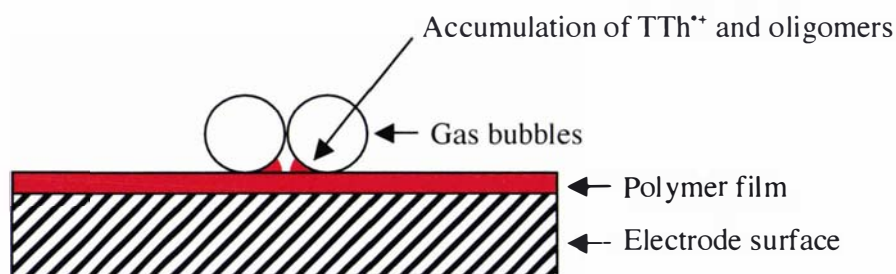


**Figure 5.45 Schematic diagram of terthiophene hemicrown surface deposition**

Samples of the three hemicrowns, from both solvent systems, were grown on ITO-coated glass in the oxidised and reduced states. The positions of the absorption maxima are tabulated in Table 5.3, and an example of the spectra obtained is shown in Fig. 5.46.

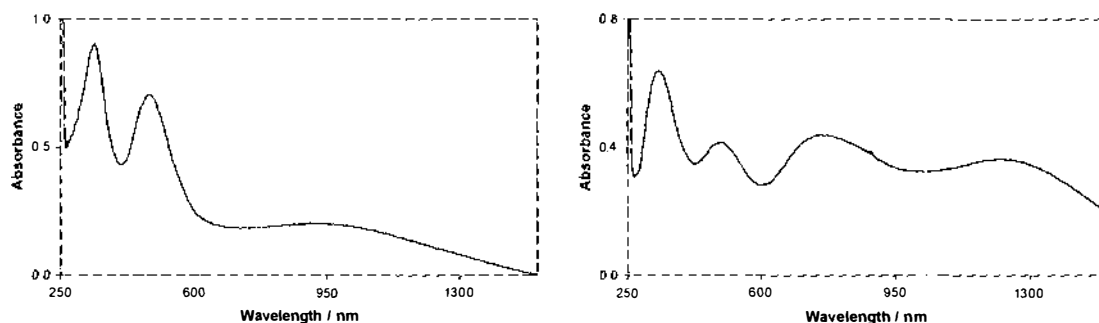


**Figure 5.46 UV/VIS/NIR spectra of hemicrown LXI in the neutral (left) and oxidised (right) forms**

The data in Table 5.3 shows that two absorbance maxima are seen for the neutral films from each of the terthiophene hemicrowns, and that the position of these peaks is not substantially changed by the solvent the films were grown from. The peak at 334-341 nm is due to the presence of the thiophene-styryl moiety, and the peak at 468-480 nm is attributed to the presence of sexithiophene groups. The fact that there are no apparent peaks corresponding to longer oligomers suggests that these monomers, like those containing only one terthiophene group, polymerise preferentially at one of the available  $\alpha$ -positions. The difference in reactivity between the head and tail  $\alpha$ -positions means that regardless of the degree of polymerisation, the maximum conjugation length will never exceed 6 thiophene units.

#### **5.2.4.6 Styryl-15-crown-5 terthiophene copolymer formation**

The majority of the monomers characterised so far lack stability on post-polymerisation cycling, so a brief investigation into stabilizing the films by forming copolymers was carried out. The ‘sensing’ monomer chosen was styryl-15-crown-5 terthiophene **I**, as it had previously shown the greatest response to metal cations. Both terthiophene and a terthiophene hemicrown were evaluated in copolymers with **I**, since the films formed from these compounds were comparatively stable.

The growth CV for an equimolar solution of styryl-15-crown-5 terthiophene **I** and terthiophene is shown in Fig. 5.47. Polymerisation under these conditions led to the formation of an adherent red film on the working electrode surface.

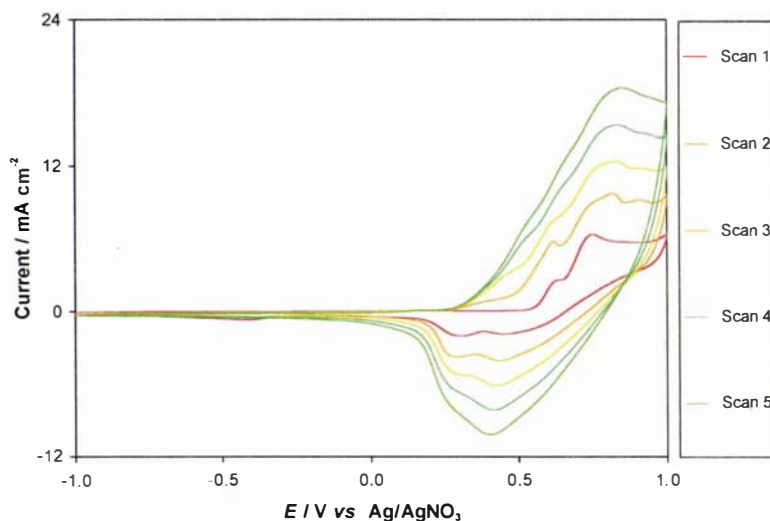


**Figure 5.47** Cyclic voltammetry for styryl-15-crown-5 terthiophene:terthiophene copolymer

( $\nu = 100 \text{ mV s}^{-1}$ , 5 mM **I**, 5 mM terthiophene, 0.1 M TBAP, MeCN)

Two peaks are seen on the first oxidative sweep in Fig. 5.47, at 0.65 and 0.77 V. These are the same peak oxidation potentials observed for homopolymers of styryl-15-crown-5 terthiophene and terthiophene respectively (Table 5.4). This indicates that at least some of each monomer has been oxidised. Subsequent oxidation scans show an increase in both peaks, and a gradual merging. The first reduction shows two peaks, at 0.44 and 0.29 V, as well as a broad shallow peak at  $-0.44 \text{ V}$ . These are very similar to the position of peaks seen for 15-crown-5 terthiophene **I**. As for the oxidation peaks, the reduction peaks increase and gradually merge over subsequent scans. The shape of the CV after 5 scans resembles that seen for terthiophene (Fig. 5.8) more than styryl-15-crown-5 terthiophene (Fig. 5.26).

Post-polymerisation CVs were carried out in TBAP and a number of different metal cation perchlorates ( $\text{LiClO}_4$ ,  $\text{NaClO}_4$ ,  $\text{Mg}(\text{ClO}_4)_2$ ,  $\text{Mn}(\text{ClO}_4)_2$ ), and two of these are shown in Fig. 5.48.

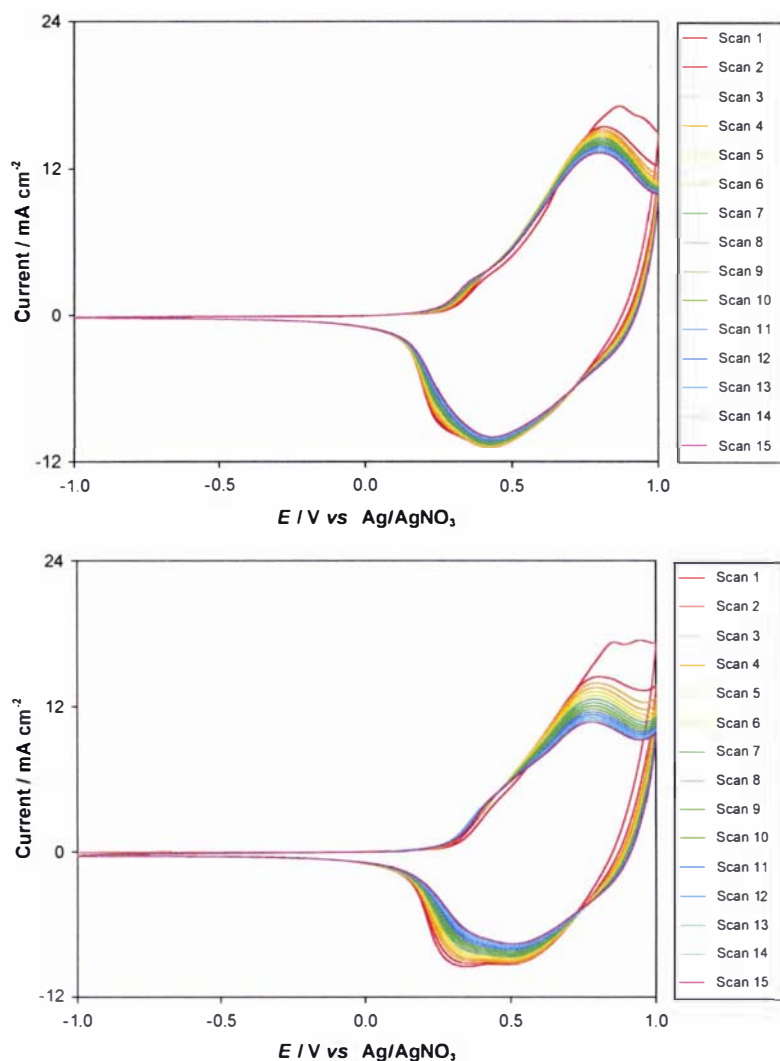


**Figure 5.48 Post-polymerisation CVs of 15-crown-5 terthiophene: terthiophene copolymer in 0.1 M TBAP (top) and 0.1 M LiClO<sub>4</sub> (bottom) ( $\nu = 100 \text{ mV s}^{-1}$ , MeCN)**

It can be seen in Fig. 5.48 that the post-polymerisation CVs of this copolymer are very similar to those previously observed for a terthiophene homopolymer (Fig. 5.9). The current decline is somewhat more rapid in the presence of Li<sup>+</sup> (26 % loss over 14 cycles) than TBAP (13% loss over 14 cycles). It is likely that this is due to an interaction between the lithium cations and the crown ether moiety, leading to increased dissolution as seen for the 15-crown-5 homopolymer (Section 5.2.4.2). While this polymer is certainly more stable than the 15-crown-5 homopolymer, the lack of response to cations and shape of the post-polymerisation CVs suggest that terthiophene is the major component.

A sample of the film was grown onto ITO-coated mylar under the same conditions. The growth CV and SEM of the film are presented in Fig. 5.49.

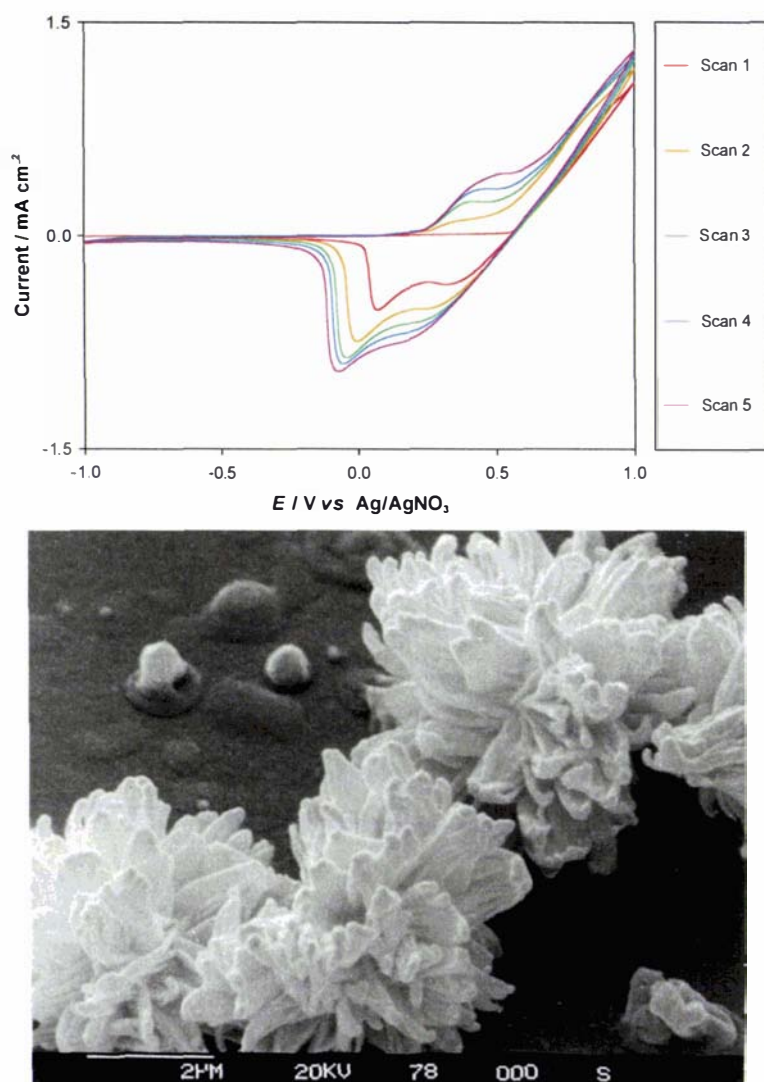


**Figure 5.49 Growth CV and surface morphology of 15-crown-5 terthiophene:terthiophene copolymer film on ITO-coated mylar**  
( $\nu = 100 \text{ mV s}^{-1}$ , 5 mM terthiophene, 5 mM I, 0.1 M TBAP, MeCN)

The SEM image for the copolymer shows coral-like structures similar to those seen for 15-crown-5 terthiophene (Fig. 5.28). However, it can also be seen that in this case the surface is covered with a comparatively smooth polymer layer as well.

Samples of the film in both the neutral and oxidised state were grown onto ITO glass as described in Section 5.2.2, and their UV/VIS/NIR spectra are presented below in Fig. 5.50.

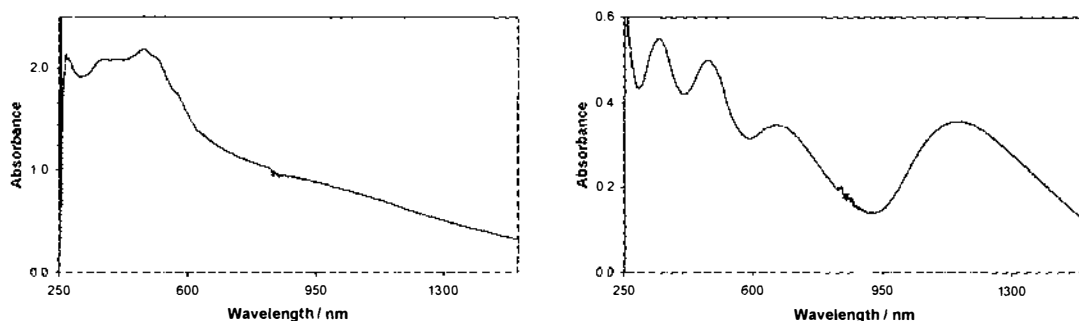


**Figure 5.50 UV/VIS/NIR spectra of 15-crown-5 terthiophene: terthiophene copolymer in the neutral (left) and oxidised (right) forms**

The spectrum of the film in the neutral state consists of a peak at 484 nm with a shoulder at 372 nm. A comparison of these values with those presented for other films in Table 5.3 shows that this is an average value for a film containing a sexithienyl moiety. The spectrum of the film in the oxidised state has absorbance maxima at 353, 484, 674 and 1158 nm. Again, these values are no different from those previously observed (Table 5.3). Styryl terthiophenes have been shown to couple preferentially at one of the available  $\alpha$ -positions (Section 5.1.2), whereas terthiophene has equal reactivity at both ends due to its symmetry. It seems that the longest likely oligomer would then consist of a central terthiophene group with one styryl-15-crown-5 terthiophene monomer attached at each end. This would give a maximum conjugation length of 9 thiophene rings. However, the UV/VIS/NIR data provides no evidence for a conjugation length any longer than 6 thiophene units, and it appears that once again coupling has halted with the formation of a dimer. The exact composition of this copolymer is uncertain, although it appears to contain both monomers. This copolymer was more stable to cyclic voltammetry than a homopolymer of 15-crown-5 terthiophene, but did not display any exploitable response to metal cations.

A copolymer was also formed between 15-crown-5 terthiophene **I** and hemicrown **LXIII**. The cyclic voltammetry for this copolymer is shown in Fig. 5.51.

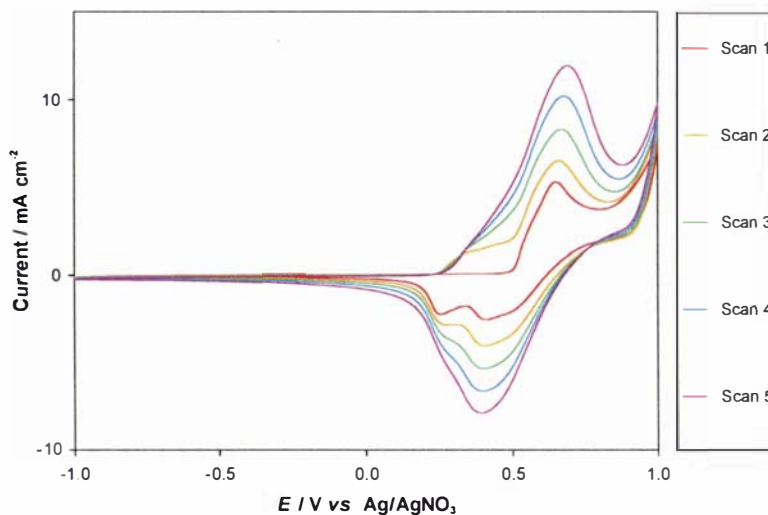


**Figure 5.51 Cyclic voltammetry for styryl-15-crown-5 terthiophene:terthiophene hemicrown copolymer**

( $\nu = 100 \text{ mV s}^{-1}$ , 5mM I, 2.5 mM LXIII, 0.1 M TBAP, 3:1 MeCN:CH<sub>2</sub>Cl<sub>2</sub>)

The initial oxidation peak for this copolymer is seen at 0.66 V, the same potential as both the component monomers. On subsequent oxidation scans, growth is seen at 0.34 V, indicating the formation of longer chain material. The reduction peaks are seen at 0.34 and 0.24 V, again very similar to those seen for the substituent monomers. This is not surprising given the structural similarity of the monomers used. As the polyether chain is not conjugated, it electronically insulates the two dialkoxystyryl-substituted terthiophenes that it physically tethers together.

Post-polymerisation CVs of the copolymer were carried out in TBAP and several metal cation solutions, and examples are presented in Fig. 5.52.

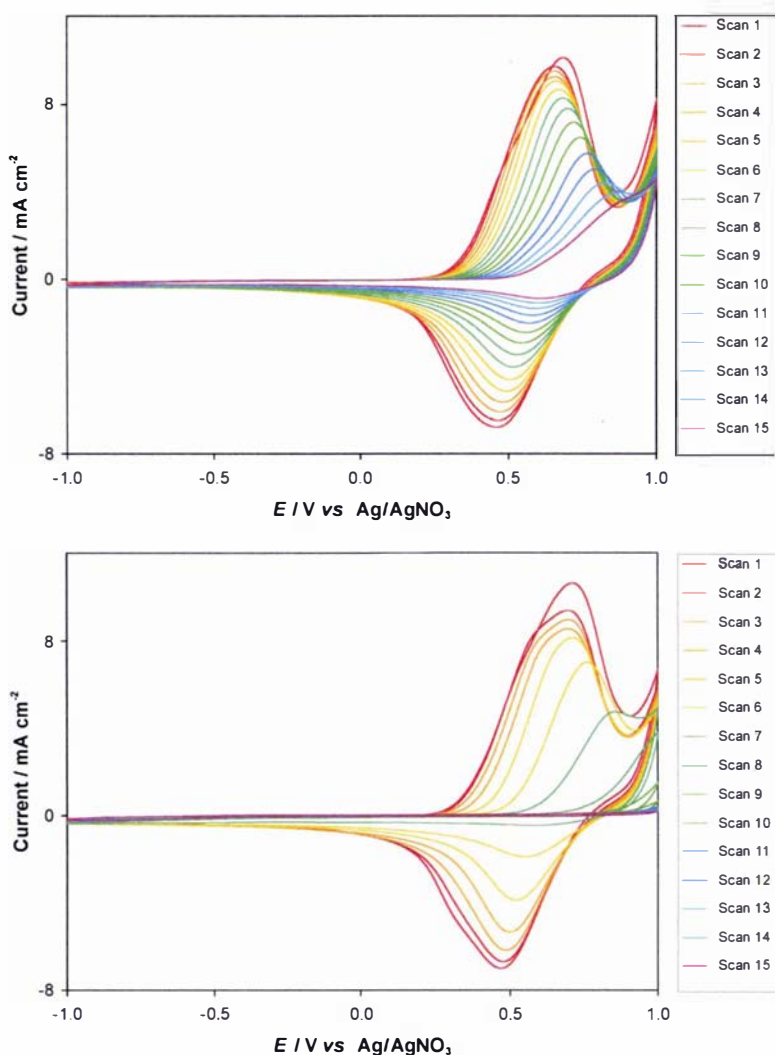


**Figure 5.52** Post-polymerisation CVs of 15-crown-5 terthiophene hemicrown copolymer in 0.1 M TBAP (top) and 0.1 M LiClO<sub>4</sub> (bottom) ( $\nu = 100 \text{ mV s}^{-1}$ , MeCN)

Figure 5.52 shows that, while the response of the copolymer to TBAP and LiClO<sub>4</sub> is similar in form, the polymer degrades more quickly in the presence of Li<sup>+</sup>. This effect has also been seen for the styryl-15-crown-5 terthiophene homopolymer (Section 5.2.4.2) and its copolymer with terthiophene, and is attributed to complexation between the crown ether moiety and the lithium cations. The degradation was slightly faster in the presence of Na<sup>+</sup> than Li<sup>+</sup>.

A sample of the copolymer was grown onto ITO-coated mylar in order to examine its surface morphology. The growth CV and SEM are presented in Fig. 5.53.

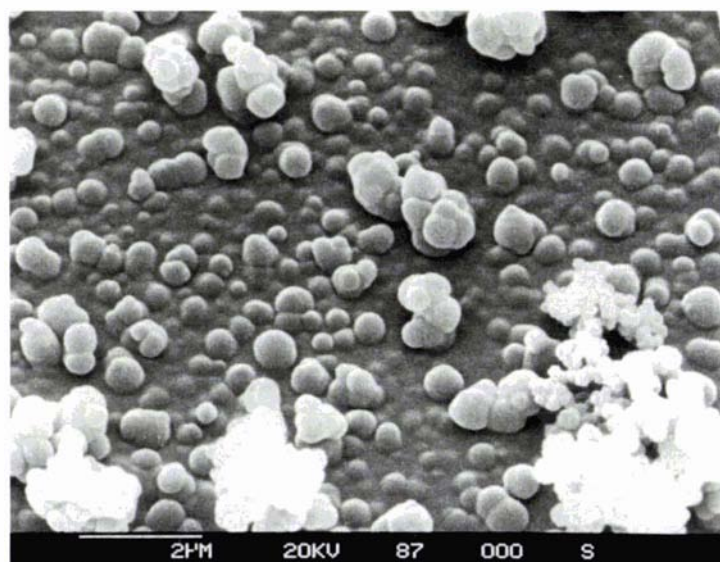
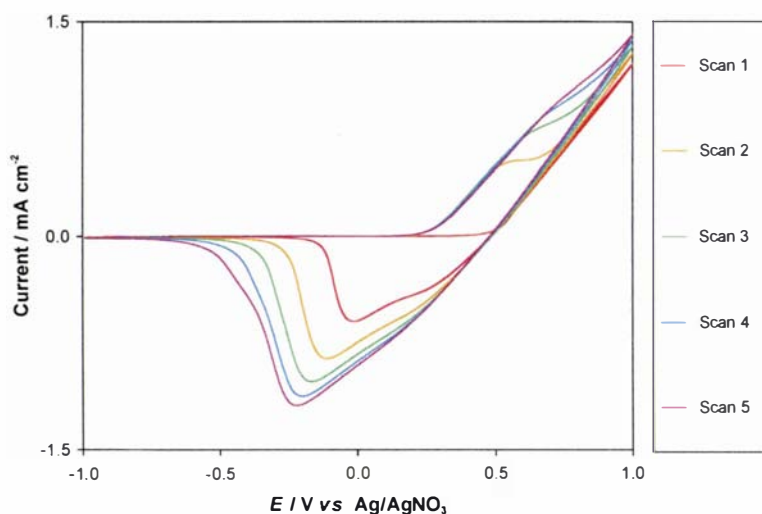


**Figure 5.53 Growth CV and surface morphology of 15-crown-5 terthiophene:hemicrown copolymer film on ITO-coated mylar**

( $v = 100 \text{ mV s}^{-1}$ , 5 mM I, 2.5 mM LXIII, 0.1 M TBAP, 3:1 MeCN:CH<sub>2</sub>Cl<sub>2</sub>)

The growth CV for this copolymer onto ITO-coated mylar is more similar to that of the hemicrowns (Fig. 5.43 and Fig. 5.44), than to that seen for styryl-15-crown-5 terthiophene **I** (Fig. 5.28). The copolymer film appeared, on a macroscopic scale, to be covered with a uniform coating. Figure 5.53 shows that this coating is a continuous film, with small bubble-like and larger globular surface features. A similar film grown with hemicrown **LXI** had cracks visible to the naked eye, whereas microscopic cracks were evident in a film grown using hemicrown **LXII**.

In order to investigate the degree of conjugation in the film, samples in both the neutral and oxidised form were grown onto ITO-coated glass for analysis by UV/VIS/NIR spectroscopy. The spectra obtained from these samples are shown below in Fig. 5.54.

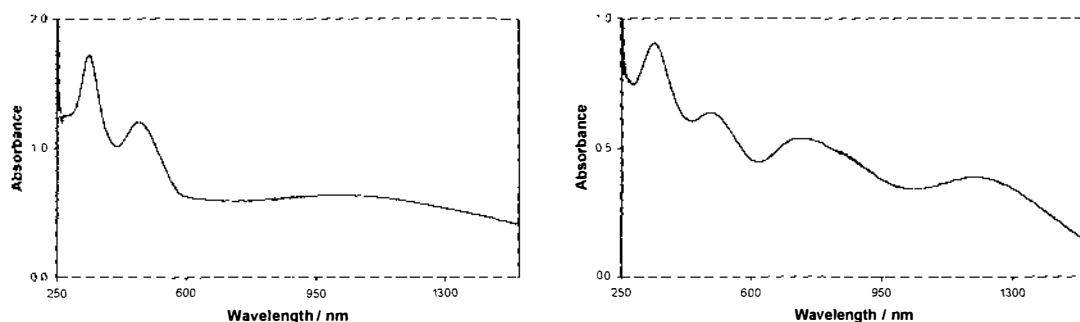


**Figure 5.54** UV/VIS/NIR spectra of styryl-15-crown-5 terthiophene: hemicrown copolymer in the neutral (left) and oxidised (right) forms

The absorption peaks in the neutral film are at 347 and 480 nm. Comparing these values with those in Table 5.3 shows that this is typical of this type of sexithiophene derivative. This is also true of the peaks seen at 349, 499, 740 and 1210 nm for the oxidised film. Once again, there is no evidence for films containing oligothiophenes longer than 6 thiophene units. This is not surprising given the asymmetric reactivity of the terthiophene monomers, and their proven tendency to form dimers.

**Table 5.3 Absorption maxima for electrochemically produced films and chemically produced dimer films**

( $\nu = 100 \text{ mV s}^{-1}$ , in MeCN unless otherwise noted,  $E/V$  vs  $\text{Ag}/\text{AgNO}_3$ )

<b>Compound</b>	$\lambda_{\text{max}} / \text{nm}$ <b>Neutral film</b>	$\lambda_{\text{max}} / \text{nm}$ <b>Oxidised film</b>	$\lambda_{\text{max}} / \text{nm}$ <b>Dimer film (neutral)</b>
TTh	393	478, 595, 1075	
TTh=-Bz <b>LXXVI</b>		358, 482, 727, 1185	338, 514
TTh=-BzOMe <b>LXXVII</b>	287, 357, 489, 524, 563	345, 482, 689, 1135	336, 488
TTh=-Bz(OMe) <sub>2</sub> <b>XXIV</b>	280, 347, 513, 555(s)	350, 496, 749, 1147	285, 343, 510, 555 (s)
TTh=-BzOCOCOC <b>XXIII</b>	499 (s), 523, 578 (s)	345, 516, 752, 995 (s)	290, 353, 528
TTh=-BzOCOCOC <b>XXVI</b>		357, 510, 695, 978 (s)	291, 380, 511
TTh=-BzOCOCOCOC <b>XXIV</b>			279, 348, 500
TTh=-BzOCOCOCOC <b>XXVII</b>			280, 349, 489
TTh=-BzOCOCOCOCOC <b>XXV</b>			282, 343, 485
TTh=-BzOCOCOCOCOC <b>XXVIII</b>			285, 345, 478
TTh=-Bz15c5 <b>I</b>	348, 480	333, 469, 753, 1254	357, 499
TTh=-Bz18c6 <b>II</b>			346, 480
TTh=-BzOCOCOBz=-TTh <b>LXI</b> $\text{CH}_2\text{Cl}_2$	337, 480	331, 491, 758, 1225	
TTh=-BzOCOCOBz=-TTh <b>LXI</b> $\text{CH}_2\text{Cl}_2/\text{MeCN}$	341, 476	341, 489, 778, 1270	
TTh=-BzOCOCOBz=-TTh <b>LXII</b> $\text{CH}_2\text{Cl}_2$	336, 478	321, 494, 765, 1219	
TTh=-BzOCOCOBz=-TTh <b>LXII</b> $\text{CH}_2\text{Cl}_2/\text{MeCN}$	339, 477	334, 489, 756, 1206	
TTh=-BzOCOCOBz=-TTh <b>LXIII</b> $\text{CH}_2\text{Cl}_2$	334, 475	333, 496, 789, 1221	
TTh=-BzOCOCOBz=-TTh <b>LXIII</b> $\text{CH}_2\text{Cl}_2/\text{MeCN}$	341, 468	344, 473, 758, 1250	

**Table 5.4 Peak oxidation and reduction potentials obtained on electropolymerisation by cyclic voltammetry over the range  $\pm 1.0$  V**

( $\nu = 100 \text{ mV s}^{-1}$ , in MeCN unless otherwise noted,  $E/V$  vs  $\text{Ag}/\text{AgNO}_3$ )

Compound	Peak Potential Oxidation 1 <sup>st</sup> scan	Peak Potential Reduction 1 <sup>st</sup> scan	Peak Potential Oxidation 2 <sup>nd</sup> scan	Film?
TTh	0.76, 0.88	0.33	0.75 (s), 0.94	Yes
TTh--Bz <b>LXXVI</b>	0.72	0.58, 0.24	0.58, 0.84	Yes
TTh--BzOMe <b>LXXVII</b>	0.66	0.94, 0.48, 0.16, -0.39	0.28, 0.71	Yes
TTh--Bz(OMe) <sub>2</sub> <b>XXIV</b>	0.65	0.84, 0.43, 0.18, 0.11, - 0.32	0.68	Yes
TTh--BzOCOCOC <b>XXIII</b>	0.65	0.86, 0.41, 0.23, -0.45	0.60, 0.67	Yes
TTh--BzOCOCOC <b>XXVI</b>	0.64	0.87, 0.42, 0.19, -0.38	0.54, 0.67	Yes
TTh--BzOCOCOCOC <b>XXIV</b>	0.65	0.87, 0.43, 0.22, -0.44	0.65	No
TTh--BzOCOCOCOC <b>XXVII</b>	0.66	0.86, 0.43, 0.23, -0.40	0.35, 0.66	No
TTh--BzOCOCOCOCOC <b>XXV</b>	0.66	0.89, 0.44, 0.23, -0.46	0.33, 0.66	No
TTh--BzOCOCOCOCOC <b>XXVIII</b>	0.67	0.86, 0.40, 0.25, -0.42	0.36, 0.66	No
TTh--Bz15c5 <b>I</b>	0.65	0.91, 0.44, 0.23, -0.41	0.30, 0.66	Yes
TTh--Bz18c6 <b>II</b>	0.66	0.94, 0.45, 0.23, -0.59	0.33, 0.66	No
TTh--BzOCOCOBz--TTh <b>LXI</b> CH <sub>2</sub> Cl <sub>2</sub>	0.88	0.38 (s), 0.23, 0.14 (s), -0.34	0.31, 0.90	Yes
TTh--BzOCOCOBz--TTh <b>LXI</b> CH <sub>2</sub> Cl <sub>2</sub> /MeCN	0.68	0.89, 0.44 (s), 0.33, 0.23 (s)	0.30, 0.69	Yes
TTh--BzOCOCOBz--TTh <b>LXII</b> CH <sub>2</sub> Cl <sub>2</sub>	0.82	0.40, 0.22, - 0.38	0.30, 0.83	Yes
TTh--BzOCOCOBz--TTh <b>LXII</b> CH <sub>2</sub> Cl <sub>2</sub> /MeCN	0.67	0.92, 0.46, 0.25	0.40 (s), 0.68	Yes
TTh--BzOCOCOBz--TTh <b>LXIII</b> CH <sub>2</sub> Cl <sub>2</sub>	0.88	0.40, 0.19, - 0.21	0.37, 0.90	Yes
TTh--BzOCOCOBz--TTh <b>LXIII</b> CH <sub>2</sub> Cl <sub>2</sub> /MeCN	0.67	0.89, 0.47, 0.29	0.33, 0.68	Yes

## 5.2.5 Electropolymerisation of thiophene monomers

Previous research carried out by Cutler *et al.*,<sup>164-166, 322</sup> Smith *et al.*<sup>160</sup> and Welzel *et al.*<sup>162</sup> indicates that 3-styryl substituted thiophene compounds do not polymerise to form conducting polymers (Section 1.5). An attempt was made to polymerise each of the thiophene monomers synthesised, to confirm that this was also the case for these new monomers.

### 5.2.5.1 Electropolymerisation of dialkoxystyryl-substituted thiophene compounds

Dimethoxystyryl thiophene **XXXVI**, styryl-15-crown-5 thiophene **XV**, styryl-18-crown-6 thiophene **XVI** and open-chain thiophenes **XXX-XXV** were polymerised under the same conditions. In all cases, cyclic voltammograms virtually identical to that shown below were obtained.

As can be seen from Fig. 5.55, while oxidation occurs, there is no corresponding reduction. In addition, no visible material was deposited on the electrode, and no discolouration of the monomer solution was evident. Extending the upper limit to +1.5 V resulted in a faster loss of current. The initial oxidation peak occurred at 0.73 V for every compound except 18-crown-6 thiophene, where it was seen at 0.78 V. These results are in agreement with previously published research on the electropolymerisation of 3-styryl substituted thiophenes. Smith *et al.* attribute the initial oxidation peak to oxidation of the alkene bond, and the second peak to oxidation of the thiophene ring itself.<sup>160</sup>

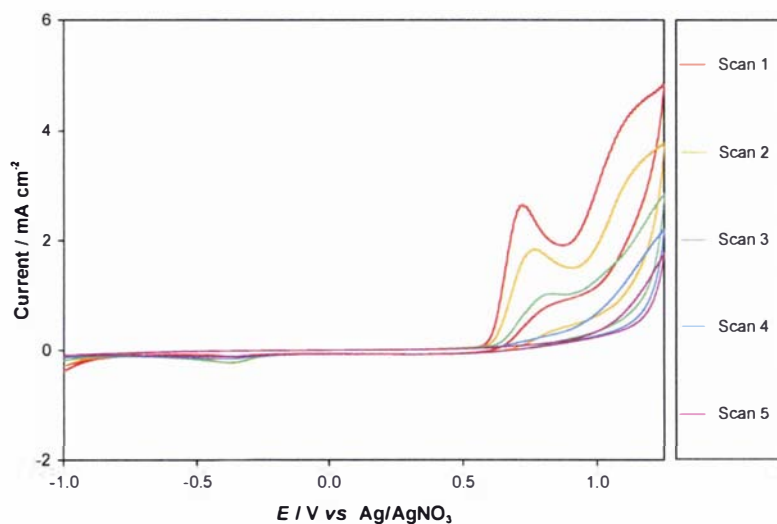


**Figure 5.55** Cyclic voltammetry for styryl-15-crown-5 thiophene **XV**  
( $\nu = 100 \text{ mV s}^{-1}$ , 10 mM **XV**, 0.1 M TBAP, MeCN)

### 5.2.5.2 Electropolymerisation of thiophene hemicrown compounds

An attempt was also made to electropolymerise the three thiophene hemicrown compounds **LXIV-LXVI**. This was unsuccessful, as seen in the growth CV below (Fig. 5.56). As in the case of the dialkoxystyryl-substituted thiophenes, only oxidation peaks were observed with no corresponding reduction peaks. The initial oxidation peak in both  $\text{CH}_2\text{Cl}_2$  and MeCN/ $\text{CH}_2\text{Cl}_2$  solution was at *ca.* 0.9 V, at a higher potential than the monomers investigated in MeCN alone. This is consistent with results seen earlier for the equivalent terthiophene compounds. Cycling up to +1.5 V did not lead to any increase in reversibility. When the cathodic limit was extended to -1.0 V, a peak was seen at -0.3 V. The nature of the species giving rise to this peak is uncertain.

Since no films were formed on the electrode surface, UV/VIS/NIR and SEM analysis could not be performed.

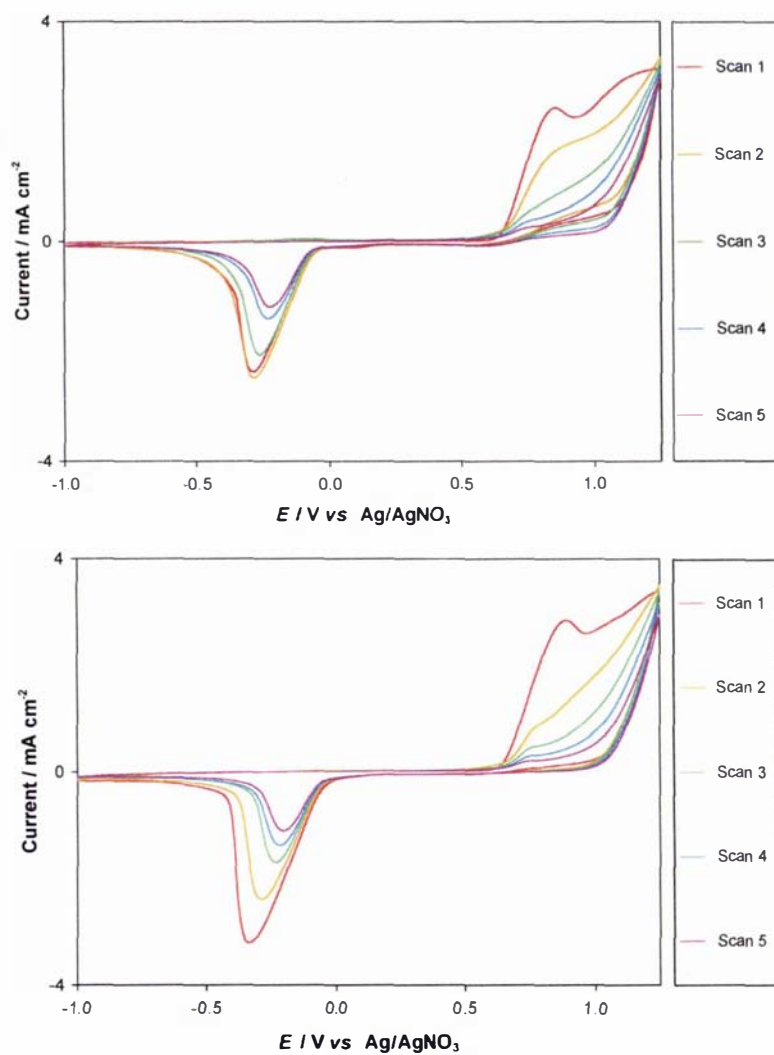


**Figure 5.56** Cyclic voltammetry for thiophene hemicrown LXV

( $\nu = 100 \text{ mV s}^{-1}$ , 5 mM LXV, 0.1 M TBAP,  $\text{CH}_2\text{Cl}_2$  - top)

( $\nu = 100 \text{ mV s}^{-1}$ , 5 mM LXV, 0.1 M TBAP, 1:1  $\text{CH}_2\text{Cl}_2$ :MeCN - bottom)

### 5.2.5.3 Styryl-15-crown-5 thiophene copolymer formation

A brief investigation was carried out on the feasibility of creating copolymers of thiophene monomers with terthiophene. The compound chosen was styryl-15-crown-5 thiophene **XV**. It was envisaged that this monomer would give the largest interaction with metal cations due to the preorganisation of the polyether chain, as seen for the corresponding terthiophene analogues (Chapter 4). A growth CV of 1:1 15-crown-5 thiophene:terthiophene is shown below in Fig. 5.57.

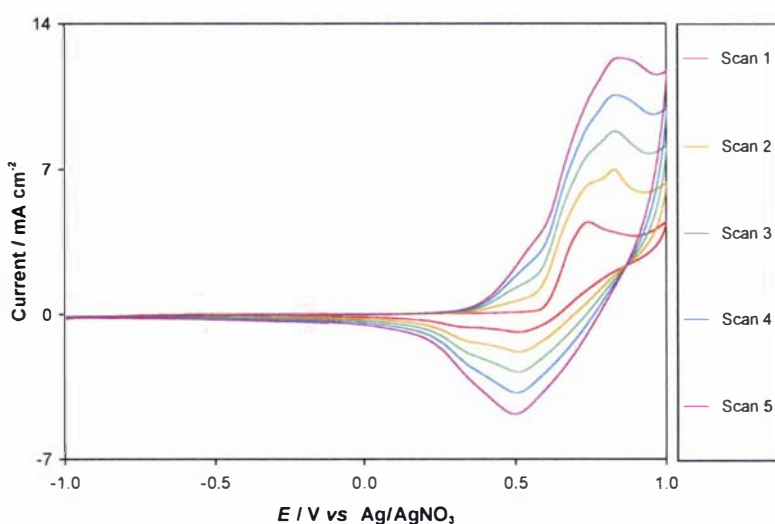


**Figure 5.57** Cyclic voltammetry for styryl-15-crown-5 thiophene:terthiophene copolymer

( $\nu = 100 \text{ mV s}^{-1}$ , 5 mM terthiophene, 5 mM **XV**, 0.1 M TBAP, MeCN)

It can be interpreted from the increasing current with scan number shown in Fig. 5.57, that an electroactive material can be formed from a 1:1 mixture of terthiophene and styryl-15-crown-5 thiophene under these conditions. The initial oxidation peak, at 0.75 V, is similar to that seen on oxidation of terthiophene (Section 5.2.1.1), however the reduction peak (0.50 V) is shifted considerably. This implies that there is a different species being formed on oxidation, perhaps due to some sort of coupling between the terthiophene and styryl thiophene monomers.

Post-polymerisation CVs of the copolymer in TBAP and LiClO<sub>4</sub> are shown below in Fig. 5.58.

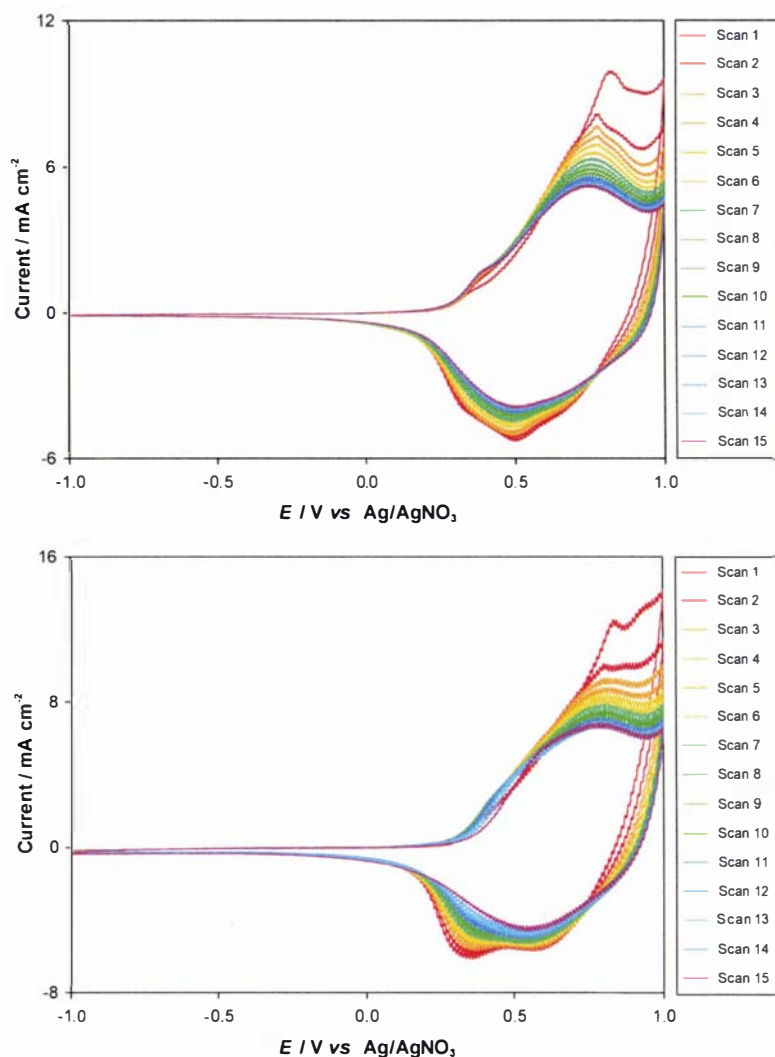


**Figure 5.58** Post-polymerisation CVs of thiophene crown:terthiophene copolymer in 0.1 M TBAP (top) and 0.1 M LiClO<sub>4</sub> (bottom) ( $v = 100 \text{ mV s}^{-1}$ , MeCN)

No significant differences can be seen between the post-polymerisation CVs in TBAP and LiClO<sub>4</sub>, as seen in Fig. 5.58. In addition, the shape of these electrochemical responses is similar to that exhibited by terthiophene (Fig. 5.9), suggesting that the polymer may consist predominantly of terthiophene.

A sample of this copolymer was grown onto ITO-coated mylar for analysis by SEM. The growth CV and SEM image of this film are shown in Fig. 5.59.

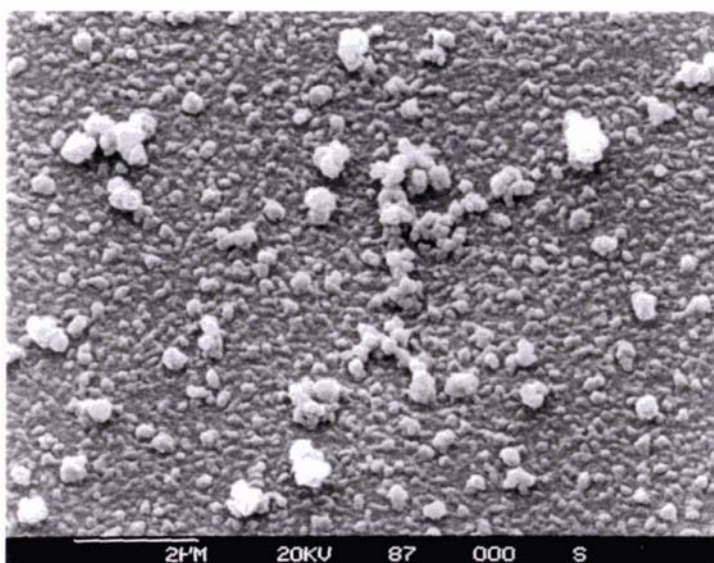
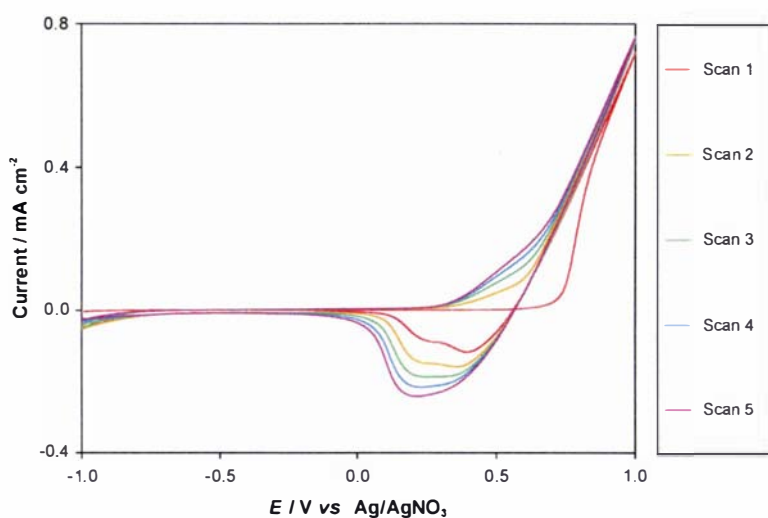


**Figure 5.59 Growth CV and SEM of terthiophene:thiophene crown copolymer on ITO-coated mylar**

( $v = 100 \text{ mV s}^{-1}$ , 5 mM terthiophene, 5 mM **XV**, 0.1 M TBAP, MeCN)

The onset of oxidation seen in Fig. 5.59 is at the same potential as that seen for terthiophene under the same conditions (Fig. 5.10). The SEM image above shows that this copolymer forms a relatively smooth, continuous film on ITO-coated mylar.

In order to more fully investigate the properties of this copolymer, samples in both the oxidised and neutral forms were grown onto ITO-coated glass for UV/VIS/NIR analysis (Fig. 5.60).

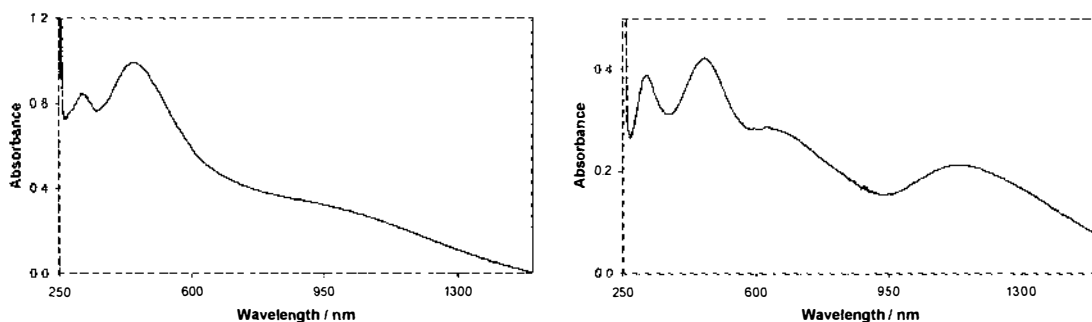


**Figure 5.60 UV/VIS/NIR spectra of thiophene crown:terthiophene copolymer in the neutral (left) and oxidised (right) forms**

The UV spectrum of the copolymer in the neutral form shows two peaks, at 317 and 452 nm. The lowest energy peak, while at a longer wavelength than that seen for films of terthiophene alone, is still only indicative of the presence of a sexithienyl chromophore. This indicates that there is no extensive conjugation in this copolymer. Peaks are seen in the spectrum of the copolymer in the oxidised form at 317, 471 and 1147 nm, with a shoulder at 647 nm. Again, these are similar for those obtained for other terthiophene monomers (Table 5.3), which have been proven to primarily form dimers. Structural and compositional uncertainty is always an issue when forming copolymers. In this case, the electrochemical, spectroscopic and morphological evidence suggests that the copolymer consists predominantly of terthiophene. Varying the ratios of monomer used could lead to a higher percentage of styryl-thiophene being incorporated, although there is no certainty that monomer **XV** would polymerise at these potentials. Replacing terthiophene in this system with a monomer that has a higher oxidation potential may be preferable. 3-styryl substituted thiophenes synthesised by other researchers have been shown to form copolymers,<sup>162-166</sup> so it seems likely that an optimization of conditions could lead to films containing the styryl thiophene monomers synthesised in this research.

## 5.2.6 Electropolymerisation of sexithiophene compounds

An attempt was also made to electropolymerise the sexithiophene compounds that had been produced *via* chemical oxidation of terthiophene monomers (Section 5.1.2). It seemed unlikely that these compounds would polymerise, given the lack of evidence seen for the production of oligothiophenes longer than sexithiophene during chemical or electrochemical polymerisation of terthiophene monomers. However, if the compounds were to oxidise electrochemically, the potential at which this occurred would be lower than that needed for terthiophene monomers, due to the extended conjugation in these molecules. For this reason, the anodic limit for cyclic voltammetry was set at + 0.75 V. Due to the low solubility of the substituted sexithiophenes in organic solvents, experiments were carried out with a monomer concentration of 0.5 - 1.0 mM in CH<sub>2</sub>Cl<sub>2</sub>, giving rise to a much smaller current response than those observed for the terthiophene-based monomers. Although the exact form of the cyclic voltammograms varied from compound to compound, similar features were evident. The onset of oxidation for all compounds was between 0.4 - 0.5 V. In most cases there was a single peak, although compound **LXXII** showed two distinct peaks, and compounds **LXX** and **LXXIV** two very close peaks. The reduction peaks were very similar for all compounds, with a distinct peak at 0.4 - 0.5 V. The only exception to this was monomer **LXXII**, which showed two reduction peaks corresponding to the two observed oxidation peaks. There was no increase in current with scan number observed for any of the monomers tested, and nor was any visible film deposited on the working electrode. Instead, the redox peaks appear to be those for oxidation and reduction of the sexithiophenes in solution, with no coupling to form higher oligomers. Examples of the cyclic voltammetry for these compounds are shown in Figs. 5.61 – 5.63.

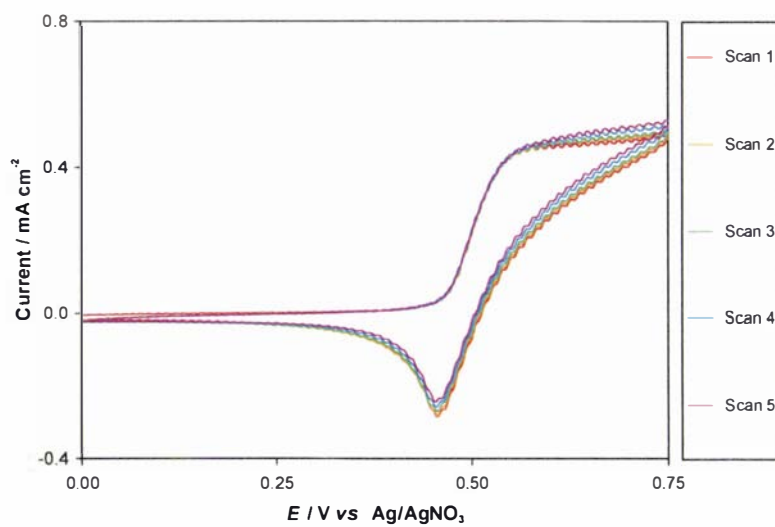


**Figure 5.61** Cyclic voltammetry for open-chain sexithiophene LXXIII  
 ( $\nu = 100 \text{ mV s}^{-1}$ , 1 mM LXXIII, 0.1 M TBAP,  $\text{CH}_2\text{Cl}_2$ )

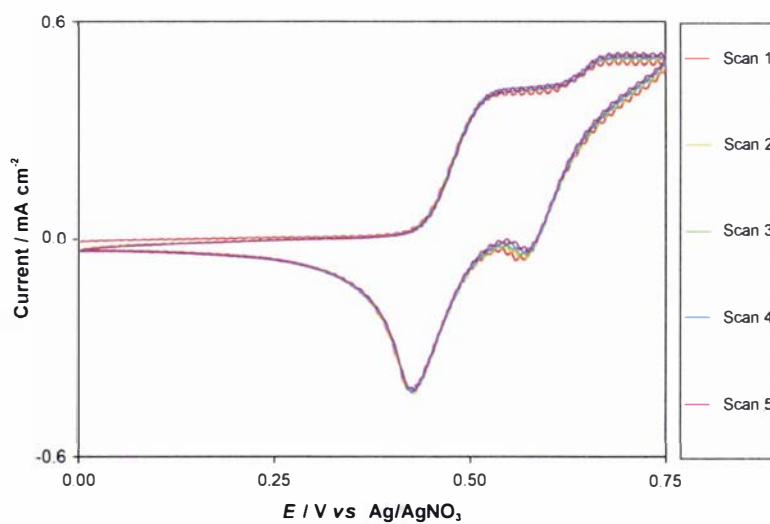


**Figure 5.62** Cyclic voltammetry for open-chain sexithiophene LXXII  
 ( $\nu = 100 \text{ mV s}^{-1}$ , 1 mM LXXII, 0.1 M TBAP,  $\text{CH}_2\text{Cl}_2$ )

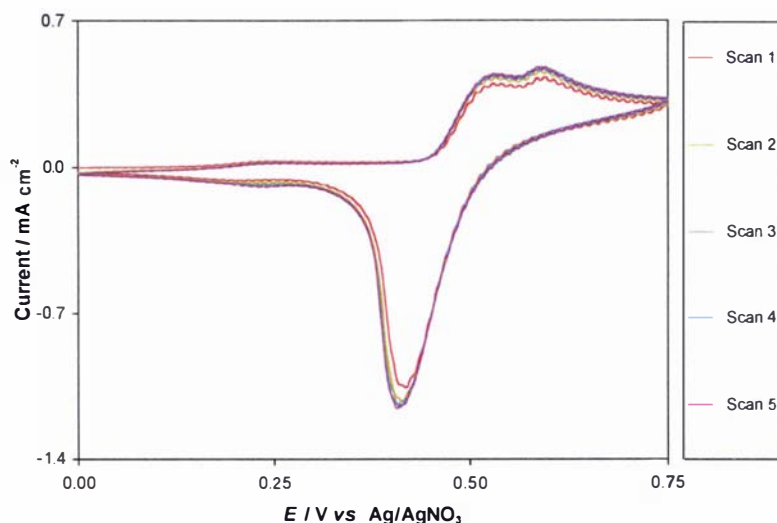


**Figure 5.63** Cyclic voltammetry for open-chain sexithiophene LXX

( $\nu = 100 \text{ mV s}^{-1}$ , 1 mM LXX, 0.1 M TBAP,  $\text{CH}_2\text{Cl}_2$ )

The lack of reactivity of these oxidised sexithiophene derivatives is consistent with the rest of the results presented in this thesis. In no case is there evidence for production of oligomers longer than sexithiophenes, from the dialkoxy-styryl-substituted terthiophenes synthesised.

Similar results have been reported by Roncali *et al.*<sup>314</sup> who investigated the electro-oxidation of three different alkyl- and alkoxy-substituted sexithiophenes. Cyclic voltammetry of these compounds gave current responses with two oxidation and two reduction peaks, which were attributed to the sexithiophene radical and dication. Repetitive cycling in  $\text{CH}_2\text{Cl}_2$  led to the deposition of some material on the working electrode surface. However, this was shown to consist of the sexithienyl dication salt, rather than higher oligomers, as evidenced by the lack of new peaks in the CV. When the compounds were cycled in a more polar solvent (MeCN), new oxidation and reduction peaks were observed at lower potentials than seen for the monomer. Although the species giving rise to the new peaks were not identified, they were believed to consist of an extensively conjugated material, produced by radical cation coupling.

Xu and Horowitz<sup>323</sup> investigated the response of sexithiophene to cyclic voltammetry. Two slight oxidation and reduction peaks were observed, which they attributed to the

formation of the radical cation and dication. No film was deposited on the surface of the electrode, and the peak-to-peak separations of *ca.* 60 mV for each set of peaks showed that both reactions involved one electron. They then vacuum evaporated sexithiophene onto an ITO-coated glass electrode. UV/VIS spectra were obtained before and after the sample was subjected to an oxidizing potential, a red-shift of the absorption maxima indicating that polymerisation did occur in the solid-state.

## 5.2.7 Summary

The electrochemical oxidation of a series of new dialkoxystyryl-substituted terthiophene monomers was investigated using cyclic voltammetry. In general, those with shorter polyether chains tended to form films on the working electrode surface, whereas those with longer polyether chains did not. In most cases where films could be formed, UV/VIS/NIR data (Table 5.3) showed no evidence for the production of oligothiophenes longer than sexithiophene. It has been shown previously (Section 5.1) that these compounds form isolable dimers when chemically polymerised, due to an asymmetric reactivity of the terthiophene-based monomer. This leads to the formation of regioselective dimers in very high yields. An increase in the length of the attached polyether chain increases the solubility of these dimers in MeCN. It is believed that in most cases electrochemical oxidation led only to dimers, and that electrochemical films are not formed from monomers bearing long polyether chains due to the solubility of the dimers in the electrochemical solvent.

Hemicrown compounds, consisting of two dialkoxystyryl-substituted terthiophenes linked by a polyether chain, were also electrochemically oxidised. The extent of polymerisation for films produced from these monomers was unable to be determined, however it is known from UV/VIS/NIR data that the maximum conjugation length in the polymers produced was six thiophene units. It appears that each terthiophene moiety contained in these monomers reacts preferentially at one of

the two available  $\alpha$ -positions, in the same way as seen for the terthiophene-based monomers.

Analogous monomers containing thienyl or sexithienyl moieties did not form films under the conditions employed. It is believed that this is caused by oxidation of the alkene bond for the thiophene-based monomers, and by the stability of the sexithienyl dication species for the sexithiophene-based monomers. These results are consistent with those obtained by previous researchers,<sup>160, 162-166, 314, 322, 323</sup> and with the results of chemical polymerisation presented in Section 5.1.

**6**

# **CONCLUSIONS**

The aim of this research was to synthesise conducting polymer precursors that could be used as alkali metal sensors. These compounds include either crown ethers or polyether chains designed to complex metal cations, and a polymerisable terthiophene moiety. The two functionalities are connected *via* a conjugated styryl spacer unit to reduce unfavourable steric interactions that may inhibit polymerisation. A number of novel dialkoxystyryl-substituted terthiophenes were successfully synthesised. This methodology was extended to the formation of cross-linked bis(terthiophene) crown ethers, as it was believed that these compounds would form more stable network-type polymers, and may also show an actuation effect on ion complexation. The insolubility of these compounds meant that they could not be investigated further, so the structurally-similar hemicrown compounds became the synthetic focus. The hemicrown compounds consist of two styryl-terthiophene units linked by an ether chain, and as such can form network-type polymers in the same way. Three isomeric hemicrowns were successfully synthesised, and were sufficiently soluble to be of use in further investigations. In order to more fully understand the spectroscopic properties of the target terthiophenes, the thiophene analogues of the crown ether, open-chain ether, bis(terthiophene) crown ether and hemicrown compounds were also successfully synthesised and characterised.

As the terthiophene moiety is both a chromophore and a fluorophore, the response of the terthiophene crown compounds, open-chain compounds and hemicrowns to a range of metal cations was investigated by both UV/VIS and fluorescence spectroscopy. The position of the UV/VIS absorbance maxima was blue-shifted on complexation of appropriate metal ions, the magnitude of the shift giving an indication of the binding affinity. Complexation-enhanced quenching of fluorescence was also observed on addition of metal ions to these compounds. The results obtained from both UV/VIS and fluorescence studies were in agreement, and consistent with complexation based on size-fit and charge density of ions. Of the metal ions studied, a unique response to  $\text{Pb}^{2+}$  was observed. This is believed to be due to the soft nature of the  $\text{Pb}^{2+}$  allowing it to interact with both the thienyl sulphur atoms and the polyether oxygen atoms. In addition, a particularly striking fluorescence response of styryl-15-crown-5 terthiophene **I** to  $\text{Mn}^{2+}$  was observed. It is

believed that, with some further work, spectroscopic sensors for  $\text{Pb}^{2+}$  or  $\text{Mn}^{2+}$  could be developed from these compounds.

As the terthiophene monomers were designed as precursors for conducting polymers, their polymerisation by both chemical and electrochemical means was explored. Chemical polymerisation of the terthiophene crown monomers and open-chain ether terthiophene compounds carried out using  $\text{FeCl}_3$  led to the isolation of dimeric sexithiophene compounds in high yield. While there are three possible isomeric products that could be formed from dimerisation, characterisation of the pure sexithiophene products showed that they consisted of a single regiospecific isomer. It was elucidated that this unusual regiospecificity was caused by an asymmetric reactivity of the terthiophene-based monomers. Geometry optimizations on the monomer radical cations confirmed that electron spin density is unevenly distributed between the two available  $\alpha$ -positions, directing new bond formation to occur between the two head- $\alpha$  positions. Thus this was discovered to be an excellent high-yielding synthetic route toward isomerically pure dialkoxy-styryl-substituted sexithiophenes. This dimerisation was investigated further by chemically oxidising the terthiophene compounds using  $\text{Cu}(\text{ClO}_4)_2$  in MeCN, and following the reaction with UV/VIS/NIR spectroscopy. This allowed the identification of the oxidised sexithienyl species present. No oxidised terthienyl species were observed, showing that the terthiophene radical cation is extremely reactive. This is not the case for the sexithiophene radical cation, which did not react further, even in the presence of an excess of oxidant. Reduction of these species led to sexithiophene dimers, as seen for chemical polymerisation using  $\text{FeCl}_3$ .

Electrochemical polymerisation of the terthiophene compounds was carried out by cyclic voltammetry. The incorporation of oxygen atoms onto the phenyl ring led to a lowering of the initial oxidation potential, indicating that the alkoxy-styryl compounds were more easily oxidised than styryl-terthiophene. In general, the compounds with shorter polyether chains formed adherent films, whereas those with longer chains did not. This is believed to be due to the solubility of the sexithienyl species formed. Those that formed adherent films were analysed by UV/VIS/NIR spectroscopy in both the neutral and oxidised form. The electrochemical and

spectroscopic evidence again pointed to the formation of dimers as the primary product of oxidation. Styryl-15-crown-5 terthiophene **I** formed an adherent electroactive film under the same conditions used for other samples, however the film appeared to undergo oxidative degradation at the high potential limit. Growing this film using a lower oxidation potential led to a film that dissolved slowly on post-polymerisation cycling in TBAP, and almost instantly in the presence of metal ions. While this shows that the dimer-film formed is sensitive to metal ions, the tendency of the film to dissolve limits its analytical utility. As expected due to their structure, the hemicrown compounds formed films that were considerably more mechanically stable. However, the films did not show any change in response in the presence of different metal ions. In addition, due to the asymmetric reactivity common to all dialkoxystyryl-terthiophenes studied, the maximum conjugation length in the hemicrown films was still only six thiophene units. The surface morphology of all of the films formed was investigated by scanning electron microscopy, and showed a variety of morphologies ranging from discrete coral-like structures, to continuous films. The electrochemical polymerisation of the thiophene monomers and sexithiophene dimers was also investigated. None of the thiophene compounds formed electroactive films on the working electrode surface, rather these compounds appeared to undergo over-oxidation as seen by other researchers for similar compounds. The sexithiophene dimers did not couple further, although their oxidation and reduction in solution could be observed. This result was expected, given the lack of polymerisation obtained by chemical means.

In order to continue this work to form conducting polymers, the design of the monomers needs to be readdressed. Currently, a large difference in reactivity between the head and tail  $\alpha$ -positions leads to the formation of dimers. From literature results, it is believed that grafting long alkoxy chains onto the 4 and 4'' carbons would increase the reactivity of the terminal  $\alpha$ -positions, and could lead to a higher degree of polymerisation. This would also likely increase the solubility of the resultant polymers, simplifying their processing.

**7**

**EXPERIMENTAL**

**DETAILS**

## General Experimental Procedures:

$^1\text{H}$  NMR spectra were obtained either at 270.19 MHz using a JEOL JMN-GX270 FT-NMR Spectrometer with Tecmag Libra upgrade, or at 400.13 MHz using a Bruker 400 Avance running X-WIN NMR software. The chemical shifts are relative to TMS or to the residual proton signal in deuterated solvents ( $\text{CDCl}_3$   $\delta$  7.27,  $\text{CD}_2\text{Cl}_2$   $\delta$  5.32) when TMS was not present.  $^{13}\text{C}$  NMR shifts are relative to  $\text{CDCl}_3$  ( $\delta$  77.0) or  $\text{CD}_2\text{Cl}_2$  ( $\delta$  53.1). Chemical shifts are reported as position ( $\delta$ ), multiplicity (s = singlet, d = doublet, t = triplet, q = quartet, dd = doublet of doublets, m = multiplet), coupling constant ( $J$  Hz), relative integral and assignment.

UV/VIS/NIR spectra were collected on a Shimadzu UV-3101PC UV-VIS-NIR Scanning Spectrophotometer controlled by a PC running Shimadzu software. AR, HPLC or spectroscopy grade solvents were always used.

HRMS (FAB and EI) was carried out by John Allen at HortResearch, Palmerston North using a Varian VG70-250S double focusing magnetic sector mass spectrometer.

Elemental Analysis was carried out in the Campbell Microanalytical Laboratory at the University of Otago using a Carlo Erba Elemental Analyser EA 1108.

Melting point determinations were performed on a Cambridge Instruments Kofler hot-stage, and are uncorrected.

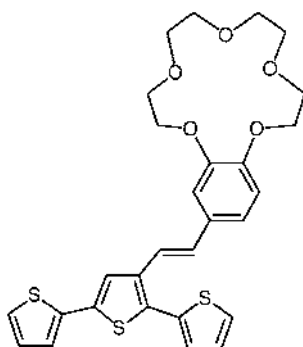
Column chromatography was performed using Merck Kieselgel 60 (230-400 mesh), and thin-layer chromatography using precoated silica gel plates (Merck Kieselgel  $^{60}\text{F}_{254}$ ).

The reagents and solvents used in this work came from many different sources, and were generally AR grade. Chromatography solvents were laboratory grade and were distilled before use.  $\text{H}_2\text{O}$  was reverse osmosis for most applications. Higher purity  $\text{H}_2\text{O}$  was obtained by distilling Milli-Q  $\text{H}_2\text{O}$  off activated charcoal. Dry degassed

$\text{CH}_2\text{Cl}_2$  and DMF were prepared by distillation of AR grade solvent over  $\text{CaH}_2$  under a  $\text{N}_2$  atmosphere. Dry toluene, ether, benzene and THF were prepared by passing argon-degassed solvent through activated alumina columns.  $\text{N}_2$  (oxygen-free) was passed through a KOH drying column to remove moisture.

Thiophene-3-carbaldehyde, thiophen-3-ylmethyl-phosphonic acid diethyl ester (thiophene phosphonate), [2,2';5',2'']terthiophene-3'-carbaldehyde and [2,2';5',2'']terthiophen-3'-ylmethyl-phosphonic acid diethyl ester (terthiophene phosphonate) were routinely synthesised in our laboratories. Samples for this research were provided by S. Gambhir, G. Collis and E. Smith.

**2-(2'-[2'',2''';5''',2''']Terthiophen-3''-yl-vinyl)-6,7,9,10,12,13,15,16-octahydro-5,8,11,14,17-pentaoxa-benzocyclopentadecene (I)**



**a) From crown ether phosphonium salt**

10,12,13,15,16-Octahydro-5,8,11,14,17-pentaoxa-benzocyclopentadecen-2-ylmethyl)-triphenyl-phosphonium chloride (104.1 mg, 0.180 mmol) and [2,2';5',2'']terthiophene-3'-carbaldehyde (63.8 mg, 0.231 mmol, 1.3 eq) were dissolved in 1,2-dichloroethane under N<sub>2</sub> and heated to reflux. 1,8-diazabicyclo[5.4.0]undec-7-ene (80 mL, 0.535 mmol, 3.0 eq) was added in 10 mL aliquots over 1.25 hours. The solution was left to reflux for 1.75 hours before the solvent was removed under reduced pressure. Excess terthiophene aldehyde was removed by column chromatography in CH<sub>2</sub>Cl<sub>2</sub> before the product was eluted in 1% MeOH. Several fractions were collected and individually analysed by NMR spectroscopy and TLC (5% MeOH in CH<sub>2</sub>Cl<sub>2</sub>). Fractions containing little or no triphenylphosphine oxide were pooled and recollected under the same conditions to yield a pure fraction. Mass = 16.1 mg (17%).

**b) From crown ether phosphonate**

6,7,9,10,12,13,15,16-Octahydro-5,8,11,14,17-pentaoxa-benzocyclopentadecen-2-ylmethyl)-phosphonic acid diethyl ester (2.5395 g, max 96.6% pure, 5.86 mmol) and [2,2';5',2'']terthiophene-3'-carbaldehyde (2.0790 g, 7.52 mmol, 1.3 eq) were dissolved in dry tetrahydrofuran (40 mL) and stirred under N<sub>2</sub>. Potassium tert-butoxide (1.6539 g, 14.7 mmol, 2.5 eq) rinsed in with dry tetrahydrofuran (20 mL) was added and the solution left to stir for 3 hours before the tetrahydrofuran was removed under reduced pressure. Dichloromethane (100 mL) and water (100 mL) were added, then a small amount of HCl to bring the solution to neutral pH. The CH<sub>2</sub>Cl<sub>2</sub> layer was

separated, before the aqueous layer was washed with  $\text{CH}_2\text{Cl}_2$  (2 x 50 mL). The combined organic layers were washed with water (100 mL), dried over  $\text{MgSO}_4$ , filtered and evaporated under reduced pressure. The residue was dissolved in  $\text{CH}_2\text{Cl}_2$  and loaded onto a silica column. [2,2';5',2'']Terthiophene was eluted in  $\text{CH}_2\text{Cl}_2$  before the product was eluted in 1.5% MeOH. Mass = 2.3103 g (73%, containing approximately 4% *cis* isomer). The product was dissolved in dry benzene (90 mL) under Ar. Three portions of thiophenol (46  $\mu\text{L}$ ) and 1,1'-azobis(cyclohexanecarbonitrile) (52 mg) were added at hourly intervals and the solution irradiated and heated for three hours. The benzene solution was washed with 1M NaOH (60 mL) and  $\text{H}_2\text{O}$  (60 mL) before the benzene layer was separated. The combined aqueous layer were washed with  $\text{CH}_2\text{Cl}_2$  (2 x 60 mL) before the combined organic layers were washed with  $\text{H}_2\text{O}$  (60 mL), dried over  $\text{MgSO}_4$ , filtered and evaporated under reduced pressure. Analysis of NMR spectra at this point showed no *cis* isomer remained. The product was redissolved in  $\text{CH}_2\text{Cl}_2$  and recolumned. The pure *trans* product was eluted in 5% MeOH. Removal of the solvent afforded a thick yellow oil (2.1115 g, 67%).

### c) From terthiophene phosphonate

6,7,9,10,12,13,15,16-Octahydro-5,8,11,14,17-pentaoxa-benzocyclopentadecene-2-carbaldehyde (0.8368 g, 2.82 mmol) and terthiophene phosphonate (20 mL x 0.14 mmol/mL solution in THF, 2.80 mmol) were dissolved in dry  $\text{CH}_2\text{Cl}_2$  (20 mL) and stirred under  $\text{N}_2$ . On addition of potassium tert-butoxide (1.2750 g, 11.36 mmol), the solution turned briefly dark red, before being left to stir for 30 minutes.  $\text{H}_2\text{O}$  (40 mL) was added, then the solution neutralized with aq. HCl. The organic layer was separated, before the aqueous layer was washed with  $\text{CH}_2\text{Cl}_2$  (3 x 30 mL). The combined organic layers were washed with water (50 mL) and evaporated under reduced pressure. The yellow residue was dissolved in  $\text{CH}_2\text{Cl}_2$  and loaded onto a silica column. A small amount of 1,2-bis([2',2'';5'',2''']terthiophen-3''-yl)ethene was eluted in  $\text{CH}_2\text{Cl}_2$  before the pure *trans* product was eluted in 2% MeOH and evaporated to yield a yellow sticky oil (1.4712 g, 97%).

$^1\text{H}$  NMR (400 MHz,  $\text{CD}_2\text{Cl}_2$ )  $\delta$  3.76-3.80 (m, 8H,  $\text{OCH}_2$ 9, 10, 12, 13); 3.91-3.95 (m, 4H,  $\text{OCH}_2$ 7, 15); 4.14-4.20 (m, 4H,  $\text{OCH}_2$ 6, 16); 6.86 (d, 1H,  $^3J = 8.1$  Hz, ArH4);

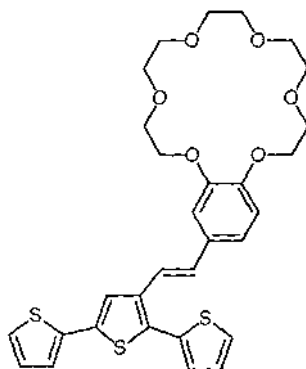
6.97 (d, 1H,  $^3J = 16.1$  Hz,  $H_{\text{vinyl}1'}$ ); 7.03-7.06 (m, 2H, ArH1,3); 7.05 (dd, 1H,  $^3J = 5.1$  Hz,  $^4J = 3.6$  Hz, ThH4'''); 7.13 (dd, 1H,  $^3J = 5.2$  Hz,  $^4J = 3.6$  Hz, ThH4''); 7.20 (dd, 1H,  $^3J = 3.6$  Hz,  $^4J = 1.2$  Hz, ThH3''); 7.21 (d, 1H,  $^3J = 16.1$  Hz,  $H_{\text{vinyl}2'}$ ); 7.22 (dd, 1H,  $^3J = 3.6$  Hz,  $^4J = 1.2$  Hz, ThH3'''); 7.26 (dd, 1H,  $^3J = 5.1$ ,  $^4J = 1.2$  Hz, ThH5'''); 7.39 (dd, 1H,  $^3J = 5.1$  Hz,  $^4J = 1.2$  Hz, ThH5''); 7.40 (s, 1H, ThH4'').

$^{13}\text{C}$  NMR (100.6 MHz,  $\text{CD}_2\text{Cl}_2$ )  $\delta$  68.3 OCH<sub>2</sub>; 68.5 OCH<sub>2</sub>; 68.9 OCH<sub>2</sub>; 69.0 OCH<sub>2</sub>; 69.8 OCH<sub>2</sub>; 69.8 OCH<sub>2</sub>; 70.4 OCH<sub>2</sub>; 70.4 OCH<sub>2</sub>; 111.2 ArC1; 113.2 ArC4; 119.3 C<sub>vinyl</sub>2'; 119.8 ArC3; 121.9 ThC4'''; 123.8 ThC3'''; 124.6 ThC5'''; 126.0 ThC5''; 126.5 ThC3''; 127.5 ThC4''; 127.6 ThC4'''; 130.1 ArC2; 130.3 C<sub>vinyl</sub>1'; 130.4 ThC2'''; 134.9 ThC2''; 135.5 ThC5'''; 136.2 ThC3'''; 136.3 ThC2'''; 148.9 ArCO; 148.9 ArCO.

Electronic spectrum (MeCN)  $\lambda_{\text{max}}$  nm/(log  $\epsilon$ ) 329.0 (4.57).

HRMS (FAB)  $M^+$  calc 540.1099, found 540.1128.

**2-(2'-[2'',2''';5''',2''''']Terthiophen-3'''-yl-vinyl)-6,7,9,10,12,13,15,16,18,19-decahydro-5,8,11,14,17,20-hexaoxa-benzocyclooctadecene (II)**



**a) From crown ether phosphonate**

(6,7,9,10,12,13,15,16,18,19-Decahydro-5,8,11,14,17,20-hexaoxabenzocyclooctadecen-2-ylmethyl)-phosphonic acid diethyl ester (1.5467 g,

3.34 mmol) and [2,2';5',2'']terthiophene-3'-carbaldehyde (1.2026 g, 4.35 mmol, 1.3 eq) were dissolved in dry tetrahydrofuran (30 mL) and stirred under N<sub>2</sub>. Potassium tert-butoxide (0.5600 g, 4.99 mmol, 1.5 eq) was added in five portions at half-hourly intervals and the solution left to stir for a further 30 minutes before the tetrahydrofuran was removed under reduced pressure. The product was redissolved in CH<sub>2</sub>Cl<sub>2</sub> and loaded onto a silica column. A small amount of [2,2';5',2'']terthiophene was eluted in CH<sub>2</sub>Cl<sub>2</sub> before the product was eluted as a *cis:trans* mixture (1:49) in 5% MeOH. The product was then dissolved in dry benzene (40 mL) under Ar. Three portions of thiophenol (20 μL) and 1,1'-azobis(cyclohexanecarbonitrile) (22 mg) were added at hourly intervals and the solution irradiated with heating for a total of 3 hours. The solution was washed with 1 M NaOH (30 mL) and H<sub>2</sub>O (30 mL) before the combined aqueous extracts were washed with CH<sub>2</sub>Cl<sub>2</sub> (2 x 30 mL). The combined organic layers were then washed with H<sub>2</sub>O (50 mL), dried over MgSO<sub>4</sub>, filtered and evaporated. Analysis by NMR spectroscopy at this point showed no *cis* isomer remaining. The product was dissolved in CH<sub>2</sub>Cl<sub>2</sub> and columned on silica. Evaporation of the pure *trans* product eluted in 5% MeOH gave a yellow sticky oil (0.8023 g, 41%).

#### **b) From terthiophene phosphonate**

Terthiophene phosphonate (40 mL x 0.135 mmol/mL solution in THF, 5.40 mmol) and 6,7,9,10,12,13,15,16,18,19-decahydro-5,8,11,14,17,20-hexaoxabenzocyclooctadecene-2-carbaldehyde (1.8380 g, 5.40 mmol) were stirred in dry CH<sub>2</sub>Cl<sub>2</sub> (40 mL) under N<sub>2</sub> before potassium tert-butoxide (2.4140 g, 21.5 mmol) was added, causing the solution to go temporarily dark red. After stirring at room temperature for 30 minutes, CH<sub>2</sub>Cl<sub>2</sub> (20 mL) and H<sub>2</sub>O (100 mL) were added and the solution acidified with aq. HCl. The organic layer was separated and the aqueous layer extracted with CH<sub>2</sub>Cl<sub>2</sub> (50 mL) before the combined organic layers were washed with H<sub>2</sub>O (80 mL) and the solvent removed under reduced pressure. The sticky orange/brown residue was dissolved in CH<sub>2</sub>Cl<sub>2</sub> and purified by flash column chromatography on silica. 1,2-bis([2',2'';5'',2''']Terthiophen-3''-yl)ethene was eluted in CH<sub>2</sub>Cl<sub>2</sub> (85.8 mg, 6%) before the desired product was eluted in 2% MeOH. Removal of the solvent afforded 2-(2'-[2'',2''';5''',2''''']terthiophen-3''-yl-vinyl)-

6,7,9,10,12,13,15,16,18,19-decahydro-5,8,11,14,17,20-hexaoxa-benzocyclooctadecene as a dark yellow oil (2.8342 g, 89%).

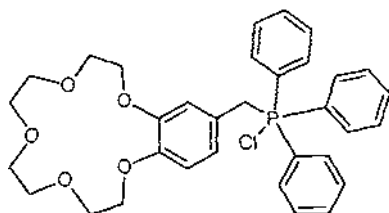
$^1\text{H}$  NMR (400 MHz,  $\text{CD}_2\text{Cl}_2$ )  $\delta$  3.61 (s, 4H,  $\text{OCH}_2$ 12, 13); 3.62-3.65 (m, 4H,  $\text{OCH}_2$ 10, 15); 3.68-3.70 (m, 4H,  $\text{OCH}_2$ 9, 16); 3.83-3.87 (m, 4H,  $\text{OCH}_2$ 7, 18); 4.12-4.17 (m, 4H,  $\text{OCH}_2$ 6, 19); 6.84 (d, 1H,  $^3J = 8.2$  Hz, ArH4); 7.00 (d, 1H,  $^3J = 16.3$  Hz,  $\text{H}_{\text{vinyl}}1'$ ); 7.01-7.05 (m, 2H, ArH1, 3); 7.05 (dd, 1H,  $^3J = 5.1$  Hz,  $^4J = 3.6$  Hz, ThH4'''); 7.13 (dd, 1H,  $^3J = 5.1$  Hz,  $^4J = 3.6$  Hz, ThH4'''); 7.22 (dd, 1H,  $^3J = 3.6$  Hz,  $^4J = 1.2$  Hz, ThH3''); 7.23 (d, 1H,  $^3J = 16.1$  Hz,  $\text{H}_{\text{vinyl}}2'$ ); 7.23 (dd, 1H,  $^3J = 3.7$  Hz,  $^4J = 1.1$  Hz, ThH3'''); 7.28 (dd, 1H,  $^3J = 5.1$  Hz,  $^4J = 1.1$  Hz, ThH5'''); 7.41 (dd, 1H,  $^3J = 5.1$  Hz,  $^4J = 1.2$  Hz, ThH5'''); 7.44 (s, 1H, ThH4''').

$^{13}\text{C}$  NMR (100.6 MHz,  $\text{CD}_2\text{Cl}_2$ )  $\delta$  68.0  $\text{OCH}_2$ ; 68.0  $\text{OCH}_2$ ; 68.8  $\text{OCH}_2$ ; 68.9  $\text{OCH}_2$ ; 69.9  $\text{OCH}_2$ ; 69.9  $\text{OCH}_2$ ; 70.0  $\text{OCH}_2$ ; 70.0  $\text{OCH}_2$ ; 70.1  $\text{OCH}_2$ ; 70.1  $\text{OCH}_2$ ; 110.4 ArC1; 112.4 ArC4; 119.2  $\text{C}_{\text{vinyl}}2'$ ; 119.5 ArC3; 121.9 ThC4'''; 123.8 ThC3'''; 124.5 ThC5'''; 126.0 ThC5''; 126.5 ThC3''; 127.5 ThC4''; 127.6 ThC4'''; 130.0 ArC2; 130.1  $\text{C}_{\text{vinyl}}1'$ ; 130.3 ThC2''; 134.9 ThC2''; 135.4 ThC5''; 136.2 ThC3''; 136.3 ThC2'''; 148.4 ArCO; 148.4 ArCO.

Electronic spectrum (MeCN)  $\lambda_{\text{max}}$  nm/(log  $\epsilon$ ) 330.0 (4.58).

HRMS (FAB)  $\text{M}^+$  calc 584.1361, found 584.1387.

**(6,7,9,10,12,13,15,16-Octahydro-5,8,11,14,17-pentaoxa-benzocyclopentadecen-2-ylmethyl)-triphenyl-phosphonium chloride (III)**



2-Chloromethyl-6,7,9,10,12,13,15,16-octahydro-5,8,11,14,17-pentaoxa-benzocyclopentadecene (1.0924 g, 3.45 mmol) and triphenylphosphine (1.5203 g, 5.80 mmol) were dissolved in toluene (10 mL), then heated to reflux for 21 hours. The reaction mixture was diluted with hexane (15 mL) and cooled to room temperature before cooling in ice. The precipitate that formed was separated by filtration and dried under vacuum. The dry precipitate was then ground up, recrystallised from CH<sub>2</sub>Cl<sub>2</sub>/toluene, and recovered by filtration on a 0.45 μm HVLP membrane (Millipore) to give the 15-crown-5 phosphonium salt as a white solid (1.239 g, 62%).

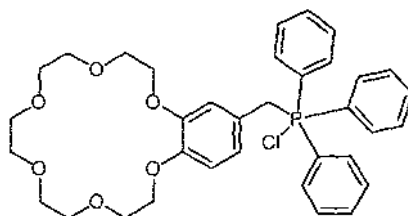
<sup>1</sup>H NMR (400 MHz, CDCl<sub>3</sub>) δ 3.62-3.67 (m, 12H, OCH<sub>2</sub>); 3.79-3.80 (m, 2H, OCH<sub>2</sub>); 3.95-3.96 (m, 2H, OCH<sub>2</sub>); 5.14 (d, 2H, <sup>2</sup>J<sub>H,P</sub> = 13.8 Hz, CH<sub>2</sub>P); 6.44 (dd, 1H, <sup>3</sup>J = 8.3 Hz, <sup>4</sup>J = 2.4 Hz, ArH3); 6.51 (d, 1H, <sup>3</sup>J = 8.3 Hz, ArH4); 6.70 (d, 1H, <sup>4</sup>J = 2.0 Hz, ArH1); 7.54-7.69 (m, 15H, ArH).

<sup>31</sup>P NMR (162.0 MHz, CDCl<sub>3</sub>) δ 23.8 PPh<sub>3</sub>.

Electronic spectrum (CHCl<sub>3</sub>) λ<sub>max</sub> nm/(log ε) 269.0 (3.77), 276.0 (3.78).

HRMS (FAB) (M-Cl)<sup>+</sup> calc 543.2300, found 543.2325.

**(6,7,9,10,12,13,15,16,18,19-Decahydro-5,8,11,14,17,20-hexaoxa-benzocyclooctadecen-2-ylmethyl)-triphenyl-phosphonium chloride (IV)**



2-Chloromethyl-6,7,9,10,12,13,15,16,18,19-decahydro-5,8,11,14,17,20-hexaoxa-benzocyclooctadecene (0.6230 g, 1.727 mmol) and triphenylphosphine (0.7651 g, 2.917 mmol, 1.7 eq) were dissolved in dry toluene (10 mL). The solution was heated to reflux for 20 hours before being diluted with toluene (10 mL) and cooled to room temperature. The solution was cooled in ice before being filtered through a 0.45  $\mu\text{m}$  HVLP membrane filter (Millipore). After drying under vacuum, the phosphonium salt was obtained as a white solid (0.731 g, 68%).

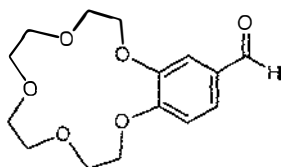
$^1\text{H}$  NMR (400 MHz,  $\text{CDCl}_3$ )  $\delta$  3.57-3.69 (m, 12H,  $\text{OCH}_2$ ); 3.79-3.81 (m, 4H,  $\text{OCH}_2$ ); 3.96-3.98 (m, 4H,  $\text{OCH}_2$ ); 5.14 (d, 2H,  $^2J_{\text{CP}} = 13.8$  Hz,  $\text{CH}_2\text{P}$ ); 6.44 (d, 1H,  $^3J = 8.6$  Hz, ArH); 6.50 (d, 1H,  $^3J = 8.4$  Hz, ArH); 6.68 (s, 1H, ArH1); 7.54-7.69 (m, 15H, ArH).

$^{31}\text{P}$  NMR (162.0 MHz,  $\text{CDCl}_3$ )  $\delta$  23.6.

Electronic spectrum ( $\text{CHCl}_3$ )  $\lambda_{\text{max}}$  nm/(log  $\epsilon$ ) 269.5 (3.83), 276.0 (3.83).

HRMS (FAB) ( $\text{M}-\text{Cl}$ ) $^+$  calc 587.2563, found 587.2559.

**6,7,9,10,12,13,15,16-Octahydro-5,8,11,14,17-pentaoxa-benzocyclopentadecene-2-carbaldehyde (V)**

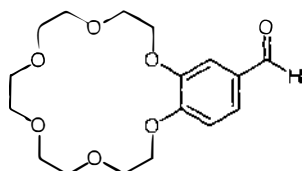


6,7,9,10,12,13,15,16-Octahydro-5,8,11,14,17-pentaoxa-benzocyclopentadecene-2-carbaldehyde was prepared according to the method of Ungaro, El Haj and Smid.<sup>16</sup> 3,4-dihydroxybenzaldehyde (5.00 g, 0.036 mol) and sodium hydroxide (3.00 g, 0.075 mol) were stirred under  $\text{N}_2$  in 1-butanol (50 mL). 1,1-dichloro-3,6,9-

trioxaundecane (8.32 g, 0.036 mol) was added and the mixture refluxed for 27 hours before cooling to room temperature. The solution was acidified with 18% HCl, the solids filtered out and washed with methanol and the solvent removed under reduced pressure. The oily residue was adsorbed onto silica and extracted with heptane for 26 hours using a soxhlet apparatus. The heptane was removed and the product solidified from 3:2 isopropyl alcohol:hexane. After the product was filtered, washed with hexane and dried under vacuum, 6,7,9,10,12,13,15,16-octahydro-5,8,11,14,17-pentaoxa-benzocyclopentadecene-2-carbaldehyde was obtained as a white solid (4.37 g, 41%, lit. 40%<sup>16</sup>).

Spectroscopic properties were in agreement with published data.<sup>16</sup>

**6,7,9,10,12,13,15,16,18,19-Decahydro-5,8,11,14,17,20-hexaoxa-benzocyclooctadecene-2-carbaldehyde (VI)**

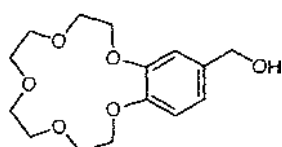


6,7,9,10,12,13,15,16,18,19-Decahydro-5,8,11,14,17,20-hexaoxa-benzocyclooctadecene-2-carbaldehyde was prepared according to the method of Ungaro, El Haj and Smid.<sup>16</sup> 3,4-dihydroxybenzaldehyde (5.00 g, 0.036 mol) and sodium hydroxide (3.00 g, 0.075 mol) were stirred under N<sub>2</sub> in 1-butanol (50 mL). 1,14-dichloro-3,6,9,12-tetraoxaundecane (9.91 g, 0.036 mol) was added and the mixture refluxed for 27 hours before cooling to room temperature. The solution was acidified with 18% HCl, the solids filtered and washed with methanol and the solvent removed under reduced pressure. The oily residue was adsorbed onto silica and extracted with heptane for 26 hours using a soxhlet apparatus. The heptane was removed and the product solidified from 3:2 isopropyl alcohol:hexane. After the product was filtered, washed with hexane and dried under vacuum, the title compound

was obtained as a white solid (6.669 g, 54%, lit. 25%<sup>16</sup>).

Spectroscopic properties were in agreement with published data.<sup>16</sup>

**(6,7,9,10,12,13,15,16-Octahydro-5,8,11,14,17-pentaoxa-benzocyclopentadecen-2-yl)-methanol (VII)**

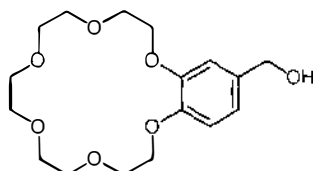


6,7,9,10,12,13,15,16-Octahydro-5,8,11,14,17-pentaoxa-benzocyclopentadecene-2-carbaldehyde (6.0400 g, 20.38 mmol) was dissolved in 1:1 THF:ethanol (60 mL) before sodium borohydride (0.8045 g, 21.27 mmol) was added and the solution left to stir under Ar for 17 hours. The reaction was quenched by the slow addition of 1M HCl (50 mL). After the cessation of effervescence, the product was extracted with CH<sub>2</sub>Cl<sub>2</sub> (3 x 50 mL). The combined organic extracts were washed with H<sub>2</sub>O (50 mL), dried with MgSO<sub>4</sub>, filtered and evaporated to yield the title compound as an oil which could be solidified by treatment with isopropyl alcohol and hexane (5.43 g, 89%, lit. 64% using LiAl<sub>4</sub><sup>211</sup>).

<sup>1</sup>H NMR (270.2 MHz, CDCl<sub>3</sub>) δ 2.52 (br s, 1H, OH); 3.74 (s, 8H, OCH<sub>2</sub>9, 10, 12, 13); 3.86-3.90 (m, 4H, OCH<sub>2</sub>7, 17); 4.09-4.12 (m, 4H, OCH<sub>2</sub>6, 16); 4.56 (s, 2H, ArCH<sub>2</sub>); 6.78-6.88 (m, 3H, ArH1, 3, 4)

<sup>13</sup>C NMR (68.1 MHz, CDCl<sub>3</sub>) δ 65.0 CH<sub>2</sub>OH; 68.8 OCH<sub>2</sub>; 69.1 OCH<sub>2</sub>; 69.5 OCH<sub>2</sub>; 70.4 OCH<sub>2</sub>; 71.0 OCH<sub>2</sub>; 112.9 ArC; 113.8 ArC; 119.7 ArC; 134.3 ArC; 148.3 ArCO; 149.0 ArCO.

**(6,7,9,10,12,13,15,16,18,19-Decahydro-5,8,11,14,17,20-hexaoxa-benzocyclooctadecen-2-yl)-methanol (VIII)**

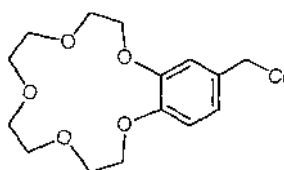


Formylbenzo-18-crown-6 (3.6131 g, 10.6 mmol) was dissolved in 1:1 THF:ethanol (60 mL) before sodium borohydride (0.4030 g, 10.7 mmol) was added and the solution left to stir under Ar for 20 hours. The reaction was quenched by the slow addition of 1M HCl (50 mL), and after the cessation of effervescence, was extracted with CH<sub>2</sub>Cl<sub>2</sub> (3 x 45 mL). The combined organic extracts were washed with H<sub>2</sub>O (60 mL), dried with MgSO<sub>4</sub>, filtered and evaporated to leave an oil. Some further impurities were removed by vacuum distillation, leaving the title compound (2.5305 g, 70%).

<sup>1</sup>H NMR (270.2 MHz, CDCl<sub>3</sub>) δ 2.82 (br s, 1H, OH); 3.64-3.77 (m, 12H, OCH<sub>2</sub>, 9, 10, 12, 13, 15, 16); 3.89-3.92 (m, 4H, OCH<sub>2</sub>, 7, 18); 4.12-4.16 (m, 4H, OCH<sub>2</sub>, 6, 19); 4.57 (s, 2H, ArCH<sub>2</sub>); 6.80-6.90 (m, 3H, ArH, 3, 4).

<sup>13</sup>C NMR (68.1 MHz, CDCl<sub>3</sub>) δ 65.0 CH<sub>2</sub>OH; 69.0 OCH<sub>2</sub>; 69.1 OCH<sub>2</sub>; 69.6 OCH<sub>2</sub>; 70.5 OCH<sub>2</sub>; 70.6 OCH<sub>2</sub>; 70.7 OCH<sub>2</sub>; 70.8 OCH<sub>2</sub>; 113.0 ArC; 113.8 ArC; 119.8 ArC; 134.2 ArC; 148.3 ArCO; 148.8 ArCO.

**2-Chloromethyl-6,7,9,10,12,13,15,16-octahydro-5,8,11,14,17-pentaoxa-benzocyclopentadecene (IX)**

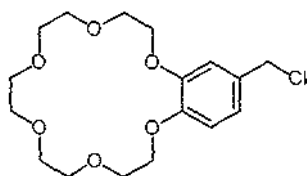


The title compound was prepared according to the method of Hyde *et al.*<sup>211</sup> Hydroxymethylbenzo-15-crown-5 (5.43 g, 18.2 mmol) was dissolved in dry benzene (10 mL) and thionyl chloride (2.8 mL, 4.57 g, 38.4 mmol) in benzene (10 mL) added. The solution was left to stir under Ar for 2 hours before H<sub>2</sub>O (50 mL) was added and the benzene layer separated. The aqueous layer was extracted with CH<sub>2</sub>Cl<sub>2</sub> (3 x 50 mL) before the combined organic extracts were washed with H<sub>2</sub>O (50 mL), dried over MgSO<sub>4</sub>, filtered and evaporated. The title compound was obtained by recrystallisation with petroleum ether (b.p. 40-60°C) to yield a white solid (1.7912 g, 28%).

<sup>1</sup>H NMR (270.2 MHz, CDCl<sub>3</sub>) δ 3.75 (s, 8H, OCH<sub>2</sub>9, 10, 12, 13); 3.88-3.92 (m, 4H, OCH<sub>2</sub>7, 15); 4.11-4.16 (m, 4H, OCH<sub>2</sub>6, 16); 4.53 (s, 2H, CH<sub>2</sub>Cl); 6.81 (d, <sup>3</sup>J = 8.8 Hz, ArH4); 6.89-6.93 (m, 2H, ArH1, 3).

<sup>13</sup>C NMR (68.1 MHz, CDCl<sub>3</sub>) δ 46.6 CH<sub>2</sub>Cl; 69.0 OCH<sub>2</sub>; 69.5 OCH<sub>2</sub>; 70.5 OCH<sub>2</sub>; 71.1 OCH<sub>2</sub>; 113.6 ArC; 114.3 ArC; 121.6 ArC; 130.3 ArC; 149.0 ArCO; 149.2 ArCO.

**2-Chloromethyl-6,7,9,10,12,13,15,16,18,19-decahydro-5,8,11,14,17,20-hexaoxa-benzocyclooctadecene (X)**



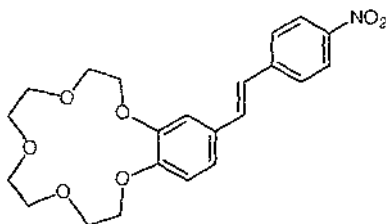
The title compound was prepared according to a method similar to that published by Hyde *et al.*<sup>211</sup> Hydroxymethylbenzo-18-crown-6 (2.5305 g, 7.39 mmol) was dissolved in dry benzene (20 mL) and thionyl chloride (1.10 mL, 1.79 g, 15.08 mmol) in benzene (15 mL) added. The solution was left to stir under Ar for 2 hours before H<sub>2</sub>O (20 mL) was added and the benzene layer separated. The aqueous layer was

extracted with  $\text{CH}_2\text{Cl}_2$  (5 x 20 mL) before the combined organic extracts were washed with  $\text{H}_2\text{O}$  (50 mL), dried over  $\text{MgSO}_4$ , filtered and evaporated. The title compound was obtained by recrystallisation with petroleum ether (b.p. 40-60°C) to yield a white solid (0.7725 g, 29%).

$^1\text{H}$  NMR (270.2 MHz,  $\text{CDCl}_3$ )  $\delta$  3.63-3.76 (m, 12H,  $\text{OCH}_2$ , 9, 10, 12, 13, 15, 16); 3.88-3.92 (m, 4H,  $\text{OCH}_2$ , 7, 18); 4.12-4.17 (m, 4H,  $\text{OCH}_2$ , 6, 19); 4.52 (s, 2H,  $\text{CH}_2\text{Cl}$ ); 6.81 (d,  $^3J = 8.8$  Hz, ArH4); 6.87-6.90 (m, 2H, ArH1, 3).

$^{13}\text{C}$  NMR (68.1 MHz,  $\text{CDCl}_3$ )  $\delta$  46.5  $\text{CH}_2\text{Cl}$ ; 69.1  $\text{OCH}_2$ ; 69.5  $\text{OCH}_2$ ; 70.5  $\text{OCH}_2$ ; 70.6  $\text{OCH}_2$ ; 70.7  $\text{OCH}_2$ ; 70.8  $\text{OCH}_2$ ; 113.7 ArC; 114.4 ArC; 121.6 ArC; 130.3 ArC; 148.9 ArCO; 149.0 ArCO.

**2-[2'-(4''-Nitro-phenyl)-vinyl]-6,7,9,10,12,13,15,16-octahydro-5,8,11,14,17-pentaoxa-benzocyclopentadecene (XI)**



10,12,13,15,16-Octahydro-5,8,11,14,17-pentaoxa-benzocyclopentadecen-2-ylmethyl)-triphenyl-phosphonium chloride (100.9 mg, 0.174 mmol) and 4-nitrobenzaldehyde (39.8 mg, 0.263 mmol, 1.5 eq) were dissolved in dry  $\text{CH}_2\text{Cl}_2$  (5 mL) and stirred under  $\text{N}_2$ . 1,8-diazabicyclo[5.4.0]undec-7-ene (130 mL, 0.869 mmol, 5.0 eq) was added and the solution left to stir for 4.5 hours. The product was subjected to column chromatography, and fractions collected in  $\text{CH}_2\text{Cl}_2$ , 1%  $\text{MeOH}/\text{CH}_2\text{Cl}_2$  and 2%  $\text{MeOH}/\text{CH}_2\text{Cl}_2$ . The fractions collected in  $\text{CH}_2\text{Cl}_2$  and 1%  $\text{MeOH}$  were separately subjected to column chromatography (1%  $\text{MeOH}/\text{CH}_2\text{Cl}_2$ ) and several subfractions collected from each. Subfractions were individually analysed by

NMR spectroscopy and TLC (5% MeOH/CH<sub>2</sub>Cl<sub>2</sub>), and those containing only product were combined and the solvent removed by reduced pressure to yield the *trans* product as a yellow solid (21.1 mg, 29%).

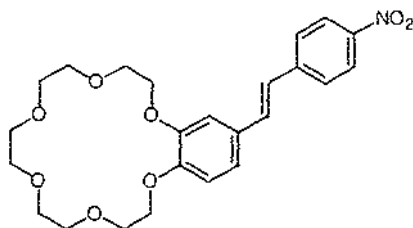
<sup>1</sup>H NMR (400 MHz, CDCl<sub>3</sub>) δ 3.78 (s, 8H, OCH<sub>2</sub>9, 10, 12, 13); 3.92-3.96 (m, 4H, OCH<sub>2</sub>7, 15); 4.17-4.23 (m, 4H, OCH<sub>2</sub>6, 16); 6.88 (d, 1H, <sup>3</sup>J = 8.8 Hz, ArH4); 6.99 (d, 1H, <sup>3</sup>J = 16.2 Hz, H<sub>vinyl</sub>2'); 7.09-7.11 (m, 2H, ArH1, 3); 7.19 (d, 1H, <sup>3</sup>J = 16.2 Hz, H<sub>vinyl</sub>1'); 7.60 (d, 2H, <sup>3</sup>J = 8.8 Hz, ArH2'', 6''); 8.21 (d, 2H, <sup>3</sup>J = 8.6 Hz, ArH3'', 5'').

<sup>13</sup>C NMR (100.6 MHz, CDCl<sub>3</sub>) δ 68.7 OCH<sub>2</sub>; 69.1 OCH<sub>2</sub>; 69.4 OCH<sub>2</sub>; 69.5 OCH<sub>2</sub>; 70.3 OCH<sub>2</sub>; 70.4 OCH<sub>2</sub>; 71.0 OCH<sub>2</sub>; 71.0 OCH<sub>2</sub>; 111.9 ArC3; 113.4 ArC4; 121.4 ArC1; 124.1 ArC3'', 5''; 124.3 C<sub>vinyl</sub>2'; 126.5 ArC2'', 6''; 129.6 ArC2; 133.1 C<sub>vinyl</sub>1'; 144.1 ArC1''; 146.4 ArC4''; 149.2 ArCO; 150.1 ArCO.

Electronic spectrum (MeCN) λ<sub>max</sub> nm/(log ε) 278.5 (3.54), 382.5 (3.86).

HRMS (EI) M<sup>+</sup> calc 415.1631, found 415.1626.

**2-[2'-(4''-Nitro-phenyl)-vinyl]-6,7,9,10,12,13,15,16,18,19-decahydro-5,8,11,14,17,20-hexaoxa-benzocyclooctadecene (XII)**



(6,7,9,10,12,13,15,16,18,19-Decahydro-5,8,11,14,17,20-hexaoxa-benzocyclooctadecen-2-ylmethyl)-triphenyl-phosphonium chloride (106.4 mg, 0.1708 mmol) and 4-nitrobenzaldehyde (35.3 mg, 0.2336 mmol, 1.4 eq) were stirred in dry CH<sub>2</sub>Cl<sub>2</sub> under Ar. 1,8-diazabicyclo[5.4.0]undec-7-ene (75 mL, 0.502 mmol,

2.9 eq) was added and the solution was left to stir for 4 hours. The solvent was removed under reduced pressure to give a yellow oily/solid. This material was subjected to column chromatography and the product eluted in 2% MeOH/CH<sub>2</sub>Cl<sub>2</sub> to give a 1:1 mixture of *cis* and *trans* products as a yellow solid (104.8 mg). The product was dissolved in dry CH<sub>2</sub>Cl<sub>2</sub> (10 mL) and stirred under N<sub>2</sub>. I<sub>2</sub> (140 mg, 3 eq) was added and the solution left to stir, shielded from light, for 3.5 hours. Saturated Na<sub>2</sub>S<sub>2</sub>O<sub>3</sub> (25 mL) was added and the solution left to stir overnight before the mixture was diluted with H<sub>2</sub>O (30 mL) and the yellow organic layer was separated. The aqueous layer was washed with CH<sub>2</sub>Cl<sub>2</sub> (3 x 10 mL), before the combined organic layers were washed with H<sub>2</sub>O (20 mL), dried over MgSO<sub>4</sub>, filtered and evaporated. The yellow solid product was purified by column chromatography (CH<sub>2</sub>Cl<sub>2</sub>, 1% MeOH/CH<sub>2</sub>Cl<sub>2</sub>, 2% MeOH/CH<sub>2</sub>Cl<sub>2</sub>) and multiple fractions collected. Fractions were analysed by TLC (5% MeOH/CH<sub>2</sub>Cl<sub>2</sub>) and <sup>1</sup>H NMR spectroscopy, and those containing pure product were combined to leave the title compound as a yellow solid (7.0 mg, 9%).

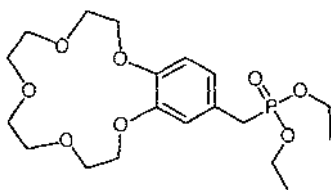
<sup>1</sup>H NMR (400 MHz, CD<sub>2</sub>Cl<sub>2</sub>) δ 3.62 (s, 4H, OCH<sub>2</sub>12, 13); 3.64-3.67 (m, 4H, OCH<sub>2</sub>10, 15); 3.69-3.71 (m, 4H, OCH<sub>2</sub>9, 16); 3.85-3.90 (m, 4H, OCH<sub>2</sub>7, 18); 4.15-4.21 (m, 4H, OCH<sub>2</sub>6, 19); 6.88 (d, 1H, <sup>3</sup>J = 8.8 Hz, ArH4); 7.04 (d, 1H, <sup>3</sup>J = 16.3 Hz, H<sub>vinyl</sub>2'); 7.11 (dd, 1H, <sup>3</sup>J = 8.8 Hz, <sup>4</sup>J = 1.9 Hz, ArH3); 7.11 (d, 1H, <sup>4</sup>J = 2.0 Hz, ArH1); 7.24 (d, 1H, <sup>3</sup>J = 16.3 Hz, H<sub>vinyl</sub>1'); 7.63 (d, 2H, <sup>3</sup>J = 8.7 Hz, ArH2'', 6''); 8.19 (d, 2H, <sup>3</sup>J = 8.9 Hz, ArH3'', 5'').

<sup>13</sup>C NMR (100.6 MHz, CD<sub>2</sub>Cl<sub>2</sub>) δ 67.9 OCH<sub>2</sub>; 68.0 OCH<sub>2</sub>; 68.8 OCH<sub>2</sub>; 68.8 OCH<sub>2</sub>; 69.9 OCH<sub>2</sub>; 69.9 OCH<sub>2</sub>; 70.0 OCH<sub>2</sub>; 70.1 OCH<sub>2</sub>; 110.2 ArC1; 112.2 ArC4; 120.6 ArC3; 123.7 ArC3'', 5''; 123.8 C<sub>vinyl</sub>2'; 126.2 ArC2'', 6''; 128.9 ArC2; 132.7 C<sub>vinyl</sub>1'; 144.0 ArC1''; 146.1 ArC4''; 148.5 ArCO; 149.3 ArCO.

Electronic spectrum (MeCN) λ<sub>max</sub> nm/(log ε) 383.5 (4.27), 280.5 (3.95).

HRMS (FAB) M<sup>+</sup> calc 459.1893, found 459.1881.

**(6,7,9,10,12,13,15,16-Octahydro-5,8,11,14,17-pentaoxa-benzocyclopentadecen-2-ylmethyl)-phosphonic acid diethyl ester (XIII)**



2-Chloromethyl-6,7,9,10,12,13,15,16-octahydro-5,8,11,14,17-pentaoxa-benzocyclopentadecene (4.8371 g, 15.3 mmol) was heated to reflux with triethyl phosphite (80 mL, as the solvent) and allowed to reflux for 24 hours under Ar. The reaction mixture was cooled to room temperature before the majority of the triethyl phosphite was removed under vacuum (0.01 mm Hg) at room temperature, with subsequent heating to 100°C. This yielded the impure 15-crown-5 phosphonate as a pale oil (6.6133 g, <100%).

$^1\text{H}$  NMR (400.1 MHz,  $\text{CDCl}_3$ )  $\delta$  1.23 (t, 6H,  $^3J = 7.1$  Hz,  $\text{CH}_3$ ); 3.05 (d, 2H,  $^2J_{\text{H,P}} = 21.2$  Hz,  $\text{CH}_2\text{P}$ ); 3.74 (s, 8H,  $\text{OCH}_2$ ); 3.87-3.89 (m, 4H,  $\text{OCH}_2$ ); 3.99 (q, 4H,  $^3J = 7.0$  Hz,  $\text{POCH}_2$ ); 4.08-4.13 (m, 4H,  $\text{OCH}_2$ ); 6.78-6.83 (m, 3H, ArH 1, 3, 4).

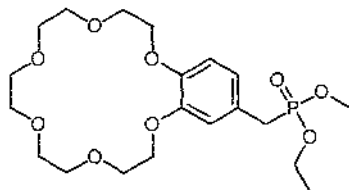
$^{13}\text{C}$  NMR (100.6 MHz,  $\text{CDCl}_3$ )  $\delta$  16.3  $\text{CH}_3$ ; 33.0  $^1J_{\text{C,P}} = 138.8$  Hz,  $\text{CH}_2\text{P}$ ; 62.1  $\text{POCH}_2$ ; 68.7  $\text{OCH}_2$ ; 68.9  $\text{OCH}_2$ ; 69.4  $\text{OCH}_2$ ; 69.5  $\text{OCH}_2$ ; 70.3  $\text{OCH}_2$ ; 70.3  $\text{OCH}_2$ ; 70.9  $\text{OCH}_2$ ; 113.9 ArC; 115.4 ArC; 122.4 ArC; 124.2 ArC; 148.0 ArCO; 148.9 ArCO.

$^{31}\text{P}$  NMR (162.0 MHz,  $\text{CDCl}_3$ )  $\delta$  28.0.

Electronic spectrum (MeCN)  $\lambda_{\text{max}}$  nm/(log  $\epsilon$ ) 203.0 (4.59), 231.5 (3.88), 282.0 (3.44).

HRMS (FAB)  $\text{MH}^+$  calc 419.1835, found 419.1842.

**(6,7,9,10,12,13,15,16,18,19-Decahydro-5,8,11,14,17,20-hexaoxabenzocyclooctadecen-2-ylmethyl)-phosphonic acid diethyl ester  
(XIV)**



2-Chloromethyl-6,7,9,10,12,13,15,16,18,19-decahydro-5,8,11,14,17,20-hexaoxabenzocyclooctadecene (5.0458 g, 14.0 mmol) was heated to reflux with triethyl phosphite (80 mL, as the solvent) and allowed to reflux for 23 hours under Ar. The reaction mixture was cooled to room temperature before the majority of the triethyl phosphite was removed under vacuum (0.01 mm Hg) at room temperature, then with heating up to 100°C. This yielded the impure (6,7,9,10,12,13,15,16,18,19-decahydro-5,8,11,14,17,20-hexaoxabenzocyclooctadecen-2-ylmethyl)-phosphonic acid diethyl ester as a pale oil (5.8276 g, 90%).

$^1\text{H}$  NMR (400.1 MHz,  $\text{CDCl}_3$ )  $\delta$  1.22 (t, 6H,  $^3J = 7.1$  Hz,  $\text{CH}_3$ ); 3.05 (d, 2H,  $^2J_{\text{H,P}} = 21.2$  Hz,  $\text{CH}_2\text{P}$ ); 3.66 (s, 4H,  $\text{OCH}_2$ ); 3.69-3.71 (m, 4H,  $\text{OCH}_2$ ); 3.74-3.75 (m, 4H,  $\text{OCH}_2$ ); 3.88-3.91 (m, 4H,  $\text{OCH}_2$ ); 3.96-3.99 (m, 4H,  $\text{POCH}_2$ ); 4.10-4.13 (m, 4H,  $\text{OCH}_2$ ); 6.79-6.84 (m, 3H, ArH), 3, 4).

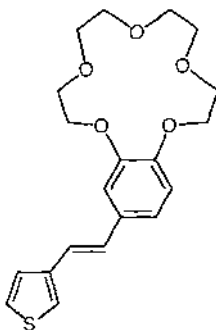
$^{13}\text{C}$  NMR (100.6 MHz,  $\text{CDCl}_3$ )  $\delta$  16.3  $\text{CH}_3$ ; 32.6  $^1J_{\text{C,P}} = 138.8$  Hz,  $\text{CH}_2\text{P}$ ; 62.0  $\text{POCH}_2$ ; 69.0  $\text{OCH}_2$ ; 69.1  $\text{OCH}_2$ ; 69.5  $\text{OCH}_2$ ; 69.6  $\text{OCH}_2$ ; 70.6  $\text{OCH}_2$ ; 70.7  $\text{OCH}_2$ ; 70.7  $\text{OCH}_2$ ; 70.8  $\text{OCH}_2$ ; 114.1 ArC; 115.6 ArC; 122.4 ArC; 124.3 ArC; 147.9 ArCO; 148.8 ArCO.

$^{31}\text{P}$  NMR (162.0 MHz,  $\text{CDCl}_3$ )  $\delta$  27.8.

Electronic spectrum (MeCN)  $\lambda_{\text{max}}$  nm/(log  $\epsilon$ ) 203.5 (4.57), 233.0 (3.91), 281.0 (3.56).

HRMS (FAB)  $\text{M}^+$  calc 462.2019, found 462.2025.

**2-(2'-Thiophen-3''-yl-vinyl)-6,7,9,10,12,13,15,16-octahydro-5,8,11,14,17-pentaoxa-benzocyclopentadecene (XV)**



(6,7,9,10,12,13,15,16-Octahydro-5,8,11,14,17-pentaoxa-benzocyclopenta-decen-2-ylmethyl)-phosphonic acid diethyl ester (2.0055 g, max 96.6% pure, 4.63 mmol) and thiophene-3-carbaldehyde (0.6019 g, 5.37 mmol) were stirred in dry THF (35 mL) before potassium tert-butoxide (1.0822 g, 9.64 mmol) was added and the solution left to stir at room temperature under N<sub>2</sub> for 3 hours. The reaction mixture was neutralized with 2M HCl and the solvent removed under reduced pressure. The product was dissolved in CH<sub>2</sub>Cl<sub>2</sub> (40 mL) and H<sub>2</sub>O (40 mL), the organic layer separated and the aqueous washed with CH<sub>2</sub>Cl<sub>2</sub> (20 mL). The combined organic layers were washed with H<sub>2</sub>O (20 mL), dried with activated neutral Al<sub>2</sub>O<sub>3</sub>, filtered and dried under vacuum to give a creamy coloured solid. Recrystallisation from CH<sub>2</sub>Cl<sub>2</sub>/hexane afforded an off-white solid, melting point = 139-142°C (0.7162 g, 41%).

<sup>1</sup>H NMR (400 MHz, CDCl<sub>3</sub>) δ 3.77 (s, 8H, OCH<sub>2</sub>9, 10, 12, 13); 3.91-3.95 (m, 4H, OCH<sub>2</sub>7, 15); 4.14-4.16 (m, 2H, OCH<sub>2</sub>6); 4.18-4.20 (m, 2H, OCH<sub>2</sub>16); 6.83 (d, 1H, <sup>3</sup>J = 8.2 Hz, ArH4); 6.87 (d, 1H, <sup>3</sup>J = 16.3 Hz, H<sub>vinyl</sub>1'); 6.98 (d, 1H, <sup>3</sup>J = 16.2 Hz, H<sub>vinyl</sub>2'); 7.00 (dd, 1H, <sup>3</sup>J = 8.2 Hz, <sup>4</sup>J = 2.0 Hz, ArH3); 7.02 (d, 1H, <sup>4</sup>J = 1.9 Hz, ArH1); 7.21-7.22 (m, 1H, ThH4''); 7.30-7.33 (m, 2H, ThH2'', 5'').

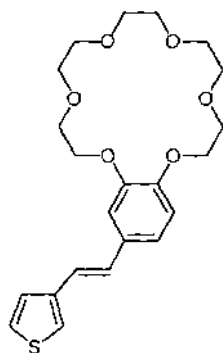
<sup>13</sup>C NMR (100.6 MHz, CDCl<sub>3</sub>) δ 68.8 OCH<sub>2</sub>; 69.0 OCH<sub>2</sub>; 69.4 OCH<sub>2</sub>; 69.5 OCH<sub>2</sub>; 70.3 OCH<sub>2</sub>; 70.4 OCH<sub>2</sub>; 70.9 OCH<sub>2</sub>; 71.0 OCH<sub>2</sub>; 111.3 ArC1; 113.8 ArC4; 120.1 ArC3; 121.2 C<sub>vinyl</sub>2'; 121.6 ThC4''; 124.8 ThC2''; 126.1 ThC5''; 128.3 C<sub>vinyl</sub>1'; 130.8 ArC2; 140.1 ThC3''; 148.8 ArCO; 149.1 ArCO.

Electronic spectrum (MeCN)  $\lambda_{\text{max}}$  nm/(log  $\epsilon$ ) 216.0 (4.27), 298.5 (4.39), 318.0 (4.41).

HRMS (FAB)  $M^+$  calc 376.1344, found 376.1340.

Anal. Calculated for  $C_{20}H_{24}O_5S$ : C, 63.81; H, 6.43; S, 8.52. Found: C, 62.72; H, 6.78; S, 7.99.

**2-(2'-Thiophen-3''-yl-vinyl)-6,7,9,10,12,13,15,16,18,19-decahydro-5,8,11,14,17,20-hexaoxa-benzocyclooctadecene (XVI)**



Thiophen-3-ylmethyl-phosphonic acid diethyl ester (0.2063 g, 0.88 mmol) and formylbenzo-18-crown-6 (0.3066 g, 0.90 mmol) were dissolved in dry  $CH_2Cl_2$  (5 mL) before potassium tert-butoxide (0.1980 g, 1.76 mmol) was added and the solution left to stir at room temperature under  $N_2$  for 1 hour.  $H_2O$  (10 mL) was added and neutralized with 2M HCl.  $CH_2Cl_2$  (10 mL) was added and the organic layer separated. The aqueous layer was washed with  $CH_2Cl_2$  (10 mL) before the combined organic layers were washed with  $H_2O$  (20 mL) and the solvent removed under reduced pressure. The yellow residue was dissolved in  $CH_2Cl_2$  and purified by column chromatography on silica. A cream-coloured fraction eluted in 2:98 MeOH: $CH_2Cl_2$  was washed with distilled  $H_2O$ , then dried to yield an off-white solid, melting point = 80-83°C (0.2300 g, 62%).

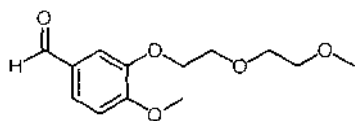
$^1\text{H}$  NMR (400 MHz,  $\text{CD}_2\text{Cl}_2$ )  $\delta$  3.62 (s, 4H,  $\text{OCH}_2$ 12, 13); 3.63-3.66 (m, 4H,  $\text{OCH}_2$ 10, 15); 3.68-3.71 (m, 4H,  $\text{OCH}_2$ 9, 16); 3.83-3.88 (m, 4H,  $\text{OCH}_2$ 7, 18); 4.12-4.14 (m, 2H,  $\text{OCH}_2$ 6); 4.16-4.19 (m, 2H,  $\text{OCH}_2$ 19); 6.83 (d, 1H,  $^3J = 8.2$  Hz, ArH4); 6.89 (d, 1H,  $^3J = 16.3$  Hz,  $\text{H}_{\text{vinyl}1'}$ ); 6.99-7.01 (m, 1H, ArH3); 7.01 (d, 1H,  $^3J = 16.0$  Hz,  $\text{H}_{\text{vinyl}2'}$ ); 7.03 (d, 1H,  $^4J = 2.0$  Hz, ArH1); 7.24-7.25 (m, 1H, ThH 4''); 7.32-7.35 (m, 2H, ThH 2'', 5'').

$^{13}\text{C}$  NMR (100.6 MHz,  $\text{CD}_2\text{Cl}_2$ )  $\delta$  68.0  $\text{OCH}_2$ ; 68.0  $\text{OCH}_2$ ; 68.9  $\text{OCH}_2$ ; 68.9  $\text{OCH}_2$ ; 69.9  $\text{OCH}_2$ ; 69.9  $\text{OCH}_2$ ; 70.0  $\text{OCH}_2$ ; 70.1  $\text{OCH}_2$ ; 109.8 ArC1; 112.4 ArC4; 119.3 ArC3; 120.5  $\text{C}_{\text{vinyl}2'}$ ; 121.3 ThC4''; 124.4 ThC2''; 125.8 ThC5''; 128.0  $\text{C}_{\text{vinyl}1'}$ ; 130.1 ArC2; 140.0 ThC3''; 148.2 ArCO; 148.4 ArCO.

Electronic spectrum (MeCN)  $\lambda_{\text{max}}$  nm/(log  $\epsilon$ ) 217.5 (4.21), 298.5 (4.31), 318.5 (4.34).

HRMS (FAB)  $M^+$  calc 420.1607, found 420.1612.

#### 4-Methoxy-3-[2'-(2''- methoxy-ethoxy)-ethoxy]-benzaldehyde (XVII)



Toluene-4-sulfonic acid 2-(2-methoxy-ethoxy)-ethyl ester (9.0356 g, 32.9 mmol), isovanillin (4.9993 g, 32.9 mmol) and anhydrous potassium carbonate (4.5445 g, 32.9 mmol) were heated to 110°C in dry DMF (40 mL) under  $\text{N}_2$  for 92 hours. The mixture was cooled and the solids filtered off and washed with  $\text{CH}_2\text{Cl}_2$ . The solvent was removed under reduced pressure before the residue was redissolved in  $\text{H}_2\text{O}$  (200 mL) and  $\text{CH}_2\text{Cl}_2$  (100 mL). The organic layer was separated, washed with  $\text{H}_2\text{O}$  (100 mL), dried over  $\text{MgSO}_4$ , filtered and evaporated. The crude product was purified by column chromatography on silica and eluted with  $\text{CH}_2\text{Cl}_2$  to yield a pale orange oil (5.9955 g, 72%).

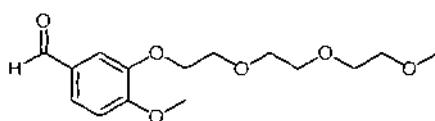
$^1\text{H}$  NMR (400 MHz,  $\text{CDCl}_3$ )  $\delta$  3.36 (s, 3H,  $2''\text{OCH}_3$ ); 3.54-3.57 (m, 2H,  $\text{OCH}_22''$ ); 3.70-3.72 (m, 2H,  $\text{OCH}_21''$ ); 3.89-3.91 (m, 2H,  $\text{OCH}_22'$ ); 3.92 (s, 3H,  $\text{ArOCH}_3$ ); 4.22-4.25 (m, 2H,  $\text{OCH}_21'$ ); 6.95 (d, 1H,  $^3J = 8.2$  Hz,  $\text{ArH5}$ ); 7.42 (d, 1H,  $^4J = 1.9$  Hz,  $\text{ArH2}$ ); 7.45 (dd, 1H,  $^3J = 8.2$  Hz,  $^4J = 1.9$  Hz,  $\text{ArH6}$ ); 9.81 (s, 1H, CHO).

$^{13}\text{C}$  NMR (100.6 MHz,  $\text{CDCl}_3$ )  $\delta$  56.0  $\text{ArOCH}_3$ ; 58.9  $2''\text{OCH}_3$ ; 68.3  $\text{OCH}_21'$ ; 69.4  $\text{OCH}_22'$ ; 70.7  $\text{OCH}_21''$ ; 71.8  $\text{OCH}_22''$ ; 110.6  $\text{ArC5}$ ; 111.0  $\text{Ar2}$ ; 126.7  $\text{ArC6}$ ; 129.9  $\text{ArC1}$ ; 148.8  $\text{ArC3}$ ; 154.8  $\text{ArC4}$ ; 190.7 CHO.

Electronic spectrum (MeCN)  $\lambda_{\text{max}}$  nm/(log  $\epsilon$ ) 204.0 (4.09), 229.5 (4.23), 273.5 (4.03), 306.0 (3.91).

HRMS (FAB)  $M^+$  calc 254.1154, found 254.1143.

**4-Methoxy-3-[2'-(2''-{2'''-methoxy-ethoxy}-ethoxy)-ethoxy]-benzaldehyde  
(XVIII)**



Toluene-4-sulfonic acid 2-(2-[2-methoxy-ethoxy]-ethoxy)-ethyl ester (10.4922 g, 33.0 mmol), isovanillin (4.9982 g, 32.9 mmol) and anhydrous potassium carbonate (4.5469 g, 32.9 mmol) were heated to  $110^\circ\text{C}$  in dry DMF (40 mL) under  $\text{N}_2$  for 77 hours. The mixture was cooled and the solids filtered off and washed with  $\text{CH}_2\text{Cl}_2$ . The solvent was removed under reduced pressure before the residue was redissolved in  $\text{H}_2\text{O}$  (100 mL) and  $\text{CH}_2\text{Cl}_2$  (100 mL). The organic layer was separated and the aqueous layer extracted with  $\text{CH}_2\text{Cl}_2$  (2 x 50 mL). The combined organic extracts were then washed with  $\text{H}_2\text{O}$  (50 mL), dried over  $\text{MgSO}_4$ , filtered and evaporated. The



aqueous washed with  $\text{CH}_2\text{Cl}_2$  (2 x 50 mL), then the combined organic extracts were washed with  $\text{H}_2\text{O}$  (50 mL), dried over  $\text{MgSO}_4$ , filtered and the solvent evaporated. The crude product was purified by column chromatography on silica and eluted with  $\text{CH}_2\text{Cl}_2$  to yield a yellow oil (5.4996 g, 49%).

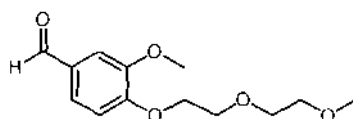
$^1\text{H}$  NMR (400 MHz,  $\text{CDCl}_3$ )  $\delta$  3.36 (s, 3H,  $2''''\text{OCH}_3$ ); 3.52-3.54 (m, 2H,  $\text{OCH}_22''''$ ); 3.62-3.63 (m, 2H,  $\text{OCH}_21''''$ ); 3.64-3.66 (m, 4H,  $\text{OCH}_21''''$ ,  $2''''$ ); 3.66-3.68 (m, 2H,  $\text{OCH}_22''$ ); 3.71-3.74 (m, 2H,  $\text{OCH}_21''$ ); 3.89-3.92 (m, 2H,  $\text{OCH}_22'$ ); 3.93 (s, 3H,  $\text{ArOCH}_3$ ); 4.22-4.24 (m, 2H,  $\text{OCH}_21'$ ); 6.96 (d, 1H,  $^3J = 8.2$  Hz,  $\text{ArH5}$ ); 7.42 (d, 1H,  $^4J = 1.8$  Hz,  $\text{ArH2}$ ); 7.46 (dd, 2H,  $^3J = 8.2$  Hz,  $^4J = 1.9$  Hz,  $\text{ArH6}$ ); 9.83 (s, 1H, CHO).

$^{13}\text{C}$  NMR (100.6 MHz,  $\text{CDCl}_3$ )  $\delta$  56.0  $\text{ArOCH}_3$ ; 58.9  $2''''\text{OCH}_3$ ; 68.3  $\text{OCH}_21'$ ; 69.4  $\text{OCH}_22'$ ; 70.4  $\text{OCH}_21''''$ ; 70.5  $\text{OCH}_22''$ ; 70.5  $\text{OCH}_22''''$ ; 70.5  $\text{OCH}_21''$ ; 70.8  $\text{OCH}_21''$ ; 71.8  $\text{OCH}_22''''$ ; 110.7  $\text{ArC5}$ ; 110.9  $\text{Ar2}$ ; 126.8  $\text{ArC6}$ ; 129.9  $\text{ArC1}$ ; 148.8  $\text{ArC3}$ ; 154.8  $\text{ArC4}$ ; 190.8 CHO.

Electronic spectrum (MeCN)  $\lambda_{\text{max}}$  nm/(log  $\epsilon$ ) 203.5 (4.20), 229.5 (4.34), 273.5 (4.14), 306.0 (4.02).

HRMS (FAB)  $\text{MH}^+$  calc 343.1757, found 343.1761.

### 3-Methoxy-4-[2'-(2''-methoxy-ethoxy)-ethoxy]-benzaldehyde (XX)



Toluene-4-sulfonic acid 2-(2-methoxy-ethoxy)-ethyl ester (9.0209 g, 32.9 mmol), vanillin (5.0031 g, 32.9 mmol) and anhydrous potassium carbonate (4.5571 g, 33.0 mmol) were heated to  $110^\circ\text{C}$  in dry DMF (40 mL) under  $\text{N}_2$  for 69 hours. The mixture was cooled and the solids filtered off and washed with  $\text{CH}_2\text{Cl}_2$ . The solvent

was removed under reduced pressure before the residue was redissolved in H<sub>2</sub>O (100 mL) and CH<sub>2</sub>Cl<sub>2</sub> (100 mL). The organic layer was separated, and the aqueous layer extracted with CH<sub>2</sub>Cl<sub>2</sub> (2 x 50 mL). The combined organic layers were washed with H<sub>2</sub>O (50 mL), dried over MgSO<sub>4</sub>, filtered and evaporated. The crude product was purified by column chromatography on silica and eluted with CH<sub>2</sub>Cl<sub>2</sub> to yield a pale oil (6.9615 g, 83%).

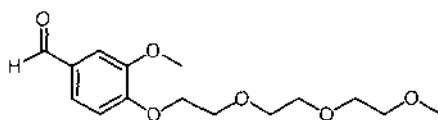
<sup>1</sup>H NMR (400.1 MHz, CDCl<sub>3</sub>) δ 3.36 (s, 3H, 2''OCH<sub>3</sub>); 3.54-3.56 (m, 2H, OCH<sub>2</sub>2''); 3.70-3.72 (m, 2H, OCH<sub>2</sub>1''); 3.89 (s, 3H, ArOCH<sub>3</sub>); 3.90-3.93 (m, 2H, OCH<sub>2</sub>2'); 4.25-4.27 (m, 2H, OCH<sub>2</sub>1'); 6.99 (d, 1H, <sup>3</sup>J = 8.2 Hz, ArH5); 7.38 (d, 1H, <sup>4</sup>J = 1.9 Hz, ArH2); 7.41 (dd, 1H, <sup>3</sup>J = 8.2 Hz, <sup>4</sup>J = 1.9 Hz, ArH6); 9.83 (s, 1H, CHO).

<sup>13</sup>C NMR (100.6 MHz, CDCl<sub>3</sub>) δ 55.9 ArOCH<sub>3</sub>; 59.0 2''OCH<sub>3</sub>; 68.4 OCH<sub>2</sub>1'; 69.3 OCH<sub>2</sub>2'; 70.8 OCH<sub>2</sub>1''; 71.8 OCH<sub>2</sub>2''; 109.2 ArC2; 111.8 ArC5; 126.6 ArC6; 130.2 ArC1; 149.8 ArC3; 153.8 ArC4; 190.8 CHO.

Electronic spectrum (MeCN) λ<sub>max</sub> nm/(log ε) 203.0 (4.08), 229.5 (4.17), 274.0 (4.01), 307.0 (3.92).

HRMS (FAB) M<sup>+</sup> calc 254.1154, found 254.1152.

### 3-Methoxy-4-[2'-(2''-{2'''-methoxy-ethoxy}-ethoxy)-ethoxy]-benzaldehyde (XXI)



Toluene-4-sulfonic acid 2-(2-[2-methoxy-ethoxy]-ethoxy)-ethyl ester (10.5100 g, 33.0 mmol), vanillin (5.0131 g, 32.9 mmol) and anhydrous potassium carbonate (4.5507 g, 32.9 mmol) were heated to 110°C in dry DMF (40 mL) under N<sub>2</sub> for

77 hours. The mixture was cooled and the solids filtered off and washed with CH<sub>2</sub>Cl<sub>2</sub>. The solvent was removed under reduced pressure before the residue was redissolved in H<sub>2</sub>O (100 mL) and CH<sub>2</sub>Cl<sub>2</sub> (100 mL). The organic layer was separated and the aqueous layer extracted with CH<sub>2</sub>Cl<sub>2</sub> (2 x 50 mL). The combined organic extracts were washed with H<sub>2</sub>O (50 mL), dried over MgSO<sub>4</sub>, filtered and evaporated. The crude product was purified by column chromatography on silica and eluted with CH<sub>2</sub>Cl<sub>2</sub> to yield a pale oil (5.4275 g, 55%).

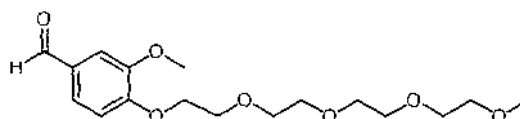
<sup>1</sup>H NMR (400 MHz, CDCl<sub>3</sub>) δ 3.36 (s, 3H, 2'''OCH<sub>3</sub>); 3.51-3.54 (m, 2H, OCH<sub>2</sub>2'''); 3.62-3.64 (m, 2H, OCH<sub>2</sub>1'''); 3.64-3.67 (m, 2H, OCH<sub>2</sub>2''); 3.72-3.75 (m, 2H, OCH<sub>2</sub>1''); 3.90 (s, 3H, ArOCH<sub>3</sub>); 3.90-3.93 (m, 2H, OCH<sub>2</sub>2'); 4.25-4.27 (m, 2H, OCH<sub>2</sub>1'); 7.00 (d, 1H, <sup>3</sup>J = 8.2 Hz, ArH5); 7.39 (d, 1H, <sup>4</sup>J = 1.9 Hz, ArH2); 7.42 (dd, 1H, <sup>3</sup>J = 8.2 Hz, <sup>4</sup>J = 1.9 Hz, ArH6); 9.83 (s, 1H, CHO).

<sup>13</sup>C NMR (100.6 MHz, CDCl<sub>3</sub>) δ 55.9 ArOCH<sub>3</sub>; 58.9 2'''OCH<sub>3</sub>; 68.4 OCH<sub>2</sub>1'; 69.3 OCH<sub>2</sub>2'; 70.5 OCH<sub>2</sub>1'''; 70.5 OCH<sub>2</sub>2''; 70.8 OCH<sub>2</sub>1''; 71.8 OCH<sub>2</sub>2'''; 109.2 ArC2; 111.8 ArC5; 126.6 ArC6; 130.1 ArC1; 149.8 ArC3; 153.8 ArC4; 190.9 CHO.

Electronic spectrum (MeCN) λ<sub>max</sub> nm/(log ε) 203.0 (4.13), 229.5 (4.22), 274.0 (4.06), 307.0 (3.97).

HRMS (FAB) M<sup>+</sup> calc 298.1416, found 298.1415.

**3-Methoxy-4-[2'-(2''-{2'''-methoxy-ethoxy}-ethoxy)-ethoxy]-ethoxy)-benzaldehyde (XXII)**



Toluene-4-sulfonic acid 2-(2-[2-methoxy-ethoxy]-ethyl)-ethyl ester (11.9267 g, 32.9 mmol), vanillin (5.0086 g, 32.9 mmol) and anhydrous potassium carbonate (4.5545 g, 33.0 mmol) were heated to 110°C in dry DMF (40 mL) under N<sub>2</sub> for 96 hours. The mixture was cooled and the solids filtered off and washed with CH<sub>2</sub>Cl<sub>2</sub>. The solvent was removed under reduced pressure before the residue was redissolved in H<sub>2</sub>O (100 mL) and CH<sub>2</sub>Cl<sub>2</sub> (100 mL). The organic layer was separated, and the aqueous washed with CH<sub>2</sub>Cl<sub>2</sub> (2 x 50 mL) before the combined organic extracts were washed with H<sub>2</sub>O (80 mL), dried over MgSO<sub>4</sub>, filtered and evaporated. The crude product was purified by column chromatography on silica and eluted with CH<sub>2</sub>Cl<sub>2</sub> to yield a yellow oil (6.070 g, 54%).

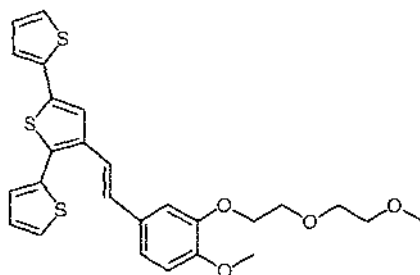
<sup>1</sup>H NMR (400 MHz, CDCl<sub>3</sub>) δ 3.36 (s, 3H, 2''''OCH<sub>3</sub>); 3.51-3.54 (m, 2H, OCH<sub>2</sub>2'''''); 3.61-3.63 (m, 2H, OCH<sub>2</sub>1'''''); 3.64-3.65 (m, 4H, OCH<sub>2</sub>1''', 2'''); 3.66-3.67 (m, 2H, OCH<sub>2</sub>2''); 3.71-3.74 (m, 2H, OCH<sub>2</sub>1''); 3.90 (s, 3H, ArOCH<sub>3</sub>); 3.90-3.93 (m, 2H, OCH<sub>2</sub>2'); 4.25-4.27 (m, 2H, OCH<sub>2</sub>1'); 7.00 (d, 1H, <sup>3</sup>J = 8.2 Hz, ArH5); 7.39 (d, 1H, <sup>4</sup>J = 1.9 Hz, ArH2); 7.42 (dd, 1H, <sup>3</sup>J = 8.1 Hz, <sup>4</sup>J = 1.9 Hz, ArH6); 9.83 (s, 1H, CHO).

<sup>13</sup>C NMR (100.6 MHz, CDCl<sub>3</sub>) δ 55.9 ArOCH<sub>3</sub>; 58.9 2''''OCH<sub>3</sub>; 68.4 OCH<sub>2</sub>1'; 69.3 OCH<sub>2</sub>2'; 70.4 OCH<sub>2</sub>1'''''; 70.5 OCH<sub>2</sub>2''; 70.5 OCH<sub>2</sub>2'''; 70.5 OCH<sub>2</sub>1'''; 70.8 OCH<sub>2</sub>1''; 71.8 OCH<sub>2</sub>2''''; 109.2 ArC2; 111.8 ArC5; 126.6 ArC6; 130.2 ArC1; 149.8 ArC3; 153.8 ArC4; 190.9 CHO.

Electronic spectrum (MeCN) λ<sub>max</sub> nm/(log ε) 203.0 (4.16), 229.5 (4.26), 274.0 (4.10), 307.0 (4.01).

HRMS (FAB) MH<sup>+</sup> calc 343.1757, found 343.1750.

**3'-(2''-{4'''-Methoxy-3''''-[2''''''-(2''''''-methoxy-ethoxy)-ethoxy]-phenyl}-vinyl)-[2,2';5',2'']terthiophene (XXIII)**



4-Methoxy-3-[2''-(2''-methoxy-ethoxy)-ethoxy]-benzaldehyde (0.3583 g, 1.41 mmol) and terthiophene phosphonate (10 mL x 0.140 mmol/mL solution in THF, 1.40 mmol) were stirred under N<sub>2</sub> in dry CH<sub>2</sub>Cl<sub>2</sub> (10 mL) before KO<sup>t</sup>Bu (0.3970 g, 3.54 mmol) was added and the solution left to stir at room temperature for 1 hour. H<sub>2</sub>O (20 mL) was added and neutralized with aqueous HCl. H<sub>2</sub>O (20 mL) and CH<sub>2</sub>Cl<sub>2</sub> (20 mL) were added, and the organic layer separated. The aqueous layer was extracted with CH<sub>2</sub>Cl<sub>2</sub> (20 mL), then the combined organic layers washed with H<sub>2</sub>O (20 mL) and the solvent removed under reduced pressure. The residue was dissolved in CH<sub>2</sub>Cl<sub>2</sub> and purified using flash column chromatography on silica. After 1,2-bis([2',2'';5'',2''']terthiophen-3''-yl)ethene (20.1 mg, 3%) was eluted in CH<sub>2</sub>Cl<sub>2</sub>, the desired product was eluted in 2% MeOH. Removal of the solvent under reduced pressure yielded 3'-(2''-{4'''-methoxy-3''''-[2''''''-(2''''''-methoxy-ethoxy)-ethoxy]-phenyl}-vinyl)-[2,2';5',2'']terthiophene as a dark yellow oil (0.6144 g, 88%).

<sup>1</sup>H NMR (400.1 MHz, CD<sub>2</sub>Cl<sub>2</sub>) δ 3.35 (s, 3H, 2''''''OCH<sub>3</sub>); 3.52-3.55 (m, 2H, OCH<sub>2</sub>2'''''''); 3.66-3.68 (m, 2H, OCH<sub>2</sub>1'''''''); 3.82-3.84 (m, 2H, OCH<sub>2</sub>2'''''''); 3.86 (s, 3H, ArOCH<sub>3</sub>); 4.14-4.16 (m, 2H, OCH<sub>2</sub>1'''''''); 6.88 (d, 1H, <sup>3</sup>J = 8.2 Hz, ArH5'''''); 7.00 (d, 1H, <sup>3</sup>J = 16.1 Hz, H<sub>vinyl</sub>2'''''); 7.05 (dd, 1H, <sup>3</sup>J = 5.1 Hz, <sup>4</sup>J = 3.6 Hz, ThH4''); 7.05-7.09 (m, 2H, ArH2''''', 6'''''); 7.13 (dd, 1H, <sup>3</sup>J = 5.2 Hz, <sup>4</sup>J = 3.6 Hz, ThH4); 7.22 (dd, 1H, <sup>3</sup>J = 3.6 Hz, <sup>4</sup>J = 1.2 Hz, ThH3); 7.23 (d, 1H, <sup>3</sup>J = 16.2 Hz, H<sub>vinyl</sub>1'''''); 7.24 (dd, 1H, <sup>3</sup>J = 3.6 Hz, <sup>4</sup>J = 1.2 Hz, ThH3''); 7.29 (dd, 1H, <sup>3</sup>J = 5.1 Hz, <sup>4</sup>J = 1.2 Hz, ThH5''); 7.41 (dd, 1H, <sup>3</sup>J = 5.1 Hz, <sup>4</sup>J = 1.2 Hz, ThH5); 7.44 (s, 1H, ThH4').



2% MeOH. Removal of the solvent under reduced pressure yielded 3'-(2''-{4'''-methoxy-3'''-[2''''-(2'''''-{2''''''-methoxy-ethoxy}-ethoxy)-ethoxy]-phenyl}-vinyl)-[2,2';5',2'']terthiophene as a dark yellow oil (0.6477 g, 88%).

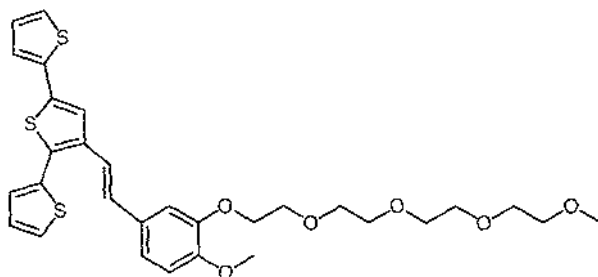
<sup>1</sup>H NMR (400.1 MHz, CD<sub>2</sub>Cl<sub>2</sub>) δ 3.33 (s, 3H, 2''''''OCH<sub>3</sub>); 3.49-3.51 (m, 2H, OCH<sub>2</sub>2'''''''); 3.58-3.60 (m, 2H, OCH<sub>2</sub>1'''''''); 3.61-3.64 (m, 2H, OCH<sub>2</sub>2'''''''); 3.67-3.70 (m, 2H, OCH<sub>2</sub>1'''''''); 3.83-3.85 (m, 2H, OCH<sub>2</sub>2'''''''); 3.86 (s, 3H, ArOCH<sub>3</sub>); 4.15-4.17 (m, 2H, OCH<sub>2</sub>1'''''''); 6.88 (d, 1H, <sup>3</sup>J = 8.2 Hz, ArH5'''''); 7.01 (d, 1H, <sup>3</sup>J = 16.1 Hz, H<sub>vinyl</sub>2'''''); 7.05 (dd, 1H, <sup>4</sup>J = 2.0 Hz, ArH2'''''); 7.06 (dd, 1H, <sup>3</sup>J = 5.1 Hz, <sup>4</sup>J = 3.6 Hz, ThH4''); 7.08 (dd, 1H, <sup>3</sup>J = 8.2 Hz, <sup>4</sup>J = 2.0 Hz, ArH6'''''); 7.14 (dd, 1H, <sup>3</sup>J = 5.1 Hz, <sup>4</sup>J = 3.6 Hz, ThH4); 7.22 (dd, 1H, <sup>3</sup>J = 3.6 Hz, <sup>4</sup>J = 1.2 Hz, ThH3); 7.23 (d, 1H, <sup>3</sup>J = 16.2 Hz, H<sub>vinyl</sub>1'''''); 7.24 (dd, 1H, <sup>3</sup>J = 3.6 Hz, <sup>4</sup>J = 1.2 Hz, ThH3''); 7.29 (dd, 1H, <sup>3</sup>J = 5.2 Hz, <sup>4</sup>J = 1.1 Hz, ThH5''); 7.42 (dd, 1H, <sup>3</sup>J = 5.2 Hz, <sup>4</sup>J = 1.2 Hz, ThH5); 7.45 (s, 1H, ThH4').

<sup>13</sup>C NMR (100.6 MHz, CD<sub>2</sub>Cl<sub>2</sub>) δ 55.5 ArOCH<sub>3</sub>; 58.3 2''''''OCH<sub>3</sub>; 68.0 OCH<sub>2</sub>1'''''''; 69.3 OCH<sub>2</sub>2'''''''; 70.1 OCH<sub>2</sub>1'''''''; 70.1 OCH<sub>2</sub>2'''''''; 70.4 OCH<sub>2</sub>1'''''''; 71.5 OCH<sub>2</sub>2'''''''; 110.8 ArC2'''''; 111.4 ArC5'''''; 119.2 C<sub>vinyl</sub>1'''''; 119.8 ArC6'''''; 121.9 ThC4'; 123.8 ThC3''; 124.6 ThC5''; 126.0 ThC5; 126.5 ThC3; 127.5 ThC4; 127.6 ThC4''; 129.9 ArC1'''''; 130.1 C<sub>vinyl</sub>2'''''; 130.4 ThC2'; 134.9 ThC2; 135.4 ThC5'; 136.2 ThC3'; 136.3 ThC2''; 148.1 ArC3'''''; 149.3 ArC4''''.

Electronic spectrum (MeCN) λ<sub>max</sub> nm/(log ε) 328.5 (4.60).

HRMS (FAB) M<sup>+</sup> calc 542.1255, found 542.1278.

**3'-(2''-{4'''-Methoxy-3'''-[2''''-(2'''''-{2''''''-methoxy-ethoxy}-ethoxy)-ethoxy]-phenyl}-vinyl)-[2,2';5',2'']terthiophene (XXV)**



4-Methoxy-3-[2'-(2''-{2''''-[2''''-methoxy-ethoxy]-ethoxy}-ethoxy)-ethoxy]-benzaldehyde (0.4624 g, 1.35 mmol) and terthiophene phosphonate (10 mL x 0.135 mmol/mL solution in dry THF, 1.35 mmol) were stirred under N<sub>2</sub> in dry CH<sub>2</sub>Cl<sub>2</sub> (10 mL) before KO<sup>t</sup>Bu (0.3909 g, 3.48 mmol) was added. The solution was left to stir at room temperature for 30 minutes before H<sub>2</sub>O (20 mL) was added and neutralized with aqueous HCl. CH<sub>2</sub>Cl<sub>2</sub> (20 mL) was added, and the organic layer separated. The aqueous layer was extracted with CH<sub>2</sub>Cl<sub>2</sub> (20 mL) before the combined organic layers were washed with H<sub>2</sub>O (20 mL) and the solvent removed under reduced pressure. The residue was dissolved in CH<sub>2</sub>Cl<sub>2</sub> and purified using flash column chromatography. After 1,2-bis([2',2';5'',2''']terthiophen-3''-yl)ethene (21.6 mg, 6%) was eluted in CH<sub>2</sub>Cl<sub>2</sub>, the desired product was eluted in 2% MeOH. Removal of the solvent under reduced pressure yielded 3'-(2''-{4'''-methoxy-3'''-[2''''-(2'''''-{2''''''-methoxy-ethoxy}-ethoxy)-ethoxy]-phenyl}-vinyl)-[2,2';5',2'']terthiophene as a dark yellow oil (0.7363 g, 93%).

<sup>1</sup>H NMR (400.1 MHz, CD<sub>2</sub>Cl<sub>2</sub>) δ 3.32 (s, 3H, 2''''''OCH<sub>3</sub>); 3.47-3.50 (m, 2H, OCH<sub>2</sub>2'''''''); 3.56-3.58 (m, 2H, OCH<sub>2</sub>1'''''''); 3.58-3.60 (m, 4H, OCH<sub>2</sub>1''''''', 2'''''''); 3.62-3.64 (m, 2H, OCH<sub>2</sub>2'''''''); 3.68-3.70 (m, 2H, OCH<sub>2</sub>1'''''''); 3.83-3.85 (m, 2H, OCH<sub>2</sub>2'''''''); 3.86 (s, 3H, ArOCH<sub>3</sub>); 4.15-4.17 (m, 2H, OCH<sub>2</sub>1'''''''); 6.87 (d, 1H, <sup>3</sup>J = 8.1 Hz, ArH5'''''); 7.00 (d, 1H, <sup>3</sup>J = 16.1 Hz, H<sub>vinyl</sub>2'''''); 7.05-7.08 (m, 2H, ArH2''''', 6'''''); 7.06 (dd, 1H, <sup>3</sup>J = 5.1 Hz, <sup>4</sup>J = 3.6 Hz, ThH4''); 7.13 (dd, 1H, <sup>3</sup>J = 5.2 Hz, <sup>4</sup>J = 3.6 Hz, ThH4); 7.22 (dd, 1H, <sup>3</sup>J = 3.6 Hz, <sup>4</sup>J = 1.2 Hz, ThH3); 7.23 (d, 1H, <sup>3</sup>J = 16.2 Hz, H<sub>vinyl</sub>1'''''); 7.24 (dd, 1H, <sup>3</sup>J = 3.6 Hz, <sup>4</sup>J = 1.2 Hz, ThH3''); 7.29 (dd, 1H, <sup>3</sup>J =

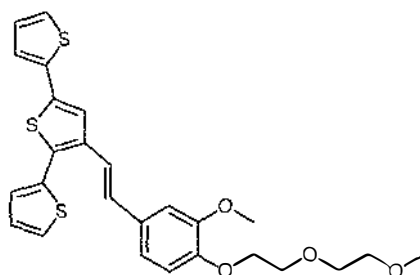
5.1 Hz,  $^4J = 1.2$  Hz, ThH5''); 7.41 (dd, 1H,  $^3J = 5.2$  Hz,  $^4J = 1.2$  Hz, ThH5); 7.44 (s, 1H, ThH4').

$^{13}\text{C}$  NMR (100.6 MHz,  $\text{CD}_2\text{Cl}_2$ )  $\delta$  55.5 ArOCH<sub>3</sub>; 58.2 2''''''''OCH<sub>3</sub>; 68.0 OCH<sub>2</sub>1''''''; 69.3 OCH<sub>2</sub>2''''''; 70.0 OCH<sub>2</sub>1''''''; 70.1 OCH<sub>2</sub>2''''''; 70.2 OCH<sub>2</sub>2''''''; 70.2 OCH<sub>2</sub>1''''''; 70.4 OCH<sub>2</sub>1''''''; 71.5 OCH<sub>2</sub>2''''''; 110.8 ArC2''''; 111.4 ArC5''''; 119.2 C<sub>vinyl</sub>1''''; 119.8 ArC6''''; 121.9 ThC4'; 123.8 ThC3''; 124.6 ThC5''; 126.0 ThC5; 126.5 ThC3; 127.5 ThC4; 127.6 ThC4''; 129.9 ArC1''''; 130.1 C<sub>vinyl</sub>2''''; 130.4 ThC2'; 134.9 ThC2; 135.4 ThC5'; 136.2 ThC3'; 136.3 ThC2''; 148.1 ArC3''''; 149.3 ArC4''''.

Electronic spectrum (MeCN)  $\lambda_{\text{max}}$  nm/(log  $\epsilon$ ) 328.5 (4.59).

HRMS (FAB) M<sup>+</sup> calc 586.1518, found 586.1529.

**3'-(2'''-{3''''-Methoxy-4''''-[2''''-(2''''''-methoxy-ethoxy)-ethoxy]-phenyl}-vinyl)-[2,2';5,2'']terthiophene (XXVI)**



3-Methoxy-4-[2-(2-methoxyethoxy)-ethoxy]-benzaldehyde (0.3593 g, 1.41 mmol) and terthiophene phosphonate (10 mL x 0.140 mmol/mL solution in THF, 1.40 mmol) were stirred under N<sub>2</sub> in dry CH<sub>2</sub>Cl<sub>2</sub> (10 mL) before KO<sup>t</sup>Bu (0.3997 g, 3.56 mmol) was added and the solution left to stir at room temperature for 30 minutes. H<sub>2</sub>O (20 mL) was added and neutralized with aqueous HCl. H<sub>2</sub>O (20 mL) and CH<sub>2</sub>Cl<sub>2</sub> (20 mL) were added, and the organic layer separated. The aqueous layer was extracted with CH<sub>2</sub>Cl<sub>2</sub> (2 x 15 mL), before the combined organic layers were washed

with H<sub>2</sub>O (15 mL), dried over MgSO<sub>4</sub>, filtered and evaporated. The residue was dissolved in CH<sub>2</sub>Cl<sub>2</sub>, and purified using flash column chromatography. After 1,2-bis([2',2'';5'',2''']terthiophen-3''-yl)ethene (32.7 mg, 9%) was eluted in CH<sub>2</sub>Cl<sub>2</sub>, the desired product was eluted in 2% MeOH. Removal of the solvent under reduced pressure yielded 3'-(2''-{3''-methoxy-4''-[2''''-(2''''-methoxy-ethoxy)-ethoxy]-phenyl}-vinyl)-[2,2';5',2'']terthiophene as a dark orange oil (0.6227 g, 89%).

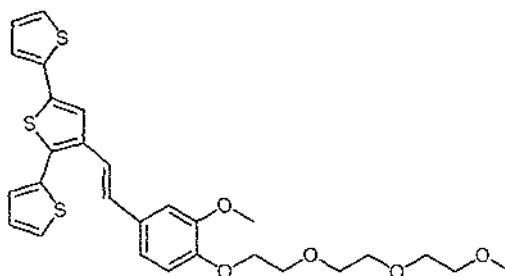
<sup>1</sup>H NMR (400.1 MHz, CD<sub>2</sub>Cl<sub>2</sub>) δ 3.35 (s, 3H, 2''''''OCH<sub>3</sub>); 3.53-3.55 (m, 2H, OCH<sub>2</sub>2'''''''); 3.65-3.68 (m, 2H, OCH<sub>2</sub>1'''''''); 3.81-3.83 (m, 2H, OCH<sub>2</sub>2'''''''); 3.88 (s, 3H, ArOCH<sub>3</sub>); 4.12-4.14 (m, 2H, OCH<sub>2</sub>1'''''''); 6.87 (d, 1H, <sup>3</sup>J = 8.9 Hz, ArH5'''''); 7.02 (d, 1H, <sup>3</sup>J = 16.5 Hz, H<sub>vinyl</sub>2'''''); 7.02-7.05 (m, 2H, ArH2''''', 6'''''); 7.06 (dd, 1H, <sup>3</sup>J = 5.2 Hz, <sup>4</sup>J = 3.6 Hz, ThH4''); 7.13 (dd, 1H, <sup>3</sup>J = 5.1 Hz, <sup>4</sup>J = 3.6 Hz, ThH4); 7.22 (dd, 1H, <sup>3</sup>J = 3.6 Hz, <sup>4</sup>J = 1.2 Hz, ThH3); 7.24 (dd, 1H, <sup>3</sup>J = 3.6 Hz, <sup>4</sup>J = 1.2 Hz, ThH3''); 7.25 (d, 1H, <sup>3</sup>J = 16.6 Hz, H<sub>vinyl</sub>1'''''); 7.29 (dd, 1H, <sup>3</sup>J = 5.1 Hz, <sup>4</sup>J = 1.2 Hz, ThH5''); 7.41 (dd, 1H, <sup>3</sup>J = 5.2 Hz, <sup>4</sup>J = 1.2 Hz, ThH5); 7.45 (s, 1H, ThH4').

<sup>13</sup>C NMR (100.6 MHz, CD<sub>2</sub>Cl<sub>2</sub>) δ 55.4 ArOCH<sub>3</sub>; 58.3 2''''''OCH<sub>3</sub>; 68.0 OCH<sub>2</sub>1'''''''; 69.2 OCH<sub>2</sub>2'''''''; 70.2 OCH<sub>2</sub>1'''''''; 71.5 OCH<sub>2</sub>2'''''''; 109.2 ArC2'''''; 112.8 ArC5'''''; 119.2 ArC6'''''; 119.3 C<sub>vinyl</sub>1'''''; 121.9 ThC4'; 123.8 ThC3''; 124.6 ThC5''; 126.0 ThC5; 126.5 ThC3; 127.5 ThC4; 127.6 ThC4''; 130.1 C<sub>vinyl</sub>2''''; 130.3 ArC1'''''; 130.4 ThC2'; 134.9 ThC2; 135.5 ThC5'; 136.2 ThC3'; 136.3 ThC2''; 148.0 ArC4''''; 149.3 ArC3''''.

Electronic spectrum (MeCN) λ<sub>max</sub> nm/(log ε) 329.0 (4.59).

HRMS (FAB) M<sup>+</sup> calc 498.0993, found 498.1019.

**3'-(2''-{3'''-Methoxy-4''''-[2'''''-(2''''''-{2''''''''-methoxy-ethoxy}-ethoxy)-ethoxy]-ethoxy]-phenyl)-vinyl)-[2,2';5',2'']terthiophene (XXVII)**



3-Methoxy-4-[2'-{(2''-{3'''-methoxy-ethoxy}-ethoxy)-ethoxy]-benzaldehyde (0.4054 g, 1.36 mmol) and terthiophene phosphonate (10 mL x 0.135 mmol/mL solution in dry THF, 1.35 mmol) were stirred under N<sub>2</sub> in dry CH<sub>2</sub>Cl<sub>2</sub> (10 mL) before KO<sup>t</sup>Bu (0.4096 g, 3.65 mmol) was added and the solution left to stir at room temperature for 30 minutes. H<sub>2</sub>O (20 mL) was added and neutralized with aqueous HCl. H<sub>2</sub>O (20 mL) and CH<sub>2</sub>Cl<sub>2</sub> (20 mL) were added, and the organic layer separated. The aqueous layer was extracted with CH<sub>2</sub>Cl<sub>2</sub> (20 mL), before the combined organic layers were washed with H<sub>2</sub>O (20 mL) and the solvent removed under reduced pressure. The resulting residue was dissolved in CH<sub>2</sub>Cl<sub>2</sub> and purified using flash column chromatography on silica. 1,2-bis([2',2'';5'',2''']terthiophen-3''-yl)ethene (31.1 mg, 9%) was eluted in CH<sub>2</sub>Cl<sub>2</sub>, the desired product was eluted in 2% MeOH. Removal of the solvent under reduced pressure yielded 3'-(2''-{3'''-methoxy-4''''-[2'''''-(2''''''-{2''''''''-methoxy-ethoxy}-ethoxy)-ethoxy]-ethoxy]-phenyl)-vinyl)-[2,2';5',2'']terthiophene as a dark orange oil (0.6811 g, 93%).

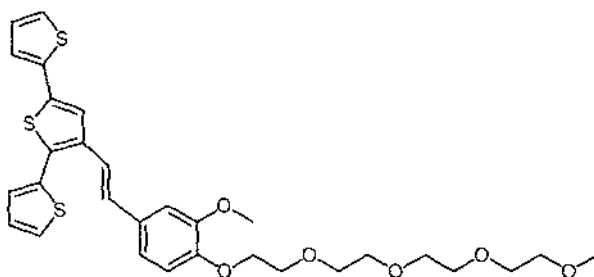
<sup>1</sup>H NMR (400.1 MHz, CD<sub>2</sub>Cl<sub>2</sub>) δ 3.33 (s, 3H, 2''''''OCH<sub>3</sub>); 3.49-3.52 (m, 2H, OCH<sub>2</sub>2'''''''); 3.58-3.60 (m, 2H, OCH<sub>2</sub>1'''''''); 3.61-3.64 (m, 2H, OCH<sub>2</sub>2'''''''); 3.67-3.69 (m, 2H, OCH<sub>2</sub>1'''''''); 3.82-3.84 (m, 2H, OCH<sub>2</sub>2'''''''); 3.88 (s, 3H, ArOCH<sub>3</sub>); 4.13-4.15 (m, 2H, OCH<sub>2</sub>1'''''''); 6.88 (d, 1H, <sup>3</sup>J = 8.9 Hz, ArH5'''''); 7.02 (d, 1H, <sup>3</sup>J = 16.6 Hz, H<sub>vinyl</sub>2'''''); 7.03-7.05 (m, 2H, ArH2''''', 6'''''); 7.06 (dd, 1H, <sup>3</sup>J = 5.2 Hz, <sup>4</sup>J = 3.6 Hz, ThH4''); 7.14 (dd, 1H, <sup>3</sup>J = 5.2 Hz, <sup>4</sup>J = 3.6 Hz, ThH4); 7.23 (dd, 1H, <sup>3</sup>J = 3.7 Hz, <sup>4</sup>J = 1.2 Hz, ThH3); 7.24 (dd, 1H, <sup>3</sup>J = 3.6 Hz, <sup>4</sup>J = 1.2 Hz, ThH3''); 7.25 (d, 1H, <sup>3</sup>J = 16.6 Hz, H<sub>vinyl</sub>1'''''); 7.29 (dd, 1H, <sup>3</sup>J = 5.1 Hz, <sup>4</sup>J = 1.2 Hz, ThH5''); 7.41 (dd, 1H, <sup>3</sup>J = 5.2 Hz, <sup>4</sup>J = 1.2 Hz, ThH5); 7.45 (s, 1H, ThH4').

$^{13}\text{C}$  NMR (100.6 MHz,  $\text{CD}_2\text{Cl}_2$ )  $\delta$  55.5 ArOCH<sub>3</sub>; 58.3 2''''''OCH<sub>3</sub>; 68.0 OCH<sub>2</sub>1''''''; 69.2 OCH<sub>2</sub>2''''''; 70.1 OCH<sub>2</sub>1''''''; 70.2 OCH<sub>2</sub>2''''''; 70.4 OCH<sub>2</sub>1''''''; 71.5 OCH<sub>2</sub>2''''''; 109.2 ArC2''''''; 112.8 ArC5''''''; 119.2 ArC6''''''; 119.3 C<sub>vinyl</sub>1''''''; 121.9 ThC4'; 123.8 ThC3''; 124.6 ThC5''; 126.0 ThC5; 126.5 ThC3; 127.5 ThC4; 127.6 ThC4''; 130.1 C<sub>vinyl</sub>2''''; 130.3 ArC1''''''; 130.4 ThC2'; 134.9 ThC2; 135.5 ThC5'; 136.2 ThC3'; 136.3 ThC2''; 148.1 ArC4''''''; 149.3 ArC3''''.

Electronic spectrum (MeCN)  $\lambda_{\text{max}}$  nm/(log  $\epsilon$ ) 329.0 (4.60).

HRMS (FAB)  $M^+$  calc 542.1255, found 542.1233.

**3'-(2''-{3''''-Methoxy-4''''-[2''''''-(2''''''-{2''''''''-[2''''''''''-methoxy-ethoxy]-ethoxy}-ethoxy)-ethoxy]-phenyl)-vinyl)-[2,2';5',2'']terthiophene (XXVIII)**



3-Methoxy-4-[2'-(2''-{2''''-[2''''''-methoxy-ethoxy]-ethoxy}-ethoxy)-ethoxy]-benzaldehyde (0.4634 g, 1.35 mmol) and terthiophene phosphonate (10 mL x 0.135 mmol/mL solution in dry THF, 1.35 mmol) were stirred under  $\text{N}_2$  in dry  $\text{CH}_2\text{Cl}_2$  (10 mL) before KO<sup>t</sup>Bu (0.3856 g, 3.44 mmol) was added and the solution left to stir at room temperature for 30 minutes.  $\text{H}_2\text{O}$  (20 mL) was added and the reaction mixture acidified with aqueous HCl.  $\text{CH}_2\text{Cl}_2$  (20 mL) was added, and the organic layer separated. The aqueous layer was extracted with  $\text{CH}_2\text{Cl}_2$  (20 mL), before the combined organic layers were washed with  $\text{H}_2\text{O}$  (20 mL) and the solvent removed under reduced pressure. The residue was dissolved in  $\text{CH}_2\text{Cl}_2$ , and purified using

flash column chromatography. After 1,2-bis(2',5''-thiophen-3''-yl)ethene (24.8 mg, 7%) was eluted in CH<sub>2</sub>Cl<sub>2</sub>, the desired product was eluted in 2% MeOH. Removal of the solvent under reduced pressure yielded 3'-(2''-{3''-methoxy-4''-[2''-(2''''-{2''''''-[2''''''-methoxy-ethoxy]-ethoxy}-ethoxy)-ethoxy]-phenyl}-vinyl)-[2,2';5',2'']terthiophene as a dark orange oil (0.7463 g, 94%).

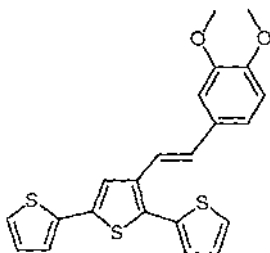
<sup>1</sup>H NMR (400.1 MHz, CD<sub>2</sub>Cl<sub>2</sub>) δ 3.33 (s, 3H, 2''''''OCH<sub>3</sub>); 3.48-3.50 (m, 2H, OCH<sub>2</sub>2'''''''); 3.56-3.58 (m, 2H, OCH<sub>2</sub>1'''''''); 3.58-3.61 (m, 4H, OCH<sub>2</sub>1''''''', 2'''''''); 3.62-3.64 (m, 2H, OCH<sub>2</sub>2'''''''); 3.67-3.70 (m, 2H, OCH<sub>2</sub>1'''''''); 3.82-3.84 (m, 2H, OCH<sub>2</sub>2'''''''); 3.88 (s, 3H, ArOCH<sub>3</sub>); 4.13-4.15 (m, 2H, OCH<sub>2</sub>1'''''''); 6.87 (d, 1H, <sup>3</sup>J = 8.8 Hz, ArH5'''); 7.01 (d, 1H, <sup>3</sup>J = 16.6 Hz, H<sub>vinyl</sub>2'''); 7.02-7.04 (m, 2H, ArH2''', 6'''); 7.06 (dd, 1H, <sup>3</sup>J = 5.2 Hz, <sup>4</sup>J = 3.6 Hz, ThH4''); 7.13 (dd, 1H, <sup>3</sup>J = 5.2 Hz, <sup>4</sup>J = 3.6 Hz, ThH4); 7.22 (dd, 1H, <sup>3</sup>J = 3.6 Hz, <sup>4</sup>J = 1.2 Hz, ThH3); 7.24 (dd, 1H, <sup>3</sup>J = 3.7 Hz, <sup>4</sup>J = 1.2 Hz, ThH3''); 7.25 (d, 1H, <sup>3</sup>J = 15.8 Hz, H<sub>vinyl</sub>1'''); 7.29 (dd, 1H, <sup>3</sup>J = 5.2 Hz, <sup>4</sup>J = 1.1 Hz, ThH5''); 7.41 (dd, 1H, <sup>3</sup>J = 5.1 Hz, <sup>4</sup>J = 1.2 Hz, ThH5); 7.45 (s, 1H, ThH4').

<sup>13</sup>C NMR (100.6 MHz, CD<sub>2</sub>Cl<sub>2</sub>) δ 55.4 ArOCH<sub>3</sub>; 58.3 2''''''OCH<sub>3</sub>; 67.9 OCH<sub>2</sub>1'''''''; 69.2 OCH<sub>2</sub>2'''''''; 70.0 OCH<sub>2</sub>1'''''''; 70.1 OCH<sub>2</sub>2'''''''; 70.2 OCH<sub>2</sub>2'''''''; 70.2 OCH<sub>2</sub>1'''''''; 70.3 OCH<sub>2</sub>1'''''''; 71.5 OCH<sub>2</sub>2'''''''; 109.2 ArC2''''; 112.8 ArC5''''; 119.2 ArC6''''; 119.3 C<sub>vinyl</sub>1''''; 121.9 ThC4'; 123.8 ThC3''; 124.6 ThC5''; 126.0 ThC5; 126.5 ThC3; 127.5 ThC4; 127.6 ThC4''; 130.1 C<sub>vinyl</sub>2''''; 130.3 ArC1''''; 130.4 ThC2'; 134.9 ThC2; 135.5 ThC5'; 136.2 ThC3'; 136.3 ThC2''; 148.1 ArC4''''; 149.3 ArC3''''.

Electronic spectrum (MeCN) λ<sub>max</sub> nm/(log ε) 329.0 (4.64).

HRMS (FAB) M<sup>+</sup> calc 586.1518, found 586.1510.

### 3'-[2'''-(3''',4'''-Dimethoxy-phenyl)-vinyl]-[2,2';5',2'']terthiophene (XXIX)



3,4-dimethoxybenzaldehyde (0.5152 g, 3.10 mmol) and terthiophene phosphonate (16.5 mL x 0.190 mmol/mL solution in CH<sub>2</sub>Cl<sub>2</sub>, 3.14 mmol) were stirred under N<sub>2</sub> in 1:1 dry THF:CH<sub>2</sub>Cl<sub>2</sub> (20 mL) before KO<sup>t</sup>Bu (1.0329 g, 9.204 mmol) was added. The solution was left to stir at room temperature for 30 minutes before H<sub>2</sub>O (20 mL) was added and acidified with aqueous HCl. H<sub>2</sub>O (20 mL) and CH<sub>2</sub>Cl<sub>2</sub> (20 mL) were added, and the organic layer separated. The aqueous layer was extracted with CH<sub>2</sub>Cl<sub>2</sub> (2 x 40 mL), the combined organic layers washed with H<sub>2</sub>O (50 mL), and the solvent removed under reduced pressure. The residue was dissolved in 1:1 hexane:CH<sub>2</sub>Cl<sub>2</sub> and purified using flash column chromatography. After a small amount of 1,2-bis([2',2'';5'',2''']terthiophen-3''-yl)ethene was eluted in 1:1 CH<sub>2</sub>Cl<sub>2</sub>:hexane, the desired product was eluted in 3:1 CH<sub>2</sub>Cl<sub>2</sub>:hexane. Removal of the solvent under reduced pressure yielded 3'-[2'''-(3''',4'''-dimethoxy-phenyl)-vinyl]-[2,2';5',2'']terthiophene as a yellow solid, melting point = 114-116°C (1.0938 g, 86%).

<sup>1</sup>H NMR (400.1 MHz, CD<sub>2</sub>Cl<sub>2</sub>) δ 3.87 (s, 3H, 4''''OCH<sub>3</sub>); 3.90 (s, 3H, 3''''OCH<sub>3</sub>); 6.88 (d, 1H, <sup>3</sup>J = 8.4 Hz, ArH5'''); 7.04 (d, 1H, <sup>3</sup>J = 16.1 Hz, H<sub>vinyl</sub>2'''); 7.06-7.09 (m, 2H, ArH2''', 6'''); 7.08 (dd, 1H, <sup>3</sup>J = 5.1 Hz, <sup>4</sup>J = 3.6 Hz, ThH4''); 7.16 (dd, 1H, <sup>3</sup>J = 5.2 Hz, <sup>4</sup>J = 3.6 Hz, ThH4); 7.25 (dd, 1H, <sup>3</sup>J = 3.6 Hz, <sup>4</sup>J = 1.2 Hz, ThH3); 7.26 (dd, 1H, <sup>3</sup>J = 3.6 Hz, <sup>4</sup>J = 1.1 Hz, H3''); 7.30 (d, 1H, <sup>3</sup>J = 16.1 Hz, H<sub>vinyl</sub>1'''); 7.31 (dd, 1H, <sup>3</sup>J = 5.1 Hz, <sup>4</sup>J = 1.2 Hz, ThH5''); 7.43 (dd, 1H, <sup>3</sup>J = 5.1 Hz, <sup>4</sup>J = 1.2 Hz, ThH5); 7.48 (s, 1H, ThH4').

<sup>13</sup>C NMR (100.6 MHz, CD<sub>2</sub>Cl<sub>2</sub>) δ 55.3 3''''OCH<sub>3</sub>; 55.3 4''''OCH<sub>3</sub>; 108.8 ArC2'''; 111.0 ArC5'''; 119.1 C<sub>vinyl</sub>1'''; 119.3 ArC6'''; 121.8 ThC4'; 123.7 ThC3''; 124.5 ThC5''; 125.9 ThC5; 126.4 ThC3; 127.5 ThC4; 127.6 ThC4''; 129.8 ArC1'''; 130.1

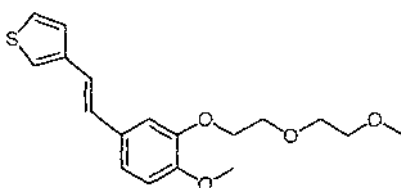
$C_{\text{vinyl}2''''}$ ; 130.3 ThC2'; 134.9 ThC2; 135.4 ThC5'; 136.2 ThC3'; 136.3 ThC2''; 148.9 ArC4''''; 148.9 ArC3''''.

Electronic spectrum (MeCN)  $\lambda_{\text{max}}$  nm/(log  $\epsilon$ ) 329.0 (4.65).

HRMS (FAB)  $M^+$  calc 410.0469, found 410.0450.

Anal. Calculated for  $C_{22}H_{18}O_2S_3$ ; C, 64.36; H, 4.42; S, 23.43. Found: C, 64.27; H, 4.15; S, 23.16.

**3-(2'-{4''-Methoxy-3''-[2'''-(2''''-methoxy-ethoxy)-ethoxy]-phenyl}-vinyl)-thiophene (XXX)**



4-Methoxy-3-[2'-(2''-methoxy-ethoxy)-ethoxy]-benzaldehyde (0.5510 g, 2.17 mmol) and thiophene phosphonate (0.5055 g, 2.16 mmol) were stirred under  $N_2$  in dry  $CH_2Cl_2$  (20 mL) before KO<sup>t</sup>Bu (0.6948 g, 6.19 mmol) was added and the solution left to stir at room temperature for 1 hour.  $H_2O$  (20 mL) was added and neutralized with aqueous HCl.  $CH_2Cl_2$  (20 mL) was added, and the organic layer separated before the aqueous layer was extracted with  $CH_2Cl_2$  (20 mL), and the combined organic layers were washed with  $H_2O$  (20 mL). The solvent was removed under reduced pressure before the residue was dissolved in  $CH_2Cl_2$ , and purified using flash column chromatography. After initially eluting in  $CH_2Cl_2$ , the solvent was changed to 1% MeOH to elute the desired product as a pale yellow band. Removal of the solvent under reduced pressure yielded 3-(2'-{4''-methoxy-3''-[2'''-(2''''-methoxy-ethoxy)-ethoxy]-phenyl}-vinyl)-thiophene as a beige solid, melting point = 56-58°C (0.5650 g, 78%).

$^1\text{H}$  NMR (400.1 MHz,  $\text{CDCl}_3$ )  $\delta$  3.39 (s, 3H,  $2''''\text{OCH}_3$ ); 3.57-3.59 (m, 2H,  $\text{OCH}_22''''$ ); 3.73-3.75 (m, 2H,  $\text{OCH}_21''''$ ); 3.86 (s, 3H,  $\text{ArOCH}_3$ ); 3.90-3.93 (m, 2H,  $\text{OCH}_22''$ ); 4.24-4.27 (m, 2H,  $\text{OCH}_21''$ ); 6.83 (d, 1H,  $^3J = 8.3$  Hz,  $\text{ArH}5''$ ); 6.87 (d, 1H,  $^3J = 16.3$  Hz,  $\text{H}_{\text{vinyl}2'}$ ); 6.98 (d, 1H,  $^3J = 16.3$  Hz,  $\text{H}_{\text{vinyl}1'}$ ); 7.01 (dd, 1H,  $^3J = 8.3$  Hz,  $^4J = 2.0$  Hz,  $\text{ArH}6''$ ); 7.10 (d, 1H,  $^4J = 2.0$  Hz,  $\text{ArH}2''$ ); 7.21-7.22 (m, 1H,  $\text{ThH}4$ ); 7.29-7.33 (m, 2H,  $\text{ThH}2$ , 5).

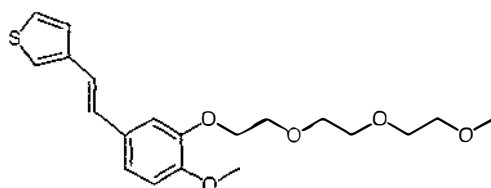
$^{13}\text{C}$  NMR (100.6 MHz,  $\text{CDCl}_3$ )  $\delta$  55.8  $\text{ArOCH}_3$ ; 58.9  $2''''\text{OCH}_3$ ; 68.4  $\text{OCH}_21''''$ ; 69.6  $\text{OCH}_22''$ ; 70.6  $\text{OCH}_21''$ ; 71.8  $\text{OCH}_22''$ ; 111.0  $\text{ArC}2''$ ; 111.6  $\text{ArC}5''$ ; 120.1  $\text{ArC}6''$ ; 121.0  $\text{C}_{\text{vinyl}1'}$ ; 121.5  $\text{ThC}4$ ; 124.7  $\text{ThC}2$ ; 126.0  $\text{ThC}5$ ; 128.2  $\text{C}_{\text{vinyl}2'}$ ; 130.3  $\text{ArC}1''$ ; 140.1  $\text{ThC}3$ ; 148.2  $\text{ArC}3''$ ; 149.2  $\text{ArC}4''$ .

Electronic spectrum (MeCN)  $\lambda_{\text{max}}$  nm/(log  $\epsilon$ ) 317.0 (4.38), 298.0 (4.36), 216.0 (4.26).

HRMS (FAB)  $M^+$  calc 334.1239, found 334.1228.

Anal. Calculated for  $\text{C}_{18}\text{H}_{22}\text{O}_4\text{S}$ ; C, 64.64; H, 6.63; S, 9.59. Found: C, 63.48; H, 6.88; S, 9.36.

**3-(2'-(4''-Methoxy-3''-[2'''-(2''''-(2''''''-methoxy-ethoxy)-ethoxy)-ethoxy]-phenyl)-vinyl)-thiophene (XXXI)**



4-Methoxy-3-[2'-(2''-(2'''-(2''''-(2''''''-methoxy-ethoxy)-ethoxy)-ethoxy)-ethoxy]-benzaldehyde (0.6755 g, 2.26 mmol) and thiophene phosphonate (0.5168, 2.21 mmol) were stirred

in dry  $\text{CH}_2\text{Cl}_2$  (20 mL) under  $\text{N}_2$  before KO<sup>t</sup>Bu (0.8103 g, 7.22 mmol) was added. The solution was left to stir at room temperature for 1 hour before  $\text{H}_2\text{O}$  (20 mL) was added and acidified with aqueous HCl.  $\text{CH}_2\text{Cl}_2$  (20 mL) was added, and the organic layer separated. The aqueous layer was extracted with  $\text{CH}_2\text{Cl}_2$  (20 mL) before the combined organic layers were washed with  $\text{H}_2\text{O}$  (30 mL), and the solvent removed under reduced pressure. The resulting residue was subsequently dissolved in  $\text{CH}_2\text{Cl}_2$ , and purified using flash column chromatography on silica. The column was initially washed with  $\text{CH}_2\text{Cl}_2$ , then the desired product eluted in 1% MeOH. Removal of the solvent under reduced pressure yielded 3-(2'-{4"-methoxy-3"-[2'''-(2''''-{2'''''-methoxy-ethoxy}-ethoxy)-ethoxy]-phenyl}-vinyl)-thiophene as a pale orange oil (0.6475 g, 78%).

$^1\text{H}$  NMR (400.1 MHz,  $\text{CDCl}_3$ )  $\delta$  3.37 (s, 3H, 2''''OCH<sub>3</sub>); 3.53-3.55 (m, 2H, OCH<sub>2</sub>2'''''); 3.64-3.66 (m, 2H, OCH<sub>2</sub>1'''''); 3.67-3.70 (m, 2H, OCH<sub>2</sub>2'''''); 3.74-3.77 (m, 2H, OCH<sub>2</sub>1'''''); 3.86 (s, 3H, ArOCH<sub>3</sub>); 3.90-3.92 (m, 2H, OCH<sub>2</sub>2'''''); 4.23-4.25 (m, 2H, OCH<sub>2</sub>1'''''); 6.84 (d, 1H,  $^3J = 8.4$  Hz, ArH5''); 6.87 (d, 1H,  $^3J = 16.8$  Hz, H<sub>vinyl</sub>2'); 6.98 (d, 1H,  $^3J = 16.0$  Hz, H<sub>vinyl</sub>1'); 7.01 (dd, 1H,  $^3J = 8.3$  Hz,  $^4J = 2.0$  Hz, ArH6''); 7.09 (d, 1H,  $^4J = 2.0$  Hz, ArH2''); 7.21-7.22 (m, 1H, ThH4); 7.29-7.33 (m, 2H, ThH2, 5).

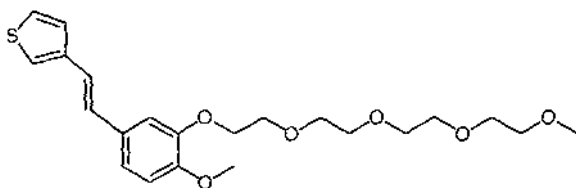
$^{13}\text{C}$  NMR (100.6 MHz,  $\text{CDCl}_3$ )  $\delta$  55.9 ArOCH<sub>3</sub>; 58.9 2''''OCH<sub>3</sub>; 68.4 OCH<sub>2</sub>1'''''; 69.6 OCH<sub>2</sub>2'''''; 70.5 OCH<sub>2</sub>1'''''); 70.6 OCH<sub>2</sub>2'''''); 70.7 OCH<sub>2</sub>1'''''); 71.8 OCH<sub>2</sub>2'''''); 111.0 ArC2''; 111.7 ArC5''; 120.1 ArC6''; 121.0 C<sub>vinyl</sub>1'; 121.6 ThC4; 124.7 ThC2; 126.0 ThC5; 128.2 C<sub>vinyl</sub>2'; 130.3 ArC1''; 140.1 ThC3; 148.3 ArC3''; 149.2 ArC4''.

Electronic spectrum (MeCN)  $\lambda_{\text{max}}$  nm/(log  $\epsilon$ ) 317.0 (4.30), 298.0 (4.28), 216.5 (4.25), 205.0 (4.24).

HRMS (FAB)  $M^+$  calc 378.1501, found 378.1492.

Anal. Calculated for  $\text{C}_{20}\text{H}_{26}\text{O}_5\text{S}$ ; C, 63.47; H, 6.92; S, 8.47. Found: C, 60.84; H, 7.37; S, 7.63.

**3-(2'-(4''-Methoxy-3''-[2'''-(2''''-{2''''''-methoxy-ethoxy]-ethoxy}-ethoxy)-ethoxy)-phenyl)-vinyl)-thiophene (XXXII)**



4-Methoxy-3-[2'-(2''-{2'''-[2''''-methoxy-ethoxy]-ethoxy}-ethoxy)-ethoxy]-ethoxy]-benzaldehyde (0.7644 g, 2.23 mmol) and thiophene phosphonate (0.5065, 2.16 mmol) were stirred in dry  $\text{CH}_2\text{Cl}_2$  (20 mL) under  $\text{N}_2$  before KO<sup>t</sup>Bu (0.7542 g, 6.72 mmol) was added. The solution was left to stir at room temperature for 30 minutes before  $\text{H}_2\text{O}$  (20 mL) was added and acidified with aqueous HCl.  $\text{CH}_2\text{Cl}_2$  (20 mL) was added, and the organic layer separated. The aqueous layer was extracted with  $\text{CH}_2\text{Cl}_2$  (20 mL) before the combined organic layers were washed with  $\text{H}_2\text{O}$  (30 mL) and the solvent removed under reduced pressure. The residue was dissolved in  $\text{CH}_2\text{Cl}_2$  and purified using flash column chromatography on silica. The column was initially washed with  $\text{CH}_2\text{Cl}_2$ , then the desired product eluted in 1% MeOH. Removal of the solvent under reduced pressure yielded 3-(2'-(4''-methoxy-3''-[2'''-(2''''-{2''''''-methoxy-ethoxy]-ethoxy)-ethoxy)-ethoxy)-phenyl)-vinyl)-thiophene as a pale yellow oil (0.4991 g, 55%).

$^1\text{H}$  NMR (400.1 MHz,  $\text{CDCl}_3$ )  $\delta$  3.37 (s, 3H, 2''''''OCH<sub>3</sub>); 3.53-3.55 (m, 2H, OCH<sub>2</sub>2'''''''); 3.62-3.64 (m, 2H, OCH<sub>2</sub>1'''''''); 3.64-3.68 (m, 4H, OCH<sub>2</sub>1''''''', 2'''''''); 3.68-3.70 (m, 2H, OCH<sub>2</sub>2'''''''); 3.74-3.76 (m, 2H, OCH<sub>2</sub>1'''''''); 3.87 (s, 3H, ArOCH<sub>3</sub>); 3.90-3.93 (m, 2H, OCH<sub>2</sub>2'''''''); 4.23-4.26 (m, 2H, OCH<sub>2</sub>1'''''''); 6.85 (d, 1H,  $^3J = 8.3$  Hz, ArH5''); 6.88 (d, 1H,  $^3J = 16.2$  Hz, H<sub>vinyl</sub>2'); 6.99 (d, 1H,  $^3J = 16.2$  Hz, H<sub>vinyl</sub>1'); 7.02 (dd, 1H,  $^3J = 8.3$  Hz,  $^4J = 2.0$  Hz, ArH6''); 7.10 (d, 1H,  $^4J = 2.0$  Hz, ArH2''); 7.22-7.23 (m, 1H, ThH4); 7.30-7.34 (m, 2H, ThH2, 5).

$^{13}\text{C}$  NMR (100.6 MHz,  $\text{CDCl}_3$ )  $\delta$  55.9 ArOCH<sub>3</sub>; 59.0 2''''''''OCH<sub>3</sub>; 68.4 OCH<sub>2</sub>1'''''''; 69.6 OCH<sub>2</sub>2'''''''; 70.4 OCH<sub>2</sub>1'''''''''; 70.5 OCH<sub>2</sub>2'''''''''; 70.5 OCH<sub>2</sub>2'''''''''; 70.6 OCH<sub>2</sub>1'''''''''; 70.8 OCH<sub>2</sub>1'''''''''; 71.9 OCH<sub>2</sub>2'''''''''''; 111.1 ArC2''; 111.7 ArC5''; 120.1 ArC6''; 121.1 C<sub>vinyl</sub>1'';

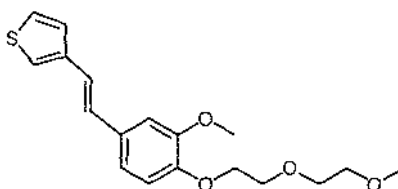
121.6 ThC4; 124.8 ThC2; 126.0 ThC5; 128.3 C<sub>vinyl</sub>2'; 130.4 ArC1''; 140.2 ThC3; 148.3 ArC3''; 149.3 ArC4''.

Electronic spectrum (MeCN)  $\lambda_{\max}$  nm/(log  $\epsilon$ ) 317.0 (4.37), 298.0 (4.35), 216.0 (4.25).

HRMS (FAB) M<sup>+</sup> calc 422.1763, found 422.1754.

Anal. Calculated for C<sub>22</sub>H<sub>30</sub>O<sub>6</sub>S; C, 62.54; H, 7.16; S, 7.59. Found: C, 61.26; H, 7.42; S, 7.30.

**3-(2'-{3''-Methoxy-4''-[2'''-(2''''-methoxy-ethoxy)-ethoxy]-phenyl}-vinyl)-thiophene (XXXIII)**



3-Methoxy-4-[2'-{2''-methoxy-ethoxy)-ethoxy]-benzaldehyde (0.5718 g, 2.25 mmol) and thiophene phosphonate (0.5078 g, 2.17 mmol) were stirred under N<sub>2</sub> in dry CH<sub>2</sub>Cl<sub>2</sub> (20 mL) before KO<sup>t</sup>Bu (0.7158 g, 6.38 mmol) was added. The solution was left to stir at room temperature for 90 minutes before H<sub>2</sub>O (20 mL) was added and neutralized with aqueous HCl. CH<sub>2</sub>Cl<sub>2</sub> (20 mL) was added and the organic layer separated. The aqueous layer was extracted with CH<sub>2</sub>Cl<sub>2</sub> (20 mL), before the combined organic layers were washed with H<sub>2</sub>O (30 mL) and the solvent removed under reduced pressure. The residue was dissolved in CH<sub>2</sub>Cl<sub>2</sub>, and purified using flash column chromatography on a silica column. After initially eluting with CH<sub>2</sub>Cl<sub>2</sub>, the solvent was changed to 1% MeOH to elute the product as a pale yellow band. Removal of the solvent under reduced pressure yielded 3-(2'-{3''-methoxy-4''-[2'''-(2''''-methoxy-ethoxy)-ethoxy]-phenyl}-vinyl)-thiophene as iridescent beige flakes (0.5709 g, 79%, melting point = 90-93°C).

$^1\text{H}$  NMR (400.1 MHz,  $\text{CDCl}_3$ )  $\delta$  3.39 (s, 3H,  $2''''\text{OCH}_3$ ); 3.57-3.59 (m, 2H,  $\text{OCH}_22''''$ ); 3.72-3.74 (m, 2H,  $\text{OCH}_21''''$ ); 3.89-3.91 (m, 2H,  $\text{OCH}_22'''$ ); 3.91 (s, 3H,  $\text{ArOCH}_3$ ); 4.20-4.22 (m, 2H,  $\text{OCH}_21'''$ ); 6.89 (d, 1H,  $^3J = 8.3$  Hz,  $\text{ArH5}''$ ); 6.89 (d, 1H,  $^3J = 16.2$  Hz,  $\text{H}_{\text{vinyl}2'}$ ); 6.99 (dd, 1H,  $^3J = 8.2$  Hz,  $^4J = 2.1$  Hz,  $\text{ArH6}''$ ); 7.00 (d, 1H,  $^3J = 16.5$  Hz,  $\text{H}_{\text{vinyl}1'}$ ); 7.02 (d, 1H,  $^4J = 2.0$  Hz,  $\text{ArH2}''$ ); 7.22-7.23 (m, 1H,  $\text{ThH4}$ ); 7.30-7.34 (m, 2H,  $\text{ThH2, 5}$ ).

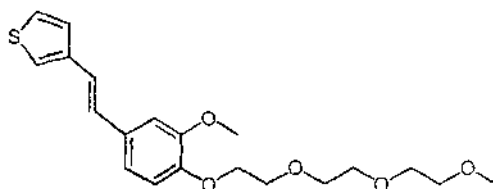
$^{13}\text{C}$  NMR (100.6 MHz,  $\text{CDCl}_3$ )  $\delta$  55.8  $\text{ArOCH}_3$ ; 59.0  $2''''\text{OCH}_3$ ; 68.4  $\text{OCH}_21''''$ ; 69.5  $\text{OCH}_22''''$ ; 70.7  $\text{OCH}_21'''$ ; 71.8  $\text{OCH}_22'''$ ; 109.1  $\text{ArC2}''$ ; 113.6  $\text{ArC5}''$ ; 119.4  $\text{ArC6}''$ ; 121.2  $\text{C}_{\text{vinyl}1'}$ ; 121.6  $\text{ThC4}$ ; 124.7  $\text{ThC2}$ ; 126.0  $\text{ThC5}$ ; 128.3  $\text{C}_{\text{vinyl}2'}$ ; 130.9  $\text{ArC1}''$ ; 140.1  $\text{ThC3}$ ; 147.9  $\text{ArC4}''$ ; 149.6  $\text{ArC3}''$ .

Electronic spectrum (MeCN)  $\lambda_{\text{max}}$  nm/(log  $\epsilon$ ) 317.0 (4.35), 298.0 (4.33), 216.0 (4.24).

HRMS (FAB)  $M^+$  calc 334.1239, found 334.1248.

Anal. Calculated for  $\text{C}_{18}\text{H}_{22}\text{O}_4\text{S}$ ; C, 64.64; H, 6.63; S, 9.59. Found: C, 63.59; H, 6.96; S, 9.46.

**3-(2'-{3''-Methoxy-4''-[2'''-(2''''-{2'''''-methoxy-ethoxy}-ethoxy)-ethoxy]-ethoxy}-phenyl)-vinyl)-thiophene (XXXIV)**



3-Methoxy-4-[2'-{2''-(2'''-methoxy-ethoxy)-ethoxy]-ethoxy]-benzaldehyde (0.6990 g, 2.34 mmol) and thiophene phosphonate (0.5224 g, 2.23 mmol) were stirred

in dry CH<sub>2</sub>Cl<sub>2</sub> (20 mL) under N<sub>2</sub> before KO<sup>t</sup>Bu (0.8301 g, 7.40 mmol) was added and the solution left to stir at room temperature for 60 minutes. H<sub>2</sub>O (20 mL) was added and acidified with aqueous HCl before CH<sub>2</sub>Cl<sub>2</sub> (20 mL) was added, and the organic layer separated. The aqueous layer was extracted with CH<sub>2</sub>Cl<sub>2</sub> (20 mL), after which the combined organic layers were washed with H<sub>2</sub>O (30 mL) and the solvent removed under reduced pressure. The residue was dissolved in CH<sub>2</sub>Cl<sub>2</sub>, then purified using flash column chromatography on silica. The column was initially eluted in CH<sub>2</sub>Cl<sub>2</sub>, then the desired product eluted in 1% MeOH. Removal of the solvent under reduced pressure yielded 3-(2'-{3"-methoxy-4"-[2"'-(2"'-{2""'-methoxy-ethoxy}-ethoxy)-ethoxy]-phenyl}-vinyl)-thiophene as a beige semi-solid (0.6702 g, 79%).

<sup>1</sup>H NMR (400.1 MHz, CDCl<sub>3</sub>) δ 3.38 (s, 3H, 2""OCH<sub>3</sub>); 3.54-3.56 (m, 2H, OCH<sub>2</sub>2"""); 3.64-3.67 (m, 2H, OCH<sub>2</sub>1"""); 3.67-3.69 (m, 2H, OCH<sub>2</sub>2"""); 3.73-3.76 (m, 2H, OCH<sub>2</sub>1"""); 3.88-3.90 (m, 2H, OCH<sub>2</sub>2"""); 3.90 (s, 3H, ArOCH<sub>3</sub>); 4.18-4.21 (m, 2H, OCH<sub>2</sub>1"""); 6.89 (d, 1H, <sup>3</sup>J = 8.3 Hz, ArH5"); 6.89 (d, 1H, <sup>3</sup>J = 16.2 Hz, H<sub>vinyl</sub>2'); 6.98 (dd, 1H, <sup>3</sup>J = 8.1 Hz, <sup>4</sup>J = 2.1 Hz, ArH6"); 7.00 (d, 1H, <sup>3</sup>J = 16.5 Hz, H<sub>vinyl</sub>1'); 7.02 (d, 1H, <sup>4</sup>J = 1.9 Hz, ArH2"); 7.22-7.23 (m, 1H, ThH4); 7.29-7.33 (m, 2H, ThH2, 5).

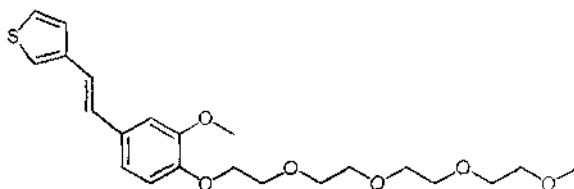
<sup>13</sup>C NMR (100.6 MHz, CDCl<sub>3</sub>) δ 55.8 ArOCH<sub>3</sub>; 58.9 2""OCH<sub>3</sub>; 68.4 OCH<sub>2</sub>1"""; 69.5 OCH<sub>2</sub>2"""; 70.4 OCH<sub>2</sub>1"""; 70.5 OCH<sub>2</sub>2"""; 70.7 OCH<sub>2</sub>1"""; 71.8 OCH<sub>2</sub>2"""; 109.1 ArC2"; 113.6 ArC5"; 119.4 ArC6"; 121.2 C<sub>vinyl</sub>1'; 121.6 ThC4; 124.7 ThC2; 126.0 ThC5; 128.3 C<sub>vinyl</sub>2'; 130.9 ArC1"; 140.1 ThC3; 148.0 ArC4"; 149.6 ArC3".

Electronic spectrum (MeCN) λ<sub>max</sub> nm/(log ε) 317.5 (4.42), 298.0 (4.38), 216.0 (4.26).

HRMS (FAB) M<sup>+</sup> calc 378.1501, found 378.1491.

Anal. Calculated for C<sub>20</sub>H<sub>26</sub>O<sub>5</sub>S; C, 63.47; H, 6.92; S, 8.47. Found: C, 62.95; H, 7.28; S, 8.16.

**3-(2'-{3''-Methoxy-4''-[2'''-(2''''-{2''''''-methoxy-ethoxy]-ethoxy}-ethoxy)-ethoxy]-phenyl)-vinyl)-thiophene (XXXV)**



3-Methoxy-4-[2'-{2''-(2'''-(2''''-methoxy-ethoxy)-ethoxy)-ethoxy}-ethoxy]-ethoxy]-benzaldehyde (0.7782 g, 2.27 mmol) and thiophene phosphonate (0.5167 g, 2.21 mmol) were stirred in dry  $\text{CH}_2\text{Cl}_2$  (20 mL) under  $\text{N}_2$  before KO<sup>t</sup>Bu (0.7971 g, 7.10 mmol) was added and the solution left to stir at room temperature for 1 hour.  $\text{H}_2\text{O}$  (20 mL) was added and acidified with aqueous HCl before  $\text{CH}_2\text{Cl}_2$  (20 mL) was added, and the organic layer separated. The aqueous layer was extracted with  $\text{CH}_2\text{Cl}_2$  (20 mL), after which the combined organic layers were washed with  $\text{H}_2\text{O}$  (30 mL) and the solvent removed under reduced pressure. The residue was dissolved in  $\text{CH}_2\text{Cl}_2$ , and purified using flash column chromatography on silica. The column was initially eluted in  $\text{CH}_2\text{Cl}_2$ , then the desired product eluted in 1% MeOH. Removal of the solvent under reduced pressure yielded 3-(2'-{3''-methoxy-4''-[2'''-(2''''-{2''''''-methoxy-ethoxy]-ethoxy}-ethoxy)-ethoxy]-phenyl)-vinyl)-thiophene as a beige semi-solid (0.5954 g, 64%).

$^1\text{H}$  NMR (400.1 MHz,  $\text{CDCl}_3$ )  $\delta$  3.37 (s, 3H, 2''''''OCH<sub>3</sub>); 3.53-3.55 (m, 2H, OCH<sub>2</sub>2'''''''); 3.63-3.65 (m, 2H, OCH<sub>2</sub>1'''''''); 3.65-3.67 (m, 4H, OCH<sub>2</sub>1''''''', 2'''''''); 3.68-3.69 (m, 2H, OCH<sub>2</sub>2'''''''); 3.72-3.74 (m, 2H, OCH<sub>2</sub>1'''''''); 3.88-3.91 (m, 2H, OCH<sub>2</sub>2'''''''); 3.91 (s, 3H, ArOCH<sub>3</sub>); 4.19-4.21 (m, 2H, OCH<sub>2</sub>1'''''''); 6.89 (d, 1H,  $^3J = 8.3$  Hz, ArH5''); 6.89 (d, 1H,  $^3J = 16.2$  Hz,  $\text{H}_{\text{vinyl}2'}$ ); 6.99 (dd, 1H,  $^3J = 8.2$  Hz,  $^4J = 2.0$  Hz, ArH6''); 7.00 (d, 1H,  $^3J = 16.1$  Hz,  $\text{H}_{\text{vinyl}1'}$ ); 7.02 (d, 1H,  $^4J = 1.9$  Hz, ArH2''); 7.22-7.23 (m, 1H, ThH4); 7.30-7.34 (m, 2H, ThH2, 5).

$^{13}\text{C}$  NMR (100.6 MHz,  $\text{CDCl}_3$ )  $\delta$  55.8 ArOCH<sub>3</sub>; 59.0 2''''''''OCH<sub>3</sub>; 68.4 OCH<sub>2</sub>1'''''''; 69.5 OCH<sub>2</sub>2'''''''; 70.4 OCH<sub>2</sub>1'''''''''; 70.5 OCH<sub>2</sub>2'''''''''; 70.5 OCH<sub>2</sub>2'''''''''; 70.5 OCH<sub>2</sub>1'''''''''; 70.7 OCH<sub>2</sub>1'''''''''; 71.8 OCH<sub>2</sub>2'''''''''''; 109.1 ArC2''; 113.6 ArC5''; 119.4 ArC6''; 121.2  $\text{C}_{\text{vinyl}1'}$ ;

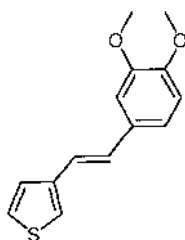
121.6 ThC4; 124.7 ThC2; 126.0 ThC5; 128.3 C<sub>vinyl</sub>2'; 130.9 ArC1''; 140.1 ThC3; 148.0 ArC4''; 149.6 ArC3''.

Electronic spectrum (MeCN)  $\lambda_{\max}$  nm/(log  $\epsilon$ ) 317.5 (4.41), 298.0 (4.38), 216.0 (4.26).

HRMS (FAB) M<sup>+</sup> calc 422.1763, found 422.1782.

Anal. Calculated for C<sub>22</sub>H<sub>30</sub>O<sub>6</sub>S; C, 62.54; H, 7.16; S, 7.59. Found: C, 61.58; H, 7.56; S, 7.27.

### 3-[2'-(3'',4''-Dimethoxy-phenyl)-vinyl]-thiophene (XXXVI)



Thiophen-3-ylmethyl-phosphonic acid diethyl ester (0.5040 g, 2.15 mmol) and 3,4-dimethoxybenzaldehyde (0.3573 g, 2.15 mmol) were dissolved in dry CH<sub>2</sub>Cl<sub>2</sub> (10 mL) before potassium tert-butoxide (0.6997 g, 6.23 mmol) was added and the solution left to stir at room temperature under N<sub>2</sub> for 30 minutes. H<sub>2</sub>O (20 mL) was added and acidified with 2M HCl. The organic layer was separated and the aqueous layer washed with CH<sub>2</sub>Cl<sub>2</sub> (20 mL), before the combined organic layers were washed with H<sub>2</sub>O (25 mL) and the solvent removed under reduced pressure. The residue was dissolved in CH<sub>2</sub>Cl<sub>2</sub> and rinsed through a plug of silica with CH<sub>2</sub>Cl<sub>2</sub>. The eluent was dried to yield an off-white solid, melting point = 87-89°C, (0.2859 g, 54%).

<sup>1</sup>H NMR (400 MHz, CD<sub>2</sub>Cl<sub>2</sub>)  $\delta$  3.84 (s, 3H, 4''OCH<sub>3</sub>); 3.88 (s, 3H, 3''OCH<sub>3</sub>); 6.85 (d, 1H, <sup>3</sup>J = 8.2 Hz, ArH5''); 6.91 (d, 1H, <sup>3</sup>J = 16.3 Hz, H<sub>vinyl</sub>2'); 7.01 (dd, 1H, <sup>3</sup>J =

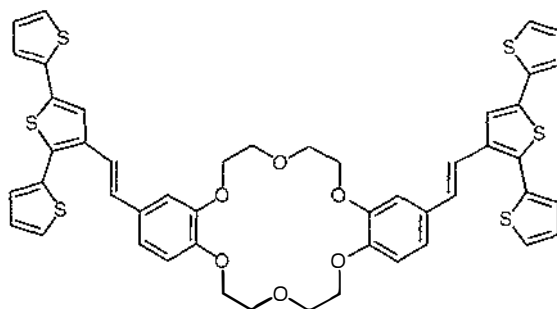
8.2 Hz,  $^4J = 2.0$  Hz, ArH2"); 7.03 (d, 1H,  $^3J = 16.2$  Hz,  $H_{\text{vinyl}1'}$ ); 7.04 (d, 1H,  $^4J = 2.2$  Hz, ArH2"); 7.25-7.26 (m, 1H, ThH 4"); 7.32-7.36 (m, 2H, ThH 2", 5").

$^{13}\text{C}$  NMR (100.6 MHz,  $\text{CD}_2\text{Cl}_2$ )  $\delta$  55.3 3"OCH<sub>3</sub>, 55.4 4"OCH<sub>3</sub>; 108.3 ArC2"; 111.1 ArC5"; 119.2 ArC6"; 120.5  $C_{\text{vinyl}1'}$ ; 121.3 ThC4; 124.4 ThC2; 125.8 ThC5; 128.0  $C_{\text{vinyl}2'}$ ; 130.0 ArC1"; 140.0 ThC3; 148.7 ArC4"; 149.0 ArC3".

Electronic spectrum (MeCN)  $\lambda_{\text{max}}$  nm/(log  $\epsilon$ ) 216.5 (4.26), 297.5 (4.38), 318.0 (4.40).

HRMS (FAB)  $M^+$  calc 246.0715, found 246.0711.

**2,14-Bis-(2-[2,2';5',2'']terthiophen-3'-yl-vinyl)-6,7,9,10,17,18,20,21-octahydro-5,8,11,16,19,22-hexaoxa-dibenzo[a,j]cyclooctadecene (XXXVII)**



6,7,9,10,17,18,20,21-Octahydro-5,8,11,16,19,22-

hexaoxadibenzo[a,j]cyclooctadecene-2,14-dicarbaldehyde (101.6 mg, 0.24 mmol) was dissolved in dry  $\text{CH}_2\text{Cl}_2$  (50 mL) under  $\text{N}_2$  by sonication. Terthiophene phosphonate (2 mL x 0.264 mol/L solution in THF, 0.53 mmol) was added, followed by potassium tert-butoxide (0.5476 g, 4.88 mmol) causing the reaction mixture to turn briefly dark red, then cloudy yellow. The solution was sonicated for 20 minutes, then diluted with  $\text{CH}_2\text{Cl}_2$  (100 mL).  $\text{H}_2\text{O}$  (20 mL) was added and acidified with 2M HCl before the organic layer was separated and washed with  $\text{H}_2\text{O}$  (20 mL). The solvent

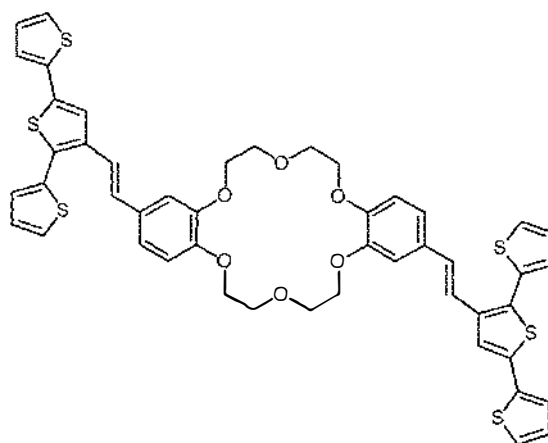
was removed, and the yellow residue suspended in CH<sub>2</sub>Cl<sub>2</sub> (1000 mL) then loaded onto a short, wide silica column. After 1,2-bis([2',2'';5'',2''']terthiophen-3''-yl)ethene (17.1 mg, 27%) was eluted in CH<sub>2</sub>Cl<sub>2</sub>, the product was eluted as a yellow band in 3% MeOH. Removal of solvent under reduced pressure yielded an insoluble yellow solid (114.7 mg, 52%).

HRMS (FAB) (M+Na)<sup>+</sup> calc 927.1047, found 927.1039.

Anal. Calculated for C<sub>48</sub>H<sub>40</sub>O<sub>6</sub>S<sub>6</sub>Na; C, 62.11; H, 4.34; S, 20.73. Found: C, 62.35; H, 4.48; S, 20.98.

Further characterisation was not possible due to insolubility of the material in a wide variety of common solvents including alkanes, alcohols, ethers, esters, ketones, chlorinated solvents, aromatics, DMF and THF.

**2,13-Bis-(2-[2,2';5',2'']terthiophen-3'-yl-vinyl)-6,7,9,10,17,18,20,21-octahydro-5,8,11,16,19,22-hexaoxa-dibenzo[a,j]cyclooctadecene (XXXVIII)**



6,7,9,10,17,18,20,21-Octahydro-5,8,11,16,19,22-hexaoxadibenzo[a,j]cyclooctadecene-2,13-dicarbaldehyde (50.1 mg, 0.12 mmol) was dissolved in dry CH<sub>2</sub>Cl<sub>2</sub> (50 mL) under N<sub>2</sub> by sonication. Terthiophene phosphonate

(1 mL x 0.26 mol/L solution in THF, 0.26 mmol) was added, followed by potassium tert-butoxide (0.2899 g, 2.6 mmol) causing the reaction mixture to turn briefly dark red, then cloudy yellow. The solution was sonicated for 1 hour and subsequently washed with 2M HCl (20 mL). The solvent was removed, and the yellow residue suspended in CH<sub>2</sub>Cl<sub>2</sub> (150 mL), before being loaded onto a short, wide silica column. After 1,2-bis([2',2'';5'',2''']terthiophen-3''-yl)ethene (7.5 mg, 24%) was eluted in CH<sub>2</sub>Cl<sub>2</sub>, the product was eluted as a yellow band in 3% MeOH. Removal of solvent under reduced pressure yielded an insoluble yellow solid (77.5 mg, 71%).

HRMS (FAB) M<sup>+</sup> calc 904.1149, found 904.1147.

Anal. Calculated for C<sub>48</sub>H<sub>40</sub>O<sub>6</sub>S<sub>6</sub>; C, 63.69; H, 4.45; S, 21.25. Found: C, 63.37; H, 5.13; S, 18.61.

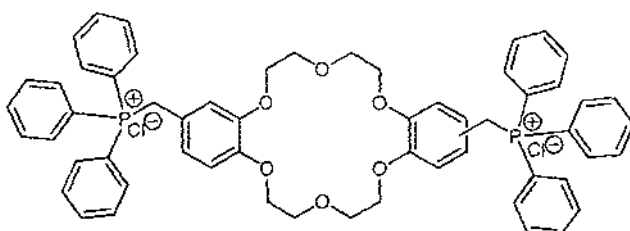
Further characterisation was not possible due to insolubility of the material in a wide variety of common solvents, including alkanes, alcohols, ethers, esters, ketones, chlorinated solvents, aromatics, DMF and THF.

**[13-(Diethoxy-phosphorylmethyl)-6,7,9,10,17,18,20,21-octahydro-5,8,11,16,19,22-hexaoxa-dibenzo[a,j]cyclooctadecen-2-ylmethyl]-triphenyl-phosphonium chloride**

and

**[14-(Diethoxy-phosphorylmethyl)-6,7,9,10,17,18,20,21-octahydro-5,8,11,16,19,22-hexaoxa-dibenzo[a,j]cyclooctadecen-2-ylmethyl]-triphenyl-phosphonium chloride**

**(XXXIX)**



Dichloromethylbenzo-18-crown-6 (1.5530 g, 3.40 mmol) was stirred in toluene (20 mL) and triphenylphosphine (2.8297 g, 10.79 mmol) added. The mixture was heated to reflux for 3 hours after which the solid was filtered, washed with toluene and excess solvent removed under reduced pressure. 1,2-dichloroethane (20 mL) and triphenylphosphine (1.8129 g, 6.91 mmol) were added and the solution refluxed for a further 3 hours. After cooling the solution was diluted with hexane, the solid removed by filtration, washed with toluene and dried under vacuum to yield the title compound as an off-white powder (2.7342 g, 82%).

$^1\text{H}$  NMR (400 MHz,  $\text{CDCl}_3$ )  $\delta$  3.65-3.68(m, 16H,  $\text{OCH}_2$ ); 5.16 (d, 4H,  $^2J_{\text{H,P}} = 8.9$  Hz,  $\text{CH}_2\text{P}$ ); 6.45-6.46 (m, 2H, ArH); 7.13-7.20 (m, 4H, ArH); 7.54-7.71 (m, 30H, ArH).

$^{31}\text{P}$  NMR (162.0 MHz,  $\text{CDCl}_3$ )  $\delta$  23.7.

Electronic spectrum ( $\text{CHCl}_3$ )  $\lambda_{\text{max}}$  nm/(log  $\epsilon$ ) 269.5 (4.07), 276.0 (4.08).

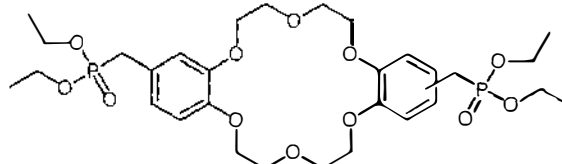
HRMS (FAB) ( $\text{M}-\text{Cl}$ ) $^+$  calc 945.3241, found 945.3274.

**[13-(Diethoxy-phosphorylmethyl)-6,7,9,10,17,18,20,21-octahydro-5,8,11,16,19,22-hexaoxa-dibenzo[a,j]cyclooctadecen-2-ylmethyl]-phosphonic acid diethyl ester**

and

**[14-(Diethoxy-phosphorylmethyl)-6,7,9,10,17,18,20,21-octahydro-5,8,11,16,19,22-hexaoxa-dibenzo[a,j]cyclooctadecen-2-ylmethyl]-phosphonic acid diethyl ester**

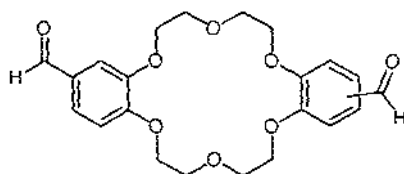
(XL)



Dichloromethylbenzo-18-crown-6 **XLIII** (1.5530 g, 3.40 mmol) was heated to reflux with triethyl phosphite (40 mL, as the solvent) under Ar for 16 hours, before excess triethyl phosphite was removed under vacuum. Purification by chromatography and distillation failed, so the product was used without further purification.

HRMS (FAB) (MH)<sup>+</sup> calc 661.2543, found 661.2550.

**6,7,9,10,17,18,20,21-Octahydro-5,8,11,16,19,22-hexaoxa-  
dibenzo[a,j]cyclooctadecene-2,14-dicarbaldehyde**  
and  
**6,7,9,10,17,18,20,21-Octahydro-5,8,11,16,19,22-hexaoxa-  
dibenzo[a,j]cyclooctadecene-2,13-dicarbaldehyde**  
(XLI)



Dibenzo-18-crown-6 was formylated using the Smith modification of the Duff reaction according to the method of Wada *et al.*<sup>177</sup> Phosphorus oxychloride (6.95 mL, 11.44 g, 0.075 mol) was added to N-methylformanilide (9.20 mL, 10.08 g, 0.075 mol) under Ar and left to stir at room temperature for 20 minutes. Dibenzo-18-crown-6 (6.49 g, 0.018 mol) was added and the solution heated for 5 hours at 90°C before leaving to cool overnight. The solution was heated to 60°C and H<sub>2</sub>O added (100 mL). The aqueous solution was extracted with CHCl<sub>3</sub> (6 x 50 mL), and the organic extracts dried over MgSO<sub>4</sub> and solvent removed. The solid was washed with acetone and dried to yield a 1:1 isomeric mixture of the title compounds (5.757 g, 77%, lit 90%<sup>177</sup>).

$^1\text{H}$  NMR (400.1 MHz,  $\text{CDCl}_3$ )  $\delta$  4.00-4.04 (m, 8H,  $\text{OCH}_2$ ); 4.20-4.24 (m, 8H,  $\text{OCH}_2$ ); 6.92 (d, 1H,  $^3J = 8.2$  Hz, ArH); 6.93 (d, 1H,  $^3J = 8.2$  Hz, ArH); 7.35 (d, 2H,  $^4J = 1.7$  Hz, ArH); 7.42 (dd, 2H,  $^3J = 8.2$  Hz,  $^4J = 1.8$  Hz, ArH); 9.82 (s, 1H, CHO); 9.82 (s, 1H, CHO).

$^{13}\text{C}$  NMR (68.1 MHz,  $\text{CDCl}_3$ )  $\delta$  68.1  $\text{OCH}_2$ ; 68.2  $\text{OCH}_2$ ; 68.3  $\text{OCH}_2$ ; 68.4  $\text{OCH}_2$ ; 69.2  $\text{OCH}_2$ ; 69.3  $\text{OCH}_2$ ; 69.4  $\text{OCH}_2$ ; 109.7 ArC; 109.8 ArC; 111.1 ArC; 111.1 ArC; 126.7 ArC; 126.9 ArC; 129.9 ArC; 130.0 ArC; 148.8 ArC; 148.8 ArC; 153.8 ArC; 153.8 ArC; 190.7 CHO.

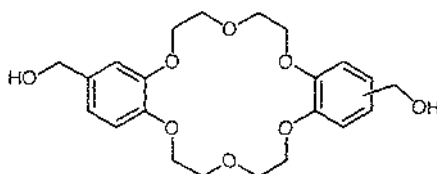
Electronic spectrum ( $\text{CH}_2\text{Cl}_2$ )  $\lambda_{\text{max}}$  nm/(log  $\epsilon$ ) 232.5 (4.41), 276.0 (4.26), 308.0 (4.14).

**(13-Hydroxymethyl-6,7,9,10,17,18,20,21-octahydro-5,8,11,16,19,22-hexaoxa-dibenzo[*a,j*]cyclooctadecen-2-yl)-methanol**

and

**(14-Hydroxymethyl-6,7,9,10,17,18,20,21-octahydro-5,8,11,16,19,22-hexaoxa-dibenzo[*a,j*]cyclooctadecen-2-yl)-methanol**

**(XLII)**



Diformylbenzo-18-crown-6 **XLI** (2.5084 g, 6.02 mmol) was stirred under Ar in 1:1 THF:ethanol (60 mL) before sodium borohydride (0.4702 g, 12.43 mmol) was added and the solution left to stir for 24 hours. The reaction was quenched with 1M HCl (50 mL) before the reaction mixture was extracted with  $\text{CH}_2\text{Cl}_2$  (3 x 45 mL). The organic extracts were washed with  $\text{H}_2\text{O}$  (50 mL), dried over  $\text{MgSO}_4$ , filtered and

evaporated to yield the desired dialcohol **XLII** as an off-white powder (1.8971 g, 75%).

$^1\text{H NMR}$  (270.2 MHz,  $\text{CDCl}_3$ )  $\delta$  3.99-4.04 (m, 8H,  $\text{OCH}_2$ ); 4.12-4.17 (m, 8H,  $\text{OCH}_2$ ); 4.58 (s, 4H,  $\text{ArCH}_2$ ); 6.80-6.88 (m, 6H, 6 x  $\text{ArH}$ ).

$^{13}\text{C NMR}$  (68.1 MHz,  $\text{CDCl}_3$ )  $\delta$  65.0  $\text{CH}_2\text{OH}$ ; 68.1  $\text{OCH}_2$ ; 69.6  $\text{OCH}_2$ ; 112.5  $\text{ArC}$ ; 119.3  $\text{ArC}$ ; 120.9  $\text{ArC}$ ; 133.7  $\text{ArC}$ ; 147.7  $\text{ArCO}$ ; 148.3  $\text{ArCO}$ .

Electronic spectrum ( $\text{CH}_2\text{Cl}_2$ )  $\lambda_{\text{max}}$  nm/(log  $\epsilon$ ) 280.5 (3.76).

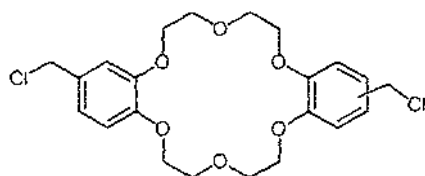
HRMS (FAB)  $\text{M}^+$  calc 420.1784, found 420.1781.

**2,14-Dichloromethyl-6,7,9,10,17,18,20,21-octahydro-5,8,11,16,19,22-hexaoxa-dibenzo[*a,j*]cyclooctadecene**

and

**2,13-Dichloromethyl-6,7,9,10,17,18,20,21-octahydro-5,8,11,16,19,22-hexaoxa-dibenzo[*a,j*]cyclooctadecene**

**(XLIII)**



Dihydroxymethylbenzo-18-crown-6 **XLII** (1.8670 g, 4.44 mmol) was stirred under Ar in dry benzene (15 mL) before thionyl chloride (1.40 mL, 2.28 g, 19.2 mmol) in dry benzene (30 mL) was added and the solution left to stir for 1 hour. The reaction was quenched with  $\text{H}_2\text{O}$  (50 mL) before the reaction mixture was extracted with  $\text{CH}_2\text{Cl}_2$  (3 x 50 mL). The organic extracts were dried over  $\text{MgSO}_4$ , filtered and evaporated to yield the desired dichloro crown **XLIII** as an off-white powder (1.7904 g, 88%).

$^1\text{H}$  NMR (270.2 MHz,  $\text{CDCl}_3$ )  $\delta$  3.99-4.04 (m, 8H,  $\text{OCH}_2$ ); 4.14-4.19 (m, 8H,  $\text{OCH}_2$ ); 4.54 (s, 4H,  $\text{CH}_2\text{Cl}$ ); 6.78-6.91 (m, 6H, 6 x ArH).

$^{13}\text{C}$  NMR (68.1 MHz,  $\text{CDCl}_3$ )  $\delta$  46.7  $\text{CH}_2\text{Cl}$ ; 68.6  $\text{OCH}_2$ ; 69.7  $\text{OCH}_2$ ; 112.7 ArC; 113.5 ArC; 121.4 ArC; 130.2 ArC; 148.6 ArCO; 148.7 ArCO.

Electronic spectrum ( $\text{CH}_2\text{Cl}_2$ )  $\lambda_{\text{max}}$  nm/(log  $\epsilon$ ) 237.5 (4.12), 282.0 (3.83).

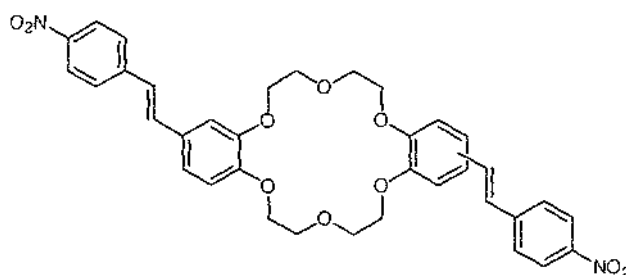
HRMS (FAB)  $\text{M}^+$  calc 458.1077, found 458.1095.

**2,13-Bis-[2'-(4''-nitro-phenyl)-vinyl]-6,7,9,10,17,18,20,21-octahydro-5,8,11,16,19,22-hexaoxa-dibenzo[a,j]cyclooctadecene**

and

**2,14-Bis-[2'-(4''-nitro-phenyl)-vinyl]-6,7,9,10,17,18,20,21-octahydro-5,8,11,16,19,22-hexaoxa-dibenzo[a,j]cyclooctadecene**

**(XLIV)**



Bis(phosphonate)-18-crown-6 (101.0 mg, 0.15 mmol max.) and 4-nitrobenzaldehyde (69.4 mg, 0.46 mmol) were dissolved in dry THF (10 mL) and stirred under  $\text{N}_2$ . Potassium tert-butoxide (55.4 mg, 0.49 mmol) was added and the solution left to stir for 2.5 hours before being neutralized with 2M HCl. The product was evaporated and redissolved in  $\text{CH}_2\text{Cl}_2$ , then subjected to column chromatography on silica. Gradient elution from  $\text{CH}_2\text{Cl}_2$  to 10% MeOH/ $\text{CH}_2\text{Cl}_2$  yielded 3 identifiable fractions. Fraction

1 (2.2 mg, 2%) and fraction 2 (6.9 mg, 7%) consisted of the title compounds, while a third fraction appeared to be 2-[2'-(4"-nitro-phenyl)-vinyl]-6,7,9,10,17,18,20,21-octahydro-5,8,11,16,19,22-hexaoxa-dibenzo[*a,j*]cyclooctadecene (5.3 mg, 7%).

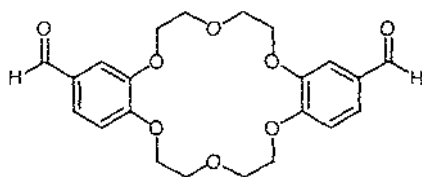
<sup>1</sup>H NMR (270 MHz, CDCl<sub>3</sub>) δ 4.06-4.09 (m, 8H, OCH<sub>2</sub>); 4.20-4.26 (m, 8H, ArOCH<sub>2</sub>); 6.87 (d, 2H, <sup>3</sup>*J* = 8.6 Hz, ArH); 6.99 (d, 2H, <sup>3</sup>*J* = 16.0 Hz, H<sub>vinyl</sub>2'); 7.08-7.10 (m, 4H, ArH); 7.19 (d, 2H, *J* = 16.0 Hz, H<sub>vinyl</sub>1'); 7.60 (d, 4H, <sup>3</sup>*J* = 8.6 Hz, ArH2'', 6''); 8.21 (d, 2H, <sup>3</sup>*J* = 8.8 Hz, ArH3'', 5'').

<sup>13</sup>C NMR (100.6 MHz, CDCl<sub>3</sub>) δ 68.6 OCH<sub>2</sub>; 68.6 OCH<sub>2</sub>; 68.7 OCH<sub>2</sub>; 68.8 OCH<sub>2</sub>; 68.8 OCH<sub>2</sub>; 68.9 OCH<sub>2</sub>; 69.8 OCH<sub>2</sub>; 69.9 OCH<sub>2</sub>; 111.0 ArC; 112.9 ArC; 121.2 ArC; 124.1 ArC3'', 5''; 124.3 C<sub>vinyl</sub>2'; 126.4 ArC2'', 6''; 129.5 ArC; 133.0 C<sub>vinyl</sub>1'; 144.0 ArC1''; 146.4 ArC4''; 148.7 ArCO; 149.5 ArCO.

Electronic spectra (CH<sub>2</sub>Cl<sub>2</sub>) λ<sub>max</sub> nm/(log ε) 281.5 (4.10), 388.0 (4.39) and 275.0 (4.11), 379.5 (4.32).

Mass spectra (FAB) M<sup>+</sup> calc 654.2213, found 654.2181 and 654.2216.

**6,7,9,10,17,18,20,21-Octahydro-5,8,11,16,19,22-hexaoxadibenzo[*a,j*]cyclooctadecene-2,14-dicarbaldehyde (XLV)**



1,5-bis(2'-hydroxy,5'-formylphenoxy)-3-oxapentane (3.5040 g, 10.1 mmol) and potassium hydroxide (1.1677 g, 20.8 mmol) were brought to reflux in 1-butanol (350 mL). After 2 hours the solution was cooled and di(ethylene glycol)-di-*p*-tosylate (4.1900 g, 10.1 mmol) was added. The solution was then refluxed for 43 hours before

the solvent was removed under reduced pressure. The residue was dissolved in H<sub>2</sub>O (100 mL) and CH<sub>2</sub>Cl<sub>2</sub> (100 mL), and the CH<sub>2</sub>Cl<sub>2</sub> layer separated. The aqueous layer was extracted with CH<sub>2</sub>Cl<sub>2</sub> (25 mL), after which the combined CH<sub>2</sub>Cl<sub>2</sub> layers were washed with H<sub>2</sub>O (100 mL), dried over activated neutral Al<sub>2</sub>O<sub>3</sub>, filtered and the solvent removed under vacuum. The solid was suspended in acetone, filtered, and washed with acetone to yield a white microcrystalline powder, melting point = 214-218°C (1.4989 g, 36%).

<sup>1</sup>H NMR (400.1 MHz, CDCl<sub>3</sub>) δ 4.01-4.06 (m, 8H, OCH<sub>2</sub>); 4.22-4.25 (m, 8H, ArOCH<sub>2</sub>); 6.93 (d, 2H, <sup>3</sup>J = 8.2 Hz, ArH4, 12); 7.37 (d, 2H, <sup>4</sup>J = 1.8 Hz, ArH1, 15); 7.43 (dd, 2H, <sup>3</sup>J = 8.2 Hz, <sup>4</sup>J = 1.8 Hz, ArH3, 13); 9.83 (s, 2H, CHO).

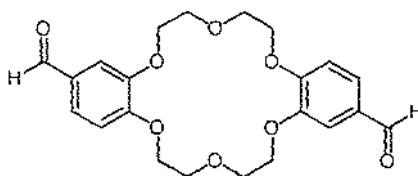
<sup>13</sup>C NMR (100.6 MHz, CDCl<sub>3</sub>) δ 68.1 ArOCH<sub>2</sub>; 68.3 ArOCH<sub>2</sub>; 69.3 OCH<sub>2</sub>; 69.3 OCH<sub>2</sub>; 109.6 ArC; 111.0 ArC; 126.9 ArC; 130.0 ArC; 148.9 ArCO; 153.8 ArCO; 191.0 CHO.

Electronic spectrum (MeCN) λ<sub>max</sub> nm/(log ε) 204.0 (4.45), 230.5 (4.57), 274.0 (4.37), 307.0 (4.28).

HRMS (FAB) MH<sup>+</sup> calc 417.1549, found 417.1530.

Anal. Calculated for C<sub>22</sub>H<sub>24</sub>O<sub>8</sub>; C, 63.45; H, 5.81. Found: C, 62.52; H, 5.79.

**6,7,9,10,17,18,20,21-Octahydro-5,8,11,16,19,22-hexaoxadibenzo[a,j]cyclooctadecene-2,13-dicarbaldehyde (XLVI)**



1-(2'-Hydroxy-4'-formylphenoxy)-5-(2''-hydroxy-5'''-formylphenoxy)-3-oxapentane (108.8 mg, 0.314 mmol) and sodium hydroxide (29.8 mg, 0.745 mmol) were brought to reflux in 1-butanol (100 mL). After 4 hours the solution was cooled and di(ethylene glycol)-di-*p*-tosylate (132.3 mg, 0.319 mmol) was added. The solution was then refluxed for 40 hours before the solvent was removed under reduced pressure. The residue was dissolved in H<sub>2</sub>O (20 mL) and CH<sub>2</sub>Cl<sub>2</sub> (20 mL), and the CH<sub>2</sub>Cl<sub>2</sub> layer separated. The aqueous layer was washed with CH<sub>2</sub>Cl<sub>2</sub> (20 mL), the combined CH<sub>2</sub>Cl<sub>2</sub> layers washed with H<sub>2</sub>O (20 mL), dried with activated neutral aluminium oxide, filtered and the solvent evaporated. The solid was suspended in acetone, filtered, washed with acetone and dried to give a cream powder, melting point 232-235 C (17.2 mg, 13%).

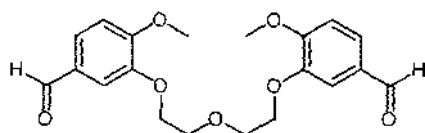
<sup>1</sup>H NMR (400.1 MHz, CDCl<sub>3</sub>) δ 4.02-4.06 (m, 8H, OCH<sub>2</sub>); 4.22-4.25 (m, 8H, ArOCH<sub>2</sub>); 6.94 (d, 2H, <sup>3</sup>*J* = 8.2 Hz, ArH<sub>4</sub>, 15); 7.37 (d, 2H, <sup>4</sup>*J* = 1.8 Hz, ArH<sub>1</sub>, 12); 7.43 (dd, 2H, <sup>3</sup>*J* = 8.2 Hz, <sup>4</sup>*J* = 1.8 Hz, ArH<sub>3</sub>, 14); 9.83 (s, 2H, CHO).

<sup>13</sup>C NMR (68.0 MHz, CDCl<sub>3</sub>) δ 68.3 ArOCH<sub>2</sub>; 68.4 ArOCH<sub>2</sub>; 69.3 OCH<sub>2</sub>; 69.5 OCH<sub>2</sub>; 109.8 ArC; 111.1 ArC; 127.0 ArC; 130.0 ArC; 148.8 ArCO; 153.9 ArCO; 190.8 CHO.

Electronic spectrum (CH<sub>2</sub>Cl<sub>2</sub>) λ<sub>max</sub> nm/(log ε) 232.5 (4.51), 276.0 (4.35), 309.0 (4.27).

HRMS (FAB) MH<sup>+</sup> calc 417.1549, found 417.1557.

### 1,5-bis(2'-Methoxy-5'-formylphenoxy)-3-oxapentane (XLVII)



1,5-bis(2'-Methoxy-5'-formylphenoxy)-3-oxapentane was prepared according to the method of Kumar and Mashraqui.<sup>239</sup> Isovanillin (12.1792 g, 80.0 mmol), potassium carbonate (11.0818 g, 80.2 mmol) and di(ethylene glycol)-di-*p*-tosylate (16.5940 g, 40.0 mmol) were heated in dry dimethylformamide (100 mL) under nitrogen at 110°C for 137 hours. The solution was poured into water (500 mL), causing a white precipitate to form. The precipitate was isolated by filtering through a 0.5 μm FH membrane (Millipore) that had been pre-saturated with methanol. The product was re-suspended in water (300 mL) and filtered again, before being recrystallised from ethanol to yield white crystals (11.5152 g, 77%).

<sup>1</sup>H NMR (400.1 MHz, CDCl<sub>3</sub>) δ 3.89 (s, 6H, OCH<sub>3</sub>); 3.96-3.99 (m, 4H, OCH<sub>2</sub>, 4); 4.22-4.25 (m, 4H, OCH<sub>2</sub>, 5); 6.93 (d, 2H, <sup>3</sup>J = 8.2 Hz, ArH3'); 7.39 (d, 2H, <sup>4</sup>J = 1.9 Hz, ArH6'); 7.43 (dd, 2H, <sup>3</sup>J = 8.2 Hz, <sup>4</sup>J = 1.9 Hz, ArH4'); 9.79 (s, 2H, CHO).

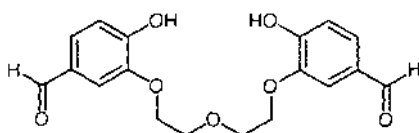
<sup>13</sup>C NMR (100.6 MHz, CDCl<sub>3</sub>) δ 56.0 OCH<sub>3</sub>; 68.4 OCH<sub>2</sub>, 5; 69.5 OCH<sub>2</sub>, 4; 110.6 Ar3'; 110.8 ArC6'; 126.7 ArC4'; 129.8 ArC5'; 148.6 ArC1'; 154.8 ArC2'; 190.7 CHO.

Electronic spectrum (CHCl<sub>3</sub>) λ<sub>max</sub> nm/(log ε) 204.0 (4.41), 230.0 (4.56), 273.5 (4.35), 305.5 (4.23).

HRMS (FAB) MH<sup>+</sup> calc 375.1443, found 375.1452.

Anal. Calculated for C<sub>20</sub>H<sub>22</sub>O<sub>7</sub>: C, 64.16; H, 5.92. Found: C, 63.85; H, 5.95.

### 1,5-bis(2'-Hydroxy-5'-formylphenoxy)-3-oxapentane (XLVIII)



Sodium hydride in 20% paraffin oil (3.2649 g, 0.109 mol) was stirred under Ar with dry DMF (150 mL). Ethanethiol (8.3 mL, 0.112 mol) was added and the mixture left to stir for 10 minutes before 1,5-bis(2-methoxy-5-formylphenoxy)-3-oxapentane (10.5021 g, 0.028 mol) was added. The solution was heated to 160°C for 3.5 hrs before evaporating under vacuum with heating to 50°C. 1M HCl (100 mL) was added, followed by CH<sub>2</sub>Cl<sub>2</sub> (100 mL) and the mixture left to stir until it had completely dissolved. The organic layer was separated, and the aqueous layer extracted with CH<sub>2</sub>Cl<sub>2</sub> (2 x 50 mL). The combined CH<sub>2</sub>Cl<sub>2</sub> layers were washed with H<sub>2</sub>O (100 mL), dried with MgSO<sub>4</sub>, filtered and the solvent removed under reduced pressure. The residue was purified by flash column chromatography on silica (gradient elution 0% - 1.5% MeOH in CH<sub>2</sub>Cl<sub>2</sub>), and the product recrystallised from MeOH, yielding a pale tan product, mass = 7.2206 g (75%).

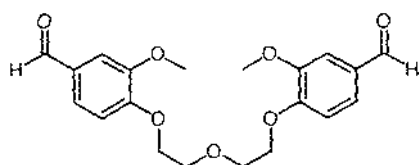
<sup>1</sup>H NMR (400.1 MHz, CDCl<sub>3</sub>) δ 3.94-3.96 (m, 4H, OCH<sub>2</sub>2, 4); 4.28-4.30 (m, 4H, OCH<sub>2</sub>1, 5); 7.08 (d, 2H, <sup>3</sup>J = 7.0 Hz, ArH3'); 7.48 (s, 2H, ArH6'); 7.49 (dd, 2H, <sup>3</sup>J = 7.5 Hz, <sup>4</sup>J = 1.9 Hz, ArH4'); 9.81 (s, 2H, CHO).

<sup>13</sup>C NMR (100.6 MHz, CDCl<sub>3</sub>) δ 69.0 OCH<sub>2</sub>1, 5; 69.3 OCH<sub>2</sub>2, 4; 113.5 ArC6'; 116.0 ArC3'; 128.6 ArC4'; 129.7 ArC5'; 146.3 ArC1'; 153.3 ArC2'; 190.7 CHO.

Electronic spectrum (MeCN) λ<sub>max</sub> nm/(log ε) 203.0 (4.44), 227.0 (4.45), 273.0 (4.31), 300.5 (4.14).

HRMS (FAB) MH<sup>+</sup> calc 347.1131, found 347.1147.

### 1,5-bis(2'-Methoxy-4'-formylphenoxy)-3-oxapentane (XLIX)



1,5-bis(2'-Methoxy-4'-formylphenoxy)-3-oxapentane was prepared according to the method of Tuncer and Erk.<sup>234</sup> Vanillin (15.2271 g, 0.100 mol) and potassium carbonate (13.8487 g, 0.100 mol) were stirred in dimethylformamide (80 mL) before dichlorodiethyl ether (5.9 mL, 0.050 mol) was added and the solution heated to 95°C for 235 hours. After cooling, the solution was diluted with water (120 mL) and 2M HCl (40 mL) added slowly. The white precipitate that formed was removed by filtering through a 0.5 µm FH membrane (Millipore) that had been pre-saturated with methanol. The precipitate was re-suspended in H<sub>2</sub>O and filtered as previously. The solid residue was dissolved in CH<sub>2</sub>Cl<sub>2</sub> (200 mL), washed with H<sub>2</sub>O (50 mL), dried with MgSO<sub>4</sub>, filtered and dried under vacuum. Recrystallisation from methanol gave white crystals, melting point = 130-131°C (15.49 g, 83%).

<sup>1</sup>H NMR (400.1 MHz, CDCl<sub>3</sub>) δ 3.90 (s, 6H, OCH<sub>3</sub>); 4.00-4.03 (m, 4H, OCH<sub>2</sub>2, 4); 4.27-4.30 (m, 4H, OCH<sub>2</sub>1, 5); 7.00 (d, 2H, <sup>3</sup>J = 8.1 Hz, ArH6'); 7.39 (d, 2H, <sup>4</sup>J = 1.7 Hz, ArH3'); 7.41 (dd, 2H, <sup>3</sup>J = 8.0 Hz, <sup>4</sup>J = 1.9 Hz, ArH5'); 9.83 (s, 2H, CHO).

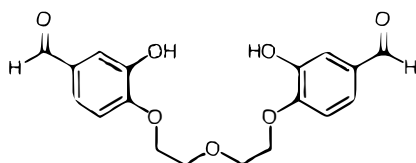
<sup>13</sup>C NMR (100.6 MHz, CDCl<sub>3</sub>) δ 55.9 OCH<sub>3</sub>; 68.5 OCH<sub>2</sub>1, 5; 69.6 OCH<sub>2</sub>2, 4; 109.2 ArC3'; 111.8 ArC6'; 126.5 ArC5'; 130.2 ArC4'; 149.8 ArC2'; 153.7 ArC1'; 190.9 CHO.

Electronic spectrum (MeCN) λ<sub>max</sub> nm/(log ε) 203.5 (4.43), 229.5 (4.53), 274.0 (4.38), 306.5 (4.28).

HRMS (FAB) MH<sup>+</sup> calc 375.1444, found 375.1429.

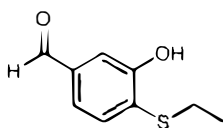
Anal. Calculated for C<sub>20</sub>H<sub>22</sub>O<sub>7</sub>; C, 64.16; H, 5.92. Found: C, 64.15; H, 5.91.

## Attempted preparation of 1,5-bis(2'-hydroxy-4'-formylphenoxy)-3-oxapentane (L)



Sodium hydride in 20% paraffin oil (1.2902 g, 43.0 mmol) was stirred under Ar in dry DMF (100 mL) for 5 minutes before ethanethiol (3.30 mL, 44.6 mmol) was added. After 15 minutes, when the solution had gone clear, 1,5-bis(2'-methoxy-4'-formylphenoxy)-3-oxapentane (4.0889 g, 10.92 mmol) was added and the solution heated to 160°C for 4 hours. After removing excess thiol, solvent and by-product under vacuum, the residue was dissolved in CH<sub>2</sub>Cl<sub>2</sub> (100 mL) and 1M HCl (50 mL). The organic layer was separated and the aqueous layer extracted with CH<sub>2</sub>Cl<sub>2</sub> (2 x 40 mL). The combined organic layers were washed with H<sub>2</sub>O (60 mL), dried with MgSO<sub>4</sub>, filtered and evaporated. The residue was purified by flash column chromatography on silica utilizing gradient elution from 0% - 1.5% MeOH/CH<sub>2</sub>Cl<sub>2</sub>, yielding 4-ethylsulfanyl-3-hydroxy-benzaldehyde **LI** (0.8735 g, 44%, melting point = 72-73°C) and 3-hydroxy-4-[2-(2-hydroxy-ethoxy)-ethoxy]-benzaldehyde **LII** (0.2335 g, 9%, melting point = 70-73°C). Characterisation for these two compounds follows. The desired product was not isolated.

### 4-Ethylsulfanyl-3-hydroxy-benzaldehyde (LI)



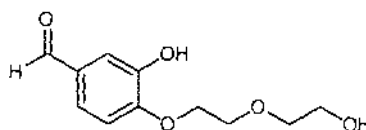
<sup>1</sup>H NMR (400.1 MHz, CDCl<sub>3</sub>) δ 1.27 (t, 3H, <sup>3</sup>J = 7.4 Hz, CH<sub>3</sub>); 2.85 (q, 2H, <sup>3</sup>J = 7.4 Hz, CH<sub>2</sub>); 6.89 (s, 1H, OH); 7.40 (dd, 1H, <sup>3</sup>J = 7.9 Hz, <sup>4</sup>J = 1.7 Hz, ArH<sub>6</sub>); 7.45 (d, 1H, <sup>4</sup>J = 1.7 Hz, ArH<sub>2</sub>); 7.57 (d, 1H, <sup>3</sup>J = 7.9 Hz, ArH<sub>5</sub>); 9.93 (s, 1H, CHO).

$^{13}\text{C}$  NMR (100.6 MHz,  $\text{CDCl}_3$ )  $\delta$  14.7  $\text{CH}_3$ ; 29.8  $\text{CH}_2$ ; 114.9 ArC2; 121.8 ArC6; 127.8 ArC4; 134.3 ArC5; 137.5 ArC1; 156.6 ArC3; 191.6 CHO.

Electronic spectrum (MeCN)  $\lambda_{\text{max}}$  nm/(log  $\epsilon$ ) 209.5 (4.19), 245.0 (3.88), 298.5 (3.91), 329.0 (4.10).

HRMS (EI)  $\text{MH}^+$  calc 182.0402, found 182.0400.

### 3-Hydroxy-4-[2'-(2''-hydroxy-ethoxy)-ethoxy]-benzaldehyde (LII)



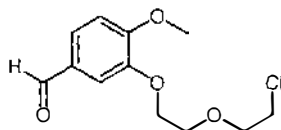
$^1\text{H}$  NMR (400.1 MHz,  $\text{CDCl}_3$ )  $\delta$  3.68-3.70 (m, 2H,  $\text{OCH}_21''$ ); 3.80-3.82 (m, 2H,  $\text{OCH}_22''$ ); 3.89-3.91 (m, 2H,  $\text{OCH}_22'$ ); 4.18-4.21 (m, 2H,  $\text{OCH}_21'$ ); 6.88 (d, 1H,  $^3J = 8.2$  Hz, ArH5); 7.33 (dd, 1H,  $^3J = 8.2$  Hz,  $^4J = 2.0$  Hz, ArH6); 7.38 (d, 1H,  $^4J = 2.0$  Hz, ArH2); 9.80 (s, 1H, CHO).

$^{13}\text{C}$  NMR (100.6 MHz,  $\text{CDCl}_3$ )  $\delta$  61.4  $\text{OCH}_22''$ ; 67.7  $\text{OCH}_21''$ ; 69.1  $\text{OCH}_22'$ ; 72.5  $\text{OCH}_21'$ ; 111.8 ArC5; 115.2 ArC2; 124.0 ArC6; 130.9 ArC1; 146.9 ArC3; 151.4 ArC4; 191.2 CHO.

Electronic spectrum (MeCN)  $\lambda_{\text{max}}$  nm/(log  $\epsilon$ ) 205.0 (4.20), 228.0 (4.19), 271.5 (4.03), 308.0 (3.89).

HRMS (EI)  $\text{M}^+$  calc 226.0841, found 226.0843.

### 3-[2'-(2''-Chloro-ethoxy)-ethoxy]-4-methoxy-benzaldehyde (LIII)



Isovanillin (19.4756 g, 0.128 mol) and potassium carbonate (17.6872 g, 0.128 mol) were heated in dimethylformamide (100 mL) to 90°C before 2-chloroethyl ether (15 mL, 0.128 mol) was added. The reaction mixture was heated for a further 113 hours, before filtering and evaporating under vacuum. The tan coloured solid was dissolved in CH<sub>2</sub>Cl<sub>2</sub> and purified by flash column chromatography on silica. Gradient elution (100:0 to 98:2 CH<sub>2</sub>Cl<sub>2</sub>:MeOH) gave the desired product as a white crystalline solid, melting point = 61-63°C, (13.8724 g, 42%). A second fraction yielded 1,5-bis(2'-methoxy-5'-formylphenoxy)-3-oxapentane **XLVII** as iridescent flakes after recrystallisation from ethanol, melting point = 130-132°C (11.0463 g, 46%).

<sup>1</sup>H NMR (400.1 MHz, CDCl<sub>3</sub>) δ 3.61-3.64 (m, 2H, OCH<sub>2</sub>2''); 3.82-3.79 (m, 2H, OCH<sub>2</sub>1''); 3.90 (s, 3H, OCH<sub>3</sub>); 3.89-3.91 (m, 2H, OCH<sub>2</sub>2'); 4.20-4.22 (m, 2H, OCH<sub>2</sub>1'); 6.94 (d, 1H, <sup>3</sup>J = 8.2 Hz, ArH5); 7.39 (d, 1H, <sup>4</sup>J = 1.9 Hz, ArH2); 7.44 (dd, 1H, <sup>3</sup>J = 8.2 Hz, <sup>4</sup>J = 1.7 Hz, ArH6); 9.80 (s, 1H, CHO).

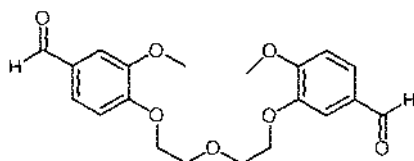
<sup>13</sup>C NMR (100.6 MHz, CDCl<sub>3</sub>) δ 42.5 OCH<sub>2</sub>2''; 56.0 OCH<sub>3</sub>; 68.3 OCH<sub>2</sub>1'; 69.3 OCH<sub>2</sub>2'; 71.4 OCH<sub>2</sub>1''; 110.6 ArC5; 110.8 ArC2; 126.8 ArC6; 129.8 ArC1; 148.5 ArC3; 154.7 ArC4; 190.7 CHO.

Electronic spectrum (CHCl<sub>3</sub>) λ<sub>max</sub> nm/(log ε) 204.0 (4.14), 229.5 (4.27), 273.5 (4.07), 305.5 (3.95).

HRMS (FAB) M<sup>+</sup> calc 258.0659, found 258.0657.

Anal. Calculated for C<sub>12</sub>H<sub>15</sub>ClO<sub>4</sub>; C, 55.71; H, 5.84. Found: C, 55.07; H, 5.68.

**1-(2'-Methoxy-4'-formylphenoxy)-5-(2''-methoxy-5''-formylphenoxy)-3-oxapentane (LIV)**



Sodium hydride in 20% paraffin oil (0.8361 g, 27.9 mmol) was stirred in dry dimethylformamide (50 mL) before vanillin (4.2616 g, 28.0 mmol) was added and the solution heated to 40°C for 30 minutes. 3-[2-(2-Chloroethoxy)-ethoxy]-4-methoxybenzaldehyde (7.2158 g, 27.9 mmol) was added and the solution heated to 95°C under nitrogen for a further 256 hours. After cooling, the reaction mixture was diluted with water (50 mL) and 1M HCl (100 mL), and CH<sub>2</sub>Cl<sub>2</sub> (50 mL) added. The organic layer was separated, and the aqueous extracted with CH<sub>2</sub>Cl<sub>2</sub> (2 x 50 mL) before the combined organic layers were washed with H<sub>2</sub>O (100 mL), dried with MgSO<sub>4</sub>, filtered and evaporated under reduced pressure. The brown solid thus obtained was dissolved in CH<sub>2</sub>Cl<sub>2</sub> and purified by flash column chromatography on silica. Fractions containing product only were combined and evaporated, then the solid recrystallised from methanol to yield 1-(2'-methoxy-4'-formylphenoxy)-5-(2''-methoxy-5''-formylphenoxy)-3-oxapentane as a white solid, melting point = 99-100°C, (5.7243 g, 55%).

<sup>1</sup>H NMR (400.1 MHz, CDCl<sub>3</sub>) δ 3.88 (s, 3H, OCH<sub>3</sub>''); 3.90 (s, 3H, OCH<sub>3</sub>''); 3.97-4.01 (m, 4H, OCH<sub>2</sub>2, 4); 4.23-4.25 (m, 2H, OCH<sub>2</sub>5); 4.26-4.29 (m, 2H, OCH<sub>2</sub>1); 6.95 (d, 1H, <sup>3</sup>J = 8.2 Hz, ArH3''); 6.99 (d, 1H, <sup>3</sup>J = 8.2 Hz, ArH6'); 7.36 (d, 1H, <sup>4</sup>J = 1.8 Hz, ArH3'); 7.39 (dd, 1H, <sup>3</sup>J = 8.1 Hz, <sup>4</sup>J = 1.9 Hz, ArH5'); 7.41 (d, 1H, <sup>4</sup>J = 1.9 Hz, ArH6''); 7.44 (dd, 1H, <sup>3</sup>J = 8.1 Hz, <sup>4</sup>J = 1.9 Hz, ArH4''); 9.80 (s, 1H, CHO''); 9.81 (s, 1H, CHO').

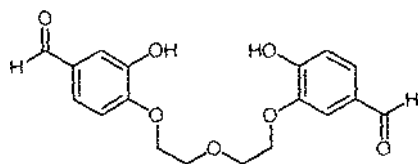
<sup>13</sup>C NMR (100.6 MHz, CDCl<sub>3</sub>) δ 55.8 OCH<sub>3</sub>''; 56.0 OCH<sub>3</sub>''; 68.4 OCH<sub>2</sub>1; 68.4 OCH<sub>2</sub>5; 69.5 OCH<sub>2</sub>4; 69.7 OCH<sub>2</sub>2; 109.1 ArC3'; 110.6 ArC3''; 110.7 ArC6''; 111.8 ArC6'; 126.5 ArC5'; 126.9 ArC4''; 129.8 ArC5''; 130.1 ArC4'; 148.7 ArC1''; 149.7 ArC2'; 153.7 ArC1'; 154.8 ArC2''; 190.7 CHO''; 190.9 CHO'.

Electronic spectrum (MeCN)  $\lambda_{\max}$  nm/(log  $\epsilon$ ) 204.0 (4.43), 229.5 (4.55), 274.0 (4.37), 306.5 (4.26).

HRMS (FAB)  $MH^+$  calc 375.1444, found 375.1438.

Anal. Calculated for  $C_{20}H_{22}O_7$ : C, 64.14; H, 5.92. Found: C, 64.44; H, 6.00.

**1-(2'-Hydroxy-4'-formylphenoxy)-5-(2''-hydroxy-5''-formylphenoxy)-3-oxapentane (LV)**



Sodium hydride in 20% paraffin oil (0.8086 g, 27.0 mmol) was stirred under Ar in dry DMF (150 mL). Ethanethiol (2.0 mL, 27.0 mmol) was added and the mixture left to stir for 10 minutes before 1-(2'-methoxy-4'-formylphenoxy)-5-(2''-methoxy-5''-formylphenoxy)-3-oxapentane (4.0147 g, 10.7 mmol) was added. The solution was heated to 160°C for 3 hours before the solvent was removed under vacuum. 1 M HCl (100 mL) was added, followed by  $CH_2Cl_2$  (100 mL) and the mixture left to stir until it had completely dissolved. The organic layer was separated, and the aqueous layer extracted with  $CH_2Cl_2$  (2 x 50 mL). The combined  $CH_2Cl_2$  layers were washed with  $H_2O$  (100 mL), dried with  $MgSO_4$ , filtered and the solvent removed under reduced pressure. The residue was purified by flash column chromatography on silica. Gradient elution from 0% to 1.5% MeOH in  $CH_2Cl_2$  yielded 4-ethylsulfanyl-3-methoxy-benzaldehyde **LVII** (0.4698 g, 22%), 4-ethylsulfanyl-3-hydroxy-benzaldehyde **LI** (0.5736 g, 29%, melting point = 72-73°C), 1-(2'-hydroxy-4'-formylphenoxy)-5-(2''-hydroxy-5''-formylphenoxy)-3-oxapentane **LV** (0.9686 g,

26%, melting point = 55-66°C) and 4-hydroxy-3-[2-(2-hydroxy-ethoxy)-ethoxy]-benzaldehyde **LVIII** (0.8781 g, 36%, melting point = 79-81°C).

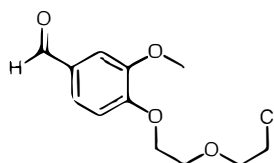
<sup>1</sup>H NMR (400.1 MHz, CDCl<sub>3</sub>) δ 3.89-3.94 (m, 4H, OCH<sub>2</sub>, 4); 4.24-4.29 (m, 4H, OCH<sub>2</sub>, 5); 7.00 (d, 1H, <sup>3</sup>J = 8.2 Hz, ArH6'); 7.07 (d, 1H, <sup>3</sup>J = 8.6 Hz, ArH3''); 7.38 (dd, 1H, <sup>3</sup>J = 8.2 Hz, <sup>4</sup>J = 2.0 Hz, ArH5'); 7.47-7.50 (m, 3H, ArH3', 4'', 6''); 9.79 (s, 1H, CHO''); 9.83 (s, 1H, CHO').

<sup>13</sup>C NMR (100.6 MHz, CDCl<sub>3</sub>) δ 69.1 OCH<sub>2</sub>; 69.2 OCH<sub>2</sub>; 69.3 OCH<sub>2</sub>; 69.6 OCH<sub>2</sub>; 114.2 ArC6''; 114.3 ArC6'; 115.8 ArC3''; 116.0 ArC3'; 123.8 ArC5'; 128.5 ArC4''; 129.7 ArC5''; 131.7 ArC4'; 146.3 ArC1''; 147.3 ArC2'; 151.0 ArC1'; 153.3 ArC2''; 190.7 CHO''; 191.1 CHO'.

Electronic spectrum (MeCN) λ<sub>max</sub> nm/(log ε) 203.5 (4.47), 227.5 (4.48), 272.0 (4.32), 303.5 (4.15).

HRMS (FAB) M<sup>+</sup> calc 347.1131, found 347.1121.

#### 4-[2'-(2''-Chloro-ethoxy)-ethoxy]-3-methoxy-benzaldehyde (**LVI**)



Vanillin (19.476 g, 0.128 mol) and potassium carbonate (17.700 g, 0.128 mol) were dissolved in DMF (100 mL) with heating to 80°C for 60 minutes. 2-Chloroethyl ether (15 mL, 0.128 mol) was added, and the solution heated for a further 119 hours at 90°C. After cooling, the solution was filtered using a buchner funnel, the solids washed with CH<sub>2</sub>Cl<sub>2</sub>, and the filtrate evaporated under vacuum. The solid residue was dissolved in CH<sub>2</sub>Cl<sub>2</sub> (200 mL) and purified by flash column chromatography on silica.

The title compound was eluted in  $\text{CH}_2\text{Cl}_2$ , and dried to yield white needles, melting point = 55-56°C (10.2651 g, 31%). A second fraction was eluted in 98:2  $\text{CH}_2\text{Cl}_2$ :MeOH and was identified as 1,5-bis(2'-methoxy-4'-formylphenoxy)-3-oxapentane **XLIX** (10.4212 g, 43%).

$^1\text{H}$  NMR (400.1 MHz,  $\text{CDCl}_3$ )  $\delta$  3.63-3.66 (m, 2H,  $\text{OCH}_2$ "); 3.82-3.85 (m, 2H,  $\text{OCH}_2$ "); 3.90 (s, 3H,  $\text{OCH}_3$ ); 3.93-3.95 (m, 2H,  $\text{OCH}_2$ "); 4.25-4.28 (m, 2H,  $\text{OCH}_2$ "); 7.00 (d, 1H,  $^3J = 8.2$  Hz, ArH5); 7.39 (d, 1H,  $^4J = 1.8$  Hz, ArH2); 7.42 (dd, 1H,  $^3J = 8.2$  Hz,  $^4J = 1.9$  Hz, ArH6); 9.84 (s, 1H, CHO).

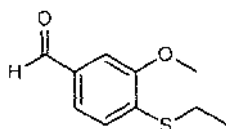
$^{13}\text{C}$  NMR (100.6 MHz,  $\text{CDCl}_3$ )  $\delta$  42.7  $\text{OCH}_2$ "); 55.9  $\text{OCH}_3$ ; 68.4  $\text{OCH}_2$ "); 69.3  $\text{OCH}_2$ "); 71.5  $\text{OCH}_2$ "); 109.2 ArC2; 111.8 ArC5; 126.5 ArC6 6; 130.3 ArC1; 149.8 ArC3; 153.6 ArC4; 190.9 CHO.

Electronic spectrum (MeCN)  $\lambda_{\text{max}}$  nm/(log  $\epsilon$ ) 202.5 (4.17), 229.0 (4.25), 274.0 (4.10), 307.0 (3.99).

HRMS (EI)  $M^+$  calc 258.0659, found 258.0655.

Anal. Calculated for  $\text{C}_{12}\text{H}_{15}\text{ClO}_4$ : C, 55.71; H, 5.84. Found: C, 55.62; H, 5.79.

#### 4-Ethylsulfanyl-3-methoxy-benzaldehyde (LVII)



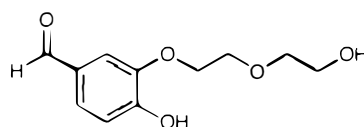
$^1\text{H}$  NMR (400.1 MHz,  $\text{CDCl}_3$ )  $\delta$  1.40 (t, 3H,  $^3J = 7.4$  Hz,  $\text{CH}_3$ ); 2.99 (q, 2H,  $^3J = 7.4$  Hz,  $\text{CH}_2$ ); 3.95 (s, 3H,  $\text{OCH}_3$ ); 7.25 (d, 1H,  $^3J = 7.9$  Hz, ArH5); 7.30 (d, 1H,  $^4J = 1.5$  Hz, ArH2); 7.41 (dd, 1H,  $^3J = 7.9$  Hz,  $^4J = 1.6$  Hz, ArH6); 9.89 (s, 1H, CHO).

$^{13}\text{C}$  NMR (100.6 MHz,  $\text{CDCl}_3$ )  $\delta$  13.4  $\text{CH}_3$ ; 24.7  $\text{CH}_2$ ; 55.9  $\text{OCH}_3$ ; 107.4 ArC2; 124.7 ArC5; 125.0 ArC6; 133.9 ArC1; 136.1 ArC4; 155.1 ArC3; 191.2 CHO.

Electronic spectrum (MeCN)  $\lambda_{\text{max}}$  nm/(log  $\epsilon$ ) 206.5 (4.23), 244.0 (3.94), 300.0 (3.98), 328.0 (4.20).

HRMS (FAB)  $\text{MH}^+$  calc 196.0558, found 196.0554.

#### 4-Hydroxy-3-[2'-(2''-hydroxy-ethoxy)-ethoxy]-benzaldehyde (LVIII)



$^1\text{H}$  NMR (400.1 MHz,  $\text{CDCl}_3$ )  $\delta$  3.69-3.72 (m, 2H,  $\text{OCH}_21''$ ); 3.82-3.84 (m, 2H,  $\text{OCH}_22''$ ); 3.89-3.91 (m, 2H,  $\text{OCH}_22'$ ); 4.19-4.21 (m, 2H,  $\text{OCH}_21'$ ); 7.00 (d, 1H,  $^3J = 8.1$  Hz, ArH5); 7.37 (d, 1H,  $^4J = 1.8$  Hz, ArH2); 7.41 (dd, 1H,  $^3J = 8.1$  Hz,  $^4J = 1.8$  Hz, ArH6); 9.78 (s, 1H, CHO).

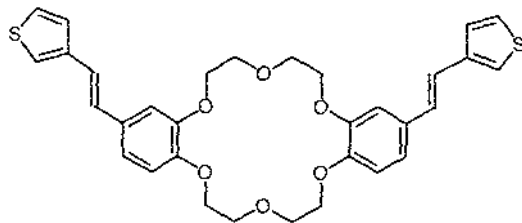
$^{13}\text{C}$  NMR (100.6 MHz,  $\text{CDCl}_3$ )  $\delta$  61.4  $\text{OCH}_22''$ ; 67.9  $\text{OCH}_21''$ ; 69.3  $\text{OCH}_22'$ ; 72.5  $\text{OCH}_21'$ ; 111.2 ArC2; 115.6 ArC5; 128.1 ArC6; 129.4 ArC1; 146.5 ArC3; 153.0 ArC4; 190.8 CHO.

Electronic spectrum (MeCN)  $\lambda_{\text{max}}$  nm/(log  $\epsilon$ ) 204.0 (4.15), 228.0 (4.21), 273.5 (4.05), 301.0 (3.89).

HRMS (FAB)  $\text{MH}^+$  calc 227.0919, found 227.0927.

Anal. Calculated for  $\text{C}_{11}\text{H}_{14}\text{O}_5$ : C, 58.40; H, 6.24. Found: C, 58.59; H, 6.14.

**2,14-Bis-(2'-thiophen-3''-yl-vinyl)-6,7,9,10,17,18,20,21-octahydro-5,8,11,16,19,22-hexaoxa-dibenzo[a,j]cyclooctadecene (LIX)**



6,7,9,10,17,18,20,21-Octahydro-5,8,11,16,19,22-

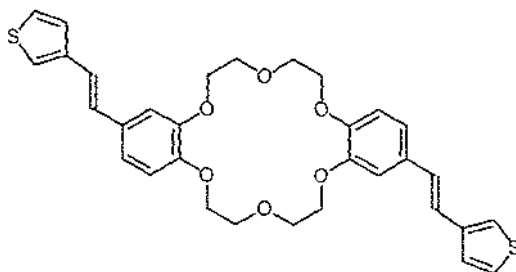
hexaoxadibenzo[a,j]cyclooctadecene-2,14-dicarbaldehyde (155.3 mg, 0.373 mmol) and thiophene phosphonate (191.8 mg, 0.819 mmol) were dissolved in dry CH<sub>2</sub>Cl<sub>2</sub> (30 mL) and stirred under N<sub>2</sub>. Potassium tert-butoxide (0.9658 g, 8.606 mmol) was added and the solution left to stir at room temperature for 30 minutes. The reaction mixture was diluted with CH<sub>2</sub>Cl<sub>2</sub> (10 mL) and H<sub>2</sub>O (40 mL), then neutralized with aqueous HCl. The organic layer was separated and the aqueous layer extracted with CH<sub>2</sub>Cl<sub>2</sub> (2 x 30 mL) before the combined organic extracts were washed with H<sub>2</sub>O (100 mL), dried over activated neutral Al<sub>2</sub>O<sub>3</sub>, filtered, and dried under vacuum. The residue was dissolved in CH<sub>2</sub>Cl<sub>2</sub> and purified by flash column chromatography on silica. After initially eluting in CH<sub>2</sub>Cl<sub>2</sub>, the product was removed as a pale yellow band in 2% MeOH. Removal of solvent under reduced pressure yielded 2,14-bis-(2-thiophen-3-yl-vinyl)-6,7,9,10,17,18,20,21-octahydro-5,8,11,16,19,22-hexaoxa-dibenzo[a,j]cyclooctadecene as a cream powder, melting point = 241-243°C (82.4 mg, 38%).

<sup>1</sup>H NMR (400.1 MHz, CD<sub>2</sub>Cl<sub>2</sub>) δ 3.94-3.99 (m, 8H, OCH<sub>2</sub>); 4.14-4.16 (m, 4H, ArOCH<sub>2</sub>); 4.18-4.21 (m, 4H, ArOCH<sub>2</sub>); 6.83 (d, 2H, <sup>3</sup>J = 8.1 Hz, ArH<sub>4</sub>, 12); 6.90 (d, 2H, <sup>3</sup>J = 16.3 Hz, H<sub>vinyl</sub>1'); 6.99-7.04 (m, 4H, ArH<sub>1</sub>, 3, 13, 15); 7.02 (d, 2H, <sup>3</sup>J = 16.6 Hz, H<sub>vinyl</sub>2'); 7.25 (dd, 2H, <sup>3</sup>J = 2.5 Hz, <sup>4</sup>J = 1.5 Hz, ThH<sub>4</sub>''); 7.32-7.36 (m, 4H, ThH<sub>2</sub>'', 5'').

Electronic spectrum (CH<sub>2</sub>Cl<sub>2</sub>) λ<sub>max</sub> nm/(log ε) 299.5 (4.55), 320.0 (4.57).

HRMS (FAB) M<sup>+</sup> calc 576.1640, found 576.1655.

**2,13-Bis-(2'-thiophen-3''-yl-vinyl)-6,7,9,10,17,18,20,21-octahydro-5,8,11,16,19,22-hexaoxa-dibenzo[a,j]cyclooctadecene (LX)**



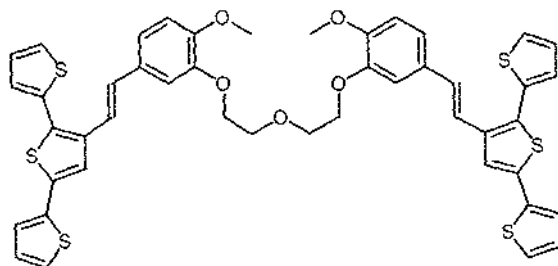
6,7,9,10,17,18,20,21-Octahydro-5,8,11,16,19,22-hexaoxadibenzo[a,j]cyclooctadecene-2,13-dicarbaldehyde (153.6 mg, 0.37 mmol) and thiophene phosphonate (186.5 mg, 0.80 mmol) were dissolved in dry  $\text{CH}_2\text{Cl}_2$  (50 mL) and stirred under  $\text{N}_2$ . Potassium tert-butoxide (0.9888 g, 8.81 mmol) was added and the solution left to stir at room temperature for 30 minutes.  $\text{H}_2\text{O}$  (50 mL) was added, then acidified with aqueous HCl. The organic layer was separated and the aqueous layer extracted with  $\text{CH}_2\text{Cl}_2$  (50 mL) before the combined organic extracts were washed with  $\text{H}_2\text{O}$  (100 mL) and dried under vacuum. The residue was dissolved in  $\text{CH}_2\text{Cl}_2$  with sonication, and filtered on a buchner funnel to remove insoluble material. The filtrate was then purified by flash column chromatography on silica. After initially eluting in  $\text{CH}_2\text{Cl}_2$ , the product was removed as a pale yellow band in 2% MeOH. The solution was concentrated and the product precipitated with hexane. After collection on a 0.5  $\mu\text{m}$  FH membrane (Millipore) and removal of solvent under reduced pressure, 2,13-bis-(2-thiophen-3-yl-vinyl)-6,7,9,10,17,18,20,21-octahydro-5,8,11,16,19,22-hexaoxa-dibenzo[a,j]cyclooctadecene was obtained as a cream powder, melting point = 220-222°C (83.6 mg, 39%).

$^1\text{H}$  NMR (400.1 MHz,  $\text{CD}_2\text{Cl}_2$ )  $\delta$  3.95-3.98 (m, 8H,  $\text{OCH}_2$ ); 4.14-4.17 (m, 4H,  $\text{ArOCH}_2$ ); 4.18-4.20 (m, 4H,  $\text{ArOCH}_2$ ); 6.82 (d, 1H,  $^3J = 8.0$  Hz, ArH); 6.83 (d, 1H,  $^3J = 8.0$  Hz, ArH); 6.90 (d, 2H,  $^3J = 16.4$  Hz,  $\text{H}_{\text{vinyl}1'}$ ); 7.00-7.04 (m, 4H, ArH1, 3, 12, 14); 7.02 (d, 2H,  $J = 16.2$  Hz,  $\text{H}_{\text{vinyl}2'}$ ); 7.24-7.25 (m, 2H, ThH4''); 7.32-7.37 (m, 4H, ThH2'', 5'').

Electronic spectrum ( $\text{CH}_2\text{Cl}_2$ )  $\lambda_{\text{max}}$  nm/(log  $\epsilon$ ) 300.0 (4.49), 320.0 (4.51).

HRMS (FAB)  $M^+$  calc 576.1674, found 576.1661.

**1,5-bis-(2'-Methoxyphenyl-5'-{2''-[2''',2''';5''',2''''']terthiophen-3'''-yl-vinyl})-3-oxapentane (LXI)**



1,5-bis-(2'-Methoxy-5'-formylphenoxy)-3-oxapentane (0.0523 g, 0.14 mmol) and terthiophene phosphonate (2 mL x 0.14 mmol/mL solution in THF, 0.28 mmol) were stirred in dry  $\text{CH}_2\text{Cl}_2$  (4 mL) under  $\text{N}_2$ . Potassium tert-butoxide (0.1460 g, 1.30 mmol) was added, and the solution left to stir at room temperature for 30 minutes.  $\text{H}_2\text{O}$  (20 mL) was added, and the solution acidified with aq. HCl. The organic layer was separated and the aqueous extracted with  $\text{CH}_2\text{Cl}_2$  (2 x 15 mL), before the combined organic layers were washed with  $\text{H}_2\text{O}$  (15 mL) and evaporated. The crude yellow residue was dissolved in  $\text{CH}_2\text{Cl}_2$  and subjected to flash column chromatography on silica. After the removal of 1,2-bis([2',2'';5'',2''']terthiophen-3''-yl)ethene (3.4 mg, 2%) in  $\text{CH}_2\text{Cl}_2$ , the desired product was eluted in 2% MeOH, melting point = 55-58°C (0.1180 g, 98%).

$^1\text{H}$  NMR (400.1 MHz,  $\text{CD}_2\text{Cl}_2$ )  $\delta$  3.83 (s, 6H,  $\text{OCH}_3$ ); 3.91-3.94 (m, 4H,  $\text{OCH}_2$ , 4); 4.17-4.20 (m, 4H,  $\text{OCH}_2$ , 5); 6.85 (d, 2H,  $^3J = 8.5$  Hz,  $\text{ArH}3'$ ); 6.96 (d, 2H,  $^3J = 16.1$  Hz,  $\text{H}_{\text{vinyl}}1''$ ); 7.03-7.06 (m, 4H,  $\text{ArH}4'$ , 6'); 7.04 (dd, 2H,  $^3J = 5.1$  Hz,  $^4J = 3.6$  Hz,  $\text{ThH}4''''$ ); 7.10 (dd, 2H,  $^3J = 5.2$  Hz,  $^4J = 3.6$  Hz,  $\text{ThH}4''''$ ); 7.19 (dd, 2H,  $^3J = 3.6$  Hz,  $^4J = 1.2$  Hz,  $\text{ThH}3''$ ); 7.20 (d, 2H,  $^3J = 16.2$  Hz,  $\text{ThH}2''$ ); 7.21 (dd, 2H,  $^3J =$

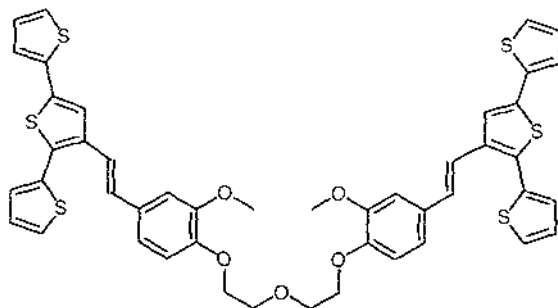
3.6 Hz,  $^4J = 1.2$  Hz, ThH3'''''); 7.26 (dd, 2H,  $^3J = 5.1$  Hz,  $^4J = 1.2$  Hz, ThH5'''''); 7.38 (dd, 2H,  $^3J = 5.1$  Hz,  $^4J = 1.2$  Hz, ThH5'''); 7.40 (s, 2H, ThH4''').

$^{13}\text{C}$  NMR (100.6 MHz,  $\text{CD}_2\text{Cl}_2$ )  $\delta$  55.5  $\text{OCH}_3$ ; 68.2  $\text{OCH}_2$ , 1, 5; 69.6  $\text{OCH}_2$ , 4; 111.1  $\text{ArC6}'$ ; 111.4  $\text{Ar3}'$ ; 119.2  $\text{C}_{\text{vinyl}2''}$ ; 119.9  $\text{ArC4}'$ ; 121.9  $\text{ThC4}''''$ ; 123.8  $\text{ThC3}''''$ ; 124.5  $\text{ThC5}''''$ ; 126.0  $\text{ThC5}'''$ ; 126.5  $\text{ThC3}'''$ ; 127.5  $\text{ThC4}'''$ ; 127.6  $\text{ThC4}''''$ ; 129.9  $\text{ArC5}'$ ; 130.0  $\text{C}_{\text{vinyl}1''}$ ; 130.2  $\text{ThC2}''''$ ; 134.9  $\text{ThC2}'''$ ; 135.4  $\text{ThC5}''''$ ; 136.2  $\text{ThC3}''''$ ; 136.4  $\text{ThC2}''''$ ; 148.1  $\text{ArC1}'$ ; 149.4  $\text{ArC2}'$ .

Electronic spectrum ( $\text{CH}_2\text{Cl}_2$ )  $\lambda_{\text{max}}$  nm/(log  $\epsilon$ ) 330 (4.88).

HRMS (FAB)  $\text{M}^+$  calc 862.1044, found 862.1021.

**1,5-bis-(2'-Methoxyphenyl-4'-{2''-[2''',2'''';5''''',2''''']terthiophen-3''''-yl-vinyl})-3-oxapentane (LXII)**



1,5-bis-(2'-Methoxy-4'-formylphenoxy)-3-oxapentane (0.5230 g, 1.40 mmol) and terthiophene phosphonate (20 mL x 0.140 mmol/mL solution in THF, 2.80 mmol) were stirred in dry  $\text{CH}_2\text{Cl}_2$  (40 mL) under  $\text{N}_2$ . Potassium tert-butoxide (1.4538 g, 13.0 mmol) was added, and the solution left to stir at room temperature for 1 hour.  $\text{H}_2\text{O}$  (50 mL) was added, and the solution acidified with aq. HCl. The organic layer was separated and the aqueous extracted with  $\text{CH}_2\text{Cl}_2$  (2 x 50 mL), before the combined organic layers were washed with  $\text{H}_2\text{O}$  (100 mL) and evaporated. The crude

yellow residue was dissolved in  $\text{CH}_2\text{Cl}_2$  and subjected to flash column chromatography on silica. After the removal of 1,2-bis([2',2'';5'',2''']terthiophen-3''-yl)ethene (18.0 mg, 2%) in  $\text{CH}_2\text{Cl}_2$ , the desired product was eluted in 2% MeOH and dried under vacuum to yield a yellow solid, melting point = 68-70°C (1.0617 g, 88%).

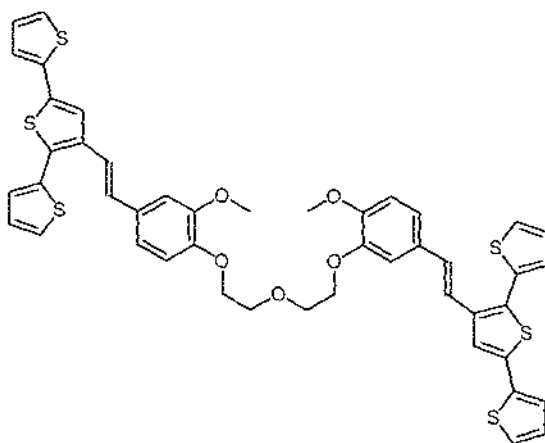
$^1\text{H}$  NMR (400.1 MHz,  $\text{CD}_2\text{Cl}_2$ )  $\delta$  3.87 (s, 6H,  $\text{OCH}_3$ ); 3.90-3.92 (m, 4H,  $\text{OCH}_2$ , 4); 4.15-4.18 (m, 4H,  $\text{OCH}_2$ , 5); 6.88 (d, 2H,  $^3J = 8.8$  Hz, ArH6'); 7.00 (d, 2H,  $^3J = 16.1$  Hz,  $\text{H}_{\text{vinyl}1''}$ ); 7.01-7.03 (m, 2H, ArH5'); 7.03 (s, 2H, ArH3'); 7.05 (dd, 2H,  $^3J = 5.1$  Hz,  $^4J = 3.6$  Hz, ThH4'''''); 7.12 (dd, 2H,  $^3J = 5.2$  Hz,  $^4J = 3.6$  Hz, ThH4'''''); 7.21 (dd, 2H,  $^3J = 3.6$  Hz,  $^4J = 1.2$  Hz, ThH3'''''); 7.22 (dd, 2H,  $^3J = 3.6$  Hz,  $^4J = 1.1$  Hz, ThH3'''''); 7.24 (d, 2H,  $^3J = 16.1$  Hz,  $\text{H}_{\text{vinyl}2''}$ ); 7.27 (dd, 2H,  $^3J = 5.1$  Hz,  $^4J = 1.2$  Hz, ThH5'''''); 7.40 (dd, 2H,  $^3J = 5.1$  Hz,  $^4J = 1.2$  Hz, ThH5'''''); 7.43 (s, 2H, ThH4''''').

$^{13}\text{C}$  NMR (100.6 MHz,  $\text{CD}_2\text{Cl}_2$ )  $\delta$  55.4  $\text{OCH}_3$ ; 68.1  $\text{OCH}_2$ , 1, 5; 69.5  $\text{OCH}_2$ , 2, 4; 109.3 ArC3'; 113.0 ArC6'; 119.2 ArC5'; 119.4  $\text{C}_{\text{vinyl}2''}$ ; 121.9 ThC4'''''; 123.8 ThC3'''''; 124.6 ThC5'''''; 126.0 ThC5'''''; 126.5 ThC3'''''; 127.5 ThC4'''''; 127.6 ThC4'''''; 130.1  $\text{C}_{\text{vinyl}1''}$ ; 130.4 ArC4'; 130.4 ThC2'''''; 134.9 ThC2'''''; 135.5 ThC5'''''; 136.2 ThC3'''''; 136.3 ThC2'''''; 148.0 ArC1'; 149.3 ArC2'.

Electronic spectrum ( $\text{CH}_2\text{Cl}_2$ )  $\lambda_{\text{max}}$  nm/(log  $\epsilon$ ) 330 (4.86).

HRMS (FAB)  $\text{M}^+$  calc 862.1044, found 862.1027.

**1-(2'-Methoxyphenyl-4'-{2''- [2''',2''',5''',2''']terthiophen-3''''-yl-vinyl }-5-(2''''-methoxyphenyl-5''''''-{2''''''''- [2''''''''',2''''''''',5''''''''',2''''''''']terthiophen-3''''''''-yl-vinyl })-3-oxapentane (LXIII)**



1-(2'-Hydroxy-4'-formylphenoxy)-5-(2''-hydroxy-5''-formylphenoxy)-3-oxapentane (0.5628 g, 1.503 mmol) and terthiophene phosphonate (7 mL x 0.140 mmol/mL + 15 mL x 0.135 mmol/mL solution in THF, 3.005 mmol) were stirred in dry CH<sub>2</sub>Cl<sub>2</sub> (40 mL) under N<sub>2</sub>. Potassium tert-butoxide (1.4838 g, 13.2 mmol) was added, and the solution left to stir at room temperature for 1.5 hours. H<sub>2</sub>O (50 mL) was added, and the solution acidified with aq. HCl. The organic layer was separated and the aqueous extracted with CH<sub>2</sub>Cl<sub>2</sub> (50 mL), before the combined organic layers were washed with H<sub>2</sub>O (50 mL) and evaporated. The crude yellow residue was dissolved in CH<sub>2</sub>Cl<sub>2</sub> and subjected to flash column chromatography on silica. After the removal of 1,2-bis([2',2'';5'',2''']terthiophen-3''-yl)ethene (14.2 mg, 2%) in CH<sub>2</sub>Cl<sub>2</sub>, the desired product was eluted in 2% MeOH, melting point = 59-61 °C (1.2035 g, 93%).

<sup>1</sup>H NMR (400.1 MHz, CD<sub>2</sub>Cl<sub>2</sub>) δ 3.83 (s, 3H, OCH<sub>3</sub>); 3.83 (s, 3H, OCH<sub>3</sub>); 3.89-3.92 (m, 4H, OCH<sub>2</sub>, 4); 4.13-4.19 (m, 4H, OCH<sub>2</sub>, 5); 6.85 (d, 2H, <sup>3</sup>J = 8.6 Hz, ArH6', 3'''''''); 6.96 (d, 2H, <sup>3</sup>J = 16.0 Hz, H<sub>vinyl</sub>1'', 1'''''''); 6.98-7.00 (m, 1H, ArH); 6.99 (d, 2H, <sup>3</sup>J = 6.9 Hz, ArH); 7.00 (s, 1H, ArH3'); 7.02 (dd, 1H, <sup>3</sup>J = 5.2 Hz, <sup>4</sup>J = 3.6 Hz, ThH); 7.03 (dd, 1H, <sup>3</sup>J = 5.1 Hz, <sup>4</sup>J = 3.6 Hz, ThH); 7.04-7.06 (m, 1H, ArH); 7.06 (s, 1H, ArH6'''''''); 7.10 (dd, 1H, <sup>3</sup>J = 5.2 Hz, <sup>4</sup>J = 3.6 Hz, ThH); 7.10 (dd, 1H, <sup>3</sup>J = 5.2 Hz, <sup>4</sup>J = 3.6 Hz, ThH); 7.18 (dd, 1H, <sup>3</sup>J = 3.7 Hz, <sup>4</sup>J = 1.2 Hz, ThH); 7.19 (dd, 1H,

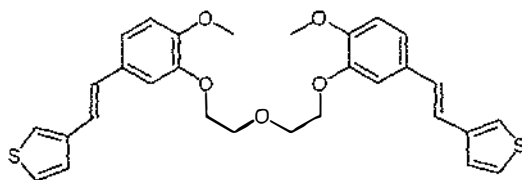
$^3J = 3.7$  Hz,  $^4J = 1.3$  Hz, ThH); 7.19 (dd, 1H,  $^3J = 3.6$  Hz,  $^4J = 1.2$  Hz, ThH); 7.20 (d, 2H,  $^3J = 16.1$  Hz,  $H_{\text{vinyl}}$ ); 7.21 (dd, 1H,  $^3J = 3.6$  Hz,  $^4J = 1.2$  Hz, ThH); 7.24 (dd, 1H,  $^3J = 5.1$  Hz,  $^4J = 1.1$  Hz, ThH); 7.26 (dd, 1H,  $^3J = 5.2$  Hz,  $^4J = 1.1$  Hz, ThH); 7.37 (dd, 1H,  $^3J = 5.1$  Hz,  $^4J = 1.2$  Hz, ThH); 7.38 (dd, 1H,  $^3J = 5.1$  Hz,  $^4J = 1.2$  Hz, ThH); 7.40 (s, 1H, ThH); 7.41 (s, 1H, ThH).

$^{13}\text{C}$  NMR (100.6 MHz,  $\text{CD}_2\text{Cl}_2$ )  $\delta$  55.4  $\text{OCH}_3$ ; 55.4  $\text{OCH}_3$ ; 68.1  $\text{OCH}_2$ ; 68.1  $\text{OCH}_2$ ; 69.4  $\text{OCH}_2$ ; 69.5  $\text{OCH}_2$ ; 109.2 ArC3'; 111.1 ArC6''''''; 111.4 ArC3''''''; 113.0 Ar6'; 119.2  $\text{C}_{\text{vinyl}}$ ; 119.2 ArC5'; 119.3  $\text{C}_{\text{vinyl}}$ ; 119.9 ArC4''''''; 121.9 ThC4''''', 4''''''''; 123.7 ThC3''''', 3''''''''; 124.5 ThC5''''''; 124.5 ThC5''''''''; 126.0 ThC5''''', 5''''''''; 126.5 ThC3''''', 3''''''''; 127.5 ThC4''''', 4''''''''; 127.6 ThC4''''''', 4''''''''''; 129.9 ArC5''''''; 130.0  $\text{C}_{\text{vinyl}}$ ; 130.0  $\text{C}_{\text{vinyl}}$ ; 130.3 ThC2''''''''; 130.4 ArC4'; 130.4 ThC2''''''; 134.9 ThC2''''', 2''''''''; 135.4 ThC5''''', 5''''''''; 136.2 ThC3''''', 3''''''''; 136.3 ThC2''''''', 2''''''''''; 148.0 ArC1'; 148.1 ArC1''''''; 149.3 ArC2'; 149.3 ArC2''''''.

Electronic spectrum ( $\text{CH}_2\text{Cl}_2$ )  $\lambda_{\text{max}}$  nm/(log  $\epsilon$ ) 331 (4.91).

HRMS (FAB)  $M^+$  calc 862.1044, found 862.1017.

**1,5-bis(2'-Methoxy-5'-{2''-thiophen-3'''-yl-vinyl}-phenoxy)-3-oxapentane  
(LXIV)**



Thiophen-3-ylmethyl-phosphonic acid diethyl ester (0.5157 g, 2.201 mmol) and 1,5-bis(2'-methoxy-5'-formylphenoxy)-3-oxapentane (0.4108 g, 1.097 mmol) were stirred in dry  $\text{CH}_2\text{Cl}_2$  (10 mL) and THF (5 mL) under  $\text{N}_2$ . Potassium tert-butoxide (1.2227 g, 10.90 mmol) was added and the solution left to stir at room temperature for

1.5 hours. H<sub>2</sub>O (20 mL) was added and acidified with HCl before the crude product was extracted with CH<sub>2</sub>Cl<sub>2</sub> (3 x 30 mL). After evaporation, the residue was dissolved in CH<sub>2</sub>Cl<sub>2</sub> and purified by flash column chromatography on silica with CH<sub>2</sub>Cl<sub>2</sub> as eluent. Removal of the solvent under reduced pressure yielded the title compound as a white powder, melting point = 153-155°C (0.1623 g, 28%).

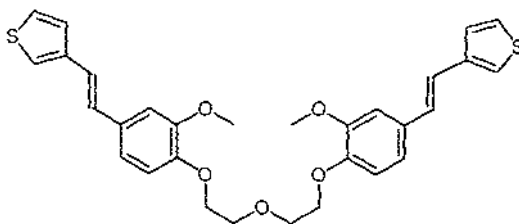
<sup>1</sup>H NMR (400.1 MHz, CDCl<sub>3</sub>) δ 3.86 (s, 6H, OCH<sub>3</sub>); 4.01-4.03 (m, 4H, OCH<sub>2</sub>2, 4); 4.28-4.30 (m, 4H, OCH<sub>2</sub>1, 5); 6.85 (d, 2H, <sup>3</sup>J = 8.3 Hz, ArH3'); 6.86 (d, 2H, <sup>3</sup>J = 16.3 Hz, H<sub>vinyl</sub>1''); 6.98 (d, 2H, <sup>3</sup>J = 16.2 Hz, H<sub>vinyl</sub>2''); 7.03 (dd, 2H, <sup>3</sup>J = 8.6 Hz, <sup>4</sup>J = 2.0 Hz, ArH4'); 7.12 (d, 2H, <sup>4</sup>J = 2.0 Hz, ArH6'); 7.19-7.20 (m, 2H, ThH4'''); 7.29-7.32 (m, 4H, ThH2''', 5''').

<sup>13</sup>C NMR (100.6 MHz, CDCl<sub>3</sub>) δ 56.0 OCH<sub>3</sub>; 68.7 OCH<sub>2</sub>1, 5; 70.0 OCH<sub>2</sub>2, 4; 111.3 ArC6'; 111.8 Ar3'; 120.2 ArC4'; 121.1 C<sub>vinyl</sub>2''; 121.6 ThC4'''; 124.8 ThC5'''; 126.0 ThC2'''; 128.3 C<sub>vinyl</sub>1''; 130.5 ArC5'; 140.2 ThC3'''; 148.4 ArC1'; 149.4 ArC2'.

Electronic spectrum (CH<sub>2</sub>Cl<sub>2</sub>) λ<sub>max</sub> nm/(log ε) 300.5 (4.63), 319.0 (4.67).

HRMS (FAB) M<sup>+</sup> calc 534.1535, found 534.1563.

**1,5-bis(2'-Methoxy-4'-{2''-thiophen-3'''}-yl-vinyl)-phenoxy)-3-oxapentane  
(LXV)**



Thiophen-3-ylmethyl-phosphonic acid diethyl ester (0.5146 g, 2.197 mmol) and 1,5-bis(2'-methoxy-4'-formylphenoxy)-3-oxapentane (0.4106 g, 1.097 mmol) were stirred in dry CH<sub>2</sub>Cl<sub>2</sub> (10 mL) and THF (5 mL) under N<sub>2</sub>. Potassium tert-butoxide

(1.1975 g, 10.67 mmol) was added and the solution left to stir at room temperature for 2 hours. H<sub>2</sub>O (15 mL) was added and acidified with HCl before the crude product was extracted with CH<sub>2</sub>Cl<sub>2</sub> (3 x 30 mL). After evaporation, the residue was dissolved in CH<sub>2</sub>Cl<sub>2</sub> and purified by flash column chromatography (eluent = CH<sub>2</sub>Cl<sub>2</sub>). Removal of the solvent under reduced pressure yielded the title compound as a white powder, melting point = 143-145°C (0.2998 g, 51%).

<sup>1</sup>H NMR (400.1 MHz, CD<sub>2</sub>Cl<sub>2</sub>) δ 3.89 (s, 6H, OCH<sub>3</sub>); 3.91-3.93 (m, 4H, OCH<sub>2</sub>, 4); 4.16-4.19 (m, 4H, OCH<sub>2</sub>, 5); 6.88 (d, 2H, <sup>3</sup>J = 8.3 Hz, ArH6'); 6.91 (d, 2H, <sup>3</sup>J = 16.5 Hz, H<sub>vinyl</sub>1''); 6.99 (dd, 2H, <sup>3</sup>J = 8.3 Hz, <sup>4</sup>J = 2.0 Hz, ArH5'); 7.03 (d, 2H, <sup>3</sup>J = 15.9 Hz, H<sub>vinyl</sub>2''); 7.05 (d, 2H, <sup>4</sup>J = 1.8 Hz, ArH3'); 7.25-7.26 (m, 2H, ThH4'''); 7.32-7.36 (m, 4H, ThH2''', 5''').

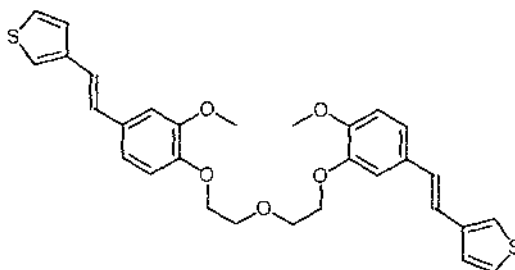
<sup>13</sup>C NMR (100.6 MHz, CDCl<sub>3</sub>) δ 55.4 OCH<sub>3</sub>; 68.1 OCH<sub>2</sub>, 5; 69.5 OCH<sub>2</sub>, 4; 108.7 ArC3'; 113.1 Ar6'; 119.1 ArC5'; 120.7 C<sub>vinyl</sub>2''; 121.4 ThC4'''; 124.4 ThC5'''; 125.8 ThC2'''; 128.0 C<sub>vinyl</sub>1''; 130.5 ArC4'; 140.0 ThC3'''; 147.8 ArC1'; 149.4 ArC2'.

Electronic spectrum (CH<sub>2</sub>Cl<sub>2</sub>) λ<sub>max</sub> nm/(log ε) 300.5 (4.70), 320.0 (4.75).

HRMS (FAB) M<sup>+</sup> calc 534.1535, found 534.1522.

Anal. Calculated for C<sub>30</sub>H<sub>30</sub>O<sub>5</sub>S<sub>2</sub>; C, 67.39; H, 5.66; S, 11.99. Found: C, 66.61; H, 5.36; S, 11.69.

**1-(2'-Methoxyphenyl-4'-{2''-thiophen-3'''-yl-vinyl})-5-(2''''-methoxyphenyl-5''''-{2''''''-thiophen-3''''''-yl-vinyl})-3-oxapentane (LXVI)**



Thiophen-3-ylmethyl-phosphonic acid diethyl ester (0.5113 g, 2.181 mmol) and 1-(2'-methoxy-4'-formylphenoxy)-5-(2''-methoxy-5''-formylphenoxy)-3-oxapentane (0.4116 g, 1.099 mmol) were stirred in dry  $\text{CH}_2\text{Cl}_2$  (10 mL) and THF (5 mL) under  $\text{N}_2$ . Potassium tert-butoxide (1.2595 g, 11.22 mmol) was added and the solution left to stir at room temperature for 3 hours.  $\text{H}_2\text{O}$  (15 mL) was added and acidified with HCl before the layers were separated and the aqueous layer was extracted with  $\text{CH}_2\text{Cl}_2$  (2 x 15 mL). After evaporation, the residue was dissolved in  $\text{CH}_2\text{Cl}_2$  and purified by flash column chromatography (eluent =  $\text{CH}_2\text{Cl}_2$ ). Removal of the solvent under reduced pressure yielded the title compound as a white powder, melting point = 162-165°C (0.3129 g, 53%).

$^1\text{H}$  NMR (400.1 MHz,  $\text{CD}_2\text{Cl}_2$ )  $\delta$  3.85 (s, 3H,  $\text{OCH}_3$ '''''); 3.88 (s, 3H,  $\text{OCH}_3$ ); 3.92-3.95 (m, 4H,  $\text{OCH}_2$ , 4); 4.17-4.20 (m, 2H,  $\text{OCH}_2$ 1); 4.21-4.23 (m, 2H,  $\text{OCH}_2$ 5); 6.87 (d, 1H,  $^3J = 8.3$  Hz, ArH3'''''); 6.88 (d, 1H,  $^3J = 8.4$  Hz, ArH6'); 6.89 (d, 1H,  $^3J = 15.8$  Hz,  $\text{H}_{\text{vinyl}}1$ '''''); 6.91 (d, 1H,  $^3J = 16.2$  Hz,  $\text{H}_{\text{vinyl}}1$ ''); 6.99 (dd, 1H,  $^3J = 8.3$  Hz,  $^4J = 2.0$  Hz, ArH5'); 7.01 (d, 1H,  $^3J = 16.3$  Hz,  $\text{H}_{\text{vinyl}}2$ '''''); 7.04 (dd, 1H,  $^3J = 8.3$  Hz,  $^4J = 2.0$  Hz, ArH4'''''); 7.03 (d, 1H,  $^3J = 16.1$  Hz,  $\text{H}_{\text{vinyl}}2$ ''); 7.05 (d, 1H,  $^4J = 2.0$  Hz, ArH3'); 7.09 (d, 1H,  $^4J = 1.8$  Hz, ArH6'''''); 7.22-7.23 (m, 1H, ThH4'''''''); 7.25-7.26 (m, 1H, ThH4'''); 7.32-7.36 (m, 4H, ThH2''', 2''''''', 5''', 5''''''').

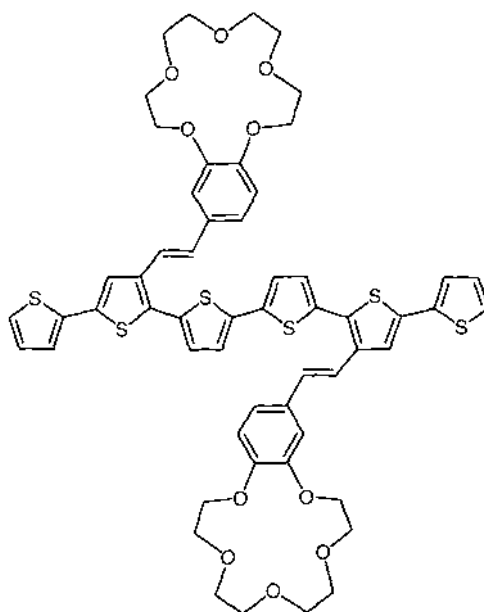
$^{13}\text{C}$  NMR (100.6 MHz,  $\text{CDCl}_3$ )  $\delta$  55.4  $\text{OCH}_3$ ; 55.5  $\text{OCH}_3$ '''''; 68.1  $\text{OCH}_2$ 1; 68.1  $\text{OCH}_2$ 5; 69.5  $\text{OCH}_2$ 2; 69.5  $\text{OCH}_2$ 4; 108.7 ArC3'; 110.5 ArC6'''''; 111.4 Ar3'''''; 113.1 Ar6'; 119.1 ArC5'; 119.7 ArC4'''''; 120.6  $\text{C}_{\text{vinyl}}2$ '''''''; 120.7  $\text{C}_{\text{vinyl}}2$ ''); 121.3 ThC4'''''''; 121.4 ThC4'''; 124.4 ThC5'''; 124.4 ThC5'''''''; 125.8 ThC2'''; 125.8 ThC2'''''''; 127.9

$C_{\text{vinyl}}1''$ ; 128.0  $C_{\text{vinyl}}1''''$ ; 130.0  $\text{ArC}5''''$ ; 130.5  $\text{ArC}4'$ ; 140.0  $\text{ThC}3'''$ ; 140.0  $\text{ThC}3''''''$ ; 147.8  $\text{ArC}1'$ ; 148.1  $\text{ArC}1''''$ ; 149.1  $\text{ArC}2''''$ ; 149.4  $\text{ArC}2'$ .

Electronic spectrum ( $\text{CH}_2\text{Cl}_2$ )  $\lambda_{\text{max}}$  nm/(log  $\epsilon$ ) 300.5 (4.68), 319.5 (4.72).

HRMS (FAB)  $M^+$  calc 534.1535, found 534.1555.

**5''-Bis-{2-(2'-[2'',2''';5''',2''''}]terthiophen-3''-yl-vinyl)-6,7,9,10,12,13,15,16-octahydro-5,8,11,14,17-pentaoxa-benzocyclopentadecene} (LXVII)**



2-(2'-[2'',2''';5''',2''''}]Terthiophen-3''-yl-vinyl)-6,7,9,10,12,13,15,16-octahydro-5,8,11,14,17-pentaoxa-benzocyclopentadecene (0.1638 g, 0.303 mmol) was dissolved in dry  $\text{CH}_2\text{Cl}_2$  (5 mL) under  $\text{N}_2$  before anhydrous  $\text{FeCl}_3$  (0.2603 g, 1.605 mmol) in dry  $\text{CH}_2\text{Cl}_2$  (10 mL) was added slowly. The reaction mixture was stirred for 50 hours before being poured into MeOH (100 mL), causing a red precipitate to form. The precipitate was collected on a 0.45  $\mu\text{m}$  HVLP membrane filter (Millipore) and dried under vacuum, then extracted with  $\text{CH}_2\text{Cl}_2$  for 22 hours in a soxhlet apparatus. The  $\text{CH}_2\text{Cl}_2$  was then concentrated and the product precipitated with MeOH, collected on

a membrane filter as previously and dried under vacuum. This yielded the title compound as a red solid, melting point = 213-215°C, (0.1188 g, 73%)

$^1\text{H}$  NMR (400 MHz,  $\text{CD}_2\text{Cl}_2$ )  $\delta$  3.66-3.72 (m, 16H,  $\text{OCH}_2$ 9, 10, 12, 13); 3.85-3.87 (m, 8H,  $\text{OCH}_2$ 7, 15); 4.10-4.16 (m, 8H,  $\text{OCH}_2$ 6, 16); 6.87 (d, 2H,  $^3J = 8.2$  Hz, ArH4); 7.04 (d, 2H,  $^3J = 16.3$  Hz,  $\text{H}_{\text{vinyl}1'}$ ); 7.06-7.10 (m, 4H, ArH1, 3); 7.08 (dd, 2H,  $^3J = 5.1$ ,  $^4J = 3.6$  Hz, ThH4'''); 7.17 (d, 2H,  $^3J = 3.8$  Hz, ThH3''); 7.26 (d, 2H,  $^3J = 3.8$  Hz, ThH4''); 7.27 (dd, 2H,  $^3J = 3.6$ , 1.2 Hz, ThH3'''); 7.28 (d, 2H,  $^3J = 16.3$  Hz,  $\text{H}_{\text{vinyl}2'}$ ); 7.31 (dd, 2H,  $^3J = 5.1$ ,  $^4J = 1.2$  Hz, ThH5'''); 7.46 (s, 2H, ThH4'').

$^{13}\text{C}$  NMR (100.6 MHz,  $\text{CD}_2\text{Cl}_2$ )  $\delta$  68.3  $\text{OCH}_2$ ; 68.5  $\text{OCH}_2$ ; 68.9  $\text{OCH}_2$ ; 69.0  $\text{OCH}_2$ ; 69.8  $\text{OCH}_2$ ; 69.8  $\text{OCH}_2$ ; 70.4  $\text{OCH}_2$ ; 70.4  $\text{OCH}_2$ ; 111.3 ArC1; 113.2 ArC4; 119.2  $\text{C}_{\text{vinyl}2'}$ ; 119.8 ArC3; 122.1 ThC4''; 123.9 ThC3'''; 124.2 ThC4''; 124.7 ThC5'''; 127.2 ThC3''; 127.7 ThC4'''; 130.0 ArC2; 130.2ThC2''; 130.5  $\text{C}_{\text{vinyl}1'}$ ; 134.2 ThC2''; 135.7 ThC5''; 136.3ThC2'''; 136.6 ThC3''; 137.1 ThC5''; 148.9 ArC4; 149.0 ArC18.

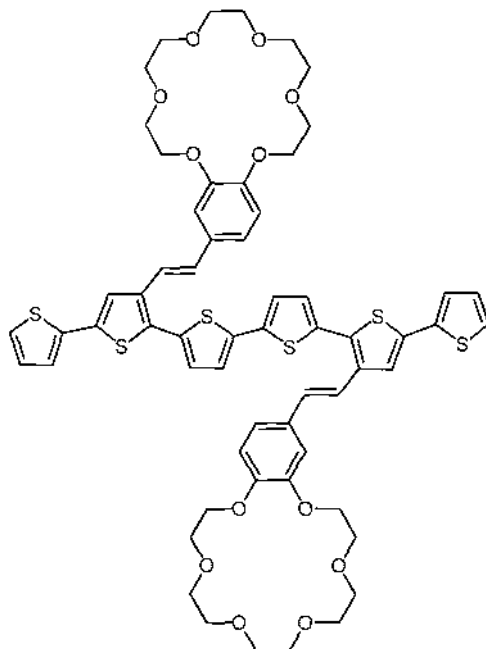
Electronic spectrum ( $\text{CH}_2\text{Cl}_2$ )  $\lambda_{\text{max}}$  nm/(log  $\epsilon$ ) 336.0 (4.82), 450.0 (4.59).

Electronic spectrum (thin film)  $\lambda_{\text{max}}$  nm 357.0, 499.0.

HRMS (FAB)  $M^+$  calc 1078.2041, found 1078.1985.

Anal. Calculated for  $\text{C}_{56}\text{H}_{54}\text{O}_{10}\text{S}_6$ ; C, 62.31; H, 5.04; S, 17.82. Found: C, 61.78; H, 5.29; S, 17.35; Cl, 0.70.

**5''-Bis-{2-(2'-[2'',2''';5''',2''''']terthiophen-3'''-yl-vinyl)-  
6,7,9,10,12,13,15,16,18,19-decahydro-5,8,11,14,17,20-hexaoxa-  
benzocyclooctadecene} (LXVIII)**



2-(2'-[2'',2''';5''',2''''']Terthiophen-3'''-yl-vinyl)-6,7,9,10,12,13,15,16,18,19-decahydro-5,8,11,14,17,20-hexaoxa-benzocyclooctadecene (0.1445 g, 0.247 mmol) was dissolved in dry  $\text{CH}_2\text{Cl}_2$  (10 mL) under  $\text{N}_2$  before anhydrous  $\text{FeCl}_3$  (0.2340 g, 1.443 mmol) in dry  $\text{CH}_2\text{Cl}_2$  (10 mL) was added slowly. The reaction mixture was stirred for 50 hours then poured into MeOH (100 mL), causing a red precipitate to form. The precipitate was collected on a 0.45  $\mu\text{m}$  HVLP membrane filter (Millipore) and dried under vacuum, then extracted with  $\text{CH}_2\text{Cl}_2$  for 18 hours in a soxhlet apparatus. The  $\text{CH}_2\text{Cl}_2$  was then concentrated and the product precipitated with MeOH, collected on a membrane filter as previously and dried under vacuum. This yielded the title compound as a red solid, melting point = 208-210°C, (0.0796 g, 55%).

$^1\text{H}$  NMR (400 MHz,  $\text{CD}_2\text{Cl}_2$ )  $\delta$  3.61-3.70 (m, 24H,  $\text{OCH}_2$ 9, 10, 12, 13, 15, 16); 3.85-3.87 (m, 8H,  $\text{OCH}_2$ 7, 18); 4.14-4.16 (m, 4H,  $\text{OCH}_2$ 19); 4.18-4.20 (m, 4H,  $\text{OCH}_2$ 6); 6.87 (d, 2H,  $^3J = 8.3$  Hz, ArH4); 7.04 (d, 2H,  $^3J = 16.2$  Hz,  $\text{H}_{\text{vinyl}}1'$ ); 7.08 (dd, 2H,  $^3J = 5.1$ ,  $^4J = 3.5$  Hz, ThH4'''); 7.08-7.10 (m, 4H, ArH1, 3); 7.17 (d, 2H,  $^3J = 3.7$ , ThH3'');

7.26 (d, 2H,  $^3J = 3.6$ , ThH4''); 7.27 (dd, 2H,  $^3J = 3.4$ , 1.1 Hz, ThH3'''); 7.28 (d, 2H,  $^3J = 16.2$  Hz, H<sub>vinyl</sub>2'); 7.31 (dd, 2H,  $^3J = 5.1$ ,  $^4J = 1.1$  Hz, ThH5'''); 7.46 (s, 2H, ThH4''').

$^{13}\text{C}$  NMR (100.6 MHz,  $\text{CD}_2\text{Cl}_2$ )  $\delta$  68.0 OCH<sub>2</sub>; 68.1 OCH<sub>2</sub>; 68.9 OCH<sub>2</sub>; 68.9 OCH<sub>2</sub>; 69.9 OCH<sub>2</sub>; 70.0 OCH<sub>2</sub>; 70.0 OCH<sub>2</sub>; 70.1 OCH<sub>2</sub>; 70.1 OCH<sub>2</sub>; 70.1 OCH<sub>2</sub>; 111.2 ArC1; 113.2 ArC4; 119.2 C<sub>vinyl</sub>2'; 119.8 ArC3; 122.1 ThC4''; 123.9 ThC3'''; 124.2 ThC4''; 124.7 ThC5'''; 127.2 ThC3''; 127.7 ThC4'''; 129.9 ArC2; 130.2ThC2''; 130.5 C<sub>vinyl</sub>1'; 134.2 ThC2''; 135.7 ThC5''; 136.2ThC2'''; 136.6 ThC3''; 137.1 ThC5''; 148.9 ArC4; 149.0 ArC18.

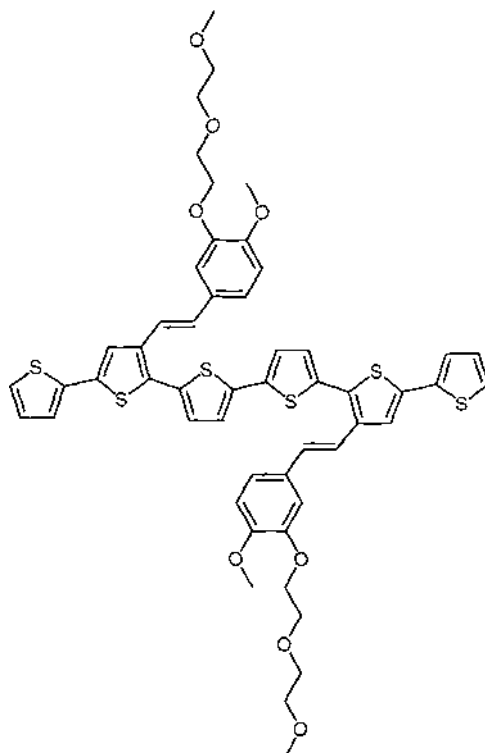
Electronic spectrum ( $\text{CH}_2\text{Cl}_2$ )  $\lambda_{\text{max}}$  nm/(log  $\epsilon$ ) 274.5 (4.50), 335.5 (4.83), 445.5 (4.56).

Electronic spectrum (thin film)  $\lambda_{\text{max}}$  nm 346.0, 480.0.

HRMS (FAB)  $M^+$  calc 1166.2566, found 1166.2626.

Anal. Calculated for  $\text{C}_{60}\text{H}_{62}\text{O}_{12}\text{S}_6$ ; C, 61.72; H, 5.35; S, 16.48. Found: C, 60.70; H, 5.27; S, 16.10.

**4',3'''-Bis-(2''''''-{4''''''-methoxy-3''''''-[2''''''-(2''''''-methoxy-ethoxy)-ethoxy]-phenyl}-vinyl)-[2,2';5',2'';5'',2''';5''',2'''';5''''',2''''']sexithiophene  
(LXIX)**

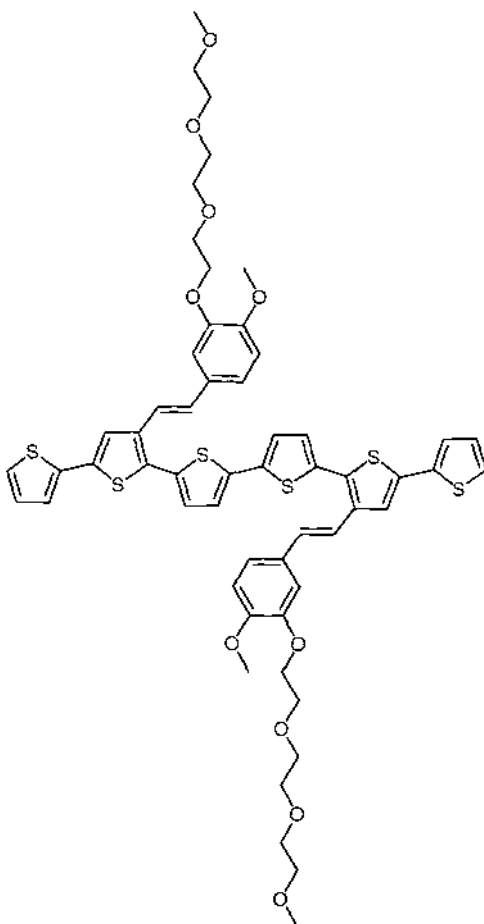


3'-(2''''-{4''''-methoxy-3''''-[2''''-(2''''-methoxy-ethoxy)-ethoxy]-phenyl}-vinyl)-[2,2';5',2'']terthiophene (0.0558 g, 0.112 mmol) was dissolved in  $\text{CHCl}_3$  (2 mL) before anhydrous  $\text{FeCl}_3$  (0.1061 g, 0.654 mmol) in  $\text{CHCl}_3$  (7 mL) was added dropwise. The solution was stirred under  $\text{N}_2$  at room temperature for 66 hours. After this time the solution was poured into MeOH (50 mL) and the resulting brown-red precipitate was filtered off on a 0.45  $\mu\text{m}$  HVLP membrane (Millipore). The precipitate was dried under vacuum, then extracted with MeOH in a soxhlet apparatus for 17 hours. The residual red powder was dried to yield 4',3'''-bis-(2''''''-{4''''''-methoxy-3''''''-[2''''''-(2''''''-methoxy-ethoxy)-ethoxy]-phenyl}-vinyl)-[2,2';5',2'';5'',2''';5''',2'''';5''''',2''''']sexithiophene (48.2 mg, 87%, melting point = 172-173°C).

$^1\text{H}$  NMR (400.1 MHz,  $\text{CD}_2\text{Cl}_2$ )  $\delta$  3.32 (s, 6H, 2''''''''OCH<sub>3</sub>); 3.50-3.52 (m, 4H, OCH<sub>2</sub>2'''''''''); 3.63-3.66 (m, 4H, OCH<sub>2</sub>1'''''''''); 3.81-3.84 (m, 4H, OCH<sub>2</sub>2'''''''''); 3.86



**4',3'''-Bis-[2''''-(4''''-methoxy-3''''-{2''''-(2''''-methoxy-ethoxy)-ethoxy]-phenyl)-vinyl]-[2,2';5,2'';5'',2''';5''',2'''';5'''';2''''']sexithiophene (LXX)**



3'-(2''-{4''-methoxy-3''-{2''-(2''-methoxy-ethoxy)-ethoxy]-phenyl}-vinyl)-[2,2';5,2'']terthiophene (0.1250 g, 0.230 mmol) was dissolved in dry  $\text{CH}_2\text{Cl}_2$  (5 mL) before anhydrous  $\text{FeCl}_3$  (0.1802 g, 1.111 mmol) in  $\text{CH}_2\text{Cl}_2$  (10 mL) was added dropwise. The solution was stirred under  $\text{N}_2$  at room temperature for 114 hours. After this time the solution was poured into MeOH (100 mL) and the resulting brown-red precipitate was filtered off on a 0.45  $\mu\text{m}$  HVLP membrane (Millipore). The precipitate was dried under vacuum, and subsequently extracted with  $\text{CH}_2\text{Cl}_2$  in a soxhlet apparatus for 21 hours. The  $\text{CH}_2\text{Cl}_2$  was concentrated and the product precipitated with MeOH, before being collected on a 0.45  $\mu\text{m}$  HVLP membrane (Millipore) and dried under vacuum. This yielded 4',3'''-bis-[2''''-(4''''-methoxy-3''''-{2''''-(2''''-methoxy-ethoxy)-ethoxy]-ethoxy)-ethoxy]-phenyl)-vinyl]-

[2,2';5',2";5",2'';5''',2'''';5''''',2''''']sexithiophene as a red solid (86.3 mg, 69%, melting point = 158-160°C).

<sup>1</sup>H NMR (400.1 MHz, CD<sub>2</sub>Cl<sub>2</sub>) δ 3.30 (s, 6H, 2''''''''''OCH<sub>3</sub>); 3.46-3.49 (m, 4H, OCH<sub>2</sub>2'''''''''''); 3.56-3.58 (m, 4H, OCH<sub>2</sub>1'''''''''''); 3.58-3.61 (m, 4H, OCH<sub>2</sub>2'''''''''''); 3.65-3.67 (m, 4H, OCH<sub>2</sub>1'''''''''''); 3.82-3.85 (m, 4H, OCH<sub>2</sub>2'''''''''''); 3.87 (s, 6H, ArOCH<sub>3</sub>); 4.17-4.19 (m, 4H, OCH<sub>2</sub>1'''''''''''); 6.90 (d, 2H, <sup>3</sup>J = 8.3 Hz, ArH5'''''''''); 7.04 (d, 2H, <sup>3</sup>J = 16.1 Hz, H<sub>vinyl</sub>2'''''''''); 7.08 (dd, 2H, <sup>3</sup>J = 5.1 Hz, <sup>4</sup>J = 3.6 Hz, ThH4, 4'''''''); 7.09 (d, 2H, <sup>4</sup>J = 2.0 Hz, ArH2'''''''''); 7.12 (dd, 2H, <sup>3</sup>J = 8.3 Hz, <sup>4</sup>J = 2.0 Hz, ArH6'''''''''); 7.17 (d, 2H, <sup>3</sup>J = 3.8 Hz, ThH3'', 4'''); 7.26 (d, 2H, <sup>3</sup>J = 3.8 Hz, ThH4'', 3'''); 7.27 (dd, 2H, <sup>3</sup>J = 3.6 Hz, <sup>4</sup>J = 1.2 Hz, ThH3, 3'''''); 7.28 (d, 2H, <sup>3</sup>J = 16.2 Hz, H<sub>vinyl</sub>1'''''''''); 7.31 (dd, 2H, <sup>3</sup>J = 5.2 Hz, <sup>4</sup>J = 1.1 Hz, ThH5, 5'''''''); 7.46 (s, 2H, ThH3', 4''').

<sup>13</sup>C NMR (100.6 MHz, CD<sub>2</sub>Cl<sub>2</sub>) δ 55.5 ArOCH<sub>3</sub>; 58.3 2''''''''''OCH<sub>3</sub>; 68.1 OCH<sub>2</sub>1'''''''''''; 69.3 OCH<sub>2</sub>2'''''''''''; 70.1 OCH<sub>2</sub>1'''''''''''; 70.2 OCH<sub>2</sub>2'''''''''''; 70.4 OCH<sub>2</sub>1'''''''''''; 71.6 OCH<sub>2</sub>2'''''''''''; 111.1 ArC2'''''''''''; 111.6 ArC5'''''''''''; 119.2 C<sub>vinyl</sub>1'''''''''''; 119.8 ArC6'''''''''''; 122.2 ThC3', 4'''); 124.0 ThC3, 3'''''); 124.3 ThC4'', 3'''); 124.8 ThC5, 5'''''); 127.3 Th3'', 4'''); 127.7 ThC4, 4'''''); 129.9 ArC1'''''''''''; 129.9 ThC5', 2'''''); 130.5 C<sub>vinyl</sub>2'''''''''''; 134.3 ThC2'', 5'''); 135.7 ThC2', 5'''''); 136.3 ThC2, 2'''''); 136.7 ThC4', 3'''''); 137.1 ThC5'', 2'''); 148.2 ArC3'''''''''''; 149.5 ArC4'''''''''''.

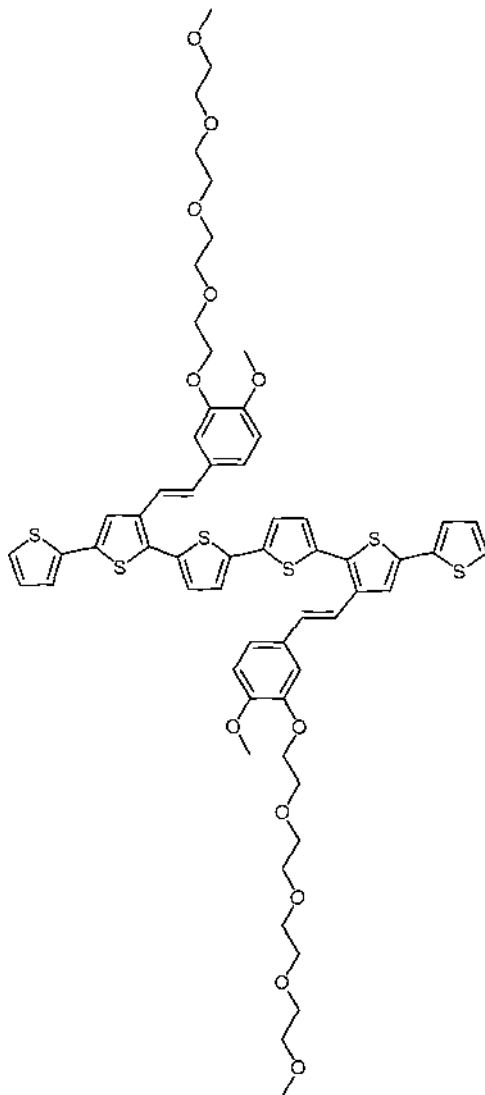
Electronic spectrum (CH<sub>2</sub>Cl<sub>2</sub>) λ<sub>max</sub> nm/(log ε) 334.5 (4.81), 446.0 (4.57).

Electronic spectrum (thin film) λ<sub>max</sub> nm 278.5, 348.0, 499.5.

HRMS (FAB) M<sup>+</sup> calc 1082.2354, found 1082.2381.

Anal. Calculated for C<sub>56</sub>H<sub>58</sub>O<sub>10</sub>S<sub>6</sub>; C, 62.08; H, 5.40; S, 17.76. Found: C, 61.85; H, 5.27; S, 17.85.

**4',3'''-Bis-{2''''-[4''''-methoxy-3''''-(2''''-[2''''-[2''''-(2''''-methoxy-ethoxy)-ethoxy]-ethoxy)-ethoxy]-phenyl}-vinyl)-[2,2';5',2'';5'',2''';5''',2'''';5''''',2''''']sexithiophene (LXXI)**



3'-(2''-[4''-Methoxy-3''-[2''-(2''-[2''-[2''-(2''-methoxy-ethoxy)-ethoxy]-ethoxy)-ethoxy]-phenyl]-vinyl)-[2,2';5',2'']terthiophene (0.1286 g, 0.219 mmol) was dissolved in CH<sub>2</sub>Cl<sub>2</sub> (5 mL) before anhydrous FeCl<sub>3</sub> (0.1698 g, 1.047 mmol) in CH<sub>2</sub>Cl<sub>2</sub> (10 mL) was added dropwise. The solution was stirred under N<sub>2</sub> at room temperature for 112 hours. After this time the solution was poured into MeOH (100 mL) and the resulting brown-red precipitate was filtered off on a 0.45 μm HVLP membrane (Millipore). The precipitate was dried under vacuum, then extracted with CH<sub>2</sub>Cl<sub>2</sub> in a soxhlet apparatus for 18 hours. The CH<sub>2</sub>Cl<sub>2</sub> was concentrated and the

product precipitated with MeOH before being collected on a membrane as previously. The collected red solid was dried to yield 4',3''-bis-{2''''''-[4''''''-methoxy-3''''''-(2''''''-{2''''''''-[2''''''''-(2''''''''-methoxy-ethoxy)-ethoxy]-ethoxy}-ethoxy)-phenyl]-vinyl}-[2,2';5',2";5",2'';5''',2'''';5''''',2'''''']sexithiophene (75.6 mg, 59%, melting point = 160-163°C).

$^1\text{H}$  NMR (400.1 MHz,  $\text{CD}_2\text{Cl}_2$ )  $\delta$  3.30 (s, 6H, 2''''''''''OCH<sub>3</sub>); 3.46-3.48 (m, 4H, OCH<sub>2</sub>2'''''''''''); 3.53-3.55 (m, 4H, OCH<sub>2</sub>1'''''''''''); 3.56-3.57 (m, 8H, OCH<sub>2</sub>1''''''''''', 2'''''''''''); 3.60-3.62 (m, 4H, OCH<sub>2</sub>2'''''''''''); 3.66-3.68 (m, 4H, OCH<sub>2</sub>1'''''''''''); 3.83-3.85 (m, 4H, OCH<sub>2</sub>2'''''''''''); 3.87 (s, 6H, ArOCH<sub>3</sub>); 4.17-4.20 (m, 4H, OCH<sub>2</sub>1'''''''''''); 6.90 (d, 2H,  $^3J = 8.4$  Hz, ArH5'''''''''); 7.04 (d, 2H,  $^3J = 16.2$  Hz, H<sub>vinyl</sub>2'''''''''); 7.08 (dd, 2H,  $^3J = 5.1$  Hz,  $^4J = 3.6$  Hz, ThH4, 4'''''); 7.09 (d, 2H,  $^4J = 2.5$  Hz, ArH2'''''''''); 7.13 (dd, 2H,  $^3J = 8.6$  Hz,  $^4J = 2.0$  Hz, ArH6'''''''''); 7.17 (d, 2H,  $^3J = 3.8$  Hz, ThH3'', 4'''); 7.26 (d, 2H,  $^3J = 3.8$  Hz, ThH4'', 3'''); 7.27 (dd, 2H,  $^3J = 3.6$  Hz,  $^4J = 1.3$  Hz, ThH3, 3'''''); 7.28 (d, 2H,  $^3J = 16.1$  Hz, H<sub>vinyl</sub>1'''''''''); 7.31 (dd, 2H,  $^3J = 5.1$  Hz,  $^4J = 1.1$  Hz, ThH5, 5'''''); 7.46 (s, 2H, ThH3', 4''').

$^{13}\text{C}$  NMR (100.6 MHz,  $\text{CD}_2\text{Cl}_2$ )  $\delta$  55.5 ArOCH<sub>3</sub>; 58.3 2''''''''''OCH<sub>3</sub>; 68.1 OCH<sub>2</sub>1'''''''''''; 69.3 OCH<sub>2</sub>2'''''''''''; 70.0 OCH<sub>2</sub>1'''''''''''; 70.1 OCH<sub>2</sub>1'''''''''''; 70.2 OCH<sub>2</sub>2'''''''''''; 70.2 OCH<sub>2</sub>2'''''''''''; 70.4 OCH<sub>2</sub>1'''''''''''; 71.5 OCH<sub>2</sub>2'''''''''''; 111.2 ArC2'''''''''''; 111.6 ArC5'''''''''''; 119.2 C<sub>vinyl</sub>1'''''''''''; 119.8 ArC6'''''''''''; 122.2 ThC3', 4'''; 124.0 ThC3, 3'''''; 124.3 ThC4'', 3'''; 124.8 ThC5, 5'''''; 127.2 ThC3'', 4'''; 127.7 ThC4, 4'''''; 129.8 ArC1'''''''''''; 129.9 ThC5', 2'''''; 130.5 C<sub>vinyl</sub>2'''''''''''; 134.3 ThC2'', 5'''; 135.7 ThC2', 5'''''; 136.3 ThC2, 2'''''; 136.7 ThC4', 3'''''; 137.1 ThC5'', 2'''''; 148.2 ArC3'''''''''''; 149.5 ArC4'''''''''''.

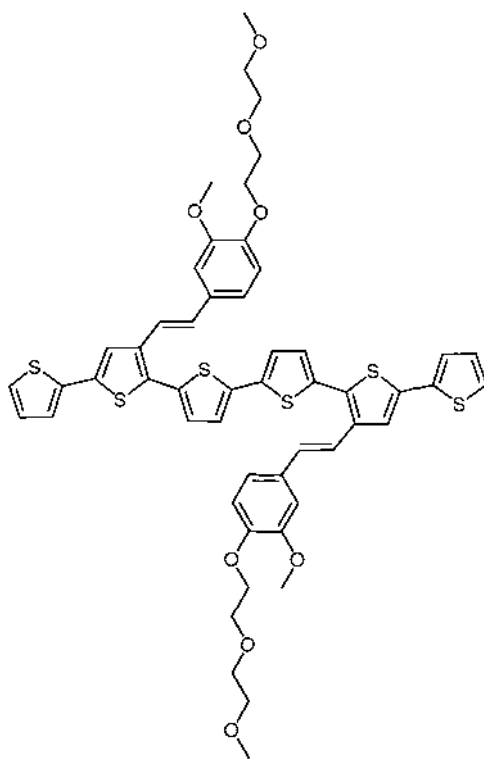
Electronic spectrum ( $\text{CH}_2\text{Cl}_2$ )  $\lambda_{\text{max}}$  nm/(log  $\epsilon$ ) 335.5 (4.80), 450.5 (4.61).

Electronic spectrum (thin film)  $\lambda_{\text{max}}$  nm 281.5, 342.5, 485.0.

HRMS (FAB)  $\text{M}^+$  calc 1170.2879, found 1170.2919.

Anal. Calculated for  $C_{60}H_{66}O_{12}S_6$ ; C, 61.51; H, 5.68; S, 16.42. Found: C, 61.36; H, 5.64; S, 16.40.

**4',3'''-Bis-(2''''''-{3''''''-methoxy-4''''''-[2''''''-(2''''''''-methoxy-ethoxy)-ethoxy]-phenyl}-vinyl)-[2,2';5',2'';5'',2''' ;5''',2'''' ;5''''',2'''''']sexithiophene (LXXII)**



3'-(2''''-{3''''-Methoxy-4''''-[2''''-(2''''''-methoxy-ethoxy)-ethoxy]-phenyl}-vinyl)-[2,2';5',2'']terthiophene (0.1152 g, 0.231 mmol) was dissolved in dry  $CH_2Cl_2$  (5 mL) before anhydrous  $FeCl_3$  (0.1714 g, 1.057 mmol) in dry  $CH_2Cl_2$  (10 mL) was added dropwise. The solution was stirred under  $N_2$  at room temperature for 30 minutes. After this time the solution was poured into MeOH (100 mL) and the resulting brown-red precipitate was filtered off on a 0.45  $\mu m$  HVLP membrane (Millipore). The precipitate was dried under vacuum, before being extracted with  $CH_2Cl_2$  in a soxhlet apparatus for 1 hour. The  $CH_2Cl_2$  was concentrated by evaporation and sufficient

MeOH added to precipitate the product, which was subsequently collected on a membrane filter as before and dried under vacuum. This gave 4',3''-bis-(2''''''-  
{3''''''-methoxy-4''''''-[2''''''-(2''''''-methoxy-ethoxy)-ethoxy]-phenyl}-vinyl)-  
[2,2';5',2";5",2'';5''',2'''';5''''',2''''']sexithiophene as a red solid (94.6 mg, 82%, melting  
point = 128-130°C).

<sup>1</sup>H NMR (400.1 MHz, CD<sub>2</sub>Cl<sub>2</sub>) δ 3.35 (s, 6H, 2''''''''OCH<sub>3</sub>); 3.53-3.55 (m, 4H, OCH<sub>2</sub>2'''''''''); 3.66-3.68 (m, 4H, OCH<sub>2</sub>1'''''''''); 3.82-3.84 (m, 4H, OCH<sub>2</sub>2'''''''''); 3.90 (s, 6H, ArOCH<sub>3</sub>); 4.13-4.15 (m, 4H, OCH<sub>2</sub>1'''''''''); 6.89 (d, 2H, <sup>3</sup>J = 8.9 Hz, ArH5'''''''''); 7.06 (d, 2H, <sup>3</sup>J = 16.7 Hz, H<sub>vinyl</sub>2'''''''''); 7.08 (dd, 2H, <sup>3</sup>J = 5.1 Hz, <sup>4</sup>J = 3.6 Hz, ThH4, 4'''''); 7.06-7.09 (m, 4H, ArH2''''''''', 6'''''''''); 7.17 (d, 2H, <sup>3</sup>J = 3.8 Hz, ThH3'', 4'''); 7.25 (d, 2H, <sup>3</sup>J = 3.8 Hz, ThH4'', 3'''); 7.27 (dd, 2H, <sup>3</sup>J = 3.6 Hz, <sup>4</sup>J = 1.2 Hz, ThH3, 3'''''); 7.30 (d, 2H, <sup>3</sup>J = 16.3 Hz, H<sub>vinyl</sub>1'''''''''); 7.31 (dd, 2H, <sup>3</sup>J = 5.1 Hz, <sup>4</sup>J = 1.1 Hz, ThH5, 5'''''); 7.46 (s, 2H, ThH3', 4''').

<sup>13</sup>C NMR (100.6 MHz, CD<sub>2</sub>Cl<sub>2</sub>) δ 55.5 ArOCH<sub>3</sub>; 58.3 2''''''''''OCH<sub>3</sub>; 68.0 OCH<sub>2</sub>1''''''''''; 69.2 OCH<sub>2</sub>2''''''''''; 70.2 OCH<sub>2</sub>1''''''''''; 71.6 OCH<sub>2</sub>2''''''''''; 109.3 ArC2''''''''''; 112.9 ArC5''''''''''; 119.2 C<sub>vinyl</sub>1''''''''''; 119.3 ArC6''''''''''; 122.1 ThC3', 4''''; 124.0 ThC3, 3''''; 124.2 ThC4'', 3'''; 124.8 ThC5, 5''''; 127.2 ThC3'', 4''; 127.7 ThC4, 4''''; 130.0 ThC5', 2''''; 130.2 ArC1''''''''''; 130.5 C<sub>vinyl</sub>2''''''''''; 134.2 ThC2'', 5''; 135.7 ThC2', 5''; 136.3 ThC2, 2''''; 136.6 ThC4', 3''; 137.1 ThC5'', 2''; 148.2 ArC4''''''''''; 149.3 ArC3''''''''''.

Electronic spectrum (CH<sub>2</sub>Cl<sub>2</sub>) λ<sub>max</sub> nm/(log ε) 336.0 (4.78), 458.5 (4.62).

Electronic spectrum (thin film) λ<sub>max</sub> nm 291.0, 380.0, 510.5.

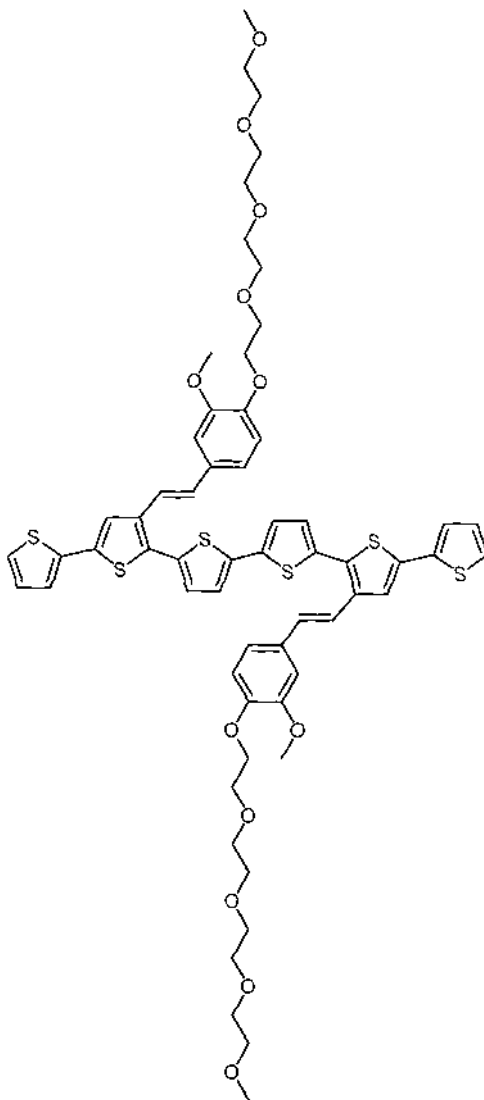
HRMS (FAB) M<sup>+</sup> calc 994.1830, found 994.1826.

Anal. Calculated for C<sub>52</sub>H<sub>50</sub>O<sub>8</sub>S; C, 62.75; H, 5.06; S, 19.33. Found: C, 60.96; H, 5.06; S, 19.09.





**4',3'''-Bis-{2''''-[3''''-methoxy-4''''-(2''''-[2''''-[2''''-[2''''-methoxy-ethoxy]-ethoxy]-ethoxy)-ethoxy]-phenyl]-vinyl}-[2,2';5',2'';5'',2''';5''',2'''';5''''',2''''']sexithiophene (LXXIV)**



3'-(2''-{3''-Methoxy-4''-[2''-(2''-[2''-[2''-[2''-methoxy-ethoxy]-ethoxy]-ethoxy)-ethoxy]-phenyl}-vinyl)-[2,2';5',2'']terthiophene (0.1294 g, 0.221 mmol) was dissolved in  $\text{CH}_2\text{Cl}_2$  (5 mL) before anhydrous  $\text{FeCl}_3$  (0.1736 g, 1.070 mmol) in  $\text{CH}_2\text{Cl}_2$  (10 mL) was added dropwise. The solution was stirred under  $\text{N}_2$  at room temperature for 112 hours. After this time the solution was poured into MeOH (100 mL), and the resulting brown-red precipitate filtered off on a 0.45  $\mu\text{m}$  HVLP membrane (Millipore). The precipitate was dried under vacuum, then extracted with  $\text{CH}_2\text{Cl}_2$  in a soxhlet apparatus for 16 hours. The  $\text{CH}_2\text{Cl}_2$  was concentrated and the

product precipitated with MeOH. After filtering as previously, the red solid was dried under vacuum to give 4',3''-bis-{2''''''-|3''''''-methoxy-4''''''-(2''''''-|2''''''- (2''''''''-methoxy-ethoxy)-ethoxy|-ethoxy)-ethoxy}-phenyl|-vinyl}- [2,2';5',2'';5'',2''' ;5''',2'''';5''''',2''''']sexithiophene as a red powder (108.4 mg, 84%, melting point = 99-101 °C).

<sup>1</sup>H NMR (400.1 MHz, CD<sub>2</sub>Cl<sub>2</sub>) δ 3.32 (s, 6H, 2''''''''''OCH<sub>3</sub>); 3.48-3.50 (m, 4H, OCH<sub>2</sub>2''''''''''); 3.56-3.58 (m, 4H, OCH<sub>2</sub>1''''''''''); 3.59-3.60 (m, 8H, OCH<sub>2</sub>1'''''''''', 2''''''''''); 3.63-3.65 (m, 4H, OCH<sub>2</sub>2''''''''''); 3.68-3.69 (m, 4H, OCH<sub>2</sub>1''''''''''); 3.83-3.85 (m, 4H, OCH<sub>2</sub>2''''''''''); 3.90 (s, 6H, ArOCH<sub>3</sub>); 4.14-4.16 (m, 4H, OCH<sub>2</sub>1''''''''''); 6.90 (d, 2H, <sup>3</sup>J = 8.9 Hz, ArH5'''''''''); 7.06 (d, 2H, <sup>3</sup>J = 16.4 Hz, H<sub>vinyl</sub>2'''''''''); 7.07-7.09 (m, 4H, ArH2''''''''', 6'''''''''); 7.08 (dd, 2H, <sup>3</sup>J = 5.1 Hz, <sup>4</sup>J = 3.6 Hz, H4, 4'''''''); 7.17 (d, 2H, <sup>3</sup>J = 3.8 Hz, H3'', 4'''); 7.25 (d, 2H, <sup>3</sup>J = 3.8 Hz, H4'', 3'''); 7.27 (dd, 2H, <sup>3</sup>J = 3.6 Hz, <sup>4</sup>J = 1.2 Hz, H3, 3'''''); 7.30 (d, 2H, <sup>3</sup>J = 16.7 Hz, H<sub>vinyl</sub>1'''''''''); 7.31 (dd, 2H, <sup>3</sup>J = 5.1 Hz, <sup>4</sup>J = 1.1 Hz, H5, 5'''''); 7.46 (s, 2H, H3', 4''').

<sup>13</sup>C NMR (100.6 MHz, CD<sub>2</sub>Cl<sub>2</sub>) δ 55.4 ArOCH<sub>3</sub>; 58.2 2''''''''''OCH<sub>3</sub>; 67.9 OCH<sub>2</sub>1''''''''''; 69.2 OCH<sub>2</sub>2''''''''''; 70.0 OCH<sub>2</sub>1''''''''''; 70.1 OCH<sub>2</sub>1''''''''''; 70.1 OCH<sub>2</sub>2''''''''''; 70.2 OCH<sub>2</sub>2''''''''''; 70.3 OCH<sub>2</sub>1''''''''''; 71.5 OCH<sub>2</sub>2''''''''''; 109.2 ArC2''''''''''; 112.8 ArC5''''''''''; 119.2 C<sub>vinyl</sub>1''''''''''; 119.3 ArC6''''''''''; 122.1 C3', 4''''; 123.9 C3, 3''''; 124.1 C4'', 3''; 124.7 C5, 5''''; 127.1 C3'', 4''; 127.7 C4, 4''''; 129.9 C5', 2''; 130.2 ArC1''''''''''; 130.5 C<sub>vinyl</sub>2''''''''''; 134.2 C2'', 5''; 135.6 C2', 5''''; 136.2 C2, 2''''; 136.5 C4', 3''; 137.0 C5'', 2''; 148.1 ArC4''''''''''; 149.2 ArC3''''''''''.

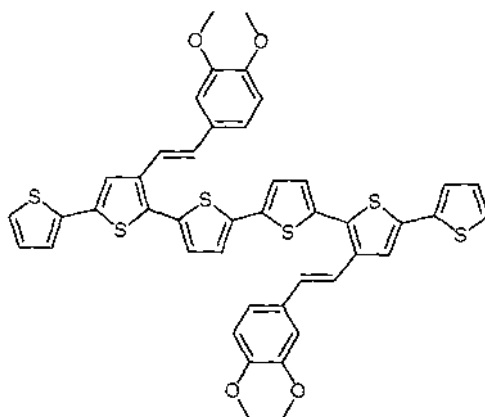
Electronic spectrum (CH<sub>2</sub>Cl<sub>2</sub>) λ<sub>max</sub> nm/(log ε) 336.5 (4.81), 454.0 (4.63).

Electronic spectrum (thin film) λ<sub>max</sub> nm 285.0, 344.5, 478.0.

HRMS (FAB) M<sup>+</sup> calc 1170.2879, found 1170.2900.

Anal. Calculated for C<sub>66</sub>H<sub>66</sub>O<sub>12</sub>S<sub>6</sub>; C, 61.51; H, 5.68; S, 16.42. Found: C, 61.24; H, 5.60; S, 16.26.

**4',3'''-Bis-[2''''-(3''''',4'''''-dimethoxy-phenyl)-vinyl]-  
[2,2';5,2'';5'',2''';5''',2'''';5''''',2''''']sexithiophene (LXXV)**



3'-(2''-{3''',4''''-Dimethoxy-phenyl}-vinyl)-[2,2';5,2'']terthiophene (0.1001 g, 0.244 mmol) was dissolved in CH<sub>2</sub>Cl<sub>2</sub> (5 mL) before anhydrous FeCl<sub>3</sub> (0.1437 g, 0.886 mmol) in CH<sub>2</sub>Cl<sub>2</sub> (10 mL) was added dropwise. The solution was stirred under N<sub>2</sub> at room temperature for 30 minutes. After this time the solution was poured into MeOH (100 mL), and the resulting brown-red precipitate filtered off on a 0.45 μm HVLP membrane (Millipore). The precipitate was dried under vacuum, then extracted with CH<sub>2</sub>Cl<sub>2</sub> in a soxhlet apparatus for 22 hours. The CH<sub>2</sub>Cl<sub>2</sub> was concentrated and the product precipitated with MeOH. After filtering as previously, the red solid was dried under vacuum to give 4',3'''-bis-[2''''-(3''''',4'''''-dimethoxy-phenyl)-vinyl]-[2,2';5,2'';5'',2''';5''',2'''';5''''',2''''']sexithiophene as a red powder (78.8 mg, 79%, melting point = 216-218°C).

Electronic spectrum (CH<sub>2</sub>Cl<sub>2</sub>) λ<sub>max</sub> nm/(log ε) 275.0 (4.48), 335.5 (4.80), 445.0 (4.55).

Electronic spectrum (thin film) λ<sub>max</sub> nm 284.5, 342.5, 510.0, 555.0.

HRMS (FAB) M<sup>+</sup> calc 818.0781, found 818.0794.

Further characterisation was not possible due to insolubility of the material in a wide variety of common solvents, including alkanes, alcohols, ethers, esters, ketones, chlorinated solvents, aromatics, DMF and THF.

*“Out of every fruition of success,  
no matter what,  
comes forth something  
to make a new effort necessary”*

*Walt Whitman*



## References

- 1 P. R. Teasdale and G. G. Wallace, *Analyst*, **118**, 329-334 (1993).
- 2 C. J. Pedersen, *J. Am. Chem. Soc.*, **89**(26), 7017-7036 (1967).
- 3 C. J. Pedersen, *J. Am. Chem. Soc.*, **89**(10), 2495-2496 (1967).
- 4 J.-M. Lehn, 'Supramolecular Chemistry Concepts and Perspectives', VCH, (1995).
- 5 P. W. Atkins, 'Physical Chemistry', Oxford University Press, (1994).
- 6 H. C. Brown, D. Basavaiah, S. U. kulkarni, N. G. Bhat, and J. V. N. V. Prasad, *J. Org. Chem.*, **53**(2), 239-246 (1988).
- 7 C. J. Pedersen, *J. Am. Chem. Soc.*, **92**(2), 386-391 (1970).
- 8 J. J. Christensen, J. O. Hill, and R. M. Izatt, *Science*, **174**, 459-467 (1971).
- 9 M. Hiraoka, 'Crown Compounds, their characteristics and applications', Kodansha Ltd. and Elsevier Scientific Publishing Company, (1982).
- 10 D. J. Cram, *Angew. Chem. Int. Ed. Eng.*, **27**(8), 1009-1112 (1988).
- 11 V. P. Barannikov, S. S. Guseinov, and A. I. V'ugin, *Russ. J. Coord. Chem.*, **28**(3), 153-162 (2002).
- 12 H. K. Frensdorff, *J. Am. Chem. Soc.*, **93**(3), 600-606 (1971).
- 13 F. de Jong and D. N. Reinhoudt, 'Stability and Reactivity of Crown-Ether Complexes', Academic Press, (1981).
- 14 E. Shchori, J. Jagur-Grodzinski, and M. Shporer, *J. Am. Chem. Soc.*, **95**(12), 3842-3846 (1973).
- 15 H. Tsukube, K. Takagi, T. Higashiyama, T. Iwachido, and N. Hayama, *Bull. Chem. Soc. Jpn.*, **58**(12), 3659-3660 (1985).
- 16 R. Ungaro, B. E. Haj, and J. Smid, *J. Am. Chem. Soc.*, **98**(17), 5198-5202 (1976).
- 17 K. H. Pannell, W. Yee, G. S. Lewandos, and D. C. Hambrick, *J. Am. Chem. Soc.*, **99**(5), 1457-1461 (1977).
- 18 K. H. Wong, G. Konizer, and J. Smid, *J. Am. Chem. Soc.*, **92**(3), 666-670 (1970).
- 19 G. W. Gokel, *Chem. Soc. Rev.*, **21**, 39-47 (1992).

- 20 Y. Liu, H.-Y. Zhang, X.-P. Bai, T. Wada, and Y. Inoue, *J. Org. Chem.*, **65**, 7105-7109 (2000).
- 21 C.-C. Su, M.-C. Chang, and L. K. Liu, *Anal. Chim. Acta*, **432**, 261-267 (2001).
- 22 R. B. Davidson, R. M. Izatt, J. J. Christensen, R. A. Schultz, D. M. Dishong, and G. W. Gokel, *J. Org. Chem.*, **49**(26), 5080-5084 (1984).
- 23 J.-M. Lehn, *Acc. Chem. Res.*, **11**(2), 49-57 (1978).
- 24 D. J. Cram, T. Kaneda, R. C. Helgeson, and G. M. Lein, *J. Am. Chem. Soc.*, **101**(22), 6752-6754 (1979).
- 25 D. J. Sam and H. E. Simmons, *J. Am. Chem. Soc.*, **96**(7), 2252-2253 (1974).
- 26 T. Nakamura, T. Ueda, and K. Fujimori, *Bull. Chem. Soc. Jpn.*, **65**, 19-22 (1992).
- 27 M. Shamsipur and F. Raoufi, *Sep. Sci. Techol.*, **37**(2), 481-492 (2002).
- 28 Y. K. Agrawal and S. Sudhakar, *Sep. Purif. Technol.*, **27**, 111-119 (2002).
- 29 T. Fujii, H. Moriyama, T. Hirata, and K. Nishizawa, *Bull. Chem. Soc. Jpn.*, **74**, 1031-1032 (2001).
- 30 H. Tsukube, H. Fukui, and S. Shinoda, *Tetrahedron Lett.*, **42**, 7583-7585 (2001).
- 31 Z. Zeng, W. Qiu, M. Yang, X. Wei, Z. Huang, and F. Li, *J. Chromatogr. A*, **934**, 51-57 (2001).
- 32 V. K. Gupta, S. Chandra, and R. Mangla, *Electrochim. Acta*, **47**, 1579-1586 (2002).
- 33 A. Haidekker and C. G. Huber, *J. Chromatogr. A*, **921**, 217-226 (2001).
- 34 E. Blasius and K.-P. Janzen, *Host Guest Complex Chem., Macrocycles* 189-215 (1985).
- 35 R. J. Steffek, Y. Zelechonok, and K. H. Gahm, *J. Chromatogr. A*, **947**, 301-305 (2002).
- 36 Y. Gong, G. Xue, J. S. Bradshaw, M. L. Lee, and H. K. Lee, *J. Heterocyc. Chem.*, **38**, 1317-1321 (2001).
- 37 Y.-S. Jane and J.-S. Shih, *Analyst*, **120**, 517-522 (1995).
- 38 C. K. Chiang, M. A. Druy, S. C. Gau, A. J. Heeger, E. J. Louis, A. G. MacDiarmid, Y. W. Park, and H. Shirakawa, *J. Am. Chem. Soc.*, **100**(3), 1013-1015 (1977).

- 39 C. K. Chiang, C. R. Fincher, Y. W. Park, A. J. Heeger, H. Shirakawa, E. J. Louis, S. C. Gau, and A. G. MacDiarmid, *Phys. Rev. Lett.*, **39**(17), 1098-1101 (1977).
- 40 D. MacInnes Jr., M. A. Druy, P. J. Nigrey, D. P. Nairns, A. G. MacDiarmid, and A. J. Heeger, *J. Chem. Soc., Chem. Commun.* 317-319 (1981).
- 41 P. J. Nigrey, A. G. MacDiarmid, and A. J. Heeger, *J. Chem. Soc., Chem. Commun.* 594-595 (1979).
- 42 A. J. Heeger, *Angew. Chem. Int. Ed. Eng.*, **40**, 2591-2611 (2001).
- 43 A. G. MacDiarmid, *Angew. Chem. Int. Ed. Eng.*, **40**, 2581-2590 (2001).
- 44 H. Shirakawa, *Angew. Chem. Int. Ed. Eng.*, **40**, 2574-2580 (2001).
- 45 A. J. Heeger, *Synth. Met.*, **125**(1), 23-42 (2002).
- 46 A. G. MacDiarmid, *Synth. Met.*, **125**(1), 11-22 (2002).
- 47 H. Shirakawa, *Synth. Met.*, **125**(1), 3-10 (2002).
- 48 A. J. Epstein, *MRS Bull.*, **22**(6), 16-23 (1997).
- 49 G. M. Spinks, P. C. Innis, T. W. Lewis, L. A. P. Kane-Maguire, and G. G. Wallace, *Mater. Forum*, **24**, 125-166 (2000).
- 50 F. Garnier, G. Tourillon, M. Gazard, and J. C. Dubois, *J. Electroanal. Chem.*, **148**, 299-303 (1983).
- 51 R. D. McCullough, *Adv. Mater.*, **10**(2), 93-116 (1998).
- 52 R. J. Mortimer, *Chem. Soc. Rev.*, **26**, 147-156 (1997).
- 53 J. R. Reynolds, B. Sankaran, G. A. Sotzing, D. J. Irvin, J. A. Irvin, J. L. Reddinger, and S. A. Sapp, *Mater. Res. Soc. Symp. Proc.*, **413**, 373-376 (1996).
- 54 G. A. Sotzing, J. L. Reddinger, and J. R. Reynolds, *Synth. Met.*, **84**, 199-201 (1997).
- 55 M. Frechette, M. Belletete, J.-Y. Bergeron, G. Durocher, and M. Leclerc, *Macromol. Chem. Phys.*, **198**, 1709-1722 (1997).
- 56 B. Krische and M. Zagorska, *Synth. Met.*, **28**, C263-C268 (1989).
- 57 R. J. Waltman and J. Bargon, *Can. J. Chem.*, **64**, 76-95 (1986).
- 58 Y. Furukawa, *J. Phys. Chem.*, **100**(39), 15644-15653 (1996).
- 59 R. B. Kaner and A. G. MacDiarmid, *Sci. Am.*, **258**(2), 60-65 (1988).
- 60 S. Akoudad and J. Roncali, *Chem. Comm.*, 2081-2082 (1998).
- 61 M. G. Kanatzidis, *Chem. Eng.*, 36-54 (1990).

- 62 A. G. MacDiarmid and W. Zheng, *MRS Bull.*, **22**(6), 24-30 (1997).
- 63 G. Tourillon, in 'Polythiophene and Its Derivatives', ed. T. A. Skotheim, (1986).
- 64 T.-C. Chung, J. H. Kaufman, A. J. Heeger, and F. Wudl, *Phys. Rev. B*, **30**(2), 702-710 (1984).
- 65 K. C. Gordon, Personal Communication, (2003).
- 66 R. M. Eales and A. R. Hillman, *J. Electroanal. Chem.*, **250**, 219-223 (1988).
- 67 S. J. Higgins, *Chem. Soc. Rev.*, **26**, 247-257 (1997).
- 68 H. S. O. Chan and S. C. Ng, *Prog. Polym. Sci.*, **23**, 1167-1231 (1998).
- 69 F. Martinez, J. Retuert, and G. Neculqueo, *Int. J. Polymeric Mater.*, **28**(1-4), 51-59 (1995).
- 70 P. T. Henderson and D. M. Collard, *Chem. Mater.*, **7**, 1879-1889 (1995).
- 71 E. Naudin, N. E. Mehdi, C. Soucy, L. Breau, and D. Belanger, *Chem. Mater.*, **13**, 634-642 (2001).
- 72 B. Rasch and W. Vielstich, *J. Electroanal. Chem.*, **370**, 109-117 (1994).
- 73 J. Roncali, *J. Mater. Chem.*, **9**, 1875-1893 (1999).
- 74 R. M. Souto Maior, K. Hinkelmann, H. Eckert, and F. Wudl, *Macromol.*, **23**, 1268-1279 (1990).
- 75 M.-A. Sato and M. Hiroi, *Chem. Lett.*, 985-988 (1994).
- 76 K. Faid, R. Cloutier, and M. Leclerc, *Synth. Met.*, **55-57**, 1272-1277 (1993).
- 77 R. D. McCullough, S. P. Williams, S. Tristram-Nagle, M. Jayaraman, P. C. Ewbank, and L. Miller, *Synth. Met.*, **69**, 279-282 (1995).
- 78 A. Boldea, I. Levesque, and M. Leclerc, *J. Mater. Chem.*, **9**, 2133-2138 (1999).
- 79 K. Faid, M. Frechette, M. Ranger, L. Mazerolle, I. Levesque, and M. Leclerc, *Chem. Mater.*, **7**, 1390-1396 (1995).
- 80 F. Goldoni, D. Larossi, A. Mucci, and L. Schenetti, *J. Chem. Soc., Chem. Commun.*, 2175-2176 (1997).
- 81 M. Leclerc, F. M. Diaz, and G. Wegner, *Makromol. Chem.*, **190**, 3105-3116 (1989).
- 82 M. R. Andersson, D. Selse, M. Berggren, H. Jarvinen, T. Hjertberg, O. Inganas, O. Wennerstrom, and J.-E. Osterholm, *Macromol.*, **27**(22), 6503-6506 (1994).

- 83 Y. Miyazaki and T. Yamamoto, *Synth. Met.*, **64**, 69-76 (1994).
- 84 J.-P. Lere-Porte, J. J. E. Moreau, and C. Torreilles, *Eur. J. Org. Chem.* (7), 1249-1258 (2001).
- 85 R. Cloutier and M. Leclerc, *J. Chem. Soc., Chem. Commun.*, 1194-1195 (1991).
- 86 M. Hasik, J. E. Laska, A. Pron, I. Kulszewicz-Bajer, K. Koziel, and M. Lapkowski, *J. Polym. Sci., Part A: Polym. Chem.*, **30**, 1741-1746 (1992).
- 87 A. Pron, G. Louarn, M. Lapkowski, M. Zagorska, J. Glowczyk-Zubek, and S. Lefrant, *Macromol.*, **28**, 4644-4649 (1995).
- 88 B. Krische, J. Hellberg, and C. Lilja, *J. Chem. Soc., Chem. Commun.*, 1476-1478 (1987).
- 89 M. Lapkowski, M. Zagorska, I. Kulszewicz-Bajer, K. Koziel, and A. Pron, *J. Electroanal. Chem.*, **310**, 57-70 (1991).
- 90 M. Zagorska, I. Kulszewicz-Bajer, M. Lapkowski, J. Laska, M. Hasik, and A. Pron, *Synth. Met.*, **41-43**, 3009-3012 (1991).
- 91 M. C. Gallazzi, L. Castellani, R. A. Marin, and G. Zerbi, *J. Polym. Sci., Part A: Polym. Chem.*, **31**, 3339-3349 (1993).
- 92 G. Zotti, M. C. Gallazzi, G. Zerbi, and S. V. Meille, *Synth. Met.*, **73**, 217-225 (1995).
- 93 B. Krische, M. Zagorska, and J. Hellberg, *Synth. Met.*, **58**, 295-307 (1993).
- 94 M. Lapkowski, M. Zagorska, I. Kulszewicz-Bajer, and A. Pron, *Synth. Met.*, **55-57**, 1580-1583 (1993).
- 95 J. Tanguy, A. Pron, M. Zagorska, and I. Kulszewicz-Bajer, *Synth. Met.*, **45**, 81-105 (1991).
- 96 I. Kulszewicz-Bajer, M. Zagorska, F. Genoud, J. Kruszka, K. Stocka, A. Pron, and M. Nechtschein, *Synth. Met.*, **35**, 129-133 (1990).
- 97 C. Wang, M. E. Benz, E. LeGoff, J. L. Schindler, J. Allbritton-Thomas, C. R. Kannewurf, and M. G. Kanatzidis, *Chem. Mater.*, **6**, 401-411 (1994).
- 98 M. C. Gallazzi, L. Castellani, and G. Zerbi, *Synth. Met.*, **41-43**, 495-498 (1991).
- 99 R. D. McCullough and R. D. Lowe, *J. Chem. Soc., Chem. Commun.*, 70-72 (1992).

- 100 R. D. McCullough and S. P. Williams, *J. Am. Chem. Soc.*, **115**(24), 11608-11609 (1993).
- 101 R. D. McCullough, S. Tristram-Nagle, S. P. Williams, R. D. Lowe, and M. Jayaraman, *J. Am. Chem. Soc.*, **115**(11), 4910-4911 (1993).
- 102 R. D. McCullough, R. D. Lowe, M. Jayaraman, and D. L. Anderson, *J. Org. Chem.*, **58**(4), 904-912 (1993).
- 103 R. D. McCullough and M. Jayaraman, *J. Chem. Soc., Chem. Commun.*, 135-136 (1995).
- 104 T.-A. Chen and R. D. Rieke, *J. Am. Chem. Soc.*, **114**, 10087-10088 (1992).
- 105 T.-A. Chen, R. A. O'Brien, and R. D. Rieke, *Macromol.*, **26**(13), 3462-3463 (1993).
- 106 T.-A. Chen and R. D. Rieke, *Synth. Met.*, **60**, 175-177 (1993).
- 107 T.-A. Chen, X. Wu, and R. D. Rieke, *J. Am. Chem. Soc.*, **117**, 233-244 (1995).
- 108 H. Jarvinen, J. Laakso, T. Taka, and J. E. Osterholm, *Synth. Met.*, **55**(2-3), 1260-1265 (1993).
- 109 M. Miyasaka, T. Yamazaki, E. Tsuchida, and H. Nishide, *Macromol.*, **33**(22), 8211-8217 (2000).
- 110 I. Levesque and M. Leclerc, *Chem. Mater.*, **8**, 2843-2849 (1996).
- 111 G. Daoust and M. Leclerc, *Macromol.*, **24**, 455-459 (1991).
- 112 S.-C. Ng and P. Miao, *Macromol. Chem. Phys.*, **200**(9), 2166-2172 (1999).
- 113 S.-A. Chen and C.-C. Tsai, *Macromol.*, **26**(9), 2234-2239 (1993).
- 114 A. K. Narula, R. Singh, K. L. Yadav, K. B. Ravat, and S. Chandra, *App. Biochem. Biotech.*, **96**(1-3), 109-117 (2001).
- 115 S. C. Ng, P. Fu, W.-L. Yu, H. S. O. Chan, and K. L. Tan, *Synth. Met.*, **87**(2), 119-122 (1997).
- 116 S. C. Ng, L. G. Xu, and H. S. O. Chan, *Synth. Met.*, **94**(2), 185-191 (1998).
- 117 J. A. Irvin and J. R. Reynolds, *Polymer*, **39**(11), 2339-2347 (1998).
- 118 N. DiCesare, M. Belletete, A. Donat-Bouillud, M. Leclerc, and G. Durocher, *Macromol.*, **31**(18), 6289-6296 (1998).
- 119 J. Kowalik, L. M. Tolbert, S. Narayan, and A. S. Abhiraman, *Macromol.*, **34**(16), 5471-5479 (2001).
- 120 R. L. Elsenbaumer, K.-Y. Jen, G. G. Miller, H. Eckhardt, L. W. Shacklette, and R. Jow, in 'Poly(alkyl thiophenes) and Poly(substituted heteroaromatic

- vinylenes): Versatile, Highly Conductive, Processible Polymers with Tunable Properties', ed. H. Kuzmany, M. Mehring, and S. Roth, (1987).
- 121 G. Barbarella, A. Bongini, and M. Zambianchi, *Macromol.*, **27**(11), 3039-3045 (1994).
- 122 N. Somanathan, S. Radhakrishnan, M. Thelakkat, and H. W. Schmidt, *Macromol. Mater. Eng.*, **287**(4), 236-242 (2002).
- 123 J. H. Schon, A. Dodabalapur, Z. Bao, C. Kloc, O. Schenker, and B. Batlogg, *Nature*, **410**, 189-192 (2001).
- 124 M. Lemaire and R. Garreau, *New J. Chem.*, **13**, 863-871 (1989).
- 125 J. Roncali, *Chem. Rev.*, **92**, 711-738 (1992).
- 126 J. Roncali, R. Garreau, and M. Lemaire, *J. Electroanal. Chem.*, **278**(1-2), 373-378 (1990).
- 127 J. Kankare, J. Lukkari, P. Pasanen, R. Sillanpaa, H. Laine, and K. Harmaa, *Macromol.*, **27**(15), 4327-4334 (1994).
- 128 M. R. Bryce, A. Chissel, P. Kathirgamanathan, D. Parker, and N. R. M. Smith, *J. Chem. Soc., Chem. Commun.*, 466-467 (1987).
- 129 J. Roncali, R. Garreau, D. Delabouglise, F. Garnier, and M. Lemaire, *Synth. Met.*, **28**, C341-C348 (1989).
- 130 J. Roncali, L. H. Shi, R. Garreau, F. Garnier, and M. Lemaire, *Synth. Met.*, **36**, 267-273 (1990).
- 131 A.-C. Chang, R. L. Blankespoor, and L. L. Miller, *J. Electroanal. Chem.*, **236**, 239-252 (1987).
- 132 J. Roncali, R. Garreau, D. Delabouglise, F. Garnier, and M. Lemaire, *J. Chem. Soc., Chem. Commun.*, 679-681 (1989).
- 133 J. Roncali, P. Marque, R. Garreau, F. Garnier, and M. Lemaire, *Macromol.*, **23**, 1347-1352 (1990).
- 134 J. Roncali, L. H. Shi, and F. Garnier, *J. Phys. Chem.*, **95**, 8983-8989 (1991).
- 135 L. H. Shi, F. Garnier, and J. Roncali, *Synth. Met.*, **41-43**, 547-550 (1991).
- 136 L. H. Shi, F. Garnier, and J. Roncali, *Solid State Commun.*, **77**(10), 811-815 (1991).
- 137 D. T. McQuade, A. E. Pullen, and T. M. Swager, *Chem. Rev.*, **100**, 2537-2574 (2000).

- 138 R. D. McCullough and S. P. Williams, *Chem. Mater.*, **7**(11), 2001-2003 (1995).
- 139 M. Feldhues, G. Kampf, H. Litterer, T. Mecklenburg, and P. Wegener, *Synth. Met.*, **28**, C487-C493 (1989).
- 140 S. Scheib and P. Bauerle, *J. Mater. Chem.*, **9**, 2139-2150 (1999).
- 141 B. Fabre and J. Simonet, *Coord. Chem. Rev.*, **178-180**, 1211-1250 (1998).
- 142 P. Marrec, B. Fabre, and J. Simonet, *J. Electroanal. Chem.*, **437**, 245-253 (1997).
- 143 P. Blanchard, L. Huchet, E. Levillain, and J. Roncali, *Electrochem. Comm.*, **2**(1), 1-5 (2000).
- 144 I. F. Perepichka, M. Besbes, E. Levillain, M. Salle, and J. Roncali, *Chem. Mater.*, **14**(1), 449-457 (2002).
- 145 M. J. Marsella and T. M. Swager, *J. Am. Chem. Soc.*, **115**(25), 12214-12215 (1993).
- 146 M. J. Marsella and T. M. Swager, *Polym. Prepr. (Am. Chem. Soc., Div. Polym. Chem.)*, **35**(1), 271-272 (1994).
- 147 M. J. Marsella, R. J. Newland, and T. M. Swager, *Polym. Prepr. (Am. Chem. Soc., Div. Polym. Chem.)*, **36**(1), 594-595 (1995).
- 148 B. Fabre, P. Marrec, and J. Simonet, *J. Electrochem. Soc.*, **145**(12), 4110-4119 (1998).
- 149 P. Bauerle and S. Scheib, *Adv. Mater.*, **5**(11), 848-853 (1993).
- 150 F. Sannicolo, E. Brenna, T. Benincori, G. Zotti, S. Zecchin, G. Schiavon, and T. Pilati, *Chem. Mater.*, **10**, 2167-2176 (1998).
- 151 L. K. Bicknell, M. J. Marsella, and T. M. Swager, *Polym. Prepr. (Am. Chem. Soc., Div. Polym. Chem.)*, **35**(1), 269-270 (1994).
- 152 P. Bauerle and S. Scheib, *Acta Polym.*, **46**(2), 124-129 (1995).
- 153 T. Sone, K. Sato, and Y. Ohba, *Bull. Chem. Soc. Jpn.*, **62**(3), 838-844 (1989).
- 154 A. Berlin, G. Zotti, S. Zecchin, and G. Schiavon, *Synth. Met.*, **131**(1-3), 149-160 (2002).
- 155 G. Zotti and G. Schiavon, *Synth. Met.*, **39**, 183-190 (1990).
- 156 T. Yamamoto, M. Omote, Y. Miyazaki, A. Kashiwazaki, B.-L. Lee, T. Kanbara, K. Osakada, T. Inoue, and K. Kubota, *Macromol.*, **30**(23), 7158-7165 (1997).

- 157 Y. Miyazaki, T. Kanbara, K. Osakada, and T. Yamamoto, *Polym. Prepr., Jpn.*, **42**(3), 724 (1993).
- 158 Y. Miyazaki and T. Yamamoto, *Chem. Lett.*, (1), 41-44 (1994).
- 159 M. Bouachrine, J.-P. Lere-Porte, J. J. E. Moreau, F. Serein-Spirau, and C. Torrelles, *J. Mater. Chem.*, **10**(2), 263-268 (2000).
- 160 J. R. Smith, S. A. Campbell, N. M. Ratcliffe, and M. Dunleavy, *Synth. Met.*, **63**(3), 233-243 (1994).
- 161 J. R. Smith, N. M. Ratcliffe, and S. A. Campbell, *Synth. Met.*, **73**, 171-182 (1995).
- 162 H.-P. Welzel, G. Kossmehl, G. Engelmann, and W. Plieth, *Eur. Polym. J.*, **33**(3), 299-301 (1997).
- 163 C. A. Cutler, 'Electrochemical and Photoelectrochemical Studies of Functionalised Polythiophenes', PhD Thesis, Department of Chemistry, The University of Wollongong, (2000).
- 164 C. A. Cutler, A. K. Burrell, G. E. Collis, P. C. Dastoor, D. L. Officer, C. O. Too, and G. G. Wallace, *Synth. Met.*, **123**(2), 225-237 (2001).
- 165 J. Chen, A. K. Burrell, G. E. Collis, D. L. Officer, G. F. Swiegers, C. O. Too, and G. G. Wallace, *Electrochim. Acta*, **47**, 2715-2724 (2002).
- 166 C. O. Too, G. G. Wallace, A. K. Burrell, G. E. Collis, D. L. Officer, E. W. Boge, S. G. Brodie, and E. J. Evans, *Synth. Met.*, **123**, 53-60 (2001).
- 167 J. Kagan and H. Liu, *Synth. Met.*, **82**, 75-81 (1996).
- 168 K. Nawa, I. Imae, N. Noma, and Y. Shirota, *Macromol.*, **28**(3), 723-729 (1995).
- 169 I. Imae, K. Nawa, Y. Ohsedo, N. Noma, and Y. Shirota, *Macromol.*, **30**(3), 380-386 (1997).
- 170 M. Pagels, J. Heinze, B. Geschke, and V. Rang, *Electrochim. Acta*, **46**, 3943-3954 (2001).
- 171 K. Kikukawa, S. Takamura, H. Hirayama, H. Namiki, F. Wada, and T. Matsuda, *Chem. Lett.*, (5), 511-514 (1980).
- 172 L. Yi, Z. Zhuangyu, and H. Hongwen, *Synth. Commun.*, **25**(4), 595-601 (1995).
- 173 P. D. Beer, O. Kocian, R. J. Mortimer, and C. Ridgway, *J. Chem. Soc., Chem. Commun.*, (20), 1460-1463 (1991).

- 174 P. D. Beer, O. Kocian, R. J. Mortimer, and C. Ridgway, *Analyst*, **117**(8), 1247-1249 (1992).
- 175 P. D. Beer, O. Kocian, R. J. Mortimer, and C. Ridgway, *J. Chem. Soc., Faraday Trans.*, **89**(2), 333-338 (1993).
- 176 P. D. Beer, O. Kocian, R. J. Mortimer, and C. Ridgway, *J. Chem. Soc., Dalton Trans.: Inorg. Chem.*, (17), 2629-2638 (1993).
- 177 F. Wada, H. Hirayama, H. Namiki, K. Kikukawa, and T. Matsuda, *Bull. Chem. Soc. Jpn.*, **53**, 1473-1474 (1980).
- 178 O. Kocian, R. J. Mortimer, and P. D. Beer, *J. Chem. Soc., Perkin Trans. 1*, (11), 3203-3205 (1990).
- 179 O. Kocian, R. J. Mortimer, and P. D. Beer, *Tetrahedron Lett.*, **31**(35), 5069-5072 (1990).
- 180 G. R. Brown and A. J. Foubister, *J. Med. Chem.*, **22**(8), 997-999 (1979).
- 181 M. Shirai, M. Kuwahara, and M. Tanaka, *Eur. Polym. J.*, **24**(5), 403-410 (1988).
- 182 M. Shirai, M. Kuwahara, and M. Tanaka, *J. Polym. Sci., Part A: Polym. Chem.*, **28**(9), 2563-2567 (1990).
- 183 M. Shirai, T. Orikata, and M. Tanaka, *Makromol. Chem., Rapid Commun.*, **4**(2), 65-69 (1983).
- 184 M. Shirai, A. Ueda, and M. Tanaka, *Makromol. Chem.*, **186**(3), 493-500 (1985).
- 185 M. Shirai, A. Ueda, and M. Tanaka, *Makromol. Chem.*, **186**(12), 2519-2527 (1985).
- 186 M. Shirai, A. Ueda, and M. Tanaka, *J. Polym. Sci., Part A: Polym. Chem.*, **25**(7), 1811-1823 (1987).
- 187 E. Luboch, A. Cygan, and J. F. Biernat, *Tetrahedron*, **47**(24), 4101-4112 (1991).
- 188 M. V. Alfimov, S. P. Gromov, and I. K. Lednev, *Chem. Phys. Lett.*, **185**(5-6), 455-460 (1991).
- 189 E. A. Baryshnikova, T. I. Sergeeva, U. Oertel, J. Nagel, and S. Y. Zaitsev, *Macromol. Rapid Commun.*, **21**(1), 45-47 (2000).

- 190 A. V. Barzykin, M. A. Fox, E. N. Ushakov, O. B. Stanislavsky, S. P. Gromov, O. A. Fedorova, and M. V. Alfimov, *J. Am. Chem. Soc.*, **114**(16), 6381-6385 (1992).
- 191 A. Feofanov, A. Ianoul, V. Oleinikov, S. Gromov, O. Fedorova, M. Alfimov, and I. Nabiev, *J. Phys. Chem.*, **100**(6), 2154-2160 (1996).
- 192 S. P. Gromov, O. A. Fedorova, E. N. Ushakov, I. I. Baskin, A. V. Lindeman, E. V. Malysheva, T. A. Balashova, A. S. Arsenev, and M. V. Alfimov, *Russ. Chem. Bull.*, **47**(1), 97-106 (1998).
- 193 E. N. Ushakov, S. P. Gromov, A. V. Buevich, I. I. Baskin, O. A. Fedorova, A. I. Vedernikov, M. V. Alfimov, B. Eliasson, and U. Edlund, *J. Chem. Soc., Perkin Trans. 2*, (3), 601-608 (1999).
- 194 S. Y. Zaitsev, T. I. Sergeeva, E. A. Baryshnikova, W. Zeib, D. Mobius, O. V. Yescheulova, S. P. Gromov, O. A. Fedorova, and M. V. Alfimov, *Mater. Sci. Eng. C: Biomim. Supramol. Sys.*, **C8-C9**, 469-473 (1999).
- 195 S. Y. Zaitsev, V. P. Vereschetin, E. A. Baryshnikova, S. P. Gromov, O. A. Fedorova, M. V. Alfimov, H. Huesmann, and D. Mobius, *Thin Solid Films*, **327-329**, 821-823 (1998).
- 196 S. Gromov, O. Fedorova, and M. Alfimov, *Mol. Cryst. Liq. Cryst.*, **246**, 183-186 (1994).
- 197 M. V. Alfimov, Y. V. Fedorov, O. A. Fedorova, S. P. Gromov, R. E. Hester, I. K. Lednev, J. N. Moore, V. P. Oleshko, and A. I. Vedernikov, *Spectrochim. Acta, Part A*, **53**(11), 1853-1865 (1997).
- 198 M. V. Alfimov, Y. V. Fedorov, O. A. Fedorova, S. S. Gromov, R. E. Hester, I. K. Lednev, J. N. Moore, V. P. Oleshko, and A. I. Vedernikov, *J. Chem. Soc., Perkin Trans. 2*, (7), 1441-1447 (1996).
- 199 I. K. Lednev and M. C. Petty, *Thin Solid Films*, **284-285**, 683-686 (1996).
- 200 V. P. Tsybyshev, V. A. Livshits, B. B. Meshkov, O. A. Fedorova, S. P. Gromov, and M. V. Alfimov, *Russ. Chem. Bull.*, **46**(7), 1239-1244 (1997).
- 201 S. Y. Zaitsev, S. P. Gromov, O. A. Fedorova, E. A. Baryshnikova, V. P. Vereschetin, W. Zeiss, H. Huesmann, M. V. Alfimov, and D. Mobius, *Colloids Surf., A*, **131**(1-3), 325-332 (1998).

- 202 S. Y. Zaitsev, V. P. Vereschetin, S. P. Gromov, O. A. Fedorova, M. V. Alfimov, H. Heusmann, and D. Mobius, *Supramol. Sci.*, **4**(3-4), 519-524 (1997).
- 203 S. P. Gromov, O. A. Fedorova, E. N. Ushakov, A. V. Buevich, I. I. Baskin, Y. V. Pershina, B. Eliasson, U. Edlund, and M. V. Alfimov, *J. Chem. Soc., Perkin Trans. 2*, (7), 1323-1329 (1999).
- 204 E. N. Ushakov, S. P. Gromov, O. A. Fedorova, Y. V. Pershina, M. V. Alfimov, F. Barigelletti, L. Flamigni, and V. Balzani, *J. Phys. Chem. A*, **103**(50), 11188-11193 (1999).
- 205 G. Lindsten, O. Wennerstrom, and B. Thulin, *Acta Chem. Scand., Ser. B.*, **B40**(7), 545-554 (1986).
- 206 P. D. Beer, C. Blackburn, J. F. McAleer, and H. Sikanyika, *Inorg. Chem.*, **29**(3), 378-381 (1990).
- 207 P. D. Beer, H. Sikanyika, C. Blackburn, and J. F. McAleer, *J. Chem. Soc., Chem. Commun.*, (23), 1831-1833 (1989).
- 208 B. Winkler, A. W. H. Mau, and L. Dai, *Phys. Chem. Chem. Phys.*, **2**(2), 291-295 (2000).
- 209 G. E. Collis, A. K. Burrell, and D. L. Officer, *Tetrahedron Lett.*, **42**(49), 8733-8735 (2001).
- 210 K. H. Wong and H. L. Ng, *Tetrahedron Lett.*, **44**, 4295-4296 (1979).
- 211 E. M. Hyde, B. L. Shaw, and I. Shepherd, *J. Chem. Soc., Dalton Trans.*, 1696-1705 (1978).
- 212 G. E. Collis, Personal Communication, (2002).
- 213 R. M. Silverstein, G. C. Bassler, and T. C. Morrill, 'Spectrometric Identification of Organic Compounds', John Wiley & Sons, Inc., (1991).
- 214 F. Demanze, J. Cornil, F. Garnier, G. Horowitz, P. Valat, A. Yassar, R. Lazzaroni, and J.-L. Bredas, *J. Phys. Chem. B*, **101**(23), 4553-4558 (1997).
- 215 J. March, 'Advanced Organic Chemistry', John Wiley & Sons, (1985).
- 216 K. U. I. Ulyanov, *Pure App. Chem.*, **9**, 307-335 (1964).
- 217 J.-F. Carpentier, Y. Castanet, J. Brocard, A. Mortreux, and F. Petit, *Tetrahedron Lett.*, **32**(36), 4705-4708 (1991).
- 218 A. K. Mohanakrishnan, M. V. Lakshmikanthan, C. McDougal, M. P. Cava, J. W. Baldwin, and R. M. Metzger, *J. Org. Chem.*, **63**, 3105-3112 (1998).

- 219 A. K. Mohanakrishnan, M. V. Lakshmikantham, and M. P. Cava, *Sulfur Lett.*, **21**(6), 247-252 (1998).
- 220 F. L. Cook, C. W. Bowers, and C. L. Liotta, *J. Org. Chem.*, **39**(23), 3416-3418 (1974).
- 221 C. L. Liotta and H. P. Harris, *J. Am. Chem. Soc.*, **96**(7), 2250-2252 (1974).
- 222 C. L. Liotta, H. P. Harris, M. McDermott, T. Gonzalez, and K. Smith, *Tetrahedron Lett.*, (28), 2417-2420 (1974).
- 223 D. C. W. Reid, *A Building Block Approach to Porphyrin Arrays*, PhD Thesis, Department of Chemistry, Massey University (1998).
- 224 U. Lauter, W. H. Meyer, and G. Wegner, *Macromol.*, **30**, 2092-2101 (1997).
- 225 Samples provided by A. Ballantyne.
- 226 Z. Ge, Y. Li, C. Du, S. Wang, and D. Zhu, *Thin Solid Films*, **368**, 147-150 (2000).
- 227 Z. Ge, Y. Li, Z. Shi, F. Bai, and D. Zhu, *J. Phys. Chem.*, **61**, 1075-1079 (2000).
- 228 Z. Ge, Y. Li, N. Sun, S. Wang, and D. Zhu, *Supramol. Chem.*, **12**, 451-455 (2001).
- 229 J.-P. Bourgeois, L. Echegoyen, M. Fibbioli, E. Pretsch, and F. Diederich, *Angew. Chem. Int. Ed.*, **37**(15), 2118-2121 (1998).
- 230 J.-P. Bourgeois, P. Seiler, M. Fibbioli, E. Pretsch, and F. Diederich, *Helv. Chim. Acta*, **82**, 1572-1595 (1999).
- 231 W. W. Parish, P. E. Stott, and C. W. McCausland, *J. Org. Chem.*, **43**(24), 4577-4581 (1978).
- 232 N. Z. Saifullina, A. D. Grebenyuk, I. A. Stempnevskaya, K. M. Valikhanov, V. I. Vinogradova, M. G. Levkovich, and A. K. Tashmukhamedova, *Chem. Nat. Compd.*, **34**(6), 711-714 (1998).
- 233 P. E. Stott, J. S. Bradshaw, and W. W. Parish, *J. Am. Chem. Soc.*, **102**, 4810-4815 (1980).
- 234 H. Tuncer and C. Erk, *Dyes Pigm.*, **44**(2), 81-86 (2000).
- 235 G. I. Feutrill and R. N. Mirrington, *Tetrahedron Lett.*, (16), 1327-1328 (1970).
- 236 G. I. Feutrill and R. N. Mirrington, *Aust. J. Chem.*, **25**, 1719-1729 (1972).
- 237 J. M. Lansinger and R. C. Ronald, *Synth. Commun.*, **9**(4), 341-349 (1979).

- 238 M. Ouchi, Y. Inoue, T. Kanzaki, and T. Hakushi, *J. Org. Chem.*, **49**, 1408-1412 (1984).
- 239 S. Kumar and S. H. Mashraqui, *Indian J. Chem., Sect. B: Org. Chem. Incl. Med. Chem.*, **40**(1), 5-10 (2001).
- 240 P. Garcia, J. M. Pernaut, P. Hapiot, V. Wintgens, P. Valat, F. Garnier, and D. Delabougliuse, *J. Phys. Chem.*, **97**(2), 513-516 (1993).
- 241 M. Belletete, L. Mazerolle, N. Desrosiers, M. Leclerc, and G. Durocher, *Macromol.*, **28**(25), 8587-8597 (1995).
- 242 N. DiCesare, M. Belletete, A. Donat-Bouillud, M. Leclerc, and G. Durocher, *J. Lumin.*, **81**(2), 111-125 (1999).
- 243 N. DiCesare, M. Belletete, M. Leclerc, and G. Durocher, *Synth. Met.*, **98**(1), 31-40 (1998).
- 244 N. DiCesare, M. Belletete, C. Marrano, M. Leclerc, and G. Durocher, *J. Phys. Chem. A*, **103**(7), 795-802 (1999).
- 245 N. DiCesare, M. Belletete, C. Marrano, M. Leclerc, and G. Durocher, *J. Phys. Chem. A*, **102**(26), 5142-5149 (1998).
- 246 R. Rossi, M. Ciofalo, A. Carpita, and G. Ponterini, *J. Photochem. Photobiol. A., Chem.*, **70**(1), 59-67 (1993).
- 247 S. A. Lee, S. Hotta, and F. Nakanishi, *J. Phys. Chem. A*, **104**(9), 1827-1833 (2000).
- 248 N. R. Krishnaswamy and C. S. S. R. Kumar, *Indian J. Chem., Sect. B: Org. Chem. Incl. Med. Chem.*, **32B**(7), 766-771 (1993).
- 249 P. Hrdlovic, J. Krajcovic, and D. Vegh, *J. Photochem. Photobiol. A., Chem.*, **144**(2-3), 73-81 (2001).
- 250 C. Visy, J. Lukkari, and J. Kankare, *Macromol.*, **27**(12), 3322-3329 (1994).
- 251 E. J. Shin, *Chem. Lett.*, (7), 686-687 (2002).
- 252 F. Vogtle, 'Supramolecular Chemistry', John Wiley & Sons, (1991).
- 253 R. C. Weast, in 'CRC Handbook of Chemistry and Physics', 1989.
- 254 H.-G. Lohr and F. Vogtle, *Acc. Chem. Res.*, **18**, 65-72 (1985).
- 255 S. Fery-Forgues, M.-T. Le Bris, J.-P. Guette, and B. Valeur, *J. Phys. Chem.*, **92**(22), 6233-6237 (1988).
- 256 J. Bourson and B. Valeur, *J. Phys. Chem.*, **93**(9), 3871-3876 (1989).

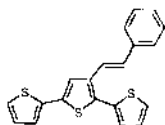
- 257 L. Cazaux, M. Faher, A. Lopez, C. Picard, and P. Tisnes, *J. Photochem. Photobiol. A., Chem.*, **77**, 217-225 (1994).
- 258 M. Leclerc, M. Frechette, J.-Y. Bergeron, M. Ranger, I. Levesque, and K. Faid, *Macromol. Chem. Phys.*, **197**, 2077-2087 (1996).
- 259 I. Levesque and M. Leclerc, *J. Chem. Soc., Chem. Commun.*, (22), 2293-2294 (1995).
- 260 A. K. Burrell, D. L. Officer, G. E. Collis, and S. M. Scott, *J. Org. Chem.*, submitted for publication (2003).
- 261 T. M. Clarke, Personal Communication, (2003).
- 262 R. A. J. Janssen, L. Smilowitz, N. S. Sariciftci, and D. Moses, *J. Chem. Phys.*, **101**(3), 1787-1798 (1994).
- 263 S. Hotta, S. D. D. V. Rughooputh, A. J. Heeger, and F. Wudl, *Macromol.*, **20**(1), 212-215 (1987).
- 264 L. R. Sousa, B. Son, T. E. Trehearne, R. W. Stevenson, S. J. Ganion, B. E. Beeson, S. Barnell, T. E. Mabry, M. Yao, C. Chakrabarty, P. L. Bock, C. C. Yoder, and S. Pope, *ACS Symposium Series*, **538**, 10-24 (1993).
- 265 J. Kim, D. T. McQuade, S. K. McHugh, and T. M. Swager, *Angew. Chem. Int. Ed.*, **39**(21), 3868-3873 (2000).
- 266 S. Iwata and K. Tanaka, *J. Chem. Soc., Chem. Commun.*, (15), 1491-1492 (1995).
- 267 K. Kimura, S. Iketani, and T. Shono, *Anal. Chim. Acta*, **203**(1), 85-89 (1987).
- 268 L. Tarazi, H. Choi, J. C. Mason, J. Sowell, L. Strekowski, and G. Patonay, *Microchem. J.*, **72**(1), 55-62 (2002).
- 269 A. Gocmen and C. Erk, *J. Inclusion Phenom. Macrocyclic Recog. Chem.*, **26**(1-3), 67-72 (1996).
- 270 J. H. Chang, Y. M. Choi, and Y.-K. Shin, *Bull. Korean Chem. Soc.*, **22**(5), 527-530 (2001).
- 271 H.-J. Xu, *J. Photochem. Photobiol. A., Chem.*, **92**(1-2), 35-38 (1995).
- 272 S. Shinkai, Y. Ishikawa, H. Shinkai, T. Tsuno, H. Makishima, K. Ueda, and O. Manabe, *J. Am. Chem. Soc.*, **106**(6), 1801-1808 (1984).
- 273 N. Mateeva, T. Deligeorgiev, M. Mitewa, S. Simova, and I. Dimov, *J. Inclusion Phenom. Macrocyclic Recog. Chem.*, **17**(1), 81-91 (1994).
- 274 H. Warmke, W. Wiczak, and T. Ossowski, *Talanta*, **52**(3), 449-456 (2000).

- 275 N. M. Richardson and I. O. Sutherland, *Tetrahedron Lett.*, **26**(31), 3739-3742 (1985).
- 276 A. Tahri, E. Cielen, K. J. Van Aken, G. J. Hoornaert, F. C. De Schryver, and N. Boens, *J. Chem. Soc., Perkin Trans. 2*, (8), 1739-1748 (1999).
- 277 J. Si, Y. Wu, L. Cai, Y. Liu, B. Du, T. Xu, and H. An, *J. Inclusion Phenom. Macrocyclic Recog. Chem.*, **17**(3), 249-258 (1994).
- 278 R. Colditz, D. Grebner, M. Helbig, and S. Rentsch, *Chem. Phys.*, **201**(2-3), 309-320 (1995).
- 279 R. S. Becker, J. Seixas de Melo, A. L. Macanita, and F. Elisei, *Pure App. Chem.*, **67**(1), 9-16 (1995).
- 280 D. Grebner, M. Helbig, and S. Rentsch, *J. Phys. Chem.*, **99**(46), 16991-16998 (1995).
- 281 D. V. Lap, D. Grebner, S. Rentsch, and H. Naarmann, *Chem. Phys. Lett.*, **211**(1), 135-139 (1993).
- 282 J. Seixas de Melo, F. Elisei, C. Gartner, G. G. Aloisi, and R. S. Becker, *J. Phys. Chem. A*, **104**(30), 6907-6911 (2000).
- 283 J. J. Apperloo, L. B. Groenendaal, H. Verheyen, M. Jayakannan, R. A. J. Janssen, A. Dkhissi, D. Beljonne, R. Lazzaroni, and J.-L. Bredas, *Chem. Eur. J.*, **8**(10), 2384-2396 (2002).
- 284 H. Chosrovian, S. Rentsch, D. Grebner, D. U. Dahm, E. Birckner, and H. Naarmann, *Synth. Met.*, **60**(1), 23-26 (1993).
- 285 D. Oelkrug, H.-J. Engelhaaf, D. R. Worrall, and F. Wilkinson, *J. Fluorescence*, **5**(2), 165-170 (1995).
- 286 S. Rentsch, J. P. Yang, W. Paa, E. Birckner, J. Schiedt, and R. Weinkauff, *Phys. Chem. Chem. Phys.*, **1**(8), 1707-1714 (1999).
- 287 D. Birnbaum and B. E. Kohler, *J. Chem. Phys.*, **90**(7), 3506-3510 (1989).
- 288 R. S. Becker, J. S. d. Melo, A. L. Macanita, and F. Elisei, *J. Phys. Chem.*, **100**(48), 18683-18695 (1996).
- 289 B. Xu and S. Holdcroft, *J. Am. Chem. Soc.*, **115**(18), 8447-8448 (1993).
- 290 C. Evans, D. Weir, J. C. Scaiano, A. MacEachern, J. T. Arnason, P. Morand, B. Hollebhone, L. C. Leitch, and B. J. R. Philogene, *Photochem. Photobiol.*, **44**(4), 441-451 (1986).

- 291 J. P. Reyftmann, J. Kagan, R. Santus, and P. Morliere, *Photochem. Photobiol.*, **41**(1), 1-7 (1985).
- 292 E. Cielen, A. Tahri, K. Ver Heyen, G. J. Hoornaert, F. C. De Schryver, and N. Boens, *J. Chem. Soc., Perkin Trans. 2*, (7), 1573-1580 (1998).
- 293 C. A. Parker, 'Photoluminescence of Solutions', Elsevier Publishing Company, (1968).
- 294 S. G. Schulman, 'Fluorescence and Phosphorescence Spectroscopy: Physicochemical Principles and Practice', ed. R. Belcher and H. Freiser, Pergamon Press, (1977).
- 295 M. C. Gallazzi, F. Toscano, D. Paganuzzi, C. Bertarell, A. Farina, and G. Zotti, *Macromol. Chem. Phys.*, **202**(10), 2074-2085 (2001).
- 296 M. Dietrich and J. Heinze, *Synth. Met.*, **41-43**, 503-506 (1991).
- 297 S. Ando and M. Ueda, *Synth. Met.*, **129**, 207-213 (2002).
- 298 T. Yamamoto and H. Hayashi, *J. Polym. Sci., Part A: Polym. Chem.*, **35**, 463-474 (1997).
- 299 T. M. Clarke, K. C. Gordon, D. L. Officer, S. B. Hall, G. E. Collis, and A. K. Burrell, *J. Phys. Chem.*, submitted for publication (2003).
- 300 M. Ciofalo and G. La Manna, *Chem. Phys. Lett.*, **263**, 73-78 (1996).
- 301 A. F. Diaz and J. Bargon, in 'Electrochemical Synthesis of Conducting Polymers', ed. T. A. Skotheim, New York, (1986).
- 302 D. Fichou, G. Horowitz, B. Xu, and F. Garnier, *Synth. Met.*, **39**, 243-259 (1990).
- 303 D. Fichou, G. Horowitz, and F. Garnier, *Synth. Met.*, **39**, 125-131 (1990).
- 304 J. Guay, P. Kasai, A. Diaz, R. Wu, J. M. Tour, and L. H. Dao, *Chem. Mater.*, **4**(5), 1097-1105 (1992).
- 305 M. G. Hill, J.-F. Penneau, B. Zinger, K. R. Mann, and L. L. Miller, *Chem. Mater.*, **4**(5), 1106-1113 (1992).
- 306 B. Zinger, K. R. Mann, M. G. Hill, and L. L. Miller, *Chem. Mater.*, **4**(5), 1113-1118 (1992).
- 307 P. Bauerle, U. Segelbacher, K.-U. Gaudl, D. Huttenlocher, and M. Mehring, *Angew. Chem. Int. Ed. Eng.*, **32**(1), 76-78 (1993).
- 308 J. J. Apperloo, R. A. J. Janssen, P. R. L. Malenfant, L. Groenendaal, and J. M. J. Frechet, *J. Am. Chem. Soc.*, **122**(29), 7042-7051 (2000).

- 309 M.-A. Sato and M. Hiroi, *Synth. Met.*, **69**(1-3), 307-308 (1995).
- 310 M.-A. Sato and M. Hiroi, *Chem. Lett.*, 745-748 (1994).
- 311 M. G. Hill, K. R. Mann, L. L. Miller, and J.-F. Penneau, *J. Am. Chem. Soc.*, **114**(7), 2728-2730 (1992).
- 312 D. R. Crow, 'Principles and Applications of Electrochemistry', Blackie Academic & Professional, (1994).
- 313 P. H. Rieger, 'Electrochemistry', Chapman & Hall, (1994).
- 314 J. Roncali, M. Giffard, M. Jubault, and A. Gorgues, *J. Electroanal. Chem.*, **361**, 185-191 (1993).
- 315 J. Salbeck, *J. Electroanal. Chem.*, **340**, 169-195 (1992).
- 316 K. Kaneto, Y. Kohno, K. Yoshino, and Y. Inuishi, *J. Chem. Soc., Chem. Commun.*, 382-383 (1983).
- 317 H. Harada, T. Fuchigami, and T. Nonaka, *J. Electroanal. Chem.*, **303**, 139-150 (1991).
- 318 J. Roncali, F. Garnier, M. Lemaire, and R. Garreau, *Synth. Met.*, **15**, 323-331 (1986).
- 319 G. Zotti, R. A. Marin, and M. C. Gallazzi, *Chem. Mater.*, **9**(12), 2945-2950 (1997).
- 320 I. Mukoyama, K. Aoki, and J. Chen, *J. Electroanal. Chem.*, **531**(2), 133-139 (2002).
- 321 G. G. Wallace, Personal Communication to D. L. Officer, (2003).
- 322 C. A. Cutler, A. K. Burrell, D. L. Officer, C. O. Too, and G. G. Wallace, *Synth. Met.*, **128**, 35-42 (2002).
- 323 Z.-G. Xu and G. Horowitz, *J. Electroanal. Chem.*, **335**123-134 (1992).

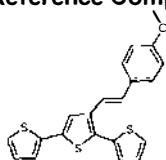
### Reference Compounds



styryl terthiophene LXXVI

TTh=-Bz

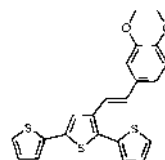
dimer = LXXVIII



methoxystyryl terthiophene LXXVII

TTh=-BzOMe

dimer = LXXIX

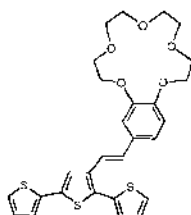


dimethoxystyryl terthiophene XXIX

TTh=-Bz(OMe)<sub>2</sub>

dimer = LXXV

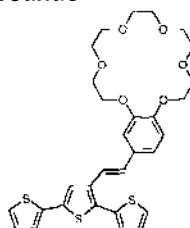
### Crown Compounds



styryl-15-crown-5 terthiophene I

TTh=-Bz15c5

dimer = LXVII

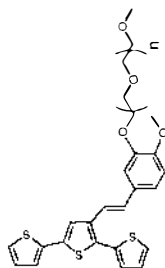


styryl-18-crown-6 terthiophene II

TTh=-Bz18c6

dimer = LXVIII

### Open-Chain Compounds

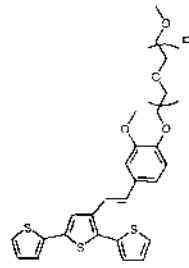


isovanillin-derived

n = 1 TTh=-BzOCOCOC XXIII dimer = LXIX

n = 2 TTh=-BzOCOCOCOC XXIV dimer = LXX

n = 3 TTh=-BzOCOCOCOCOC XXV dimer = LXXI



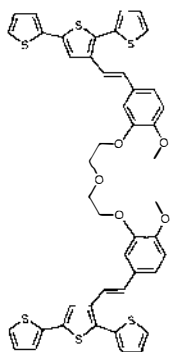
vanillin derived

TTh=-BzOCOCOC XXVI dimer = LXXII

TTh=-BzOCOCOCOC XXVII dimer = LXXIII

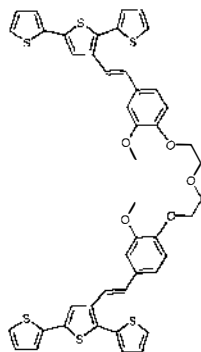
TTh=-BzOCOCOCOCOC XXVIII dimer = LXXIV

### Hemicrown Compounds



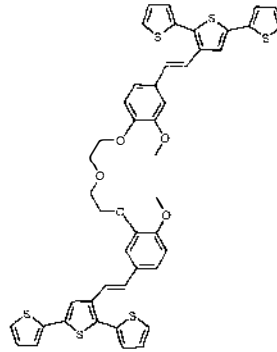
Isovanillin-derived hemicrown LXI

TTh=-BzOCOCOBz=-TTh



Vanillin-derived hemicrown LXII

TTh=-BzOCOCOBz=-TTh



Mixed hemicrown LXIII

TTh=-BzOCOCOBz=-TTh